

Camila Machado de Azevedo Correia

**Positive Energy Schools with Cool Materials and Passive  
Strategies: Scenarios and Perspectives for the Brazilian  
Context**

Thesis submitted to the Postgraduate Program in  
Architecture and Urbanism from the University of  
Brasilia as a requirement for obtaining the  
Academic Doctorate Degree in Architecture and  
Urbanism.

Advisor: Prof. PhD Claudia Naves David Amorim

Co-advisor: Prof. PhD Mattheos Santamouris

Brasília, 2024.

Camila Machado de Azevedo Correia

**Escolas de Energia Positiva com Materiais Frios e  
Estratégias Passivas: Cenários e Perspectivas para o  
Contexto Brasileiro**

Tese submetida ao Programa de Pós-Graduação  
em Arquitetura e Urbanismo da Universidade de  
Brasília como requisito para obtenção do título  
de Doutorado em Arquitetura e Urbanismo.

Orientadora: Profa. Dra. Claudia Naves David  
Amorim

Co-orientador: Prof. Dr. Mattheos Santamouris

Brasília, 2024.

## CATALOG CARD

MC824p Machado de Azevedo Correia, Camila  
Positive Energy Schools with Cool Materials and Passive Strategies: Scenarios and Perspectives for the Brazilian Context / Camila Machado de Azevedo Correia; orientador Cláudia Naves David Amorim; co-orientador Mattheos Santamouris. -- Brasília, 2024.  
298 p.

Tese (Doutorado em Arquitetura e Urbanismo) --  
Universidade de Brasília, 2024.

1. Educational Buildings. 2. Cool Materials. 3. Positive Energy Buildings. 4. Passive Survivability. I. Naves David Amorim, Cláudia, orient. II. Santamouris, Mattheos, co-orient. III. Título.

## REFERENCE

CORREIA, Camila Machado de Azevedo. Positive energy schools with cool materials and passive strategies: scenarios and perspectives for the brazilian context. 2024. 298 f. Tese (Doutorado) - Curso de Arquitetura e Urbanismo, Universidade de Brasília, Brasília, 2024.

## ASSIGNMENT OF RIGHTS

A University of Brasília is granted permission to reproduce copies of this doctoral thesis and to lend or sell such copies only for academic and scientific purposes. The author reserves other publication rights and no part of this master's dissertation may be reproduced without the author's permission.

Doctoral thesis submitted as a partial requirement for the attainment of the Academic Doctorate degree by the Research and Postgraduate Program of the Faculty of Architecture and Urbanism at the University of Brasília, under the supervision of the committee comprised of professors:

---

Prof. PhD Cláudia Naves David Amorim (advisor)  
University of Brasília (UnB)

---

Prof. PhD Mattheos Santamouris (co-advisor)  
University of New South Wales (UNSW)

---

Prof. PhD Fabrizio Ascione  
Università degli Studi di Napoli Federico II (UNINA)

---

Prof. PhD Denia Kolokotsa  
Technical University of Crete (TUC)

---

Prof. PhD Joara Cronemberger Ribeiro Silva  
University of Brasília (UnB)



"The important thing is not to stop questioning.  
Curiosity has its own reason for existing."

Albert Einstein

## **ACKNOWLEDGMENTS**

Firstly, I thank God for His constant care and sustenance, for giving me strength in every moment and for leading me to paths much better than I could plan.

Thanks to Professor Cláudia Amorim, for her dedicated and consistent guidance, insights that fundamentally shaped, directed and refined the entire thesis, for her patience throughout this process and for inspiring me to be a persistent researcher. My appreciation to my co-advisor, Professor Mattheos Santamouris, who provided essential guidance during the sandwich period at UNSW (University of New South Wales) from August to December 2022. He not only deepened my understanding of cool materials but also supervised pilot simulations, contributed to the methodological foundation and continued overseeing the thesis development.

I am thankful to the evaluators who kindly accepted to assess and make valuable contributions. Thanks to Professor Joara Cronemberger from UnB (University of Brasília) for suggestions during meetings at LACAM (Built Environment Comfort Laboratory) and the intermediate evaluation, which were important in refining the focus of the research. Thanks to Professor Fabrizio Ascione from UNINA (Università degli Studi di Napoli Federico II) for an accurate and detailed analysis that enhanced the quality of all parts of the thesis. Also, thanks to Professor Denia Kolokotsa from TUC (Technical University of Crete Kounoupidiana) for accepting the invitation to the final defense and dedicating her time to the evaluation.

I express my gratitude to CNPq (National Council for Scientific and Technological Development) for the scholarship for the sandwich doctorate program abroad, which made it possible to conduct part of the studies at UNSW, a significant period for enhancing the quality of this thesis.

Thanks to Professor Paulo Menezes from UnB for providing soil data references. Thanks to architects and engineers from other Brazilian universities who shared relevant information: Matheus Geraldi from UFSC (Federal University of Santa Catarina) for energy consumption data of Brazilian public schools and Marcela Andrade from USP (University of São Paulo) for technical information on Brazilian cool paintings. Gratitude to various researchers who kindly answered questions: including Mário Silva from UFV (Federal University of Viçosa) on optimization

processes, Ana Carolina Veloso from UFMG (Federal University of Minas Gerais) on soil modeling for thermoenergetic simulations, Letícia Gabriela Eli from UFSC on the interpretation of thermal-energetic performance of buildings through heat balance graphs, Emeli Guarda from USFC on future weather generator software and Amanda Krelling from UFSC on software outputs for passive survivability analysis.

I appreciate colleagues at UNSW: Jianxiu Wen for friendship, experience exchange in scientific research and great patience in teaching simulation software, Hassan Khan for exchanging experiences in cool materials and Alessia Boccalatte for sharing references on photovoltaic systems.

Thanks also to colleagues at UnB, including Thiago Goes, who assisted me numerous times in using simulation software and calculating occupied hours in thermal comfort, Adriano Silva, who shared data and models of standardized schools from FNDE, Jader Freitas and João Walter for sharing experiences in zero energy buildings simulations, Túlio Bones and Juliana Andrade for learning exchanges and Marcílio Sudério and Isabella Gaspar for support in developing oratory skills for intermediate and final thesis defense panels.

Thanks to DesignBuilder software support team, who kindly helped correct errors, answered questions and suggested alternative paths for obtaining relevant outputs for the analyses in this thesis, with special thanks to Vangelis Karagiannis, Luis Sousa and Marco Passarelli. Also, thanks to Aaron Boranian from Big Ladder Software for suggestions on simulation configurations using thermochromic cool coatings.

Thanks to my mother, Nelma Correia, for constant and unconditional support in all stages of my life and especially during the thesis development. Thanks also to Renato Medeiros, Fábio Areias and all other family members who provided moral support during the challenges faced throughout this academic journey.

This thesis is the result of a collective journey and I am profoundly grateful for each contribution that shaped this work, made by so many people who believe that science can help to build a better world.

## ABSTRACT

Standardized replicable buildings can cause discomfort and increased air conditioning usage currently and in the future. Besides, supercool materials are effective passive cooling solutions to enhance the potential for positive energy buildings and passive survivability. Therefore, It is hypothesized that it is possible to achieve positive energy, adequate thermal comfort, thermal resilience and passive survivability in Brazilian standardized public schools of the FNDE with easy replicability in eight bioclimatic zones using cool materials, other passive strategies and local energy production from photovoltaic system. Hence, this thesis is structured by the following specific objectives and methods: identify thermoenergetic performance of current standardized brazilian public schools in 8 bioclimatic zones through DesignBuilder simulations and ASHRAE 55 adaptive thermal comfort analysis, verify suitable cool materials and passive strategies to achieve thermal comfort by optimization simulations with EnergyPlus and JEA Algorithm, sensitivity and heat balance analysis, evaluate the thermal resilience and passive survivability of the schools in present and future (Typical Meteorological Year – TMY, 2050 and 2080) with frequency, intensity and severity indicators and assess achieving a positive energy balance. Results showed that the current school models lack thermal comfort. Thus, different cool paints are recommended: Thermochromic for Heating-dominated; Spectrally Selective for Cooling-dominated dry and High Broadband Emissivity for Extreme-cooling-dominated humid zones. Regarding opaque envelope, thermal mass flat roofs and insulated walls are advised. In 7 out of the 8 climates, the cool paint on thermal mass flat roof was the most influential passive strategy on thermal comfort, followed by natural ventilation. The optimized school model ensures thermal comfort and passive survivability across all bioclimatic zones in TMY without artificial air conditioning, easily achieving a positive energy balance with PV system. Despite improved results in thermal comfort and passive autonomy in all scenarios, the optimized model exhibits higher percentage of occupied hours in dangerous heat. Consequently, artificial conditioning and a PV system increase of up to 18.75% are necessary to ensure thermal comfort, passive survivability and positive energy.

**Keywords:** Educational Buildings, Cool Materials, Positive Energy Buildings, Passive Survivability

## RESUMO

Edifícios padronizados replicáveis podem causar desconforto e aumento no uso de ar-condicionado atualmente e no futuro. Além disso, materiais super frios são soluções passivas eficazes para aprimorar o potencial de edifícios com energia positiva e sobrevivência passiva. Portanto, hipotetiza-se que seja possível alcançar energia positiva, conforto térmico, resiliência térmica e sobrevivência passiva em escolas públicas brasileiras padronizadas do FNDE, com fácil replicabilidade em oito zonas bioclimáticas, utilizando materiais frios, outras estratégias passivas e produção de energia local a partir de sistemas fotovoltaicos. Portanto, esta tese é estruturada pelos seguintes objetivos específicos e métodos: identificar o desempenho termoenergético das atuais escolas públicas brasileiras padronizadas em oito zonas bioclimáticas por meio de simulações do DesignBuilder e análise de conforto térmico adaptativo da ASHRAE 55; verificar materiais frios adequados e estratégias passivas para alcançar conforto térmico por meio de simulações de otimização com o EnergyPlus e o algoritmo JEA, análise de sensibilidade e balanço térmico; avaliar a resiliência térmica e a sobrevivência passiva das escolas no presente e futuro (Ano Meteorológico Típico - TMY, 2050 e 2080) com indicadores de frequência, intensidade e severidade; e avaliar o alcance de um balanço energético positivo. Os resultados mostraram que os modelos escolares atuais carecem de conforto térmico. Assim, recomendam-se diferentes tipos de tintas frias: Termocrômicas para áreas dominadas por aquecimento; Espectralmente Seletivas para áreas secas dominadas por resfriamento e Alta Emissividade de Banda Larga para áreas úmidas dominadas por resfriamento extremo. Em relação ao envelope opaco, recomendam-se telhados planos de massa térmica e paredes isoladas. Em 7 das 8 zonas climáticas, a tinta fria sobre o telhado plano de massa térmica foi a estratégia passiva mais influente no conforto térmico, seguida pela ventilação natural. O modelo escolar otimizado garante conforto térmico e sobrevivência passiva em todas as zonas bioclimáticas em TMY sem ar-condicionado, alcançando facilmente um balanço energético positivo com o sistema fotovoltaico. Apesar dos resultados melhorados no conforto térmico e na autonomia passiva em todos os cenários, o modelo otimizado apresenta uma maior porcentagem de horas ocupadas em condições perigosas de calor. Conseqüentemente, é necessário o uso de

condicionamento artificial e um aumento de até 18,75% no sistema fotovoltaico para garantir conforto térmico, sobrevivência passiva e energia positiva.

**Palavras-chaves:** Edifícios Educacionais, Materiais Frios, Edifícios de Energia Positiva, Sobrevivência Passiva

## LIST OF FIGURES

Figure 1 - Thesis Structure.....	35
Figure 2 - Solar reflectivity and emissivity scale of materials.....	42
Figure 3 - Reflectivity and Emissivity Wavelengths .....	42
Figure 4 - History of cool materials for cooling the built.....	43
Figure 5 - Cool Materials Cooling Potential and Forms of Application.....	44
Figure 6 - Surface temperature variation according to color composition and roughness.....	45
Figure 7 - Surface temperature measurement of cool pavement and conventional sidewalk .....	45
Figure 8 - Inorganic and non-toxic pigments with high near-infrared reflectance (>65%) and solar reflectance (>53.51%).....	46
Figure 10 - Glass beads for retro-reflective property .....	48
Figure 11 - Retro-reflective coatings with glass spheres .....	48
Figure 12 - Inks with leuco dyes, from four different manufacturers, which show variable reflectivity according to temperature transition.....	49
Figure 13 - Experimental tests of spectrally selective multilayer silica and aluminum materials.....	51
Figure 14 - Brazilian Bioclimatic Zoning .....	55
Figure 15 - Brazilian Bioclimatic Chart .....	55
Figure 16 - Classification of Brazilian climates according to Roriz (2014) .....	59
Figure 17 - Suitable cool materials according to temperature and humidity variation.....	61
Figure 18 - Predominant forms of public school buildings in Brazil .....	65
Figure 19 - Types of Building Compositions.....	65
Figure 20 - Characterization of the school building in terms of operating shifts (a), installations (b) and year of construction (c).....	67
Figure 21 - Histograms of continuous variables: annual energy consumption (a), floor plan area (b) and number of students (c) .....	68
Figure 22 - EUI of schools according to each bioclimatic zone in Brazil.....	70
Figure 23 - EUI of brazilian schools in each bioclimatic region and thermal satisfaction .....	71
Figure 24 - EUI versus environmental satisfaction with year-round temperature in classrooms (a) and lighting and airflow in office rooms and classrooms (b).....	72

Figure 25 - Typical energy end uses for schools for each climate zone in Brazil. (a) End uses for schools with high air conditioning; (b) End uses for schools with low level of air conditioning.....	74
Figure 26 - Discretisation and average EUI of (a) Log EUI, (b) Floor-plan area, (c) Occupation and (d) Cooling capacity.....	75
Figure 27 - Types of schools financed by the FNDE until 2022.....	79
Figure 28 - Shape of FNDE schools – PAR and Proinfancia.....	79
Figure 29 - Perspectives of FNDE Schools.....	80
Figure 30 - Percentage of Rectangular and Multi-buildings Schools.....	80
Figure 31 - Materials evaluated in computer simulations.....	85
Figure 32 - Place of application of cool materials.....	88
Figure 33 - Most used softwares cor computer simulations.....	88
Figure 34 - Possible Objective functions and variables in Optimization Method.....	99
Figure 35 - Pareto front curve.....	103
Figure 36 - Key indicators for indoor thermal performance.....	112
Figure 37 - Building Diagnosis Example.....	113
Figure 38 - Dimensions for selecting scenarios to assess thermal resilience.....	114
Figure 39 - Future annual emissions of CO <sub>2</sub> and Contribution to global surface temperature increase from illustrative scenarios.....	117
Figure 40 – Methods Steps.....	119
Figure 41 - Flowchart: Systematic Review of Literature on cool materials applied to zero and positive energy contexts.....	121
Figure 42 - Flowchart: Systematic Review of Literature on cool materials and applicability analysis to the Brazilian context.....	124
Figure 43 - Flowchart: Systematic Review of Literature on brazilian school patterns and SWOT analysis.....	126
Figure 44 - Flowchart: Systematic Review of Literature on multiobjective optimization analysis.....	128
Figure 45 - Flowchart: Systematic Review of Literature on Thermal Resilience in Buildings.....	129
Figure 46 - Standardized 1 Classroom School Floor Plan, Perspective and Sections.....	130
Figure 47 - Variables and possible combinations of the algorithmic optimization process.....	135



Figure 48 - Details of variables tested in optimization simulations .....	136
Figure 49 - Adjusted R-squared Value Accuracy in Sensitivity Analysis .....	141
Figure 50 - Recommendations for minimum ground clearances .....	146
Figure 51 - PV support suitable for flat roofs .....	147
Figure 52 - PV inclination and PV Rows Spacing.....	148
Figure 53 - Graph model for Energy Balance Achievement Analysis .....	149
Figure 54 – Summary of Current State 1 Classroom School Heat Balance .....	152
Figure 55 - Summary of Optimized 1 Classroom School Heat Balance .....	161
Figure 56 - Impact of Variables on Thermal Comfort.....	162
Figure 57 - Impact of Cool Materials and Reflectivities on Thermal Comfort.....	162
Figure 58 - Variations in Wall Type .....	165
Figure 59 - Variations in Roof Type.....	166
Figure 60 - Energy Balance Achievement Analysis of Optimized 1 Classroom School .....	171
Figure 61 - Thermal Resilience and Passive Survivability Results .....	172
Figure 62 - Final Energy Balance in Optimized 1 Classroom School in TMY, 2050 and 2080 .....	177

## LIST TABLES

Table 1 – Types of Energy Balance, Geographical Limit, Location of Energy Production .....	38
Table 2 - Summary Table of Characteristics of Cool Materials and Climatic Indication .....	52
Table 3 - Technical-construction recommendations for the 8 Brazilian bioclimatic zones.....	56
Table 4 - Wall and roof properties recommended by ABNT (2005a).....	57
Table 5 - Bioclimatic Zones, Strategies, Predominant Needs Most suitable Cool Materials.....	62
Table 6 – Prices of Cool and Conventional Paints .....	63
Table 7 - Areas of Subspaces in Brazilian Public Schools .....	66
Table 8 - Summary statistics of continuous variables.....	67
Table 9 - Climates considered in the parametric simulation in recent studies .....	69
Table 10 - Characteristics of Brazilian public schools .....	73
Table 11 - Parameters used in the simulations in previous studies.....	76
Table 12 - SWOT analysis of the current stock of brazilian school buildings .....	77
Table 13 - Areas of PAR-FNDE Standard Schools .....	81
Table 14 - Areas of Proinfancia-FNDE Standard Schools.....	81
Table 15 - Building Materials – FNDE Standard schools.....	82
Table 16 - Characteristics of Standard Schools in relation to ABNT parameters (2005a).....	83
Table 17 - Type of artificial conditioning system proposed by the FNDE in standardized projects .....	84
Table 18 - Installed lighting power.....	84
Table 19 - Electrical Equipment Power Density.....	85
Table 20 - Evaluated cool materials and respective climatic contexts considered on computer simulations .....	86
Table 21 - Summary of optimization studies.....	94
Table 22 - Main Characteristics of Resilient Buildings.....	107
Table 23 - Standard Effective Temperatures Limits .....	111
Table 24 - Examples of thermal resilience studies, scenarios mentioned and the weather data generator softwares .....	116

Table 25 - Selected cities TMY climate files used in the thesis .....	130
Table 26 - Kiva Foundation Settings .....	131
Table 27 - Settings of Super Cool Coatings (Paints) tested in each Climatic Group	136
Table 28 - Summary of optimization algorithm settings.....	139
Table 29 - Bitumen Felt Thermal Properties.....	145
Table 30 - Summary of occupied hours in comfort and discomfort and Heat Balance of Current State 1 Classroom School .....	151
Table 31 - Optimal solutions for extreme cooling dominated zones .....	155
Table 32 - Worse solutions for extreme cooling dominated zones .....	155
Table 33 - Optimal solutions for cooling dominated zones .....	157
Table 34 - Worse solutions for cooling dominated zones .....	157
Table 35 - Optimal solutions for heating dominated zones: Summer .....	158
Table 36 - Optimal solutions for heating dominated zones: Winter .....	159
Table 37 - Worse solutions for heating dominated zones: Summer .....	159
Table 38 - Worse solutions for heating dominated zones: Winter .....	159
Table 39 - Comparison of heat balances due to roof composition variations of 1 classroom school.....	164
Table 40 - Comparison of heat balances due to wall composition variations of 1 classroom school.....	164
Table 41 - Summary of Strategies and Comfort Results .....	168
Table 42 - Monthly Loads Sizing .....	170
Table 43 - Photovoltaic System Dimensioning .....	170

## LIST OF ACRONYMS AND ABBREVIATIONS

ABNT	Brazilian Association of Technical Standards
ANEEL	National Electric Energy Agency
ANN	Artificial Neural Network
AR	Assessment Report
Autonomous ZEB	Autonomous or Self-Sufficient Building
AWD	Ambient Warmness Degree
BAU	Business as Usual
BPO	Building Performance Optimization
CB3E	Center for Excellence in Energy Efficiency
DBT	Dry Bulb Temperature
EA	Evolutionary Algorithms
ELETROBRÁS	Brazilian Electric Power Company
EMS	Energy Management System
END	Energy Neutral District
EPE	Energy Research Office
EPN	Energy Positive Neighborhood
FDE	Foundation for the Development of Education
FNDE	National Education Development Fund
GA	Genetic Algorithm
HI	Heat Index
IBGE	Brazilian Institute of Geography and Statistics
IEA	International Energy Agency
INEP	National Institute of Educational Studies and Research Anísio Teixeira
INI-C	Normative Instruction Inmetro for the Classification of Energy Efficiency of Commercial, Service and Public Buildings
INMET	National Institute of Meteorology
INMETRO	National Institute of Metrology, Quality and Technology
IOD	Indoor Overheating Degree
IPCC	Intergovernmental Panel on Climate Change
ISO	International Organization for Standardization

jEPlus	EnergyPlus Simulation Manager
KPI	Key Performance Indicator
LHS	Latin Hypercube Sampling
LC-ZEB	Life Cycle Zero Energy Building
LEED	Leadership in Energy and Environmental Design
MEC	Ministry of Education
MMA	Ministry of the Environment
NED	Neutral Energy District
Net ZEB or NZEB	Net Zero Energy Building
NOCT	Nominal Operating Cell Temperature
NSGA	Non-dominated Sorting Genetic Algorithm
nZEB	Nearly Zero Energy Building
PAR	Plan of Articulated Actions
PBE Edifica	National Energy Conservation Label of the Brazilian Building Labeling Program
PEB	Positive or Plus Energy Building or Positive Energy Blocks
PED	Positive Energy District
PEN	Positive Energy Neighborhood
PMV	Predicted Mean Vote
PPD	Predicted Percentage of Dissatisfied
PROCEL	National Program for Electricity Conservation
PROCEL INFO	PROCEL's Information Center
PROINFÂNCIA	National Program for Restructuring and Acquisition of Equipment for the Public School Network of Early Childhood Education
PROJETEEE	Designing Energy-Efficient Buildings
PV	Photovoltaic
PSO	Particle Swarm Optimization
SINAPI	National System of Prices and Indices for Civil Construction
SA	Simulated Annealing
SE	Energy Department
SET	Standard Effective Temperature
SRC	Standardized Regression Coefficient

SRES	Special Report on Emissions Scenarios
SSP	Shared Socioeconomic Pathways
TA	Thermal Autonomy
TAR	Technical Assessment Report
TMY	Typical Meteorological Year
TRY	Test Reference Year
UFSC	Federal University of Santa Catarina
UN	United Nations
WBGT	Wet-Bulb Globe Temperature
WSM	Weighted Sum Method
XMY	Extreme Meteorological Year
ZBBR	Brazilian Bioclimatic Zone
ZEB	Zero Energy Building
ZED	Zero Energy District

# SUMMARY

<b>1. INTRODUCTION .....</b>	<b>21</b>
1.1. Problem.....	29
1.2. Justification .....	32
1.3. Originality .....	33
1.4. Hypothesis .....	33
1.5. Objectives .....	34
1.6. Thesis Structure .....	34
<b>2. LITERATURE REVIEW .....</b>	<b>35</b>
2.1. Zero and Positive Energy Buildings and Districts: Definitions and compatibility with Cool Materials .....	35
2.2. Cool Materials as a Passive Strategy: State of the art of international research .....	41
2.3. Bioclimatic zones and passive strategies recommended for the Brazilian context .....	54
2.4. Analysis of Applicability of Cool Materials to the Brazilian Context and Costs of Brazilian Supercool paints.....	60
2.5. Costs of Brazilian Supercool paints and comparison with conventional paints .....	62
2.6. Brazilian School Building Stock: Construction and Energy Consumption Patterns.....	64
2.7. FNDE standard schools: Buildings characteristics .....	78
2.8. Computer Simulation of Cool Materials .....	85
2.9. Building Thermoenergetic Optimization.....	92
2.10. Thermal Resilience and Passive Survivability in Buildings.....	106
<b>3. METHODS.....</b>	<b>118</b>
3.1. Literature Review .....	120
3.2. Optimization Process .....	129
3.3. Transformation of Optimized Schools in ZEB.....	143
3.4. Thermal Resilience and Passive Survivability Analysis.....	149
<b>4. RESULTS .....</b>	<b>151</b>
4.1. Pilot Simulation Results.....	151
4.2. Optimization Results .....	154
4.4. Final Stage results.....	167
4.5. Transformation of Optimized Schools in ZEB.....	169
4.6. Thermal Resilience and Passive Survivability Analysis.....	171
<b>5. CONCLUSIONS .....</b>	<b>178</b>
<b>REFERENCES.....</b>	<b>188</b>

<b>APPENDICES .....</b>	<b>205</b>
-------------------------	------------



## 1. INTRODUCTION

Currently more than 55% of the world population lives in cities and this percentage is predicted to increase to 68% by 2050 (PISELLO, 2017). This continuous growth of built-up areas potentiates the phenomenon of heat islands, reduces the levels of comfort in external and internal spaces and increases: the energy consumption of buildings with cooling, the urban ecological footprint, the concentration of polluting gases and the occurrence of problems of heat-related health or mortality (MORINI *et al.*, 2017; PISELLO, 2017; SANTAMOURIS; YUN, 2020). Another aggravating factor is climate change and extreme weather events, representing a significant challenge in the built environment, becoming more frequent (FLORES-LARSEN; FILIPPÍN; BRE, 2023; KRELLING *et al.*, 2023), intense and longer-lasting (HONG *et al.*, 2023), as evidenced by unprecedented record temperatures in many parts of the world over the last two decades (SERDAR; MACAULEY; AL-GHAMDI, 2022) and more than 12,000 extreme events recorded in the last 50 years resulting in over 2 million deaths and more than 4.3 trillion dollars in economic losses (HONG *et al.*, 2023). The increase in heatwaves due to climate change is generating various consequences, such as increased ambient temperatures, reduced heating energy demand (TAVAKOLI *et al.*, 2022), compromised energy and environmental performance of buildings (CIRRINCIONE; MARVUGLIA; SCACCIANOCE, 2021), adverse effects on health (heatstroke, heat exhaustion and other heat-related illnesses) (ZHANG *et al.*, 2021), increased mortality (MEHMOOD *et al.*, 2022), social security issues, geopolitical instability (climate refugees), reduced biodiversity safeguards (CIRRINCIONE; MARVUGLIA; SCACCIANOCE, 2021), a growing demand for cooling and increased greenhouse gas emissions (SIU *et al.*, 2023; TAVAKOLI *et al.*, 2022). Furthermore, the high energy demand during extreme events can coincide with or even cause power outages, exposing residents to health risks and further endangering building occupants (HONG *et al.*, 2023; ZHANG *et al.*, 2021).

Regarding to the energy consumption, the construction and industry sectors are responsible for 36% of final energy consumption and 40% of greenhouse gas emissions, which could reach 50% if the energy consumption in buildings continues growing at current rates (LIU *et al.*, 2019; ZHANG *et al.*, 2021). In Brazil, residential, commercial, public and service buildings represent more than 40% of the national energy demand (EPE, 2019).

This context has led to the emergence of several international initiatives (SHIRINBAKHS; HARVEY, 2021) to achieve the decarbonization targets of the Paris Agreement (ZHANG *et al.*, 2021) and Clean and Affordable Energy and Sustainable Cities and Communities of the Goals of the Sustainable Development (DERKENBAEVA *et al.*, 2022). Consequently, were developed design strategies and advanced technologies to reduce energy consumption and environmental impacts (HUANG, P.; HUANG, G.; SUN, 2018; PARKIN; HERRERA; A COLEY, 2018; PIDERIT *et al.*, 2019; HAWILA *et al.* 2022) such as Zero Energy Buildings and Districts<sup>1</sup>, which have high energy efficiency and produce, through renewable sources, the same amount of energy they consume (SARTORI; NAPOLITAN; VOSS, 2012; LIU *et al.*, 2019), or Positive Energy Buildings and Districts<sup>2</sup>, which produce more energy than they use (HAWILA *et al.* 2022). In Brazil, definitions of these design strategies are also outlined in the Application Manual of Inmetro Instruction INI-C, which regulates the Brazilian Building Labeling Program – PBE Edifica. According to this guide, a Nearly Zero Energy Building (NZEB) is an energy-efficient building where 50% or more of its annual energy demand is supplied by renewable energy generated on-site or within the building's lot. Meanwhile, a Positive Energy Building (PEB) generates renewable energy on-site or within its lot boundaries, exceeding its annual energy demand (INMETRO, 2021).

These constructions are based on three cardinal strategies: passive climate technologies (such as bioclimatic design, envelope solutions, solar orientation of the building), active technologies (with artificial climate and efficient equipment) and renewable energy technologies (COLLADO *et al.*, 2019; BANDEIRAS *et al.*, 2020; FRANCÉS *et al.*, 2020; ZHANG *et al.*, 2021).

Among the international initiatives that include Zero or Positive Energy, the following stand out: Executive Order 13,514 in the USA that requires all new buildings to be Net ZEB by 2030 (LIU *et al.*, 2019) and the requirements of the European Union (UE 2010/31) for a Near Zero Energy Buildings<sup>3</sup> for new or renovated buildings (HAWILA *et al.* 2022). Due to the fact that 85% of the buildings were constructed before 2000,

---

<sup>1</sup> Zero Energy Building – ZEB, Net Zero Energy Building – Net ZEB or NZEB, Zero Energy District – ZED and Energy Neutral District – END

<sup>2</sup> Positive or Plus Energy Building – PEB, Positive Energy Blocks – PEB, Positive Energy District – PED, Energy Positive Neighborhood – EPN

<sup>3</sup> Nearly Zero Energy Building – nZEB

with 75% of them displaying poor energy performance, the latest regulatory updates (EU Directive 844/2018 and the Provisional Agreement on EPBD Recast/2023) focus on the existing building stock. These updates mandate the complete decarbonization (80-95%) of all buildings by 2050 (EUROPEAN COMMISSION, n/d).

The school ZEB theme has been applied by government intervention plans in schools in Europe and the United States: School of the Future: Towards Zero Emission with High Performance Indoor Environment (2011-2016), Renew School (2014-2017), ZEMedS: Zero Energy MEDiterranean Schools (2013-2016), Kentucky Zero Energy Schools (2012). These established improvements in comfort with passive strategies; replacement of equipment by more efficient ones; production of local energy from renewable sources; use of computer softwares to verify the economic feasibility of implementing solutions, user training programs, recycling and water conservation (DETWILER, 2012, GAITANI *et al.*, 2015). In Brazil, there are no programs to achieve zero or positive energy in schools, but there are government initiatives regarding mandatory building standards to improve comfort and energy efficiency (FDE, 1990 *apud* KOWALTOWSKI; LABAKI; PINA, 2001; ABNT, 2005a; ME, 2007; BRITO *et al.*, 2019, PROCELINFO, n/d), energy saving with equipment efficiency (SE, n/d) and laws to encourage local production from renewable sources (ANEEL, 2012).

Other advances on zero energy in elementary schools were achieved in the United States, through a zero energy plan by Kentucky institutions, with wall insulation strategies, use of natural light, implementation of a geothermal heating and cooling system, energy efficiency, use of efficient light bulbs, use of renewable sources such as photovoltaic systems and recycling and water conservation (DETWILER, 2012).

In the national scenario, regarding the first stage of Zero or Positive Energy which is the constructive adaptation to the climate, there is NBR 15,220 normative, divided into five parts, which deals with the thermal performance of buildings. The third part of the document classifies the Brazilian territory into eight bioclimatic zones, based on a grouping of cities with similar temperatures and humidity and defines constructive guidelines for single-family housing of social interest, with recommendations for transmittance and thermal delay for walls and roofs and passive air conditioning strategies (ABNT, 2005a). Minimum performance and

comfort requirements are also established in Brazilian normatives (ABNT, 2021a; 2021b; 2021c).

The current schools follow a standardized model defined by the Foundation for the Development of Education – FDE, with minimum comfort parameters: room size, natural lighting and ventilation area, illuminance, types of lamp (FDE, 1990 *apud* KOWALTOWSKI; LABAKI; PINA, 2001). In addition to these requirements, there is a set of guidelines determined in the Technical Guidelines Manual of the National Program for Restructuring and Acquisition of Equipment for the Public School Network of Early Childhood Education – PROINFÂNCIA, used for renovations and construction of new school buildings, which requires a minimum height of the ceiling according to the region, thermal insulation of the roof, height of the windows for ventilation, sun protection by constructive elements or vegetation according to climatic needs and air renewal between roof and ceiling (ME, 2007). However, the characteristics defined in these programs are generic and superficial, which do not explore the maximum potential of each region for energy savings.

As for the second aspect, the reduction of consumption with equipment, a Manual for Saving Electric Energy at Schools was published by the Government of the State of São Paulo. This suggests regular monitoring of bills, reduction of unnecessary lighting, strategies for optimizing the lighting system, taking advantage of natural light, enhancing luminous comfort, energy savings with optimization of water use, rational use of equipment such as refrigerators, drinking fountains, computers, copiers, air conditioners and finally, electrical system and equipment maintenance recommendations (SE, n/d). Even with this initiative, not all Brazilian states have adopted similar projects and therefore, cases of great energy waste with obsolete equipment can be identified in other regions; operation of active air conditioning systems throughout the day, even when the environments are not occupied; and activation of artificial lighting by circuit breakers, depriving individual shutdown when there is no occupation (BASTOS *et al.*, 2012).

As for the third stage, related to renewable energies, on April 17, 2012, the Normative Resolution 482 was published by the National Electric Energy Agency – ANEEL, which stipulates conditions for distributed microgeneration and minigeneration and regulates the credit compensation system with the public

electricity grid. This decision was a small step forward to stimulate local production from renewable sources (ANEEL, 2012).

Since the emergence of design solutions in 1976 in Denmark, the concept of Zero and Positive Energy has received several variations in terms of physical or geographic limits (building, neighborhood or district), location of energy production, period of time for assessing the energy balance (period of balance), ways of interacting with the grid, energy assessment metrics, assessment of carbon dioxide emission and environmental impacts (WELLS; RISMANCHI; AYE, 2018; COLLADO *et al.*, 2019; LIN *et al.*, 2019; LIN *et al.*, 2020; SHIRINBAKHS; HARVEY, 2021; ZHANG *et al.*, 2021; DERKENBAEVA *et al.*, 2022; HAWILA *et al.*, 2022).

In addition to zero and positive energy initiatives, recent studies highlight the need to enhance the thermal resilience and the passive survivability of buildings to make them more adaptable and prepared for climate-change-related extreme events that are expected to become more frequent, intense and severe (SIU *et al.*, 2023). These buildings feature designs and possibilities for passive cooling, low-energy consumption systems, backup power and conscious human behavior (MEHMOOD *et al.*, 2022; ZHANG *et al.*, 2021; HONG *et al.*, 2023). These essential strategies for thermal resilience and passive survivability in buildings, alternatives to the common active method of upgrading and resizing HVAC systems, help avoid grid overloads during peak hours that could lead to power outages in extreme temperature events (ATTIA *et al.*, 2021; HONG *et al.*, 2023; SIU *et al.*, 2023) and maintain safe internal environmental conditions for occupants during such events (HONG *et al.*, 2023; ZHANG *et al.*, 2021), especially in regions with extremely high temperatures (MEHMOOD *et al.*, 2022). In addition to these advantages, buildings with thermal resilience and passive survivability offer various other benefits, such as improved air quality, increased comfort and enhanced productivity, sparking increased interest in studies evaluating building performance through resilience, aiming to surpass minimum standards and meet future performance targets (ISMAIL; OUAHRANI; TOUMA, 2023).

Although the concept of building thermal resilience and passive survivability is not yet part of building codes, there is growing interest in this area (HONG *et al.*, 2023), as reflected in current scientific discussions (FLORES-LARSEN; FILIPPÍN; BRE, 2023),

in the Sustainable Development Goals – SDGs (ATTIA *et al.*, 2021; CIRRINCIONE; MARVUGLIA; SCACCIANOCE, 2021; KHAN *et al.*, 2022), in RELi building ratings in Leadership in Energy and Environmental Design – LEED, in the practical guide for climate-resilient buildings by the United Nations Environment Programme and in indicators for resilient cities developed by International Organization for Standardization – ISO 37123 (HONG *et al.*, 2023). These initiatives align with the argument presented by Attia *et al.* (2021) that, while addressing the root cause of the climate change problem, it is crucial to deal with its effects. Given that the most critical future challenge in the construction sector is to prevent extreme temperatures caused by overheating, it is necessary to conceive and construct resilient and climate-resistant buildings (ATTIA *et al.*, 2021) in addition to energy efficiency and carbon metrics (MEHMOOD *et al.*, 2022), especially in schools, where the risk of overheating is even higher due to high occupancy density (SENGUPTA *et al.*, 2023a; 2023b).

Within the international scientific development on this field, there are studies on the application of cool or supercool materials as a passive conditioning solution on urban spaces and buildings, including on Zero or Positive Energy Buildings and Thermal Resilience in Buildings, since they have high solar reflectivity, high thermal emissivity of the heat absorbed (ASCIONE *et al.*, 2018; CASTALDO *et al.*, 2018; CABEZA; GRACIA; PISELLO, 2018; CABEZA; CHÀFER, 2020; XU *et al.*, 2020; TIAN *et al.*, 2021) and consequently high cooling potential (QI; ZHU; ZHANG, 2018; BERARDI; GARAI; MORSELLI, 2020). Because of their possibility to achieve surface temperature below the air temperature, these materials can reduce heat gains, passively cool the interiors of buildings and reduce the demand for mechanical cooling (BANIASSADI; SAILOR; BAN-WEISS, 2019). Furthermore, supercool coatings also provide additional advantages when used in ZEBs or PEBs that have a photovoltaic system on the roof: these materials reduce the temperature of the roof and the surrounding air and increase the reflected radiation received by the modules, favoring an increase in efficiency and local energy production (VASILAKOPOULOU *et al.*, 2023). The supercool coatings are available as tiles, asphalt shingles, metal roofs, elastomeric coatings, single-ply membranes (ROMEO; ZINZI, 2013), paintings or can be mixed with other materials as mortar and concrete (SANTAMOURIS; YUN, 2020).

Some advances in international research on cool materials are mentioned below: a numerical simulation of cool material in a vacuum chamber showed a maximum theoretical reduction in surface temperature of 60°C (CARLOSENA *et al.*, 2021). In experiments on scaled-down models and measurements with pyranometers, thermometers and surface temperature sensors, some low-cost cool materials had a temperature 8°C below ambient temperature. In computer simulations of a high-density urban context in Kolkata (India), cool materials in building roofs enabled a cooling island with a reduction of up to 10°C in air temperature (FENG *et al.*, 2021). In computer simulations of buildings, the application of cool materials on the roof of buildings with a predominantly warm climate (Alice Springs, Australia) enabled a reduction of 46 kWh/m<sup>2</sup> in annual energy demand for cooling, equivalent to almost 50% (FENG *et al.*, 2022b).

In research in the Brazilian context, experiments in reduced models with measurements by reflectometers and emissometers indicate lime paints as cool materials with high reflectivity and emissivity and low cost (WERLE; LOH; JOHN, 2014). In computer simulations of buildings, fiber cement roofs with high reflectivity in social housing in Rio de Janeiro showed a surface temperature 22°C lower than the conventional roof, a 60% reduction in building heat gains and a payback period of less than five years (SILVA; MARINOSKI; GUTHS, 2020).

In addition to prove the effectiveness of reducing the surface temperature and temperature of the surrounding air, recent international research (2016-2022) has contributed in types of materials and physicochemical compositions (PISELLO, 2017; LIM, 2019; SANTAMOURIS; YUN, 2020), cost (CARLOSENA *et al.*, 2021; FENG *et al.*, 2022b), scalability (ways of application and possibilities of complexity reduction for industrial reproduction) (CARLOSENA *et al.*, 2021; FENG *et al.*, 2021) and durability (QI; ZHU; ZHANG, 2018; YUAN *et al.*, 2018). Other studies have focused on the performance of materials in cases of mixed climates, with warm and cold periods where an adaptable material is needed (LIM, 2019; BERARDI; GARAI; MORSELLI, 2020), or in regions with high humidity or high concentration of pollutants, where spectrally selective supercool materials tend to reduce their performance and supercool materials with high emissivity in the broadband are more suitable (SANTAMOURIS; YUN, 2020; CARLOSENA *et al.*, 2021; FENG *et al.*, 2021; FENG *et al.*, 2022b).

The most common cool materials are: light-colored natural materials, high-reflectivity white coatings, infrared high-reflectivity colored, high-reflectivity asphalt materials, phase change materials – PCM, retroreflective, thermochromic, fluorescent and spectrally selective coatings (SANTAMOURIS; YUN, 2020), applied as a coating on floors, walls or roofs (PISELLO, 2017; SANTAMOURIS; YUN, 2020) of new or existing buildings (KOLOKOTSA *et al.*, 2018), which can increase the durability of the surfaces on which are applied (KOLOKOTSA *et al.*, 2018; BERARDI; GARAI; MORSELLI, 2020), counteract the growing trends of heat islands and global warming (MORINI *et al.*, 2017; BANIASSADI; SAILOR; BAN-WEISS, 2019), pollution (YUAN *et al.*, 2018), ozone concentration in cities and urban carbon footprint (PISELLO, 2017). As cool materials are used as a coating, the cooling effect of indoor spaces is also influenced by the substrate where they are applied to.

Such materials have been recently highlighted (LASSANDRO; TURI, 2017; YANG *et al.*, 2017) as a solution to improve the microclimate in urban canyons, significantly reduce the energy consumption of buildings with cooling (XU *et al.*, 2020), increase energy efficiency and comfort conditions and facilitate the achievement of Zero Energy Buildings – ZEBs and Zero Energy Districts – ZEDs (CASTALDO *et al.*, 2018; LASSANDRO; TURI; A ZACCARO, 2019), but they have a potentiated effect when applied on the roof on direct contact with solar radiation (PISELLO, 2017). Therefore, photovoltaic modules in ZEBs and ZEDs can reduce the cool coating area of the roof in contact with solar radiation and reduce the cooling effect of the passive strategy (SAILOR; ANAND; KING, 2021; BROWN *et al.*, 2020).

Thus, there is a need for: an assessment of the applicability of cool materials in the different types of Zero and Positive Buildings and Districts, considering physical or geographic limits and location of energy production; a more in-depth analysis of the possible application of these materials to the different Brazilian climatic configurations as the main passive strategy to increase comfort and reduce the growing need for artificial air conditioning; the ideal combination of wall and roof compositions as substrates for cool materials in the Brazilian context; as well as thermal resilience and passive survivability strategies to mitigate the risk of overheating in standardized public schools in Brazil.



### 1.1. Problem

The current Brazilian energy matrix is composed of 81.7% of renewable energy, 64.5% of which refers to hydroelectric production (EPE, 2019). Although Brazil is in a positive environmental context, this configuration is vulnerable mainly in periods of drought, forcing the adoption of non-renewable energy productions, such as the additional use of thermoelectric sources in the dry periods that occurred in 2014 (GALVÃO; BERMANN, 2015). In addition, the production of electricity in power plants generates primary, transformation and secondary losses (EPE, 2019) that are almost nullified in local production systems as in cases of zero or positive energy buildings.

The environmental impact of human activities has grown considerably and a large part of it caused by Civil Construction, in terms of use of natural resources, energy consumption and emission of pollutants. Residential, commercial, public and service buildings represent 50% of the national energy demand (MMA, 2013). Within this portion, only 1.6% of final energy use refers to the public sector (EPE, 2019), but they are the only buildings that currently have mandatory energy performance standards, both in cases of new construction and in retrofit circumstances, due to the publication of the Normative Instruction for Energy Efficiency 02/2014, which requires an "A" rating on the National Energy Conservation Label of the Brazilian Building Labeling Program – PBE Edifica (PBEEDIFICA, 2014; GOMES, 2015).

The public sector is composed of different types of buildings, with different users, functions, equipment and opening hours, which directly or indirectly interfere in the energy consumption profile. The statistical survey of these aspects in educational institutions was carried out for: university centers, which present 40.9% of consumption with lighting, 14.8% with air conditioning, 2.7% with microcomputers and 41.6% with other equipment (ALVAREZ; SAIDEL, 2001); and public schools, which also have the most representative consumption of lighting (GERALDI; GHISI, 2020).

Children's schools, despite being similar to workplaces in offices, require specific intervention strategies due to the following factors: a more varied functional program, with different types of activities; constant partial use of the structure due to longer vacation periods; and partial use of functional spaces, depending on school activities (RIZZO, 2009), which reflect in different consumptions in relation to other categories.

However, such particularities have so far been little considered in investigations to achieve zero or positive energy buildings.

Although there is a Brazilian climate diversity due to the territorial extension of the country, the current school construction standard is a replicable school model that aims to solve the high educational quantity demand, with resistance to vandalism, low cost, easy maintenance and flexibility (FERREIRA; MELLO, 2006).

After the evaluation of 23 works and 59 projects by the Foundation for the Development of Education – FDE, public sector responsible for educational institutions in the State of São Paulo, it is noted that the shapes of the buildings have different compactness indexes that influence energy consumption and energy conservation: compact and vertical, horizontal with a square in the center, distributed in a set of volumes (FERREIRA; MELLO, 2006). Many have window shading with overhangs, louvres and screens on facades with a higher incidence of solar radiation, as well as cross ventilation strategies in summer.

Brazil has 137,828 basic education schools (infant, elementary and high school), of which 84,915 are urban and 52,913 are rural (INEP, 2021). Of this total, 30,181 were built or renovated by the National Education Development Fund – FNDE, which is a federal government institution with significant operations throughout Brazil and enables standardized projects for the construction of public schools (MODLER, 2017). Of all basic education schools, 5,321 were investigated in previous studies (GERALDI; GHISI, 2020), 50% operate during the morning, afternoon and night and 45% only during the morning and afternoon and therefore have more significant energy consumption outside peak hours (before 6pm or after 9pm). The lowest consumption months are December, January, February and July (due to school holidays) and the highest consumption months are March, April and May, which still have high temperatures (GERALDI; GHISI, 2020).

According to Geraldi and Ghisi (2020), many schools have more than 30 years of construction (24.38% built between 1939-1964 and 47.53% between 1964-1990), therefore, built before the regulations currently in force and probably have few guidelines related to energy efficiency. None of the analyzed buildings has a heating

system, most do not have air conditioning in the classrooms (78%) and others do not have any air conditioning system in rooms (39%) (GERALDI; GHISI, 2020).

The schools with the most satisfied users in terms of comfort have air conditioning equipment and higher installed power of artificial lighting in relation to the others, which results in a variation of Energy Use Intensity – EUI between 93.08 to 122.20 kWh/student.year, while those with more dissatisfaction vary between 63.18 to 72.55 kWh/student.year. It was identified that the “determinants factors that impact the EUI in the school building stock in Brazil were: the number of students, floor-plan area, operation time and HVAC system specifications (type and quantity)” (GERALDI; GHISI, 2020, p.211).

In most schools there is high dissatisfaction with thermal comfort and tendency to install air conditioning in classrooms. When considering this scenario, an 88% increase in the average EUI is predicted, a percentage which could increase 43% by 2080 due to the global warming effects (GERALDI; GHISI, 2020).

Therefore, one of the biggest challenges to solve issues of thermal comfort and energy efficiency in Brazilian public schools is to design more efficient passive conditioning solutions without excessively increasing the EUI, that are preferably low cost and easy to apply and replicate.

Some studies verified the comfort (RACKES, 2015; MODLER, 2017; ALMEIDA, 2018; LOPES, 2020; GONZALES, 2021) and energy efficiency (TELES *et al.*, 2019) of FNDE schools, however, not all school models were tested in all bioclimatic zones.

Standardized FNDE school buildings are the same for all Brazilian regions (ALMEIDA, 2018; LOPES, 2020). Considering the climatic diversity of the national territory, this lack of flexibility compromises the number of occupied hours in thermal comfort (LOPES, 2020), the quality of indoor spaces, the pedagogical process and the child development (MODLER, 2017).

Unlike most schools analyzed by Geraldi and Ghisi (2020), the FNDE schools are more recent, built from 2007 after the beginning of the PROINFANCIA program (FNDE, n/d) and follow more up-to-date building regulations. This means that the FNDE schools probably present better thermoenergetic performance than older

school buildings, but even so, they do not use most suitable passive strategies for each city and do not consider cool material as a passive strategy.

The FNDE schools are proposed to work in the morning and afternoon shifts, with 30 students per classroom in each period. The months of operations are not reported in the official database, but previous studies (GERALDI; GHISI, 2021) considered the standard schedule of school operation in Brazil regulated by the Ministry of Education: Monday to Friday from March to June and from August to December.

Given the above, this thesis proposes to answer the following questions:

- Cool materials are compatible strategies in which types of zero and positive energy buildings and districts?
- What are the most suitable cool materials for the Brazilian context and for each bioclimatic zone? Is it possible to provide thermal comfort in Brazilian public schools using cool materials and other passive conditioning strategies?
- What is the current thermoenergetic performance of all standardized FNDE schools in each region of Brazil?
- What are the ideal wall and roof compositions as substrates for cool material in the Brazilian context?
- Is it possible to achieve positive energy in Brazilian public schools of FNDE in all Brazilian territory?
- Do Brazilian public schools provided by FNDE offer passive survivability and safe thermal conditions for occupants currently and in long-term climate scenarios?

## 1.2. Justification

Positive energy balance is important to obtain more effective results in the performance and energy efficiency of the building than simply superficial strategies to reduce environmental impact, as already defended by Oranje (2013, p. 14, **our translation**): “By setting an absolute rather than a relative goal, we have a chance to do something good, not just less bad. Incremental efficiency is important, but it may be insufficient to deal with climate change”.

In addition to proposing the achievement of positive energy in schools as bolder long-term goals in relation to energy performance, this thesis seeks to study the application of cool materials and complementary passive conditioning strategies on FNDE standard architecture projects, that can solve the current problems of thermal comfort in Brazilian school buildings in all bioclimatic zones and increase student productivity and safety nowadays and in a long-term scenario.

Finally, the proposed study can represent a complementary bibliography for other architectural typologies with other functional programs in the national context, as well as for school programs in other countries that have climates similar to those presented in the Brazilian bioclimatic zones.

### **1.3. Originality**

Although, at present, there is a great diversity of cool materials with a high potential for cooling and achieving comfort and energy efficiency (SANTAMOURIS; YUN, 2020), few options have been tested for Brazilian climates (WERLE; LOH; JOHN, 2014; SILVA; MARINOSKI; GUTHS, 2020). Furthermore, standardized Brazilian public schools have not yet been assessed and planned to ensure occupants safety considering thermal conditions in present and future scenarios.

This thesis proposes the identification and verification of the most suitable materials for the Brazilian context, which can be part of the standard projects of Brazilian public schools and contribute to the quality of constructions and to the productivity of students (GERALDI; GHISI, 2020). Finally, this thesis conducts analyses and suggests improvements to enhance the thermal resilience and passive survivability of standardized Brazilian public schools, never previously presented.

### **1.4. Hypothesis**

The hypothesis is that it is possible to achieve positive energy, adequate thermal comfort, thermal resilience and passive survivability in Brazilian standardized public schools of the FNDE with easy replicability in eight bioclimatic zones using cool materials, other passive strategies and local production of energy from photovoltaic system.

## 1.5. Objectives

The objective of this thesis is to evaluate the possibilities of achieving positive energy balance and passive survivability in Brazilian standardized public schools, focusing mainly on the use of cool materials and passive strategies in present and future scenarios.

The thesis was structured to achieve the following specific objectives:

- a) Investigate the state of the art of international research in zero and positive energy buildings and districts and cool materials;
- b) Identify the thermoenergetic performance in the current standard school buildings of FNDE in all Brazilian zones;
- c) Verify more suitable cool materials, their costs and passive strategies to achieve comfort in public school buildings of FNDE in 8 bioclimatic Brazilian zones and evaluate the possibility to reach the positive energy in Brazilian public school buildings;
- d) Evaluate the thermal resilience and the passive survivability of the optimized schools in present, typical meteorological year – TMY and future scenarios of 2050 and 2080 and quantify the necessary increase in the PV system to enhance passive survivability.

## 1.6. Thesis Structure

The first chapter contains the introduction and as previously mentioned, it addresses the research problem, the justification, the thesis's originality and the objectives.

The second chapter pertains to the theoretical foundation of the thesis and is structured into four parts. Firstly, based on a systematic review of international literature, concepts and definitions of zero and positive energy balance, as well as the state of the art in cool materials as passive climate control strategies, are presented. Secondly, most suitable passive strategies and cool materials for the Brazilian context and their costs are discussed. Thirdly, the main architectural and energetic characteristics of the Brazilian school building stock and standardized FNDE schools are exposed, which are the subjects of the thesis. These information were obtained by consultation with official government websites and a systematic review of national and international literature. Fourthly, the results of a systematic

literature review on thermal energy simulation methods for buildings coated by cool materials and optimization processes are presented. Fifthly, are presented definitions of Thermal Resilience and Passive Survivability in Buildings, along with metrics, assessment scenarios and software related to building performance in extreme events and weather data generation.

Chapter three provides a detailed explanation of all the methods used in each part of the thesis: literature review, thermal energy simulations of the current state of FNDE standardized schools, optimization simulations, sensitivity analyses, achievement of the zero energy balance and thermal resilience and passive survivability assessments.

Chapter four focuses on the thesis results. This chapter showcases all stages of the research for the 1 classroom school from the FNDE's PAR program, considered the representative model within the group of rectangular shape schools. Among the school models updated in 2023, the rectangular shape is the most prevalent throughout Brazilian territory.

Chapter five includes the main conclusions obtained at each stage of the work completed. The structure of the thesis is summarized in the flowchart of Figure 1.

**Figure 1 - Thesis Structure**



Source: Authors.

## **2. LITERATURE REVIEW**

### **2.1. Zero and Positive Energy Buildings and Districts: Definitions and compatibility with Cool Materials**

As a fundamental principle of Zero or Positive Energy Buildings and Districts, it is necessary: to apply passive conditioning technologies (related to the design and materials of the building) to reduce energy needs, active technologies (of efficient equipment) to increase consumption efficiency and renewable energy technologies to reduce emissions and environmental impacts (CABEZA; CHÀFER, 2020), but in all

definitions and classifications, the cardinal rule is to meet the demand first and then supply (COLLADO *et al.*, 2019; ZHANG *et al.*, 2021). Therefore, the reduction of energy needs and efficiency must be prioritized (ADELI; FARAHAT; SARHADDI, 2020; BANDEIRAS *et al.*, 2020; DERKENBAEVA *et al.*, 2022) due to area limitations in buildings for collecting renewable energy, low collection efficiency and more cost-effective energy efficiency measures compared to installing renewable energy systems (SHIRINBAKHSH; HARVEY; 2020). Another important rule is that these measures should not compromise the comfort of users in the spaces (COLLADO *et al.*, 2019; CABEZA; CHÀFER, 2020) and the internal environmental quality (PIDERIT *et al.*, 2019; CABEZA; CHÀFER, 2020)

Among the methods of using renewable energy, the photovoltaic solar system is one of the most promising (ZHANG *et al.*, 2021), installed on roofs (BANDEIRAS *et al.*, 2020), in external building walls and windows (ZHANG *et al.*, 2021) or in open areas in the building limits, associated or not with wind turbines or other renewable energy sources (BANDEIRAS *et al.*, 2020). Recent research, from 2017, also presents possibilities of transparent photovoltaic cells (CABEZA; CHÀFER, 2020).

### 2.1.1 Types of energy balance, geographic limit and energy production

From the beginning of Zero and Positive Energy strategies to the present day there is no universally recognized definition or approach yet (LIU *et al.*, 2019) and the concept is in constant change and adaptation (ZHANG *et al.*, 2021).

Among the various issues surrounding the concept, the ones that most compromise or enable the use of cool materials as a passive conditioning strategy are geographic limits (building, neighborhood or district) and location of energy production.

The geographic boundary can consider Building, Community/Neighborhood or District Scale (COLLADO *et al.*, 2019; DERKENBAEVA *et al.*, 2022). When evaluating the Building Scale, it is decided to: account for the energy produced and consumed on site or at the source; for the renewable produced in relation to non-renewable consumed; or by account of credits. The building can also be connected or not to the public energy network (electricity, natural gas and district heating) (BANDEIRAS *et al.*, 2020; SHIRINBAKHSH; HARVEY; 2020; DERKENBAEVA *et al.*, 2022).



Neighborhood scale considers that the most effective method for energy gains involves not just a building, but a set of buildings, a community or even a neighborhood. This area can contain buildings of similar typologies, with similar periods and consumption loads, or different typologies (such as warehouses, office buildings and residential buildings), with a diversity of end users and energy use patterns, which facilitate the sharing of resources and renewable energy (LOVEDAY; MORRISON; MARTIN, 2022). The neighborhood's energy demand includes consumption of buildings and adjacent infrastructure such as waste and water management, green areas, street lighting and transport (BANDEIRAS *et al.*, 2020; DERKENBAEVA *et al.*, 2022). Buildings, in these cases, can optimize the production, consumption and storage of local renewable energy (DERKENBAEVA *et al.*, 2022).

The District Scale refers to a city (or an area larger than a block or neighborhood), classified as: autonomous, with energy demand supplied by renewable energy generated internally (by buildings or by a generation pole with one or more types of renewable sources) (WELLS; RISMANCHI; AYE, 2018); dynamic, that interacts with the local area, the neighboring areas and the power grid; and virtual, with renewable energy systems and energy storage outside their geographic boundaries or virtual power plants.

Energy production commonly occur in two ways: on site, in the building itself (on the roof) or on the edge of the land (as in the parking lot coverage); or off-site, with off-site supply of renewable energy by purchase or off-site production. In some cases, the building may have on-site renewable energy production and use partially external sources for remaining demands (WELLS; RISMANCHI; AYE, 2018; COLLADO *et al.*, 2019; BANDEIRAS *et al.*, 2020; DERKENBAEVA *et al.*, 2022).

Spatial variations also influence the choice of the most suitable type of renewable source: wind energy is generally used in large areas of land located in regions with higher wind speeds; while solar and thermal energy are chosen for areas of smaller scale and greater incidence of solar radiation (DERKENBAEVA *et al.*, 2022). Depending on the climate and infrastructure characteristics of the generation, transmission and distribution network, it is possible to combine more than one type of renewable energy technology to increase flexibility and minimize the fluctuating

properties of the system (BANDEIRAS *et al.*, 2020; CABEZA; CHÀFER, 2020; DERKENBAEVA *et al.*, 2022).

The main types of zero and positive energy according to the most recent references (2006-2022) and variations of geographic limit and location of energy production are shown in Table 1.

**Table 1 – Types of Energy Balance, Geographical Limit, Location of Energy Production**

Type of Energy Balance	Definition	Geographical Limit	Energy Production on Site	Bibliographic Reference
Nearly Zero Energy Building (nZEB)	A highly efficient building that produces most of its energy from renewable sources (at least 50% of demand), has a maximum annual demand of 60 kWh/m <sup>2</sup> and maximum annual CO <sub>2</sub> emissions of 8 kg CO <sub>2</sub> /m <sup>2</sup> .	Building	Onsite/ Offsite	EPBD recast 2010/31/EU <i>apud</i> Francés <i>et al.</i> (2020) and Wells, Rismanchi and Aye (2018); Szalay; Zöld (2014); Zeiler <i>et al.</i> (2016) <i>apud</i> Bandejas <i>et al.</i> (2020)
Zero Energy Building (ZEB)	(1) A building that produces the same amount of energy that it consumes annually accounted on site, (2) or accounted for at source, (3) or Zero Emissions, which produces an amount of renewable energy equivalent to what it uses from non-renewable sources (4) or Zero Energy Costs, that receives financial credit for the energy exported in the same amount in which it is charged in the utility bills.	Building	On site	Torcellini <i>et al.</i> (2006) <i>apud</i> Wells, Rismanchi and Aye (2018), Liu <i>et al.</i> (2019), Bandejas <i>et al.</i> (2020), Shirinbakhsh and Harvey (2021), Derkenbaeva <i>et al.</i> (2022)
Zero stand-alone buildings	Building that does not need to be connected to the grid and, by generating renewable energy and storage, supply the energy needs of winter and night.	Building	On site	IEA (2008) <i>apud</i> Liu <i>et al.</i> (2019)
Autonomous or Self-Sufficient Building (Autonomous ZEB)	Building designed to be independent of infrastructure services (electricity networks, water supply, sewage treatment, rainwater, telecommunications).	Building	On site	AiIB (2010) <i>apud</i> Liu <i>et al.</i> (2019)
Zero Energy Connected to the Grid (Net ZEB)	Grid connected building, which is energy efficient and capable of generating electricity or other types of energy from renewable sources to supply its demand.	Building	On site/ Offsite	Sartori <i>et al.</i> (2012); Marzal <i>et al.</i> (2011); Kolokotsa <i>et al.</i> (2011) <i>apud</i> Derkenbaeva <i>et al.</i> (2022); USDPE (2015) <i>apud</i> Bandejas <i>et al.</i> (2020)
Life Cycle Zero Energy Building (LC-ZEB)	Building in which the primary energy used and the energy embodied during its lifetime is equal to or less than the energy produced by its renewable energy systems over the same period.	Building	On site	Hernandez; Kenny (2010) <i>apud</i> Liu <i>et al.</i> (2019); Derkenbaeva <i>et al.</i> (2022)

Positive Energy Building (PEB)	A building that produces more energy than it uses annually for heating, cooling, ventilation, lighting and equipment and shares the surplus with other buildings or the public grid.	Building	On site	IEA (2008); AIIB (2010) <i>apud</i> Liu <i>et al.</i> (2019); Wronowski (2013) <i>apud</i> Hawila <i>et al.</i> (2022)
Positive Energy Block (PEB)	Set of at least three nearby buildings that have a positive average annual energy balance between them.	Community	On site/ Offsite	Ahlers <i>et al.</i> (2019); Back <i>et al.</i> (2019) <i>apud</i> Derkenbaeva <i>et al.</i> (2022)
Positive Energy Neighborhood (PEN)	Area that annually generates more electricity than it consumes.	Neighborhood/ Neighborhood	On site	Ala - Juusela <i>et al.</i> (2016); Monti <i>et al.</i> (2016) <i>apud</i> Derkenbaeva <i>et al.</i> (2022)
Neutral Energy District (NED) or Zero Energy District (ZED)	District where, annually, no energy imports from outside the district are required (refers to self-sufficiency).	District/ City	On site/ Offsite	Jablonska <i>et al.</i> (2012) <i>apud</i> Derkenbaeva <i>et al.</i> (2022)
Positive Energy District (PED)	An energy efficient and flexible urban area or group of connected buildings that has a zero balance of greenhouse gas emissions and actively manages the local or regional annual surplus production of renewable energy.	District/ City	On site/ Offsite	European Strategic Energy Technology TWG (2018); JPI Urban Europe/SET Plan Action 3.2 (2020), Lindholm <i>et al.</i> (2021) <i>apud</i> Derkenbaeva <i>et al.</i> (2022)

Source: adapted from DERKENBAEVA *et al.* (2022).

### 2.1.2 Cool Materials and Zero or Positive Energy Buildings

Cool materials can be used in two ways as a passive conditioning strategy in the energy demand reduction stage to achieve zero or positive energy balance: in urban areas to improve the outdoor microclimate and, consequently, reduce cooling needs buildings (macro-micro strategy); or in the building envelope, as a direct passive building cooling strategy, which also helps to reduce the air temperature in the urban microclimate (micro-macro strategy) (CABEZA; GRACIA; PISELLO, 2018; CASTALDO *et al.*, 2018).

As an example of the first form of application, a computer simulation was performed of the application of light-colored natural materials, high-reflectivity white coatings and high-reflectivity asphalt pavements associated with vegetation in urban areas, which resulted in a reduction of 1.5-2°C at maximum air temperature and approximately 10% energy savings with cooling in a group of 4 houses in a near-zero energy balance residential settlement in Italy (CASTALDO *et al.*, 2018). In this research, mainly in the summer period, the mitigation effect of the microclimate provided by the cool materials is comparable to other solutions, such as the increase

in the insulation of the envelope and the solar reflectivity of the roof (CASTALDO *et al.*, 2018). The proposed renewable energy solution was a combination of small wind turbines and photovoltaic modules installed on the roof of the houses (occupancy of 36m<sup>2</sup> of the roof) (CASTALDO *et al.*, 2018), which did not impair the performance of the cool materials applied to the other areas of the roof and facades, mainly due to the horizontality of the buildings.

The second way of applying cool materials, directly in buildings, is considered one of the most efficient ways to improve energy efficiency in contexts of temperate or warm climates, as exemplified in a study of the application of high reflectivity white cool tiles in Italian historic buildings, that enabled 14% energy savings with cooling (CABEZA; GRACIA; PISELLO, 2018) and in studies in China, which allowed a reduction of approximately 20°C in the surface temperature of the roof (TIAN *et al.*, 2021), but none of them mentioned the use of renewable sources in the building, inside or outside the boundaries of the lot.

Zero or Positive Energy prioritizes passive strategies, then energy demands reduced to the maximum that must be held by renewable energy sources. From this premise, the use of cool materials as a resource of energy efficiency and environmental comfort should be a priority comparing to the location of the renewable source in the system.

Authors classify the various types of Zero and Positive Energy by the place of energy production in a generic way: “on-site” or “off-site”, without specifying whether the production is on the roof or on the land limits (not on the roof). In this case, it would be possible to apply cool materials as a passive conditioning strategy in all the definitions described, as long as the energy production is not specifically on the roof of the building (in cases of small roof area) or that the renewable energy system occupies only part of the roof (in the case of horizontal buildings). However, the passive cooling effect of cool materials decreases when the area of application is reduced. Therefore, the ideal conditions for the compatibility of the two strategies are: on-site energy production with photovoltaic energy on the facades of the building; on-site in the boundaries of the land with one or more types of renewable source; or off-site with energy production by neighboring buildings as poles of renewable energy production within the neighborhood/district or by external production.

Among the existing cool materials, only a few were simulated in a zero or positive energy context (light-colored natural materials, high-reflectivity asphalt coatings and high-reflectivity white coatings).

Finally, it is noted that few studies addressed the two themes concomitantly, which is a relevant point of research in this thesis.

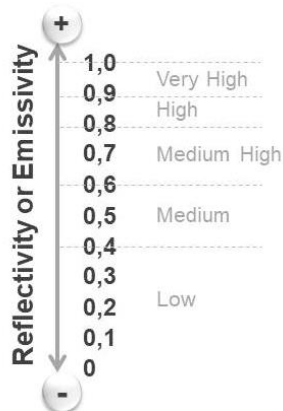
Specifically for the context of public schools standardized by the FNDE, the geographic boundary considering the building is more applicable, so that the building can achieve a positive energy balance regardless of the neighborhood or the local urban context. In this case, even though definitions of energy balance in districts have been presented, they do not apply to the context of standardized Brazilian public schools.

The system connected to the electrical grid is advisable for the Brazilian context, since local legislation favors the exchange of energy with the grid for energy credits. Energy production should preferably take place outside the roof, on the edge of the land (as in the parking lot coverage). The positioning of the photovoltaic system on the roof can be an interesting solution for small land limits, but it is important to evaluate and ensure that the modules do not reduce the effect of supercool materials on the roof.

## **2.2. Cool Materials as a Passive Strategy: State of the art of international research**

The articles shows the most consolidated definition of cool materials: those that have high solar reflectivity and high infrared emissivity, being able to reflect incident direct or diffuse sunlight and re-radiate the heat previously absorbed (PISELLO, 2017; ASCIONE *et al.*, 2018), which maintains a low surface temperature of the material under the sun, results in less heat input into the building and less overheating of the surrounding air (PISELLO, 2017; BANIASSADI; SAILOR; BAN-WEISS, 2019). This means that during the day the reflectivity is the main parameter that influences surface temperature and during the night infrared emissivity affects the surface's ability to re-radiate heat (PISELLO, 2017). The best performing cool coatings, also called supercool, generally have reflectivity and emissivity above 0.9 (very high as shown in Figure 2) (PISELLO, 2017).

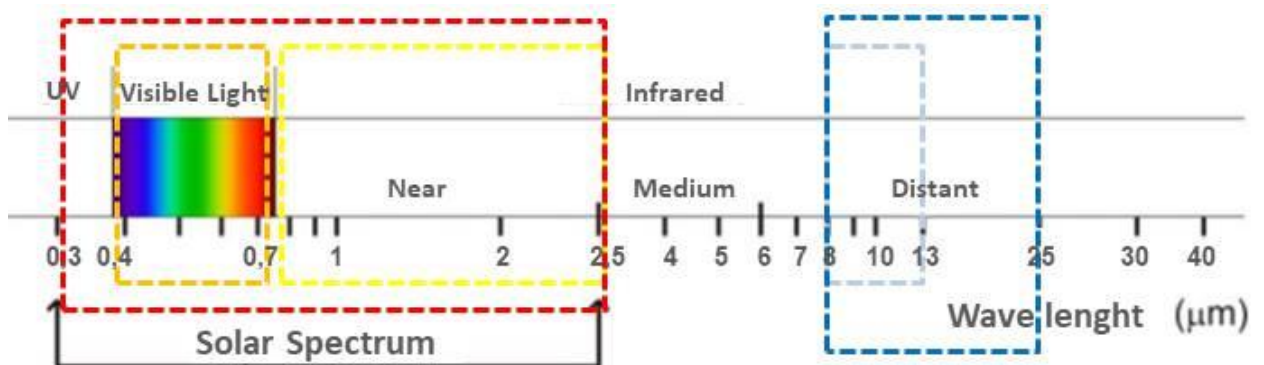
Figure 2 - Solar reflectivity and emissivity scale of materials

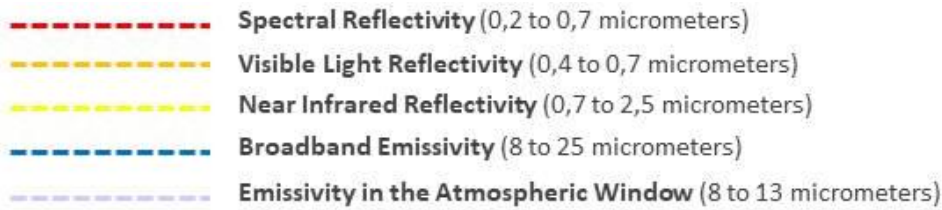


Source: Graphs based on Pisello (2017), Carlosena *et al.* (2021), Feng *et al.* (2021), e Feng *et al.* (2022b).

The reflectivity of cool materials may involve: a) reflection only in the visible spectrum, at lengths from 0.4 to 0.7 micrometers; b) in the near infrared, from 0.7 to 2.5 micrometers; or c) from the entire spectrum of incident solar radiation (spectral reflectivity), at wavelengths from 0.3 to 2.5 micrometers (YUAN *et al.*, 2018). While infrared radiation is the largest component of the solar spectrum and is the most influent parameter on heat gains (QI; ZHU; ZHANG, 2018), ultraviolet radiation represents a very narrow range, from 0.3 to 0.4 micrometers, so it has little influence (QI; ZHU; ZHANG, 2018; MANNI *et al.*, 2019) and consequently is not often cited. Emissivity is related to the re-emission of heat over a wide infrared range (broadband emissivity), at wavelengths from 8 to 25 micrometers, or only at wavelengths from 8 to 13 micrometers (atmospheric window emissivity) (SANTAMOURIS; YUN, 2020). The concepts of reflectivity and emissivity at each wavelength are summarized in Figure 3.

Figure 3 - Reflectivity and Emissivity Wavelengths





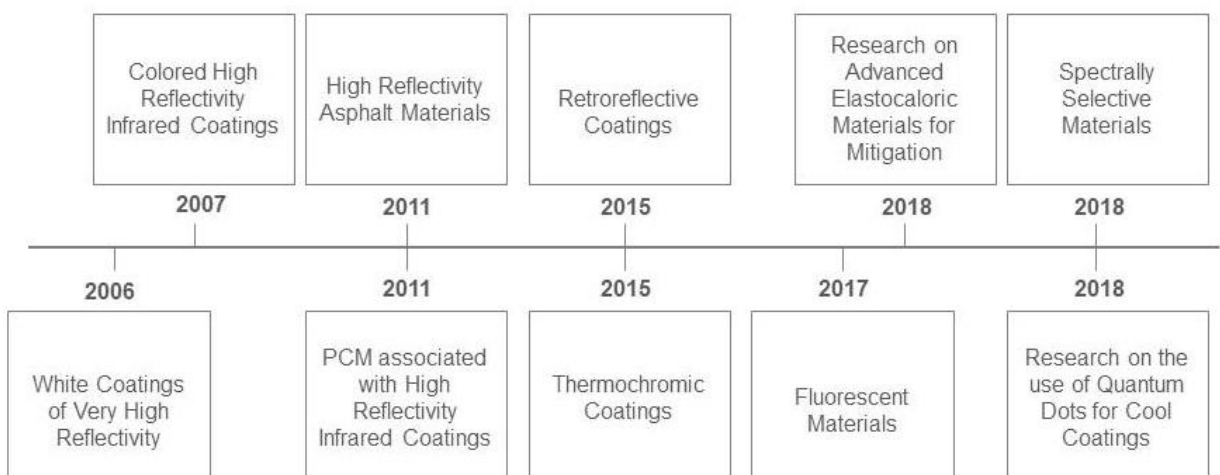
Source: adapted from Steffen, Moraes and Gama (1996).

The two key properties, reflectivity and emissivity, are sensitive to the outermost layer of the surface exposed to solar radiation, so cool materials are called “coatings” for surface applications (PISELLO, 2017). The variation of these two parameters depends on factors such as the nature of the material (natural or artificial), surface texture, color, chemical composition, type of substrate applied, thickness and quantity of material layers (SANTAMOURIS; YUN, 2020).

### 2.2.1 Summary of the main types and classification of cool materials

The historical development and progress of the most important cool materials used for cooling the built environment can be seen in Figure 4. Their cooling potential and forms of application are shown in Figure 5.

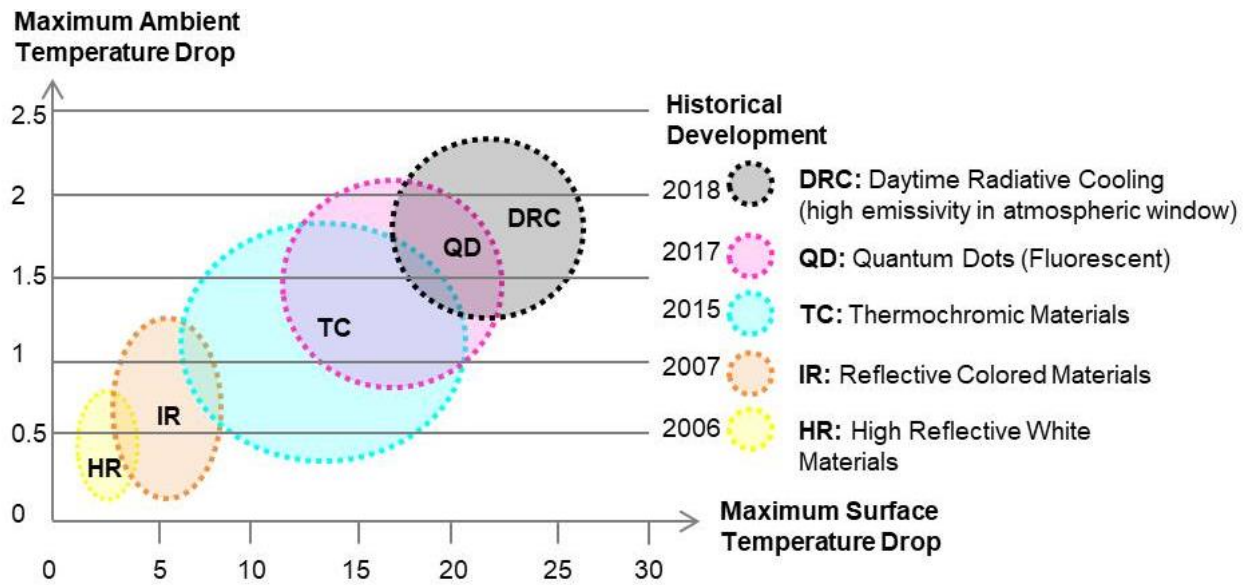
**Figure 4 - History of cool materials for cooling the built**



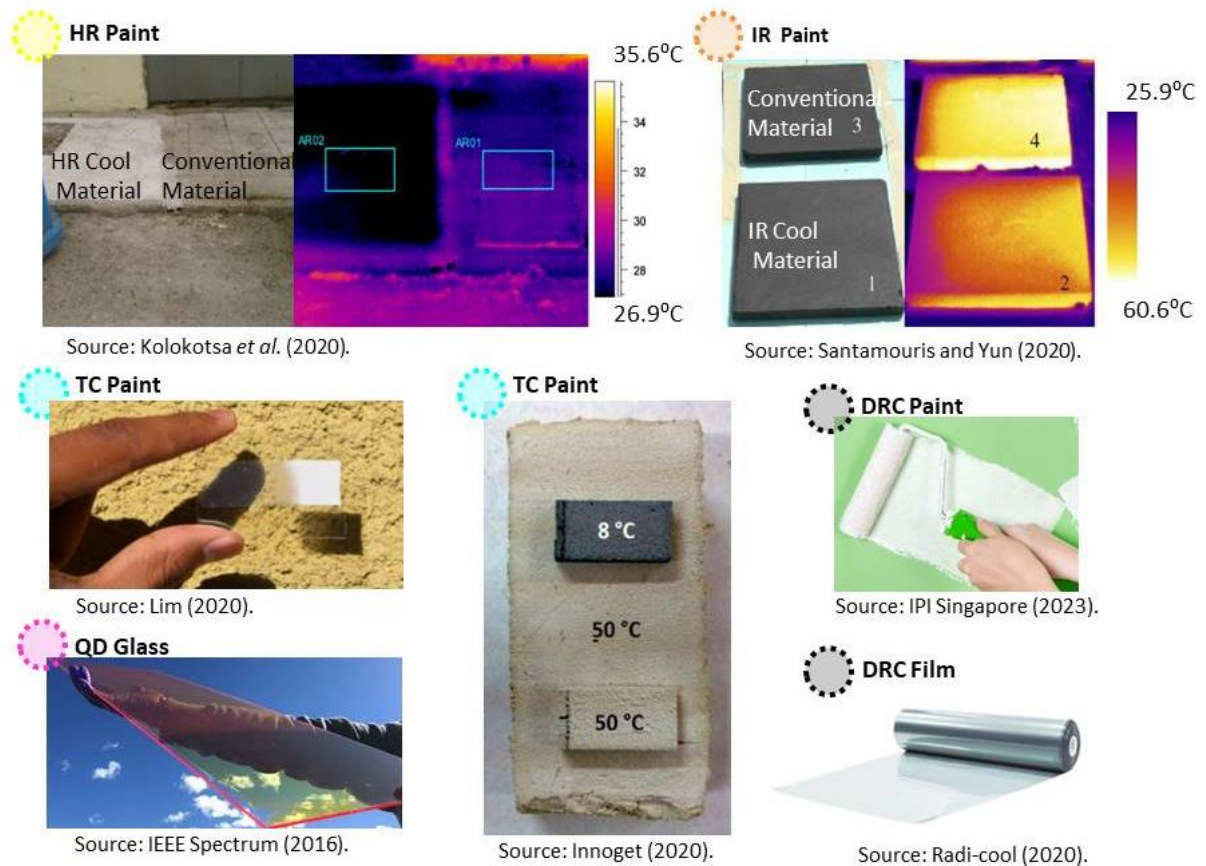
Source: adapted from Santamouris and Yun (2020).



Figure 5 - Cool Materials Cooling Potential and Forms of Application



Source: Santamouris and Vasilakopoulou (2023); Santamouris and Yun (2020).

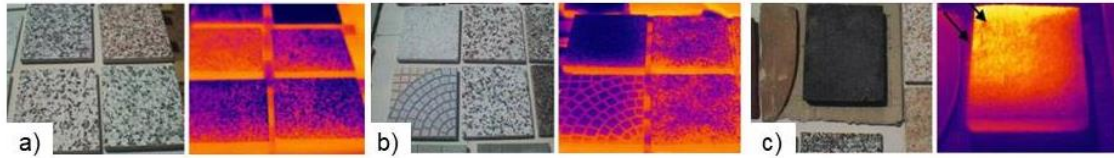


The first generation of cool materials were the conventional light-colored natural and artificial materials, such as light-colored gravel or marble (PISELLO, 2017). Studies have shown that smooth, flat and reflective surfaces have a surface temperature up to 2°C lower than similar rough and dark surfaces (SANTAMOURIS; YUN, 2020), as shown in Figure 6. Generally, conventional high-performance materials have medium



or high reflectivity only in the visible spectrum and broadband high emissivity (SANTAMOURIS; YUN, 2020).

**Figure 6 - Surface temperature variation according to color composition and roughness**

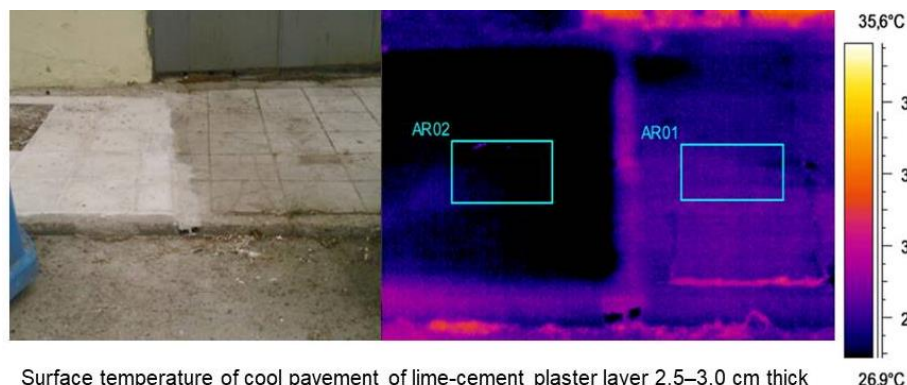


Material samples characterized by non-uniform surface temperature distribution due to contrasts in color compositions (a), roughness (b) and heat transfer phenomena (arrows show the direction of incident solar radiation) (c).

Source: adapted from Santamouris and Yun (2020).

As an alternative to conventional materials, high-reflectivity white coatings were presented, which are innovative light-colored artificial materials, with superior reflectivity compared to natural materials, available as membranes, coatings, paints, metallic coverings or tiles (PISELLO, 2017). These can be composed by elastomers, silicones, fluoropolymers and acrylics<sup>4</sup> or a combination of them (SANTAMOURIS; YUN, 2020). In studies, these materials had a surface temperature of up to 6°C below conventional cool materials (Figure 7) (SANTAMOURIS; YUN, 2020) and therefore can double the energy savings with cooling in hot periods (BANIASSADI; SAILOR; BAN-WEISS, 2019) or significantly increase the energy consumption for heating in cold periods even when associated with thermal insulation (ASCIONE *et al.*, 2018).

**Figure 7 - Surface temperature measurement of cool pavement and conventional sidewalk**



Surface temperature of cool pavement of lime-cement plaster layer 2.5–3.0 cm thick 2°C lower than conventional pavement at noon in Acharnes, Greece.

Source: adapted from Kolokotsa *et al.* (2018).

<sup>4</sup>EPDM (Ethylene-Propylene-Diene Trolimer Membrane), PVC (Poly Vinyl Chloride), CPE (Chlorated Polyethylene), CPSE (Chlorosulfonated Polyethylene) and TPO (Thermoplastic Polyolefin)

Such materials present high broadband emissivity and high reflectivity only in the visible spectrum (BANIASSADI; SAILOR; BAN-WEISS, 2019), which are significantly compromised after three to five years due to optical degradation and weathering (SANTAMOURIS; YUN, 2020). To solve such problems, alternatives are investigated for adding inorganic components to provide self-cleaning properties<sup>5</sup> (MOGHTADA; SHAHROUZIANFAR; ASHIRI, 2017; SANTAMOURIS; YUN, 2020).

In order to reduce the glare caused by clear coatings and avoid de-characterization in interventions in historic centers, colored materials with high reflectivity of near-infrared radiation (PISELLO, 2017) have emerged through the addition of organic<sup>6</sup> or inorganic pigments<sup>7</sup> to mortars, concrete or other materials, contributing more significantly to the thermoenergetic performance (SANTAMOURIS; YUN, 2020) (YUAN *et al.*, 2018; MANNI *et al.*, 2019). Inorganic pigments are the most common because they are non-toxic and have a lower cost (Figure 8) (YANG *et al.*, 2017; YUAN *et al.*, 2018).

**Figure 8 - Inorganic and non-toxic pigments with high near-infrared reflectance (>65%) and solar reflectance (>53.51%)**



Source: adapted from Yang *et al.* (2017).

Tests of application of these pigments to fiber cement tiles proved a surface temperature 10°C lower compared to the conventional material (PISELLO, 2017; YANG *et al.*, 2017; SANTAMOURIS; YUN, 2020).

Due to the potentiated cooling effect, these materials can increase the consumption for heating buildings in climates with cold periods (SANTAMOURIS; YUN, 2020). These have high broadband emissivity and high infrared reflectivity. Spectral reflectivity depends on substrate reflectivity, coating thickness, surface roughness

<sup>5</sup> TiO<sub>2</sub> (Titanium Dioxide) associated with Al (Aluminium), Li (Lithium), Ba (Barium) or K (*Kalium*)

<sup>6</sup> Anthraquinone, Quinacridone, Phthalocyanine and Dioxazine

<sup>7</sup> Chromates, Oxides, Silicates, Borates, Sulfates, Phosphates, Metals, Vanadates

and pigment backscattering potential. Generally, inorganic pigments have excellent optical stability, high durability and remain stable at high temperatures, but weathering, aging and dirt issues affect emissivity and reflectivity. Recent research focuses on two research lines: a) the development of higher spectral reflectivity pigments and advanced superhydrophobic coatings which by milling or micromolding provide self-cleaning properties (SANTAMOURIS; YUN, 2020); b) on nanopigments and nanoparticles<sup>8</sup> which can increase mechanical strength after drying, homogeneity of dispersion in the mixture, spectral reflectivity, self-cleaning and flame retardancy<sup>9</sup> (QI *et al.*, 2017; QI; ZHU; ZHANG, 2018; XIANG; ZHANG, 2018a; XIANG; ZHANG, 2018b; MAO; YANG; ZHANG, 2019; FENG *et al.*, 2022a)

Another solution regarding infrared radiation was the phase change materials – PCM, which have high latent heat (LASSANDRO; TURI, 2017) and by storing and releasing energy after a delay of up to 10 hours, it reduces its surface temperature by about 10°C under the sun when compared to conventional materials (PISELLO, 2017). Due to the thermal delay process, PCM materials shift part of the heating and cooling loads to hours when air temperatures are milder (LASSANDRO; TURI, 2017), but they do not significantly avoid heat gains like other cool materials, so they are little used for mitigation purposes (LIM, 2019; SANTAMOURIS; YUN, 2020). These materials are classified as organic<sup>10</sup>, inorganic<sup>11</sup> and eutectic<sup>12</sup>, with variations in thermal stability, conductivity and costs (LASSANDRO; TURI, 2017). Most of PCMs have high reflectivity in the visible spectrum, high reflectivity of infrared radiation and high broadband emissivity. These materials can be encapsulated and mixed with other cool materials, mortars, concrete and asphalt, which characterizes a relatively simple production process (PISELLO, 2017). Recent research seeks to address deficiencies and enhance its performance, such as minimizing leakage during the molten state, reducing aging, increasing the number of phase-change thermal cycles, decreasing peak surface temperature and improving the integration of materials into the mass of building components (SANTAMOURIS; YUN, 2020).

---

<sup>8</sup> NiTiO<sub>3</sub> (Nickel Titanate), SrTiO<sub>3</sub> (Strontium Titanate), TiO<sub>2</sub> (Titanium Dioxide), SiO<sub>2</sub> (Silicon Dioxide), BaTiO<sub>3</sub> (Barium Titanate) or Sb<sub>2</sub>O<sub>3</sub> (Antimony Trioxide)

<sup>9</sup>Sb<sub>2</sub>O<sub>3</sub> (Antimony Trioxide )

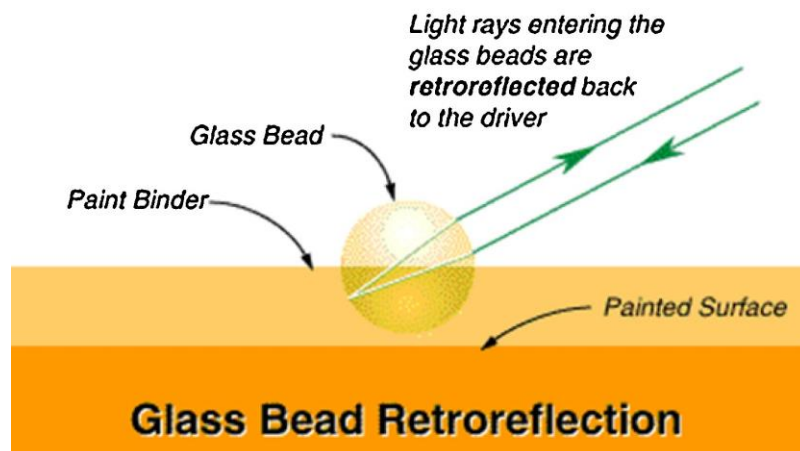
<sup>10</sup> Paraffin, Fatty Acids

<sup>11</sup> Hydrated Salt, Molten Salt, Metal

<sup>12</sup> mixtures of organic and/or inorganic components

Simultaneously, studies were started on retroreflective materials (SANTAMOURIS; YUN, 2020), which have two characteristics: they are able to reflect solar radiation back in the same direction as the incident radiation and their spectral reflectivity decreases as the angle of incidence of radiation increases (Figure 9). This means that they have variable spectral reflectivity, which can reach 100% when the sun's rays are perpendicular to the surface, so retro-reflectives can reduce part of the cooling demand with little increase in heating consumption (MAURI *et al.* 2018).

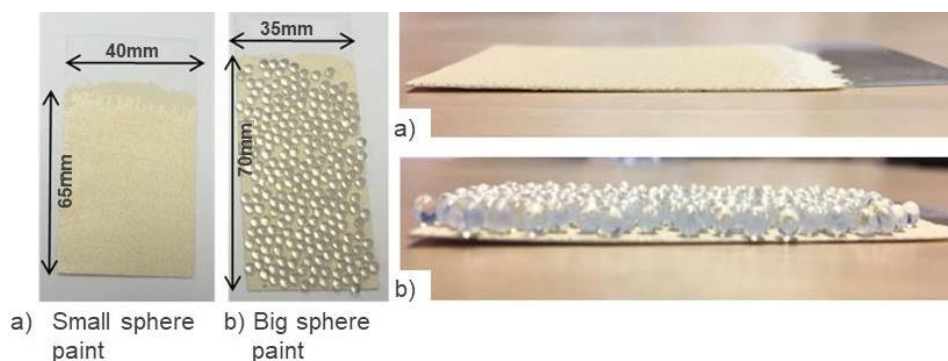
**Figure 9 - Glass beads for retro-reflective property**



Source: adapted from Morini *et al.* (2017).

These can be applied alone or together with other cool materials and are composed of small glass spheres or prisms, which instead of simply scattering light like conventional or reflective materials, reflect light and send it back into space in the same direction (Figure 10) (MORINI *et al.*, 2017). Recent research has sought to increase the durability (MORINI *et al.*, 2017) and improve the behavior of these materials to reduce solar gains during cold seasons and reduce light pollution in the urban context (LIM, 2019).

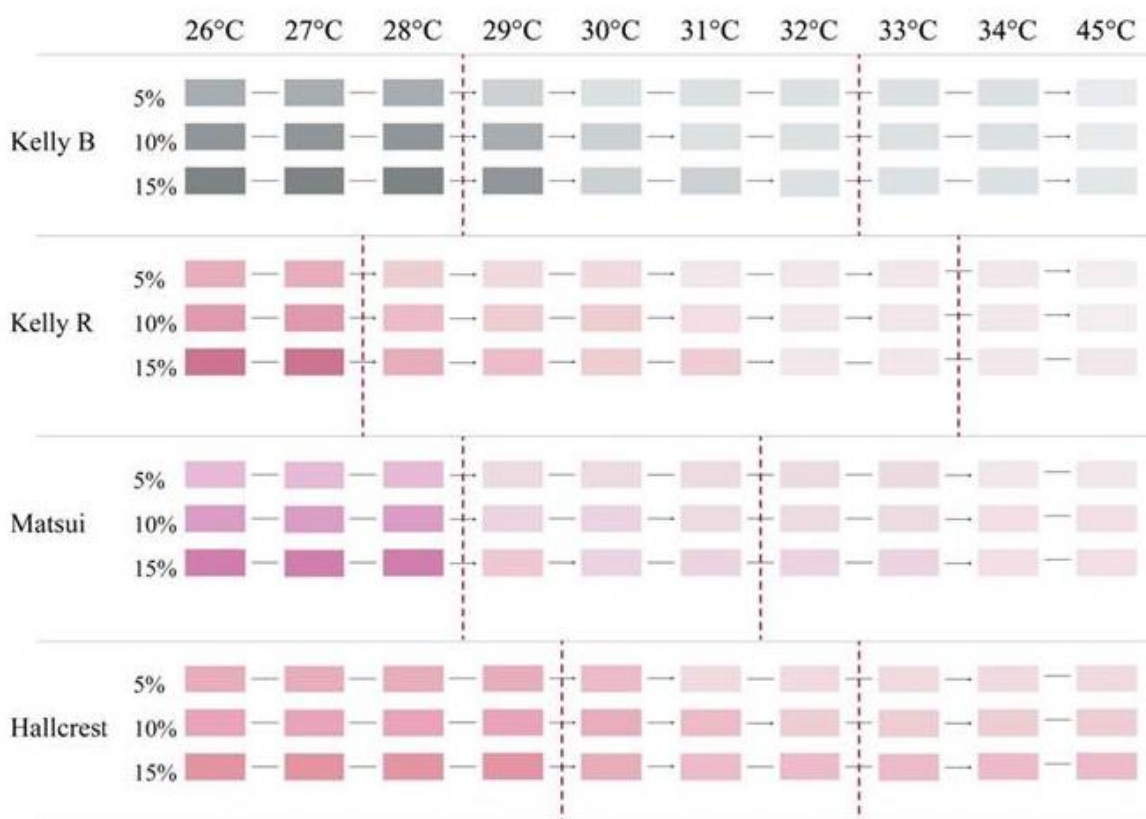
**Figure 10 - Retro-reflective coatings with glass spheres**



Source: adapted from Morini *et al.* (2017).

Cool materials can have a negative effect during cold seasons when solar gains would be beneficial (BERARDI; GARAI; MORSELLI, 2020). Therefore, for regions of mixed climate, composed of warm and cold periods, thermochromic materials emerged, which, due to their reversible characteristics, can be light and reflective in the summer or dark and absorbent in the winter (SANTAMOURIS; YUN, 2020), as shown in Figure 11, reducing excessive heating consumption (BERARDI; GARAI; MORSELLI, 2020). Figure 11 shows that thermochromic coatings become lighter and more reflective as the temperature increases. The higher the percentages of pigment, the more saturated the colors are.

**Figure 11 - Inks with leuco dyes, from four different manufacturers, which show variable reflectivity according to temperature transition**



Higher percentages of thermochromic particles led to more saturated colors.

Source: adapted from Berardi, Garai and Morselli (2020).

These materials have high spectral reflectivity and high broadband emissivity, so they have an average surface temperature 15°C lower than conventional materials (SANTAMOURIS; YUN, 2020). They are available in sol-gel films, plasmas, phase

transition in liquid crystals, mechanisms of aggregation and disaggregation between dyes and dye polymers, dyes associated with PCM, modulation of refractive index by photonic crystals and pH variation with temperature, which can be used as photonic flat surfaces for multi-layer materials, as an aqueous polymer solution or can be mixed with paints, mortars and asphalts (BERARDI; GARAI; MORSELLI, 2020; SANTAMOURIS; YUN, 2020). Among the various possibilities, *leuco* dyes are the most studied, but they are still not the most interesting option, as they present aging problems and lose their reversibility after weeks. The most promising thermochromic alternatives are based on quantum dots, plasmas or photonic crystals (SANTAMOURIS; YUN, 2020).

In order to intensify the cooling effects, fluorescent materials have emerged that have lower surface temperatures compared to common and reflective materials (up to 2°C less than non-fluorescent materials), as they have high solar reflectance in visible and infrared spectrum, high broadband emissivity associated with the photoluminescence process that corroborates the results. These can be classified as mineral photoluminescent materials (bulk) and nanoscale photoluminescent materials (quantum dots). Bulk materials often have optical aging problems, whereas quantum dot compounds attract a great deal of interest because of their superior fluorescent optical properties. Recent research seeks to enhance optical effects and reduce costs (SANTAMOURIS; YUN, 2020).

After several experimental laboratory tests and computer simulations about the cool materials reflectivity and emissivity and their influence on buildings and urban contexts (BANIASSADI; SAILOR; BAN-WEISS, 2019; FENG *et al.*, 2021; FENG *et al.*, 2022b) it was proved that materials with high emissivity in the atmospheric window or spectrally selective daytime radiative cooling materials – DTRC provided better cooling results for hot and dry climates in comparison to materials with high broadband emissivity (except in humid, polluted or cloudy regions where the results of DTRC are compromised). These materials have high emissivity in the atmospheric window but not necessarily high broadband emissivity (BERARDI; GARAI; MORSELLI, 2020) and are applied as an additional layer (composed by up to four different materials<sup>13</sup>) to a substrate of high spectral reflectivity<sup>14</sup> and therefore, are

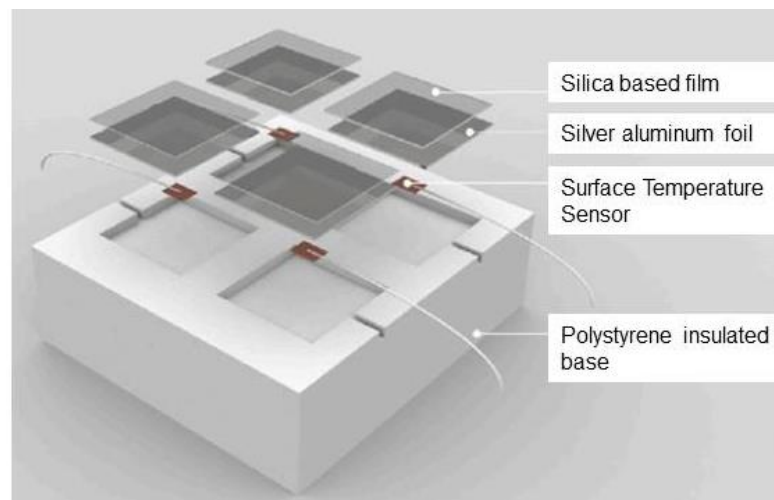
---

<sup>13</sup> SrTiO<sub>3</sub> (Strontium Titanate), SiO<sub>2</sub> (Silicon Dioxide), HfO<sub>2</sub> (Hafnium Oxide), MgF<sub>2</sub> (Magnesium Fluoride), Al<sub>2</sub>O<sub>3</sub> (Aluminium Oxide), PDMS (Dimethyl Polysiloxane), PMMA (Polymethylmethacrylate)



normally used as multilayered photonic flat surfaces (as shown in Figure 12), metamaterials photonics with two or three dimensional geometries, inks designed for radiative cooling or polymers (MOGHATA; SHAHROUZIANFAR; ASHIRI, 2017; SANTAMOURIS; YUN, 2020). There is also the possibility of multilayer photonic materials for mixed climates, through the addition of an intermediate thermochromic film with variable solar reflectivity (SANTAMOURIS; YUN, 2020). Current researches (2020-2022) focus on costs, forms of application, the improvement of thermoenergetic performance and thermochromic compositions (SANTAMOURIS; YUN, 2020). Metamaterials 2D and 3D and photonic crystals, for example, require a very sophisticated and expensive manufacturing process, whereas inks with microspheres can be easily manufactured and implemented (SANTAMOURIS; YUN, 2020).

**Figure 12 - Experimental tests of spectrally selective multilayer silica and aluminum materials**



Source: adapted from Feng *et al.* (2022a).

Table 2 shows a summary of information on the main types of cool materials, physical properties (reflectivity and emissivity), regions studied in research, climate context tested, forms of application and useful life in relation to optical degradation/weathering.

---

<sup>14</sup>Al (Aluminium) or Ag (Silver)

**Table 2 - Summary Table of Characteristics of Cool Materials and Climatic Indication**

<b>Cool Material Type</b>	<b>Examples</b>	<b>Physical properties</b>	<b>Study Regions</b>	<b>climate tested</b>	<b>Application Methods/Forms</b>	<b>Durability</b>
Natural Cool Materials	- Gravel - light marble	High average visible spectrum reflectivity and high broadband emissivity	Mediterranean area Italy Greece Montreal Los Angeles Philadelphia	Hot and dry	- Roofs - floors - Coatings	Not cited in articles
High Reflectance White	- Elastomers - Silicones - Fluoropolymers - Acrylics (EPDM, PVC, CPE, CPSE, TPO)	High visible spectrum reflectivity and high broadband emissivity	Greece London France Milan Pomegranate Portugal Spain Cairo Singapore Turkey New York Chicago Washington golden Rio de Janeiro	Hot and dry	- Membranes - Coatings - Paintings - Coverage metallic - Roof tiles	3 to 5 years
Colored high-infrared reflectance (pigments)	- Organic (anthraquinone, quinacridone, phthalocyanine, dioxazine ) - Inorganic (chromates, oxides, silicates, borates, sulfates, phosphates, metals, vanadates)	High infrared reflectivity and high broadband emissivity	California Greece Italy UK	Hot and dry	Mixing with other materials: - Mortar - Concrete - Paints - Coatings  Sol-gel thin films	3 to 5 years
Phase Change Materials (PCM)	- Organic (paraffin, fatty acids) - Inorganic (hydrated salt, molten salt, metal) - eutectic (mixtures of organic and/or inorganic)	High spectral reflectivity and high broadband emissivity	southern Italy Athens	Hot and dry with cold nights	Encapsulated materials mixed with other materials: - Mortar - Concrete - Asphalt	Not cited in articles
Retroreflective Materials	- glass beads - prisms	High spectral reflectivity (variable with solar incidence angle)	Athens Italy Oslo Cairo	Hot and dry	Applied superficially to cool or conventional materials	Not cited in articles



thermochromic	<i>leuco</i> dyes - Doped dyes PCM - polymers (PNIPAM) - quantum dots - plasmas - photonic crystals	high spectral reflectivity and high broadband emissivity (variable with temperature)	Toronto	Warm and cold periods during the year	- dyes mixed with paints, mortars and asphalts - Aqueous solution - Multilayer	weeks (dye)
fluorescent	Bulk (ruby) or nanofluorescent (quantum dots: elements of groups II and VI or III and V of the periodic table)	high spectral reflectivity, High broadband emissivity and high Fluorescent Emission	Not cited in articles	Hot (humidity not cited in articles)	Not cited in articles	Not cited in articles
Spectrally Selective	SrTiO <sub>3</sub> , SiO <sub>2</sub> , HfO <sub>2</sub> , MgF <sub>2</sub> , Al <sub>2</sub> O <sub>3</sub> , PDMS, PMMA layer applied to Al or Ag substrate	high spectral reflectivity and High emissivity in the atmospheric window	Albuquerque Atlanta Chicago Houston Los Angeles Miami Philadelphia Phoenix New York Darwin Sydney Alice Springs Shanghai Cave Creek Tempe Seoul San Pedro do Atacama Cambridge West Lafayette	Hot and dry or humid	- Multilayer - metamaterials - paints	Not cited in articles

Source: authors.

Based on the evolution of the solutions presented, the most promising materials for reducing heat island effects and energy consumption in buildings through cooling are: a) with high spectral reflectivity and high broadband emissivity (such as materials fluorescent or some multilayer photonic materials) for warm and humid or heavily polluted climates; b) with high-reflectivity and high-emissivity materials in the atmospheric window (such as DTRC) warm and dry climates and c) thermochromic materials for mixed climates (which can be applied alone or as an intermediate layer in multi-layer photonic materials). In cases of climates with greater daily thermal amplitude (warm days and cold nights), phase change materials can also be indicated.

The ways of application are diverse, such as dyes for mixtures, with simplified application; films or flat surfaces, which can be attached to a substrate, with relatively simplified application; or complex structures, with a sophisticated and expensive manufacturing process.

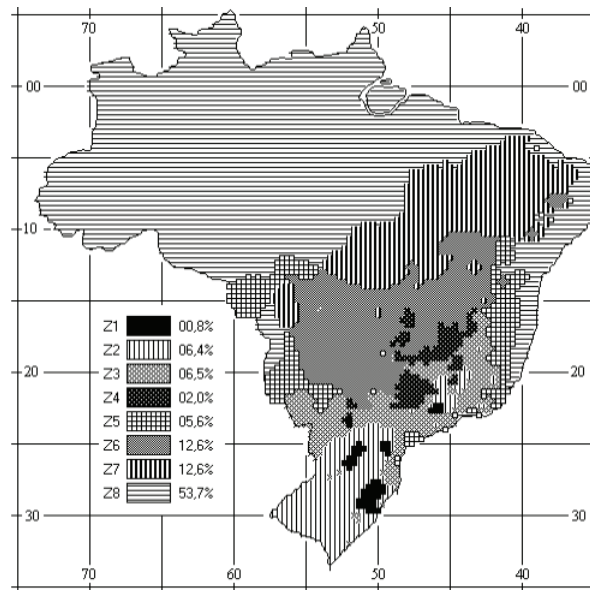
The durability of white high-reflectivity or colored high-infrared reflectivity coatings is about 3 to 5 years due to weathering and optical degradation, but can be extended by adding compounds that provide the material with self-cleaning properties. *Leuco* dye-based thermochromic coatings suffer from aging problems and lose their reversibility after weeks. The average useful life of the other materials was not mentioned in the articles chosen by the method of systematic literature review proposed.

The most promising cool materials have been studied in several international climate contexts: thermochromic in mixed climates (Toronto) and spectrally selective in cold and wet climates (Chicago), cold and dry (Darwin), mixed and dry (Albuquerque, Los Angeles, Tempe, Sydney), mixed and wet (Philadelphia, New York, West Lafayette, Shanghai, Seoul), warm and humid (Atlanta, Houston, Cambridge), very warm and humid (Miami), warm and dry (Fênix, Cave Creek, São Pedro de Atacama, Alice Springs (BANIASSADI; SAILOR; BAN-WEISS, 2019; FENG *et al.*, 2021; FENG *et al.*, 2022b), but have not been tested in Brazil yet.

The choice of the most appropriate option for the Brazilian context must be made based on a more detailed analysis of the different bioclimatic zones, which is done in the following 2.3 topic.

### **2.3. Bioclimatic zones and passive strategies recommended for the Brazilian context**

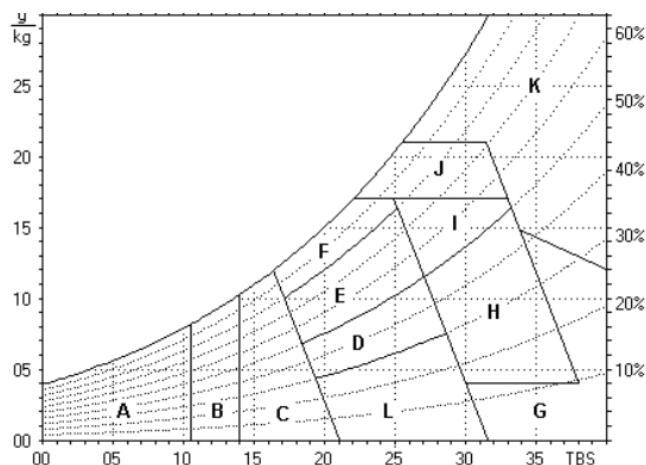
The first Brazilian bioclimatic classification was purposed by the Brazilian normative NBR 15220-3 (ABNT, 2005a) which divided 330 cities into 8 zones (ZBBR) based on the Givoni Chart (Figure 13), which considers variations in absolute air humidity, relative air humidity and dry bulb temperature. Zone 1 is the coldest and zone 8 is the warmest.

**Figure 13 - Brazilian Bioclimatic Zoning**

Source: ABNT (2005a).

The zones with predominance of extremely high temperatures throughout the year (7 and 8) represent 66.3% of the national territory. Intermediate climates (zones 4, 5 and 6) are 20.2% and those with more significant periods of cold (zones 1, 2 and 3) 13.7%.

The normative also makes technical-constructive recommendations as an orientation for single-family residential buildings that allow greater climatic adaptation and better thermal performance. The guidelines address passive strategies such as adequate size of ventilation openings, solar protection for glazing, envelope properties (walls and roofs) and passive conditioning strategies (ABNT, 2005a), shown in Figure 14 and in Table 3.

**Figure 14 - Brazilian Bioclimatic Chart**

A – artificial heating	G + H – evaporative cooling
B – passive solar heating	H + I – thermal mass (cooling)
C – thermal mass (heating)	I + J – ventilation
D – comfort (low humidity)	K – artificial cooling
E – comfort	L – air humidification
F – dehumidification (air changing)	

Source: ABNT (2005a).

**Table 3 - Technical-construction recommendations for the 8 Brazilian bioclimatic zones**

Zone	Number of Cities and the most Representative	Temperature and relative humidity annual variation	Recommendations	
1	12 Caxias do Sul (RS)	3 - 26°C 40 – 100%	G	<ul style="list-style-type: none"> <li>• Medium ventilation openings;</li> <li>• Solar radiation on windows in cold periods;</li> <li>• Light external walls;</li> <li>• Light insulated roof;</li> </ul>
			W	<ul style="list-style-type: none"> <li>B) Passive solar heating;</li> <li>C) Thermal mass internal walls;</li> <li>A) Artificial heating in cold periods;</li> </ul>
2	33 Ponta grossa (PR)	5 - 32°C 48 - 100%	G	<ul style="list-style-type: none"> <li>• Medium ventilation openings;</li> <li>• Solar radiation on Windows in winter;</li> <li>• Light external walls;</li> <li>• Light insulated roof;</li> </ul>
			S	J) cross ventilation
			W	<ul style="list-style-type: none"> <li>B) Passive solar heating;</li> <li>C) Thermal mass internal walls;</li> <li>A) Artificial heating in cold periods;</li> </ul>
3	62 Florianópolis (SC)	8 - 32°C 42 - 100%	G	<ul style="list-style-type: none"> <li>• Medium ventilation openings;</li> <li>• Solar radiation on windows in winter;</li> <li>• Light reflecting external walls;</li> <li>• Light insulated roof;</li> </ul>
			S	J) cross ventilation
			W	<ul style="list-style-type: none"> <li>B) Passive solar heating;</li> <li>C) Thermal mass internal walls;</li> </ul>
4	17 Brasília (DF)	10 - 32°C 40 – 100%	G	<ul style="list-style-type: none"> <li>• Medium ventilation openings;</li> <li>• Window shadings;</li> <li>• Thermal mass external walls;</li> <li>• Light insulated roof;</li> </ul>
			S	<ul style="list-style-type: none"> <li>H) Evaporative cooling;</li> <li>I) Thermal mass for cooling;</li> <li>J) Controlled ventilation (openings when internal temperature is higher than outside);</li> </ul>
			W	<ul style="list-style-type: none"> <li>B) Passive solar heating;</li> <li>C) Thermal mass internal walls;</li> </ul>
5	30 Santos (SP)	13 - 34°C 50 – 100%	G	<ul style="list-style-type: none"> <li>• Medium ventilation openings;</li> <li>• Window shadings;</li> <li>• Light reflecting external walls;</li> <li>• Light insulated roof;</li> </ul>
			S	J) cross ventilation
			W	C) Thermal mass internal walls;

6	38 Goiânia (GO)	10 - 35°C 34 – 100%	G	<ul style="list-style-type: none"> <li>• Medium ventilation openings;</li> <li>• Window shadings;</li> <li>• Thermal mass external walls;</li> <li>• Light insulated roof;</li> </ul>
			S	H) Evaporative cooling; I) Thermal mass for cooling; J) Controlled ventilation (openings when internal temperature is higher than outside);
			W	C) Thermal mass internal walls;
7	39 Picos (PI)	15 - 37°C 30 – 100%	G	<ul style="list-style-type: none"> <li>• Small ventilation openings;</li> <li>• Window shadings;</li> <li>• Thermal mass external walls;</li> <li>• thermal mass roof;</li> </ul>
			S	H) Evaporative cooling; I) Thermal mass for cooling; J) Controlled ventilation (openings when internal temperature is higher than outside);
8	99 Belém (PA)	18 - 37°C 50 – 100%	G	<ul style="list-style-type: none"> <li>• Large ventilation openings;</li> <li>• Window shadings;</li> <li>• Light reflecting external walls;</li> <li>• Light reflecting roof;</li> </ul>
			S	J) Permanent cross ventilation; K) Artificial cooling.

G – General construction strategies; S – Summer strategies; W – Winter strategies

Source: adapted from ABNT (2005a).

The requirement of the size of ventilation openings (A) is valid for occupied or long-stay environments and is expressed in percentage by:

(window area/floor area) x 100:

- small:  $10 < A < 15\%$
- medium:  $15 < A < 25\%$
- large:  $A > 40\%$

The wall and roof properties follow the parameters of Table 4.

**Table 4 - Wall and roof properties recommended by ABNT (2005a)**

Envelope part		Thermal transmittance – U (W/m <sup>2</sup> .K)	Heating transfer delay – $\Phi$ (hours)	Solar factor – SF <sub>o</sub> (%)
Walls	Light	$U \leq 3.0$	$\Phi \leq 4.3$	$SF_o \leq 5.0$
	Light reflecting	$U \leq 3.6$	$\Phi \leq 4.3$	$SF_o \leq 4.0$
	Thermal mass	$U \leq 2.2$	$\Phi \geq 6.5$	$SF_o \leq 3.5$
Roofs	Light insulated	$U \leq 2.0$	$\Phi \leq 3.3$	$SF_o \leq 6.5$
	Light reflecting	$U \leq 2.3$ . FT	$\Phi \leq 3.3$	$SF_o \leq 6.5$
	Thermal mass	$U \leq 2.0$	$\Phi \geq 6.5$	$SF_o \leq 6.5$

Source: ABNT (2005a).

The low temperatures are predominant in Zone 1 and passive heating strategies are indicated, as well as artificial climate control on colder days. It is suggested heat gains by solar radiation with correct orientation of glazed areas and use of dark colors on the facades (ABNT, 2005a).

Zone 2, with slightly higher temperatures than the previous zone, thus requires cross ventilation for heat losses in summer, but it is also important to apply heating strategies in the cold period, as well as those recommended for zone 1 (ABNT, 2005a).

Zone 3 has a mixed climate. In summer, it is necessary to avoid heat gains with light walls and provide losses with cross ventilation. In winter, are recommended glazed areas to provide heat gains and thermal mass on internal walls to maintain higher internal temperatures.

Zone 4 is also mixed climate, but with more cooling needs throughout the year. In addition, it is a dry climate with a wide range of temperatures in some periods. For the summer, it is suggested to avoid heat gains by shading the windows, increase losses with cross ventilation and reduce thermal amplitudes with partitions and external walls with thermal mass. In winter, the solutions are the same as in zone 3.

Zone 5 has a warm climate and therefore solutions are indicated to avoid heat gains for most of the year, such as window shading, reflecting external walls, in addition to heat loss solutions such as cross ventilation. In winter, it is recommended to maintain internal heat through thermal mass internal walls.

Zone 6 has high temperatures and low humidity, as well as a large daily temperature range in some periods. It is recommended to avoid heat gains by shading the windows, to maximize losses with controlled ventilation and evaporative cooling and to maintain the temperature in summer and winter with thermal mass in external and internal walls.

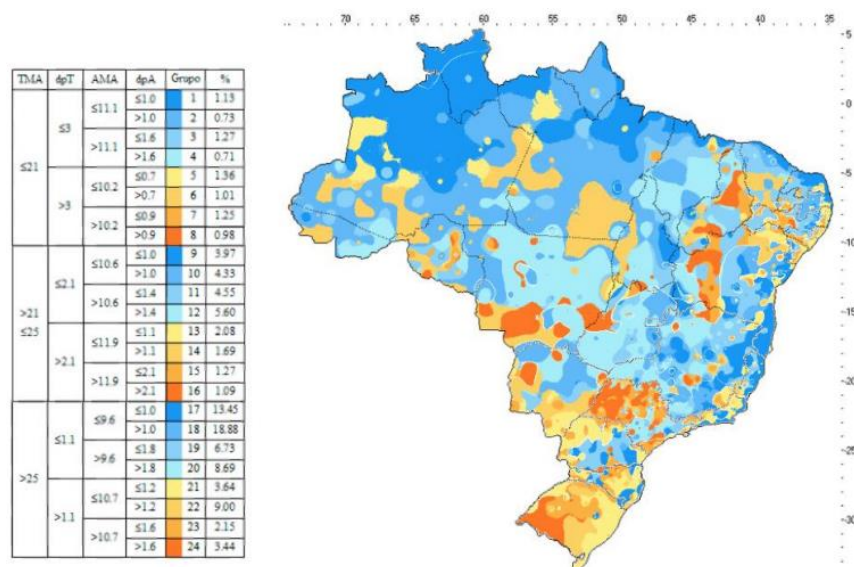
Zone 7 is very hot and dry, also with a large daily temperature range. Only cooling solutions are indicated. Window shading is recommended to avoid heat gains, thermal mass in external walls and roof associated with small window areas to mitigate thermal amplitudes and keep internal temperatures lower, as well as evaporative cooling and ventilation control to maximize heat losses and humidify.

Zone 8 is very hot and humid. It is suggested to avoid heat gains with reflective walls, window shading and potentialize losses with large openings for cross ventilation. However, according to the normative, artificial conditioning is necessary in part of the year.

As reported by ABNT (2005a), most zones only require passive strategies. Although most of the Brazilian territory needs to reduce heat gains and cooling strategies to guarantee comfort, only zone 1 and 2 need artificial heat in parts of the year and 8 needs air conditioning for artificial cooling.

ABNT (2005a) assisted in the development of several architectural projects in Brazil, including non-residential buildings. However, the methodology proposed by the first Brazilian zoning generated the grouping of cities with very different climates. Therefore, Roriz (2014) suggested a new methodology that considers mean annual temperature (TMA), mean annual amplitude (AMA), standard deviation of the monthly mean of daily mean temperatures (dpA), standard deviation of the mean monthly amplitude (dpT) and the altitude of the cities (ANDRADE, 2022). In this methodology, Brazil is divided into 24 climatic groups, as shown in Figure 15. This second zoning also became part of the Brazilian labeling system, but it has not yet been definitively implemented in all Brazilian regulations and legislations.

**Figure 15 - Classification of Brazilian climates according to Roriz (2014)**



Source: adapted from Roriz (2014).

#### **2.4. Analysis of Applicability of Cool Materials to the Brazilian Context and Costs of Brazilian Supercool paints**

The Brazilian territory is classified into eight bioclimatic zones – ZBRs based on the Givoni Chart, which considers variations in absolute air humidity, relative air humidity and dry bulb temperature (ABNT, 2005a). Although this proposed zoning has significantly contributed to the improvement of the thermal performance of popular housing in the country, the method used resulted in climatic zones with little homogenous, which do not accurately represent the climatic diversity (RORIZ, 2012).

A new bioclimatic zoning was suggested with 24 climate groups (RORIZ, 2012; RORIZ, 2014), which considers minimum, average and maximum air temperature and thermal amplitude and is currently used in the Brazilian Labeling Program – PBE Edifica (ELETROBRÁS, 2021). Although the recent proposal is more precise in terms of temperatures, it does not consider variations in relative air humidity, which also contribute to the comfort and influence design solutions.

The indication of the most suitable cool materials as a passive cooling as a complement to the others passive strategies suggested by the Brazilian legislation depends on the climatic context. According to the literature review, temperature and air humidity information must be used simultaneously, for this reason the first zoning proposal (ABNT, 2005a) was used as a reference for the selection of most suitable cool material for each Brazilian zone.

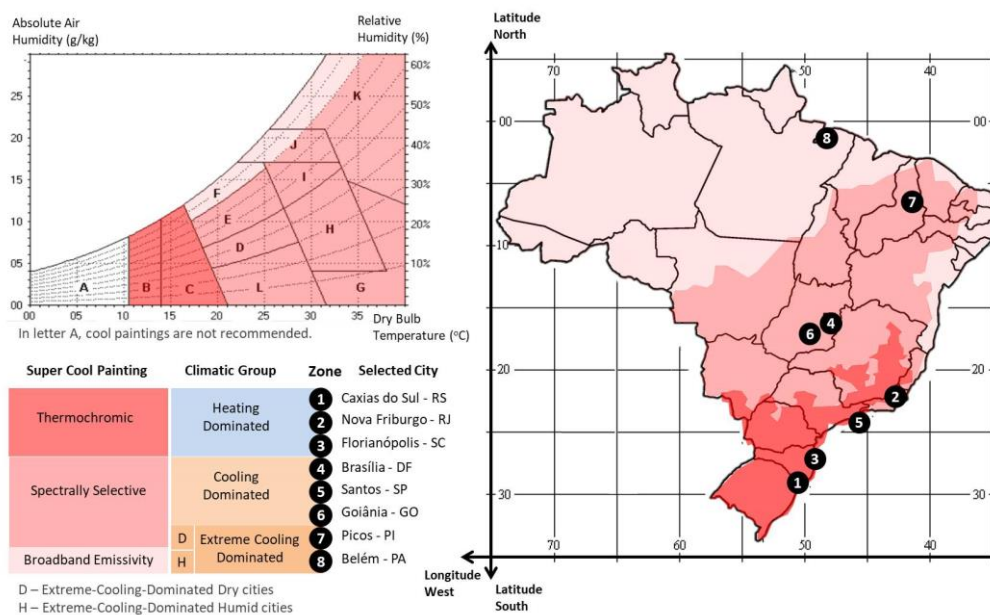
Zones 7 and 8 are very hot, however, spectrally selective materials may have reduced effectiveness in zone 8 due to high humidity. Zones 4, 5 and 6 have favorable humidity and cloudiness for spectrally selective materials. Nevertheless, due to the milder temperatures, supercool materials should be used sparingly. Zones 1, 2 and 3 have some periods with humidity above 80%. Temperatures can be high in summer but low in winter. In such cases, high broadband emissivity thermochromic material is recommended.

The current ABNT recommendations for passive strategies (2005a) can guide the determination of the most suitable cool materials for each zone. Strategy A originally refers to artificial heating, therefore, the use of cool materials is not indicated due to the high probability of generating an increase in the consumption of heating energy. Strategies B and C are related to passive heating, so thermochromic materials would



be the most suitable. The combinations of temperature and humidity of the letters D and E provide comfort, but the application of material with high spectral reflectivity and high emissivity in the atmospheric window would be interesting to help mitigate the heat island phenomenon. Strategies G, H, I and L address passive cooling at low and medium humidities, therefore, the use of material with high spectral reflectivity and high emissivity in the atmospheric window is advised. Strategy F deals with passive cooling in humid areas, therefore, the use of materials with high spectral reflectivity and high broadband emissivity is suggested. Strategies J and K are for passive or active cooling for a very large variation of humidity, therefore a subdivision was proposed, with indication of materials with high spectral reflectivity and high emissivity of broadband for high humidity and of high spectral reflectivity and high emissivity in the atmospheric window for medium or low humidity. The Figure 16 shows a summary of the most suitable cool materials for each region of Brazil. The selection of each material correlates the passive strategies indicated by NBR 15220 and the following recommendations for the use of cool materials according to international literature: 1. spectrally selective materials for cooling dominated cities with mean annual humidity levels below 80%; 2. high broadband emissivity for cooling dominated cities with mean annual humidity levels above 80%; 3. thermochromic for mixed climates or heating dominated cities.

**Figure 16 - Suitable cool materials according to temperature and humidity variation**



Source: adapted from ABNT (2005a).

Then, it was possible to identify the predominant needs in each bioclimatic zone, in order to indicate the most suitable cool materials (Table 5).

**Table 5 - Bioclimatic Zones, Strategies, Predominant Needs Most suitable Cool Materials**

Zone	Passive Strategies (ABNT, 2005a)	Cited needs	Most suitable cool material
1	A, B and C	<b>Winter:</b> Artificial and Passive Heating, Thermal Mass partitions	Thermochromic
2	A, B, C and J	<b>Winter:</b> Artificial and Passive Heating, Thermal Mass partitions <b>Summer:</b> cross ventilation	
3	B, C and J	<b>Winter:</b> Passive Heating, Thermal Mass partitions <b>Summer:</b> cross ventilation	
4	B, C, H and J	<b>Winter:</b> Passive Heating, Thermal Mass partitions <b>Summer:</b> cross ventilation, evaporative cooling and thermal mass for cooling	High Spectral Reflectivity and High Emissivity in the Atmospheric Window
5	C and J	<b>Winter:</b> Thermal Mass partitions <b>Summer:</b> cross ventilation	
6	C, H and J	<b>Winter:</b> Thermal Mass partitions <b>Summer:</b> cross ventilation, evaporative cooling and thermal mass for cooling	
7	H and J	<b>Summer:</b> cross ventilation, evaporative cooling and thermal mass for cooling	
8	K	<b>Summer:</b> Permanent cross ventilation and Artificial cooling	High Spectral Reflectivity and High Broadband Emissivity

Source: authors.

Three main climatic groups and respective most suitable cool materials were identified: for zones with a predominance of normative heating strategies (zones 1, 2 and 3), thermochromic materials were suggested; for zones with low to medium humidity and more indications of normative cooling strategies (zones 4, 5, 6 and 7), high spectral reflectivity and high emissivity materials in the atmospheric window were advised; and for the high humidity city with only normative cooling recommendation (zone 8), High Spectral Reflectivity and High Broadband Emissivity was suggested. As applying method of cool materials in standardized Brazilian schools, the use of paints is recommended, because of their ease of application and maintenance.

## **2.5. Costs of Brazilian Supercool paints and comparison with conventional paints**

Amidst the three supercool paints suitable for the Brazilian context, thermochromic are still in the development phase due to the low durability of the color-changing property in the current options under study, and therefore, they are not yet available

for purchase and application in building envelopes (SANTAMOURIS; YUN, 2020). The spectrally selective paints exhibit high emissivity at specific wavelengths (SANTAMOURIS; YUN, 2020), information not yet disclosed in the Cool Roof Rating Council – CRRC (CRRC, 2022a; 2022b) or any other publicly available database. Therefore, only commercially available supercool paintings with high spectral reflectivity and high broadband emissivity can be identified. This specific type of supercool painting is found both nationally (ANDRADE; DORNELLES, 2023) and internationally (CRRC 2022a; 2022b). Considering that the focus of this thesis is a public building that should prioritize cost-effective solutions, national supercool paintings were analyzed and the results of their cost are shown in Table 6.

Among the various options of Brazilian cool paintings recently investigated by Andrade and Dornelles (2023), only one option, acrylic-based, can be characterized as supercool, with over 90% reflectivity. This percentage is a very high value that characterizes a highly efficient supercool material according to Pisello (2017), Carlosena *et al.* (2021), Feng *et al.* (2021) and Feng *et al.* (2022b). Therefore, the Table 6 presents the average cost of this product, collected from 7 different online sources (4 different prices from manufacturer representatives and 3 from websites) in January 2024, and three different types of conventional latex acrylic paints (standard, premium and super premium) suitable for external applications (ABNT, 2021a; 2021b) in the eight different Brazilian cities studied in this thesis (PA, PI, GO, SP, DF, SC, RJ and RS) described in the latest report of the National System of Prices and Indices for Civil Construction – SINAPI published by in November 2023 (CAIXA ECONÔMICA FEDERAL, n/d).

**Table 6 – Prices of Cool and Conventional Paints**

Material Type	Average Cost (R\$/L)	Source
Super Cool Acrylic Paint Termo - T08	25.63	Mercado Livre (2024) Brand Store (2024)
Standard Conventional Acrylic Paint	19.62	Caixa Econômica Federal (n/d)
Premium Conventional Acrylic Paint	29.60	
Super Premium Conventional Acrylic Paint	36.53	

Source: authors.

The results indicate that nationally manufactured supercool paints have competitive prices compared to conventional acrylic paints for external building surfaces, with the additional advantage of optical properties that minimize heat transfer to indoor

spaces. These positive aspects makes them a favorable choice for Brazilian public buildings in predominantly warm climates (Zones 4 to 8).

## **2.6. Brazilian School Building Stock: Construction and Energy Consumption Patterns**

The current built park of Brazilian public schools is composed by 137,828 buildings, 84,915 urban and 52,913 rural. Of the urban schools, 604 are federal, 24,482 are state and 59,829 are municipal (INEP, 2021), which cover students up to 15 years of age and are distinguished mainly by size and architectural design. Generally, municipal schools are small and medium-sized (with an average of 20 students per class), while state schools are medium and large (with an average of 34 students per class) (JOTA; SOUZA; SILVA, 2017).

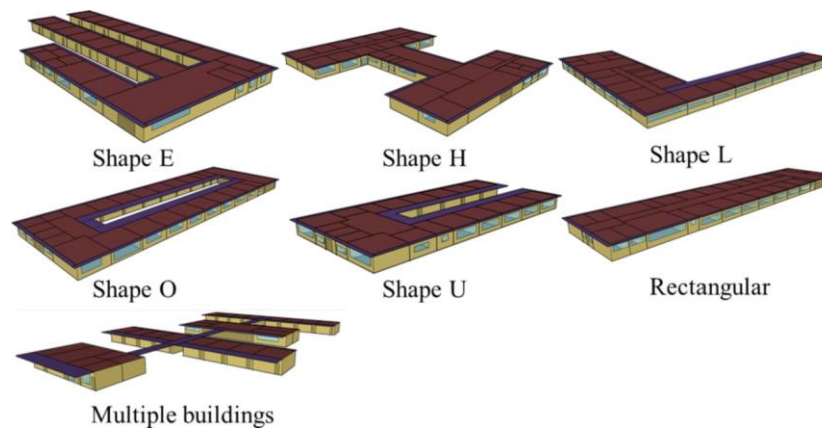
According to Geraldi and Ghisi (2020), school buildings also differ in terms of use, occupation, facilities, user behavior, education level and age of the building, which reflect a variation in energy performance. While high school buildings tend to consume more energy than primary schools (HONG *et al.*, 2014 *apud* GERALDI; GHISI, 2020), newer buildings (which follow the most current regulations and have more technology) have lower consumption (OUF; ISSA, 2017 *apud* GERALDI; GHISI, 2020).

In addition, some schools vary due to specific characteristics that reflect on the distribution of spaces, on period of operation and consequently on energy consumption: "technological schools", for example, have a greater number of laboratories, while "open schools" allow for students to study, to practice sports and to have meals on weekends (JOTA; SOUZA; SILVA, 2017).

Of the 84,915 existing urban schools, 426 were investigated by Geraldi and Ghisi (2020; 2022a; 2022b), through questionnaires, surveys and computer simulations that reveals energy consumption, building size, facilities, building systems, occupancy, routine, maintenance and occupant satisfaction with temperature, lighting and airflow.

This study shows that there are seven predominant shapes of construction (Figure 17): Shape E, L, H, O, U, Rectangular and Multiple Buildings (GERALDI; GHISI, 2022a; GERALDI; GHISI, 2022b).

**Figure 17 - Predominant forms of public school buildings in Brazil**

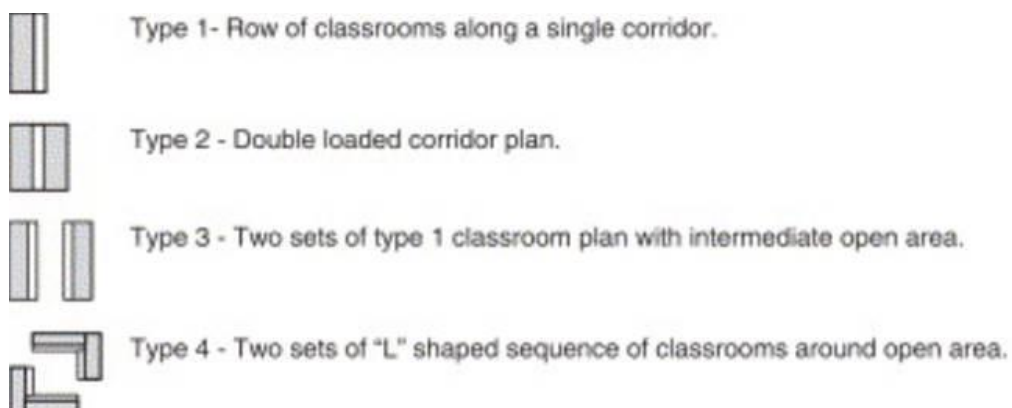


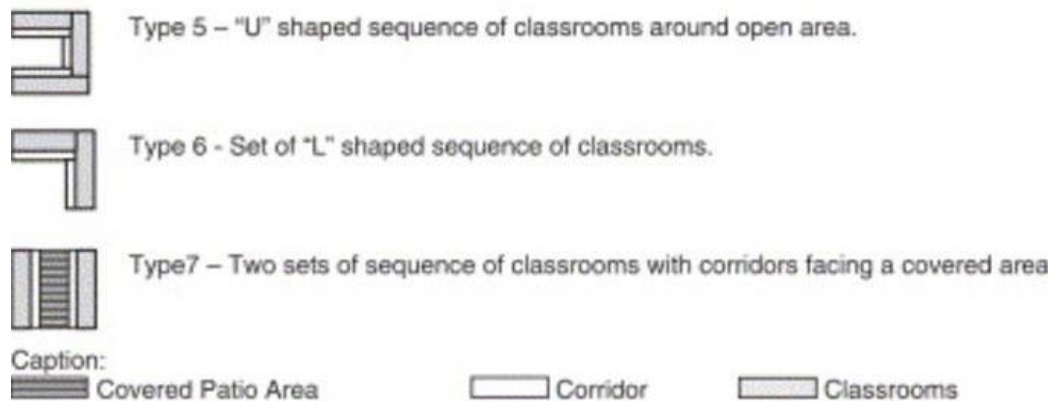
Source: Geraldi and Ghisi (2022a).

According to computer simulations and school audits, differences in the geometry of buildings mainly influence the dynamics of self-shading. However, the results show that solar orientation is not a relevant factor, since classrooms are concentrated in the central part of the building and are oriented equally in all formats (GERALDI; GHISI, 2022a).

According to the evaluation on 39 school plans in the state of São Paulo by Graça, Kowaltowski and Petreche (2007), the different formats mentioned can be presented in 7 main types of composition (Figure 18).

**Figure 18 - Types of Building Compositions**





Source: Graça, Kowaltowski and Petreche (2007).

Schools have seven typical subspaces: classrooms, library, computer cluster, office rooms, cafeteria, restrooms and corridors. Most schools have between 5 and 15 classrooms, which are grouped together and accessed through a corridor. Bathrooms, cafeteria and kitchen are next to each other, as well as office rooms, library and computer cluster are usually placed together (GERALDI; GHISI, 2022a). The average areas of each subspace can be seen in Table 7.

**Table 7 - Areas of Subspaces in Brazilian Public Schools**

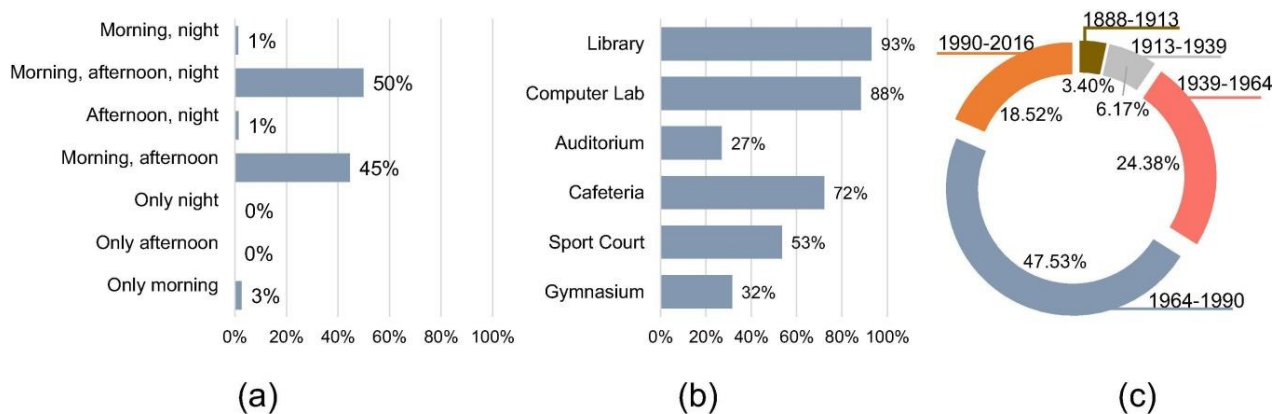
Subspace	Name	Floor plan area (m <sup>2</sup> )						
		Shape E	Shape H	Shape L	Shape O	Shape U	Rec.	Multiple Buildings
1	Classrooms	799.7	609.0	623.3	637.0	500.5	700.7	638.4
2	Library	67.8	72.0	70.0	59.5	50.1	82.0	72.0
3	Computer lab	50.0	72.0	49.0	54.6	50.1	70.0	50.0
4	Office Rooms	100.0	217.8	120.0	100.0	52.5	98.0	80.1
5	Aisles	240.9	597.7	317.7	260.5	109.8	318.3	146.0
6	Bathroom	44.8	38.8	68.6	58.8	58.9	89.0	103.0
7	Kitchen	51.0	87.8	42.0	74.2	60.0	83.3	80.0
Total		1354.1	1695.0	1290.6	1244.6	881.8	1441.3	1169.5

Source: adapted from Geraldi and Ghisi (2022a).

The most frequent school facilities are libraries, computer labs and cafeterias (Figure 20b).

Schools operate mainly in the morning, afternoon and evening or only morning and afternoon (Figure 20a) (GERALDI; GHISI, 2020). Most of them were built between 1939 and 1990, before the current requirements for comfort and energy efficiency (Figure 20c).

**Figure 19 - Characterization of the school building in terms of operating shifts (a), installations (b) and year of construction (c)**



Source: Geraldi and Ghisi (2020).

The variation in area, number of students and energy consumption of Brazilian public schools is described in the study by Geraldi and Ghisi (2020), based on information from 5,321 schools present in the 27 states of Brazil (Table 8 and Figure 20).

**Table 8 - Summary statistics of continuous variables**

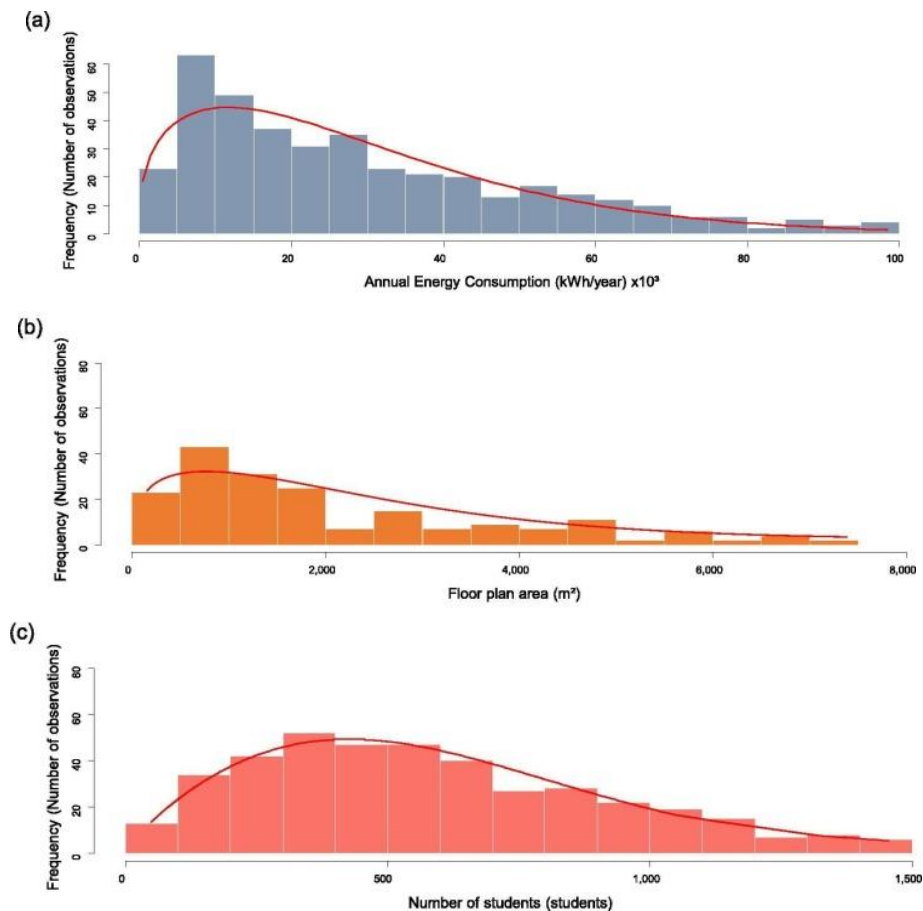
Measure	Floor-plan area (m <sup>2</sup> )	Number of students (students)	Annual energy consumption (kWh)
Minimum value	100.00	49.00	426.00
Lower Quantile (25%)	900.00	322.25	10,796.00
Average (50%)	1,501.69	534.50	23,667.00
Upper Quantile (75%)	3,065.50	817.75	42,190.00
Standard deviation	1,785.34	342.16	22,543.57
Maximum value	7,326.37	1,569.00	98,720.00

Source: adapted from Geraldi and Ghisi (2020).

The Table 8 shows that the annual energy consumption is higher as the floor plan area and the number of students increase.

In addition, it is possible to infer that most Brazilian public schools have a low energy consumption, from 0 to 40 kWh/year (Figure 21a), with a predominant area of up to 2,000 m<sup>2</sup> (Figure 21b) and generally from 0 to 700 students (Figure 21c).

**Figure 20 - Histograms of continuous variables: annual energy consumption (a), floor plan area (b) and number of students (c)**



Source: Geraldi and Ghisi (2020).

The schools are distributed unevenly in 8 Brazilian bioclimatic zones, as some areas are more urbanized and denser (such as the State of São Paulo, classified in Zones 3 and 5) than others (such as the Amazon forest, classified in the 8) (GERALDI; GHISI, 2020).

Bioclimatic zones are established by the Brazilian Standard NBR 15,220 (2005) based on monthly variations in temperature and relative humidity. According to the standard, zones 1 and 2 have lower temperatures (requiring heating strategies for parts of the year), zones 3 to 6 have intermediate temperature and humidity combinations (easily solved with passive solutions), zone 7 is characterized by high temperatures and zone 8 for high temperatures and high humidity (requiring artificial conditioning for parts of the year). Zone 1, the main region with lower temperatures in certain periods and in need of heating, represents a small portion of the Brazilian



territory and does not show the characteristic need for cooling present in the stock of Brazilian public schools (GERALDI; GHISI, 2020) .

The most representative cities of each zone and their respective climate classifications, used in studies of computer simulations of thermoenergetic performance (GERALDI; GHISI, 2022a), can be observed in Table 9.

**Table 9 - Climates considered in the parametric simulation in recent studies**

City	Brazilian climate zone (NBR 15,220 2005a)	ASHRAE classification (ASHARE 169-2013)	Lat. (°)	Long. (°)	Alt. (m)	Cooling Degree Hours*
Curitiba (PR)	1	3A (Warm Humid)	- 25.43	- 49.27	924	9397
Pelotas (RS)	2	3A (Warm Humid)	- 31.72	- 52.33	18	18,657
São Paulo (SP)	3	2A (Hot Humid)	- 23.85	- 46.64	792	14,172
Brasília (DF)	4	2A (Hot Humid)	- 15.78	- 47.93	1,160	16,624
Santos (SP)	5	2A (Hot Humid)	- 23.93	- 46.32	14	40,003
Goiânia (GO)	6	1A (Very Hot and Humid)	- 15.37	- 48.78	770	31,081
Picos (PI)	7	1A (Very Hot and Humid)	- 7.07	- 41.40	233	53,316
Cuiabá (MT)	8	0A (Extremely Hot and Humid)	- 15.62	- 56.00	151	59,551

Source: Geraldi and Ghisi (2022a).

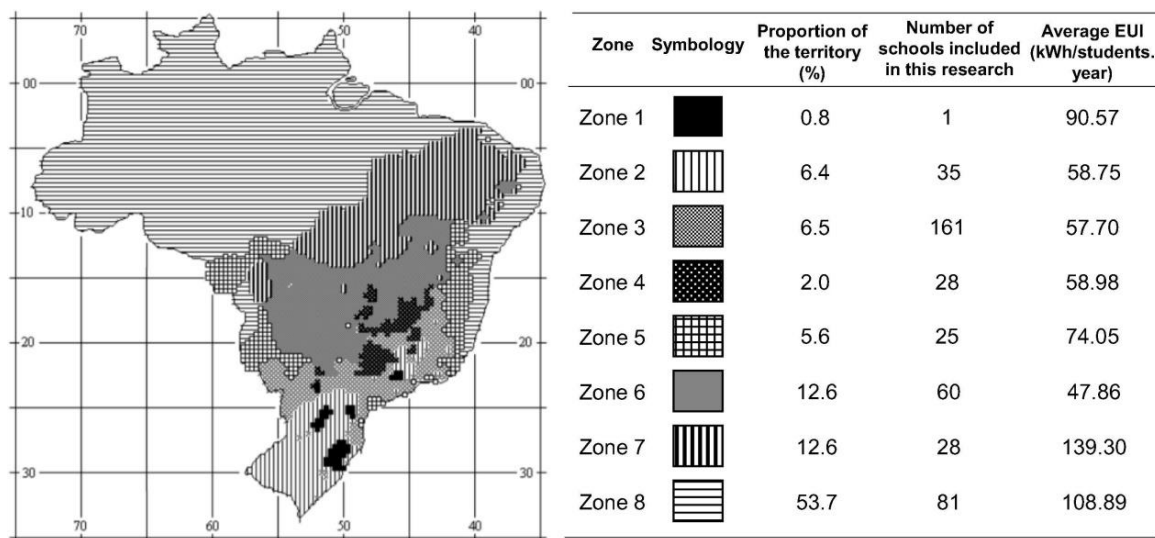
Despite the different recommendations of the Brazilian normative regarding constructive guidelines for each region, most buildings are based on a standardized project, which reaches minimum requirements about room size, constructive standard and comfort, for example, minimum window opening area based on floor area, presence of natural ventilation and floor slab in all classrooms (GRAÇA; KOWALTOWSKI; PETRECHE, 2007).

In the State of São Paulo, schools are regulated by the Foundation for the Development of Education – FDE and specific federal and state health regulations (FDE, 1997; SES-SP, 1994 *apud* GRAÇA; KOWALTOWSKI; PETRECHE, 2007). These standards provides cost reduction in the acquisition of materials and construction on a large scale and helps to solve high demand and insufficiency of Brazilian public schools. However, in most cases, the building project development does not include user participation, does not present environmental comfort as a starting point, design simulations and optimizations are not carried out and post-occupancy studies for performance evaluation are not frequent. As a reflection of

these factors, most schools experience heat discomfort throughout the year and especially in summer (GERALDI; GHISI, 2020), with records of more than 30°C of ambient temperature in the afternoon (GRAÇA; KOWALTOWSKI; PETRECHE, 2007), harming student's health and learning ability. Therefore, this is a crucial issue that needs to be improved in school buildings (GERALDI; GHISI, 2022b).

Due to climate variations, schools have different values of Energy Use Intensity – EUI (GERALDI; GHISI, 2020), which can be seen in Figure 21.

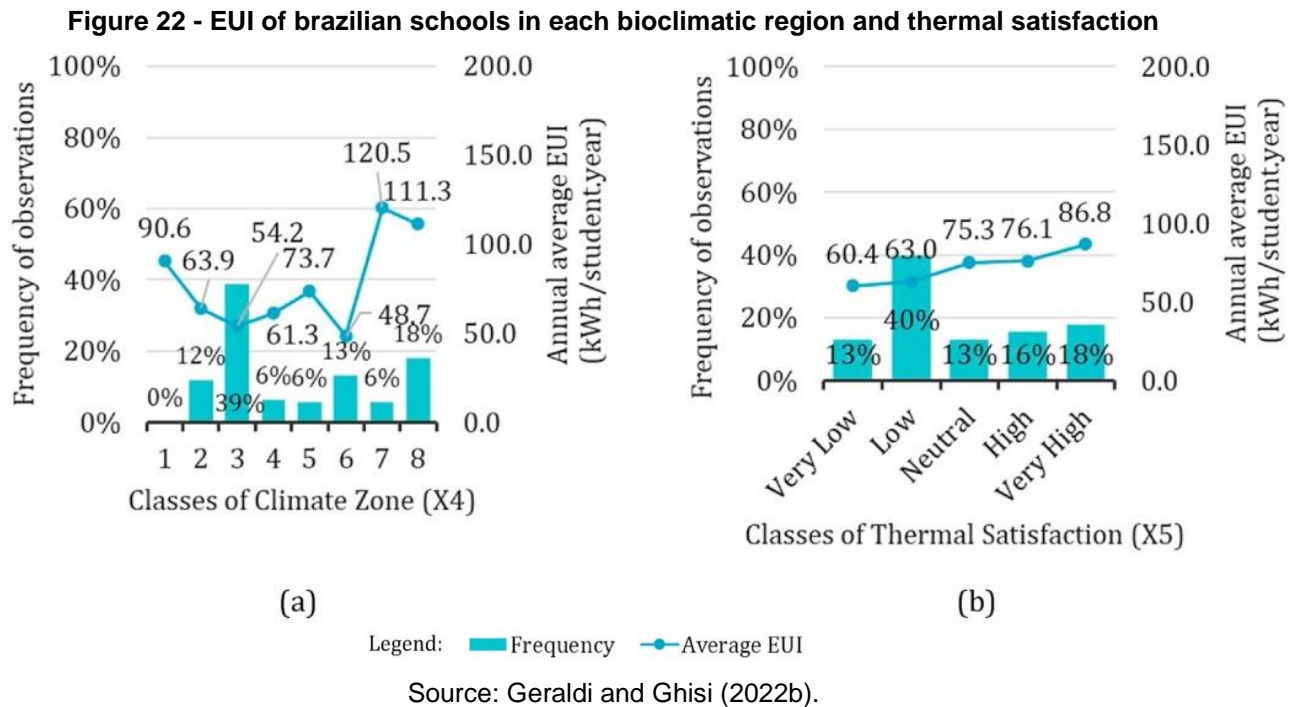
**Figure 21 - EUI of schools according to each bioclimatic zone in Brazil**



Source: Geraldi and Ghisi (2020).

The Figure 21 shows a higher average EUI in schools located in Zones 1, 7 and 8, probably due to greater needs for artificial internal climate control. However, none of the schools analyzed in previous studies have a space heating system (GERALDI; GHISI, 2020).

More recent studies (GERALDI; GHISI, 2022b) confirm the characteristic of higher average EUI of schools located in zones 7 and 8 (120.5 and 111.3 kWh/student.year respectively) than those located in other bioclimatic zones (Figure 23a). In this research, there is also an increase in thermal satisfaction in schools as the average EUI increases (Figure 23b), mainly due to artificial conditioning.

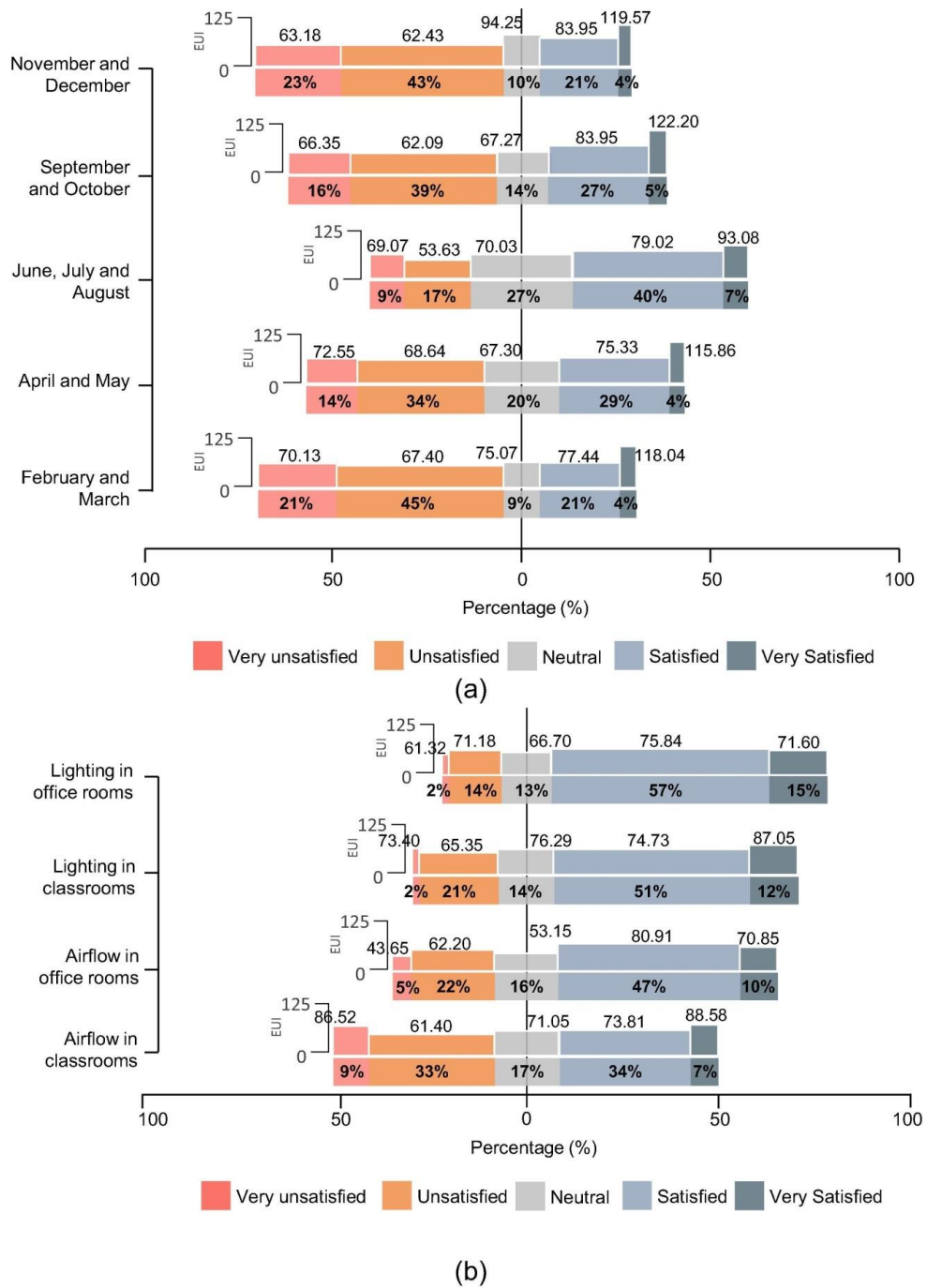


In Brazil, it is easier to obtain information on the number of students than on the built environment, therefore, the EUI indicator based on the number of students is more advantageous and reliable to represent the representative stock model than the one based on plant area (GERALDI; GHISI, 2020).

Based on a study of 416 Brazilian schools, the average EUI is 72 kWh/student.year and, in terms of planted area, 30.54 kWh/m<sup>2</sup>.year (GERALDI; GHISI, 2022b). These values are low when compared to EUIs from other more developed countries, but are similar to values from other schools in developing countries, such as the average EUI of a reference school in South Africa, which ranges from 10 to 24 kWh/m<sup>2</sup>.year (SAMUELS; BOOYSEN, 2019 *apud* GERALDI; GHISI, 2022a).

According to the results of the questionnaires applied by Geraldi and Ghisi (2020), there is a high dissatisfaction of users in relation to temperature, especially in the hottest months (February to April and October to December) and schools with higher levels of satisfaction have an EUI higher average for the use of air conditioning (Figure 23).

**Figure 23 - EUI versus environmental satisfaction with year-round temperature in classrooms (a) and lighting and airflow in office rooms and classrooms (b).**



Source: Geraldi and Ghisi (2020).

The variations in EUI, floor plan area, number of students and cooling capacity can be seen in Table 10.

**Table 10 - Characteristics of Brazilian public schools**

Variable Characteristics/unit	Classes	Average value
EUI log (kWh/student/year)	Very low	1.17
	Low	1.50
	Medium	1.70
	High	1.85
	Very high	2.18
Floor plan area (m <sup>2</sup> )	Small	734.31
	Medium	1554.35
	Great	2377.69
	Super big	3705.96
Occupation (Number of Students)	Small	298
	Medium	617
	Great	858
	Super big	1211
Cooling Capacity (BTU/h/m <sup>2</sup> )	Class 1	56.93
	Class 2	330.62
	Class 3	597.91
	Class 4	1246.39

Source : adapted from Geraldi and Ghisi (2022b).

In Brazilian public schools, the most common type of air conditioning is split (47%) (GERALDI; GHISI, 2022b) and its conditioned use happens predominantly outside the classroom: 49% in office or secretariat rooms and 50% in libraries or laboratories. Only 8% have air conditioning in the classrooms and 46.0% do not have any conditioning system (GERALDI; GHISI, 2020). Air-conditioned schools have an average annual EUI of up to 60% higher than others. The EUI varies according to annual temperature fluctuations, but there is a drop in energy use during the summer (January) and winter (July) vacation periods (GERALDI; GHISI, 2020). Those with lower EUI and apparently more efficient do not adequately provide thermal comfort conditions to users (GERALDI; GHISI, 2022b).

Currently, there is no significant use of air conditioning in Brazilian public schools, but there is a tendency to implement this air conditioning system over time, as seen worldwide in recent decades (ZHONG *et al.*, 2021 *apud* GERALDI; GHISI, 2022a) and even in developing countries (CHUNG; YEUNG, 2020 *apud* GERALDI; GHISI, 2022a). This context contradicts international guidelines for reducing energy consumption and mitigating the effects of climate change, such as the use of passive strategies and distributed generation of renewable energy (GERALDI; GHISI, 2022a), which should be explored in Brazilian public schools.

Due to the low use of air conditioning, lighting is the main end use of electricity in Brazilian public schools, as well as in similar buildings in developing countries

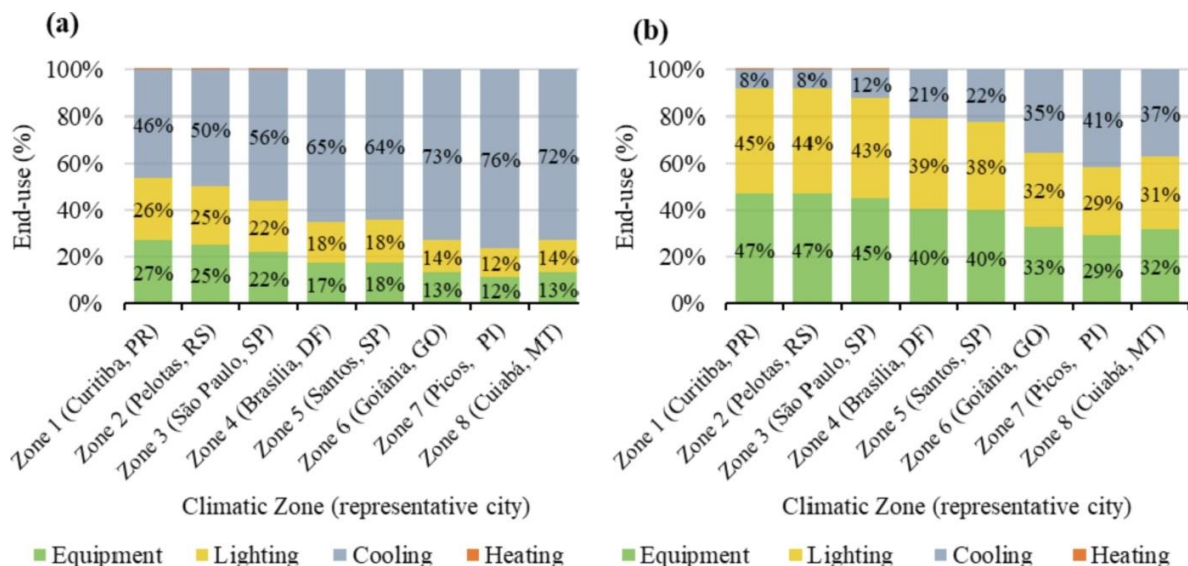
(SAMUELS; BOOYSEN, 2019 *apud* GERALDI; GHISI, 2022a). Regarding lighting in classrooms and offices, most schools have a high level of satisfaction (GERALDI; GHISI, 2020). However, lighting systems and equipment are inefficient, with old equipment and lack of planning and management in the implementation of new appliances (GERALDI; GHISI, 2022a).

The others end uses refer to computers, electronic equipment, water heating and cafeteria equipment (JOTA; SOUZA; SILVA, 2017). 15% of schools have electric showers, 85% do not have a water heating system and gas is used only for cooking (GERALDI; GHISI, 2022a).

Based on a decomposition of the average EUI from a benchmarking model of computer simulations, the typical end uses of Brazilian public schools in each bioclimatic zone can be seen in Figure 24.

The calculation of specific consumption (CS) involves usable area, number of school days, number of students, number of shifts, number of classrooms and number of classes (GERALDI; GHISI, 2022a).

**Figure 24 - Typical energy end uses for schools for each climate zone in Brazil. (a) End uses for schools with high air conditioning; (b) End uses for schools with low level of air conditioning**

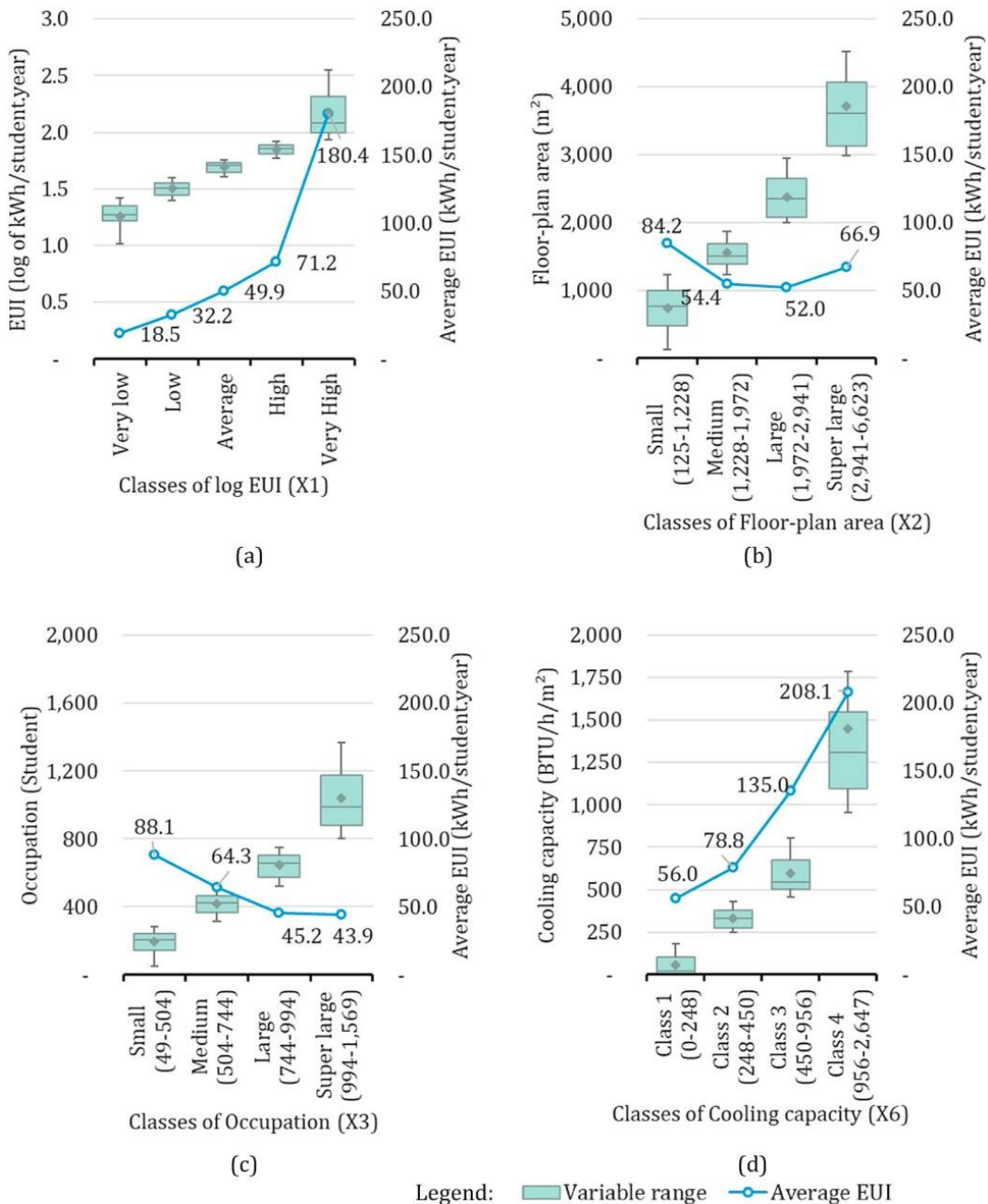


Source: Geraldi and Ghisi (2022a).

It is possible to observe in Figure 26b that small and super-large schools have a slightly larger EUI than the intermediate-sized ones. In Figure 26c, it can be seen that the EUI reduces with the increase in the number of students due to residual office

and refrigerator loads that do not depend on the size of the school or the number of students. In addition, the increase in installed cooling capacity reflects the increase in EUI (Figure 26d) (GERALDI ; GHISI, 2022b).

**Figure 25 - Discretisation and average EUI of (a) Log EUI, (b) Floor-plan area, (c) Occupation and (d) Cooling capacity**



Source: Geraldi and Ghisi (2022b).

The parameterizations used in energy simulation studies of the representative building stock of Brazilian public schools are summarized in Table 11.

However, it is noteworthy that the simulations of previous studies do not consider the surroundings (GERALDI; GHISI, 2022a).

**Table 11 - Parameters used in the simulations in previous studies**

<b>Aspect</b>	<b>Group</b>	<b>Medians</b>	<b>Unit</b>
Building size	Subspace area	Subspace 1: 604.0 Subspace 2: 67.7 Subspace 3: 50.3 Subspace 4: 84.8 Subspace 5: 190.0 Subspace 6: 61.8 Subspace 7: 31.0	m <sup>2</sup>
	Floor height	3.0	m
Envelope (outer wall)	Thermal Transmission	2.4	W/ m <sup>2</sup> .K
	Heat Capacity	240.0	J/ m <sup>2</sup> .K
	Thermal Absorption	0.7	%
	Thickness	20.0	cm
Envelope (inner wall)	Thermal Transmission	2.4	W/ m <sup>2</sup> .K
	Heat Capacity	240.0	J/ m <sup>2</sup> .K
	Thermal Absorption	0.7	%
	Thickness	20.0	cm
Envelope (roof)	Thermal Transmission	2.1	W/ m <sup>2</sup> .K
	Heat Capacity	238.0	J/ m <sup>2</sup> .K
	Thermal Absorption	0.7	%
	Thickness	1.3	cm
Envelope (glass)	Thermal Transmission	5.7	W/ m <sup>2</sup> .K
	Window Material	0.8	%
	Opening factor	0.5	%
Envelope (WWR)	Fenestration surface	Subspace 1: 0.4 Subspace 2: 0.4 Subspace 3: 0.4 Subspace 4: 0.4 Subspace 5: 1.0 Subspace 6: 0.2 Subspace 7: 0.2	%
Envelope (horizontal shading)	Shading	All subspaces: 0.8	m <sup>2</sup>
Envelope (vertical shading)	Shading	Subspace 1 to 4: 0.4 Subspace 5 to 7: 0.0	m <sup>2</sup>
Systems	Loads of Electrical Equipment	Subspace 1 : 21.2 Subspace 2 : 20.7 Subspace 3 : 99.4 Subspace 4 : 50.5 Subspace 5 to 7: 0.0	P/m <sup>2</sup>
	Lighting Loads	Subspace 1 : 12.5 Subspace 2: 9.0 Subspace 3: 9.0 Subspace 4: 9.7 Subspace 5: 5.5 Subspace 6: 5.0 Subspace 7: 15.5	P/m <sup>2</sup>
	Air Conditioning Load (HVAC)	68.0	%
	Water heater and thermal storage	0.0	W/W



Occupation	Density of People	Subspace 1: 0.5 Subspace 2: 4.0 Subspace 3 to 4: 7.0 Subspace 5 to 7: 0.0	People/ m <sup>2</sup>
------------	-------------------	--	---------------------------

Source: adapted from Geraldi and Ghisi (2022a).

The main aspects related to the comfort and the reach of ZEB or PEB were summarized in form of a SWOT analysis (strengths, weaknesses, opportunities and threats) (Table 12).

**Table 12 - SWOT analysis of the current stock of brazilian school buildings**

<b>Streghths</b>	<b>Source</b>	<b>Weaknesses</b>	<b>Source</b>
-	-	Most of schools were built between 1939 and 1990, before the current requirements for comfort and energy efficiency.	Geraldi and Ghisi (2020)
Standardization of building projects provides cost and helps to solve the insufficiency of Brazilian public schools in relation to demand.	Graça, Kowaltowski and Petreche (2007)	Standardized buildings does not consider the particularities of each bioclimatic zone.	Graça, Kowaltowski and Petreche (2007)
Brazilian public schools have a low EUI (72 kWh/student.year or 30.54 kWh/m <sup>2</sup> .year) because of low presence or air conditioning.	Geraldi and Ghisi (2020); Geraldi and Ghisi (2022a); Geraldi and Ghisi (2022b)	Most schools experience heat discomfort throughout the year and especially in summer.	Geraldi and Ghisi (2020)
Most schools have a high level of satisfaction regarding lighting in classrooms and offices.	Geraldi and Ghisi (2020)	Lighting systems and equipment are inefficient and old, with lack of planning and management in new appliances.	Geraldi and Ghisi (2022a)
<b>Opportunities</b>	<b>Source</b>	<b>Threats</b>	<b>Source</b>
Passive conditioning strategies (as cool materials) and renewable energy systems are strongly indicated for brazilian school buildings.	Geraldi and Ghisi (2022a)	There is a tendency to implement air conditioning system over time in brazilian public schools.	Geraldi and Ghisi (2022a)

Source: authors.

According to the information presented, public schools vary mainly by education level, size, geometric shape, use, occupation, facilities, user behavior, bioclimatic location and building age, which reflects in a variation in energetic performance. Most schools were built before the current regulations on thermal performance and follow a standardized project that can be presented in 7 different formats, with up to 7 types of composition.

Due to the predominant characteristic of high temperatures in Brazilian territory, there is a tendency to install air conditioning in school environments, but currently very few schools are artificially conditioned and have significant thermal dissatisfaction in hot

periods, therefore, passive conditioning strategies are strongly indicated for Brazilian public school buildings.

### **2.7. FNDE standard schools: Buildings characteristics**

The National Education Development Fund – FNDE is a federal autarchy created by law in 1969, responsible for providing technical assistance to all regions of Brazil and implementing educational policies of the Ministry of Education – MEC to guarantee quality public education (FNDE, n/d).

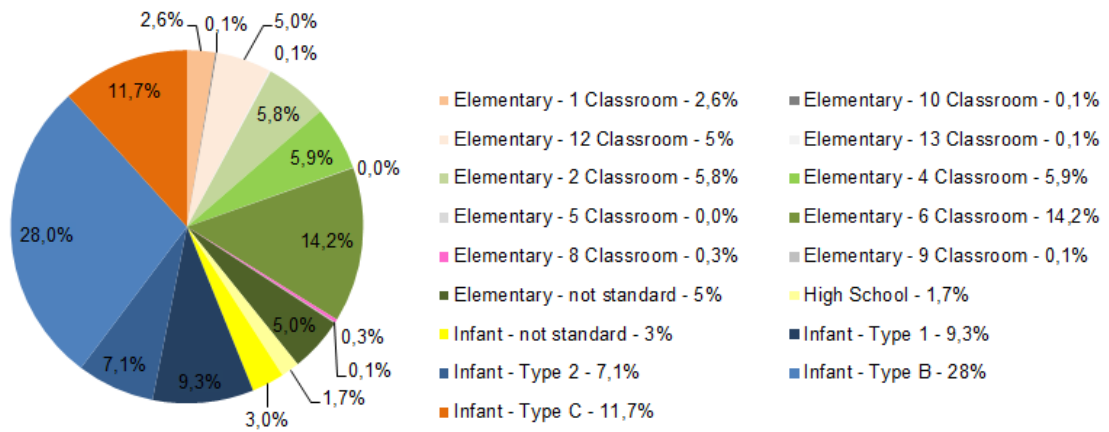
FNDE financial transfers are made through programs and agreements. The two programs currently in force that address the construction of schools are: National Program for Restructuring and Acquisition of Equipment for the Public School Network of Early Childhood Education – Proinfância and the Plan of Articulated Actions – PAR (FNDE, n/d).

Proinfância, created in 2007, works to improve the physical infrastructure of the early childhood education network with the development of two activities: a) acquisition of furniture and equipment; and b) construction of day care centers and preschools through technical and financial assistance from the FNDE with standardized architecture projects from the FNDE or own architecture projects prepared by the proponents (FNDE, n/d).

PAR, also created in 2007, offers technical and financial assistance for pedagogical actions and infrastructure development. The program covers basic education and specifically in terms of infrastructure, it operates in the expansion, construction and renovation of schools and school courts and in the acquisition of equipment (office, classrooms, kitchen and air conditioning), buses, bicycles, toys, musical instruments and furniture (FNDE, n/d).

Until 2022, the FNDE worked on the construction or renovation of 30,100 schools throughout Brazil through Proinfancia and PAR, with 26,420 multi-sports courts, 1,706 expansions, 1,974 retrofits and 15,860 complete school constructions (FNDE, n/d). Proinfancia focused on infant schools and PAR on elementary or high schools. The types of complete schools can be seen in Figure 26.

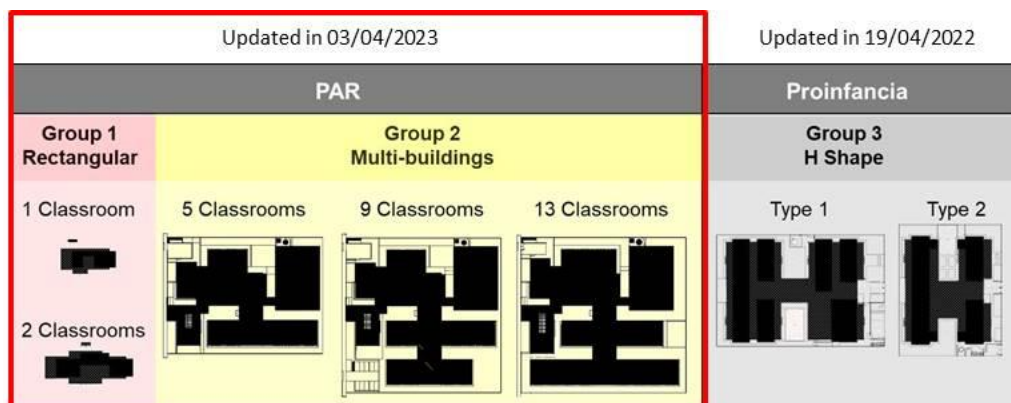
**Figure 26 - Types of schools financed by the FNDE until 2022**



Source: adapted from FNDE (n/d).

The schools with 4, 6, 8 and 12 classrooms in the PAR program and types B and C of Proinfância, despite representing a significant portion of the stock, were suspended and replaced by more update models. Currently there are 5 types of complete school projects from the PAR program and 2 types from the Proinfância program (7 models in total) that are still available to adaptation for future constructions. PAR schools with 1 and 2 classrooms are rectangular-shaped, those with 5, 9 and 13 classrooms are multi-buildings and the two Proinfância schools are H-shaped, therefore, based on shape, schools can be summarized into 3 groups (Figure 27 and Figure 28). These models are also differentiated by the level of schooling, student’s age, building size and number of students served (Table 13 and Table 14). The Proinfância schools are infant, with students from 0 to 6 years old, and the PAR models are intended for elementary and high school, with students from 7 to 17 years old (FNDE, n/d).

**Figure 27 - Shape of FNDE schools – PAR and Proinfancia**



Source: adapted from FNDE (n/a).

**Figure 28 - Perspectives of FNDE Schools**  
**Group 1 Rectangular: 1 Classroom**



**Group 2 Multi-buildings: 5 Classroom**



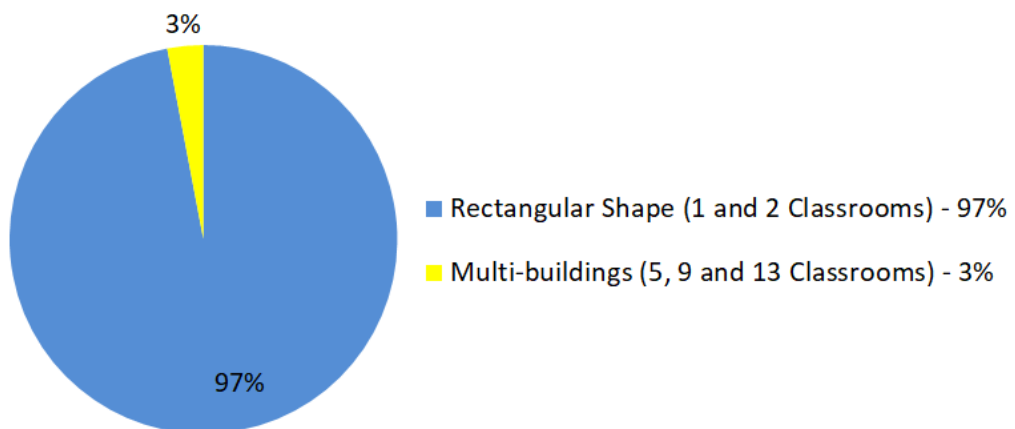
**Group 3 H Shape: Type 2**



Source: adapted from FNDE (n/a).

Among these architectural models of schools, those of the PAR program were the most recently updated (03/04/2023), and among them, the rectangular shape group is the most representative, accounting for 97% (Figure 29), and therefore, more relevant to this study.

**Figure 29 - Percentage of Rectangular and Multi-buildings Schools**



Source: adapted from FNDE (n/d).

**Table 13 - Areas of PAR-FNDE Standard Schools**

Subspace	Name	Floor plan area (m <sup>2</sup> )				
		1 classroom 60 students	2 classrooms 120 students	5 classrooms 350 students	9 Classrooms *630 students	13 classrooms 910 students
1	Classrooms	48.00	96.00	340.86	633.14	885.31
2	office rooms	11.70	12.60	105.71	105.71	112.76
3	kitchen	11.70	12.60	125.45	125.45	141.42
4	bathroom	6.56	8.10	93.05	108.85	140.40
5	aisles or Courtyard	23.59	58.12	174.16	350.74	254.64
6	Library	-	-	91.72	91.72	91.72
7	Computer or Multiuse lab	-	-	152.14	152.14	214.06
Total Built Area		101.55	187.42	1,083.09	1,567.75	1,840.31

\*The areas of 9 classrooms is an average between the 1-floor option and the 2-floor option.

Source: adapted from FNDE (n/d).

**Table 14 - Areas of Proinfancia-FNDE Standard Schools**

Subspace	Name	Floor plan area (m <sup>2</sup> )	
		Type 1 376 children	type 2 188 children
1	Classrooms	356.24	178.12
2	office rooms	62.13	35.4
3	kitchen	176.69	75.82
4	bathroom	110.18	75.55
5	aisles	513.09	366.05
6	Library	-	-
7	Computer or Multiuse lab	38.40	38.40
Total		1,256.73	769.34

Source: adapted from FNDE (n/d).

PAR schools have classrooms with very similar sizes (approximately 60m<sup>2</sup>), with 30 students each per shift (morning and afternoon). Proinfância schools have smaller classrooms, measuring around 35m<sup>2</sup> that can accommodate up to 20 students. The classrooms in all models are usually positioned next to each other, have the same solar orientation and are accessed through a covered patio or corridor. The FNDE recommends predominantly north-south orientation to provide more comfort to users (FNDE, n/d).

In schools with 1 and 2 classrooms, the bathrooms are next to the kitchen, just like the models studied by Geraldi and Ghisi (2020). In other larger models, however, there is a subdivision of the school by blocks of activity (office, classrooms, kitchen). The schools with 5 and 9 classrooms are very similar to each other, with the same office and cafeteria areas, differing only in the number of classrooms. The 13-

classroom school, in addition to the largest number of classrooms, has office areas, kitchens and multipurpose rooms that are slightly larger than the other two models.

Like PAR, Proinfância schools are subdivided into activity blocks, but have a higher percentage of kitchen areas than the PAR ones due to specific needs such as milk station, breastfeeding area, linen and laundry.

All PAR and Proinfância buildings have very similar technical and constructive characteristics, such as envelope materials, partitions, internal and external finishes and lighting equipment. The building materials of classrooms and their respective thermal and physical properties are described in Table 15. The thermal transmittance (U) data of the materials were based on Maciel *et al.* (2021) and in the library of Brazilian constructive components of the Laboratory of Energy Efficiency in Buildings – LabEEE (WEBER *et al.*, 2017), the reflectivities (R) of the paints were based on Dornelles (2008) and ABNT NBR 15220-2 (ABNT, 2005a). The emissivity ( $\epsilon$ ) of all materials described is 90% on average (ABNT, 2005a).

**Table 15 - Building Materials – FNDE Standard schools**

Building element	Description	U (W/m <sup>2</sup> .K)	R (%)
External walls	<b>1 and 2 Classrooms:</b> - Ceramic block 9x19x39cm - mortar 2.5cm each side - paint color ice white	2.37	60
	<b>5, 9, 13 Classrooms:</b> - Ceramic block 14x19x39cm - mortar 2.5cm each side - paint color light gray	1.83	40
	<b>Type 1 and 2:</b> - Ceramic block 14x19x39cm - mortar 2.5cm each side - paint color ice white	1.83	60
Internal walls	- Ceramic block 9x19x39cm - mortar 2.5cm each side - paint color light yellow	2.37	70
Roof	<b>1 and 2 Classrooms:</b> - Ceramic tile - Concrete slab 15cm	2.05	35
	<b>5, 9, 13 Classrooms:</b> - Metallic thermoacoustic tile (PIR filling) - Plaster ceiling	0.32	90

Internal Floor	<b>1 and 2 Classrooms and Type 1 and 2 (in Office):</b> - Ceramic floor 3cm - mortar 2cm - Concrete slab 10cm	3.20	40
	<b>5, 9, 13 Classrooms:</b> - Granitine floor 2cm - mortar 3cm - Concrete slab 10cm	3.20	60
	<b>Type 1 and 2 (in Classroom):</b> - Vinyl floor 2mm - mortar 2cm - Concrete slab 10cm	4.61	40*
External floor	- Concrete slab 10cm	3.74	40
Glazing	- simple transparent glass (SHGC = 89%)	5.70	-

\* Variable depending on surface color and/or material.

Source: adapted from FNDE (n/d).

In the standardized projects, some passive strategies mentioned in ABNT (2005a) were adopted, which avoid excessive heat gain and provide losses (Table 16).

**Table 16 - Characteristics of Standard Schools in relation to ABNT parameters (2005a)**

ABNT parameters	1 Class	2 Class	5 Class	9 Class	13 Class	Type 1	type 2
external wall	Light reflecting	Light reflecting	thermal mass***	thermal mass***	thermal mass***	thermal mass***	thermal mass***
Internal wall	Light reflecting	Light reflecting	Light reflecting	Light reflecting	Light reflecting	Light reflecting	Light reflecting
Roof	light	light	light insulated	light insulated	light insulated	light insulated	light insulated
window shading	overhang	overhang	Overhang Screen *sidefin	Overhang Screen *sidefin	Overhang Screen *sidefin	Overhang*	Overhang*
summer strategy	*Cross ventilation	*Cross ventilation	**Cross ventilation	**Cross ventilation	**Cross ventilation	cross ventilation	cross ventilation
winter strategy	passive solar heating	passive solar heating	-	-	-	-	-

\*Only used in classrooms.

\*\*Used in classrooms and part of office rooms.

\*\*\*Wall material meets normative thermal transmittance parameters, but does not fit in thermal mass when considering thermal delay in hours.

Source: adapted from FNDE (n/d).

Regarding artificial air conditioning, the FNDE projects consider wall fans in occupied rooms such as the secretariat, coordination, teacher's room, direction, pantry, cafeteria, library, multipurpose room and classroom. Split air conditioning equipment is also proposed in some rooms in schools with 5, 9 and 13 classrooms (PAR) and in schools type 1 and type 2 (Proinfância) according to Table 17.

**Table 17 - Type of artificial conditioning system proposed by the FNDE in standardized projects**

conditioning type	1 Class	2 Class	5 Class	9 Class	13 Class	Type 1	type 2
Wall fan	office Classroom	office Classroom	office kitchen Library multiuse Classroom	office kitchen Library multiuse Classroom	office Kitchen Library multiuse Classroom	office Kitchen multiuse Classroom	office Kitchen multiuse Classroom
Split 9,000 BTU/h	-	-	-	-	-	secretary and direction	secretary and direction
Split 12,000 BTU/h	-	-	coordinator and Direction	coordinator and Direction	Coord., Direction and Orientation	-	-
Split 22,000 BTU/h	-	-	Secretary and multifunction resources	Secretary and multifunction resources	multifunction resources	teachers room	teachers room
Split 30,000 BTU/h	-	-	Teachers room, library, multiuse and classroom	Teachers room, library, multiuse and classroom	Teachers room, library, multiuse and classroom	multiuse	multiuse

Source: adapted from FNDE (n/d).

Lighting slightly varies between schools. Schools with 1 and 2 classrooms in the PAR program and type 1 and 2 in Proinfância use fluorescent lamps and the others PAR schools use LED lamps, which are more efficient. The installed lighting power in each school model is exposed in Table 18.

**Table 18 - Installed lighting power**

Subspace	Installed lighting power (W)						
	1 Class	2 Class	5 Class	9 Class**	13 Class	Type 1	type 2
Classrooms	384	768	1,395	1,987	3,627	1,728	1,080
office rooms	64	64	434	434	558	198	144
kitchen	64	64	533	533	547	864	342
bathroom	32	32	334	466.5	712	630	342
aisles	128	192	2,563*	2,868.5*	2,776*	2.072	1,476
Library	-	-	372	372	372	-	-
Computer or Multiuse lab	-	-	465	465	651	216	216
<b>Total</b>	672	1,120	6,096	7,126	9,243	2,298	3,600

\*Significantly higher values for multi-sport court lighting;

\*\*Average values between school 9 classrooms on the ground floor and 2 floors.

Source: adapted from FNDE (n/d).

The consumption in kWh of lighting in schools can be easily calculated since the powers are cited in the electrical project and artificial lighting is generally used throughout the school's operating period (morning and afternoon from Monday to Friday, except holiday periods). On the other hand, electrical equipments are



mentioned in the projects but without power information, which makes it difficult to predict energy consumption. Due to this lack of equipment information, this thesis considers power density used in previous simulations of Brazilian public schools described in Table 19.

**Table 19 - Electrical Equipment Power Density**

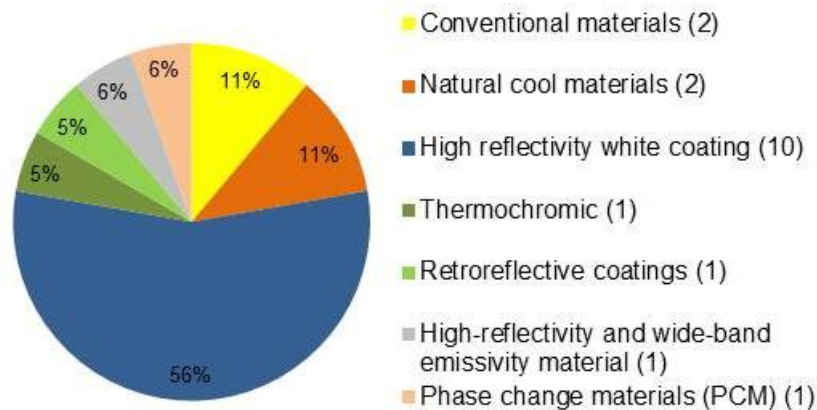
Subspace	Name	Electrical Equipment Power Density (W/m <sup>2</sup> )	Source
1	Classrooms	5.0	Lopes (2022)
2	Library	20.7	Geraldi and Ghisi (2022a)
3	Computer lab	99.4	
4	Office Rooms	50.5	
5	Aisles	0.0	
6	Bathroom	0.0	
7	Kitchen	0.0	

The information presented in this section, therefore, provides the entire database to calculate the energy consumption and to run the thermoenergetic simulations of the standardized schools of the FNDE.

## 2.8. Computer Simulation of Cool Materials

The materials evaluated in the publications can be seen in Figure 30. Seven of the ten studies address more than one material for performance comparison (FENG *et al.*, 2021; CASTALDO *et al.*, 2018; LASSANDRO; TURI; ZACCARO, 2019; LASSANDRO; TURI, 2017, BANIASSADI; SAILOR; BAN-WEISS, 2019; ASCIONE *et al.*, 2018; BERARDI; GARAI; MORSELLI, 2020).

**Figure 30 - Materials evaluated in computer simulations**



Source: authors.

White coatings of high reflectivity are the most studied. Often, these materials are compared to conventional materials (the second most present option in the studies), which are the most commonly found in buildings and cities today. Natural cool materials are frequent in research, mainly because they are an option that is easily applicable in urban environments. The other less recurrent, but no less relevant, cool materials are more recent, used mainly after 2011 (SANTAMOURIS; YUN, 2020). These materials were evaluated in several cities with different climatic contexts, which can be seen in Table 20.

**Table 20 - Evaluated cool materials and respective climatic contexts considered on computer simulations**

<b>Material</b>	<b>City</b>	<b>Climate context</b>	<b>Source</b>
Retroreflective coatings	Oslo (Norway)	Humid continental climate with warm summers and very cold winters	Manni <i>et al.</i> (2019)
	Milan (Italy)	Subtropical climate with hot and humid summers and cold winters	
	Cairo (Egypt)	Climate with hot days and cool nights year round	
High reflectivity white coating	Sydney (Australia)	Humid subtropical climate with cold winters and mild summers	Feng <i>et al.</i> (2022)
	Alice Springs (Australia)	Climate with hot summer and cold winter	
	Darwin (Australia)	Climate with similar average year-round maximum temperature	
High reflectivity white coating; High-reflectivity and wide-band emissivity material	Kolkata (India)	Hot and humid tropical climate	Feng <i>et al.</i> (2021)
Natural cool materials; High reflectivity white coating	Rimini (Central Italy)	Temperate climate with hot summers and cold winters	Castaldo <i>et al.</i> (2018)
Natural cool materials; High reflectivity white coating	Bari (Italy)	Mediterranean temperate climate with hot summers and cold winters	Lassandro, Turi and Zaccaro (2019)
Phase change material; High reflectivity white coating	Bari (Italy)	Mediterranean temperate climate with hot summers and cold winters	Lassander and Turi (2017)
	Athens (Greece)	Temperate climate with hot, dry summers and cold, rainy winters	
	Thunis (Greece)	Temperate climate with hot, dry summers and cold winters	
High reflectivity white coating	Acharnes (Greece)	Climate with hot summers and dry winters	Kolokotsa <i>et al.</i> (2018)
Conventional material; High reflectivity white coating	Albuquerque (USA)	Climate with hot summer and cold winter	Baniassadi, Sailor and Ban-Weiss (2019)
	Atlanta (USA)	Humid subtropical climate with hot summers and cold winters	
	Chicago (USA)	Continental climate with warm summers and cold winters	

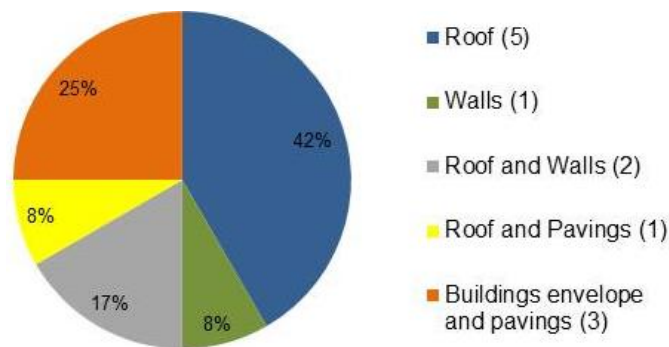
	Houston (USA)	Humid subtropical climate with hot summers and mild winters	
	Los Angeles (USA)	Subtropical climate with hot, dry summers and cold winters	
	Miami (USA)	Tropical Monsoon Climate with hot and humid summer and winter	
	Philadelphia (USA)	Humid Subtropical Climate with hot and humid summers and very cold winters	
	Phoenix (USA)	Tropical and Subtropical Desert Climate with hot, dry summers and mild, dry winters	
Conventional material; High reflectivity white coating	Lisbon, Portugal)	Mediterranean climate with mild and rainy winters and warm to hot, dry summers	Ascione <i>et al.</i> (2018)
	Seville (Spain)	Subtropical climate with hot, dry summers and cold winters	
	Naples (Italy)	Climate with slightly cold and rainy winters and hot summers	
	Athens (Greece)	Temperate climate with hot, dry summers and cold, rainy winters	
Conventional material; High reflectivity white coating; thermochromic	Toronto (Canada)	Temperate continental climate, with hot and humid summers and very cold and dry winters	Berardi, Garai and Morselli (2020)

Source: authors.

Only two of the 23 cities mentioned have a tropical climate (Darwin in Australia and Calcutta in India) and no research cites the Brazilian context.

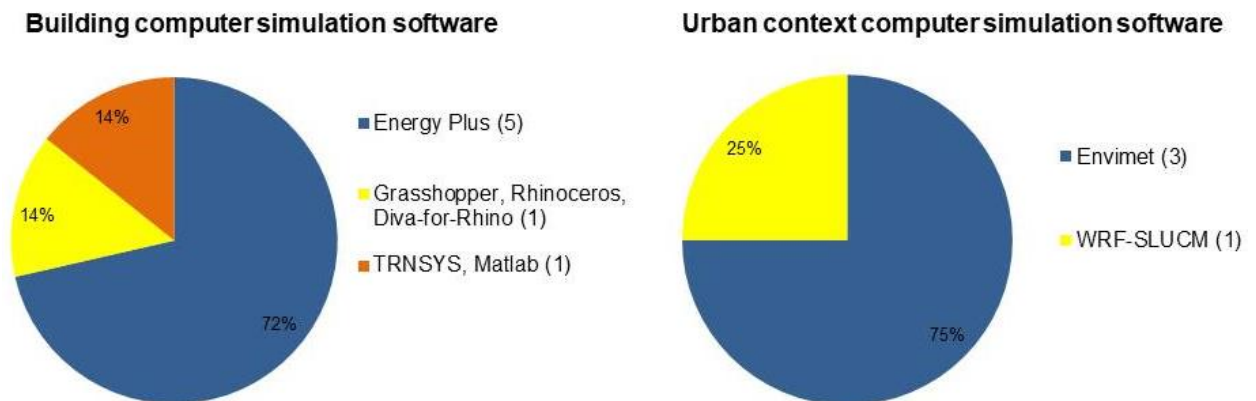
The study of the influence of cool materials only on the performance of buildings is the most frequent, since it is present in 5 of the 10 articles (50%), followed by the evaluation of the effect of materials on the building and in the urban context simultaneously, representing 3 of the 10 publications (30%). Only 2 studies evaluated the consequences of cool materials only in the urban context (20%). It is likely that this proportion is due to the more significant results of building cooling and reduced energy consumption when cool materials are applied directly to buildings.

As shown in Figure 31, the hypothesis of applying cool materials on the roof is the most recurrent (42%), since they are the surfaces with the greatest exposure to solar radiation and the least possibility of shading by neighboring buildings. The application of these solutions on the building envelope and on pavements simultaneously is the second most frequent solution (25%), as it allows the potentiated effect of cooling the urban context and buildings, as well as a significant reduction in energy consumption.

**Figure 31 - Place of application of cool materials**

Source: authors.

As shown in Figure 32, the most used software for assessing the energy performance of buildings is EnergyPlus, present in 5 of the 7 studies (LASSANDRO; TURI, 2017; KOLOKOTSA *et al.*, 2018; BANIASSADI; SAILOR; BAN-WEISS, 2019; ASCIONE *et al.*, 2018; BERARDI; GARAI; MORSELLI, 2020).

**Figure 32 - Most used softwares cor computer simulations**

Source: authors.

Lassandro and Turi (2017) used the graphical interface of DesignBuilder associated with EnergyPlus to facilitate the development of the building model. Of the studies focused on buildings, only Berardi, Garai and Morselli (2020) modeled and evaluated the influence of surrounding buildings on the object of study, using the Energy Management System (EMS) and Open Street Map tools. In this case, the adaptation of the final weather files was performed with WeatherShift.

As an alternative to EnergyPlus, Feng *et al.* (2022) also present the TRNSYS to obtain energy balance data. Manni *et al.* (2019) analyzes the effects of retroreflective materials on buildings and in the urban context. Due to the specific reflection behavior of this type of coating, which differs from other cool materials, a combination of three different softwares was used: Grasshopper, Rhinoceros, Diva-for-Rhino.

EnergyPlus, which is the most used software in the studies of cool materials in buildings, stands out for dynamically solving the mass and energy balance of all environments in a building in response to external conditions, internal loads and occupant behavior, representing precisely heat transfer phenomena on external surfaces (BANIASSADI; SAILOR; BAN-WEISS, 2019). However, this tool does not allow the insertion of data on the spectral variation of emissivity of cool materials, present mainly in spectrally selective materials, which can cause errors in the calculation of surface temperature and sensible heat flux (BANIASSADI; SAILOR; BAN-WEISS, 2019).

In simulations focusing on the evaluation of the cooling effects of materials in the urban context, the most used software is Envimet (CASTALDO *et al.*, 2018; LASSANDRO; TURI; ZACCARO, 2019; KOLOKOTSA *et al.*, 2018). WRF-SLUCM was used in the studies by Feng *et al.* (2022) and works similarly to Envimet.

Envimet is a holistic modeling software, based on Navier-Stokes equations and fluid-dynamic analysis (BRUSE; FLEER, 1998 *apud* LASSANDRO; TURI; ZACCARO, 2019) to simulate urban microclimate (TIAN *et al.*, 2021) and surface-plant-air interactions (LASSANDRO; TURI; ZACCARO, 2019). Envimet generally uses simplified numerical models with low spatial resolution (BATISTA; DE LIETO VOLLARO; ZINZI, 2021; WANG; BERARDI; AKBARI, 2015 *apud* TIAN *et al.*, 2021), but like other simulation tools, it provides data that allow comparison analysis of different scenarios. It is also noteworthy that the scale and complexity of the urban environment are represented in a simplified way in the simulation models, and therefore, the validation of the simulations is essential (TOPARLAR *et al.*, 2015 *apud* TIAN *et al.*, 2021).

In building performance simulation software (EnergyPlus and TRNSYS), the input are climate and building data, which significantly influence heat transfers and the building's heating and cooling demands: weather conditions (ambient temperature

and relative humidity, solar radiation), casual heat gain (the number of occupants, computers, equipment, lighting and air conditioning) and building characteristics (building/conditioned area, gross wall/roof area, number of thermal zones, number of conditioned zones, internal and external shading coefficients, reflectivity, emissivity, absorbance and heat transfer of the envelope, internal and external convection transfer rate and infiltration) (HUANG P.; HUANG G.; SUN, 2019; CASTALDO *et al.*, 2018; KOLOKOTSA *et al.*, 2018; BANIASSADI; SAILOR; BAN-WEISS, 2018; ASCIONE *et al.*, 2018; BERARDI; GARAI; MORSELLI, 2020).

In the urban context simulation software (ENVIMET and WRF-SLUCM), the input data are the climatic conditions, the volumetric model of the urban environment and the properties of surface coatings (CASTALDO *et al.*, 2018; LASSANDRO; TURI; ZACCARO, 2019; KOLOKOTSA *et al.*, 2018; FENG *et al.*, 2022), which influence in local climatic conditions.

The climate data entered in simulations are usually typical meteorological year files (TMY) with data from official government agencies (BERARDI; GARAI, MORSELLI, 2020; BANIASSADI; SAILOR; BAN-WEISS, 2019; KOLOKOTSA *et al.*, 2018). Castaldo *et al.* (2018) used meteorological files based on urban context mitigation scenarios, formatted by the Meteororm software. Some studies perform simulations in more than one city, with different climate configurations, for comparative analysis (LASSANDRO; TURI, 2017; BANIASSADI; SAILOR; BAN-WEISS, 2019; ASCIONE *et al.*, 2018). Air or surface temperature measurement data can also be used as boundary conditions in computer simulation calculations to compare measured data and optimization of the research process (LIU; NIU; XIA, 2017 *apud* TIAN *et al.*, 2021).

The main information obtained from building simulations are energy data of buildings, expressed in primary energy (in % or kWh/year) and energy needs for heating and cooling (FENG *et al.*, 2022; LASSANDRO; TURI, 2017; BANIASSADI; SAILOR; BAN-WEISS, 2019; ASCIONE *et al.*, 2018; BERARDI; GARAI; MORSELLI, 2020) to evaluate constructive strategies and verify the achievement of zero or positive energy balance.

In urban context simulations, the output information is related to the climate context (surface temperatures, air temperature, wind speed and direction, relative air

humidity and pressure) (CASTALDO *et al.*, 2018; LASSANDRO; TURI; ZACCARO, 2019; KOLOKOTSA *et al.*, 2018; FENG *et al.*, 2022), variables which influence comfort conditions. These results allow to identify heat or cool island phenomena and to compare intervention and mitigation solutions in the urban environment, such as natural solutions (vegetation and water bodies) or coatings on urban surfaces (paving and buildings).

The stages of carrying out the research are structured in a similar way in the studies:

1. Modeling of the object of study;
2. Collection and organization of information to insert into computer simulation software;
3. Simulation of one or more scenarios;
4. Analysis of results, comparison between the baseline scenario and the scenario with new proposals and energy performance assessment (in the case of building studies);

Step number 1 in urban context simulations is similar in all studies, since it is necessary to insert a file with the volumetry of the surroundings in the simulation software. In building simulations with EnergyPlus, which is more frequent in studies, it is only possible to entry data (KOLOKOTSA *et al.*, 2018; BANIASSADI; SAILOR; BAN-WEISS, 2019; ASCIONE *et al.*, 2018). A graphic modeling can be done with DesignBuilder as an auxiliary strategy (LASSANDRO; TURI, 2017). When there is a goal to evaluate the effects of adjacent buildings on the performance of the study object, the surrounding is also modeled (BERARDI; GARAI; MORSELLI, 2020).

Step number 2, collecting and organizing information, can be done virtually, using official data (BERARDI; GARAI, MORSELLI, 2020; BANIASSADI; SAILOR; BAN-WEISS, 2019; KOLOKOTSA *et al.*, 2018), or it may include on-site data measurement (TIAN *et al.*, 2021). Data on reflectivity, emissivity and absorbance of materials can be obtained by previous physical tests (MANNI *et al.*, 2019; FENG *et al.*, 2021; BANIASSADI; SAILOR; BAN-WEISS, 2019).

Step number 3 usually considers the simulation of the current scenario and at least 1 intervention scenario. In the intervention scenario, some parameters can be fixed equally to the reference scenarios, to assess the impact of some specific variables on the final results (MANNI *et al.*, 2019; FENG *et al.*, 2022; FENG *et al.*, 2021; LASSANDRO; TURI; ZACCARO, 2019; LASSANDRO; TURI, 2017; KOLOKOTSA *et al.*, 2018; BANIASSADI; SAILOR; BAN-WEISS, 2019; ASCIONE *et al.*, 2018; (BERARDI; GARAI, MORSELLI, 2020).

Step number 4 may involve only the comparison between the scenarios, or it may be complemented with other analysis: calculation of net energy cost savings (\$/year) and net avoided CO<sub>2</sub> emission (kgCO<sub>2</sub>/year) (BANIASSADI; SAILOR; BAN-WEISS, 2019), comparison of simulation results with on-site experiment results (KOLOKOTSA *et al.*, 2018), assessment of comfort in buildings (CASTALDO *et al.*, 2018), identification of guidelines for the best intervention strategies (LASSANDRO; TURI; ZACCARO, 2019) and future climate change impact predictions (BERARDI; GARAI; MORSELLI, 2020).

Castaldo *et al.* (2018) and Kolokotsa *et al.* (2018) apply steps 1 to 4 first for the urban context and then repeat the process for buildings. The prior assessment of interventions in the urban context allows the alteration of microclimatic data and the prior reduction of energy consumption needs for cooling the building.

The exposed publications show relevant information about the methods of computer simulations, therefore, they are used as a methodological reference for this thesis.

## **2.9. Building Thermoenergetic Optimization**

Building design involves not only the compatibility between nature and construction, but also the conciliation of numerous variables that characterize the complex system of a building (NIMLYAT; DASSAH; ALLU, 2014 *apud* MACIEL *et al.*, 2021). Given these complexities, optimizing the design and construction of buildings involves strategies that enable the greatest possible functionality and energy efficiency (NGUYEN *et al.*, 2014 *apud* VUKADINOVIC *et al.*, 2021)



Building energy optimization, therefore, is a methodology for finding the optimal solution for a building (ASCIONE *et al.*, 2019a; HONG; KIM; LEE, 2019; BRE; ROMAN; FACHINOTTI, 2020; CHEN *et al.*, 2021) according to one or more criteria (ASCIONE *et al.*, 2020; SALATA *et al.*, 2020; ZHAO; DU, 2020).

Building performance optimization studies (for new or retrofit constructions) have been widely applied worldwide, in different climatic and architectural contexts, such as: in several cities in Italy in residential (ASCIONE *et al.*, 2019a), commercial (ASCIONE *et al.*, 2019b) and industrial (ASCIONE *et al.*, 2020); in Seoul, South Korea, an East Asian monsoon climate region in a university library (HONG; KIM; LEE, 2019); in 4 different climates in Brazil in a commercial building (ZEMERO *et al.*, 2019); in a city in Brazil in a school building (MACIEL *et al.*, 2021); in six climates of Iran in office building (NADERI *et al.*, 2020), in 5 different cities in standardized residential block (BAGHOOLIZADEH *et al.*, 2021) and a typical residential building (BAGHERI-ESEF; DEGHAN, 2022); in Mediterranean climate in Kermanshah in Iran in office building (GHADERIAN; VEYSI, 2021), in moderate climate of Tehran city in residential building (BAGHERI-ESFEH; SAFIKHANI; MOTAHAR, 2020; MOSTAFAZADEH; EIRDMOUSA; TAVAKOLAN, 2023), in single-family residential building (TAVAKOLAN *et al.*, 2022) and in office buildings (BAGHOOLIZADEH *et al.*, 2023); in Argentina in standardized residential models (BRE; ROMAN; FACHINOTTI, 2020); in hot summer Mediterranean climate in Athens Greece in office building (GIOURI; TENPIERIK; TURRIN, 2020); 19 cities located from northern to southern Europe in low-density residential buildings (SALATA *et al.*, 2020); in Hohhot in China in a high-rise office typical building (ZHAO; DU, 2020); in China in a teaching building at a University (CHEN *et al.*, 2021), in Qingdao in a gymnasium (YUE *et al.*, 2021); in Nanchang, in middle and primary school (WANG, Y.; YANG; WANG, Q., 2022); in Hunan, in traditional buildings in a village (XIE *et al.*, 2022); in six climate zones in Australia in prefabricated houses (NAJU; AYE; NOGUCHI, 2021); in Niš, Serbia, (Cfa climate) in generic building (VUKADINOVIC *et al.*, 2021) ; in Paris, France, in a multiple social housing buildings (MERLET *et al.*, 2022); in Assam, North-East of India, with hot and humid summer, in a vernacular house (GUPTA; CHANDA; BISWAS, 2023).

Table 21 presents the summary of the main information on the purpose of several studies, software used, optimization objectives, variables and methodological steps.

Table 21 - Summary of optimization studies

Source	study Purpose	Software	Objectives	Variables	Methodology Steps
Ascione <i>et al.</i> (2019a)	Design optimization of a new typical Italian residential building considering Four typical Italian climates	MATLAB, DesignBuilder and EnergyPlus	Reduce primary energy consumption , energy-related global cost and discomfort hours over occupied hours	set point temperatures, radiative and thermo-physical properties of envelope, window type, building orientation	<ol style="list-style-type: none"> <li>1. Building modeling</li> <li>2. Choice of variables by initial optimization</li> <li>3. Building energy simulation</li> <li>4. Optimization</li> <li>5. Comparison of results</li> <li>6. Repetition of steps 3, 4 and 5</li> </ol> Synthesis of the final solution
Ascione <i>et al.</i> (2019b)	Optimization of a typical Italian office in Milan (north of Italy).	MATLAB, DesignBuilder and EnergyPlus	Reduce annual thermal energy demand, electrical energy demand and percentage of discomfort hours over occupied hours	Geometry (orientation, window-to-wall relationship), HVAC (heating and cooling setpoint temperature) and envelope (thermo-physical properties, window type )	<ol style="list-style-type: none"> <li>1. Execution of a genetic algorithm to achieve multi-objective optimization of design variables;</li> <li>2. Sampling of design scenarios to find optimal combinations between solutions;</li> <li>3. Final design solutions recommended according to different selection criteria.</li> </ol>
Hong, Kim and Lee (2019)	Optimization of the Yonsei University library facility located in Seoul, South Korea, an East Asian monsoon climate region	EnergyPlus	thermal energy consumption and life cycle economic-environmental values	<b>Variables:</b> window type, heating/cooling set point, ventilation/window opening type; <b>Constraints:</b> minimum IEQ level acceptance, maximum budget limit	<ol style="list-style-type: none"> <li>1. development of the basic energy model and building design scenarios;</li> <li>2. calculation of the target variables;</li> <li>3. generation of a multi-objective optimization model using an NSGA-II algorithm</li> </ol>
Zemero <i>et al.</i> (2019)	Optimization of a schematic design of a commercial building simulated for four different Brazilian weathers	EnergyPlus	find optimal solutions (OSs) with the lowest constructive cost associated with greater energy efficiency	<b>Variables:</b> orientation, walls, roof, floors and shadings, building shape <b>Constraints:</b> physical, legal and financial	<ol style="list-style-type: none"> <li>1. Formulation of the Optimization Problem</li> <li>2. Definition of objectives and variables;</li> <li>3. Building modeling;</li> <li>4. Optimization studies;</li> <li>5. Results analysis</li> </ol>
Ascione <i>et al.</i> (2020)	A tailored approach to optimize energy retrofit of an existing industrial building located in South Italy	MATLAB, DesignBuilder and EnergyPlus	Minimizing primary energy consumption and global cost	windows , solar screens, heat recovery, optimization of HVAC operation and installation of photovoltaics of different sizes	<ol style="list-style-type: none"> <li>1. Energy audit and characterization of the building (user analysis, collection of architectural and energy data of the building);</li> <li>2. Building modeling (location, envelope, activity and usage schedule);</li> <li>3. Model calibration (comparison with real measurements, evaluation and correction);</li> <li>4. Optimization ;</li> </ol>
Bagheri-Esfeh, Safikhani and Motahar	Optimization of PCM layer for a residential building in	EnergyPlus	Minimize cooling and heating loads	melting temperature and thickness of PCM, thermal	<ol style="list-style-type: none"> <li>1. Calculation of the values of objective functions and to neural network training;</li> <li>2. Application of GMDH-type</li> </ol>

(2020)	Tehran (Iran) with a moderate climate			resistance of exterior walls, internal gain and infiltration rate	neural network and obtaining of Pareto optimal points for objective functions; 3. Determination of optimum point by a financial analysis
Bre, Roman and Fachinotti (2020)	Optimization of a typical single-family house, with a typical design of the massive credit program ProCreAr supported by the Argentine national government.	EnergyPlus	optimize energy efficiency and thermal comfort	Building azimuth, window shading, external walls solar absorptivity, doors and Windows infiltration rate, window ventilation area and envelope materials	1. Obtaining a representative sample of entries; 2. Metamodel validation; 3. Evaluation of compliance with the criteria and adjustment of samples if necessary; 4. Optimization studies;
Giouri, Tenpierik and Turrin (2020)	Testing in a typical high-rise, open-plan central office building for the hot summer Mediterranean climate (Csa) of Athens, Greece	DesignBuilder, EnergyPlus, Rhino, Grasshopper, Honeybee and Ladybug	minimizing energy demand (cooling, heating, lighting and equipment), maximizing energy production (PV) and adaptive thermal comfort levels	window -to-wall ratio, wall and glazing U-value, glazing g-value, air-tightness of the facade , cooling set-point of the mechanical cooling system and PV facade surface area	1. Initial optimization simulations of floor-plan shape and building orientation; 2. Envelope optimization, PV system and building systems; 3. Data post processing; 4. Optimal combination of variables
Naderi <i>et al.</i> (2020)	Shadings and control strategies optimization of a typical office room in six climates of Iran	EnergyPlus jEPlus + EA	reduction in building energy consumption and occupant's thermal and visual discomfort	Shading control strategy and its control set-points, shading location, slat dimensions and material specifications	1. Choice of software, thermal and visual comfort parameters and shading strategies; 2. Optimization studies and analysis of results;
Salata <i>et al.</i> (2020)	Optimization of retrofitting in a low-density residential building considering climatic conditions in 19 cities located from north to south of Europe	EnergyPlus, SketchUp, OpenStudio, Python, Master, BASH and Eppy	minimization of annual energy demand, intervention costs, energy operating costs and carbon dioxide emitted	glass thermophysical properties, envelope transmittance and reflection, blinds, removable solar greenhouses, pilotis and atrium inclosing with glass, solar thermal/PV panels and their tilt angle	1. Building modeling 2. Initial energy simulation 3. Application of the genetic algorithm 4. Analysis of the results of optimal solutions
Zhao and Du (2020)	Optimization of a typical high-rise office building with a large window area, located in Hohhot, China	DesignBuilder, jEPlus + EA	optimal windows and shading, reducing energy consumption (heating, cooling and lighting) and discomfort hours	Building orientation, window inside, medium and outside layer material, overhangs installation angles and overhangs depths	1. Modeling and validation of the building model; 2. Model export in EnergyPlus format; 3. Download weather files; 4. Insertion of information in jEPlus + EA and operation of crossover and mutation for optimal solutions.
Baghoolizad	Optimization of	EnergyPlus	Optimize	Heating and	1. Model data collection and

eh <i>et al.</i> (2021)	a standard residential block (Case 600 ASHRAE) in 5 different cities in Iran (Tehran, Tabriz, Esfahan, Rasht, Bandarabbas)	us	building's total load (heating and cooling) and total cost	cooling Set Point Temperature, insulator thickness and type, geographical directions	weather data; 2. Routine estimates of occupancy, costs, internal gains and HVAC system; 3. Initial simulation and validation (comparison with other studies in cities with similar climate); 4. Sensitivity analysis; 5. Optimization Process ; 6. Choice of the optimal solution.
Chen <i>et al.</i> (2021)	Optimization of a new teaching building at Huazhong University of Science and Technology in China.	Revit, DesignBuilder, EnergyPlus and MATLAB	minimizing building energy consumption and maximizing the indoor thermal comfort	External wall U-value and solar absorptance , roof U-value and solar absorptance, external window U-value and window-to-wall ratio	1. Building energy consumption simulation (building energy consumption calculation based on BIM and DB; orthogonal experiment for obtaining dataset); 2. Building energy consumption prediction using LSSVM (data preprocessing, parameter selection and optimization 3. NSGA-II multiobjective optimization (simulation and pareto-optimal solution)
Ghaderian and Veysi (2021)	Optimization of an existing office building in Kermanshah, Iran (Csa Mediterranean climate)	SketchUp ,EnergyPlus, MATLAB	optimize the building's energy consumption and its occupant's thermal comfort simultaneously	Set-point temperature for heating and cooling, supply water temperature for heating and cooling, ventilation and infiltration rate, heat transfer of external roof	1. Building modeling and simulation of thermal and energy behavior; 2. Validation by comparison with energy bills, questionnaires applied to occupants and local measurements of temperature and humidity; 3. Choice of variables; 4. Optimization study and analysis of results.
Maciel <i>et al.</i> (2021)	Thermoenergetic optimization of a school building in Brazil	EnergyPlus, python	Optimization of Energy use intensity (IUE) for heating and cooling	thickness of thermal insulation of external walls and floor, absorptance of external walls and roof, solar orientation	1. definition of the object of study and its characteristics; 2. definition of variables and optimization approaches; 3. delimitation of implementation strategies; 4. Optimization simulations and analysis of results
Naji, Aye and Noguchi (2021)	optimization of envelope components for prefabricated house in six climate zones in Australia	Daysim TRNSYS jEPlus + EA Meteorism INSUL	Optimize life cycle cost , thermal comfort and daylight illuminance	<b>Variables:</b> wall, roof and glazing components, window size, shading factor <b>Constraints:</b> thermal/sound insulation, indoor quality	1. Selection of Australian cities based on population and climate conditions; 2. Generation of weather data; 3. Building modeling; 4. Design of objectives, variables and constraints; 5. Optimization simulations; 6. Analysis of results
Vukadinovic <i>et al.</i> (2021)	Optimization of the structural and architectural parameters of a detached passive building with a sunspace in Niš, Serbia, (Cfa climate )	DesignBuilder, EnergyPlus	Reduce heating and cooling energy, increase thermal comfort.	Window-to-wall ratio, glazing type, façade wall constructions, window shading.	1. Building modeling; 2. Sensitivity analysis to identify the most influential parameters in thermal comfort and energy consumption for heating and cooling; 3. Optimization studies; 4. Analysis of the results.

Yue <i>et al.</i> (2021)	Optimization of a campus gymnasium (indoor multi-sport facility) in Qingdao, China	EnergyPlus, Eppy, Python, MATLAB	Optimize energy consumption and thermal comfort	Roof and wall types, solar absorptance, shadings, night ventilation, displacement ventilation, air conditioning system	<ol style="list-style-type: none"> <li>1. Collection of case study information and climate data;</li> <li>2. Initial simulation and validation (comparison with measured data);</li> <li>3. Choice of optimization strategies and studies;</li> <li>4. Analysis of the results;</li> <li>5. optimization process with other variables;</li> </ol>
Bagheri-Esef and Dehghan (2022)	Optimization of a typical 3-story residential building in Bandar Abbas, Yazd, Tehran, Rasht and, Tabriz (Iran)	EnergyPlus	minimizing energy consumption and cost of insulations and maximizing thermal comfort	heating and cooling setpoint, thickness and thermal conductivity of insulations in envelopes	<ol style="list-style-type: none"> <li>1. Collection of climatic and architectural data;</li> <li>2. Building modeling;</li> <li>3. Initial simulation;</li> <li>4. Definition of variables;</li> <li>5. Optimization process ;</li> <li>6. Pareto analysis and final selection of the optimal point.</li> </ol>
Merlet <i>et al.</i> (2022)	optimization for a retrofit of multiple social housing buildings in located close to Paris, France	EnergyPlus	Optimize costs and heating demand and avoid overheating mainly in summer	Optimization of envelope (walls, ceilings, floors and Windows): U-values, solar factor and visible transmittance	<ol style="list-style-type: none"> <li>1. Choice of method, objectives and algorithms;</li> <li>2. Collection of information about buildings and climate data, initial simulation of the current state;</li> <li>3. Choice of variables;</li> <li>4. Optimization studies;</li> <li>5. Choice of the best solutions;</li> </ol>
Tavakolan <i>et al.</i> (2022)	Optimization of a single-family residence built in 1970 located in Tehran (Iran)	MATLAB, EnergyPlus, DesignBuilder	Optimization for primary energy consumption and discounted payback period	Wall and roof insulation, airtightness, Windows glazing, heating and cooling systems, photovoltaic panels (PV)	<ol style="list-style-type: none"> <li>1. First simulation of the model incorporating energy auditing data;</li> <li>2. Definition of variables and parametric model;</li> <li>3. Formulation of objectives;</li> <li>4. Process Optimization;</li> <li>5. Selection of optimal strategies</li> </ol>
Wang Y., Yang; Wang Q. (2022)	Optimization of external shading system of the classroom for the middle and primary school in Nanchang city, China	Grasshopper, Rhino, Radiance, Daysim, EnergyPlus	Optimize lighting quality, artificial lighting energy consumption, air conditioning and heating energy consumption and visual comfort	overhang length of the horizontal shading board, width of the vertical shading board, building orientations	<ol style="list-style-type: none"> <li>1. Generation of a parametric model of a classroom;</li> <li>2. Calculation of the lighting and energy performance of the integrated external shading;</li> <li>3. Process Optimization;</li> <li>4. Results analysis and synthesis of optimal solution</li> </ol>
Xie <i>et al.</i> (2022)	Retrofitting of a Traditional Raw Earth Dwellings' Envelope in Zhushan Village, Hunan, China	DesignBuilder	Optimize energy consumption, CO2 emissions, heat balance	external insulation windows, external wall insulation layer, roof insulation layer, ceiling insulation layer	<ol style="list-style-type: none"> <li>1. Analysis of the current situation of buildings through field research and initial simulations;</li> <li>2. Choice of variables;</li> <li>3. Optimization calculations ;</li> <li>4. Analysis of the results.</li> </ol>

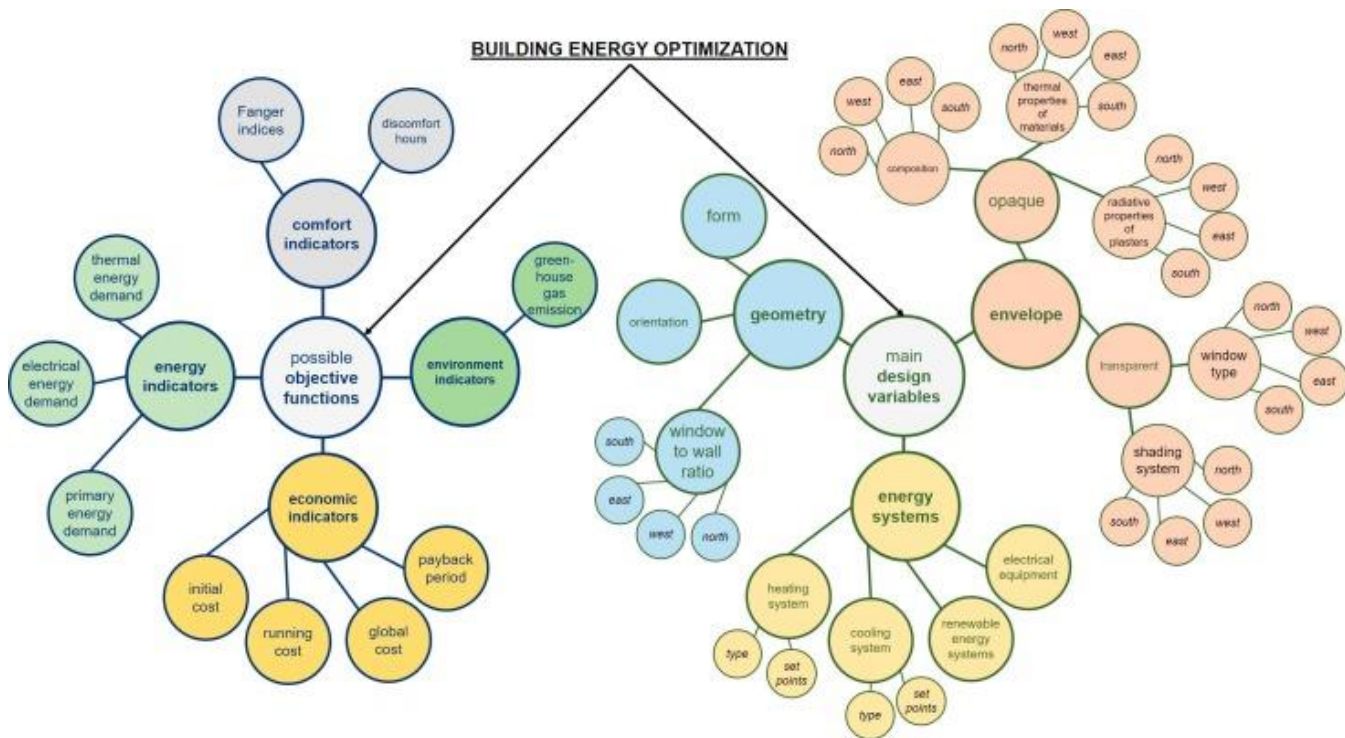
Xue, Wang and Chen (2022)	Optimization of an operational passive residential building in a severe cold climate with hybrid ventilation and light-dimming control	EnergyPlus	Minimize cost and CO2 emissions over the life cycle	insulation thickness, window type, window-to-wall ratio, overhang depth and building orientation	<ol style="list-style-type: none"> <li>1. Selection of a passive reference building and first simulation to verify energy uses;</li> <li>2. Definition of objectives and variables;</li> <li>3. Parametric simulations to establish a database of the relationship between the variables and objectives;</li> <li>4. Optimization simulations;</li> <li>5. Analysis of the results.</li> </ol>
Baghoolizadeh <i>et al.</i> (2023)	optimization of Venetian blinds in office buildings in Tehran (Iran)	Sketch Up, Open Studio, EnergyPlus, jEPlus + EA	reduce building energy consumption and improve thermal and visual comfort	Control strategies and setpoints, location and orientation of shading, slat dimensions, materials, hourly slat angle	<ol style="list-style-type: none"> <li>1. Building design and initial simulation;</li> <li>2. Choice of variables and sensitivity analysis;</li> <li>3. Optimization studies and extraction of optimal points from the Pareto front;</li> <li>4. Analysis of results and comparison with other studies.</li> </ol>
Gupta, Chanda and Biswas (2023)	Optimization of a vernacular house in Assam (North-East of India, with hot and humid summer )	DesignBuilder, EnergyPlus	Minimize CO2 emissions and cooling load demand	window to wall ratio, orientation, infiltration, shading, walls, roof and glazing type, ground floor type	<ol style="list-style-type: none"> <li>1. Collection of information about the building;</li> <li>2. Initial simulation and choice of variables;</li> <li>3. Optimization studies;</li> <li>4. Comparison and analysis of results;</li> <li>5. Choice of the optimal solution.</li> </ol>
Mostafazadeh, Eirdmoussa and Tavakolan (2023)	Optimize energy retrofit of residential buildings in Tehran (Iran)	MATLAB, EnergyPlus	maximize environmental performance (reducing emission/ water consumption), minimize life cycle costs and discomfort	envelope (Windows, thermal insulation for walls and floor), water fixtures, HVAC (heating and cooling setpoint), PV	<ol style="list-style-type: none"> <li>1. initial building model and calibration</li> <li>2. Definition of objectives;</li> <li>3. Optimization simulations;</li> <li>4. multi -criteria decision-making to find final retrofit strategies</li> </ol>

Source: Authors.

### Main objective functions and variables tested

Building energy optimization – BEO is a highly complex task that involves a huge number of potential objective functions and design variables, as schematized in Figure 33, which reports the main issues. The objective functions can refer to energy, environmental, economic and/or comfort indicators (XUE; WANG; CHEN, 2022). The design variables can be related to building geometry, envelope and energy systems (ASCIONE *et al.*, 2019b).

Figure 33 - Possible Objective functions and variables in Optimization Method



Source: Ascione *et al.* (2019b).

After combining variables in pursuit of achieving the objectives, the solutions can be standardized for all facades or individually for each part of the building according to the climate scenario, which characterize the “harlequin buildings”. These buildings have different constructive characteristics on each facade, such as: percentage of openings on the facade, reflectivity, composition of opaque and transparent envelope components and types of shading systems. The name “Arlequin”, therefore, is given due to results of buildings with differences in color and composition (ASCIONE *et al.*, 2019b).

### Genetic algorithm

The use of the computer allows the development of models that graphically represent the buildings and simulate their real current behavior (in the case of existing buildings) or future (in the planning of interventions or planning of new buildings) (DIDONÉ; PEREIRA, 2010; ZALUSKI; DANTAS, 2018 *apud* MACIEL *et al.*, 2021). This method enables further experimentation and allows for greater assertiveness in solutions to reduce energy demand in buildings.

Building performance optimization – BPO can involve simulation triggered by the designer as many times as necessary (XIE *et al.*, 2022), or by the joint action of a BPS software and a numerical optimization algorithm (BRE; ROMAN; FACHINOTTI, 2020), in which numerous computer simulations are processed automatically until the established objectives are achieved.

Optimization studies without an algorithm are processes that demand more time and are therefore less recurrent in the literature (in this systematic review, it was used only by Xie *et al.*, 2022), but they also generate satisfactory results.

Xie *et al.* (2022) identified optimal solutions based on the thermal balance calculated by DesignBuilder. In this case, the passive strategies and the thickness of the materials were individually customized and adjusted according to the needs identified in each simulation. The proposed method allows an ordering of priority solutions (with greater impact on the optimization results) and allows keeping as much as possible of the original constructive model.

Over the past 20 years, a lot of engineering research has included evolutionary computing, which is an offshoot of artificial intelligence. This technology uses optimization algorithms, such as genetic algorithms – GA, to test various architectural solutions and find optimal solutions quickly, with less energy simulation time (TAVAKOLAN *et al.*, 2022). Therefore, it has shown promise in the search for optimal solutions to complex energy efficiency problems (BAGHERI-ESFEH; SAFIKHANI; MOTAHAR, 2020; GHADERIAN; VEYSI 2021). The algorithms point out more efficient solutions from non-optimized solutions, randomly combining design variables until convergence to the optimal solutions (SALATA *et al.*, 2020).

GA, developed by Holland in the 1970s, is based on Darwin's theory of natural selection, nature's process of evolution and Mendel's theory of genetics (YU *et al.*, 2015 *apud* ZHAO; DU, 2020). In comparison to architecture, each design variable represents a gene and a combination of variables constitutes a chromosome. From the initial combinations generated arbitrarily, by random selection, crossover operation and mutation, options are generated that are more appropriate to the environment (or to the objective defined by the person responsible for the project), and the combinations evolve into increasingly better ones. In this way, they keep reproducing and evolving, and eventually converging on more suitable individuals (or



buildings) until optimal solutions are obtained (ZHAO; DU, 2020, MERLET *et al.* 2022).

The Non-dominated Sorting Genetic Algorithm – NSGA, and its NSGA-II evolution are improved variations of the basic GA (KHEIRI, 2018). They have a tournament selection strategy, which combines the parent generation with the offspring generation, and then produces the next generation through competition, in order to ensure that excellent individuals are not discarded during the evolution process (ZHAO; DU, 2020; GHADERIAN; VEYSI, 2021).

The combined platform jEplus + EA (EnergyPlus Simulation Manager for Parametrics + Evolutionary Algorithms) frequently used on studies is based on the EnergyPlus software (ZHANG; KOROLIJA, 2010 *apud* ZHAO; DU, 2020) and provides an effective approach to the architectural design and optimization process (ZHAO; DU, 2020). Currently, NSGA-III already exists, which has proven to provide improved solutions compared to previous algorithms, as it guarantees even greater diversity of optimal solutions (MOSTAFAZADEH; EIRDMOUSA; TAVAKOLAN, 2023).

### **Types of decision and criteria**

A recent research by Nguyen *et al.* (2014 *apud* MOSTAFAZADEH; EIRDMOUSA; TAVAKOLAN, 2023) classified building optimization processes and the most cited algorithms in the literature. According to this review, some of the most recurrent optimization methods include genetic algorithm – GA, simulated annealing – SA, particle swarm optimization – PSO, evolutionary algorithm – EA, artificial neural network – ANN and other lesser known methods (MOSTAFAZADEH; EIRDMOUSA; TAVAKOLAN, 2023; NGUYEN *et al.*, 2014 *apud* MOSTAFAZADEH; EIRDMOUSA; TAVAKOLAN, 2023). The study also reported the frequency of use of optimization algorithms in more than 200 evaluated works: 52% used genetic algorithm, 17% used particle swarm, 13% hybrid algorithms, 7% linear programming, 6% used Hooke-Jeeves algorithm and other less recurrent ones were used in 5% (NGUYEN *et al.*, 2014 *apud* MOSTAFAZADEH; EIRDMOUSA; TAVAKOLAN, 2023).

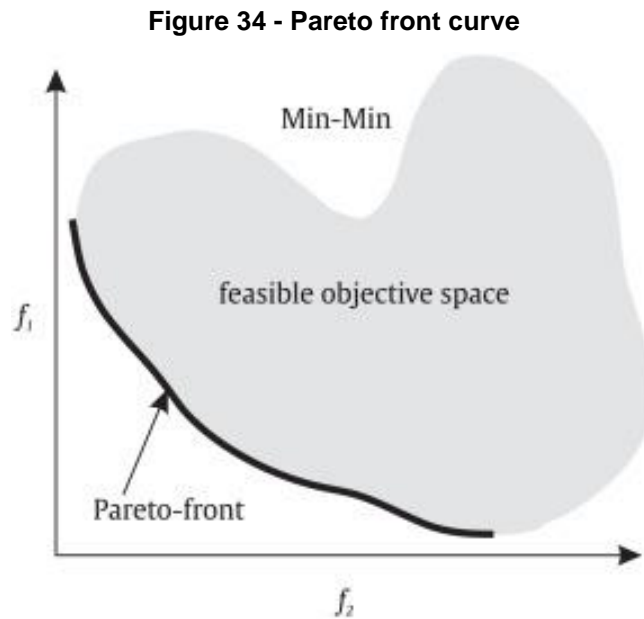
### **Multi/single criteria decision**

The optimization can be defined by a single objective function or two or more functions, which characterizes a multiobjective optimization (BAGHERI-ESFEH; SAFIKHANI; MOTAHAR, 2020). Multi-objective optimization, therefore, is a method to optimize results and simultaneously meet objectives that are often conflicting (BAGHERI-ESEF; DEHGHAN, 2022). The most common conflicting objectives are minimization of energy consumption, investment, operational cost, overall cost, polluting emissions and thermal discomfort (ASCIONE *et al.*, 2020).

Optimization objectives can be explicit, such as reducing the annual energy requirement, or implicit, such as reducing emissions or costs (SHI *et al.*, 2016 *apud* VUKADINOVIC *et al.*, 2021).

The optimal single-objective optimization solution is unique. On the other hand, the objective functions of multiobjective optimization generate a set of solutions that are not superior to each other, called the Pareto front (BAGHERI-ESEF; DEHGHAN, 2022), which allows the algorithm to optimize all objectives simultaneously and provide a set of non-dominant optimal solutions (NADERI *et al.*, 2020; ZHAO; DU, 2020).

A Pareto optimum is found by applying the theory of Pareto efficiency (GHADERIAN; VEYSI 2021) and is reached when any attempt to improve a variable worsens the other parameters (SALATA *et al.*, 2020; GHADERIAN; VEYSI 2021). In this case, the problem solution is not a single optimal design, but a set of Pareto optimal solutions that constitute the so-called Pareto front (BRE; ROMAN; FACHINOTTI, 2020; CHEN *et al.*, 2021; GHADERIAN; VEYSI 2021; MACIEL *et al.*, 2021). In the presence of only two objectives, this front can be represented as a curve (BRE; ROMAN; FACHINOTTI, 2020), as shown in Figure 34. The total set of Pareto optimal solutions is obtained when the descendant generation reaches the maximum number of generations (CHEN *et al.*, 2021).



Source: Bre, Roman and Fachinotti (2020).

After the optimization algorithm has reached the final Pareto front, a decision strategy must be adopted to choose the final optimal solution. This decision depends on the order of importance of the objective functions and the evaluation of the person responsible for the project (GHADERIAN; VEYSI 2021).

The best known multicriteria decision making approach is the weighted sum method – WSM in which different weighting coefficients are assigned to each objective, according to the needs identified by the designers (DELGARM *et al.*, 2016 *apud* ZHAO; DU, 2020).

### **Most recurrent methodology steps and softwares**

The optimization process of a building involves three main stages: preparation, optimization simulations and the final stage (NGUYEN *et al.*, 2014 *apud* VUKADINOVIC *et al.*, 2021; MACIEL *et al.*, 2021) as detailed below:

#### **Step 1: Preparation**

The preparation step involves:

- 1.1. Collection of climate information:** weather data and in some cases local climate measurements for calibration of simulations (BAGHOOLIZADEH *et al.*, 2021; YUE *et al.*, 2021; BAGHERI-ESEF; DEHGHAN, 2022; MERLET *et al.*, 2022);

- 1.2. Collection of building information:** envelope characteristics, building materials and respective thermal and optical properties, lighting load, air conditioning and equipment, occupancy schedule. In some cases, energy audits are carried out in the building for calibration (ASCIONE *et al.*, 2020; BRE; ROMAN; FACHINOTTI, 2020; GHADERIAN; VEYSI, 2021; YUE *et al.*, 2021; BAGHERI-ESEF; DEHGHAN, 2022; MERLET *et al.*, 2022; TAVAKOLA *et al.*, 2022; XIE *et al.*, 2022);
- 1.3. Modeling of the building.** Some researchers have adopted Sketch Up (SALATA *et al.*, 2020; GHADERIAN; VEISY, 2021; BAGHOOLIZADEH *et al.*, 2023) or Revit (CHEN *et al.*, 2021) or Rhino (GIOURI; TENPIERIK; TURRIN, 2020; WANG, Y.; YANG; WANG, Q., 2022) as a modeling tool and facilitator of information collection for input in performance simulation software, others have adopted DesignBuilder, which is a user-friendly graphical interface software for subsequent simulation with EnergyPlus (ASCIONE *et al.*, 2019a; ASCIONE *et al.*, 2019b; ASCIONE *et al.*, 2020; GIOURI; TENPIERIK; TURRIN, 2020; VUKADINOVIC *et al.*, 2021; TAVAKOLAN *et al.*, 2022; XIE *et al.*, 2022; GUPTA; CHANDA; BISWAS, 2023);
- 1.4. Definition of key points:** performance problem, objective function, the variables to be combined in the optimization process, scenarios to be evaluated, simulation software and, in cases of optimization made by computational algorithms, the selection of the most suitable algorithm. The variables can be chosen by a pilot simulation of the building (ASCIONE *et al.*, 2019a; ASCIONE *et al.*, 2019b) or by sensitivity analysis (BAGHOOLIZADEH *et al.*, 2021; VUKADINOVIC *et al.*, 2021; BAGHOOLIZADEH *et al.*, 2023);
- 1.5. Pilot simulation** of thermoenergetic or lighting performance with one or more softwares: EnergyPlus, used in all articles in the systematic literature review, Honeybee (GIOURI; TENPIERIK; TURRIN, 2020), Daysim (NAJI; AYE; NOGUCHI, 2021; WANG, Y.; YANG; WANG, Q., 2022), Radiance (WANG, Y.; YANG; WANG, Q., 2022) and TRNSYS (NAJI; AYE; NOGUCHI, 2021). There are also some options to be used in an auxiliary

way: Open Studio (SALATA *et al.*, 2020; BAGHOOLIZADEH *et al.*, 2023), Master, BASH (SALATA *et al.*, 2020), Eppy (SALATA *et al.*, 2020; YUE *et al.*, 2021), Python (SALATA *et al.*, 2020; MACIEL *et al.*, 2021; YUE *et al.*, 2021), MATLAB (ASCIONE *et al.*, 2019a; ASCIONE *et al.*, 2019b; ASCIONE *et al.*, 2020; CHEN *et al.*, 2021 ; GHADERIAN; VEISY, 2021; YUE *et al.*, 2021; TAVAKOLAN *et al.*, 2022; MOSTAFAZADEH; EIRDMOUSA; TAVAKOLAN, 2023), Meteonorm and INSUL (NAJI; AYE; NOGUCHI, 2021), Ladybug (GIOURI; TENPIERIK; TURRIN , 2020), Grasshopper (GIOURI; TENPIERIK; TURRIN, 2020; WANG, Y.; YANG; WANG, Q., 2022). The pilot simulation can happen before or after defining key points;

### **Step 2: Optimization simulations**

In this step, the reach or proximity to the objective function is verified through computer simulations, the duration of the simulations is monitored and possible errors in the procedure are detected and corrected (NGUYEN *et al.*, 2014 *apud* VUKADINOVIC *et al.*, 2021).

### **Stage 3: Final stage**

The third stage consists of presenting, interpreting and comparing the results (NGUYEN *et al.*, 2014 *apud* VUKADINOVIC *et al.*, 2021; MACIEL *et al.*, 2021), as well as choosing the best solution for the objectives (in cases of multiobjective analysis in which it is necessary to choose one among the several optimal solutions obtained of the Pareto front).

### **Discussion of the systematic review**

The most evaluated regions with optimization processes were cities in Iran, China and Europe, which do not have typical tropical climates. Brazil, a country with a predominance of hot climates, had only one climate type tested, among the 8 existing types, according to the Brazilian Bioclimatic Zoning.

The three main stages that involve the optimization process appear in all publications, even with different objects of study, objectives, variables and software.

Only one (XIE *et al.*, 2022) of the 27 studies did not use an algorithm for the optimization process, but presented efficient solutions with greater preservation of the original design compared to other studies. Different from the others, this method without algorithm also allowed, from the first simulations, the verification of priority and more effective alterations to reach the optimal solution.

## 2.10. Thermal Resilience and Passive Survivability in Buildings

### 2.10.1. Definitions of Thermal Resilience and Passive Survivability in Buildings

Over the years, the concept of resilience, widely applied in disaster risk management (ZHANG *et al.*, 2021), has been adapted across various scientific disciplines (KRELLING *et al.*, 2023; ISMAIL; OUAHRANI; TOUMA, 2023). It consistently advocates for a system and its component's ability to predict, absorb, adapt or efficiently recover from the impacts of a hazardous event, ensuring the preservation, restoration or enhancement of essential structures and functions (ATTIA *et al.*, 2021).

In the context of buildings, this concept, initially mentioned in the LEED scoring system as passive survivability (HONG *et al.*, 2023) and mentioned in studies by the International Energy Agency – IEA (ATTIA *et al.*, 2021), still lacks a single definition (SIU *et al.*, 2023; SERDAR, MACAULEY; AL-GHAMDI, 2022). The resilient building is often understood as one with the ability to meet occupant's needs, ensuring safe, stable and comfortable use in response to external condition changes (MEHMOOD *et al.*, 2022; SENGUPTA *et al.*, 2023a). It can also be described as capable of resisting continuous and unpredictable changes, preserving essential thermal conditions, recovering from failures within reasonable time and cost (ISMAIL; OUAHRANI; TOUMA, 2023; JI *et al.*, 2023), or resisting extreme and progressive changes in its environment (such as electrical failures, earthquakes, climate changes, heatwaves, fires, floods, soil instability) (ISMAIL; OUAHRANI; TOUMA, 2023).

According to Attia *et al.* (2021), a building's resilience against overheating and power disruptions involves stages of **vulnerability**, **resistance**, **robustness** and **recovery**

(HONG *et al.*, 2023; KRELLING *et al.*, 2023), protecting humans from the external environment (ZHANG *et al.*, 2021) and providing safe thermal conditions in case of power outages (ATTIA *et al.*, 2021). In other words, a resilient building is one that can prepare, resist, recover quickly and adapt to significant disturbances due to extreme weather conditions (FLORES-LARSEN, FILIPPÍN AND BRE, 2023). Krelling *et al.* (2023) provide further explanations about each of these stages:

- During the design phase, a **vulnerability** assessment considers potential risks;
- The **resistance** stage involves enduring various weather conditions using design features to avert critical thermal issues;
- The **robustness** stage arises when these features fail;
- In the **recovery** stage, a robust building can adapt and endure critical conditions post-failure, showcasing its capacity for recovery.

Table 22, adapted from Krelling *et al.* (2023), summarizes the main characteristics that can be identified or enhanced in resilient buildings. Among these features, those highlighted in bold are explored in this thesis.

**Table 22 - Main Characteristics of Resilient Buildings**

<b>Characteristic</b>	<b>Definition</b>	<b>Source</b>
<b>Vulnerability</b>	The inherent characteristics that make the building susceptible to negative impacts, such as the sensitivity of indoor comfort conditions in buildings to disruptions.	UN (2021); Miller <i>et al.</i> (2021); Attia <i>et al.</i> (2021); ISO (2009); ISO (2029)
<b>Adaptability</b>	The ability to adapt to potential damage and seize opportunities, focusing on anticipated future changes. This reflects the capacity of actors to influence resilience through proactive strategies aimed at protecting the system.	UN (2021); Miller <i>et al.</i> (2021); Folke <i>et al.</i> (2010); Clarke; Kuipers; Roos (2019); Grafakos <i>et al.</i> (2020); UN (2012); Pasimeni <i>et al.</i> (2019)
Transformability	The capability to rectify vulnerabilities when the current system becomes unviable, even through modifications to its fundamental attributes.	Silva; Kernaghan; Luque (2012); Folke <i>et al.</i> (2010); Clarke; Kuipers; Roos (2019); UN (2012); Walker <i>et al.</i> (2004); Privitera <i>et al.</i> (2018)
Learning capacity	The skill to extract insights from prior experiences and setbacks, facilitating adaptation, restructuring and readiness for future decisions, uncertainties and surprises.	Silva; Kernaghan; Luque (2012); Folke <i>et al.</i> (2010); UN (2012)
Dependency (on local ecosystems)	Resilient urban systems prioritize essential assets for well-being, ensuring access and quality, recognizing the value of local ecosystems (green and blue infrastructure) and taking steps to enhance their health and stability.	Silva; Kernaghan; Luque (2012)
<b>Mitigation (to climate change)</b>	Human actions aimed at decreasing emissions or bolstering the absorption of greenhouse gases.	UN (2021)
<b>Resistance</b>	The capacity to preserve original conditions and prevent disturbances from causing significant impacts.	Attia <i>et al.</i> (2021); Walker <i>et al.</i> (2004); Adger (2000)

<b>Safe failure/Robustness</b>	The capacity to absorb shocks and gradual challenges, preventing catastrophic failure if certain thresholds are surpassed. Some authors also describe Robustness as Resistance.	Silva; Kernaghan; Luque (2012); Moazami; Carlucci; Geving (2019); Attia <i>et al.</i> (2021);
Responsiveness/ Recovery	The capacity to restructure, restore functionality and establish a sense of order after a setback.	Silva; Kernaghan; Luque (2012)
<b>Flexibility</b>	The capacity to adapt, evolve and implement alternative strategies, whether in the short or long term, in response to changing conditions.	Silva; Kernaghan; Luque (2012)
<b>Smartness</b>	Contribution to sustainable development and resilience with well-informed decision-making focusing on both short- and long-term perspectives. It requires a holistic approach and innovative use of techniques and technologies. Smartness is evaluated based on technologically implementable solutions that enhance performance.	ISO (2016)
Diversity	The capacity to react to disruptions through a variety of responses.	Anderies (2014); Biggs <i>et al.</i> (2012)
Redundancy	The existence of elements, strategies, or participants capable of compensating for each other in the event of disruptions. Redundancy entails costs in terms of investment and performance that necessitate careful assessment.	Silva; Kernaghan; Luque (2012); Anderies (2014); Biggs <i>et al.</i> (2012); Stevenson; Barboska-Narozny; Chatterton (2016)
Modularity	Modularity offers a system various functional modules that can develop somewhat autonomously. These modules may have a loose connection by design, preventing the failure of one module from significantly impacting the others.	Anderies (2014);

Source: adapted from Krelling *et al.* (2023).

### 2.10.2. Building Thermal Resilience and Passive Survivability Performance Classification and Analysis Metrics

The quantitative assessment of building resilience in extreme weather conditions helps identify the capacity of a construction system to withstand disturbances and recover from extreme events (JI *et al.*, 2023). Considering the main stages of building thermal resilience, the capacity for resistance, robustness and recovery can be assessed through computational simulations, metrics and performance indicators that measure responses to risks and hazards related to internal thermal conditions. These include key indicators describing intensity, frequency, duration and severity (KRELLING *et al.*, 2023).

However, similar to the definition of resilience, researchers and practitioners have not yet reached a consensus on suitable modeling methods, performance metrics and indicators for analyzing building thermal resilience to inform decision-making (HONG *et al.*, 2023). In this context, the building's resistivity to climate change, indoor overheating risk and other resilience characteristics are generally evaluated by one



or more indicators (FLORES-LARSEN; FILIPPÍN; BRE, 2023; KRELLING *et al.*, 2023; HONG *et al.*, 2023).

Internal thermal conditions can typically be assessed using dry bulb temperature – DBT, operative temperature (which incorporates DBT and mean radiant temperature), or standard effective temperature – SET, the most complex, comprehensive and recommended metric for thermal performance evaluation (JI *et al.*, 2023; KRELLING *et al.*, 2023; HONG *et al.*, 2023; ISMAIL; OUAHRANI; TOUMA, 2023; TAVAKOLI *et al.*, 2022). SET considers internal air velocity, humidity, occupants' metabolic rate and clothing insulation, calculated in simulations with EnergyPlus or Design Builder (JI *et al.*, 2023; KRELLING *et al.*, 2023; SIU *et al.*, 2023) and is used as the thermal comfort standard by ASHRAE 55 (HONG *et al.*, 2023). Regarding thermal comfort, Predicted Mean Vote (PMV) and Predicted Percentage of Dissatisfied (PPD) have also been widely used (HONG *et al.*, 2023).

The Standard Effective Temperature – SET, recommended by authors as the most suitable metric for building thermal performance, is a rational thermal stress index based on the two-node physiological model. It is defined as the air temperature of a hypothetical standard environment with 50% relative humidity, air velocity <0.1 m/s and mean radiant temperature equal to the air temperature. This ensures that the total heat loss from the skin of an imaginary occupant with an activity level of 1.0 MET and clothing insulation of 0.6 CLO is equal to that lost by a real occupant in the actual environment with real clothing and activity level (JI *et al.*, 2023; ISMAIL; OUAHRANI; TOUMA, 2023).

Thermal stress is commonly measured by Heat Index – HI, Humidex, Wet-Bulb Globe Temperature – WBGT, or the rate of change in Indoor Overheating Degree – IOD related to the indoor environment, with an increasing Ambient Warmness Degree – AWD related to the external environment. Alternatively, the Overheating Escalation Factor can be calculated for long (annual/monthly) or short (weekly/daily) periods (HONG *et al.*, 2023; KRELLING *et al.*, 2023; FLORES-LARSEN; FILIPPÍN; BRE, 2023).

According to Sengupta *et al.* (2023b), these metrics and indices can be used to classify thermal performance into Thermal Autonomy – TA or Passive Autonomy,

represented by the percentage of occupied hours where internal operational temperature remains within thermal comfort limits without the intervention of active systems (LEVITT *et al.*, 2013). Passive Survivability Capacity (summer) or Heat Survivability refers to the period of thermal habitability, in hours, where the internal operational temperature remains within an acceptable thermal stress range, with high temperatures posing intermediate health risks. Recovery capacity is the speed at which the building and system return to normal functions, representing the time required to recover thermal comfort temperature after reaching the building's maximum temperature (ZHANG *et al.*, 2021; ISMAIL; OUAHRANI; TOUMA, 2023; SIU *et al.*, 2023).

Many studies assess the frequency of each building thermal performance phase or each level of the heat index scale, measured in hours or percentage, within a specific evaluation period and typically use bar or scatter plots to represent this data (SIU *et al.*, 2023; ISMAIL; OUAHRANI; TOUMA, 2023; HONG *et al.*, 2023):

- **Thermal Autonomy (Passive Autonomy):** Percentage of time during which natural conditioning provides thermal conditions that offer comfort to occupants;
- **Passive Survivability:** Indicates the period of comfortable and uncomfortable but still safe hours before the critical temperature is reached, combining analyses for summer and winter;
- **Critical Exceedance Time (Dangerous Cold or Heat):** The period during which the critical thermal stress limit is surpassed, when there is a high health risk rather than a range of uncomfortable temperatures and the building becomes uninhabitable;
- **Active Survivability:** Indicates the time during which an active system, such as a battery, can maintain its critical operations.

These classifications can be seen as deformation phases (TAVAKOLI *et al.*, 2022). The passive survivability (summer) or heat survivability is seen as an elastic deformation, suggesting that the building is resilient and can recover from the disturbance event. Once the internal operational temperature exceeds an acceptable limit, representing conditions of extreme thermal stress and danger to occupant's health, it is considered a plastic deformation, a condition where the internal thermal

environment may not return to equilibrium conditions. These circumstances must be avoided and require additional external intervention or the application of complementary technologies/strategies for recovery (TAVAKOLI *et al.*, 2022).

The temperature metrics considered (DBT, operative temperature and SET) and the limits characterizing each building thermal performance classification vary among studies. In studies considering SET as the most suitable metric for building thermal performance evaluation, the following classification limits are identified (Table 23):

**Table 23 - Standard Effective Temperatures Limits**

Source	Critic Cold Threshold	Cold Survivability	Passive Autonomy	Heat Survivability	Critic Heat Threshold
Siu <i>et al.</i> (2023)	< 4 °C SET	4 °C - 12 °C SET	12 °C - 30 °C SET	30 - 40 °C SET	> 40 °C SET
Tavakoli <i>et al.</i> (2022)	Not cited	Not cited	22 - 30 °C SET	30 - 38 °C SET	> 38 °C SET
Sengupta <i>et al.</i> (2023b)	Not cited	Not cited	24 °C SET	24 - 30 °C SET	> 30 °C SET
LEED <i>apud</i> Ismail, Ouahrani and Touma (2023).	< 4 °C SET	4 °C - 12 °C SET	12 °C - 30 °C SET	240 °C SET-hours	Not cited
Ismail, Ouahrani and Touma (2023).	Not cited	Not cited	Not cited	< 32 °C SET	32 - 40 °C > 40 °C SET
Khan <i>et al.</i> (2022)	Not cited	Not cited	Not cited	< 32 °C SET	> 32 °C SET

Source: Authors.

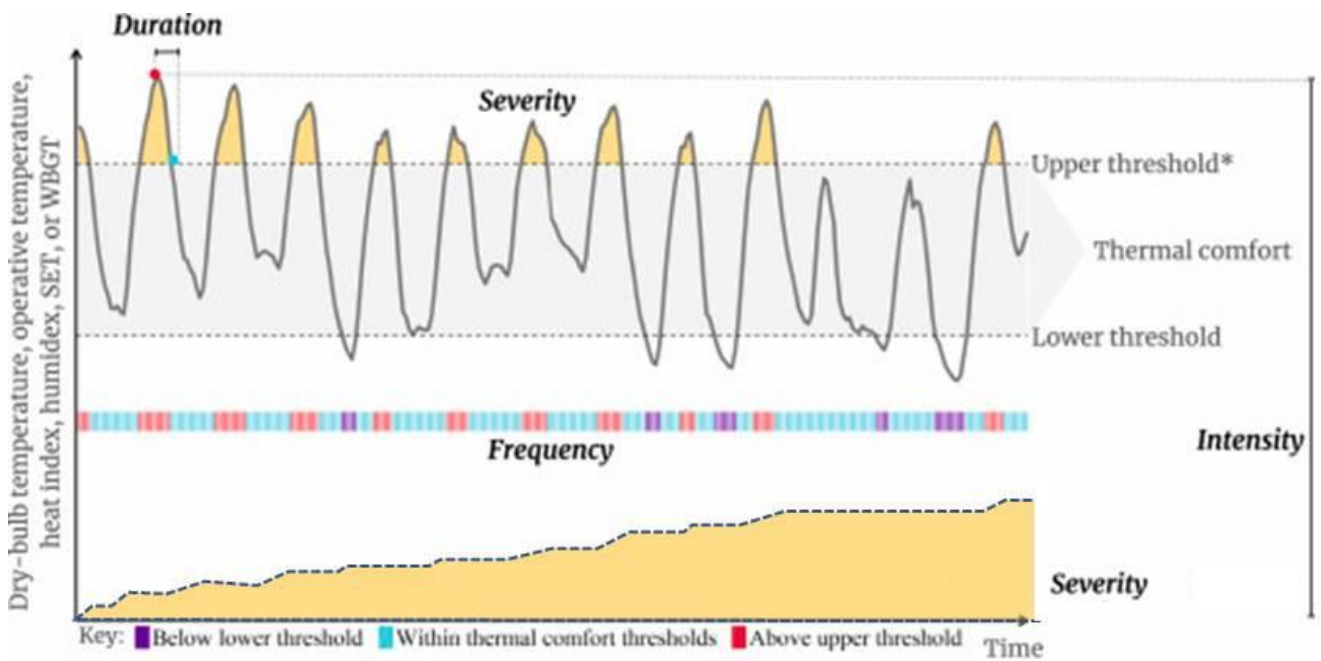
Among the mentioned thresholds, those defined by LEED are the most common. Regarding the Critical Heat Threshold, Ismail, Ouahrani and Touma (2023) and Khan *et al.* (2022) emphasize that SET variations between 32 - 40 °C can induce thermal stress, but above 40 °C SET, there is an extremely dangerous situation, rendering the building uninhabitable and evacuation is advised (ISMAIL; OUAHRANI; TOUMA, 2023).

In addition to classifying performance based on temperature limits and identifying the maximum temperature, Siu *et al.* (2023) highlight the importance of assessing the cumulative effects of continuous exposure to overheating conditions. Currently, there are still limited guidelines on temporal limits for exposure to extreme heat or cold in indoor spaces, but some recent standards consider these aspects (SIU *et al.*, 2023).

For this type of assessment, the most frequent metric is the time exposure integral (SIU *et al.*, 2023), measured in SET-degree-days or SET-degree-hours, indicating the magnitude of thermal stress by evaluating the exceedance time in relation to

comfort limits (SIU *et al.*, 2023; ATTIA *et al.*, 2021; ISMAIL; OUAHRANI; TOUMA, 2023). This metric was initially introduced by USGBC LEED system (ATTIA *et al.*, 2021). LEED sets a maximum cumulative value of 240 °C SET-hours above 30 °C in summer weeks and 120 °C SET-hours below 12.2°C in winter weeks for non-residential buildings (SIU *et al.*, 2023; ISMAIL; OUAHRANI; TOUMA, 2023). Figure 35 illustrates key indicators of thermal performance: intensity metrics (maximum temperature), severity (period outside thermal autonomy, which can also be measured as the time exposure integral in SET-hours), frequency (percentage of occurrence of thermal performance phases) and duration (building recovery time to thermal autonomy condition).

Figure 35 - Key indicators for indoor thermal performance

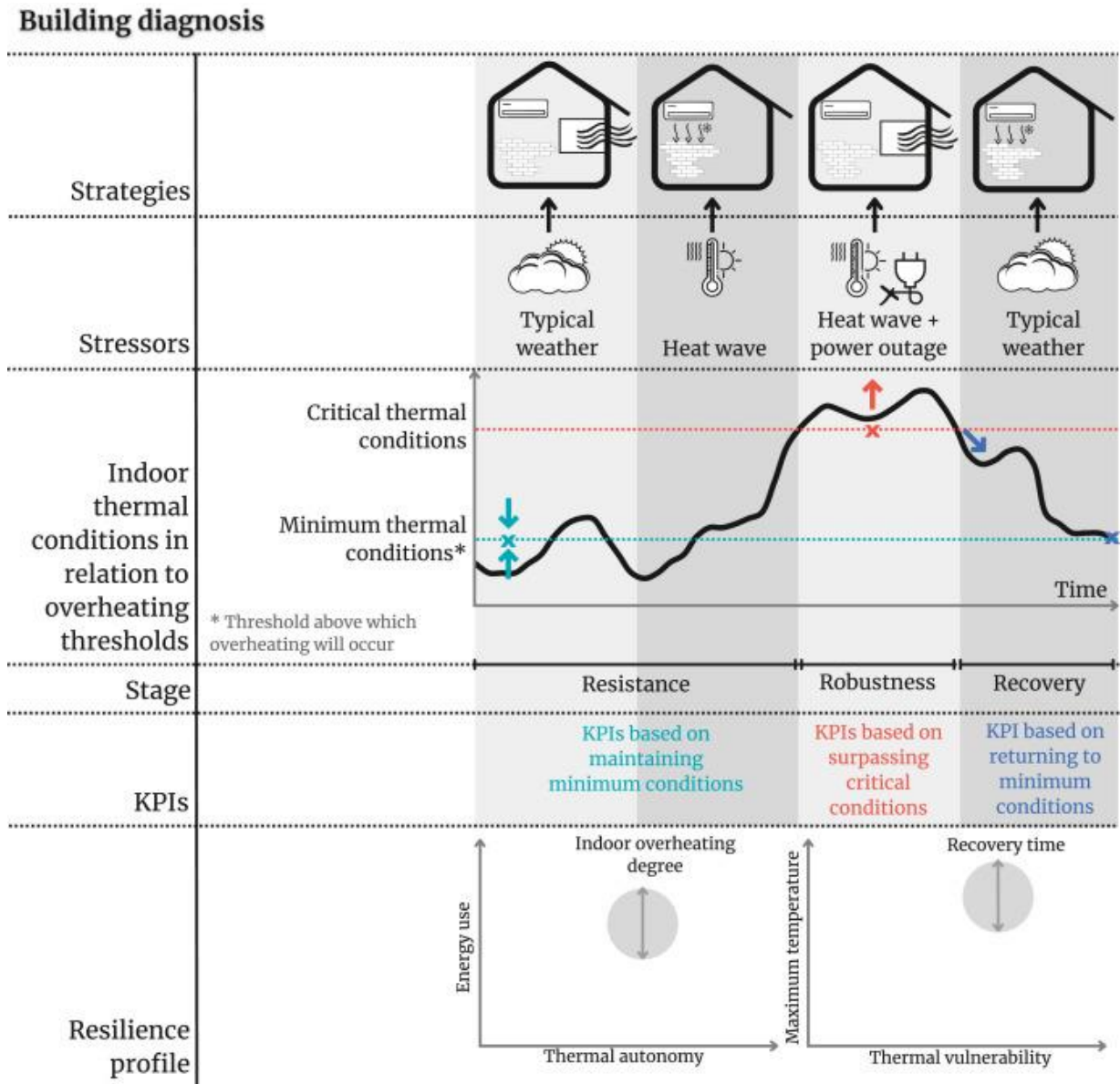


Source: adapted from Krelling *et al.* (2023).

Finally, based on the resilience stages of the building presented by Attia *et al.* (2021), it is customary to conduct assessment and diagnostic studies, followed by the evaluation of improvement strategies. The Figure 36 below illustrates the key aspects that can be considered in the diagnosis of each stage through Key Performance Indicators – KPIs (KRELLING *et al.*, 2023). Throughout the resistance stage, KPIs focusing on maintaining minimum thermal conditions are indicated; in robustness, KPIs demonstrating overcoming critical thermal conditions; and in recovery,

indicators informing the exit from critical conditions and the restoration of minimum thermal conditions (KRELLING *et al.*, 2023).

Figure 36 - Building Diagnosis Example



Source: adapted from Krelling *et al.* (2023).

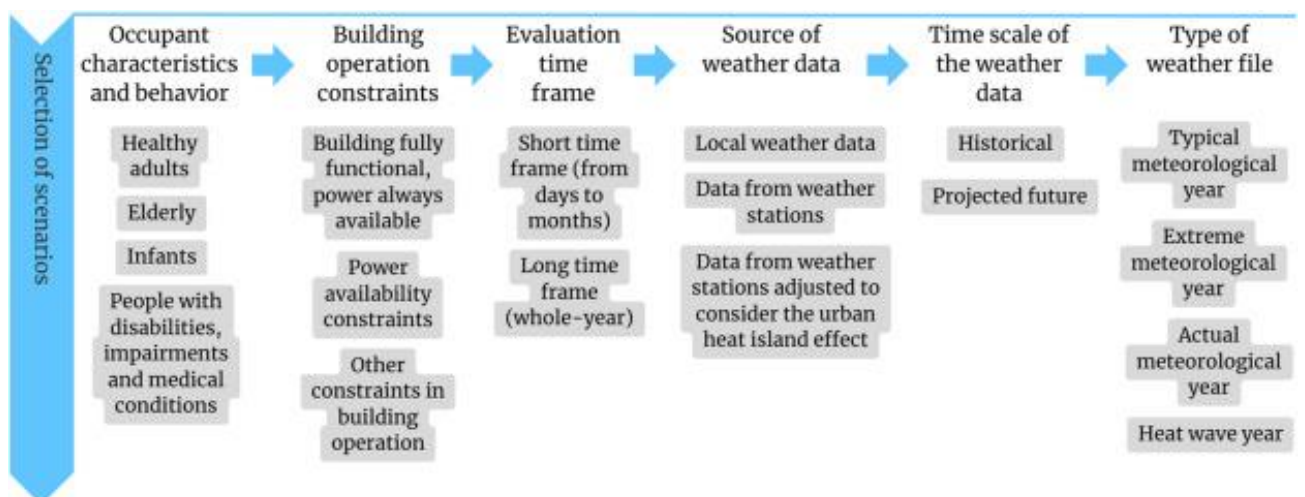
Among the improvement strategies that can be explored are: absorption capacity (minimizing the impacts of disruptive events with little difficulty), adaptive capacity (flexibility to adjust to undesirable situations through some alterations), restorative capacity (return to a normal or enhanced condition) and speed in recovery (ZHANG *et al.*, 2021). These strategies enhance thermal comfort and reduce thermal stress experienced by building occupants (JI *et al.*, 2023).

In light of all the information on the classification of Building Thermal and Passive Survivability Performance and Analysis Metrics, it is concluded that the appropriate choice of metrics is crucial for adequately assessing the thermal resilience and passive survivability of the building (HONG *et al.*, 2023). For this thesis, the evaluation of standardized public schools is proposed based on the variation in Standard Effective Temperatures. Only indicators from the resistance and robustness phases were selected. As performance indicators for the resistance phase, the frequency of thermal autonomy and passive survivability (summer) are investigated; and as indicators of robustness, the frequency of critical exceedance or dangerous heat ( $>40^{\circ}\text{C}$ ) is assessed, intensity is determined by identifying the annual maximum temperature and severity is calculated through SET-hours in a summer week to observe compliance with the requirement of a maximum accumulated  $240^{\circ}\text{C}$  SET-hours outside the range between  $12.2$  and  $30^{\circ}\text{C}$  SET. As strategies, the maximization of absorption capacity was explored through the optimization of passive strategies and adaptive capacity was enhanced with additional photovoltaics to meet future artificial air conditioning demands in extreme climatic conditions.

### 2.10.3. Assessment Scenarios, Classification of Extreme Events, Software for Weather Data Generation

In general, selecting scenarios to assess thermal resilience can be based on various dimensions, as depicted in Figure 37

Figure 37 - Dimensions for selecting scenarios to assess thermal resilience



Source: Hong *et al.* (2023).

The dimensions of occupant characteristics and behavior and building operation constraints are described not only in thermal resilience studies but also in various other building thermal performance studies.

Regarding the dimensions of evaluation time frame and time scale of weather data, Attia *et al.* (2021) highlight that extreme events can be classified into four categories, circumstances under which the thermal resilience of buildings can be assessed:

1. Extreme observed and future weather conditions (extended years)
2. Seasonal extreme weather conditions (extended months)
3. Short-term extreme weather conditions (short and extended days)
4. Power outages (covering hours)

In addition to choosing the category of extreme event, it is essential to consider the most appropriate type of weather file for conducting the simulations. Publicly accessible weather files, such as those from the Test Reference Year – TRY and Typical Meteorological Year – TMY, often do not adequately reflect urban microclimates due to the remote and rural locations of weather stations (KRELLING *et al.*, 2023). Furthermore, numerous research findings indicate that cooling solutions with low energy consumption, effective under current conditions, may exhibit suboptimal performance in the future or under extreme events such as heatwaves or power outages (MEHMOOD *et al.*, 2022; ZHANG *et al.*, 2021).

Therefore, building performance simulation for resilience assessment would benefit from including weather files covering urban microclimates, extreme conditions (such as Extreme Meteorological Year – XMY), heatwaves, cold waves and future projections based on various climate scenarios (KRELLING *et al.*, 2023; MEHMOOD *et al.*, 2022), to plan solutions that are valid in the long term as well (CIRRINCIONE; MARVUGLIA; SCACCIANOCE, 2021).

As for the source of weather data, these weather files, more suitable for thermal evaluation, are often obtained through weather data generator software. Table 24 shows some examples of thermal resilience studies with the respective scenarios mentioned or evaluated and the weather data generator softwares used.

**Table 24 - Examples of thermal resilience studies, scenarios mentioned and the weather data generator softwares**

Analysis Objective	Cited or Evaluated Scenario	Weather Data Generator Software	Source
Thermal resilience to overheating during heat waves	Historical or TMY (2010–2020), mid-term (2041–2060) and long-term (2081–2100) associated with a 24h power outage – PO scenario	Method of Weather data task force of IEA Annex 80	Sengupta <i>et al.</i> (2023)
Resilient design strategies, thermal comfort, energy usage	Mid to long-term (2070)	Meteonorm	Osman and Sevinc (2019)
Cooling resilience e eficiente cooling strategies	Years 2020 (TMY), 2050 and 2080 in the A2 emission scenario (medium-high from IPCC AR4)	CCWorldWeatherGen	Mehmood <i>et al.</i> (2022)
Evaluating the performance of passive strategies	Emission scenario A2 (medium-high from IPCC AR4) and the five emission scenarios SSP from IPCC AR6	CCWorldWeatherGen	Cirincione, Marvuglia and Scaccianoce (2021)
Thermal comfort, cooling needs and passive survivability	Synergistic impact scenario of urban overheating (UO) and heat waves (HW)	Meteonorm	Khan <i>et al.</i> (2022)
Internal thermal conditions	IPCC AR6 SSP5-8.5 emission scenarios for 2050 and 2080	Future Weather Generator	Guarda <i>et al.</i> (2023)

Source: Authors.

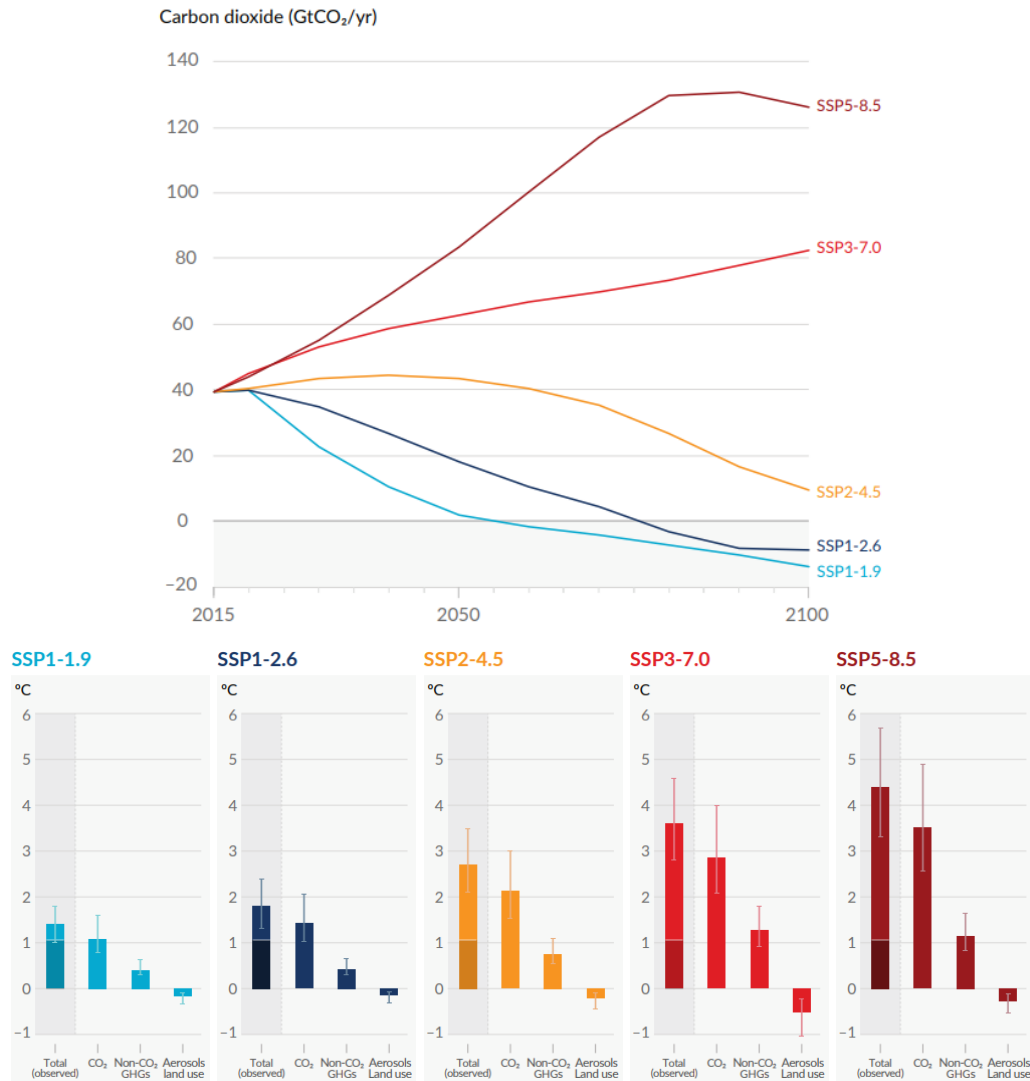
The A2 scenario from the Intergovernmental Panel on Climate Change – IPCC, which is more prevalent in the articles selected for this literature review, is one of the hypothetical climate scenarios from the Special Report on Emissions Scenarios – SRES described in the 4th Assessment Report of the IPCC AR4 (MEHMOOD *et al.*, 2022; CIRINCIONE; MARVUGLIA; SCACCIANOCE, 2021). The SRES can be classified as A1, A2, B1 and B2, with different assumptions about future emissions. The A2 scenario is considered to have medium-high emissions, resembling the Business as Usual – BAU scenario (MEHMOOD *et al.*, 2022; CIRINCIONE; MARVUGLIA; SCACCIANOCE, 2021).

The Shared Socioeconomic Pathways – SSP are more recent exploratory narratives from the IPCC, resulting from the 6th Assessment Report of the IPCC AR6, representing socio-economic and environmental futures with a more refined approach to emissions, allowing for more in-depth assessments of the impacts of



climate change. These are classified into five different narratives (Figure 38), with SSP1 being the most optimistic and SSP5 being the most pessimistic (IPCC, 2021).

**Figure 38 - Future annual emissions of CO2 and Contribution to global surface temperature increase from illustrative scenarios**



Source: IPCC (2021).

The most prevalent software tools in research are CCWorldWeatherGen and Meteororm. CCWorldWeatherGen employs the temporal series adjustment technique (morphing) based on the Technical Assessment Report – TAR models of the IPCC in the HadCM3 A2 experimental ensemble (HRM3), referring to the 3rd Assessment Report. It generates future weather data files from summarized data of an existing epw file, providing a statistical approach to downscaling (CIRRINCIONE;

MARVUGLIA; SCACCIANOCE, 2021). Despite being a recurring and effective tool, it uses outdated IPCC data.

Meteonorm is a software with reliable data sources and sophisticated calculation tools, dealing with over 30 meteorological parameters (OSMAN; SEVINC, 2019). However, the most updated version of the software constructs future weather data based on IPCC Scenarios RCP 2.6, 4.5 and 8.5 from the 5th Assessment Report of the IPCC AR5, which are also not the most recent hypothetical scenarios.

The Future Weather Generator tool used by Guarda *et al.* (2023) employs the same morphing mathematical method as CCWorldWeatherGen but utilizes more up-to-date data from the 6th Assessment Report of the IPCC AR6, making it a more suitable tool (GUARDA *et al.*, 2023).

After understanding the main potential assessment scenarios, types of extreme event classification and recurring software tools for weather data generation, this thesis proposes, based on the literature, long and short-time frame evaluations (annual and during a hot week). These evaluations will consider historical (TMY) and projected future (2050 and 2080) weather files generated by the FutureWeatherGenerator software, which incorporates the most current scenarios from IPCC AR6. Finally, the chosen scenario is SSP3-7.0, representing a context of medium-high emissions, a emission condition also opted for in previous studies by Mehmood *et al.* (2022) and Cirrincione, Marvuglia and Scaccianoce (2021).

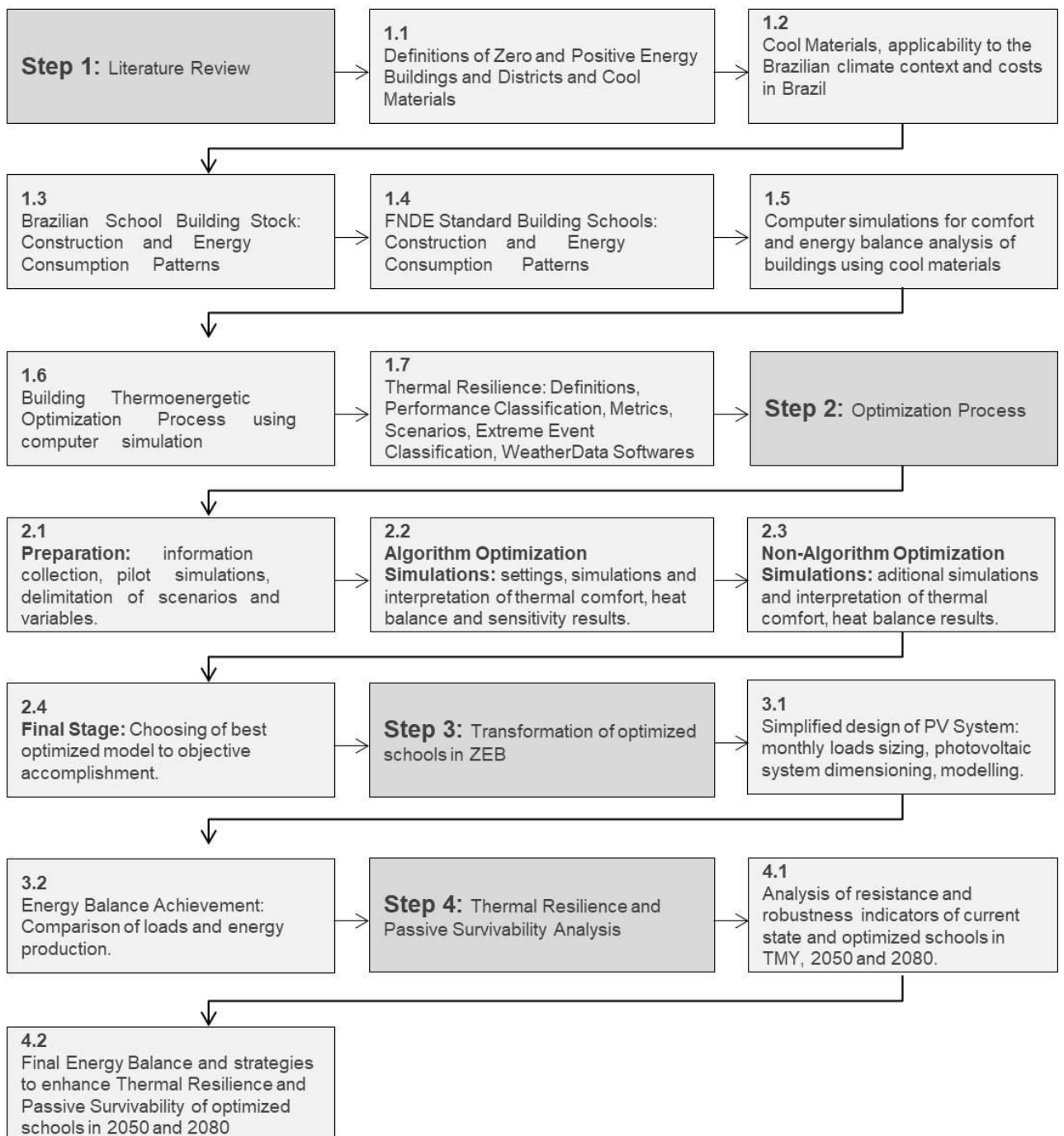
### 3. METHODS

This thesis aims to assess achieving positive energy balance and adequate thermal comfort in standardized Brazilian public schools in all bioclimatic zones by focusing on cool materials and passive strategies. The method chosen to find the most suitable solutions was the optimization process based on heat balance analysis.

The object of study is the set of projects of standardized public schools of the FNDE, which currently do not offer thermal comfort to users in all Brazilian territory, and therefore, presents a strong tendency to increase energy consumption due to artificial conditioning.

The thesis is structured in 4 steps (Figure 39), which aim to achieve the proposed objectives.

**Figure 39 – Methods Steps**



Source: authors.

### 3.1. Literature Review

The literature review was structured in two moments:

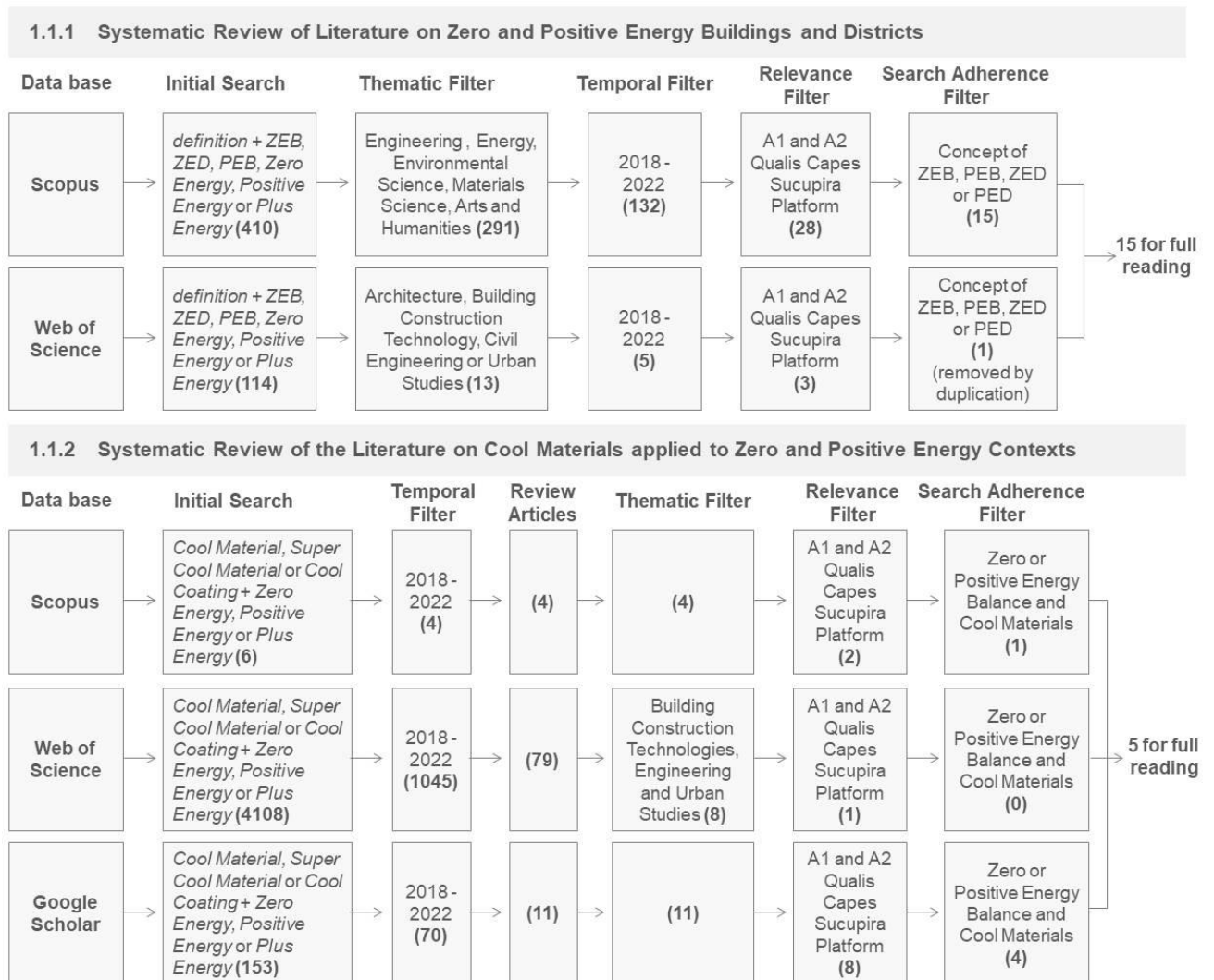
- 1.1.1 Systematic review of the literature on zero and positive energy buildings;
  - Synthesis of the fundamental principles of the concept;
  - Summary of the main types and respective variations of physical or geographic limit and location of energy production;
- 1.1.2 Systematic review of the literature on cool materials applied to zero and positive energy contexts;

The initial Systematic Literature Review includes scientific articles available in databases Scopus and Web of Science by the term *definition* conjugated with *ZEB*, *ZED*, *PEB*, *Zero Energy*, *Positive Energy* or *Plus Energy* in titles, abstracts or keywords, which shows a total of 410 and 114 publications respectively. Of the 410, only 291 refer to Engineering, Energy, Environmental Sciences, Materials Science, Arts and Humanities and of the 114, 13 involve Architecture, Building Construction Technology, Civil Engineering or Urban Studies. In this way, studies of discordant theme are discarded. The year 2018 has a peak of scientific production on the subject according to the Scopus database, therefore, the 132 and 5 publications carried out from that period are selected. Of these, 28 from the Scopus database and 3 from Web of Science are publications in A1 and A2 journals according to the Scupira Platform Classification in the area of Architecture, Urbanism and Design. From the reading of titles and abstracts, a duplication is removed and only 15 are selected for the complete reading, as they present the concept of zero or positive energy as the target subject.

The second Systematic Review includes the search for scientific articles in the databases Scopus, Web of Science and Google Scholar for the associated terms *Cool Material*, *Super Cool Material*, *Cool Coating* and *Zero Energy*, *Positive Energy* or *Plus Energy* in titles, abstracts or keywords, which shows a total of 6, 4018 and 153 publications respectively, of which 4, 1045 and 70 published between 2018 and 2022 and 4, 79 and 11 refer to review articles. The titles of publications show that those resulting from the Scopus databases and Google Scholar are similar to the

research topic, but of the 79 on the Web of Science platform, only 8 refer to Building Construction Technologies, Engineering and Urban Studies. Of the total obtained, 2, 1 and 8 are publications in journals A1 and A2 according to the Sucupira Platform Classification in the area of Architecture, Urbanism and Design. Finally, 1, 1 and 4 publications are removed because they do not contain Zero or Positive Energy or Cool Material cited throughout the research, resulting in 5 articles for full reading. The research flowchart can be seen in Figure 40.

**Figure 40 - Flowchart: Systematic Review of Literature on cool materials applied to zero and positive energy contexts**



Source: authors.

The step 1.2 was structured in three moments:

- 1.2.1 Systematic review of literature on cool or super cool materials;
  - Conceptualization and Characterization of cool materials;
  - Summary and Classification of cool materials in terms of physicochemical characteristics, performance according to the climatic context, forms of application and durability;
- 1.2.2 Analysis of applicability to the Brazilian context according to the performance of materials with variations in temperature and air humidity in Brazilian bioclimatic zones;
- 1.2.3 Cost Analysis of Brazilian Supercool paintings and comparison with conventional Brazilian paintings.

The Systematic Review includes the search for scientific articles in the databases Scopus and Web of Science databases for the terms *cool material* or *super cool material* in titles, abstracts or keywords, which results in 395 publications, 394 from the Scopus database and 1 from the Web of Science database. 195 publications are selected, only from the Scopus database, as they were published between 2016 and 2022 (a period that presents a peak of scientific production on the subject), of which only 95 have at least 10 citations. Among these, only 22 have adherence to the thesis, containing cool or super cool materials as a target subject, in contexts of literature review, studies of physical-chemical composition of the material, experimental tests in the laboratory or computer simulations of the application of materials to buildings.

The complete reading of the selected documents allows the extraction of the following information: basic concept of cool material and its fundamental characteristics, physical-chemical characteristics of the mentioned cool materials, performance in terms of surface temperature, forms of application, durability in relation to optical degradation/weathering and research trends.

Based on the Literature Review, the most suitable cool materials for each Brazilian bioclimatic zone are presented, considering the variations in temperature and air humidity annual averages portrayed in ABNT NBR 15220 (ABNT, 2005a).

The three cool paintings identified as most suitable for the Brazilian context were: thermochromic for heating-dominated zones, high spectral reflectivity and high broadband emissivity (above 90%) for extreme-cooling-dominated humid zones and high spectral reflectivity and high emissivity in the atmospheric window (above 90%), also known as spectrally selective paintings, for cooling or extreme-cooling-dominated dry zones. However, thermochromic paints are still in the development phase due to the low durability of the color-changing property in the current options under study, and therefore, they are not yet available for purchase and application in building envelopes (SANTAMOURIS; YUN, 2020).

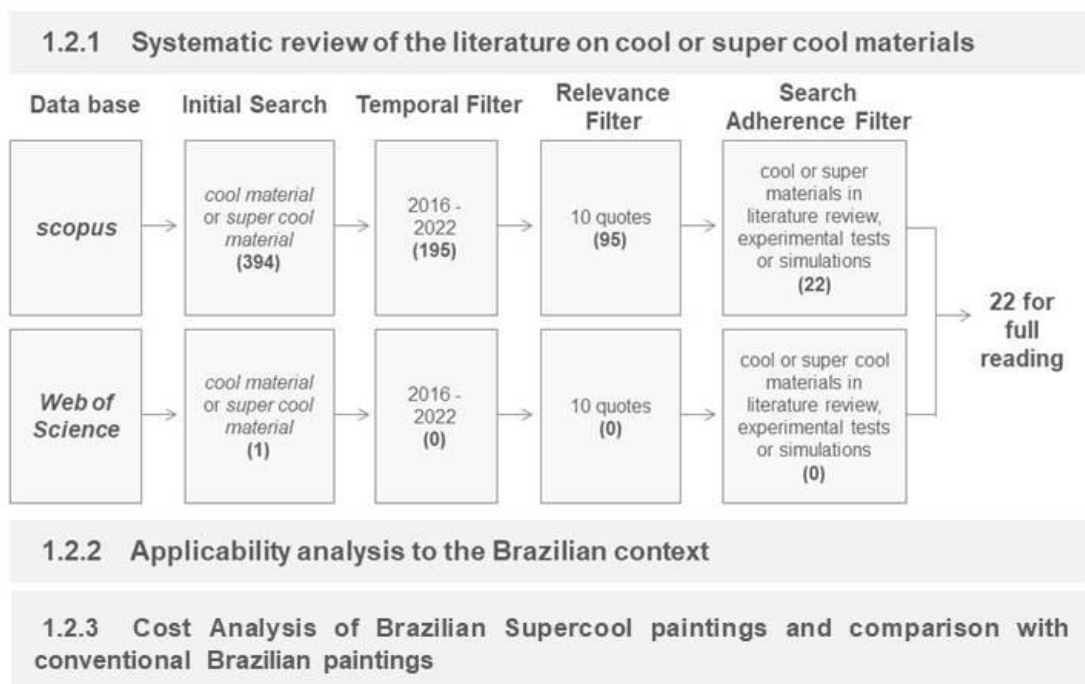
The spectrally selective paintings, which are the most recently developed and have higher cooling potential among supercool options (SANTAMOURIS; VASILAKOPOULOU, 2023), exhibit high emissivity at specific wavelengths (SANTAMOURIS; YUN, 2020), information not yet disclosed in the Cool Roof Rating Council – CRRC (CRRC, 2022a; 2022b) or any other publicly available database. Therefore, only commercially available supercool paintings with high spectral reflectivity and high broadband emissivity can be identified. This specific type of supercool painting is found both nationally (ANDRADE; DORNELLES, 2023) and internationally (CRRC 2022a; 2022b). Considering that the focus of this thesis is a public building that should prioritize cost-effective solutions, a cost analysis of national supercool paintings has been conducted.

Among the various options of Brazilian cool paintings recently investigated by Andrade and Dornelles (2023), only one option, acrylic-based, can be characterized as supercool, with over 90% reflectivity. Therefore, the cost of this product was collected from 7 different online sources (4 different prices from manufacturer representatives and 3 from websites) in January 2024 and an average market value was calculated. This value was compared with the average prices of three different types of latex acrylic paints (standard, premium and super premium) suitable for external applications (ABNT, 2021a; 2021b) in the eight different Brazilian cities studied in this thesis (PA, PI, GO, SP, DF, SC, RJ and RS) described in the latest report of the National System of Prices and Indices for Civil Construction – SINAPI published by in November 2023 (CAIXA ECONÔMICA FEDERAL, n/d). As there is currently no national classification system for cool and super cool materials and coatings, similar to the American CRRC program (ANDRADE; DORNELLES, 2023),

the specification and manufacturer of the cool paint assessed in this thesis have been concealed, following the approach taken by Andrade and Dornelles (2023).

The research flowchart can be seen in Figure 42.

**Figure 41 - Flowchart: Systematic Review of Literature on cool materials and applicability analysis to the Brazilian context**



Source: authors.

The step 1.3 was structured in two moments:

1.3.1 Systematic review of brazilian school building stock patterns of building, comfort and energy consumption. The following information was gathered:

- Number of schools in current building stock;
- Standardization of projects and common shapes of buildings;
- Most recurring subspaces;
- Predominant operating period;
- Year of construction of schools;
- Variations in the number of students;
- Quantity and Characteristics of brazilian climatic regions in wich schools are located;



- Thermal satisfaction of school users;
- Average energy consumption of schools and main end uses.

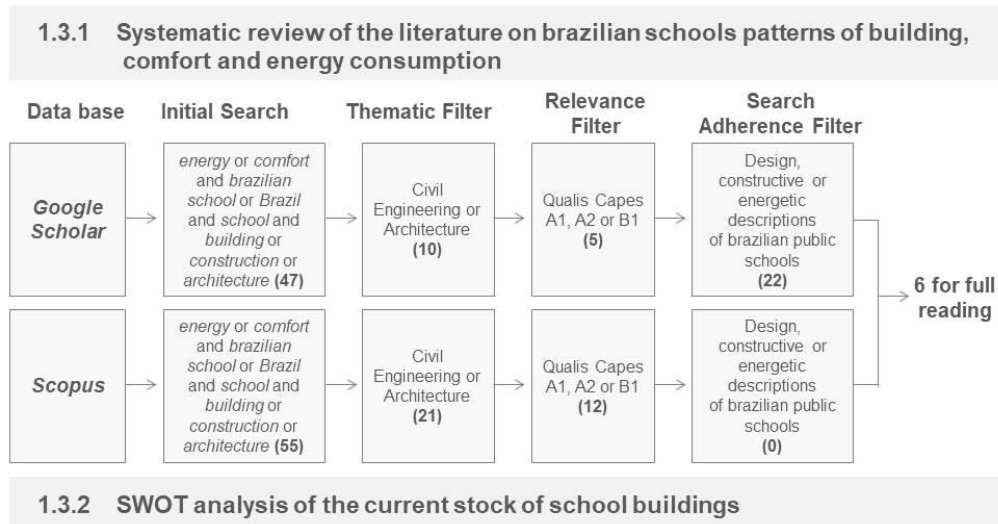
### 1.3.2 Analysis of strenghts, weaknesses, opportunities and threats of the current stock of school buildings.

The Systematic Review includes the search for scientific articles in the databases Google Scholar and Scopus databases for the terms *energy* or *comfort* associated with *brazilian school* or *Brazil* and *school* with *building* or *construction* or *architecture* in titles, abstracts or keywords, which results in 47 results in Google Scholar and 55 in the Scopus database, of which only 10 and 21 are related to Civil Engineering or Architecture. Of these, 5 and 12 respectively refer to articles published in journals and 5 and 8 were published in Qualis Capes A1, A2 or B1 journals according to the Sucupira Platform. In this case, a temporal filter is not applied, since less recent studies on the characteristics of the building stock of brazilian schools are also relevant.

From this group of publications, are discarded duplications and those that do not present design, constructive or energetic descriptions of brazilian public schools as the main information for the study (1 from Google Escolar and 2 from Scopus). Therefore, 1 and 5 (6 articles in total) were chosen for full reading.

Based on the literature review, a SWOT analysis of the current stock of school buildings was carried out in order to synthesize strengths, weaknesses, opportunities and threats related to thermal comfort and energy efficiency in current Brazilian schools. This is a strategic analysis method, used worldwide in various areas of study and even in energy-efficient building projects. It allows a comprehensive and impartial assessment of an object of study and provides valuable suggestions that can be crucial in the decision-making process (ZHANG; YUAN; KIM, 2023). In this thesis, In this thesis, this method allowed identifying positive and negative points and main opportunities and needs for intervention in the school architectural model. The research flowchart can be seen in Figure 42.

**Figure 42 - Flowchart: Systematic Review of Literature on Brazilian school patterns and SWOT analysis**



Source: authors.

The step 1.4 was a review on FNDE standard schools with the purpose of collecting the maximum amount of information about the object of study (FNDE standardized schools) to provide the necessary theoretical basis for the next stages of this thesis. The main information collected were:

- Main types of standardized schools;
- Shape, area, number of students and spaces zoning;
- Thermal and optical properties of buildings envelope;
- Type of artificial climate of standard projects, installed lighting power and equipment.

The step 1.5 was a systematic review on computer simulations of cool materials searching the following aspects:

- Cool material tested;
- Assessed city and climate;
- Object of study: urban context and/or buildings;

- Place of application of cool materials: urban paving, roofing and/or building facades;
- Software used: name of the software;
- Input data (fixed and variable);
- Output data;
- Research steps for computer simulations;

Of the articles obtained in the systematic review of the literature on cool materials and applications in a zero or positive energy balance context, it was found that 10 articles used computer simulations to analyze the effect of cool materials on the energy performance of buildings (MANNI *et al.*, 2019; FENG *et al.*, 2022; FENG *et al.*, 2021; CASTALDO *et al.*, 2018; LASSANDRO, TURI; ZACCARO, 2019; LASSANDRO; TURI, 2017; KOLOKOTSA *et al.*, 2018; BANIASSADI; SAILOR; BANWEISS, 2019; ASCIONE *et al.*, 2018; BERARDI; GARAI; MORSELLI, 2020). Of all the software used by the authors, EnergyPlus and DesignBuilder were the most frequent.

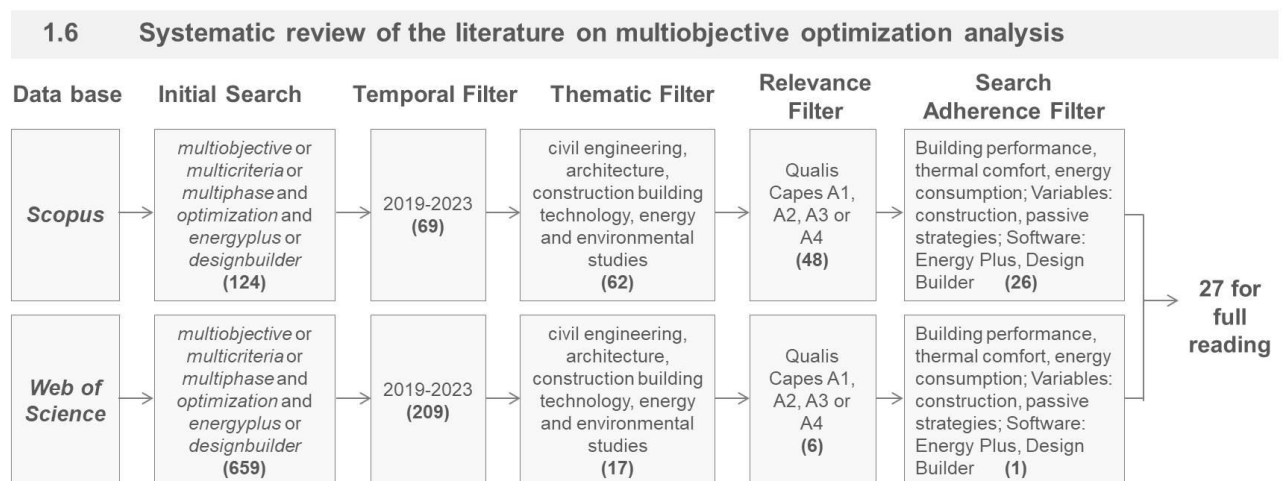
Definition and main purpose of multiobjective The step 1.6 was a systematic review on multiobjective optimization analysis following these steps:

- optimization analysis;
- Optimization objectives;
- Variables tested;
- Most recurrent methodology steps;
- Softwares used;
- Multiobjective optimization analysis applied in this thesis;

The Systematic Review includes the search for scientific articles in the databases Scopus and Web of Science databases for the terms *multiobjective* or *multicriteria* or *multiphase* and *optimization* and *energyplus* or *designbuilder* in titles, abstracts or keywords, which results in 783 publications, 124 from the Scopus database and 659 from the Web of Science database. Among these, 69 from Scopus and 209 from Web of Science were published between 2019 and 2023 (a period that presents a peak of scientific production on the subject), of which 62 and 17 are related to civil

engineering, architecture, construction building technology, energy and environmental studies. About relevance, 48 from Scopus and 6 from Web of Science are A1, A2, A3 and A4, according to Qualis Capes Scupira Platform 2017-2022 classification. After the Reading of titles and abstracts, as an adherence filter, were selected 26 and 1 publications which include the search words. The complete reading of the selected documents allows the extraction of the following information: basic concept optimization process, examples of this method application, main objective functions and variables tested in building performance optimizations, most common genetic algorithm used, types of decision and criteria, most current methodology steps and simulation tools. The research flowchart can be seen in Figure 43.

**Figure 43 - Flowchart: Systematic Review of Literature on multiobjective optimization analysis**



Source: authors.

The item 1.7 was a systematic literature review on Thermal Resilience and Passive Survivability in Buildings. The following information was gathered:

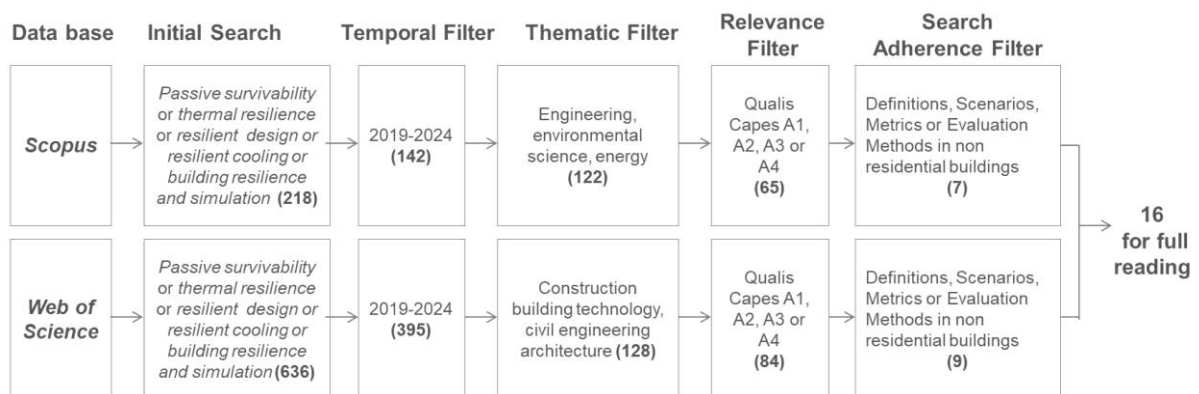
- Definitions of Thermal resilience and Passive Survivability in Buildings;
- Building Thermal Resilience and Passive Survivability Performance Classification and Analysis Metrics;
- Evaluation Scenarios, Extreme Event Classification, Weather Data Generation Software;

The Systematic Review includes the search for scientific articles in the databases Scopus and Web of Science databases for the terms *passive survivability* or *thermal*

*resilience or resilient design or resilient cooling or building resilience and simulation* in titles, abstracts or keywords, which results in 854 publications, 218 from the Scopus database and 636 from the Web of Science database. Among these, 142 from Scopus and 395 from Web of Science were published between 2019 and 2024, of which 122 and 128 are related to engineering, environmental science, energy, construction, building technology, civil engineering and architecture. About relevance, 65 from Scopus and 84 from Web of Science are A1, A2, A3 and A4, according to Qualis Capes Scupira Platform 2017-2022 classification. After the Reading of titles and abstracts, as an adherence filter, were selected 7 and 9 publications which include the search words. The research flowchart can be seen in Figure 43.

**Figure 44 - Flowchart: Systematic Review of Literature on Thermal Resilience in Buildings**

1.7 Systematic review of the literature on passive survivability and thermal resilience



Source: authors.

### 3.2. Optimization Process

The optimization process was structured in four stages (Preparation, Algorithm Optimization Simulations, Non-Algorithm Optimization Simulations and Final Step), based on Ascione *et al.* (2019a), Ascione *et al.* (2019b), Zemero *et al.* (2019), Salata *et al.* (2020), Maciel *et al.* (2021), Naji, Aye and Noguchi (2021), Vukadinovic *et al.* (2021), Yue *et al.* (2021), Bagheri-Esef and Dehghan (2022), Merlet *et al.* (2022), Tavakolan *et al.* (2022), Xie *et al.* (2022), Baghoolizadeh *et al.* (2023), Gupta, Chanda and Biswas (2023), Mostafazadeh, Eirdmoussa and Tavakolan (2023).

### 3.1.1 Preparation

The preparation stage consisted of three fundamental steps that preceded the optimization: information collection, pilot simulations, delimitation of scenarios and variables.

#### Information of climate and building modelling

The preparation involves the collection of Typical Meteorological Year – TMY Weather Data (Table 25) from cities in the 8 Brazilian bioclimatic zones – ZBBR and the modeling of buildings in DesignBuilder.

**Table 25 - Selected cities TMY climate files used in the thesis**

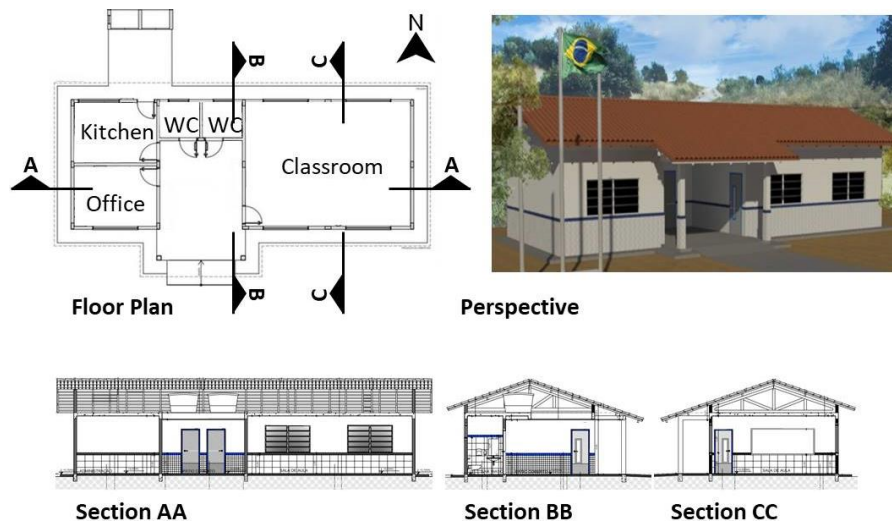
Zone	City (State)	Weather Data File
1	Caxias do Sul (RS)	BRA_RS_Caxias .do.Sul.839420_TMYx. epw
2	Nova Friburgo (RJ)	BRA_RJ_Nova .Friburgo.868890_TMYx. epw
3	Florianopolis (SC)	BRA_SC_Florianopolis .838970_TMYx. epw
4	Brasilia DF)	BRA_DF_Brasilia .867150_TMYx. epw
5	Santos (SP)	BRA_SP_Santos .837820_TMYx. epw
6	Goiania (GO)	BRA_GO_Goiania .867340_TMYx. epw
7	Picos (PI)	BRA_PI_Picos .819080_TMYx. epw
8	Belém (PA)	BRA_PA_Belem .816800_TMYx. epw

Source: adapted from ABNT (2005a) and Climate One Building (2022).

The reference cities of each Brazilian bioclimatic zone mentioned in ABNT (2005a) are selected for this study. According to the regulation, the most representative city of Zone 2 is Ponta Grossa (PR), but due to the lack of climate data on the Climate One Building platform (2022), the city of Nova Friburgo (RJ) is chosen, which is also part of the group 2.

The study focuses on a standardized 1 classroom public school of FNDE (Figure 45). The architectural and constructive data used in the pilot simulations are those explained in the chapter describing FNDE standard schools: Buildings characteristics.

**Figure 45 - Standardized 1 Classroom School Floor Plan, Perspective and Sections**



Source: Adapted from FNDE (n/d).

The orientation was north-south solar as suggested by FNDE (n/d). As for the occupation schedule, the months from February to June and from August to December in classrooms, from 8:00 am to 12:00 pm and from 2:00 pm to 6:00 pm were considered, the same of previous simulations of Brazilian school buildings (GERALDI; GHISI, 2022a).

In the simulations, soil temperatures were calculated with Kiva Basic, as it is a suitable tool for simulating smaller buildings. This is an open source tool, developed by Big Ladder Software, which is integrated into DesignBuilder and performs two-dimensional finite difference calculations to represent the heat flux between a zone and the adjacent ground. These calculations can be performed quickly and accurately (based on zone temperatures and radiation, meteorological data and solar position) without any noticeable loss of accuracy compared to a three-dimensional simulation (KRUIS; KRARTI, 2015; KRUIS; KRARTI, 2017 *apud* DESIGNBUILDER HELP, 2022). On one hand, operative temperatures are estimated based on zone setpoints, on the other hand, meteorological data and solar position are defined from input information. An insulation layer on the floor is not specified, as this material is not part of the FNDE standardized school buildings. The Kiva foundation was set up in the initial simulation as shown in Table 26.

**Table 26 - Kiva Foundation Settings**

Kiva FoundationSettings		unit	Value	Source
Soil Thermal Properties	Soil Conductivity	W/m. K	1.28	Default of DesignBuilder
	soil density	kg/m <sup>3</sup>	1460.00	
	soil specific heat	J/ Kg. K	880.00	
Surface Properties	Ground solar absorptivity	-	0.8200	Ferreira, Pereira and Labaki (2021)
	Ground thermal absorptivity	-	0.9840	
	Ground surface roughness	m	0.03	DesignBuilder Help (2022)
Extent	far-field width	m	40.00	Default of DesignBuilder
	deep-ground depth	m	autocalculate	
Options	Minimum cell dimension	m	0.02	Default of DesignBuilder
	Maximum cell growth coefficient	-	1.50	
	simulation timestep	1-hourly		
	Deep-ground boundary condition	1-Autoselect		

Source: Authors.

The soil thermal properties are the DesignBuilder's default values of “earth common”. The surface properties adjacent to the building is grass, with absorptivity values according to studies of Ferreira, Pereira and Labaki (2021) and roughness as suggested by DesignBuilder Help (2022) for grassy areas. All the other information was maintained as per the software default.

The input data described in Table 26 of Soil Thermal Properties and Surface Properties of adjacent external ground, parameters highly influential in the thermal distribution of the soil, are utilized by Kiva Basic to calculate the ground temperature under the building within a width of up to 40 meters. This is done by the software to obtain more realistic data on heat gains and losses through the building ground floor and the thermoenergetic performance results. Due to the horizontal shape of the one-classroom school under and the large area of the building in contact with the ground, associated with the architectural school standard of FNDE of lacking thermal insulation in the floor, this accurate calculation of the ground temperature beneath the building performed by Kiva Basic provides more reliable results for this thesis than other methods available in DesignBuilder, such as Ground Domain.

### Optimization objective definition

The objectives of this study are thermal comfort and low energy consumption, as well as ease of replication of the solutions in different regions of Brazil, with reduced interventions to the original standardized architecture projects. In this thesis, all rooms of all schools are modeled, but only classroom is thermally evaluated, which is the most important space in the school and has the highest occupancy



(consequently, these spaces are more critical in relation to thermal comfort in cooling dominated cities). The building was modeled with DesignBuilder Version 7.0.2.4 graphical interface and later simulated with the software's EnergyPlus engine.

The low energy consumption in this thesis is guaranteed by limiting the climatization of the occupied spaces to passive strategies and natural ventilation only. This limit also provides a future low operational cost of the buildings.

Regarding thermal comfort, the ASHRAE 55 adaptive model is adopted with 80% acceptability as a method of calculating occupant comfort. This method is recurrent in international research, is used in the calculations of the Brazilian Labeling Program – PBE Edifica (ELETROBRÁS *et al.*, 2021) and it was also the method used in previous research on comfort in standardized FNDE schools (LOPES, 2020).

PBE Edifica is regulated by the Normative Instruction Inmetro for the Classification of Energy Efficiency of Commercial, Service and Public Buildings – INI-C/2021, which explains the criteria and methods for the classification and labeling of Brazilian public buildings. This normative informs that naturally ventilated buildings without an artificial conditioning system must provide a percentage of occupied hours in thermal comfort equal to or greater than 90% during the hours of use of the building and the maximum tolerance of 10% refers only to heat discomfort (ELETROBRÁS *et al.*, 2021). It means that cold discomfort is disregarded in the calculation, which represents a problem in cold cities. Although most of the Brazilian territory has predominantly warm climates, 86.3% according to ABNT (2005a), there are also some cities with lower temperatures that are vulnerable to cold discomfort.

The main objective function of the optimization process in this thesis, therefore, is thermal comfort, with a maximum tolerance of 10% of occupied hours in discomfort due to heat (as suggested by INI-C/2021) and 10% of occupied hours in discomfort due to cold. This means that of the 1560 hours of annual occupation of the classroom in schools, there should be a maximum of 312 hours of discomfort: 156 of discomfort due to heat and 156 of discomfort due to cold.

### **Pilot simulation, selection of scenarios and key points**

The first step was an initial run of simulation of the 1 classroom school model in all 8 bioclimatic zones for verification of the thermoenergetic performance of current state buildings. Based on the internal operative temperature and external dry bulb temperature outputs from DesignBuilder, it was possible to verify the hours occupied in comfort by the adaptive comfort method of ASHRAE 55 with 80% acceptability.

The data of occupied hours in comfort of the current model allowed the identification of 3 different climatic groups: zones 1, 2 and 3 with predominant discomfort due to cold (above 10% of occupied hours) and predominant needs for heating strategies; zones 4, 5 and 6 with predominant heat discomfort (above 10% of occupied hours) with predominant cooling needs; and zones 7 and 8 with critical heat discomfort (above 70%) with extreme cooling needs. These three groups, considered as optimization scenarios, were called heating-dominated zones, cooling-dominated and extreme-cooling-dominated zones. This classification, concurrently founded on external conditions of each location and the thermal performance of the reference school building, relies on a method suggested in previous studies of the International Energy Agency (IEA) (CORY *et al.*, 2011).

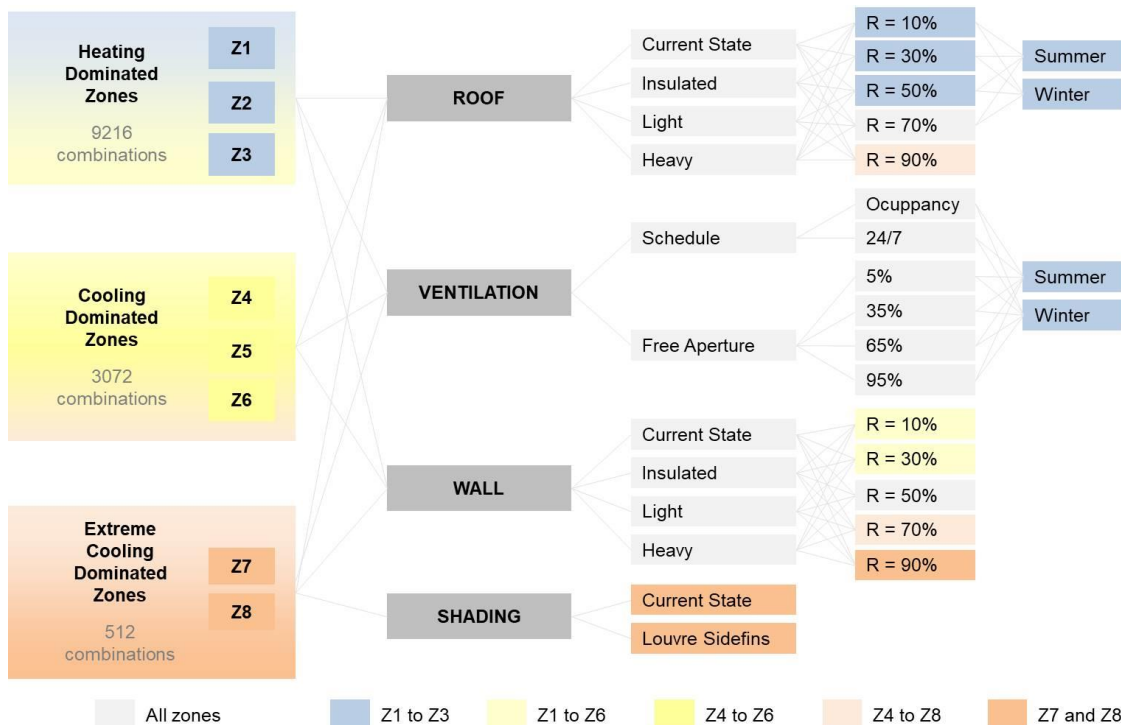
Subsequently, an assessment of the variables of greatest impact was made. According to Hens (2012), the static heat transfer coefficients as thermal transmittances do not exactly reflect the reality, since the heat exchanges are influenced by the transient temperature regime throughout the day and seasons of the year and the thermal gradient of the building surfaces. Therefore, a common technique to find the correct answer to a thermal discomfort problem is the evaluation of heat balances (HENS, 2012). DesignBuilder's heat balance output has also been used in previous optimization research (XIE *et al.*, 2022) as a key instrument to identify transient heat transfer results and investigate building energy performance.

In this thesis, annual and daily heat balance in each zone were evaluated to understand the thermoenergetic behavior of the building during the year. Two representative days were selected, one typical of winter (June 21) and the other typical of summer (December 5). Representative operative days were chosen according to the Brazilian school calendar, which at the same time were close to the summer and winter solstices. As suggested by Hens (2012), surfaces and elements that present the most influence on the heat flux were checked: opaque envelope

assemblies (roof, external walls and ground floor), Window solar gains, opaque partitions and internal gains (lighting, equipment and occupancy).

From the analysis of heat balances, the roof was identified as the main responsible for annual gains in all zones and window solar gains the second. Ventilation is the biggest cause of losses in all zones, followed by external walls. The last variable with a significant influence on the heat fluxes is the ground floor. So, three most influential variables were chosen as key points for the optimization process: Roof, Ventilation and Walls. Local shading on windows can compromise natural light in interior spaces, so it was a variable to be optimized only in the most critical cases of heat discomfort (Zones 7 and 8) to reduce window solar gains. Figure 46 shows the summary of variables and possible combinations of the algorithmic optimization process.

**Figure 46 - Variables and possible combinations of the algorithmic optimization process**



Source: Authors.

No changes were proposed to the geometry (floor plan) design and window-to-wall ratio, with the aim to avoid significant changes to the standardized architectural project. Other parameters were also considered fixed: composition of the internal

ground floor, internal partitions and the transparent envelope (type of glass of the windows).

According to the previous systematic literature review on supercool materials, spectrally selective materials would be the most suitable for zones 4 to 7 and high broadband emissivity for zone 8. However, in DesignBuilder it is not possible to input different emissivities in specific ranges of the spectrum (FENG *et al.*, 2022b), consequently, the emissivity of super cool materials are not differentiated in the simulations and a 90% value was adopted in all cases of supercool materials. Considering that the cool materials are coatings and their key properties are high reflectivity and high emissivity, in this thesis these materials were evaluated in different Brazilian climatic contexts by variations only in the external reflectivity of the building (Table 27). The same values were considered for solar and visible reflectivities.

**Table 27 - Settings of Super Cool Coatings (Paints) tested in each Climatic Group**

Climatic Group		Zone	Cool Coating (Paint)	Solar and Visible Reflectivities
Extreme-cooling Dominated	Humid	8	High Broadband Emissivity	90%
	Dry	7	Spectrally Selective	
Cooling-dominated		6		
		5		
		4		
Heating-dominated		3	Thermochromic	
		2		
		1		

Source: authors.

In order to test different possibilities of thermoenergetic behavior of the building and understand the ideal substrate for the application of cool materials in different climates, options of different thermophysical properties for the roof and the wall were evaluated: compositions of the current model, insulated compositions (with high thermal resistance), light compositions (low thermal resistance and low thermal capacity) and heavy compositions (high thermal capacity), with reflectivities ranging from 10 to 90% depending on the climate group (Figure 47).

**Figure 47 - Details of variables tested in optimization simulations**



Source: Adapted from ProjetEEE (n/d).

It was decided to test the most common homogeneous or heterogeneous envelope compositions in Brazil (WEBER *et al.*, 2017). The insulated composition of the roof with steel tile filled with polyurethane was chosen because it is already used in other models of larger FNDE standardized schools (FNDE, n/d). The insulated wall was chosen from Weber *et al.* (2017). To avoid costly solutions, compositions with aluminum or rock wool were discarded. After this filter, the wall option with the lowest transmittance was selected. Concrete was tested for light and heavy roof and wall compositions because it is a recurrent constructive solution in Brazil. For the light roof, a thickness of 5 cm was chosen because it is the minimum value recommended for roof slabs according to Brazilian regulations for concrete structures (ABNT, 2014).

The reflectivities varied according to the climatic group. On the roof of the schools in heating dominated zones, thermochromic paints were tested. Thermochromic materials cannot be configured directly in DesignBuilder simulations and to consider them in thermoenergetic performance calculations, it is necessary to write an Energy Management System – EMS code. Due to the time limitation of this thesis, the variable reflectivity option was simulated with different reflectivity values in two

different periods of the year (low reflectivity in the cold months and high reflectivity in the warm months). Options from 10 to 70% were tested in summer (November to April) and winter (May to October) separately, in order to identify an optimal value per season. Paints from 10 to 50% reflectivity were tested on the walls to identify a single optimal wall solution, without thermochromic properties.

On the roof of the cooling dominated zones, reflectivities of 70 and 90% were tested in order to obtain an optimal solution to reduce excessive heat gains through the roof. Wall reflectivities from 10 to 70% were tested.

In the extreme cooling dominated zones, only 90% of reflectivity were tested for roof and walls, since these are cities with extremely high heat discomfort and require very efficient cooling strategies. This is the only group where local shading was simulated, with louvres and sidefins of 90% reflectivity. This choice allows more accurate cooling optimization results and reduced computational simulation time demand. Horizontal (35°) and vertical (20°) angles were calculated with Sol-ar Analysis software to avoid direct solar radiation in the two cities (APPENDIX C).

As also suggested by ABNT (2005a), the different reflectivity percentage ranges of each climate group had the following objectives: to favor passive winter heat gains in heating dominated zones; provide heat gains in winter, avoid glare and excessive gains in summer in cooling dominated zones; prevent the greatest possible amount of gains and potentiate heat losses in the extreme cooling dominated zones.

As for ventilation, in each climate group the optimal solution was sought with two operation schedule options (during occupancy and windows open 24 hours 7 days a week) and 5 opening stages between 5 and 95%, which are compatible with the tilting window specified in the original building project. Specifically in heating dominated zones, these ventilation variables were tested twice: for summer and for winter.

### **3.1.2 Algorithm Optimization Simulations**

The optimization process involved three steps: algorithm settings, optimization simulations and interpretation of thermal comfort, heat balance and sensitivity analysis results.

## Algorithm settings

In the optimization simulations of all climatic groups, the JEA algorithm option was selected, which is a more powerful optimization engine than OpenBeagle, available in previous versions of the software (DESIGNBUILDER HELP, 2022). This algorithm was also used in several recent international studies on thermoenergetic optimization of buildings (NADERI *et al.*, 2020; ZHAO; DU, 2020; NAJI; AYE; NOGUCHI, 2021; BAGHOOLIZADEH *et al.*, 2023). The JEA uses a genetic operator that generates more efficient descendants through the crossing method.

The simulations were annual for cooling-dominated and extreme-cooling-dominated zones and separate periods of summer (November to April) and winter (May to October) for heating-dominated zones. The maximum generations were chosen according to the maximum number of variable combinations. 512 generations were the maximum for extreme cooling dominated zones, 3,072 for cooling-dominated and 4,608 for heating-dominated zones per period.

To ensure that the most important solutions were tested, in all climatic groups the generations for convergence were 100, which is the maximum value allowed. According to the DesignBuilder Help (2022) the maximum initial population size is 500. The other parameters were set as suggested by the software manual (DESIGNBUILDER HELP, 2022): crossover rate of 1.0, mutation rate of 0.4, tournament size 2 and objective bias 0 (Table 28).

**Table 28 - Summary of optimization algorithm settings**

Calculation Options	Climatic Group		
	Heating Dominated Zones	Cooling Dominated Zones	Extreme Cooling Dominated Zones
Simulation Periods	1 Nov to 30 Apr 2 May to 31 Oct	1 Jan to 31 Dec	
Maximum Generations and Evaluations	4,608 per period	3,072	512
Initial Population Size	500		
Generations for Convergence	100		
Mutation Rate	0,4		
Crossover Rate	1,00		
Tournament Size	2		
Objective Bias	0		

Source: Authors.

## Thermal Comfort Analysis

Thermal Comfort Analysis involved 2 steps: 1. verification of the achievement of the optimization objective (maximum 10% of occupied hours in thermal discomfort due to cold or heat); 2. identification of the thermal comfort increase of the optimized model in relation to the original model.

The percentages of occupied hours in thermal comfort were calculated using the adaptive method of 80% acceptability from ASHRAE 55, as well as in the initial simulations of the preparation stage of the optimization process.

The two steps were essential for verifying the achievement of the optimization objective in each Brazilian bioclimatic zone.

### **Heat Balance Analysis**

The Heat Balance Analysis proceeded in 2 steps: 1. identification of changes in annual and daily heat balances in relation to the original model; 2. Heat balance analysis on a typical summer and winter day of the optimized model, individually varying roof and external wall compositions.

Comparison of the heat balances of the optimized model with the results of the original model allows the evaluation of the change in heat fluxes during the year and in daytime and nighttime on typical summer and winter days. Based on this comparison, it is also possible to identify the main factors responsible for the optimized results of occupied hours in thermal comfort.

The comparison of heat balance graphs resulting from the variation of only the roof and wall substrates (original, light, insulated and heavy) in the optimized model allows the identification of the thermal behavior of the building in each case and the behavior of the ideal substrate of the standardized Brazilian school.

### **Sensitivity Analysis**

The Sensitivity Analysis occurred in two steps: 1. Sensitivity analysis of variables (comparison between original and optimized settings of roof, walls, ventilation and shadings) and 2. Sensitivity Analysis of roof and walls reflectivities in the optimized model.



Sensitivity analysis are important for a proper understanding of the relationship between design variables and the objective. This step was performed with DesignBuilder using the highly efficient Latin Hypercube Sampling – LHS (DESIGNBUILDER HELP, 2022) and which has been used in previous studies of Brazilian standardized public schools (LOPES, 2020).

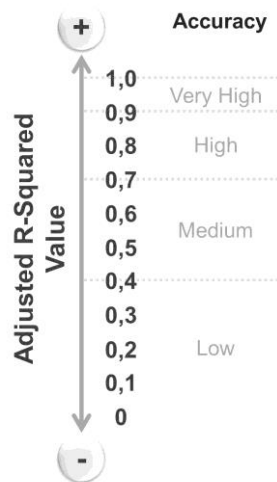
The first step of the Sensitivity analysis focused on variables (roof, walls, ventilation and shadings). In this case, the settings of the original school and the final optimized model were compared. These simulations allowed the identification of the most impactful final passive strategy in the occupied hours in thermal comfort in relation to the original standardized school model.

The second step of the Sensitivity analysis assessed the influence of cool materials on the thermal comfort of schools located in each bioclimatic zone by reflectivity variations of roof and walls. As cool materials are coatings, this analysis was carried out considering the final composition of roof and wall materials, ventilation (for all zones) and shading (for the extreme cooling dominated zones) of the optimized model, with only a variation of reflectivities from 10 to 90% of roof and external walls.

According to DesignBuilder Help (2022), the number of runs can be 10 to 20 times the number of variables. Therefore, 200 simulations were run per zone per sensitivity analysis.

In sensitivity analysis results, the higher the Standardized Regression Coefficient – SRC, the greater the relative influence of the variable on thermal comfort (DESIGNBUILDER HELP, 2022). The reliability of the final results are based on Adjusted R-Squared values and p-values (Figure 48).

**Figure 48 - Adjusted R-squared Value Accuracy in Sensitivity Analysis**



Source: DesignBuilder Help (2022).

The p-values are reliable when  $<0.05$ . However, it is common to obtain p-values above the acceptable for variables with very low SRC. In these cases, it is still possible to identify the most impactful variables, as long as the Adjusted R-Squared is above 0.4.

### 3.1.3 Non-Algorithm Optimization Simulations

After algorithmic optimizations, only two of the 8 zones did not reach the optimization objective of maximum 10% cold or heat discomfort: zone 1 (Caxias do Sul – RS) with 15.4% of cold discomfort and zone 7 (Picos – PI) with 11.8% of heat discomfort.

Therefore, this stage involved two steps: 1. complementary non-algorithm simulations and 2. interpretation of comfort and heat balance results.

#### Complementary optimizations without Algorithm

In these two cases, Caxias do Sul (RS) from Zone 1 and Picos (PI) from Zone 7, the last most significant variable for optimization was explored, the ground. The school is horizontalized with only one floor, thus, there is a large surface in contact with the ground that influences building thermal losses and gains. The ground is also influenced by the surface coverage in adjacent areas of the building.

However, the DesignBuilder software and the JEA algorithm do not have the external ground as a possible optimization variable. In this way, an optimization without an algorithm was carried out by testing different reflectivities of the floors adjacent to the building: 30 and 50% for zone 1 and 90% for zone 7. An external concrete surface was considered, with values of emissivity (90%) and surface roughness (0.002) suggested by DesignBuilder Help (2022).

### **Interpretation of Results**

The final achievement of the optimization objective of maximum hours in discomfort were analyzed. Then, the heat balances were interpreted in representative days of summer and winter (same dates of the initial simulation) and in the annual period.

#### **3.1.4 Final Stage**

Finally, an optimal school model solution was synthesized by climatic groups and extreme zones, with high thermoenergetic performance provided mainly by cool materials and easy replication in the national territory.

### **3.3. Transformation of Optimized Schools in ZEB**

The task consisted of three fundamental steps: Simplified design of PV System; Simulations and verification of the impact of the PV system on thermal comfort; and Final Energy Balance Achievement, with a comparison of loads and energy production.

#### **3.2.1 Simplified design of PV System**

This step included monthly loads sizing, photovoltaic system dimensioning, photovoltaic system modelling.

#### **Monthly Loads Sizing**

After the optimization study of standardized public schools, it is considered that there is no need for artificial air conditioning to achieve thermal comfort. Therefore, the

consumption of buildings was calculated based only on information on lighting and equipment loads obtained in the literature review on FNDE standard schools.

The sizing of the monthly loads of each of the standardized projects was based on the same values used for the computational simulations to evaluate the thermoenergetic performance. The power density of the electrical equipment in the classroom was  $5\text{W}/\text{m}^2$ , as considered by Lopes (2020) and of other spaces, as identified by Geraldi and Ghisi (2020). These values were multiplied by the area of each school model and subsequently added to the total power of the lighting system (FNDE, 2023). The final power obtained was multiplied by the monthly hours of use of the building, in an operating schedule from Monday to Friday, from 8:00 am to 12:00 pm and from 2:00 pm to 6:00 pm, according to the official calendar published by the Ministry of Education and considered in the research by Geraldi and Ghisi (2020).

### **Photovoltaic System Dimensioning**

To achieve a positive on-grid energy balance, a simplified sizing of the photovoltaic system was carried out using the Neosolar online calculator to meet the energy demand of the three standardized models representative of Brazilian public schools from the FNDE. This tool provides reliable calculation results, comparable to internationally used professional software, such as PVSyst SA, PV\*SOL, Solarius PV and SOLergo (SANTOS, 2018) and has previously been used in other studies of building zero energy balance in a Brazilian context (QUEIROZ, 2019).

The Neosolar calculator requests the following input data: location (state/city), type of building use and average monthly value of the energy bill or estimated consumption in kWh/month (NEOSOLAR, s/d). The output sizing information are: system size in kWp, number of photovoltaic modules, estimated annual production in kWh and area required for installing the modules in  $\text{m}^2$  (NEOSOLAR, n/d).

### **Photovoltaic System Modelling**

After dimensioning the loads and the necessary photovoltaic system, the modules were modeled in the DesignBuilder software to verify the influence on the thermal

comfort of the classrooms and on the cooling effect of cool and supercool roof materials in all the 8 Brazilian bioclimatic zones.

The modules were added to the optimized school models of each zone with the photovoltaic solar collector design tool and with all the tool's software default data.

The photovoltaic system designed in DesignBuilder considered the system coupled to the building, with the flat solar panel represented by the upper surface of the PV rows drawn. The default material suggested by the software, Bitumen Felt, with the thermal properties described below (Table 29), was adopted.

**Table 29 - Bitumen Felt Thermal Properties**

<b>Thermal Bulk Properties</b>	<b>Values</b>	<b>Surface Properties</b>	<b>Values</b>
Conductivity (W/m.K)	0,23	Thermal Absorptance	0,9
Specific Heat (J/Kg.K)	1,000.00	Solar Absorptance	0,87
Density (kg/m <sup>3</sup> )	1,100.00	Visible Absorptance	0,87
<b>Vapour Resistance</b>	<b>Values</b>	<b>Radiance Daylighting</b>	<b>Values</b>
Vapour Factor	50000	Absorptance	0,87
Vapour Resistivity (MNs/gm)	10	Reflectance	0,13
		Specularity, Roughness, Transmissivity, Fraction diffused	0

Source: DesignBuilder (2022).

Also as a default, a PV Constant Efficiency of 0.15 was considered, with a fraction of the surface with active solar cells of 0.9, a fixed conversion efficiency input mode, a cell efficiency value of 0.15, a rated electric power output of 48,000.00 and an availability schedule On 24 hours, 7 days a week.

Additionally, as a default, the system adopted the decoupled heat transfer integration mode, where the cell temperature of modules in the array is computed based on an energy balance relative to Nominal Operating Cell Temperature - NOCT conditions. The default generator operation scheme type was the base load, operating the generators at their rated (requested) electric power output when scheduled on. This scheme requests all generators scheduled on (available) to operate, even if the amount of electric power generated exceeds the total facility electric power demand. The electrical buss type was also considered as direct current with inverter, which is the software's basic setting for photovoltaic.

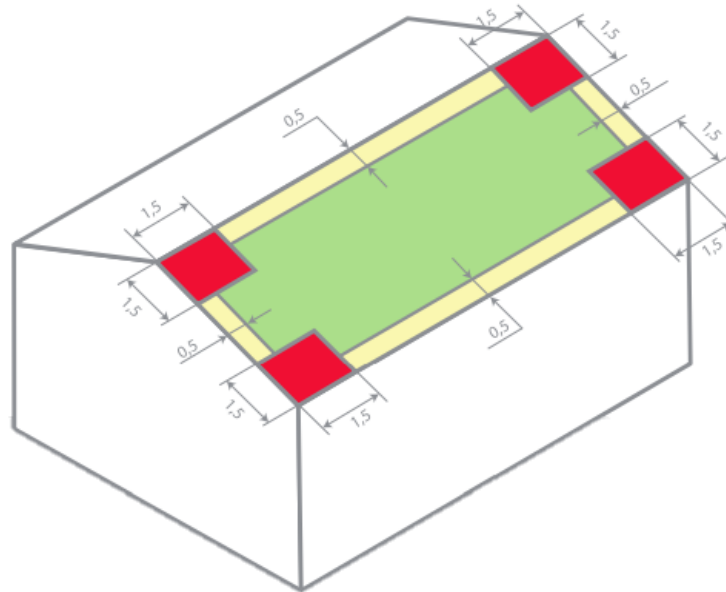
The sun's rays must reach the module perpendicularly (BYD ENERGY DO BRASIL, n/a; CANADIAN SOLAR, 2019), that is, the surface of the module must be facing the equator (IDEAL ESTUDOS E SOLUÇÕES SOLARES, 2019). Therefore, the angle of inclination should be approximately the average latitude of that country (IDEAL ESTUDOS E SOLUÇÕES SOLARES, 2019) or equal to the latitude of the location for optimal solutions (HUSSEIN *et al.*, 2004; MEHLERI *et al.*, 2010 *apud* IDEAL ESTUDOS E SOLAR SOLUTIONS, 2019).

According to IBGE (2023), the extreme points north and south of the Brazilian territory are respectively: +05° 16'19" Nascente do Rio Ailã (Roraima) and -33° 45'07" Arroio Chuí (Rio Grande do Sul). Thus, the average value of the country's latitude and consequently the appropriate inclination of the photovoltaic modules, is approximately 15°. This angle is also the minimum considered favorable for the self-cleaning effect caused by rain, which helps maintain the productivity of the system (CANADIAN SOLAR, 2019).

Specifically for this study, this fixed value of inclination of the modules was adopted for all Brazilian cities to facilitate the comparison of comfort data in classrooms in standardized projects located in different bioclimatic zones.

The positioning of the modules followed the recommendations of ESAF Solar (Figure 49), which recommends a minimum distance of 0.5m from the edges of the roof, avoiding corners in areas of 1.5m x 1.5m (IBRAP, n/d).

**Figure 49 - Recommendations for minimum ground clearances**



Source: IBRAP (n/d).

All the optimized models of the standardized schools have a flat roof with a concrete slab, therefore, according to IBRAP (n/d) it is necessary to use a support with a minimum thickness of 45 mm of Aluminum Alloy 6005-T6 (Figure 50). The supports must be at an average distance of 2.00 meters between them to resist the action of the wind.

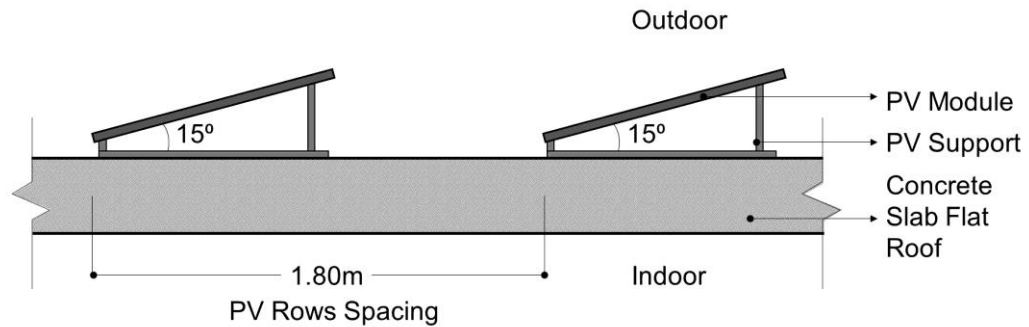
**Figure 50 - PV support suitable for flat roofs**



Source: IBRAP (n/d).

The panels were positioned in rows, with enough spacing to avoid shadows between them (Figure 51). Shading was checked individually for the latitude of each city with DesignBuilder Sunpath Tool (APPENDIX E).

Figure 51 - PV inclination and PV Rows Spacing



Source: Authors.

Considering that high temperatures in warm climates, such as those in Brazil, can negatively impact the efficiency of the PV system, the cooling solution was the consideration of supercool painting on the roof to reduce the ambient temperature around the modules. This approach aims to decrease the surface temperature, increase the reflected radiation received by the modules and simultaneously cool the indoor environments of the school, as suggested by Vasilakoupoulou *et al.* (2023).

Finally, it is emphasized that the proper planning of the PV system often relies on factors such as installation area, solar cell type and environmental conditions, including solar irradiation levels, geographical location and potential losses, as highlighted by Mussard and Amara (2018). Hence, the proposed modeling for simulations in this thesis avoided placing modules at the edges of the roof, assessed an appropriate distance between rows to prevent shading and energy production losses, adopted reliable standardized parameters for solar cell type from the DesignBuilder software and considered specific solar irradiation for each city by incorporating individual weather files into the computer simulations.

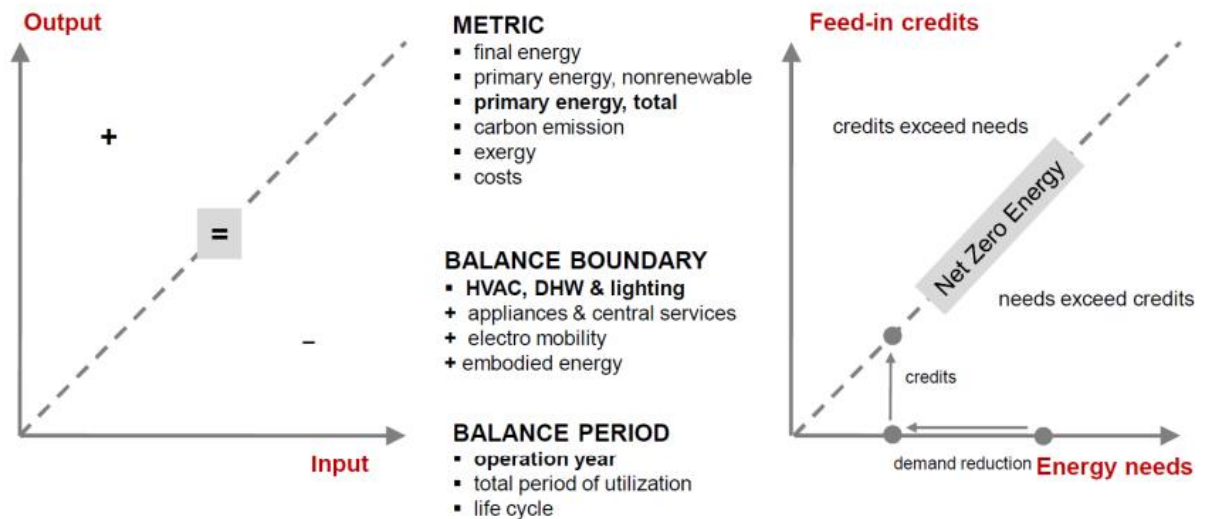
### 3.2.3 Energy Balance Achievement

For the final Energy Balance Achievement Analysis, a comparison of loads and local energy production was made by the PV System using DesignBuilder outputs and the graph proposed by IEA (2014), Figure 52. In this chart, the dashed line represents



zero energy balance. Above this line the energy balance is positive and below it is negative.

Figure 52 - Graph model for Energy Balance Achievement Analysis



Source: IEA (2014).

Among the parameters that can be considered in the different definitions of zero and positive energy buildings, for this thesis operation year was adopted as the balance period and final energy (end uses) as the energy balance evaluation metric.

### 3.4. Thermal Resilience and Passive Survivability Analysis

The thermal resilience and Passive Survivability analysis was structured in 2 steps:

#### 3.4.1 Thermal Resilience and Passive Survivability Assessment in TMY, 2050 and 2080:

- Current State standardized schools;
- Optimized standardized schools.

#### 3.4.2 Energy Balance Achievement including Thermal Resilience and Passive Survivability in TMY, 2050 and 2080:

- PV System Resizing;

- Comparison of loads and energy production.

In step 3.4.1, Standard Effective Temperatures are employed as a metric to assess thermal resilience and Passive Survivability. Indicators for the **resistance** and **robustness** phases were selected based on Siu et al. (2023), Attia et al. (2021), Ismail, Ouahrani and Touma (2023). Performance indicators for the **resistance** phase include:

- Frequency of occupied hours in thermal comfort;
- Frequency of occupied hours in thermal autonomy and passive survivability (summer), also called heat vulnerability.

For **robustness** indicators, the evaluation includes:

- Frequency of critical exceedance or dangerous heat (>40°C)
- Intensity identified by the annual maximum temperature
- Severity calculated by SET-hours in a summer week to observe compliance with the requirement of a maximum accumulated 240 °C SET-hours outside the range of 12.2 to 20°C SET in occupied hours.

Regarding the evaluation period, both long and short-time frame evaluations (annual and during hot weeks) (KRELLING *et al.*, 2023) are analyzed, considering historical (TMY) and projected future (2050 and 2080) weather files (MEHMOOD *et al.*, 2022; CIRRINCIONE; MARVUGLIA; SCACCIANOCE, 2021) generated by the FutureWeatherGenerator software, considering the SSP climate change scenarios, the most recently published in IPCC AR6. Finally, the SSP3-7.0 scenario is chosen, aligning with the selections made by Mehmood *et al.* (2022) and Cirrincione, Marvuglia and Scaccianoce (2021), representing a context of medium-high emissions.

In step 3.4.2, the previously proposed PV System was resized based on loads and local energy production outputs from DesignBuilder for the most critical overheating timeframe (2080), ensuring greater resilience to buildings in the long term. The final quantity of PV system modules was determined by climate group, based on the city with the highest cooling loads in each respective group.

In this case, simple HVAC was used in DesignBuilder, which calculates energy use involving space loads and the CoP value of the system. The input CoP was 3.78, the minimum value for A Label on the Brazilian Labeling Program (ELETROBRÁS, 2021). The Split HVAC template was also considered, which is the model used in other standardized school models from FNDE (n/d).

In simple HVAC, operational control is managed through setpoints and schedules. The setpoint temperatures were based on air temperature, with a minimum of 12°C and a maximum of 26°C, as suggested by Tavakolin *et al.* (2022). The Autosize HVAC sizing method was selected, which calculates the flow rate limit through EnergyPlus, and finally, the mixed-mode natural ventilation (referred to as hybrid ventilation in EnergyPlus) was selected, preventing simultaneous natural ventilation and HVAC system cooling operation, allowing testing various ventilation strategies to maximize natural ventilation to reduce heating/cooling loads (DESIGNBUILDER HELP, 2022). Subsequently, a comparison of loads and local energy production was conducted using the graph proposed by IEA (2014).

## 4. RESULTS

In this topic are presented the results of the thesis.

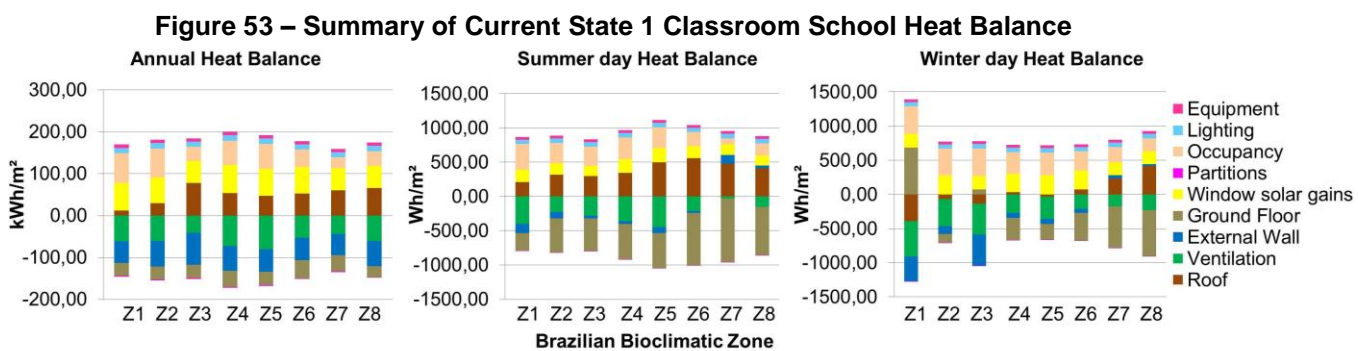
### 4.1. Pilot Simulation Results

The detailed results of percentage of occupied hours in thermal comfort and heat balance of classrooms in the 8 bioclimatic zones can be observed in the APPENDIX D. The most important data from the graphs of annual thermal comfort, main thermal gains and losses were summarized in Table 30 and Figure 53.

**Table 30 - Summary of occupied hours in comfort and discomfort and Heat Balance of Current State 1 Classroom School**

Zone	Annual Heat Discomfort (%)			Main annual heat gain	Main annual heat loss
	Annual Heat Discomfort (%)	Annual Comfort (%)	Annual Cold Discomfort (%)		
1	6,1	51,9	42	Roof Occupancy Windows	Ventilation Walls
2	7,9	76,5	15,6	Roof Windows Occupancy	Ventilation Walls
3	4,7	82,6	12,6	Roof Windows Occupancy	Ventilation Walls
4	18,4	79,9	1,7	Roof Windows Occupancy	Ventilation Walls Ground
5	21,1	76,9	2	Roof Windows Occupancy	Ventilation Walls
6	44,9	55	0,1	Roof Windows Occupancy	Ventilation Walls Ground
7	72,6	27,4	0	Roof Windows Occupancy	Ventilation Walls Ground
8	72,6	27,4	0	Roof Windows Occupancy	Walls Ventilation Ground

Source: Authors.



Source: Authors.

The 1 classroom schools located in zones 2 to 5 present most of the year in thermal comfort, with zone 3 being the most comfortable as they are milder climates with a greater predominance of air temperature and humidity within variations considered comfortable according to ABNT (2005a). The schools in zones 1, 2 and 3 tend to have more discomfort from cold than from heat, and the opposite happens for the other zones. Schools in zones 7 and 8 have long periods of heat discomfort and no periods of cold discomfort, so they are extremely hot.

The graphs of monthly variation of Percentage of occupied hours in comfort and discomfort show that in zones 1 to 3 and 5 (APPENDIX D), schools experience more significant percentages of heat from November to March, the period that includes Brazilian summer. This difference between summer and winter in the zones is clearer as these refer to cities of higher latitude. On the other hand, schools in zones 4 and 6 to 8 have more constant percentages of heat discomfort throughout the year.

In all bioclimatic zones, the roof is one of the main sources of annual heat gains, so it should be a priority intervention in all cases to reduce heat discomfort. Classrooms have windows on two opposite sides that facilitate cross ventilation, which is the main cause of heat loss.

In zones 1, 2 and 3, the greatest discomfort in winter is due to excessive thermal losses due to ventilation, so this must be a variable for optimization.

In zone 1, the walls and roof also provide thermal losses in winter due to the low external temperatures and due to low thermal insulation of the envelope. In this zone, the building ground floor is responsible for favorable thermal losses in summer and thermal gains in winter (APPENDIX D), as Brazilian schools do not have thermal insulation on the floor.

The roof, due to its low reflectivity (20%), is one of the main factors responsible for thermal gains in the summer in zones 1 to 4, causing discomfort due to heat. This part of the building is responsible for some thermal losses in the morning and for gains in the afternoon. In this second shift, the absorbed heat begins to enter the classroom (APPENDIX D).

Due to the latitude of cities 1, 2, 3 and 5 ( $29^{\circ}$ ,  $22^{\circ}$ ,  $27^{\circ}$  and  $24^{\circ}$  South respectively), window solar gains beneficially increase in the winter period, due to the higher incidence of solar radiation on the north façade (APPENDIX D). Therefore, the absence of local shading in the standardized school is favorable in these cities.

In zones 2 and 3 there is a high percentage of occupied hours in comfort in the summer period due to the well balanced heat gains and losses during the day.

Regarding cool materials, in zone 4, despite mild annual heat discomfort, heat gains and losses are balanced year-round in the occupancy period, hence the high annual

percentage of hours occupied in thermal comfort. In this zone, window solar gains slightly increase in the winter period, due to the intermediary latitude (16° South). In this case, cool materials on the roof can solve heat discomfort issues.

In zone 5, heat gains and losses are balanced during the winter occupancy period, hence the high percentage of occupied hours in comfort. In summer, there is a high heat discomfort because of the relatively high temperatures, above 24°C, associated with high humidity levels in the city during this period, above 84%. Cooling strategies and cool materials should be explored.

In zone 6, there is significant heat discomfort throughout the year, mainly due to relatively high temperatures, which on average are above 23°C, reaching up to more than 30°C in the hottest hours of the day. Cool materials on the roof can also be explored as a cooling strategy.

In zones 7 and 8 there is a very high heat discomfort (above 70%) due to high temperatures, generally above 25°C and 30°C. In zone 8, heat discomfort is further aggravated by high humidity, always above 80%. Maximum cooling strategies should be explored in these two zones.

In view of these results, the process of optimizing schools with 1 classroom in the 8 bioclimatic zones is developed.

## **4.2. Optimization Results**

The algorithm optimization results are presented through thermal comfort analysis, heat balance analysis and sensitivity Analysis.

### **4.2.1 Algorithm Optimization and Thermal Comfort results**

The results were divided by climate groups: extreme-cooling-dominated zones (7 and 8), cooling-dominated zones (4, 5 and 6) and heating-dominated zones (1 and 2). As the zones of greatest heat discomfort represent the majority of the Brazilian territory,

the results were presented in descending order (from zone 8 to zone 1). The description and comparison of heat balances on typical summer and winter days in all cities are in APPENDIX E.

### Extreme-Cooling-Dominated Zones (7 and 8)

Of the 512 maximum possible generations, 343 were sufficient according to the algorithm to obtain coherent optimal solutions. Hours occupied in thermal discomfort ranged from 164 to 976. The 3 options for minimum discomfort values (164 hours) were for the city of Belém (Zone 8). For the city of Picos (Zone 7), there were 2 optimal solutions with 312 hours of discomfort. In both cities, the best composition was with a heavy roof, windows open 24/7 with 95% opening for ventilation and window local shading.

In the city of Belém (Zone 8), the optimal solutions were obtained with 3 types of walls (current state, insulated or light) and in Picos (Zone 7) with the 2 types of walls (heavy or insulated). This variation only in the walls suggests that this is a variable that has little influence and that the reflectivity is less relevant for the comfort results. The insulated external walls are options common to both cities (Table 31).

**Table 31 - Optimal solutions for extreme cooling dominated zones**

City (Zone)	Discomfort (hours)	Wall	Roof	% Ventilation	Aperture Schedule	Local Shading
Belém (Z8)	164	Current State	Heavy R = 90%	95%	On 24/7	Louvre and Sidefins
		Insulated				
		Light				
Picos (Z7)	312	Heavy				
		Insulated				

Source: Authors.

**Table 32 - Worse solutions for extreme cooling dominated zones**

City (Zone)	Discomfort (hours)	Wall	Roof	% Ventilation	Aperture Schedule	Local Shading
Belém (Z8)	930	Insulated	Insulated	5%	Occupancy	No local shading
Picos (Z7)	976	Current State				
		Insulated				
		Heavy				

Source: Authors.

The combinations of greatest thermal discomfort both in Picos (976 hours) and in Belém (930 hours) were with the insulated roof, with no window local shading, openings of 5% for ventilation, restricted only to the occupancy period (Table 32). Thence, it is important to reduce solar gains through windows, provide as much ventilation as possible to maximize losses and avoid insulated roofs to allow heat to be released by the super cool roof.

The common optimal solution of this group was considered: insulated wall, heavy roof, windows open 24 hours a day with 95% openings for ventilation. Subsequently, it was evaluated individually occupied hours in comfort and thermal balance of the optimized model in Belém (Zone 8) and Picos (Zone 7) (APPENDIX E).

The thermal comfort optimization objective was reached only in Belém (Zone 8), with maximum discomfort of 7.3% due to heat and in Picos (Zone 7) it was almost reached, with 11.8% of discomfort. In Belém (Zone 8), the optimal solution obtained provided an increase of 63.3% in hours occupied in comfort and in Picos (Zone 7), 60.8%.

### Cooling Dominated Zones (4, 5 and 6)

Of the 3,072 maximum possible generations, 808 were sufficient according to the algorithm to arrive at the optimal solutions. Occupied hours in thermal discomfort ranged from 70 to 550. The 4 options of minimum discomfort values (70 hours) were for the city of Goiânia (Zone 6). There were 5 optimal solutions for Brasília (Zone 4), with 91 hours of discomfort and 5 for Santos (Zone 5) with 136 hours. In all three cities, the optimal solutions involved supercool roof with 90% reflectivity and 5%



ventilation openings (Table 33). The wall was the least influential variable in the comfort results.

**Table 33 - Optimal solutions for cooling dominated zones**

City (Zone)	Discomfort (hours)	Wall	Roof	% Ventilation	Aperture Schedule
Goiânia (Z6)	70	Current State R = 70%	Heavy R = 90%	5%	Occupancy
		Insulated R = 50%			
		Insulated R = 30%			
		Light R = 10%			
Santos (Z5)	91	Current State R = 70%	Heavy R = 90%	5%	On 24/7
		Current State R = 30%			
		Insulated R = 70%			
		Insulated R = 30%			
Brasília (Z4)	136	Current State R = 30%	Current State R = 90%	5%	Occupancy
		Insulated R = 70%			
		Light R = 50%			
		Light R = 30%			
		Heavy R = 10%			

Source: Authors.

**Table 34 - Worse solutions for cooling dominated zones**

City (Zone)	Discomfort (hours)	Wall	Roof	% Ventilation	Aperture Schedule
Goiânia (Z6)	550	Insulated R = 70%	Light R = 70%	5%	Occupancy
Santos (Z5)	423	Current State R = 10%			
		Insulated R = 10%			
		Light R = 70%			
		Light R = 30%			
Brasília (Z4)	372	Heavy R = 30%	Light R = 70%	5%	Occupancy
		Insulated R = 70%			
		Insulated R = 10%			
		Light R = 30%			
		Heavy R = 50%			

Source: Authors.

The combinations of greatest discomfort in all cities were with a light roof, with a 5 cm concrete slab (550 hours in Goiânia, 423 hours in Santos and 372 hours in Brasília). In Goiânia (Zone 6) and Santos (Zone 5), the second most uncomfortable thermal solution was the insulated roof, with 476 and 378 hours respectively (Table 34).

The optimal solution common to all cities in this group (composed of an insulated wall R = 50%, heavy roof R = 90% and windows with 5% openings for ventilation) was evaluated individually in the cities in relation to occupied hours in thermal comfort. Opening windows only during the occupancy in the simulation of Brasília and 24/7 opening in Santos (Zone 5) and Goiânia (Zone 6) were considered.

The optimization objective was reached in all of the three cities, with more than 90% of occupied hours in thermal comfort. The cities of Brasília (Zone 4) and Santos (Zone 5), which originally already had a high percentage of occupied hours in thermal comfort (above 75%), had a less expressive increase of 16.8% and 16.7% respectively. The city of Goiânia (Zone 6) had a more significant increase in thermal comfort after the optimization process (43%).

### Heating Dominated Zones (1, 2 and 3)

Of the 4,608 maximum possible generations of the summer period, 1403 were sufficient according to the algorithm to arrive at the optimal solutions. The hours of thermal discomfort ranged from 23 to 439. The 7 options for minimum thermal discomfort hours (23 hours) were for the city of Florianópolis (Zone 3). There were 4 optimal solutions for Nova Friburgo (Zone 2), with 63 hours of thermal discomfort and 4 for Caxias do Sul (Zone 1) with 115 hours. In the three cities, the optimal solutions involved a roof with 70% reflectivity and 5% ventilation openings. In the three cities, the wall was the least influential variable in the thermal comfort results. In the coldest city, Caxias do Sul (Zone 1), ventilation should only occur during occupancy hours, while in the other two (Nova Friburgo – Zone 2 and Florianópolis – Zone 3) it is more interesting to keep the windows open for 24 hours. The heavy roof was suitable for the two cooler cities while the original roof, which is slightly more insulated, was better for the colder city.

**Table 35 - Optimal solutions for heating dominated zones: Summer**

City (Zone)	Discomfort (hours)	Wall	Roof	% Ventilation	Aperture Schedule
Florianópolis (Z3)	23	Current State R = 30%	Current State R = 70%	5%	On 24/7
		Light R = 50%			
		Light R = 30%	Heavy R = 70%		
		Light R = 10%			
		Current State R = 30%			
		Heavy R = 30%			
		Heavy R = 50%			
Nova Friburgo (Z2)	63	Insulated R = 10%	Heavy R = 70%	5%	On 24/7
		Light R = 50%			
		Light R = 30%			
		Light R = 10%			
Caxias do Sul (Z1)	115	Current State R = 50%	Current State R = 70%	5%	Occupancy
		Insulated R = 10%			
		Light R = 50%			
		Heavy R = 10%			

Source: Authors.

**Table 36 - Optimal solutions for heating dominated zones: Winter**

City (Zone)	Discomfort (hours)	Wall	Roof	% Ventilation	Aperture Schedule
Florianópolis (Z3)	118	Current State R = 30%	Current State R = 70%	5%	Occupancy
		Current State R = 10%			
		Insulated R = 30%			
		Insulated R = 10%			
		Light R = 50%			
		Light R = 30%			
		Light R = 10%			
		Heavy R = 50%			
Nova Friburgo (Z2)	192	Current State R = 10%	Insulated R = 70%	5%	Occupancy
		Light R = 30%			
		Heavy R = 10%			
Caxias do Sul (Z1)	278	Insulated R = 10%	Insulated R = 70%	5%	Occupancy
		Light R = 50%			
		Light R = 30%			

Source: Authors.

**Table 37 - Worse solutions for heating dominated zones: Summer**

City (Zone)	Discomfort (hours)	Wall	Roof	% Ventilation	Aperture Schedule
Florianópolis (Z3)	413	Current State = 30%	Light R = 10%	5%	Occupancy
		Insulated R = 30%			
Nova Friburgo (Z2)	420	Insulated R = 50%			
		Insulated R = 10%			
		Heavy R = 50%			
		Heavy R = 30%			
Caxias do Sul (Z1)	439	Current State R = 50%			24/7
		Current State R = 10%			
		Light R = 30%			
		Heavy R = 30%			

Source: Authors.

**Table 38 - Worse solutions for heating dominated zones: Winter**

City (Zone)	Discomfort (hours)	Wall	Roof	% Ventilation	Aperture Schedule
Florianópolis (Z3)	419	Current State = 50%	Light R = 10%	5%	Occupancy
		Current State = 30%			
		Current State = 10%			
		Insulated R = 30%			
		Light R = 50%			
		Light R = 30%			
		Heavy R = 30%			
Nova Friburgo (Z2)	600	Current State R = 50%	Heavy R = 70%	95%	24/7
		Current State R = 10%			
		Insulated R = 50%			
		Light R = 10%			
Caxias do Sul (Z1)	704	Current State R = 50%	Heavy R = 70%	95%	24/7
		Current State R = 30%			
		Light R = 30%			
		Heavy R = 50%			
		Heavy R = 10%			

Source: Authors.

The combinations of greatest thermal discomfort during summer and winter in all cities were with a light roof, consisting of a 5 cm concrete slab (439 hours in summer and 704 in winter in Caxias do Sul (Zone 1), 420 hours in summer and 600 in winter in Nova Friburgo and 413 hours in summer and 419 in winter in Florianópolis).

The heavy roof is suitable in the summer for the cities of Florianópolis (Zone 3) and Nova Friburgo (Zone 2), while for Caxias do Sul (Zone 1), the current state roof, which is slightly more insulated, presents better results. In winter, more insulated roof options (current state and insulated) are more interesting to avoid excessive losses. Reflectivity of 70% was in all optimal roof solutions. The insulated walls, used in the optimized models of the other climate groups, also adapt to the heating dominated zones, with a reflectivity of 10%.

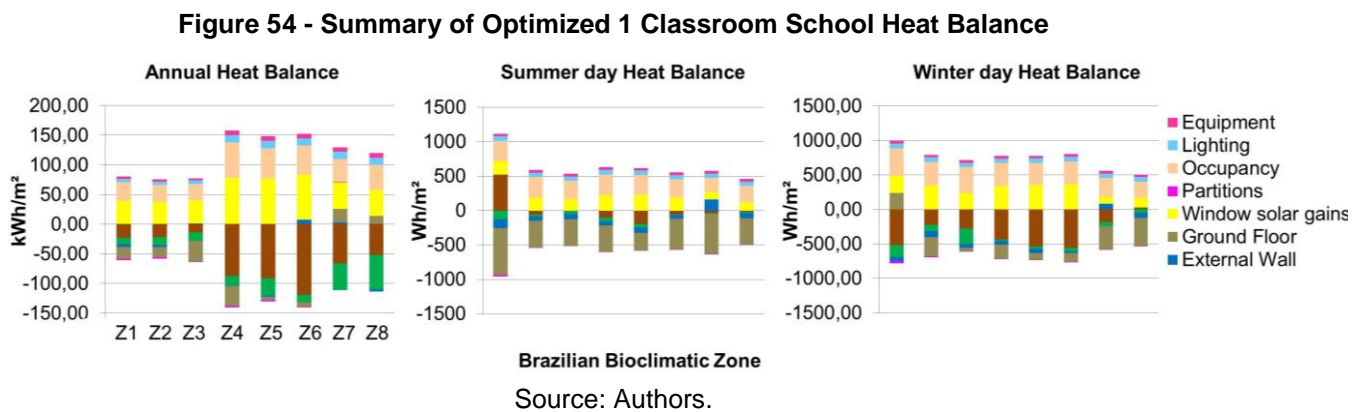
In order to maintain standardization of wall and roof compositions in all bioclimatic zones and favor the replicability of the model, the heavy roof and insulated wall were adopted, as well as cooling-dominated and extreme-cooling-dominated zones.

From the optimization results, the options with the fewest occupied hours in thermal discomfort were selected. The optimal model in this group consists of an insulated wall with 10% reflectivity, a heavy roof with thermochromic coatings (10/70% in Caxias do Sul and 50/70% in Nova Friburgo and Florianópolis), 5% window opening for ventilation. In Caxias do Sul (Zone 1), ventilation must only be during occupancy. In Florianópolis and Nova Friburgo, ventilation must be during occupancy in winter and 24/7 in summer. The thermal discomfort of this composition was 24 hours in summer and 122 in winter in Florianópolis (Zone 3), 63 in summer and 227 in winter in Nova Friburgo (Zone 2) and 131 in summer in Caxias do Sul (Zone 1).

The target objective was reached only in two cities, with maximum of 4,4% of occupied hours in thermal discomfort due to heat and 2,3% due to cold in Nova Friburgo, 0,4% due to heat and 1,5% due to cold in Florianópolis. The cities of Florianópolis (Zone 3) and Nova Friburgo (Zone 2), which originally already had a high percentage of occupied hours in thermal comfort (above 75%), had a less expressive increase of 15.5% and 16.8% respectively. The city of Caxias do Sul, which originally had greater discomfort due to the cold, had more significant increase in thermal comfort after the optimization process (34.3%).

#### 4.2.2 Heat Balance Results: Optimized 1-Classroom School Model

The optimal solution common to all cities was evaluated individually in relation to heat balance. The detailed description and comparison of heat balances on typical summer and winter days in all cities resulting from each material of roof and walls are in APPENDIX H. Figure 48 shows the summary of annual, summer and winter days heat balances Optimized 1 Classroom School.



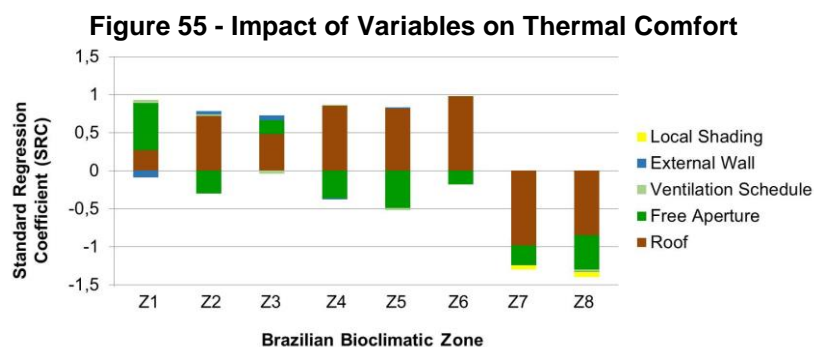
The daily thermal balance of extreme-cooling-dominated zones (7 and 8) shows that, both in summer and in winter, the main factors responsible for thermal losses during the day are: the ground floor (due to the grass cover of the ground adjacent to the building), the wall and the roof covered by the super cool material. The ground floor has a great influence on the thermal balance due to the horizontality of the building and the larger area in contact with the ground. Ventilation is a heat loss strategy, mainly in the morning and in winter, when external temperatures are not very high. Specifically in Belém (Zone 8) during the winter, night ventilation provides thermal losses during the night, quickly eliminating the heat accumulated during the day inside the classroom.

The daily heat balance of cooling dominated zones (4, 5 and 6) shows that in summer the ground is the main responsible for thermal losses, followed by roof and walls. In winter, the roof excels in heat losses. In this case, the (original) grass cover of the ground adjacent to the building and the super cool material on roof are the most efficient cooling strategies.

The daily heat balance of heating dominated zones (1, 2 and 3) shows that roof and the ground floor are the main responsible for thermal losses. The variable reflectivity of the thermochromic roof helps reduce thermal losses in winter.

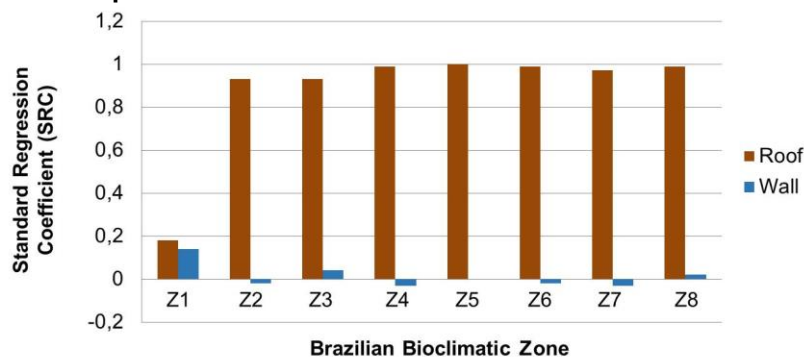
### 4.2.3 Sensitivity Analysis Results

Next, sensitivity analysis that show the impact of passive solutions and cool materials on thermal comfort are presented. Results of the influence of variables (roof, walls, ventilation and shadings) of occupants thermal comfort in all the 8 climates are illustrated in Figure 55 and findings of the effect of cool materials and reflectivities are indicated in Figure 56. Detailed results of sensitivity analyzes in each bioclimatic zone are in APPENDIX F. The results of the sensitivity analysis of Florianópolis (Zone 3) passive strategies and Caxias do Sul (Zone 1) reflectivities had Adjusted R-Squared below 0.4, therefore, it is not possible to obtain definitive conclusions regarding the most impactful variable.



Source: Authors.

**Figure 56 - Impact of Cool Materials and Reflectivities on Thermal Comfort**



Source: Authors.

The sensitivity analysis of the passive solutions in all cooling dominated zones (4 to 8: Brasília, Santos, Goiânia, Picos and Belém) shows that the roof coated by cool

material is the most impactful element in comfort, followed by the percentage of window openings for ventilation.

The sensitivity analysis of the passive solutions in heating-dominated zones shows that in Nova Friburgo (Zone 2) as in previous climate groups, the roof paint is the most impactful element in comfort, followed by the percentage of window openings for ventilation. In Caxias do Sul (Zone 1), where there is greater thermal discomfort due to cold, the percentage of window openings is more influential.

As the influence of cool materials of 90% of reflectivity on the thermal comfort of extreme-cooling-dominated and cooling-dominated zones, their application on the roof is extremely important for the adequate results and to provide the necessary thermal losses in the extreme-cooling-dominated zones. In These cities, the cool materials on the wall has little influence, as it receives a much smaller amount of solar radiation and because it is associated with an insulated wall. However, in extreme-cooling-dominated zones, wall reflectivities below 70% compromise the achievement of the optimization objective. Therefore, although the reflectivity of the walls is less impactful than the roof, they are also important for the final optimization results.

As for the influence of cool materials and the reflectivity on the thermal comfort in heating dominated zones, the results for Florianópolis (Zone 3) and Nova Friburgo (Zone 2) are similar to those of the climate group analyzed previously: the reflectivity of the roof has greater influence on results of thermal comfort than that of the walls.

#### **4.2.4 Heat Balance Results: Roof and Wall Substrate Variations**

The comparison of heat balance graphs resulting from the variation of only the roof and wall substrates (original, light, insulated and heavy) in the optimized model in each climatic group is shown below.

The summary of the performance of each composition in the three climate groups (extreme cooling dominated, cooling dominated and heating dominated zones) are represented in table format. For each group, the best composition was presented on the left and the worst on the right.

**Table 39 - Comparison of heat balances due to roof composition variations of 1 classroom school**

Group	Zone	Roof Type			
		Heavy	Original	Insulated	Light
Extreme Cooling Dominated Zones	Z8	High thermal losses in the morning and afternoon and low thermal gains in the evening during the year.		Low thermal losses in the morning and low thermal gains in non-occupied hours during the year.	Low thermal losses in the morning and high thermal gains in the afternoon. In Picos, the afternoon thermal gains are higher in summer than in winter.
	Z7				
Cooling Dominated Zones	Z6	High thermal losses in occupied hours during the year, specially in winter. Heavy roof provide more thermal losses in the afternoon than the original option.		Low thermal losses during occupied hours in winter and only in the morning in summer. Low thermal gains in non-occupied hours in summer.	In Summer, thermal losses only in the morning and high thermal gains in the afternoon, specially in Goiânia (warmer city). In winter, high thermal losses all times.
	Z5				
	Z4				
Heating Dominated Zones	Z3	Thermal losses in occupied hours and thermal gains in the evening during the year. Thermal losses are little higher with heavy roof.		Low thermal gains in summer and low thermal losses in winter in the 3 cities.	High thermal gains in summer and high thermal losses in winter. In Caxias do Sul there is a greater variation in thermal gains and losses during summer occupancy hours.
	Z2				
	Z1				

Best Option ←—————→ Worse Option

**Table 40 - Comparison of heat balances due to wall composition variations of 1 classroom school**

Group	Zone	Wall Type			
		Insulated	Heavy	Original	Light
Extreme Cooling Dominated Zones	Z8	High thermal losses in the morning and afternoon	Thermal losses in the morning and afternoon and significant thermal gains in the evening during the year.	Thermal losses only in the morning and high thermal gains in the evening during the year.	
	Z7	and low thermal gains in the evening during the year.	In summer, almost no thermal losses associated with thermal gains during non-occupied hours. In winter, thermal losses mainly in the afternoon.	In summer, thermal losses in the morning, thermal gains in the afternoon and high thermal gains in the evening. In winter, thermal losses only in the morning.	
Cooling Dominated Zones	Z6	Thermal losses in the morning and afternoon and thermal gains in the evening during the year. Insulated walls provide less thermal gains than the heavy option.		Thermal losses only in the morning and high thermal gains in the afternoon and evening during the year. Light walls provide little more thermal gains than the original option.	
	Z5				
	Z4				
Heating Dominated Zones	Z3	Thermal losses in occupied hours and few thermal gains in unoccupied hours throughout the year. The insulated option provides less nighttime gains in summer and less thermal losses during occupied hours in winter. In Caxias do Sul, the insulated wall is the one that provides the lowest thermal losses.		Thermal gains in summer afternoons and thermal losses in winter occupancy period. Light walls provide more thermal flux during the year.	
	Z1			Thermal gains in the morning and thermal losses in the afternoon in summer. The opposite occurs in winter: thermal losses in the morning and thermal gains in the afternoon.	
	Z2				

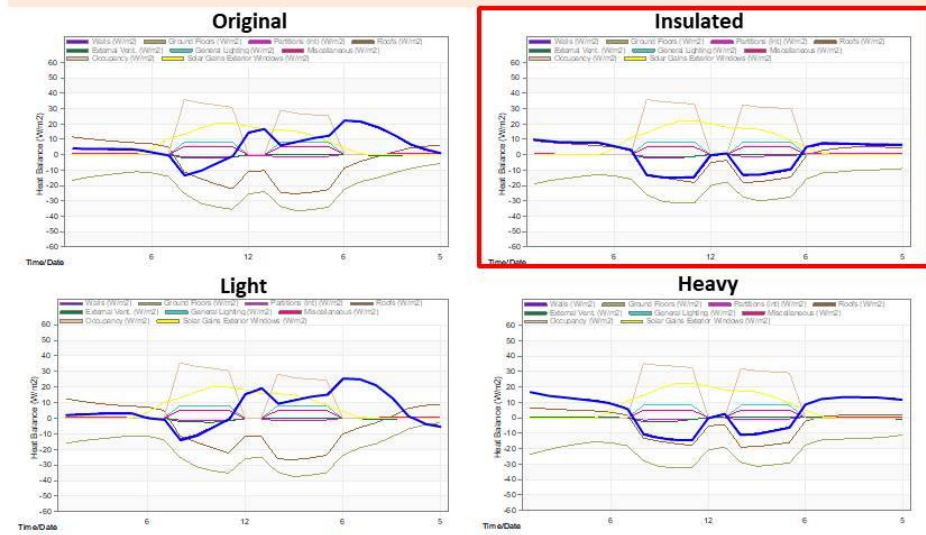
Best Option ←—————→ Worse Option



The highlights of the thermal behavior described in the tables can be observed in the heat balance graphs below considering the optimized model of the school with variations only in wall type and then only in roof type. Figure 57 shows variations in wall type with an example of Goiânia (Zone 6, Cooling-Dominated) on a Summer Representative Day and Caxias do Sul (Zone 1, Heating Dominated) on a Winter Representative Day. Figure 58 shows variations in roof type with an example of Belém (Zone 8, Extreme-Cooling-Dominated) on a Summer Representative Day and Caxias do Sul (Zone 1, Heating Dominated) on a Winter Representative Day. In all cases, the insulated wall is the best solution due to small thermal gains in summer and small losses in winter.

**Figure 57 - Variations in Wall Type**

**Example of Goiânia Summer Wall Type Variation (Zone 6, Cooling Dominated) in a Summer Representative Day**

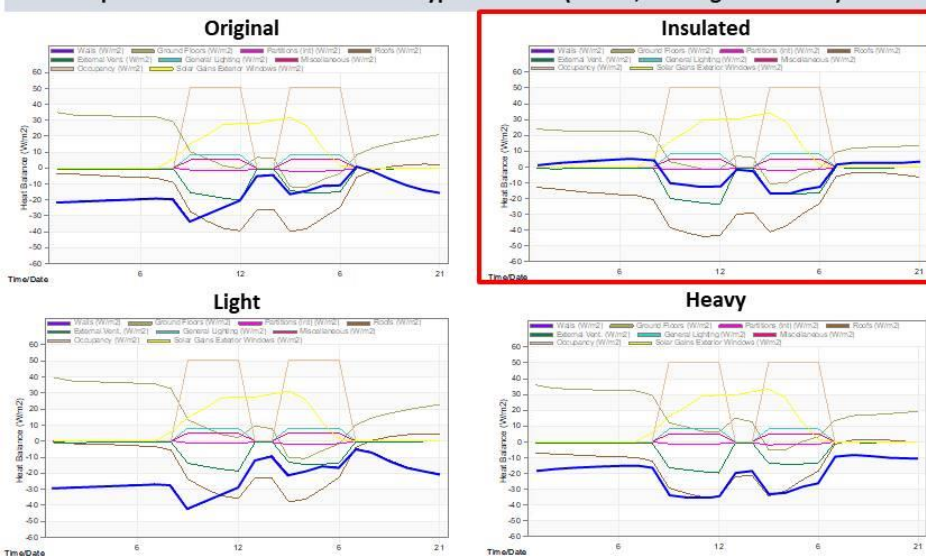


In these graphs, **walls** are represented by the **blue line**.

The **insulated** wall is the best solution for all cases.

In cooling dominated zones, it provides thermal losses during occupied hours and low thermal gains during the evening.

**Example of Caxias do Sul Winter Wall Type Variation (Zone 1, Heating Dominated) in a Winter Representative Day**



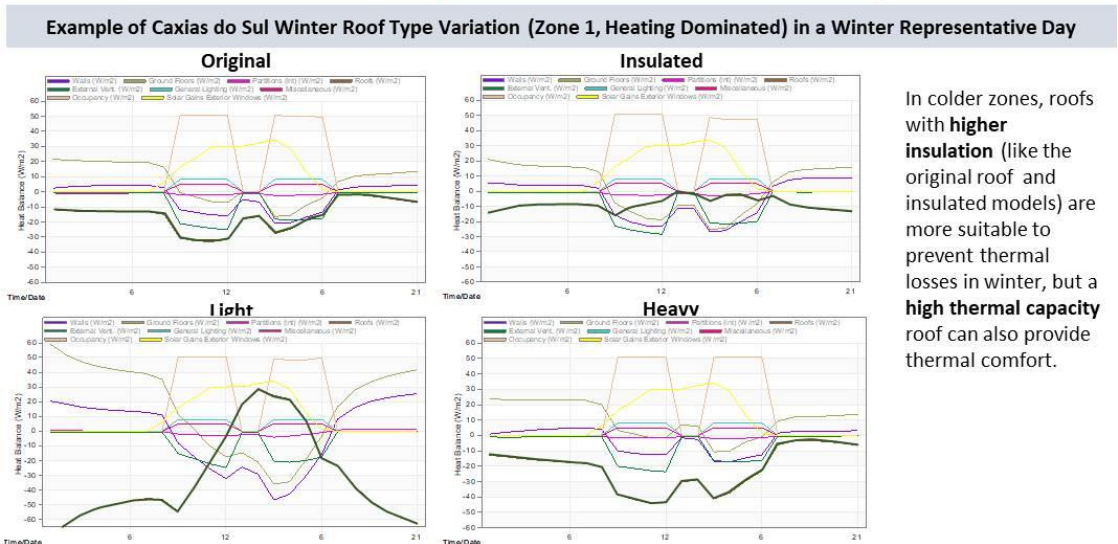
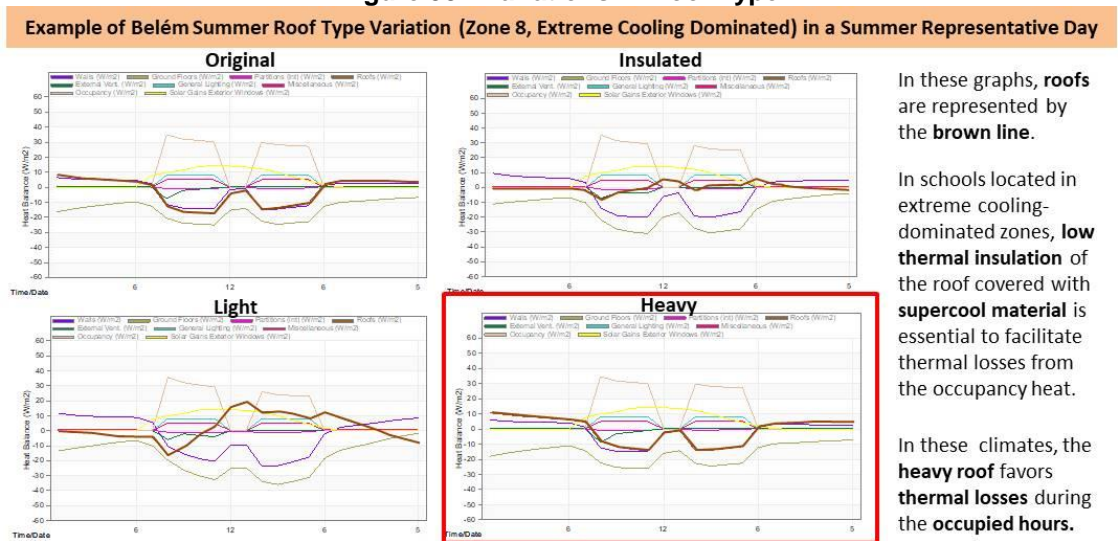
In heating dominated zones, **insulated** walls are also the best option, because they favor small thermal gains in summer and small losses in winter

Source: Authors.

In extreme-cooling-dominated and cooling-dominated zones (4 to 8), the heavy roof and insulated walls are the most favorable options, as they contribute to enhance thermal losses during the occupied hours throughout the year. These substrates facilitate heat losses through the opaque envelope, favoring thermal comfort.

The original roof composition is suitable for heating dominated zones (1 to 3), as it provides thermal losses in the summer without excessive thermal losses in the winter. However, the heavy roof is considered a more appropriate option due to the following reasons: Brazilian public school projects are standardized and in previous climate groups the heavy option was the most appropriate; Heating-dominated cities represent only a minority of Brazilian territory.

Figure 58 - Variations in Roof Type



Source: Authors.

Therefore, the ideal substrate of the standardized Brazilian school is heavy roof and insulated external walls.

### **4.3 Non-Algorithm Simulations Results**

The thermal comfort and heat balance results of the classroom in Picos (Zone 7), and Caxias do Sul (Zone 1) after non-algorithm simulation are in APPENDIX G.

In Picos (Zone7), the external concrete floor coated with a cool material of 90% reflectivity provided a small reduction in annual thermal gains due to the ground floor and increased thermal losses mainly in the months of August and September, which is the critical period of high temperatures in the city. The solution provided an increase of 0.8 in occupied hours in comfort, which made it possible to achieve the optimization objective of a maximum of 10% discomfort due to heat.

In Caxias do Sul (Zone 1), the external concrete floor with 30% reflectivity significantly reduced thermal losses in winter (May to August), but caused thermal gains in the summer period and increased heat discomfort mainly in December. In this case, the optimization objective was achieved, but the occupied hours in thermal comfort compared to algorithmic optimization rised only 0.2%.

In this heating dominated city, the option with 50% reflectivity provided more satisfactory results: it did not cause thermal gains in summer and reduced thermal losses through the ground floor in winter. This solution increased the occupied hours in thermal comfort by 0.5% and the optimization objective was achieved, with maximum discomfort due to heat of 4.4% and maximum discomfort due to cold of 9.4%.

### **4.4 Final Stage results**

The synthesis of the optimal solutions of passive strategies for the standardized 1 classroom school and the final results of occupied hours in thermal comfort are presented in Table 41.

In all cases, the objective of thermal comfort was achieved through a standardized architectural model, easy to apply throughout the Brazilian territory. The compositions

of the opaque and transparent envelope were the same for all cities. The small architectural variations between the different climates were in surface finishes (cool materials and reflectivities), window shading and external floor material adjacent to the building.

**Table 41 - Summary of Strategies and Comfort Results**

Zone	<div style="display: flex; justify-content: space-between; font-size: 0.8em;"> <span>■ Annual Heat Discomfort (%)</span> <span>■ Annual Comfort (%)</span> <span>■ Annual Cold Discomfort (%)</span> </div>			Wall Reflectivity	Roof Reflectivity (Winter/Summer)		Ventilation (Winter/Summer)		Additional Strategies
	Heat	Comfort	Cold		Winter	Summer	Winter	Summer	
1	4,4	86,2	9,4	10%	10%	70%	Occupancy 5% Aperture		Concrete ext. Ground R = 50%
2	4,4	93,3	2,2		50%		Occup. 5% Apert.	24/7 5% Apert.	
3	0,4	98,1	1,5		90%		Occupancy 5% Aperture	None	
4	0	96,7	3,3	50%	90%	24/7 5% Aperture			
5	4,8	93,6	1,6			24/7 5% Aperture			
6	0	98	2			24/7 95% Aperture			
7	10	90	0	90%	90%	24/7 95% Aperture		Local Shading, Cool ext. Ground R = 90%	
8	7,3	92,7	0			Local Shading $\alpha = 35^\circ$ and $\beta = 20^\circ$			

Source: Authors.

The interior walls of mortar and aerated ceramic block and the clear glass of the windows originally proposed in the standardized design can be maintained in all bioclimatic zones.

In all zones, ventilation is a strong recommendation for passive cooling, especially during operating hours. The main difference in the indication of ventilation in each region is the percentage of the window opening for ventilation: 95% for extreme cooling dominated zones (7 and 8) and 5% for the other zones (1 to 6). In almost all cases (zones 2 to 8), the heavy flat roof with a concrete slab is a suitable solution.

Zone 1, because of its lower temperatures, is the one that demands greater thermal insulation of the envelope (wall and roof) and dark colors on the envelope for heat absorption. Zones 1 to 3 need a thermochromic paint or dual color roof to provide thermal comfort in summer and winter. Zones 4 to 8 show gradually longer periods of heat and/or higher temperatures, thus they demand increased values of roof and wall reflectivity.

Even if window shadings are avoided to maintain original natural light conditions in classrooms, they are necessary strategies for zones 7 and 8, in order to reduce solar gains and heat discomfort. In these zones, supercool materials throughout the envelope are also needed to provide more heat losses. Specifically in zone 7, it is also necessary to cover the external ground with cool materials to decrease the temperature of the surrounding air and enhance heat losses from the building floor through contact with the ground.

The simulations show that the supercool materials offer significant cooling results in the hottest cities, as long as they are applied to as many surfaces as possible (roof, walls and surroundings) and associated with other passive cooling strategies. As suggested by Pisello (2017), applying cool materials to the roof is the most significant solution to prevent gains and enhance losses, as it is the area in closest contact with solar radiation. The use of these resources can provide thermal comfort and at the same time avoid the strong current trend of installing air conditioning in Brazilian schools identified by Geraldi and Ghisi (2020). The results obtained in this thesis considered cool paintings with high global reflectivity and high emissivity in all climates, due to limitations of the DesignBuilder software. Therefore, it may be that when using spectrally selective cool paintings in cases of real schools located in zones 4 to 7 (characterized by predominant humidities below 80%) the cooling effects are enhanced.

When comparing the optimal solutions obtained with the ABNT (2005a) constructive recommendations, it is noted that the general solutions proposed in the residential regulations are favorable to achieve thermal comfort also in educational buildings, such as: passive solar heating in cold climates; light colors and enhanced ventilation in warmer cities. However, different to the normative recommendation, the optimization research shows that in schools it is possible to achieve adequate thermal comfort in all zones only with passive strategies, without artificial heating or cooling.

#### **4.5 Transformation of Optimized Schools in ZEB**

The results of the transformation of the optimized 1 classroom schools into ZEB are described below.

### 4.5.1 Simplified Design of PV System

#### Monthly Loads Sizing

The power density of the electrical equipment in the classroom was based on Lopes (2020) and of other spaces on Geraldi and Ghisi (2020). The FNDE (2023) building areas and the occupancy suggested by the Ministry of Education (GERALDI; GHISI, 2020) were considered: 22 working days in operational months (March to June and August to December). The monthly loads sizing of the schools is detailed on Table 42. Given that FNDE's standardized 1 classroom school does not include air conditioning, the loads only refer to plugs and lighting. Since the occupancy pattern was assumed to be the same in all schools, the monthly loads are equal for all cities.

**Table 42 - Monthly Loads Sizing**

Subspace	Name	1 classroom
1	Classrooms	624 W
2	office rooms	654.85 W
3	kitchen	64 W
4	bathroom	64 W
5	aisles or courtyard	128 W
6	Library	-
7	Computer or Multiuse lab	-
Total Installed Power		1534.85 W
Total Monthly Loads		270.13 kWh

Source: Authors.

#### Photovoltaic System Dimensioning

Table 43 describes the PV system dimensioning from the Neosolar online calculator.

**Table 43 - Photovoltaic System Dimensioning**

Location	Loads (kWh/month)	System Size (kWp)	Modules Required	Estimated Annual Energy Production (kWh)	Required Area (m <sup>2</sup> )
Belém – PA (Zone 8)	270.13	2.01	7	2715	14.08
Picos – PI (Zone 7)		1.74	6	2724	12.2
Goiânia – GO (Zone 6)		1.81	7	2719	12.64
Santos – SP (Zone 5)		2.07	8	2717	14.47
Brasília – DF (Zone 4)		1.83	7	2717	12.78
Florianópolis – SC (Zone 3)		2.08	8	2717	14.53
Nova Friburgo – RJ (Zone 2)		1.91	7	2714	13.37
Caxias do Sul – RS (Zone 1)		1.90	7	2731	13.30

Source: Authors.

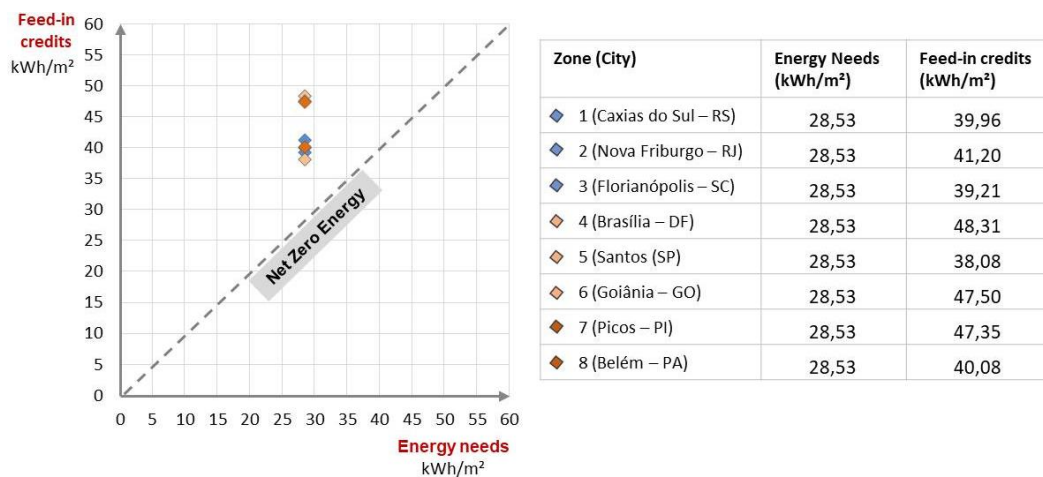
To favor standardization, the highest quantity of PV modules (8) was considered in simulations for all cities.

#### 4.5.2 Energy Balance Achievement

In all bioclimatic zones there is a significant production of energy without any consumption in the months of January, February and July, due to the school recess period. As kitchen refrigerators and freezers were not considered in the school's loads, there is no representation of baseline energy consumption in the graph.

The Figure 59 presents the positive energy balance of the school of 1 classroom in all brazilian bioclimatic zones.

**Figure 59 - Energy Balance Achievement Analysis of Optimized 1 Classroom School**



Source: Authors.

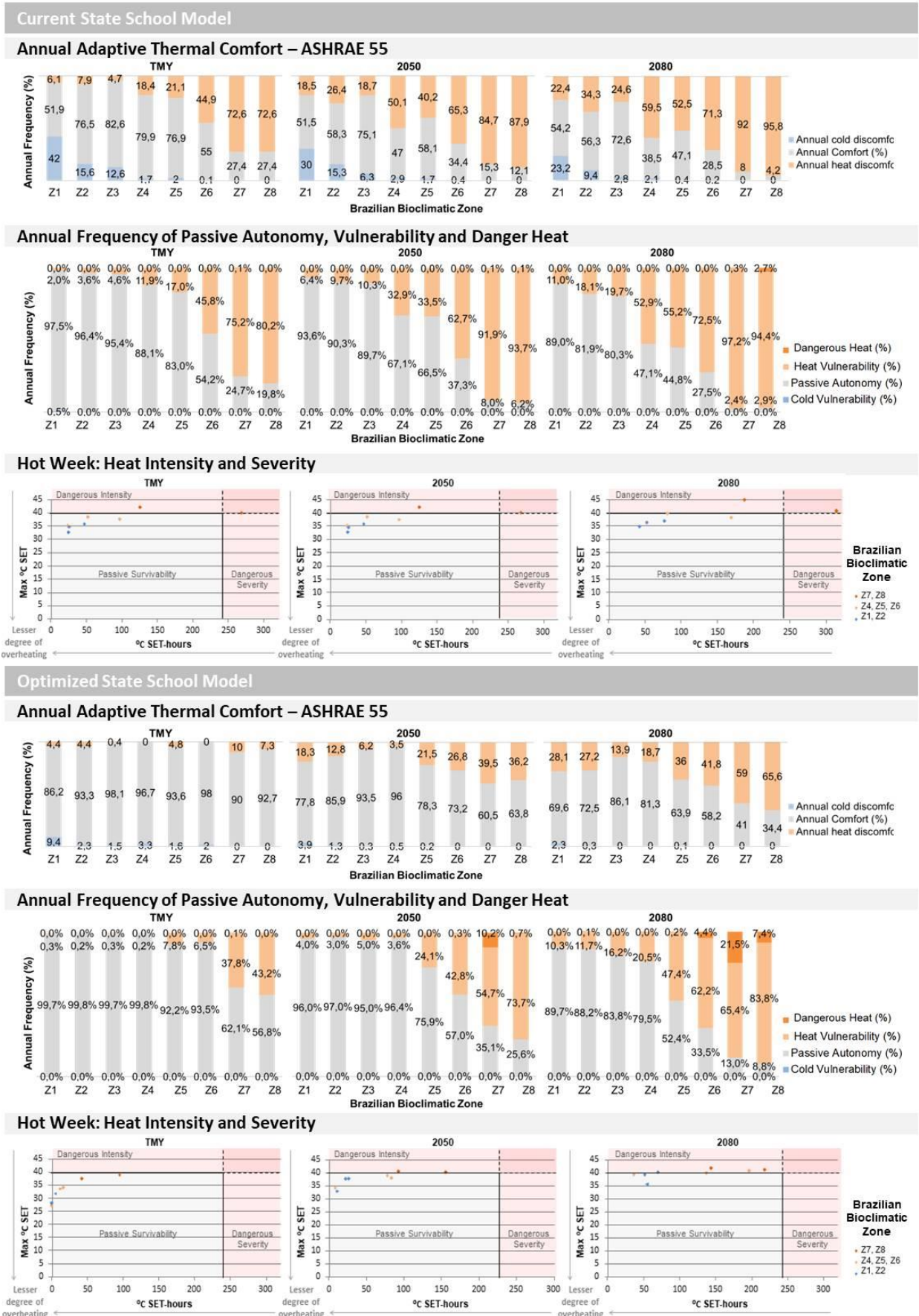
All schools were above the dashed line, with annual final energy (electricity consumption) of 28.53 kWh/m<sup>2</sup>. The cities that showed the highest production of electrical energy by the PV System were Brasília (15.78° South), Goiânia (16.68° south) and Picos (7.09° South). The first two are in latitudes close to the inclination angle of the modules (15°).

#### 4.6 Thermal Resilience and Passive Survivability Analysis

Figure 60 below provides a summary of the analysis graphs that constituted the thermal resilience and passive survivability evaluation: thermal comfort in TMY, 2050 and 2080; Passive Autonomy, Vulnerability and Dangerous Heat; Heat Intensity and Severity.



Figure 60 - Thermal Resilience and Passive Survivability Results



Source: Authors.



### **Thermal Comfort in TMY, 2050 and 2080**

In the current state school model, the normative requirements of a maximum of 10% discomfort due to cold or heat were not achieved in any of the zones, neither in TMY nor in 2050 and 2080. In all climates, the occupied hours in heat discomfort increase over the years, while cold discomfort in heating-dominated zones decreases, as evidenced in studies with future weather data by Mehmood et al. (2022). In the 2050 and 2080 weather scenarios, 7 out of 8 zones exhibit higher percentage of occupied hours in heat discomfort than in cold discomfort. In 2080, Zone 6 (Goiânia-GO) is classified as extreme-cooling-dominated (with more than 70% of hours occupied by heat discomfort), and Zones 7 and 8 (Picos-PI and Belém-PA), which originally had more than 70% heat discomfort, exceed 90%.

Considering the optimized school model on the TMY scenario, the optimization process favored compliance with Brazilian normative requirements for occupied hours in thermal comfort without the use of artificial air conditioning and all zones had a maximum of 10% of hours occupied in discomfort due to cold or heat. In 2050, only two cases (Florianópolis – Zone 3 and Brasília – Zone 4) still maintained suitable thermal comfort conditions exclusively with passive cooling. In 2080, in none of the cases would it be possible to meet normative requirements. However, even with the increase in heat discomfort over the years compared to the current state school model, the optimized model showed a lower percentage of discomfort due to heat and cold in all zones in the three weather scenarios.

The results of hours occupied in thermal comfort and discomfort in TMY, 2050 and 2080 show that the distribution of zones and the climatic grouping of heating-dominated, cooling-dominated and extreme-cooling-dominated zones proposed based on the thermal performance of the current state standardized school model in TMY do not hold in 2050 and 2080. There is a strong trend of increasing heat discomfort over the years, leading to a reduction in buildings classified as heating-dominated and an increase in cooling-dominated and extreme-cooling-dominated buildings. Therefore, Brazilian schools that currently require heating strategies will see a reduced demand and buildings will increasingly need more cooling strategies.

The optimized schools that initially had high percentages of hours occupied in comfort in TMY had these percentages reduced over the years. Although the optimized model had higher percentages of hours occupied in comfort than the current state model, it was not sufficient to meet the requirements of Brazilian regulations for buildings relying solely on passive cooling. Therefore, in the hypothesis of implementing the optimized school model proposed in this thesis, it is important to consider that while a high percentage of hours occupied in thermal comfort is possible today, in the medium and long term, artificial air conditioning will be necessary.

### **Frequency of Passive Autonomy, Vulnerability and Dangerous Heat**

In the TMY weather scenario of the current state school model, there is favorable passive autonomy exceeding 90% of the hours occupied in heating-dominated zones. In contrast, the extreme-cooling-dominated zones show unfavorable conditions, indicating an alert situation: 75.2% of hours occupied in Heat Vulnerability in Zone 7 (Picos-PI) and 80.2% in Zone 8 (Belém-PA). In the 2050 and 2080 weather scenarios, the percentages of hours occupied in Heat Vulnerability increase in all cities, reaching over 90% in zones 7 and 8. In 2080, there is a frequency of 97.2% of hours occupied in Heat Vulnerability in Zone 7 (Picos-PI) and 94.4% in Zone 8 (Belém-PA). Finally, in the current state school model, there is no significant percentage of hours occupied in dangerous heat in TMY, but dangerous heat becomes slightly more significant in Zone 8 (Belém-PA) in 2080, with 2.7% of hours occupied.

Considering the optimized school model, over 90% of the hours occupied in passive autonomy occur in 6 out of 8 zones in the TMY weather scenario. The extreme-cooling-dominated zones (7 and 8) present the most significant percentages of heat vulnerability (37.8% and 43.2%, respectively), and similar to the current state school model, there is no significant percentage of occupied hours in dangerous heat in any of the zones in this weather scenario. In both 2050 and 2080, in most zones, the optimized school model has higher passive autonomy than the current state model (except in zones 6, Goiânia - GO and 7, Picos – PI in 2050). Despite the more

favorable percentages of passive autonomy in the optimized school model, there was a more significant increase in the percentage of occupied hours in dangerous heat over the years than in the current state models. Compared to TMY, in 2050, there was an increase of over 10% in dangerous heat in Zone 7 (Picos-PI) and in 2080, an increase of over 4% in Zone 6 (Goiânia – GO), over 21% in Zone 7 (Picos – PI) and over 7% in Zone 8 (Belém – PA).

These data show that the design of the current state school model results in greater fluctuations in internal temperatures with external climatic variations, leading to more frequent conditions of heat vulnerability. However, in cases of extreme temperatures, the building can dissipate internal heat more easily. On the other hand, optimized buildings show less fluctuation in internal temperature, providing greater passive autonomy. Nevertheless, at times, there is a higher accumulation of heat that is not released quickly, making uninhabitable conditions more recurrent.

### **Heat Intensity and Severity**

In the analysis of heat intensity and severity during a hot week in the TMY weather scenario of the current state school model, situations outside the conditions of passive survivability are observed in two zones. There are dangerous heat intensity and severity in Zone 8 (Belém – PA), with temperatures frequently in heat vulnerability and peaks of 40°C SET. In 2050 and 2080, these conditions become increasingly concerning, with even higher temperatures and more consecutive hours of heat exposure. In the hot week in Zone 7 (Picos-PI), considering the TMY weather scenario, temperatures fluctuate between the passive autonomy range, heat vulnerability and dangerous intensity, but temperatures exceeding 40°C SET are the most worrisome condition. Although the current state model maintains acceptable cumulative exposure time to heat in 2050 and 2080, the temperature peaks are increasingly higher than 40°C SET. In all other zones, it was possible to meet passive survivability criteria.

In all zones, the optimized school model provides passive survivability in the TMY scenario. Additionally, this school model provides lower temperature variations over a hot week, leaving internal temperatures more stable. However, temperature peaks on specific days were more intense in the optimized model than in the current state model, which ended up increasing, although within acceptable limits, the Cumulative °C SET-hours in 2080 in Zone 6 (Goiânia – GO), Zone 5 (Santos – SP), Zone 2 (Nova Friburgo – RJ), and Zone 1 (Caxias do Sul – RS). The most concerning occurrences regarding temperature peaks were an increase in the frequency of critical exceedance (>40°C SET) of dangerous heat and compromised passive survivability due to dangerous intensity in one zone in 2050, Zone 7 (Picos – PI), and in three zones in 2080: Zone 6 (Goiânia – GO), Zone 7 (Picos – PI), and Zone 8 (Belém – PA).

Regarding the maximum annual SET intensity indicator, there is an increase over the years in both the current state school model and the optimized school model due to climate change and global warming. In all cases of the TMY weather scenario, the optimized school model provided positive results, with maximum SETs equal to or lower than the current state school model. On the other hand, maximum SETs in 2050 and 2080 were higher in 4 out of 8 zones: Zone 6 (Goiânia – GO), Zone 4 (Brasília – DF), Zone 2 (Nova Friburgo – RJ), and Zone 1 (Caxias do Sul – RS).

Overall, the results of thermal resilience indicators show that the optimized model ensured the passive survivability of schools in all bioclimatic zones in the TMY, significantly increased passive survivability in current and future climatic conditions. However, there was an increase in the percentage of dangerous intensity of Standard Effective Temperatures, with values above 40°C SET. While in 2080, the current state school model has compromised passive survivability in two cities, one due to dangerous intensity and severity, and the other only due to dangerous intensity, in the optimized school model, three cities show compromised passive survivability only due to dangerous intensity, due to higher and more frequent annual maximum temperatures.

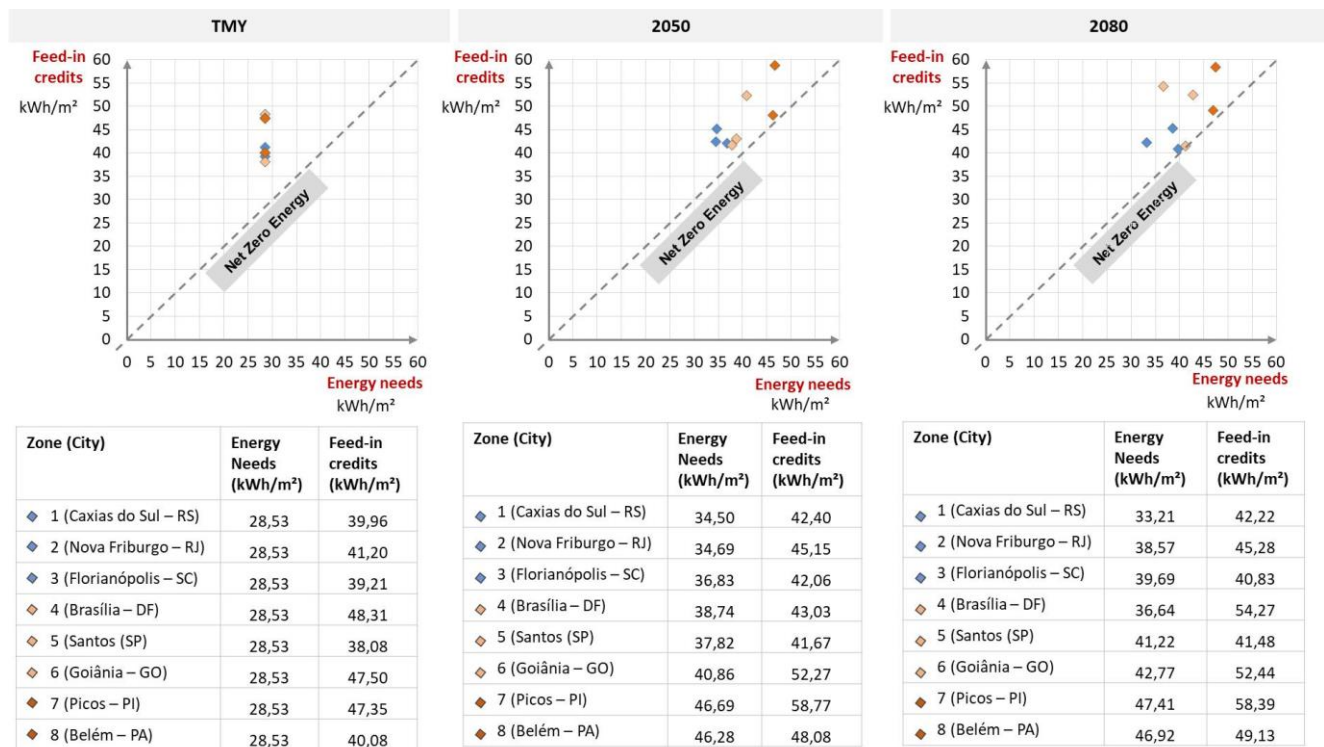
In this case, it would be possible to adopt two approaches: a new optimization process or resizing the PV System to accommodate an artificial conditioning system

to maintain safe and more comfortable internal temperatures. In the case of this thesis, the second possibility was considered.

## PV System Resizing and Comparison of Loads and Energy Production

The cities with the highest cooling loads in 2080, calculated by the Design Builder, guided the resizing of the PV System for each climatic group. The highest cooling loads were observed in the following zones: Zone 3 (Florianópolis – SC) from the heating-dominated group, Zone 5 (Santos – SP) from the cooling-dominated group, and Zone 8 (Belém – PA) from the extreme-cooling-dominated zones. An increase of 6.3% in the PV System for the heating and cooling-dominated zones and 18.8% for the extreme-cooling-dominated zones was necessary. The additional photovoltaic modules facilitated a positive energy balance in 2050 and 2080 (Figure 61), when artificial conditioning is required to prevent heat discomfort and ensure passive survivability. The system's resizing also enabled monthly electricity production that meets the monthly cooling loads depicted in the DesignBuilder outputs, detailed in APPENDIX O.

Figure 61 - Final Energy Balance in Optimized 1 Classroom School in TMY, 2050 and 2080



Source: Authors.

Therefore, it is concluded that the backup power provided by the additional PV system enhances the thermal resilience and the passive survivability of the standardized 1 classroom schools and their capacity for absorption and autonomy in relation to the public electricity grid by meeting the demand for critical HVAC loads, even during power outages coupled with extreme temperature conditions when passive measures may not be sufficient, as advocated in the studies by Hong *et al.* (2023).

## 5. CONCLUSIONS

Buildings with a net-zero energy balance or positive energy balance are characterized by high energy efficiency, achieved through passive climate control strategies and efficient equipment (CABEZA; CHÀFER, 2020). These buildings generate the same amount of energy they consume by utilizing renewable sources (SARTORI; NAPOLITAN; VOSS, 2012; LIU *et al.*, 2019).

One effective passive strategy contributing to this efficiency is the use of cool materials that are highly effective passive solutions that have gained prominence in recent years in international research to improve indoor and outdoor environmental comfort and reduce energy consumption. Moreover, supercool materials offer extra benefits when applied to Zero Energy Buildings (ZEBs) or Positive Energy Buildings (PEBs) equipped with a photovoltaic system on the roof. These materials lower the roof temperature, decrease the surrounding air temperature and enhance the reflected radiation reaching the modules, promoting heightened efficiency and local energy generation (VASILAKOPOULOU *et al.*, 2023). These materials are characterized by high values (above 90%) of reflectivity and emissivity. The most currently tested in research are thermochromic for mixed climates, high global emissivity for hot and humid climates and high emissivity at specific wavelengths (also called spectrally selective) for hot and dry climates.

There are several types of cool materials, which are available in different forms as dyes, with simplified application; as in films or flat surfaces, which can be coupled to a substrate, with relatively simplified application; or as complex structures, with a sophisticated and expensive manufacturing process.

The choice of the most suitable option must be made individually for each case, considering the physical-chemical characteristics of the materials, forms of application, durability and mainly climatic configurations. Thermochromic materials suffer from aging problems and lose their reversibility after weeks. The average durability of the other materials was not mentioned in the articles chosen by the method of systematic literature review proposed, therefore, it is a topic that can be investigated in more depth in future studies. In the case of standardized Brazilian public schools, paints are the most recommended due to their ease of application and maintenance.

Considering the Brazilian climatic context and the 8 Brazilian zones defined by ABNT (2005a), it is possible to identify three main groups for which different cool materials are recommended. For zones with normative heating strategies (Zones 1 to 3), thermochromic materials are suggested. For zones with low to medium humidity and more indications of normative cooling strategies (Zones 4 to 7), high spectral reflectivity and high emissivity materials in the atmospheric window are advised. In the high humidity city with only normative cooling recommendation (Zone 8), High Spectral Reflectivity and High Broadband Emissivity materials are suggested.

Among the options identified as most suitable, only high spectral reflectivity and high broadband emissivity paints are produced nationally. According to the research results described in this thesis, these supercool paint options have competitive prices compared to conventional acrylic paints for external building surfaces, with the additional advantage of optical properties that minimize heat transfer to indoor spaces, increase building resistance to overheating, reduce the need for artificial cooling and consequently lower the financial and environmental costs of building operation. These positive aspects make Brazilian supercool paints a favorable choice for public buildings in predominantly hot climates.

According to the results of questionnaires applied by Geraldi and Ghisi (2020), there is a high dissatisfaction among users regarding temperature, especially in the hottest months (February to April and October to December). Schools with higher levels of satisfaction tend to have a higher average Energy Use Intensity (EUI) due to the use of air conditioning. Those with lower EUI and seemingly more efficient systems do not provide adequate thermal comfort conditions to users (GERALDI; GHISI, 2022b).

This situation contradicts international guidelines for reducing energy consumption and mitigating the effects of climate change, which emphasize the use of passive strategies and distributed generation of renewable energy (GERALDI; GHISI, 2022a).

Given the high discomfort percentages due to heat in the hottest regions of current Brazilian public schools, there has been a significant surge in energy consumption for cooling and air conditioning. Consequently, there arises an urgent necessity to adapt standard architectural projects to address this challenge. Achieving the transformation of standardized FNDE schools into a positive energy balance, with a special emphasis on avoiding the use of artificial air conditioning, represents a bold objective in this thesis. Realizing this goal demands the implementation of effective solutions for passive air conditioning and ensuring the comfort of the occupants.

FNDE financial transfers are made through programs and agreements. The two programs currently in force for school construction are the National Program for Restructuring and Acquisition of Equipment for the Public School Network of Early Childhood Education – Proinfância and the Plan of Articulated Actions – PAR (FNDE, n/d). There are currently 5 types of complete school projects from the PAR program and 2 types from the Proinfância program (7 models in total) that can be summarized in three groups: rectangular-shaped, multi-buildings and H-shaped. The Proinfância schools are for infants (0 to 6 years old), and the PAR models are intended for elementary and high school (7 to 17 years old) (FNDE, n/d).

The standardized projects provided by FNDE were developed after 2007 and incorporate various recent construction guidelines to ensure minimal thermal performance suitable for the entire country. However, as identified in other research on Brazilian public schools (GERALDI; GHISI, 2020; GRAÇA; KOWALTOWSKI; PETRECHE, 2007), these standardized architectural projects do not include user participation, do not prioritize environmental comfort, lack design simulations and optimizations and have infrequent post-occupancy studies for performance evaluation. Due to these factors, the current school models do not provide adequate thermal comfort to occupants, as demonstrated in this thesis through thermal comfort simulations of the current state of a 1 classroom school of rectangular shape.



In accordance with the Inmetro Normative Instruction for the Classification of Energy Efficiency of Commercial, Service and Public Buildings – INI-C/2021, naturally ventilated buildings without artificial conditioning systems must provide a percentage of occupied hours in thermal comfort equal to or greater than 90% during the building's use hours, with a maximum tolerance of 10% for heat discomfort (ELETROBRÁS *et al.*, 2021). According to the simulations in this thesis, only 3 (Zones 1, 2 and 3) out of the 8 Brazilian bioclimatic zones meet these regulatory requirements. Although these 3 zones have a low percentage of hours occupied in heat discomfort, all of them have more than 10% of occupied hours in cold discomfort. In all bioclimatic zones, the roof is a significant source of annual heat gain and should be a priority for intervention. In Zones 1, 2 and 3, excessive thermal losses due to ventilation are the primary cause of discomfort during winter in colder cities, necessitating control measures.

Due to the identified deficiencies in the current standardized 1 classroom school project, an optimization process was conducted using computer simulations with DesignBuilder, with and without the JEA algorithm. The primary objective was to achieve thermal comfort, with a maximum tolerance of 10% of hours occupied in heat discomfort (as suggested by INI-C/2021) and 10% of hours occupied in cold discomfort. No changes were proposed to the architectural geometry (floor plan) design and window-to-wall ratio to avoid significant alterations to the standardized architectural project. Other parameters were also held constant, including the composition of the internal ground floor, internal partitions and the transparent envelope (type of window glass). Various thermophysical properties for the roof and walls were evaluated, including the compositions of the current model, insulated compositions (with high thermal resistance), light compositions (low thermal resistance and low thermal capacity) and heavy compositions (high thermal capacity). Reflectivity ranged from 10 to 90% depending on the climate group.

The results of the optimization process prove that a completely equal building is not possible for all zones due to the climatic particularities of each region of Brazil. However, it is possible to achieve objective of thermal comfort through a standardized architectural model, easy to apply throughout the Brazilian territory, with only few adaptations in each bioclimatic group (extreme cooling dominated zones, cooling dominated zones and heating dominated zones).

The FNDE's standardized model for public schools can be used to meet the high demand in the Brazilian context while promoting occupant thermal comfort and low energy consumption without the use of artificial climate control. This model should have a heavy flat roof and insulated walls, retaining the original characteristics of geometry (floor plan), window-to-wall ratio, window type (casement), window glass type (simple clear glazing) and adjacent grassy outdoor areas. The heavy roof and insulated walls are suitable substrates mainly in cooling dominated cities as they result in significant thermal losses throughout the occupancy period. It is emphasized that this optimal solution found for the envelope, despite differing from the suggestions of Brazilian normatives, was the composition that exhibited the best performance in conjunction with the other evaluated passive strategies (supercool coatings, ventilation and window shadings).

However, minor adaptations are required for each bioclimatic region, such as the reflectivity of the finish, schedule and percentage of window openings for ventilation. Schools located in extreme climatic conditions require additional passive strategies: for cities with a greater cold discomfort (Zone 1), moderately reflective external concrete floors (50%); and for cities with greater heat discomfort, local window shading (Zones 7 and 8) and supercool external floors (Zone 7).

Among all the passive strategies tested, the supercool material is one of the most effective passive strategies for cooling, especially when applied to the roof. The higher the reflectivity of the roof, the lower the need for thermal insulation in cooling-dominated cities to prevent solar radiation heat gain, as already stipulated in the Brazilian performance standard for residential buildings (ABNT, 2021). In schools located in extremely cooling-dominated zones, low thermal insulation of the roof covered with supercool material is essential to facilitate thermal losses from the heat generated by the high occupancy of classrooms. In colder zones, a roof with higher insulation (like the original roof model) is more suitable to prevent thermal losses in winter, but a high thermal inertia roof is satisfactory and enables occupant thermal comfort.

As previous international studies have suggested (PISELLO, 2017), applying cool materials to the roof is the most significant solution to prevent gains and enhance losses, as it is the area in closest contact with solar radiation. Although the roof is the

most important intervention element, especially in hotter cities, additional passive strategies are also important to ensure adequate comfort without artificial conditioning: appropriate window opening percentages and schedules for ventilation; appropriate transmittance, thermal capacity and reflectivity of the walls; and, in extreme cooling dominated zones, local window shadings. In 7 of 8 Brazilian bioclimatic zones, the second most impactful passive strategy is the natural ventilation. In Zone 1, the coldest zone, natural ventilation has a greater impact due to the higher thermal loss control requirements to ensure comfort.

The hotter the city, the larger the window openings should be to maximize thermal losses, and the colder the city, the smaller the openings should be. The reflectivity of the roof and, especially, the walls should decrease as the city's latitude increases and air temperatures are predominantly lower. As suggested by ABNT (2005a), low reflectivity favors winter heat gains. In heating-dominated Brazilian zones (1, 2 and 3), therefore, thermochromic coating on the roof to provide winter gains and summer thermal losses and dark walls to accumulate heat in winter when solar radiation strikes the north facade are advised. In extremely hot cities, the reflectivity of the walls is much less influential than the reflectivity of the roof but is essential to meet the thermal comfort requirements of the Brazilian standard for naturally air-conditioned public buildings.

Following the optimization study, it was possible to ensure thermal comfort in the standardized 1 classroom school model of FNDE solely through passive strategies, allowing for a perspective of low energy consumption in the school. Due to this reduced energy demand (which only refers to lighting and equipment), only a few photovoltaic modules were required and the school easily achieved a positive energy balance in all bioclimatic zones.

There are various definitions of net-zero and positive energy balance, depending on geographic limits (building, neighborhood, or district) and the location of energy production (DERKENBAEVA *et al.*, 2022). The ideal conditions for compatibility between these strategies include on-site energy production with photovoltaic panels on building facades, on non-occupied room roofs, within the land boundaries using multiple renewable sources, or off-site energy production by neighboring buildings, serving as renewable energy hubs within the neighborhood or district.

In the context of public schools standardized by FNDE, the building's geographic boundary is more suitable, ensuring a positive energy balance regardless of the neighborhood or local urban context. Connecting the system to the electrical grid is advisable in the Brazilian context due to favorable legislation that allows for energy exchange with the grid in conversion for energy credits.

Considering the importance of current buildings being prepared for climate change and future extreme events, this thesis assessed and proposed various adaptations to the current state 1 classroom standardized school to enhance the building's thermal resilience and passive survivability, as well as increase occupant comfort and safety.

Among the thermal resilience and passive survivability characteristics mentioned by Krelling et al. (2023), this thesis, through the optimization process, suggested strategies to reduce **vulnerabilities** related to thermal comfort. The study also demonstrated, through the application of supercool paintings and the implementation of a positive energy balance with a PV system, a potential increase in **adaptability**, **flexibility** and **smartness**. This ensures that the building is ready to meet possible additional cooling demands in the context of future climate change (KHAN et al., 2022; ZHANG et al., 2021). Moreover, the combination of supercool paintings with other passive strategies and the PV system facilitates **mitigation**, minimizing the use of artificial conditioning and associated emissions. Lastly, the PV system sized to meet potential future artificial conditioning demands enhances **resistance** and **robustness**, avoiding failure situations and overheating risks.

The results of the thermal resilience and passive survivability performance analyses of the current state standardized school model and the optimized model reveal that the proposed distribution and climatic grouping based on the thermal performance of the standard model in the TMY weather scenario do not hold in 2050 and 2080. There is a clear trend of increasing discomfort due to heat over time, indicating a reduction in buildings classified as heating-dominated and an increase in those classified as cooling-dominated and extreme-cooling dominated. This suggests that Brazilian schools, which currently require strategies for thermal loss control, will see this demand decrease, while cooling strategies become increasingly essential.

The results demonstrate that optimized schools, which initially showed very high percentages of occupied hours in thermal comfort during the Typical Meteorological Year – TMY, experienced a reduction in these percentages over the years (2050 and 2080). Despite the optimized model having higher percentages of thermal comfort hours compared to the current state model, it was insufficient to meet Brazilian regulatory requirements for buildings relying solely on passive climate control. Therefore, in the hypothetical implementation of the proposed optimized school model in this thesis, it is important to acknowledge that, even though a high percentage of hours in thermal comfort is achievable today, artificial conditioning will become necessary in the medium to long term.

These findings align with previous research, suggesting that cooling solutions with low energy consumption, effective under current conditions, may not perform optimally in the future or during extreme events like heatwaves or power outages (Mehmood *et al.*, 2022; Zhang *et al.*, 2021). Hence, based on arguments from Krelling *et al.* (2023), Mehmood *et al.* (2022) and Cirrincione, Marvuglia and Scaccianoce (2021), future research is recommended to optimize the thermoenergetic performance of buildings and thermal resilience, incorporating meteorological data covering urban microclimates, extreme conditions, heatwaves, cold waves and future projections to plan more adequate solutions in the long term.

Regarding thermal resilience and passive survivability results, the optimized model ensured passive survivability in all bioclimatic zones during the TMY and significantly improving passive autonomy in current and future climatic conditions. However, there was an increase in the percentage of dangerous intensity of Standard Effective Temperatures, surpassing 40°C SET. In contrast to the current state school model having compromised passive survivability in 2080 in two cities due to dangerous intensity and severity, the optimized school model exhibited compromised passive survivability in three cities solely due to dangerous intensity, attributed to higher and more frequent annual maximum temperatures.

This indicates that the design of the current state school model induces greater internal temperature oscillation with external climatic variations, leading to more frequent heat vulnerability conditions. Conversely, optimized buildings exhibit lower internal temperature oscillation, providing greater passive autonomy. Nevertheless, at

times, there is a more significant heat accumulation that is not rapidly dissipated, resulting in recurring inhabitable conditions.

To prevent cases of dangerous intensity of Standard Effective Temperatures, meet the electricity demand of an artificial conditioning system for safe and comfortable internal temperatures and maintain a positive energy balance in future climatic conditions (2050 and 2080), this thesis proposes resizing the PV System based on the city with the highest cooling loads in each climatic group. A 6.3% increase in the PV System is required for heating and cooling-dominated zones and an 18.8% increase for extreme-cooling-dominated zones. Aligned with Hong *et al.* (2023), the backup power provided by the additional PV system positively enhances the building's thermal resilience and its capacity to absorb and operate independently from the public electricity grid by meeting critical HVAC loads, even during power outages coupled with extreme temperature conditions when passive measures may prove insufficient.

Among the limitations of this thesis, the following points are noteworthy.

Just like in other studies, the computer simulations do not take into account the surroundings (GERALDI; GHISI, 2022a). Considering that this is a standardized public school project replicated in various regions and urban contexts, it would be interesting to conduct a future study of typical urban environments that could be considered in the computer simulations to more accurately demonstrate the thermal performance of Brazilian public schools.

EnergyPlus, which is the most commonly used software in studies of cool materials in buildings, is the software used in this thesis. It is known for dynamically solving the mass and energy balance of all environments within a building in response to external conditions, internal loads and occupant behavior, accurately representing heat transfer phenomena on external surfaces (BANIASSADI; SAILOR; BAN-WEISS, 2019). However, this tool does not allow for the inclusion of data on the spectral variation of emissivity of cool materials, which is mainly present in spectrally selective materials. This limitation can lead to errors in the calculation of surface temperature and sensible heat flux (BANIASSADI; SAILOR; BAN-WEISS, 2019). This means that in bioclimatic zones 4 to 7, where the use of spectrally selective materials is

recommended, the results obtained in this thesis for cooling schools through thermal envelope heat losses may have been underestimated.

Future research is recommended:

- Studies of cool materials and substrates suitable for other building typologies and environments with different thermal requirements and behaviors compared to the studied context. This includes spaces with lower occupancy that do not experience significant internal heat gains like classrooms, commercial buildings with shorter periods of occupancy and residential buildings with higher nighttime occupancy;
- More refined studies on the thermoenergetic performance of Brazilian public schools considering the urban context, which influences meso and microclimatic conditions, such as shading, increased ambient temperature and wind blockages;
- Assessments of the cooling effects of supercool coatings in standardized optimized school models on the microclimate of the urban surroundings, aiming to understand additional benefits of this passive technique beyond cooling the building itself;
- More detailed cost-benefit analyses of others optimal passive strategies found in this thesis for standardized Brazilian public schools, applicable to other building typologies;
- Optimization studies for other types of standardized schools with more complex shapes, which may exhibit different thermoenergetic behaviors compared to the identified rectangular 1 classroom school;
- Multiobjective optimization studies that, in addition to thermal comfort, also consider lighting comfort, costs, and CO<sub>2</sub> emissions;
- Analyses of additional strategies for nighttime passive building climate control, such as the use of geothermal heat exchangers and thermal inertia with phase change materials – PCMs;
- Evaluations of additional passive ventilation strategies, alternatives to artificial conditioning, enhancing passive survivability of standardized Brazilian public schools and occupant safety in 2050 and 2080;

- Optimization of standardized Brazilian public schools in future climate scenarios to examine the most effective passive solutions both in the current and long-term perspectives, not solely based on current conditions;
- Thermal performance analyses of current state and optimized standardized Brazilian public schools in other IPCC climate scenarios, more optimistic and pessimistic than the SSP3-7.0 considered in this thesis.

## REFERENCES

ABNT – ASSOCIAÇÃO BRASILEIRA DE NORMAS TÉCNICAS. NBR 15220: Thermal performance of buildings. Rio de Janeiro, 2005a.

\_\_\_\_\_. NBR 15575: Edificações Habitacionais – Desempenho Parte 1: Requisitos Gerais. Rio de Janeiro, 2021a.

\_\_\_\_\_. NBR 15575: Edificações Habitacionais – Desempenho Parte 4: Requisitos para os Sistemas de Vedações Verticais Internas e Externas – SVVIE. Rio de Janeiro, 2021b.

\_\_\_\_\_. NBR 15575: Edificações Habitacionais – Desempenho Parte 5: Requisitos para os Sistemas de Coberturas. Rio de Janeiro, 2021c.

\_\_\_\_\_. NBR 15215-3: Iluminação Natural – Parte 3: Procedimento de cálculo para a determinação da iluminação natural em ambientes internos. Associação Brasileira de Normas Técnicas. Rio de Janeiro, 2005b.

\_\_\_\_\_. NBR 6118: Projeto de estruturas de concreto - Procedimento. Associação Brasileira de Normas Técnicas. Rio de Janeiro, 2014.

\_\_\_\_\_. NBR 11702: Tintas para Construção Civil — Tintas, Vernizes, Texturas e Complementos Para Edificações Não Industriais — Classificação E Requisitos. Associação Brasileira de Normas Técnicas. Rio de Janeiro, 2021a.

\_\_\_\_\_. NBR 15079-1: Tintas para Construção Civil — Requisitos Mínimos de Desempenho. Associação Brasileira de Normas Técnicas. Rio de Janeiro, 2021b.

ADELI, Mohsen Mahdavi; FARAHAT, Said; SARHADDI, Faramarz. Optimization of Energy Consumption in Net-Zero Energy Buildings with Increasing Thermal Comfort of Occupants. **International Journal Of Photoenergy**, [S.L.], v. 2020, p. 1-17, 24 jan. 2020. Hindawi Limited. <http://dx.doi.org/10.1155/2020/9682428>.

ALBATAYNEH, Aiman; ALBADAINAH, Renad; JUAI, Adel; ABDALLAH, Ramez; MONTOYA, María Dolores G.; MANZANO-AGUGLIARO, Francisco. Rooftop photovoltaic system as a shading device for uninsulated buildings. **Energy Reports**, [S.L.], v. 8, p. 4223-4232, nov. 2022. Elsevier BV. <http://dx.doi.org/10.1016/j.egyr.2022.03.082>.



ALMEIDA, Mariana Barbosa Carlos de. Uma análise da implantação e da funcionalidade dos projetos padrão do FNDE: a experiência das escolas infantis tipo "B" do proinfância em Natal/RN. 2018. 232f. Dissertação (Mestrado em Arquitetura e Urbanismo) - Centro de Tecnologia, Universidade Federal do Rio Grande do Norte, Natal, 2018.

ALVAREZ, André Luiz Montero; SAIDEL, Marco Antonio. **Uso Eficiente de Energia Elétrica: Metodologia para a Determinação dos Potenciais de Conservação dos Usos Finais e Instituições e Ensino e Similares**. São Paulo: Escola Politécnica Universidade de São Paulo, Biblioteca Digital de Teses e Dissertações da USP, 2001. Disponível em: <<http://www.theses.usp.br/theses/disponiveis/3/3143/tde-17082001-000915/pt-br.php>>. Acesso em: 06 out. 2017.

AMER, Muhammad; DAIM, Tugrul U.; JETTER, Antonie. (2013). **A review of scenario planning**. Futures, 46(0), 23-40. Disponível em: < <https://www-sciencedirect-com.ez54.periodicos.capes.gov.br/science/article/pii/S0016328712001978> >. Acesso em: 25 jun. 2018.

ANDRADE, Henrique José Caravita de. Análise da eficiência energética em edificações usando os métodos RTQ-C e INI-C. 2022. Dissertação (Mestrado em Engenharia Elétrica) – Universidade Federal de São Carlos, São Carlos, 2022. Disponível em: <https://repositorio.ufscar.br/handle/ufscar/15717>.

ANDRADE, Marcela Macedo de; DORNELLES, Kelen Almeida. A influência da composição química na refletância solar e emitância térmica dos materiais frios. **XVII Encontro Nacional de Conforto no Ambiente Construído**, [S.L.], p. 1-10, 26 out. 2023. ANTAC. <http://dx.doi.org/10.46421/encac.v17i1.3743>.

ANEEL – AGÊNCIA NACIONAL DE ENERGIA ELÉTRICA. Resolução Normativa N° 482, de 17 de abril de 2012. **Estabelece as condições gerais para o acesso de microgeração e minigeração distribuída aos sistemas de distribuição de energia elétrica, o sistema de compensação de energia elétrica, e dá outras providências**. Disponível em: < <http://www2.aneel.gov.br/cedoc/ren2012482.pdf>>. Acesso em: 07 out. 2017.

ASCIONE, Fabrizio; BIANCO, Nicola; IOVANE, Teresa; MAURO, Gerardo Maria; NAPOLITANO, Davide Ferdinando; RUGGIANO, Antonio; VISCIDO, Lucio. A real industrial building: modeling, calibration and pareto optimization of energy retrofit. **Journal Of Building Engineering**, [S.L.], v. 29, p. 101186, maio 2020. Elsevier BV. <http://dx.doi.org/10.1016/j.job.2020.101186>.

ASCIONE, Fabrizio; BIANCO, Nicola; MAURO, Gerardo Maria; NAPOLITANO, Davide Ferdinando. Building envelope design: multi-objective optimization to minimize energy consumption, global cost and thermal discomfort. application to different italian climatic zones. **Energy**, [S.L.], v. 174, p. 359-374, maio 2019a. Elsevier BV. <http://dx.doi.org/10.1016/j.energy.2019.02.182>.

ASCIONE, Fabrizio; BIANCO, Nicola; MAURO, Gerardo Maria; VANOLI, Giuseppe Peter. A new comprehensive framework for the multi-objective optimization of building energy design: harlequin. **Applied Energy**, [S.L.], v. 241, p. 331-361, maio 2019b. Elsevier BV. <http://dx.doi.org/10.1016/j.apenergy.2019.03.028>.

ASCIONE, Fabrizio; MASI, Rosa Francesca de; SANTAMOURIS, Mattheos; RUGGIERO, Silvia; VANOLI, Giuseppe Peter. Experimental and numerical evaluations on the energy penalty of reflective roofs during the heating season for Mediterranean climate. **Energy**, [S.L.], v. 144, p. 178-199, fev. 2018. Elsevier BV. <http://dx.doi.org/10.1016/j.energy.2017.12.018>.

ATTIA, Shady; LEVINSON, Ronnen; NDONGO, Eileen; HOLZER, Peter; KAZANCI, Ongun Berk; HOMAIEI, Shabnam; ZHANG, Chen; OLESEN, Bjarne W.; QI, Dahai; HAMDY, Mohamed. Resilient cooling of buildings to protect against heat waves and power outages: key concepts and definition. **Energy And Buildings**, [S.L.], v. 239, p. 110869, maio 2021. Elsevier BV. <http://dx.doi.org/10.1016/j.enbuild.2021.110869>.

BANDEIRAS, F.; GOMES, M.; COELHO, P.; FERNANDES, J.. Towards net zero energy in industrial and commercial buildings in Portugal. **Renewable And Sustainable Energy Reviews**, [S.L.], v. 119, p. 109580, mar. 2020. Elsevier BV. <http://dx.doi.org/10.1016/j.rser.2019.109580>.

BAGHERI-ESFEH, Hamed; DEGHAN, Mohammad Reza. Multi-objective optimization of setpoint temperature of thermostats in residential buildings. **Energy And Buildings**, [S.L.], v. 261, p. 111955, abr. 2022. Elsevier BV. <http://dx.doi.org/10.1016/j.enbuild.2022.111955>.

BAGHERI-ESFEH, Hamed; SAFIKHANI, Hamed; MOTAHAR, Sadegh. Multi-objective optimization of cooling and heating loads in residential buildings integrated with phase change materials using the artificial neural network and genetic algorithm. **Journal Of Energy Storage**, [S.L.], v. 32, p. 101772, dez. 2020. Elsevier BV. <http://dx.doi.org/10.1016/j.est.2020.101772>.

BAGHOOLIZADEH, Mohammadreza; ROSTAMZADEH-RENANI, Mohammad; ROSTAMZADEH-RENANI, Reza; TOGHRAIE, Davood. Multi-objective optimization of Venetian blinds in office buildings to reduce electricity consumption and improve visual and thermal comfort by NSGA-II. **Energy And Buildings**, [S.L.], v. 278, p. 112639, jan. 2023. Elsevier BV. <http://dx.doi.org/10.1016/j.enbuild.2022.112639>.

BAGHOOLIZADEH, Mohammadreza; ROSTAMZADEH-RENANI, Reza; ROSTAMZADEH-RENANI, Mohammad; TOGHRAIE, Davood. A multi-objective optimization of a building's total heating and cooling loads and total costs in various climatic situations using response surface methodology. **Energy Reports**, [S.L.], v. 7, p. 7520-7538, nov. 2021. Elsevier BV. <http://dx.doi.org/10.1016/j.egyr.2021.10.092>.

BANIASSADI, Amir; SAILOR, David J.; BAN-WEISS, George A.. Potential energy and climate benefits of super-cool materials as a rooftop strategy. **Urban Climate**, [S.L.], v. 29, p. 100495, set. 2019. Elsevier BV. <http://dx.doi.org/10.1016/j.uclim.2019.100495>.

BERARDI, Umberto; GARAI, Massimo; MORSELLI, Thomas. Preparation and assessment of the potential energy savings of thermochromic and cool coatings considering inter-building effects. **Solar Energy**, [S.L.], v. 209, p. 493-504, out. 2020. Elsevier BV. <http://dx.doi.org/10.1016/j.solener.2020.09.015>.

BRE, Facundo; ROMAN, Nadia; FACHINOTTI, Víctor D.. An efficient metamodel-based method to carry out multi-objective building performance optimizations. **Energy And Buildings**, [S.L.], v. 206, p. 109576, jan. 2020. Elsevier BV. <http://dx.doi.org/10.1016/j.enbuild.2019.109576>.

BRITO, Ana Carolina Pussi de; BRITO, Carolina Moreira Barbosa de; MAURER, Vívian; FREDERICO E SILVA, Caio; AMORIM, Claudia Naves David. O Processo de Projeto de Edifício Escolar: Barreiras e Perspectivas para o Conforto e a Eficiência Energética. Anais Eletrônicos, 2019. João Pessoa: **XV Encontro Nacional de Conforto no Ambiente Construído**.

BROWN, Kyle E.; BANIASSADI, Amir; PHAM, Julie V.; SAILOR, David J.; PHELAN, Patrick E.. Effects of Rooftop Photovoltaics on Building Cooling Demand and Sensible Heat Flux Into the Environment for an Installation on a White Roof. *Journal Of Engineering For Sustainable Buildings And Cities*, [S.L.], v. 1, n. 2, p. 1-7, 12 mar. 2020. ASME International. <http://dx.doi.org/10.1115/1.4046399>.

BYD ENERGY DO BRASIL. **Manual de Instalação**: módulos fotovoltaicos vidro simples. Módulos Fotovoltaicos Vidro Simples. s/d. Disponível em: [https://www.energiasolarphb.com.br/wp-content/uploads/2021/04/Manual-de-Instalacao-Modulos-Fotovoltaicos-rev00-2019\\_5.pdf](https://www.energiasolarphb.com.br/wp-content/uploads/2021/04/Manual-de-Instalacao-Modulos-Fotovoltaicos-rev00-2019_5.pdf). Acesso em: 19 jun. 2023.

CABEZA, Luisa F.; CHÀFER, Marta. Technological options and strategies towards zero energy buildings contributing to climate change mitigation: a systematic review. **Energy And Buildings**, [S.L.], v. 219, p. 110009, jul. 2020. Elsevier BV. <http://dx.doi.org/10.1016/j.enbuild.2020.110009>.

CABEZA, Luisa F.; GRACIA, Alvaro de; PISELLO, Anna Laura. Integration of renewable technologies in historical and heritage buildings: a review. **Energy And Buildings**, [S.L.], v. 177, p. 96-111, out. 2018. Elsevier BV. <http://dx.doi.org/10.1016/j.enbuild.2018.07.058>.

CAIXA ECONÔMICA FEDERAL. Referências de preços e custos. Disponível em: [https://www.caixa.gov.br/Downloads/sinapi-composicoes-aferidas-sumario-composicoes-aferidas/SUMARIO\\_DE\\_PUBLICACOES\\_E\\_DOCUMENTACAO\\_DO\\_SINAPI.pdf](https://www.caixa.gov.br/Downloads/sinapi-composicoes-aferidas-sumario-composicoes-aferidas/SUMARIO_DE_PUBLICACOES_E_DOCUMENTACAO_DO_SINAPI.pdf). Acesso em: jan. 2024.

CANADIAN SOLAR. **Manual de Instalação de Módulos Solares Padrão**. 2019. Disponível em: [https://minhacasasolar.fbtsstatic.net//media/PT\\_Installation\\_Manual\\_of\\_Standard\\_Solar\\_Modules-v1.9a-1-min.pdf?origem=MediaCenter/PT\\_Installation\\_Manual\\_of\\_Standard\\_Solar\\_Modules-v1.9a-1-min.pdf](https://minhacasasolar.fbtsstatic.net//media/PT_Installation_Manual_of_Standard_Solar_Modules-v1.9a-1-min.pdf?origem=MediaCenter/PT_Installation_Manual_of_Standard_Solar_Modules-v1.9a-1-min.pdf). Acesso em: 19 jun. 2023.

CARBONELL-CARRERA, Carlos; SAORIN, Jose; MELIÁN-DÍAZ, Dámari; HESS-MEDLER, Stephany. Spatial Orientation Skill Performance with a Workshop Based on Green Infrastructure in Cities. **Isprs International Journal Of Geo-Information**, [SL], v. 9, no. 4, p. 216, 3 Apr. 2020. MDPI AG. <http://dx.doi.org/10.3390/ijgi9040216>.

CARLOSENA, Laura; ANDUEZA, Ángel; TORRES, Luis; IRULEGI, Olatz; HERNÁNDEZ-MINGUILLÓN, Rufino J.; SEVILLA, Joaquín; SANTAMOURIS, Mattheos. Experimental development and testing of low-cost scalable radiative cooling materials for building applications. **Solar Energy Materials And Solar Cells**, [S.L.], v. 230, p. 111209, set. 2021. Elsevier BV. <http://dx.doi.org/10.1016/j.solmat.2021.111209>.

CASTALDO, Veronica Lucia; PISELLO, Anna Laura; PISELLI, Cristina; FABIANI, Claudia; COTANA, Franco; SANTAMOURIS, Mattheos. How outdoor microclimate mitigation affects building thermal-energy performance: a new design-stage method for energy saving in residential near-zero energy settlements in Italy. **Renewable Energy**, [S.L.], v. 127, p. 920-935, nov. 2018. Elsevier BV. <http://dx.doi.org/10.1016/j.renene.2018.04.090>.

CHEN, Bin; LIU, Qiong; CHEN, Hongyu; WANG, Lei; DENG, Tingting; ZHANG, Limao; WU, Xianguo. Multiobjective optimization of building energy consumption based on BIM-DB and LSSVM-NSGA-II. **Journal Of Cleaner Production**, [S.L.], v. 294, p. 126153, abr. 2021. Elsevier BV. <http://dx.doi.org/10.1016/j.jclepro.2021.126153>.

CIRRINCIONE, Laura; MARVUGLIA, Antonino; SCACCIANOCE, Gianluca. Assessing the effectiveness of green roofs in enhancing the energy and indoor comfort resilience of urban buildings to climate change: methodology proposal and application. **Building And Environment**, [S.L.], v. 205, p. 108198, nov. 2021. Elsevier BV. <http://dx.doi.org/10.1016/j.buildenv.2021.108198>.

CLIMATE ONE BUILDING. 2022. Disponível em: [climate.onebuilding.org](http://climate.onebuilding.org). Acesso em: 10 fev. 2023

COLLADO, N; HIMPE, E; GONZÁLEZ, D; RUEDA, L. Retos para una definición de “Edificios de consumo energético casi nulo”. **Revista Ingeniería de Construcción**, [S.L.], v. 34, n. 3, p. 321-329, dez. 2019. Pontificia Universidad Católica de Chile. <http://dx.doi.org/10.4067/s0718-50732019000300321>.

CORY, Shaan; LENOIR, Aurelie; DONN, Michael; GARDE, Francois. Formulating a Building Climate Classification Method. In: 12th Conference Of International Building Performance Simulation Association, 12., 2011, Sydney. **Proceedings of Building Simulation**. Sydney: Proceedings Of Building Simulation, 2011. p. 1-8.

CRRC. COOL ROOF RATING COUNCIL. CRRC-1 Roof product rating program manual. Portland: CRRC, 2022a.

\_\_\_\_\_. COOL ROOF RATING COUNCIL. CRRC-2 Wall product rating program manual. Portland: CRRC, 2022b.

D'AGOSTINO, Delia; PARKER, Danny; MELIÀ, Paco; DOTELLI, Giovanni. Optimizing photovoltaic electric generation and roof insulation in existing residential buildings. **Energy And Buildings**, [S.L.], v. 255, p. 111652, jan. 2022. Elsevier BV. <http://dx.doi.org/10.1016/j.enbuild.2021.111652>.

DERKENBAEVA, Erkinai; VEGA, Solmaria Halleck; HOFSTEDE, Gert Jan; VAN LEEUWEN, Eveline. Positive energy districts: mainstreaming energy transition in

urban areas. **Renewable And Sustainable Energy Reviews**, [S.L.], v. 153, p. 111782, jan. 2022. Elsevier BV. <http://dx.doi.org/10.1016/j.rser.2021.111782>.

DESIGNBUILDER HELP. 2022. Disponível em: [Designbuilder.co.uk.designbuilder.co.uk/helpv7.0](http://Designbuilder.co.uk.designbuilder.co.uk/helpv7.0). Acesso em: 10 fev. 2023.

DETWILER, Peter Kelly. **Net Zero Schools in Kentucky: Models for the Future Come from Surprising Places**. Forbes, 2012. Disponível em: <<https://www.forbes.com/sites/peterdetwiler/2012/12/10/net-zero-schools-in-kentucky-models-for-the-future-come-from-surprising-places/#5e75ca79456c>>. Acesso em 07 out. 2017.

DÍAZ-LÓPEZ, Carmen; SERRANO-JIMÉNEZ, Antonio; LIZANA, Jesús; LÓPEZ-GARCÍA, Elisa; MOLINA-HUELVA, Marta; BARRIOS-PADURA, Ángela. Passive action strategies in schools: a scientific mapping towards eco-efficiency in educational buildings. **Journal Of Building Engineering**, [S.L.], v. 45, p. 103598, jan. 2022. Elsevier BV. <http://dx.doi.org/10.1016/j.jobbe.2021.103598>.

DORNELLES, Kelen Almeida. Absortância solar de superfícies opacas: métodos de determinação e base de dados para tintas látex acrílica e PVA. 2008. 160p. Tese (Doutorado) - Faculdade de Engenharia Civil, Arquitetura e Urbanismo, Universidade Estadual de Campinas, Campinas, 2008.

ELETROBRÁS; PROCEL; CB3E; UFSC. MANUAL DE APLICAÇÃO DA INI-C: Edificações Comerciais, de Serviços e Públicas. Versão 1. S.I.: **Pbe Edifica**, 2021. 240 p.

EPE – EMPRESA DE PESQUISA ENERGÉTICA. **Balanco Energético Nacional – BEN 2019, ano base 2018**. Rio de Janeiro: Ministério de Minas e Energia, p.1-303, 2019.

\_\_\_\_\_. Plano Nacional de Energia - 2050. Fu, Ran, David Feldman, and Robert Margolis. 2018. Disponível em <<http://www.epe.gov.br/pt/publicacoes-dados-abertos/publicacoes/Plano-Nacional-de-Energia-2050>>. Acesso em: 14 jul. 2022.

EUROPEAN COMMISSION. Energy Performance of Buildings Directive (EPBD). Disponível em: <[https://energy.ec.europa.eu/topics/energy-efficiency/energy-efficient-buildings/energy-performance-buildings-directive\\_en](https://energy.ec.europa.eu/topics/energy-efficiency/energy-efficient-buildings/energy-performance-buildings-directive_en)>. Acesso em: 02 jan. 2024.

FENG, Jie; GAO, Kai; JIANG, Yue; ULPIANI, Giulia; KRAJCIC, Djordje; PAOLINI, Riccardo; RANZI, Gianluca; SANTAMOURIS, Mattheos. Optimization of random silica-polymethylpentene (TPX) radiative coolers towards substantial cooling capacity. **Solar Energy Materials And Solar Cells**, [S.L.], v. 234, p. 111419, jan. 2022a. Elsevier BV. <http://dx.doi.org/10.1016/j.solmat.2021.111419>.

FENG, Jie; KHAN, Ansar; DOAN, Quang-Van; GAO, Kai; SANTAMOURIS, Mattheos. The heat mitigation potential and climatic impact of super-cool broadband radiative coolers on a city scale. **Cell Reports Physical Science**, [S.L.], v. 2, n. 7, p. 100485, jul. 2021. Elsevier BV. <http://dx.doi.org/10.1016/j.xcrp.2021.100485>.

FENG, Jie; SALIARI, Maria; GAO, Kai; SANTAMOURIS, Mattheos. On the cooling energy conservation potential of super cool roofs. **Energy And Buildings**, [S.L.], v. 264, p. 112076, jun. 2022b. Elsevier BV. <http://dx.doi.org/10.1016/j.enbuild.2022.112076>.

FERREIRA, F. L. E S.; PEREIRA, E. B.; LABAKI, L. C.. Fatores associados à distribuição da temperatura das superfícies em áreas urbanas: zonas climáticas locais e características espectrais. **Ambiente Construído**, v. 21, n. Ambient. constr., 2021 21(1), jan. 2021.

FLORES-LARSEN, Silvana; FILIPPÍN, Celina; BRE, Facundo. New metrics for thermal resilience of passive buildings during heat events. **Building And Environment**, [S.L.], v. 230, p. 109990, fev. 2023. Elsevier BV. <http://dx.doi.org/10.1016/j.buildenv.2023.109990>.

FNDE – FUNDO NACIONAL DE DESENVOLVIMENTO DA EDUCAÇÃO. Infraestrutura Física (Escolar). Disponível em: <<https://www.fnde.gov.br/index.php/programas/par/eixos-de-atuacao/infraestrutura-fisica-escolar>>. Acesso em: 19 jan. 2023.

FERREIRA, F; MELLO, M. G. Fundação para o Desenvolvimento Escolar - estruturas pré-fabricadas. Arquitetura Escolar Paulista. São Paulo: FDE, 2006.

FISCHER, PAGANI, Regina Negri; KOVALESKI, João Luiz; DE RESENDE, Luis Mauricio Martins. Avanços na composição da Methodi Ordinatio para revisão sistemática de literatura. **Ciência da Informação**, v. 46, n. 2, 2017.

FRANCÉS, Víctor Manuel Soto; LANZAROTE, A. Begoña Serrano; ESCRIBANO, Vera Valero; ESCUDERO, Miriam Navarro. Improving schools performance based on SHERPA project outcomes: valencia case (spain). **Energy And Buildings**, [S.L.], v. 225, p. 110297, out. 2020. Elsevier BV. <http://dx.doi.org/10.1016/j.enbuild.2020.110297>.

GAITANI, Niki; CASES, Laia; MASTRAPOSTOLI, Elena; ELIOPOULOU, Eftychia. Paving the way to nearly zero energy schools in Mediterranean region - ZEMedS Project. **Energy Procedia**, v. 78, p.3348-3353, 2015.

GALVÃO, Jucilene; BERMANN, Célio. **Crise hídrica e energia: conflitos no uso múltiplo das águas**. São Paulo: Instituto de Energia e Ambiente, Universidade de São Paulo, 2015. Disponível em: < [http://www.scielo.br/scielo.php?script=sci\\_arttext&pid=S0103-40142015000200043](http://www.scielo.br/scielo.php?script=sci_arttext&pid=S0103-40142015000200043)>. Acesso em: 05 out. 2017.

GERALDI, Matheus Soares; GHISI, Enedir. Data-driven framework towards realistic bottom-up energy benchmarking using an Artificial Neural Network. **Applied Energy**, [S.L.], v. 306, p. 117960, jan. 2022a. Elsevier BV. <http://dx.doi.org/10.1016/j.apenergy.2021.117960>.

GERALDI, Matheus Soares; GHISI, Enedir. Integrating evidence-based thermal satisfaction in energy benchmarking: a data-driven approach for a whole-building evaluation. **Energy**, [S.L.], v. 244, p. 123161, abr. 2022b. Elsevier BV. <http://dx.doi.org/10.1016/j.energy.2022.123161>.

GERALDI, Matheus Soares; GHISI, EneDir. Mapping the energy usage in Brazilian public schools. **Energy And Buildings**, [S.L.], v. 224, p. 110209, out. 2020. Elsevier BV. <http://dx.doi.org/10.1016/j.enbuild.2020.110209>.

GERALDI, Matheus Soares; GNECCO, Veronica Martins; BARZAN NETO, Antonio; MARTINS, Bárbara Augusta de Mafra; GHISI, EneDir; FOSSATI, Michele; MELO, Ana Paula; LAMBERTS, Roberto. Evaluating the impact of the shape of school reference buildings on bottom-up energy benchmarking. **Journal Of Building Engineering**, [S.L.], v. 43, p. 103142, nov. 2021. Elsevier BV. <http://dx.doi.org/10.1016/j.jobbe.2021.103142>.

GHADERIAN, Mohammadamin; VEYSI, Farzad. Multi-objective optimization of energy efficiency and thermal comfort in an existing office building using NSGA-II with fitness approximation: a case study. **Journal Of Building Engineering**, [S.L.], v. 41, p. 102440, set. 2021. Elsevier BV. <http://dx.doi.org/10.1016/j.jobbe.2021.102440>.

GIOURI, Evangelia Despoina; TENPIERIK, Martin; TURRIN, Michela. Zero energy potential of a high-rise office building in a Mediterranean climate: using multi-objective optimization to understand the impact of design decisions towards zero-energy high-rise buildings. **Energy And Buildings**, [S.L.], v. 209, p. 109666, fev. 2020. Elsevier BV. <http://dx.doi.org/10.1016/j.enbuild.2019.109666>.

GOMES, Anderson F. Instrução Normativa de Eficiência Energética IN SLTI-MP Nº 02-2014. SLTI/MP – **Secretaria de Logística e Tecnologia da Informação, Ministério do Planejamento**, 2015.

GONZALES, Tomaz Silva. Integração de estratégias passivas de climatização em escolas no contexto climático de Brasília (DF). 2021. 107 f., il. Dissertação (Mestrado em Arquitetura e Urbanismo) — Universidade de Brasília, Brasília, 2021.

GRAÇA, Valéria Azzi Collet da; KOWALTOWSKI, Doris Catharine Cornelie Knatz; PETRECHE, João Roberto Diego. An evaluation method for school building design at the preliminary phase with optimisation of aspects of environmental comfort for the school system of the State São Paulo in Brazil. **Building And Environment**, [S.L.], v. 42, n. 2, p. 984-999, fev. 2007. Elsevier BV. <http://dx.doi.org/10.1016/j.buildenv.2005.10.020>.

GUARDA, E. L. A. da; MIZGIER, M. G. O. .; NETO, A. H. . . Análise da severidade, intensidade e vulnerabilidade dos ocupantes de uma habitação em Cuiabá frente às mudanças climáticas. In: ENCONTRO NACIONAL DE CONFORTO NO AMBIENTE CONSTRUÍDO, 17., 2023. Anais [...]. [S. l.], 2023. p. 1–10. DOI: 10.46421/encac.v17i1.4125. Disponível em: <https://eventos.antac.org.br/index.php/encac/article/view/4125>. Acesso em: 5 jan. 2024.

GUPTA, Sudhir Kumar; CHANDA, Prayag Raj; BISWAS, Agnimitra. A 2E, energy and environment performance of an optimized vernacular house for passive cooling - Case of North-East India. **Building And Environment**, [S.L.], v. 229, p. 109909, fev. 2023. Elsevier BV. <http://dx.doi.org/10.1016/j.buildenv.2022.109909>.

HAWILA, Abed Al Waheed; PERNETTI, Roberta; POZZA, Cristian; BELLERI, Annamaria. Plus energy building: operational definition and assessment. **Energy And Buildings**, [S.L.], v. 265, p. 112069, jun. 2022. Elsevier BV. <http://dx.doi.org/10.1016/j.enbuild.2022.112069>.

HENS, Hugo S. L. C. **Building physics: heat, air and moisture: fundamentals and engineering methods with examples and exercises**. 2nd ed, Ernst & Sohn, a Wiley Company, 2012.

HONG, Taehoon; KIM, Jimin; LEE, Minhyun. A multi-objective optimization model for determining the building design and occupant behaviors based on energy, economic, and environmental performance. **Energy**, [S.L.], v. 174, p. 823-834, maio 2019. Elsevier BV. <http://dx.doi.org/10.1016/j.energy.2019.02.035>.

HONG, Tianzhen; MALIK, Jeetika; KRELLING, Amanda; O'BRIEN, William; SUN, Kaiyu; LAMBERTS, Roberto; WEI, Max. Ten questions concerning thermal resilience of buildings and occupants for climate adaptation. **Building And Environment**, [S.L.], v. 244, p. 110806, out. 2023. Elsevier BV. <http://dx.doi.org/10.1016/j.buildenv.2023.110806>.

HUANG, Pei; HUANG, Gongsheng; SUN, Yongjun. Uncertainty-based life-cycle analysis of near-zero energy buildings for performance improvements. **Applied Energy**, [S.L.], v. 213, p. 486-498, mar. 2018. Elsevier BV. <http://dx.doi.org/10.1016/j.apenergy.2018.01.059>.

IEA – INTERNATIONAL ENERGY AGENCY. Subtask C - annex 52. Net zero energy solar buildings: position paper. [S.l.], 2014. 10p.

IBGE – Instituto Brasileiro de Geografia e Estatística. **Brasil em Síntese: território: dados geográficos**. 2023. Disponível em: <https://brasilemsintese.ibge.gov.br/territorio/dados-geograficos.html>. Acesso em: 19 jun. 2023.

IBRAP. **Manual de Instalação: telhados fotovoltaicos**. Telhados Fotovoltaicos. n/d. Disponível em: <https://ibrap.com.br/arquivos/catalogos/IBRAP-Fotovoltaico---Manual-de-Instala-o-1979965996.pdf>. Acesso em: 19 jun. 2023.

IDEAL ESTUDOS E SOLUÇÕES SOLARES. **Guia de Boas Práticas em Sistemas Fotovoltaicos**. 2019. Disponível em: [https://cooperacaobrasil-alemanha.com/SEF/Guia\\_de\\_Boas\\_Praticas\\_Sistemas\\_Fotovoltaicos.pdf](https://cooperacaobrasil-alemanha.com/SEF/Guia_de_Boas_Praticas_Sistemas_Fotovoltaicos.pdf). Acesso em: 19 jun. 2023.

INEP – INSTITUTO NACIONAL DE ESTUDOS E PESQUISAS EDUCACIONAIS ANÍSIO TEIXEIRA. **Censo da Educação Básica**, 2021. Disponível em <<https://inepdata.inep.gov.br/analytics/saw.dll?Dashboard>>. Acesso em: 14 jul. 2022.

INMET – INSTITUTO NACIONAL DE METEOROLOGIA DO BRASIL. Normais Climatológicas (1961/1990), 2023. Disponível em <<https://clima.inmet.gov.br/GraficosClimatologicos/>>. Acesso em: 27 jun. 2023.

INMETRO – INSTITUTO NACIONAL DE METROLOGIA, QUALIDADE E TECNOLOGIA. Portaria nº 42, de 24 de fevereiro de 2021. Instrução Normativa



Inmetro para a Classificação de Eficiência Energética de Edificações Comerciais, de Serviços e Públicas (INI-C). Diário Oficial da União, Brasília - DF, 2021.

IPCC – Intergovernmental Panel on Climate Change. Climate change 2021: the physical science basis: summary for policymakers: working group I contribution to the sixth Assessment report of the Intergovernmental Panel on Climate Change. Geneva, Switzerland, 2021.

ISMAIL, Nagham; OUAHRANI, Djamel; TOUMA, Albert Al. Quantifying thermal resilience of office buildings during power outages: development of a simplified model metric and validation through experimentation. **Journal Of Building Engineering**, [S.L.], v. 72, p. 106564, ago. 2023. Elsevier BV. <http://dx.doi.org/10.1016/j.jobbe.2023.106564>.

JI, Lili; SHU, Chang; LAOUADI, Abdelaziz; LACASSE, Michael; WANG, Liangzhu (Leon). Quantifying improvement of building and zone level thermal resilience by cooling retrofits against summertime heat events. **Building And Environment**, [S.L.], v. 229, p. 109914, fev. 2023. Elsevier BV. <http://dx.doi.org/10.1016/j.buildenv.2022.109914>.

JOTA, Patricia Romeiro da Silva; SOUZA, Anádia Patrícia Almeida de; SILVA, Valéria Romeiro Borges da. Energy performance indexes: analysis in public schools in brazil. **Energy Efficiency**, [S.L.], v. 10, n. 6, p. 1433-1451, 31 maio 2017. Springer Science and Business Media LLC. <http://dx.doi.org/10.1007/s12053-017-9530-7>.

KHAN, Hassan Saeed; PAOLINI, Riccardo; CACCETTA, Peter; SANTAMOURIS, Mat. On the combined impact of local, regional, and global climatic changes on the urban energy performance and indoor thermal comfort—The energy potential of adaptation measures. **Energy And Buildings**, [S.L.], v. 267, p. 112152, jul. 2022. Elsevier BV. <http://dx.doi.org/10.1016/j.enbuild.2022.112152>.

KOLOKOTSA, Dionysia – Denia; GIANNARIAKIS, Gerassimos; GOBAKIS, Kostas; GIANNARAKIS, Giannis; SYNNEFA, Afroditi; SANTAMOURIS, Mat. Cool roofs and cool pavements application in Acharnes, Greece. **Sustainable Cities And Society**, [S.L.], v. 37, p. 466-474, fev. 2018. Elsevier BV. <http://dx.doi.org/10.1016/j.scs.2017.11.035>.

KOTTEK, Markus; GRIESER, Jürgen; BECK, Christoph; RUDOLF, Bruno; RUBEL, Franz. World Map of the Köppen-Geiger climate classification updated. **Meteorologische Zeitschrift**, [SL], v. 15, no. 3, p. 259-263, 10 Jul. 2006. Schweizerbart. <http://dx.doi.org/10.1127/0941-2948/2006/0130>.

KOWALTOWSKI, Doris C. C. K.; LABAKI, Lucila C; PINA, Silva A. Mikami G. **Conforto e Ambiente Escolar**. In: Arquitetura Bioclimática: Arquitetura Escolar, 2001, Bauru. Arquitetura Bioclimática: Arquitetura Escolar, 2001.

KRELLING, Amanda F.; LAMBERTS, Roberto; MALIK, Jeetika; HONG, Tianzhen. A simulation framework for assessing thermally resilient buildings and communities. **Building And Environment**, [S.L.], v. 245, p. 110887, nov. 2023. Elsevier BV. <http://dx.doi.org/10.1016/j.buildenv.2023.110887>.

LASSANDRO, Paola; TURI, Silvia. Energy efficiency and resilience against increasing temperatures in summer: the use of PCM and cool materials in buildings. **International Journal Of Heat And Technology**, [S.L.], v. 35, n. 1, p. S307-S315, 20 set. 2017. International Information and Engineering Technology Association. <http://dx.doi.org/10.18280/ijht.35sp0142>.

LASSANDRO, P; TURI, S di; A ZACCARO, S. Mitigation of rising urban temperatures starting from historic and modern street canyons towards zero energy settlement. **IOP Conference Series: Materials Science and Engineering**, [S.L.], v. 609, n. 7, p. 072036, 1 set. 2019. IOP Publishing. <http://dx.doi.org/10.1088/1757-899x/609/7/072036>.

LIM, Xiaozhi. The super-cool materials that send heat to space. **Nature**, [S.L.], v. 577, n. 7788, p. 18-20, 31 dez. 2019. Springer Science and Business Media LLC. <http://dx.doi.org/10.1038/d41586-019-03911-8>.

LIN, Yaolin; ZHONG, Shengli; YANG, Wei; HAO, Xiaoli; LI, Chun-Qing. Towards zero-energy buildings in China: a systematic literature review. **Journal Of Cleaner Production**, [S.L.], v. 276, p. 123297, dez. 2020. Elsevier BV. <http://dx.doi.org/10.1016/j.jclepro.2020.123297>.

LIU, Zhijian; ZHOU, Qingxu; TIAN, Zhiyong; HE, Bao-Jie; JIN, Guangya. A comprehensive analysis on definitions, development, and policies of nearly zero energy buildings in China. **Renewable And Sustainable Energy Reviews**, [S.L.], v. 114, p. 109314, out. 2019. Elsevier BV. <http://dx.doi.org/10.1016/j.rser.2019.109314>.

LOPES, Adriano Felipe Oliveira. Da simulação ao projeto: avaliação de conforto térmico em ambiente escolar padronizado. 2020. 130 f., il. Dissertação (Mestrado em Arquitetura e Urbanismo) — Universidade de Brasília, Brasília, 2020.

LOVEDAY, Jane; MORRISON, Gregory M.; MARTIN, David A.. Identifying Knowledge and Process Gaps from a Systematic Literature Review of Net-Zero Definitions. **Sustainability**, [S.L.], v. 14, n. 5, p. 3057, 5 mar. 2022. MDPI AG. <http://dx.doi.org/10.3390/su14053057>.

MACIEL, Thalita dos Santos; LEITZKE, Rodrigo Karini; DUARTE, Carolina de Mesquita; SCHRAMM, Fábio Kellermann; CUNHA, Eduardo Grala da. Otimização termoenergética de uma edificação escolar: discussão sobre o desempenho de quatro algoritmos evolutivos multiobjetivo. **Ambiente Construído**, [S.L.], v. 21, n. 4, p. 221-246, out. 2021. FapUNIFESP (SciELO). <http://dx.doi.org/10.1590/s1678-86212021000400567>.

MANNI, Mattia; LOBACCARO, Gabriele; GOIA, Francesco; NICOLINI, Andrea; ROSSI, Federico. Exploiting selective angular properties of retro-reflective coatings to mitigate solar irradiation within the urban canyon. **Solar Energy**, [S.L.], v. 189, p. 74-85, set. 2019. Elsevier BV. <http://dx.doi.org/10.1016/j.solener.2019.07.045>.

MAO, Zepeng; YANG, Zhangbin; ZHANG, Jun. SrTiO<sub>3</sub> as a new solar reflective pigment on the cooling property of PMMA-ceramic composites. **Ceramics International**, [S.L.], v. 45, n. 13, p. 16078-16087, set. 2019. Elsevier BV. <http://dx.doi.org/10.1016/j.ceramint.2019.05.124>.

MAURI, Luca; BATTISTA, Gabriele; VOLLARO, Emanuele de Lieto; VOLLARO, Roberto de Lieto. Retroreflective materials for building's façades: experimental characterization and numerical simulations. **Solar Energy**, [S.L.], v. 171, p. 150-156, set. 2018. Elsevier BV. <http://dx.doi.org/10.1016/j.solener.2018.06.073>.

MEC – MINISTÉRIO DA EDUCAÇÃO. Manual de Orientações Técnicas do Programa Nacional de Reestruturação e Aquisição de Equipamentos para a Rede Escolar Pública de Educação Infantil – PROINFÂNCIA. **Fundo Nacional de Desenvolvimento da Educação – FNDE**, 2007.

MEHMOOD, Sajid; LIZANA, Jesus; NÕÑEZ-PEIRÓ, Miguel; MAXIMOV, Serguey A.; FRIEDRICH, Daniel. Resilient cooling pathway for extremely hot climates in southern Asia. **Applied Energy**, [S.L.], v. 325, p. 119811, nov. 2022. Elsevier BV. <http://dx.doi.org/10.1016/j.apenergy.2022.119811>.

MERCADO LIVRE. Disponível em: <https://www.mercadolivre.com.br/>. Acesso em: 04 jan. 2024.

MERLET, Yannis; ROUCHIER, Simon; JAY, Arnaud; CELLIER, Nicolas; WOLOSZYN, Monika. Integration of phasing on multi-objective optimization of building stock energy retrofit. **Energy And Buildings**, [S.L.], v. 257, p. 111776, fev. 2022. Elsevier BV. <http://dx.doi.org/10.1016/j.enbuild.2021.111776>.

MMA – MINISTÉRIO DO MEIO AMBIENTE. Cartilha “O Que Fazer Para Tornar Mais Eficiente O Uso De Energia Elétrica Em Prédios Públicos”, 2013. Disponível em: <[http://www.mme.gov.br/documents/10584/1985241/cartilha+ ENERGIA+op1.pdf](http://www.mme.gov.br/documents/10584/1985241/cartilha+ENERGIA+op1.pdf)>. Acesso em: 05 out. 2017.

MODLER, Nébora Lazzarotto *et al.* AVALIAÇÃO DO AMBIENTE CONSTRUÍDO DE ESCOLAS DE EDUCAÇÃO INFANTIL DO PROINFÂNCIA NA REGIÃO DE ERECHIM/RS. SEPE-Seminário de Ensino, Pesquisa e Extensão da UFFS, v. 7, n. 1, 2017.

MOGHATA, Abdolmajid; SHAHROUZIANFAR, Ali; ASHIRI, Rouhollah. Facile synthesis of NiTiO<sub>3</sub> yellow nano-pigments with enhanced solar radiation reflection efficiency by an innovative one-step method at low temperature. **Dyes And Pigments**, [S.L.], v. 139, p. 388-396, abr. 2017. Elsevier BV. <http://dx.doi.org/10.1016/j.dyepig.2016.12.044>.

MORINI, Elena; CASTELLANI, Beatrice; PRESCIUTTI, Andrea; FILIPPONI, Mirko; NICOLINI, Andrea; ROSSI, Federico. Optic-energy performance improvement of exterior paints for buildings. **Energy And Buildings**, [S.L.], v. 139, p. 690-701, mar. 2017. Elsevier BV. <http://dx.doi.org/10.1016/j.enbuild.2017.01.060>.

MOSTAFAZADEH, Farzad; EIRDMOUSA, Saeed Jalilzadeh; TAVAKOLAN, Mehdi. Energy, economic and comfort optimization of building retrofits considering climate change: a simulation-based nsga-iii approach. **Energy And Buildings**, [S.L.], v. 280, p. 112721, fev. 2023. Elsevier BV. <http://dx.doi.org/10.1016/j.enbuild.2022.112721>.

MUSSARD, Maxime; AMARA, Mohamed. Performance of solar photovoltaic modules under arid climatic conditions: a review. **Solar Energy**, [S.L.], v. 174, p. 409-421, nov. 2018. Elsevier BV. <http://dx.doi.org/10.1016/j.solener.2018.08.071>.

NADERI, Ehsan; SAJADI, Behrang; BEHABADI, Mohammadali Akhavan; NADERI, Erfan. Multi-objective simulation-based optimization of controlled blind specifications to reduce energy consumption, and thermal and visual discomfort: case studies in iran. **Building And Environment**, [S.L.], v. 169, p. 106570, fev. 2020. Elsevier BV. <http://dx.doi.org/10.1016/j.buildenv.2019.106570>.

NAJI, Sareh; AYE, Lu; NOGUCHI, Masa. Multi-objective optimisations of envelope components for a prefabricated house in six climate zones. **Applied Energy**, [S.L.], v. 282, p. 116012, jan. 2021. Elsevier BV. <http://dx.doi.org/10.1016/j.apenergy.2020.116012>.

NEOSOLAR. **Simulador Solar - Calculadora Solar Fotovoltaica**. Disponível em: <https://www.neosolar.com.br/simulador-solar-calculadora-fotovoltaica>. Acesso em: 16 maio 2023.

ORANJE, Roberto. Viabilidade para Implantação de Edifícios de Balanço Energético Zero no Brasil. Anais Eletrônicos... São Paulo: **Vesta Comunicação**, p. 416-432, 2013. Disponível em: <[https://issuu.com/robertooranje/docs/anais\\_\\_ciis\\_2013\\_\\_vol\\_1](https://issuu.com/robertooranje/docs/anais__ciis_2013__vol_1)>. Acesso em: 19 ago. 2017.

OSMAN, Mobark M.; SEVINC, Harun. Adaptation of climate-responsive building design strategies and resilience to climate change in the hot/arid region of Khartoum, Sudan. **Sustainable Cities And Society**, [S.L.], v. 47, p. 101429, maio 2019. Elsevier BV. <http://dx.doi.org/10.1016/j.scs.2019.101429>.

PARKIN, Anna; HERRERA, Manuel; A COLEY, David. Energy or carbon? Exploring the relative size of universal zero carbon and zero energy design spaces. **Building Services Engineering Research And Technology**, [S.L.], v. 40, n. 3, p. 319-339, 27 nov. 2018. SAGE Publications. <http://dx.doi.org/10.1177/0143624418815780>.

PBEEDIFICA. Ministério do Planejamento, Orçamento e Gestão. Secretaria de Logística e Tecnologia da Informação. **Instrução Normativa Nº 02 de 04 de junho de 2014**.

PIDERIT, María; VIVANCO, Franklin; VAN MOESEKE, Geoffrey; ATTIA, Shady. Net Zero Buildings—A Framework for an Integrated Policy in Chile. **Sustainability**, [S.L.], v. 11, n. 5, p. 1494, 12 mar. 2019. MDPI AG. <http://dx.doi.org/10.3390/su11051494>.

PISELLO, Anna Laura. State of the art on the development of cool coatings for buildings and cities. **Solar Energy**, [S.L.], v. 144, p. 660-680, mar. 2017. Elsevier BV. <http://dx.doi.org/10.1016/j.solener.2017.01.068>.

PROCELINFO – CENTRO BRASILEIRO DE INFORMAÇÃO DE EFICIÊNCIA ENERGÉTICA. **Sobre o Programa Procel**. Disponível em: <<http://www.procelinfo.com.br/main.asp?TeamID={921E566A-536B-4582-AEAF-7D6CD1DF1AFD}>>>. Acesso em: 25 jun. 2018.

PROJETEEE. **Projetando Edificações Energeticamente Eficientes. Componentes Construtivos**. Disponível em: <http://www.mme.gov.br/projeteee/componentes-construtivos/>. Acesso em 27 jul. 2023.

QI, Yanli; XIANG, Bo; TAN, Wubin; ZHANG, Jun. Hydrophobic surface modification of TiO<sub>2</sub> nanoparticles for production of acrylonitrile-styrene-acrylate terpolymer/TiO<sub>2</sub> composited cool materials. **Applied Surface Science**, [S.L.], v. 419, p. 213-223, out. 2017. Elsevier BV. <http://dx.doi.org/10.1016/j.apsusc.2017.04.234>.

QI, Yanli; ZHU, Suoshi; ZHANG, Jun. The incorporation of modified Sb<sub>2</sub>O<sub>3</sub> and DBDPE: a new member of high solar-reflective particles and their simultaneous application in next-generation multifunctional cool material with improved flame retardancy and lower wetting behaviour. **Energy And Buildings**, [S.L.], v. 172, p. 47-56, ago. 2018. Elsevier BV. <http://dx.doi.org/10.1016/j.enbuild.2018.04.050>.

QUEIROZ, Mateus Oliveira de; TELES, Camila Correia; NUNES, Orlando Vinicius Rangel. Habitação de Interesse Social Vertical de Balanço Energético Nulo no Sol Nascente-DF. Anais Eletrônicos, 2019. João Pessoa: **XV Encontro Nacional de Conforto no Ambiente Construído**.

RACKES, Adams *et al.* Avaliação do potencial de conforto térmico em escolas naturalmente ventiladas. **Encontro Nacional de Conforto no Ambiente Construído**, v. 13, p. 1-10, 2015.

RIZZO, Gianfranco. Ricerca Sistema Elettrico: Analisi dello stato dell' arte nazionale ed Internazionale dei sistemi integrati di illuminazione naturale/artificiale in relazione all'involucro edilizio nel caso di edifici del terziario e abitativi, ai fini di un loro impiego nell'ambito della certificazione energetica degli edifici, Report RSE/2009/14. **Ente per le Nuove tecnologie, l'Energie e l'Ambiente**, 2009.

ROMEO, C.; ZINZI, M.. Impact of a cool roof application on the energy and comfort performance in an existing non-residential building. A Sicilian case study. **Energy And Buildings**, [S.L.], v. 67, p. 647-657, dez. 2013. Elsevier BV. <http://dx.doi.org/10.1016/j.enbuild.2011.07.023>.

RORIZ, Maurício. Classificação de climas do Brasil – Versão 3.0. ANTAC: São Carlos, 2014. 5 p.

RORIZ, Maurício. Uma proposta de revisão do zoneamento bioclimático brasileiro. ANTAC: São Carlos, 2012. 22 p.

SAILOR, D.J.; ANAND, J.; KING, R.R.. Photovoltaics in the built environment: a critical review. **Energy And Buildings**, [S.L.], v. 253, p. 111479, dez. 2021. Elsevier BV. <http://dx.doi.org/10.1016/j.enbuild.2021.111479>.

SALATA, Ferdinando; CIANCIO, Virgilio; DELL'OLMO, Jacopo; GOLASI, Iacopo; PALUSCI, Olga; COPPI, Massimo. Effects of local conditions on the multi-variable and multi-objective energy optimization of residential buildings using genetic algorithms. **Applied Energy**, [S.L.], v. 260, p. 114289, fev. 2020. Elsevier BV. <http://dx.doi.org/10.1016/j.apenergy.2019.114289>.

SANTAMOURIS, Mat; YUN, Geun Young. Recent development and research priorities on cool and super cool materials to mitigate urban heat island. **Renewable Energy**, [S.L.], v. 161, p. 792-807, dez. 2020. Elsevier BV. <http://dx.doi.org/10.1016/j.renene.2020.07.109>.

SANTAMOURIS, M.; VASILAKOPOULOU, K.. Recent progress on urban heat mitigation technologies. **Science Talks**, [S.L.], v. 5, p. 100105, mar. 2023. Elsevier BV. <http://dx.doi.org/10.1016/j.sctalk.2022.100105>.

SANTOS, Erica Kelly Schillemer dos. **Diretrizes para a concepção de projetos de sistema fotovoltaico conectado à rede em residências de médio padrão na cidade de Pato Branco-Paraná**. 2018. Trabalho de Conclusão de Curso. Universidade Tecnológica Federal do Paraná.

SARTORI, Igor; NAPOLITANO, Assunta; VOSS, Karsten. Net zero energy buildings: a consistent definition framework. **Energy And Buildings**, [S.L.], v. 48, p. 220-232, maio 2012. Elsevier BV. <http://dx.doi.org/10.1016/j.enbuild.2012.01.032>.

SE – SECRETARIA DE ENERGIA. Manual de Economia de Energia Elétrica na Escola. São Paulo, SP: **Governo do Estado de São Paulo**, s.d. Disponível em: <[https://www.ecoreporter.abae.pt/docs/apoio/Manual\\_de\\_Economia\\_de\\_Energia\\_Eletrica\\_na\\_Escola.pdf](https://www.ecoreporter.abae.pt/docs/apoio/Manual_de_Economia_de_Energia_Eletrica_na_Escola.pdf)>. Acesso em 07 out. 2017.

SENGUPTA, Abantika; ASSAAD, Douaa Al; BASTERO, Josué Borrajo; STEEMAN, Marijke; BREESCH, Hilde. Impact of heatwaves and system shocks on a nearly zero energy educational building: is it resilient to overheating?. **Building And Environment**, [S.L.], v. 234, p. 110152, abr. 2023a. Elsevier BV. <http://dx.doi.org/10.1016/j.buildenv.2023.110152>.

SENGUPTA, Abantika; BREESCH, Hilde; ASSAAD, Douaa Al; STEEMAN, Marijke. Evaluation of thermal resilience to overheating for an educational building in future heatwave scenarios. **International Journal Of Ventilation**, [S.L.], v. 22, n. 4, p. 366-376, jun. 2023b. Informa UK Limited. <http://dx.doi.org/10.1080/14733315.2023.2218424>.

SERDAR, Mohammad Zaher; MACAULEY, Nadine; AL-GHAMDI, Sami G.. Building thermal resilience framework (BTRF): a novel framework to address the challenge of extreme thermal events, arising from climate change. **Frontiers In Built Environment**, [S.L.], v. 8, p. 1-8, 11 nov. 2022. Frontiers Media SA. <http://dx.doi.org/10.3389/fbuil.2022.1029992>.

SHIRINBAKHSH, Mehrdad; HARVEY, L.D. Danny. Net-zero energy buildings: the influence of definition on greenhouse gas emissions. **Energy And Buildings**, [S.L.], v. 247, p. 111118, set. 2021. Elsevier BV. <http://dx.doi.org/10.1016/j.enbuild.2021.111118>.

SILVA, M. P.; MARINOSKI, D.; GUTHS, S. Simulação Termoenergética e Análise Econômica do Uso de Telhados de Fibrocimento de Alta Refletância Solar em uma Residência Unifamiliar. In: Encontro Nacional De Tecnologia No Ambiente Construído, 2020. **Anais [...]**. Porto Alegre: ANTAC, 2020. p. 1–8. Disponível em: <https://eventos.antac.org.br/index.php/entac/article/view/734>. Acesso em: 30 maio. 2022.

SIU, Chun Yin; O'BRIEN, William; TOUCHIE, Marianne; ARMSTRONG, Marianne; LAOUADI, Abdelaziz; GAUR, Abhishek; JANDAGHIAN, Zahra; MACDONALD, Iain. Evaluating thermal resilience of building designs using building performance simulation – A review of existing practices. **Building And Environment**, [S.L.], v.

234, p. 110124, abr. 2023. Elsevier BV.  
<http://dx.doi.org/10.1016/j.buildenv.2023.110124>.

STEFFEN, C. A.; MORAES, E. C.; GAMA, F. F. Radiometria óptica Espectral – Tutorial. In: VIII Simpósio Brasileiro de Sensoriamento Remoto, 1996, Salvador. Anais... Salvador: INPE, 1996.

TAVAKOLAN, Mehdi; MOSTAFAZADEH, Farzad; EIRDMOUSA, Saeed Jalilzadeh; SAFARI, Amir; MIRZAEI, Kaveh. A parallel computing simulation-based multi-objective optimization framework for economic analysis of building energy retrofit: a case study in iran. **Journal Of Building Engineering**, [S.L.], v. 45, p. 103485, jan. 2022. Elsevier BV. <http://dx.doi.org/10.1016/j.jobbe.2021.103485>.

TAVAKOLI, Elahe; O'DONOVAN, Adam; KOLOKOTRONI, Maria; O'SULLIVAN, Paul D.. Evaluating the indoor thermal resilience of ventilative cooling in non-residential low energy buildings: a review. **Building And Environment**, [S.L.], v. 222, p. 109376, ago. 2022. Elsevier BV. <http://dx.doi.org/10.1016/j.buildenv.2022.109376>.

TELES, Camila Correia; *et al.* Avaliação de Eficiência Energética e Conforto Térmico de Projetos Educacionais Padronizados do Fnde. Encontro Nacional de Conforto no Ambiente Construído. João Pessoa: [s.n.]. 2019. p. 9.

TIAN, Liu; LI, Yongcai; LU, Jun; WANG, Jue. Review on Urban Heat Island in China: methods, its impact on buildings energy demand and mitigation strategies. **Sustainability**, [S.L.], v. 13, n. 2, p. 762, 14 jan. 2021. MDPI AG. <http://dx.doi.org/10.3390/su13020762>.

VASILAKOPOULOU, K.; ULPIANI, G.; KHAN, A.; SYNNEFA, A.; SANTAMOURIS, M.. Cool roofs boost the energy production of photovoltaics: investigating the impact of roof albedo on the energy performance of monofacial and bifacial photovoltaic modules. **Solar Energy**, [S.L.], v. 265, p. 111948, nov. 2023. Elsevier BV. <http://dx.doi.org/10.1016/j.solener.2023.111948>.

VUKADINOVIĆ, Ana; RADOSAVLJEVIĆ, Jasmina; ĐORĐEVIĆ, Amelija; PROTIĆ, Milan; PETROVIĆ, Nemanja. Multi-objective optimization of energy performance for a detached residential building with a sunspace using the NSGA-II genetic algorithm. **Solar Energy**, [S.L.], v. 224, p. 1426-1444, ago. 2021. Elsevier BV. <http://dx.doi.org/10.1016/j.solener.2021.06.082>.

WANG, Yanjin; YANG, Weibin; WANG, Qian. Multi-objective parametric optimization of the composite external shading for the classroom based on lighting, energy consumption, and visual comfort. **Energy And Buildings**, [S.L.], v. 275, p. 112441, nov. 2022. Elsevier BV. <http://dx.doi.org/10.1016/j.enbuild.2022.112441>.

WEBER, F. S.; MELO, A. P.; MARINOSKI, D. L.; GUTHS, S.; LAMBERTS, R. Desenvolvimento de um modelo equivalente de avaliação de propriedades térmicas para a elaboração de uma biblioteca de componentes construtivos brasileiros para o uso no programa EnergyPlus. , p. 52, 2017

WELLS, Louise; RISMANCHI, Behzad; AYE, Lu. A review of Net Zero Energy Buildings with reflections on the Australian context. **Energy And Buildings**, [S.L.], v.

158, p. 616-628, jan. 2018. Elsevier BV. <http://dx.doi.org/10.1016/j.enbuild.2017.10.055>.

WERLE, Ana Paula; LOH, Kai; JOHN, Vanderley Moacyr. Pintura à base de cal como alternativa de revestimento frio. **Ambiente Construído**, [S.L.], v. 14, n. 3, p. 149-157, set. 2014. FapUNIFESP (SciELO). <http://dx.doi.org/10.1590/s1678-86212014000300012>.

XIANG, Bo; ZHANG, Jun. Effects of content and surface hydrophobic modification of BaTiO<sub>3</sub> on the cooling properties of ASA (acrylonitrile-styrene-acrylate copolymer). **Applied Surface Science**, [S.L.], v. 427, p. 654-661, jan. 2018a. Elsevier BV. <http://dx.doi.org/10.1016/j.apsusc.2017.08.080>.

XIANG, Bo; ZHANG, Jun. A new member of solar heat-reflective pigments: batio<sub>3</sub> and its effect on the cooling properties of asa (acrylonitrile-styrene-acrylate copolymer). **Solar Energy Materials And Solar Cells**, [S.L.], v. 180, p. 67-75, jun. 2018b. Elsevier BV. <http://dx.doi.org/10.1016/j.solmat.2018.02.027>.

XIE, Liang; LI, Zhe; LI, Jiayu; YANG, Guanglei; JIANG, Jishui; LIU, Zhezhen; TONG, Shuyuan. The Impact of Traditional Raw Earth Dwellings' Envelope Retrofitting on Energy Saving: a case study from zhushan village, in west of hunan, china. **Atmosphere**, [S.L.], v. 13, n. 10, p. 1537, 20 set. 2022. MDPI AG. <http://dx.doi.org/10.3390/atmos13101537>.

XU, Ling; DAI, Linchuan; YIN, Linzhi; SUN, Xiaoyu; XU, Wei; YANG, Rui; WANG, Xin; ZHANG, Yinping. Research on the climate response of variable thermo-physical property building envelopes: a literature review. **Energy And Buildings**, [S.L.], v. 226, p. 110398, nov. 2020. Elsevier BV. <http://dx.doi.org/10.1016/j.enbuild.2020.110398>.

XUE, Qingwen; WANG, Zhaojun; CHEN, Qingyan. Multi-objective optimization of building design for life cycle cost and CO<sub>2</sub> emissions: a case study of a low-energy residential building in a severe cold climate. **Building Simulation**, [S.L.], v. 15, n. 1, p. 83-98, 4 jun. 2021. Springer Science and Business Media LLC. <http://dx.doi.org/10.1007/s12273-021-0796-5>.

YANG, Rui; HAN, Aijun; YE, Mingquan; CHEN, Xingxing; YUAN, Lin. Synthesis, characterization and thermal performance of Fe/N co-doped MgTiO<sub>3</sub> as a novel high near-infrared reflective pigment. **Solar Energy Materials And Solar Cells**, [S.L.], v. 160, p. 307-318, fev. 2017. Elsevier BV. <http://dx.doi.org/10.1016/j.solmat.2016.10.045>.

YUAN, Lin; HAN, Aijun; YE, Mingquan; CHEN, Xingxing; DING, Cheng; YAO, Lingyun. Preparation, characterization and thermal performance evaluation of coating colored with NIR reflective pigments: bivo<sub>4</sub> coated mica-titanium oxide. **Solar Energy**, [S.L.], v. 163, p. 453-460, mar. 2018. Elsevier BV. <http://dx.doi.org/10.1016/j.solener.2018.01.009>.

YUE, Naihua; LI, Lingling; MORANDI, Alessandro; ZHAO, Yang. A metamodel-based multi-objective optimization method to balance thermal comfort and energy efficiency



in a campus gymnasium. **Energy And Buildings**, [S.L.], v. 253, p. 111513, dez. 2021. Elsevier BV. <http://dx.doi.org/10.1016/j.enbuild.2021.111513>.

ZEMERO, Bruno Ramos; TOSTES, Maria Emília de Lima; BEZERRA, Ubiratan Holanda; BATISTA, Vitor dos Santos; CARVALHO, Carminda Célia M. M.. Methodology for Preliminary Design of Buildings Using Multi-Objective Optimization Based on Performance Simulation. **Journal Of Solar Energy Engineering**, [S.L.], v. 141, n. 4, p. 1-12, 8 jan. 2019. ASME International. <http://dx.doi.org/10.1115/1.4042244>.

ZHANG, Chen; KAZANCI, Ongun Berk; LEVINSON, Ronnen; HEISELBERG, Per; OLESEN, Bjarne W.; CHIESA, Giacomo; SODAGAR, Behzad; AI, Zhengtao; SELKOWITZ, Stephen; ZINZI, Michele. Resilient cooling strategies – A critical review and qualitative assessment. **Energy And Buildings**, [S.L.], v. 251, p. 111312, nov. 2021. Elsevier BV. <http://dx.doi.org/10.1016/j.enbuild.2021.111312>.

ZHANG, Longlong; YUAN, Jingwen; KIM, Chul Soo. Application of energy-saving building's designing methods in marine cities. **Energy Reports**, [S.L.], v. 9, p. 98-110, set. 2023. Elsevier BV. <http://dx.doi.org/10.1016/j.egyr.2023.04.333>.

ZHANG, Shicong; WANG, Ke; XU, Wei; IYER-RANIGA, Usha; ATHIENITIS, Andreas; GE, Hua; CHO, Dong Woo; FENG, Wei; OKUMIYA, Masaya; YOON, Gyuyoung. Policy recommendations for the zero energy building promotion towards carbon neutral in Asia-Pacific Region. **Energy Policy**, [S.L.], v. 159, p. 112661, dez. 2021. Elsevier BV. <http://dx.doi.org/10.1016/j.enpol.2021.112661>.

ZHAO, Jing; DU, Yahui. Multi-objective optimization design for windows and shading configuration considering energy consumption and thermal comfort: a case study for office building in different climatic regions of china. **Solar Energy**, [S.L.], v. 206, p. 997-1017, ago. 2020. Elsevier BV. <http://dx.doi.org/10.1016/j.solener.2020.05.090>.

## APPENDICES

The appendices are organized into 15 parts:

- A: Architectural data of FNDE standardized 1 classroom public schools;
- B: Climate Characterization Maps;
- C: Shading Dimensioning for Belém – PA (Zone 8) and Picos – PI (Zone 7);
- D: Thermal Comfort and Heat Balance of Current State 1 Classroom School;
- E: Thermal Comfort and Heat Balance of Algorithm Optimized 1 Classroom School;
- F: Sensitivity Analysis Results of Optimized 1 Classroom School;
- G: Thermal Comfort and Heat Balance of Non-Algorithm Optimized 1 Classroom School;
- H: Heat Balance Results of Roof and Wall Type Variantion;
- I: Data used in computer simulations;

J: Sunpath studies to avoid shadings on PV System;

K: Annual loads and local energy production;

L: Thermal Comfort of Current State 1 Classroom School in 2050 and 2080;

M: Thermal Comfort of Optimized 1 Classroom School in 2050 and 2080;

N: Results of Passive Survivability: Degree Hour ( $^{\circ}\text{C SET-hr}$ ) Limits Compliance

O: Annual loads and local energy production to maintain Passive Survivability in 2050 and 2080.

## APPENDIX A

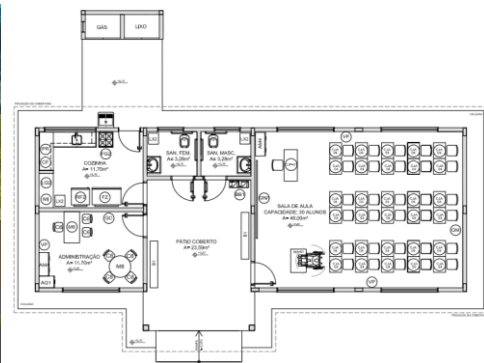
All drawings in this appendix were made available by FNDE (n/d), regarding to the 1 classroom school, chosen to this thesis.

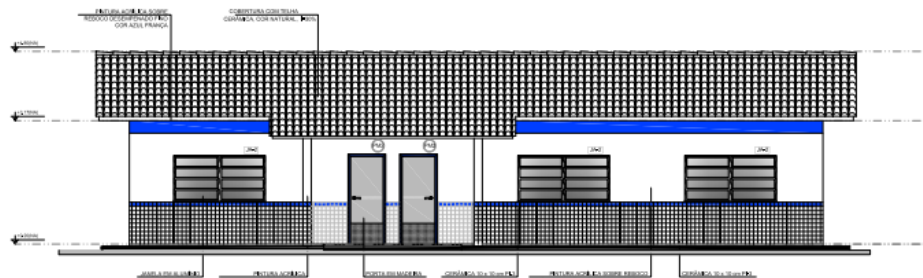
External View: 1 Classroom School



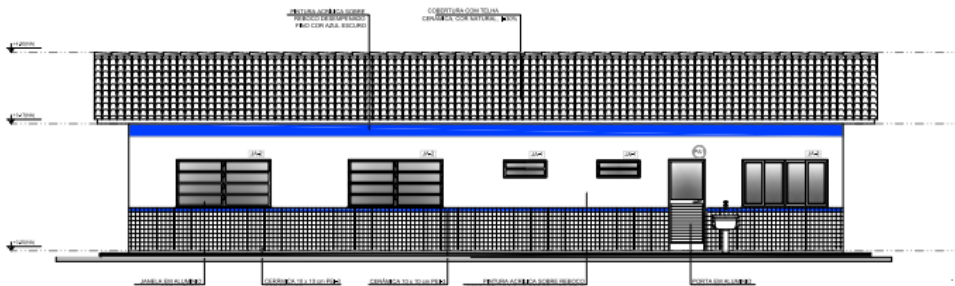
Facades: 1 Classroom School

Floor Plan: 1 Classroom School

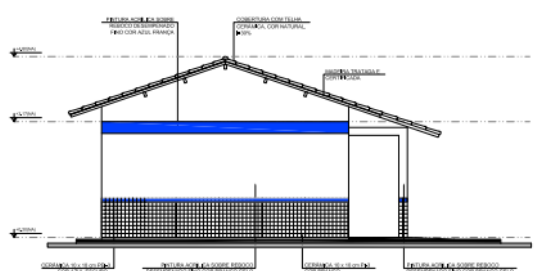




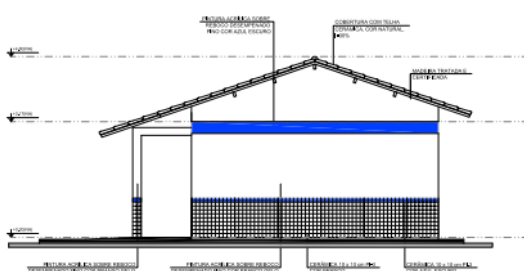
1 FACHADA 1  
ESCALA 1/50



2 FACHADA 2  
ESCALA 1/50



3 FACHADA 3  
ESCALA 1/50

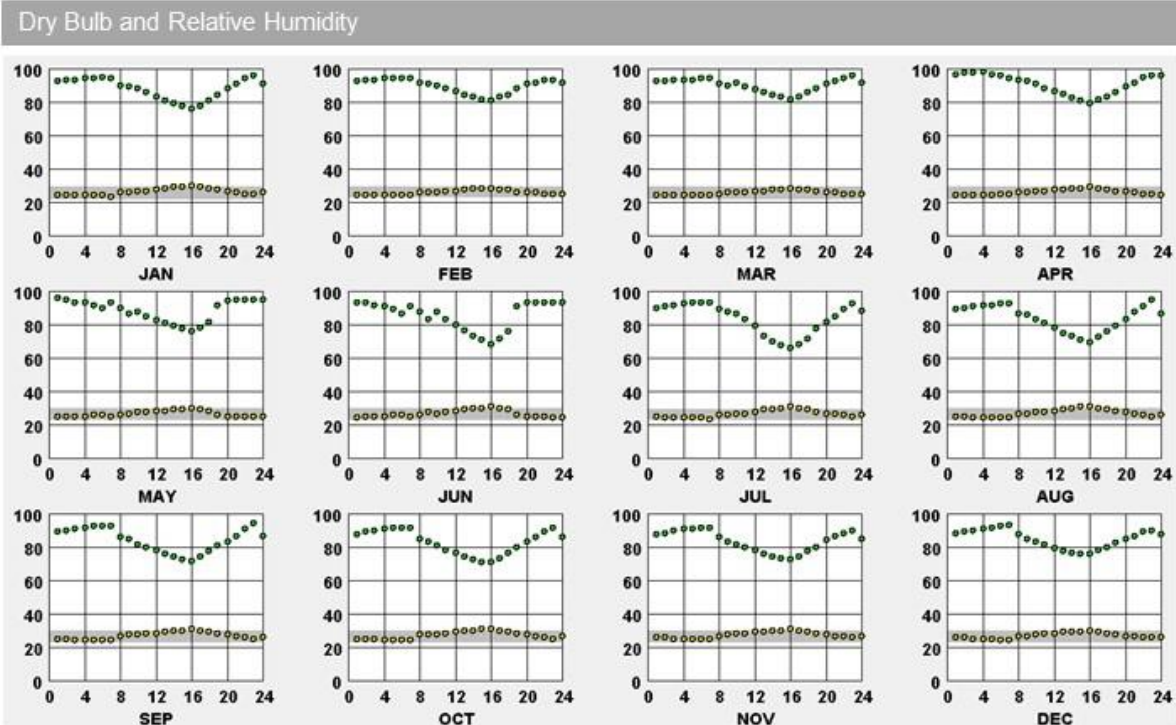
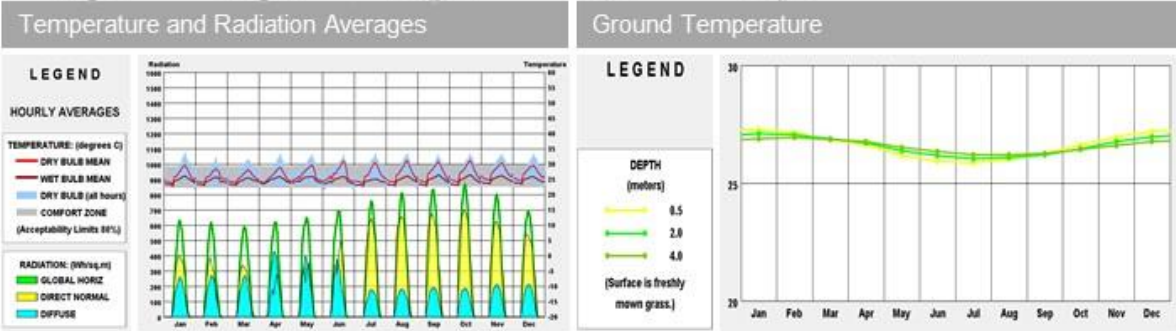
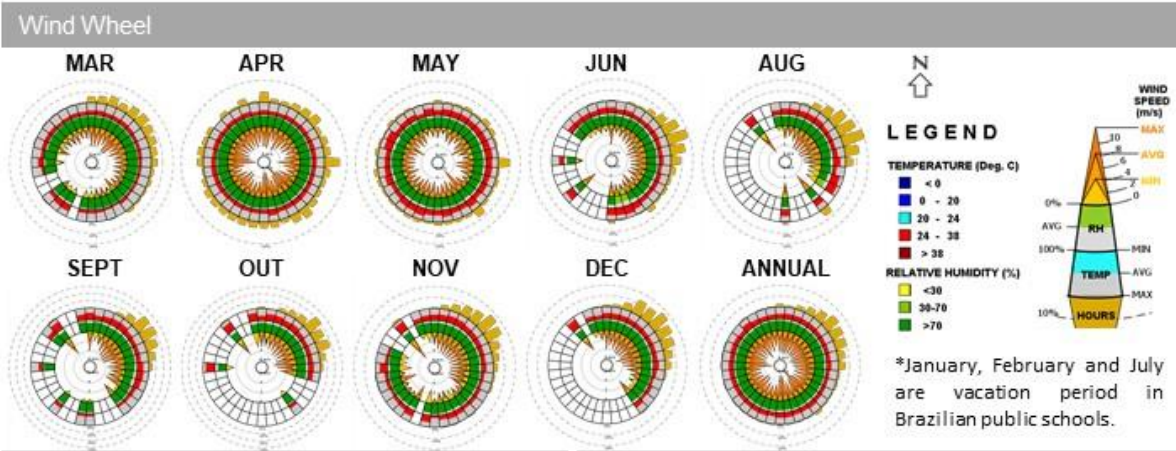


4 FACHADA 4  
ESCALA 1/50

APPENDIX B

Belém (PA) – Zone 8

Source: ClimateConsultant (2021).



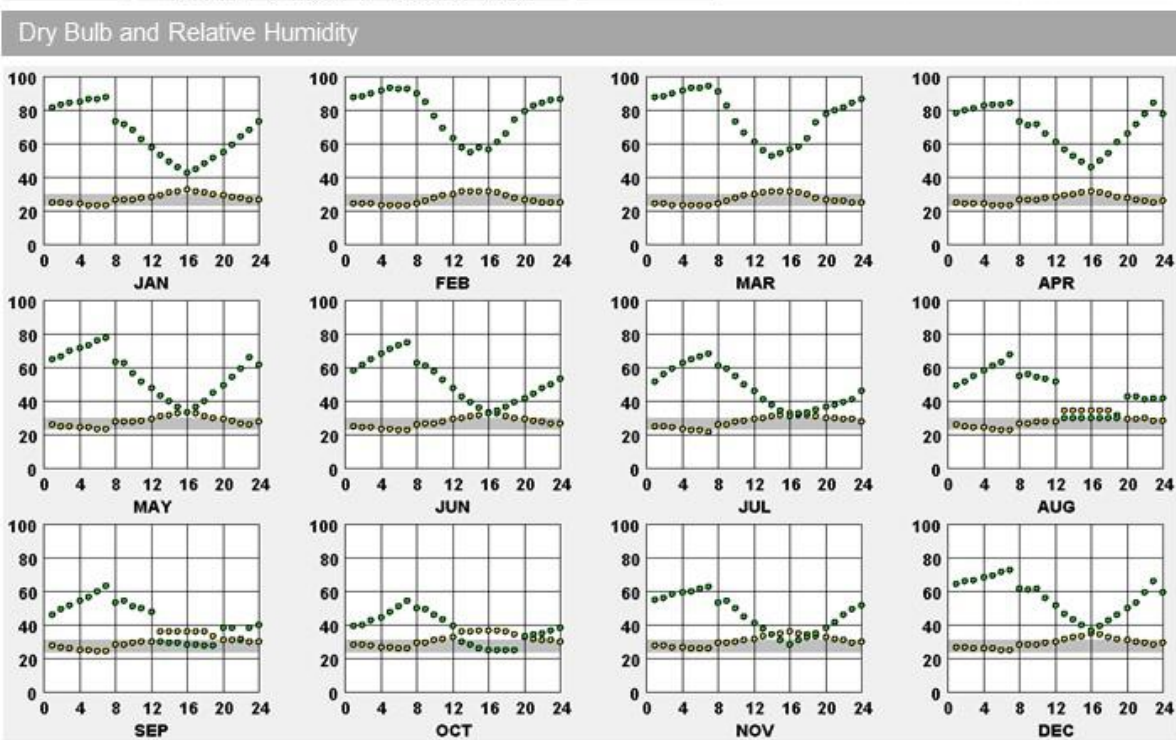
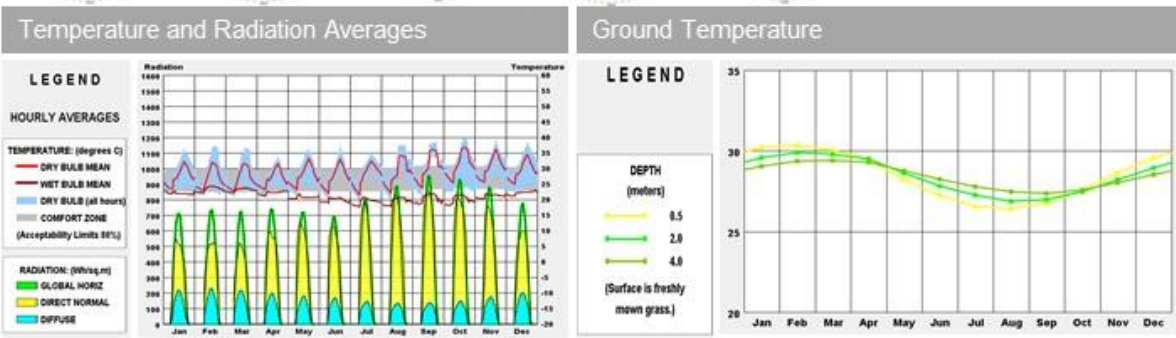
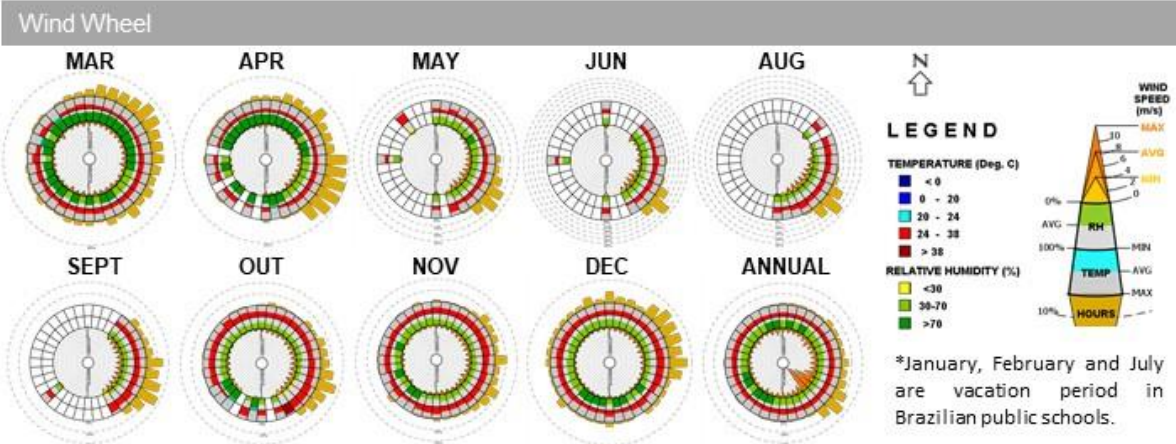
INTERPRETATION

Most frequent winds are northeast of 2 to 5 m/s. Belém is hot and humid (air temp. 24 - 38 °C and RH > 70%). The second half of the year is warmer, with more direct solar radiation and slightly lower relative humidity. Temperature peaks and relative humidity troughs are around 4 pm. Ground temperature is always close to 27 degrees, with a slight drop in the middle of the year.



# Picos (PI) – Zone 7

Source: ClimateConsultant (2021).

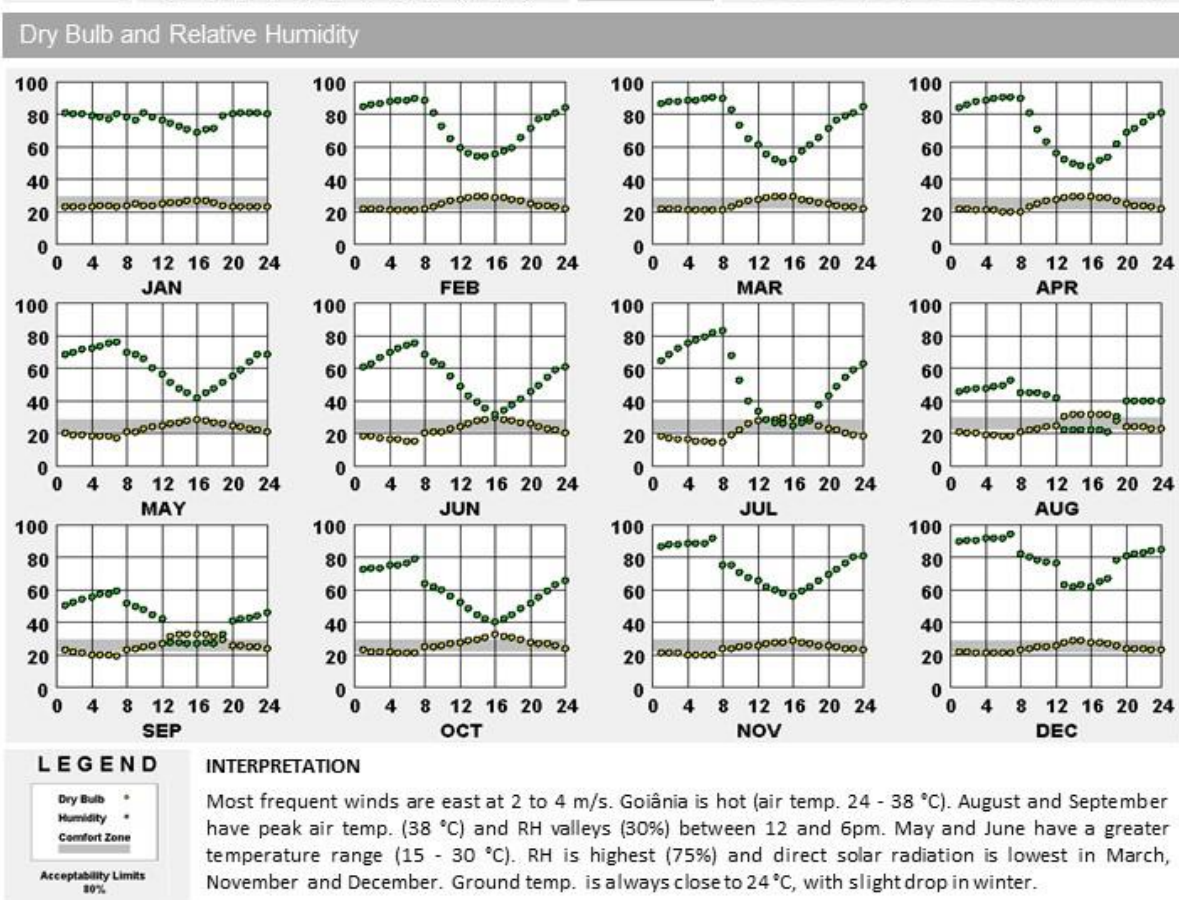
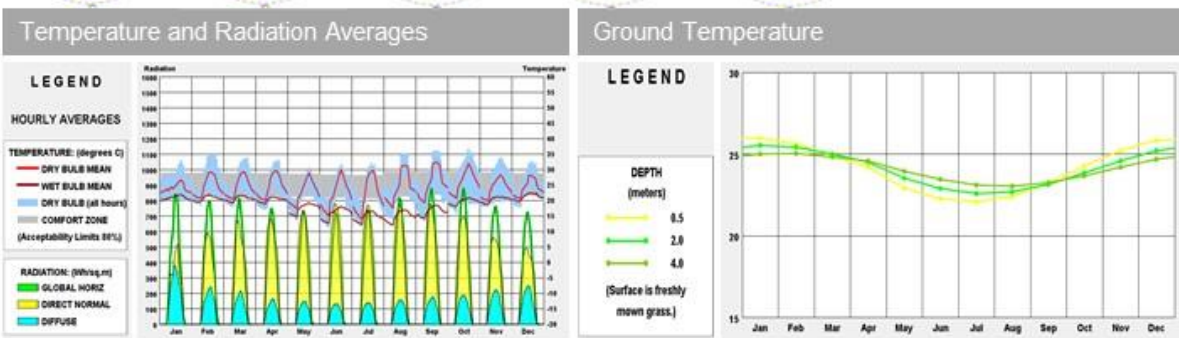
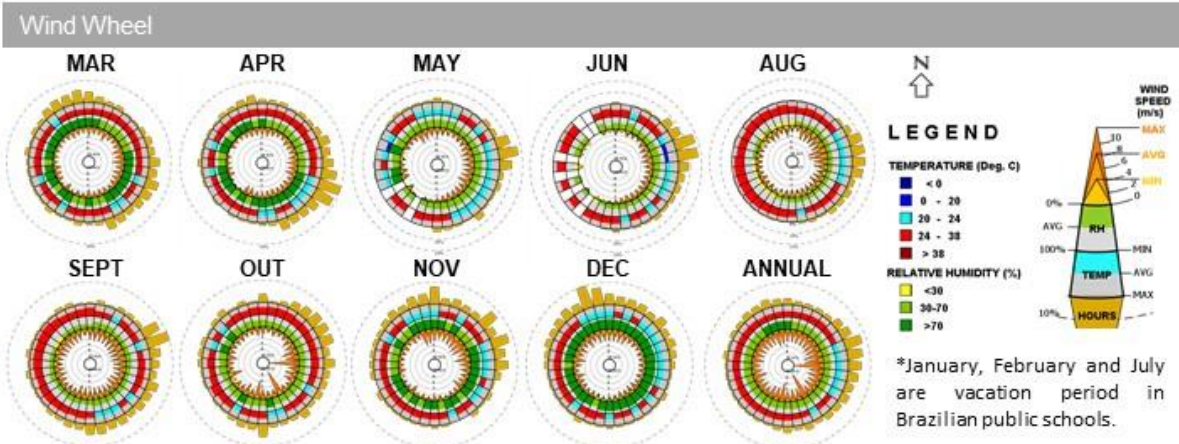


**INTERPRETATION**

Most frequent winds are east at 4 to 6 m/s. Picos is very hot (air temp. 24 - 38 °C), with extremes in October (air temp > 38 °C) and more direct solar radiation. Predominant RH is 50%, with more than 70% in March and April. Temp. peaks and RH valleys are in the afternoon, mainly at 4 pm. Ground temp. has less variation at a depth of 4 meters, with 29 °C in summer and 27 °C in winter.

# Goiania (GO) – Zone 6

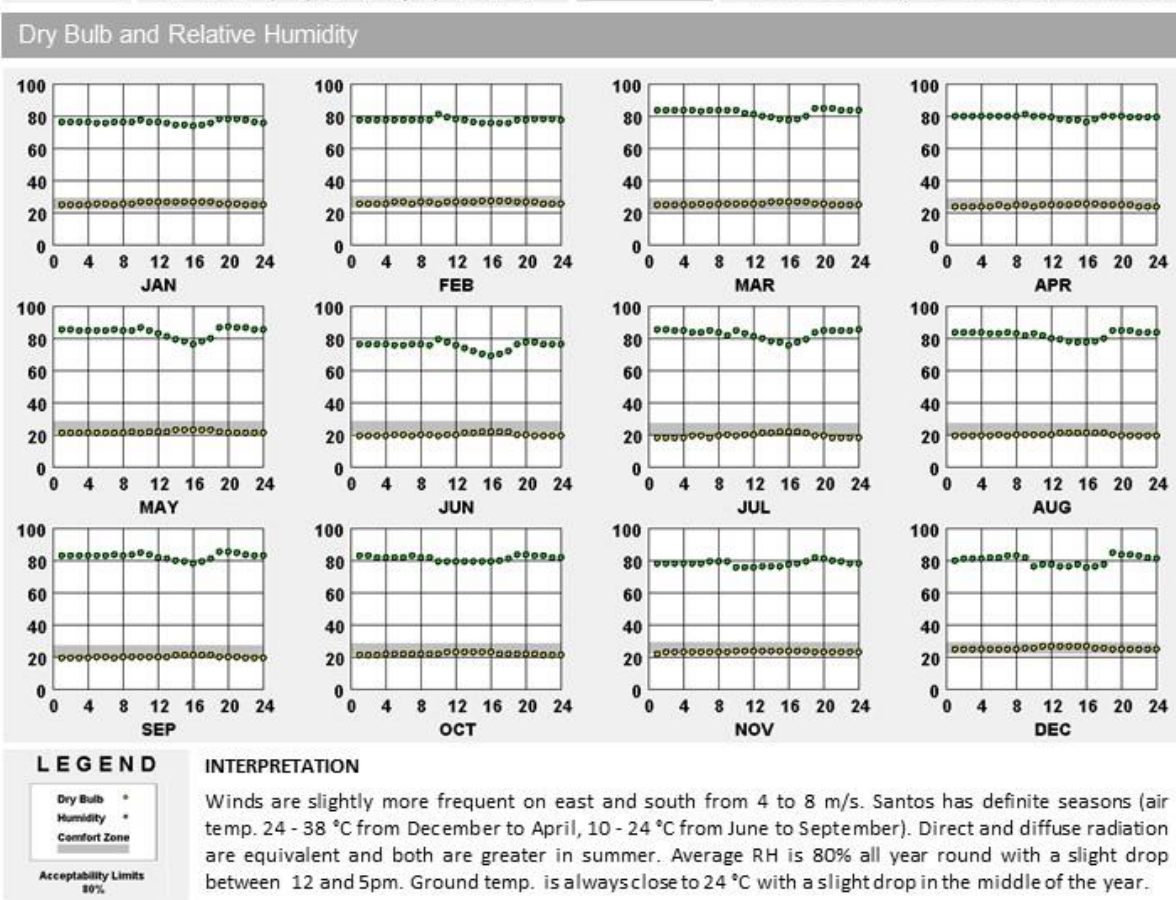
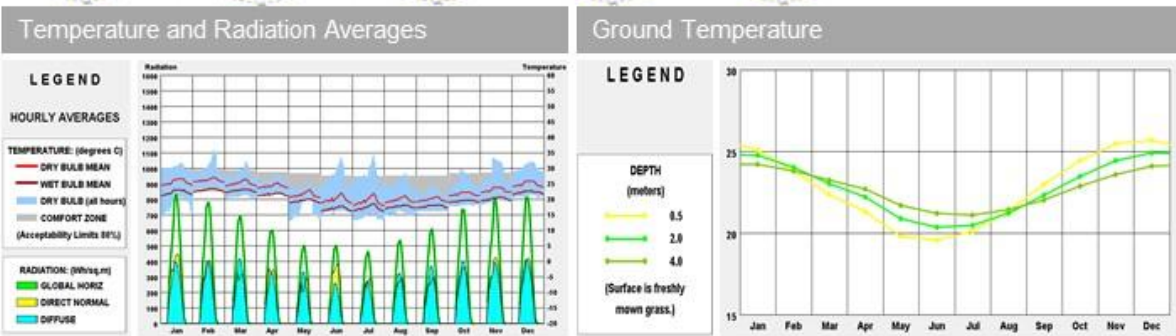
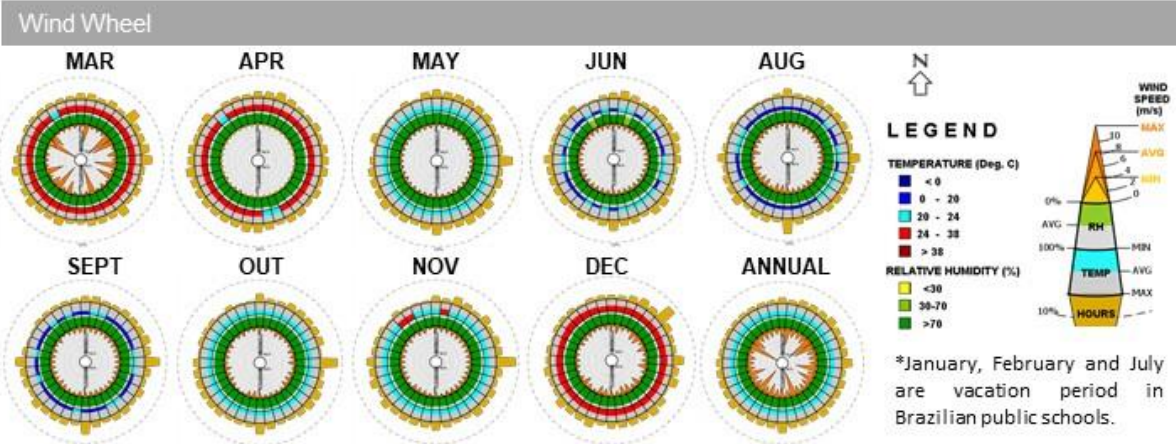
Source: ClimateConsultant (2021).





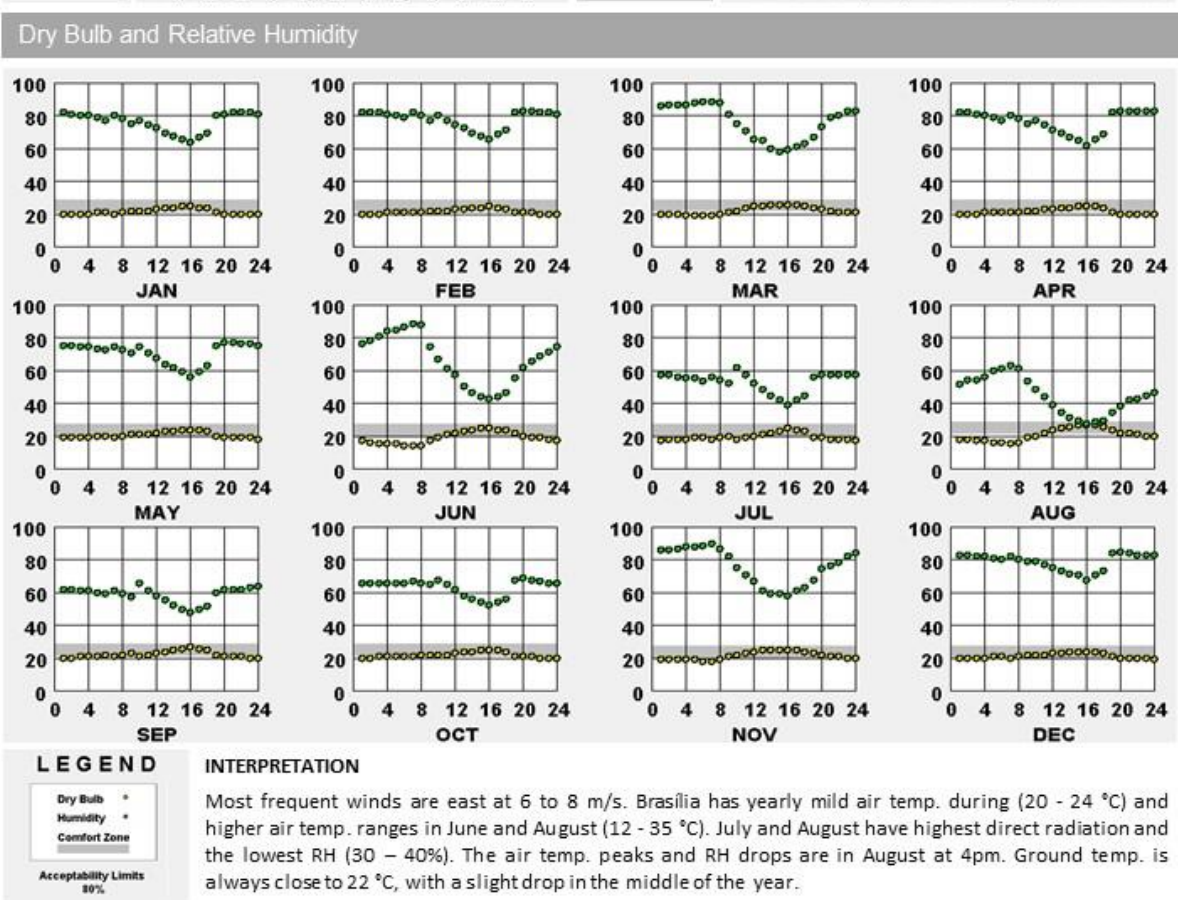
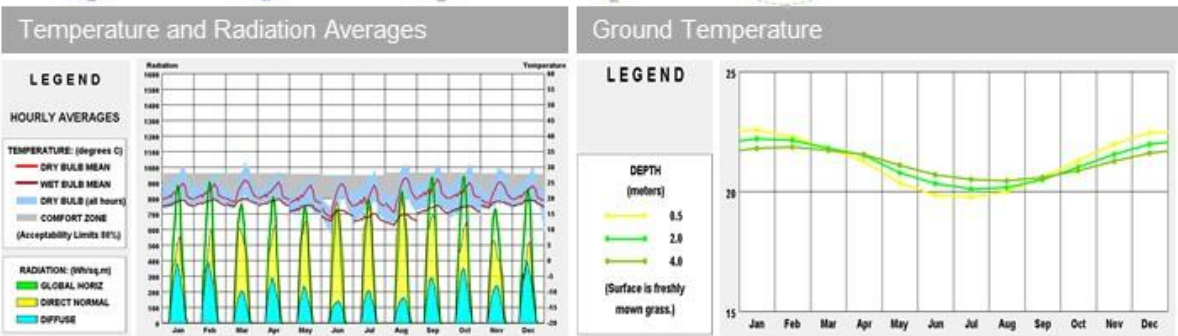
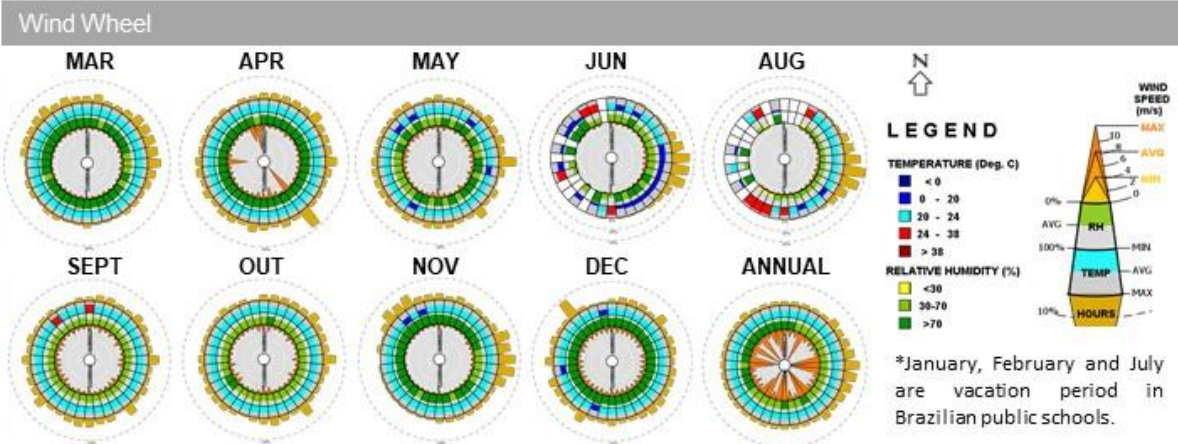
# Santos (SP) – Zone 5

Source: ClimateConsultant (2021).



# Brasilia (DF) – Zone 4

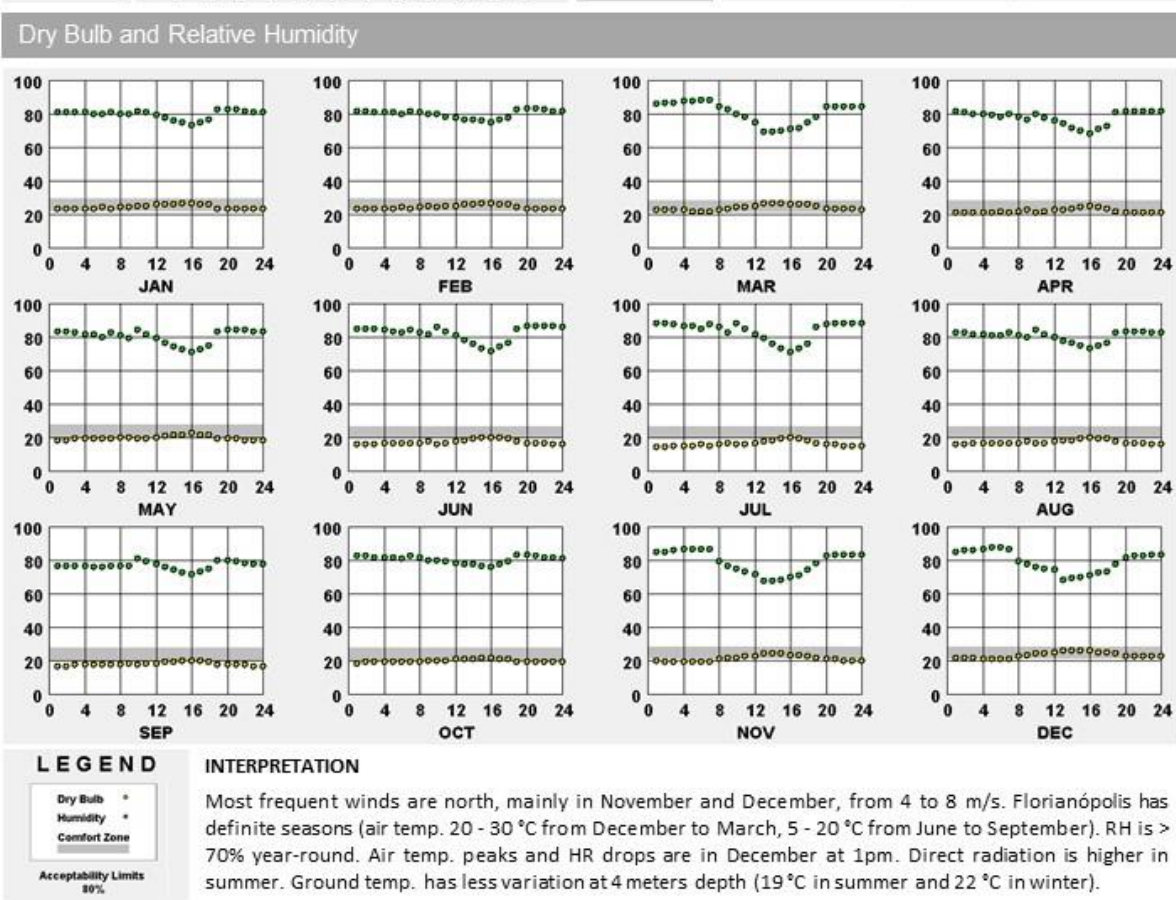
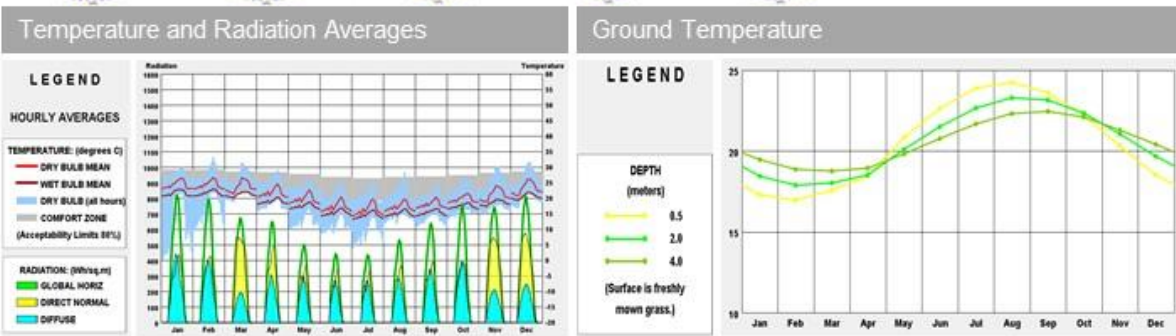
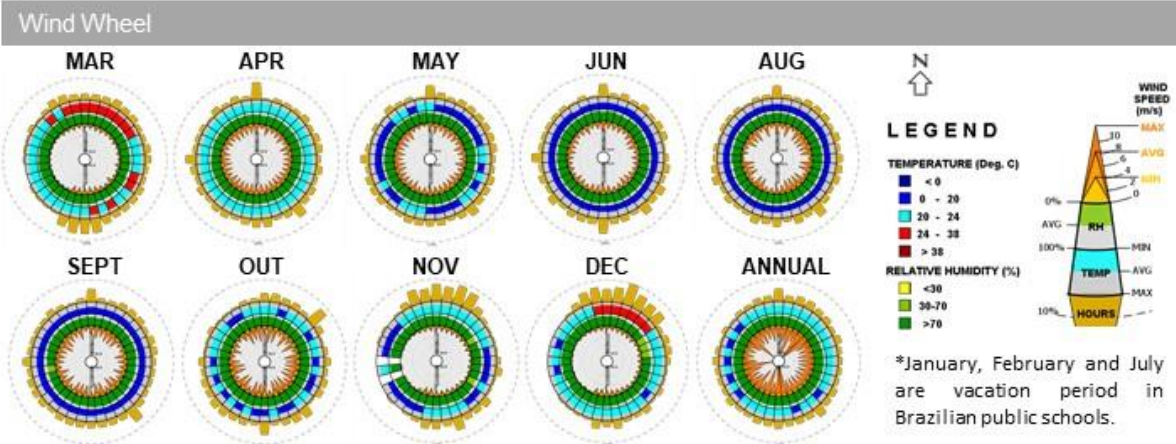
Source: ClimateConsultant (2021).





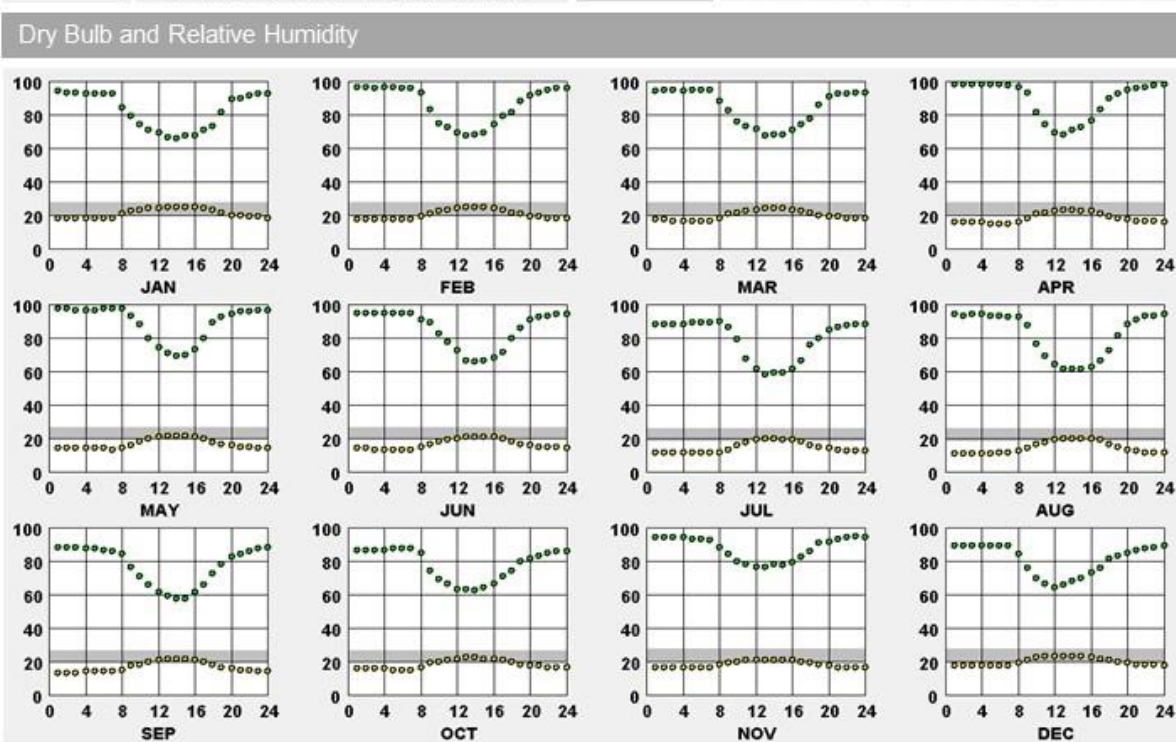
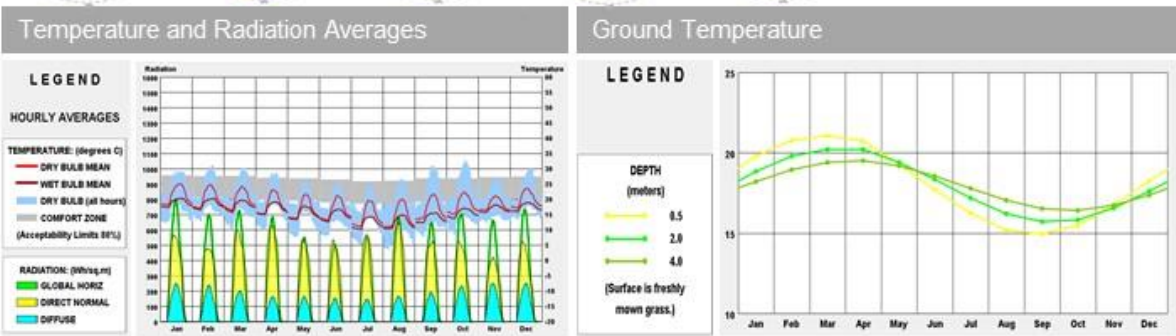
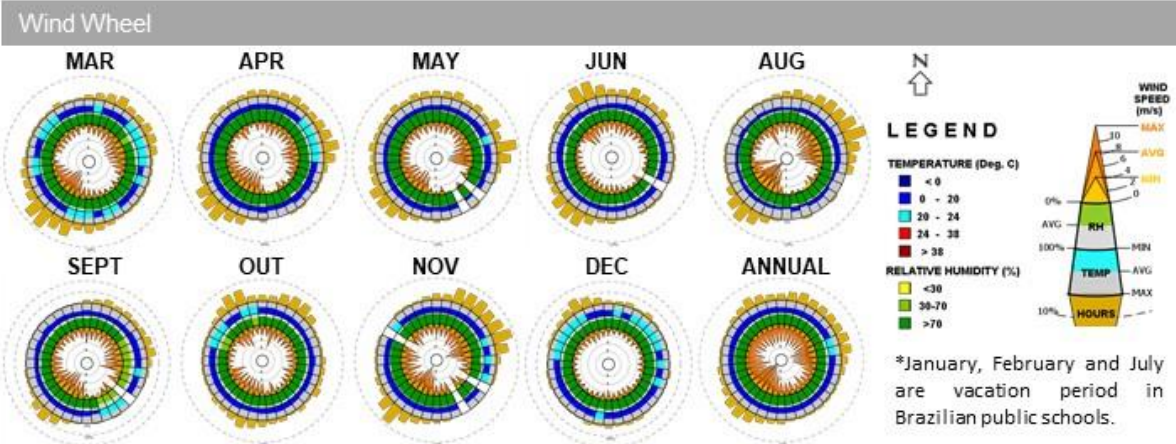
# Florianópolis (SC) – Zone 3

Source: ClimateConsultant (2021).



# Nova Friburgo (RJ) – Zone 2

Source: ClimateConsultant (2021).



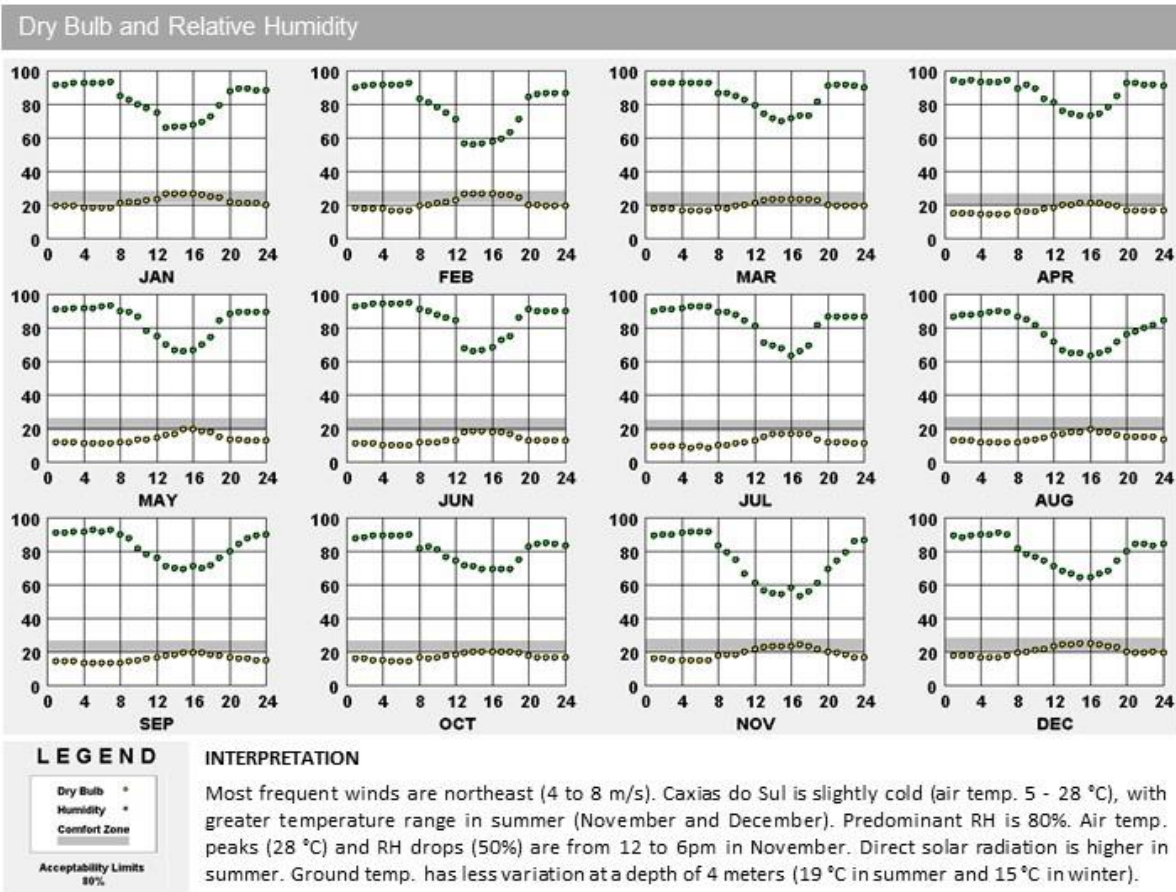
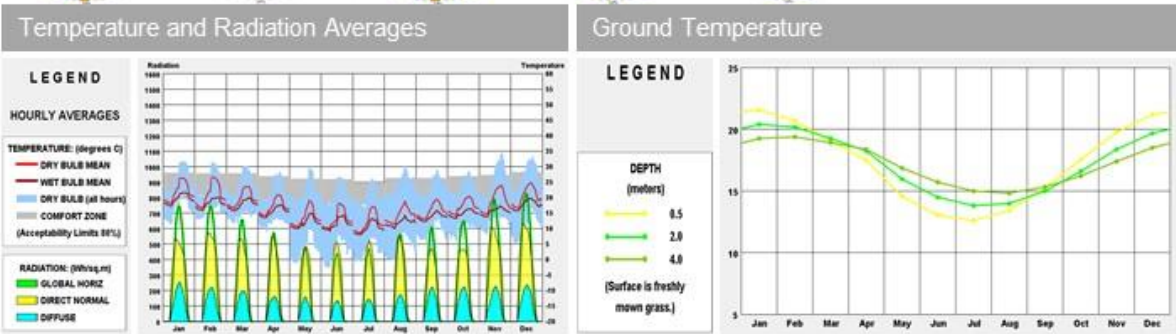
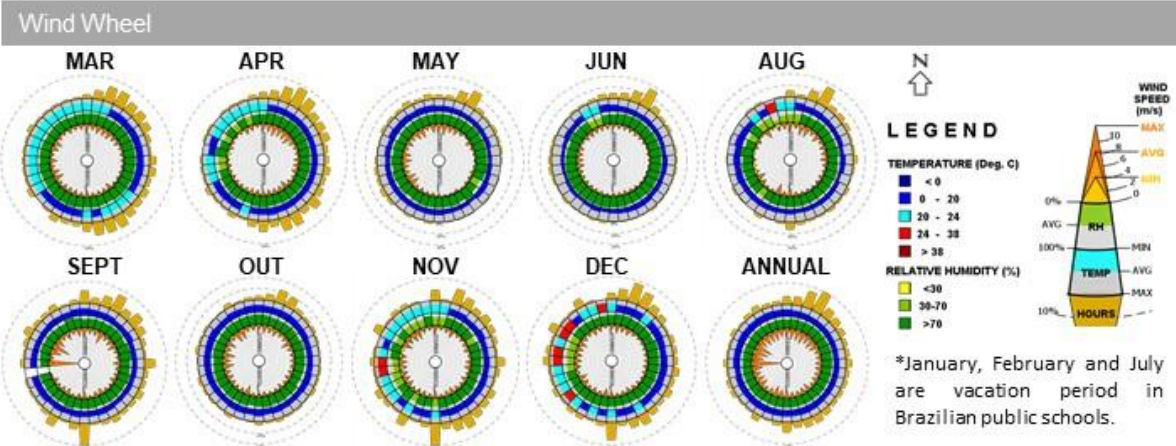
#### INTERPRETATION

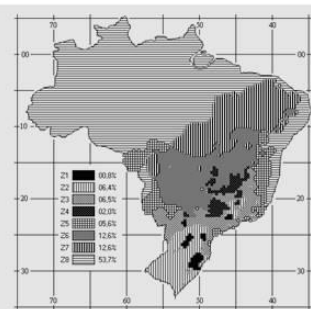
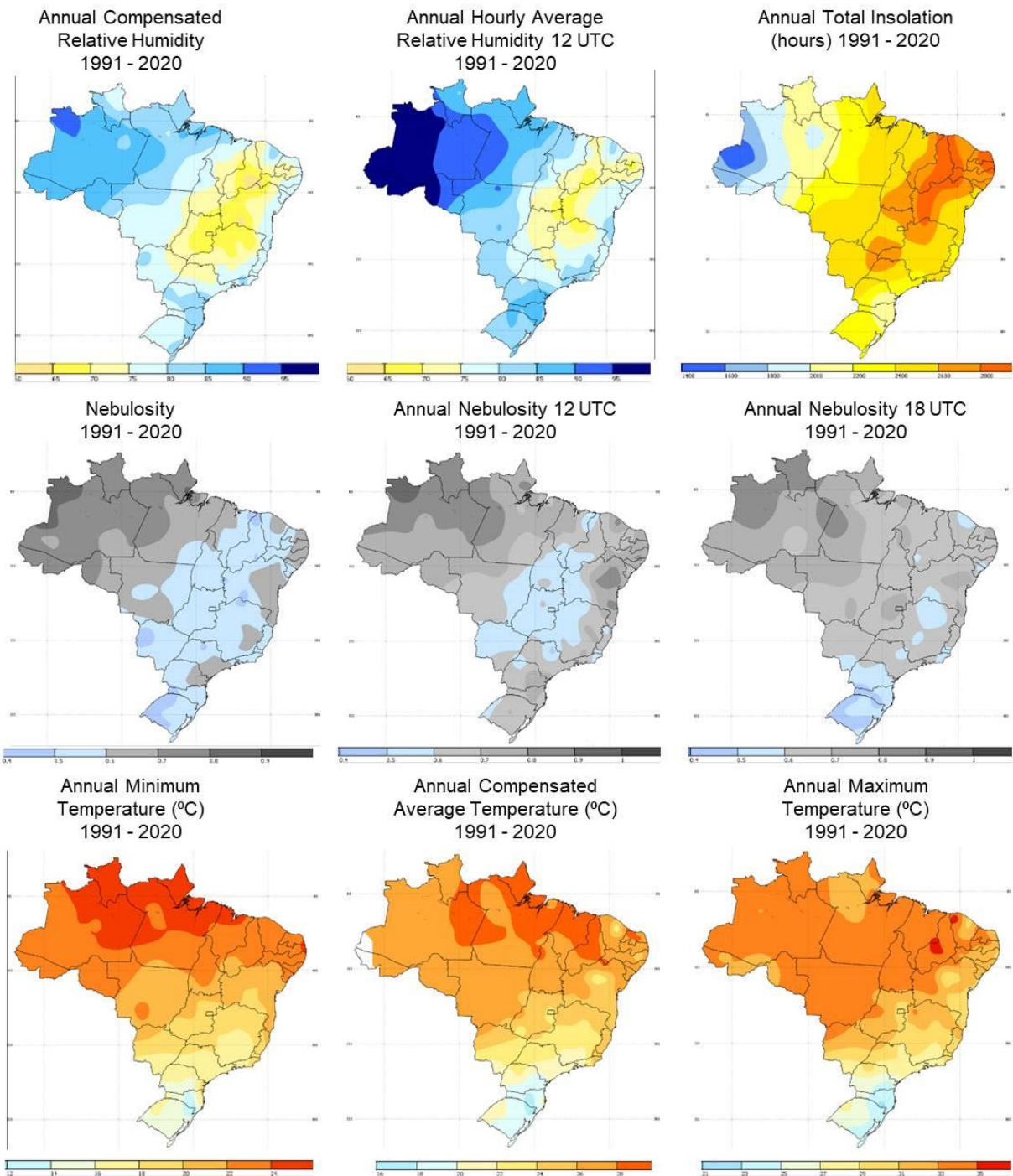
Most frequent winds are Northeast and Southeast (2 to 6 m/s). Nova Friburgo is slightly cold (air temp. 8 - 24 °C), min. in August and max. in December. RH is almost always > 70%, with drops in September (58%). Air temp. peaks and HR drops (30%) are 12 and 4pm. Direct radiation is high, with a slight increase in April and August. Ground temp. has less variation at 4 meters depth (19 °C in autumn and 17 °C in spring).



# Caxias do Sul (RS) – Zone 1

Source: ClimateConsultant (2021).





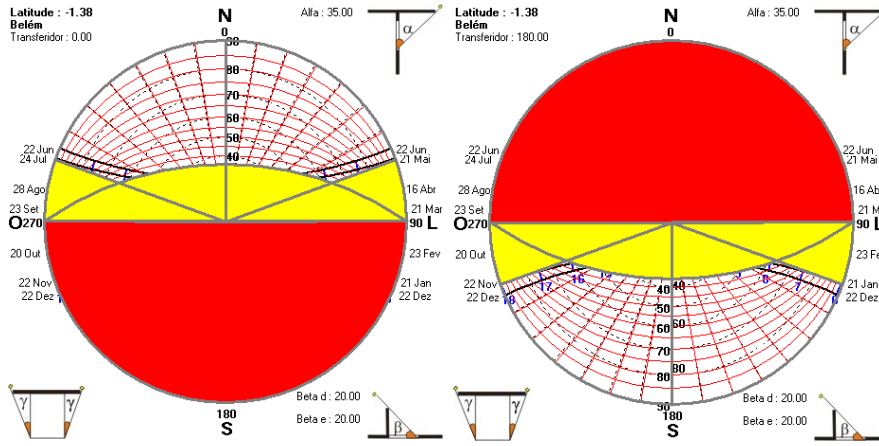
Source: ABNT(n/d).

**INTERPRETATION**

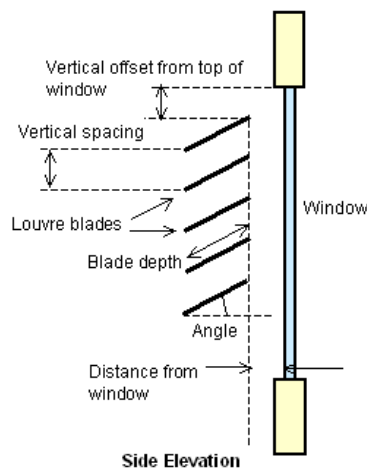
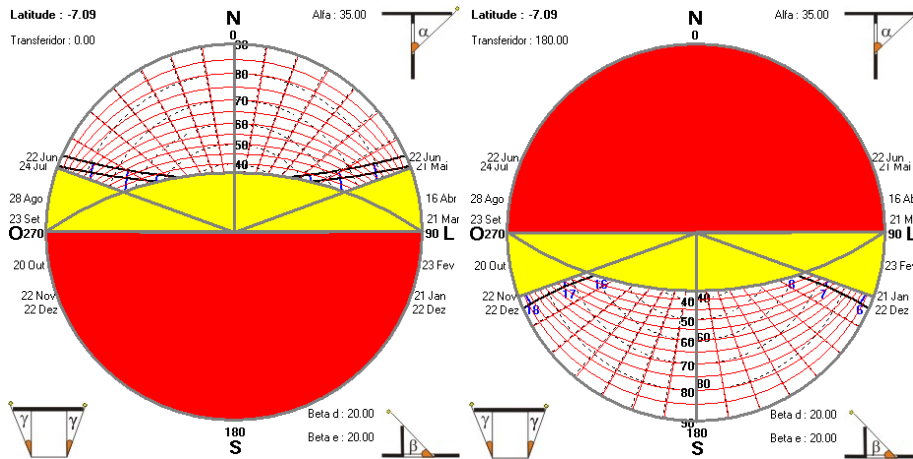
Zone 8, composed mainly of cities in the north of Brazil, has high annual values of humidity (> 80%), nebulosity(>0.6) and temperature (> 26 °C). Zone 7, which covers part of the Midwest and Northeast, involves cities with high annual temperature (> 26 °C), lower humidity (65 - 75%) and nebulosity(< 0.6) and many hours of sun (>2600). Zones 4, 5 and 6 also have lower humidity (65 - 75%) and nebulosity (< 0.6), but with more pleasant annual temperatures (18 - 31 °C). Zones 1, 2 and 3 with cities in the south and southeast have medium to high humidity (75 - 85%) (14 - 29°C) with cool winter temperatures and mild summer temperatures (12 - 29°C).

## APPENDIX C

### Z8 – Belém (PA)



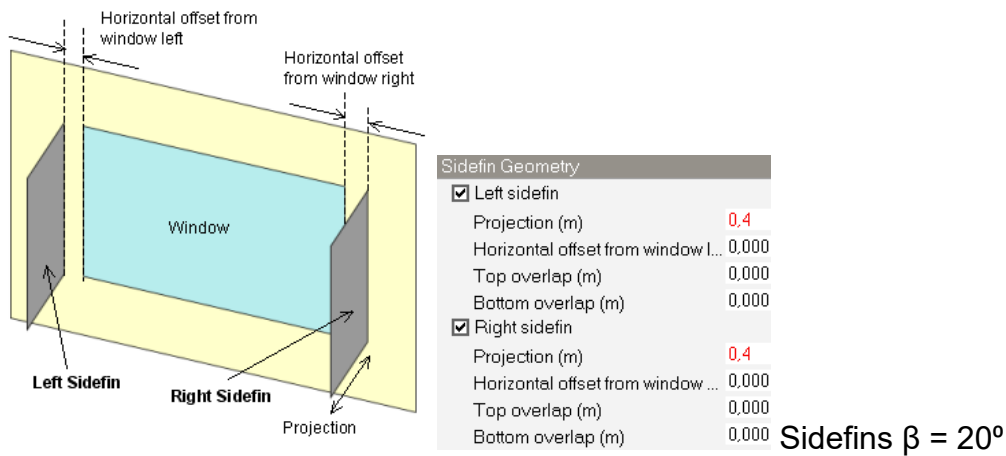
### Z7 – Picos (PI)



Louvre Blade Geometry	
<input checked="" type="checkbox"/> Louvres	
Number of blades	4
Vertical spacing (m)	0.27
Angle (°)	0.000
Distance from window (m)	0.0
Blade depth (m)	0.19
Vertical offset from window top (m)	0.000
Horizontal window overlap (m)	0.000

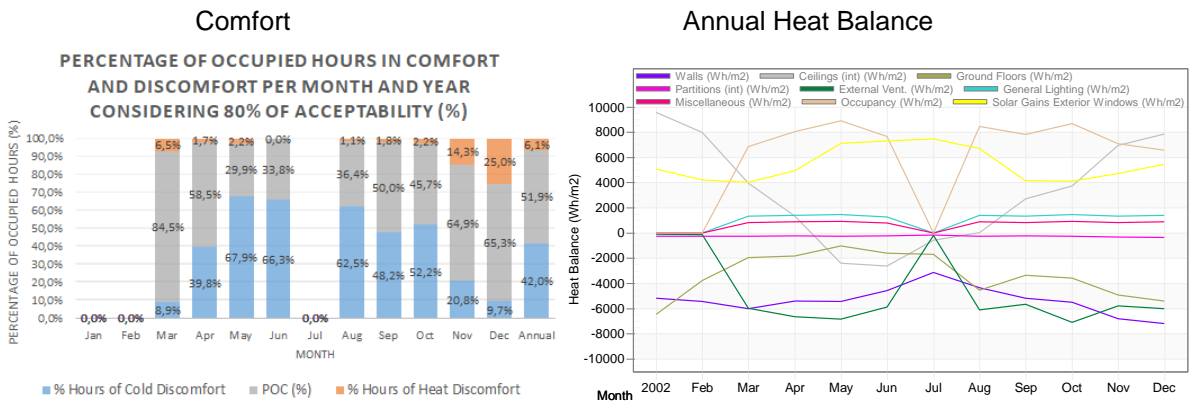
Louvre  $\alpha = 35^\circ$



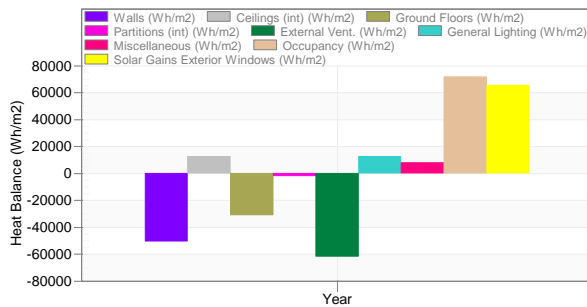


## APPENDIX D

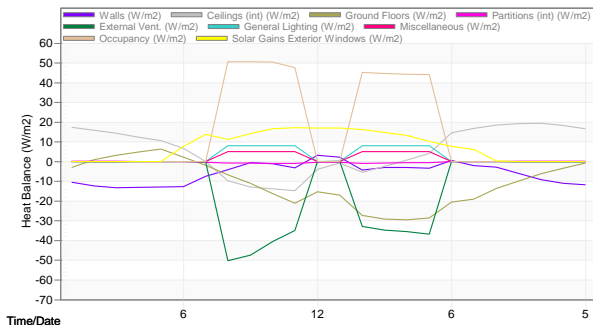
### Percentage of occupied hours in comfort and discomfort and Heat balance of classroom in 1 classroom school in Caxias do Sul (RS) – Zone 1



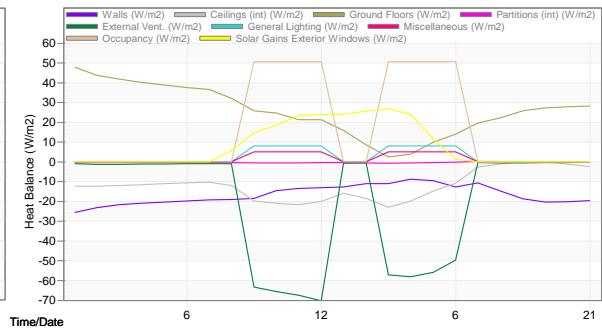
#### Annual Heat Balance Summary



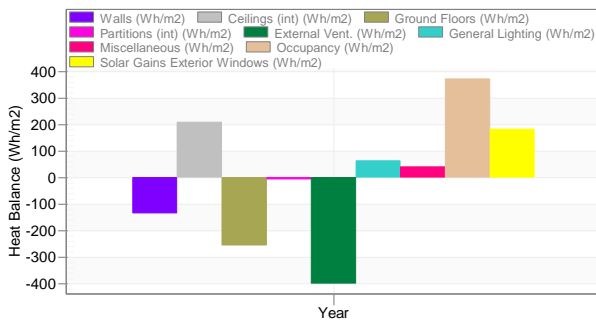
Summer Heat Balance (5 December)



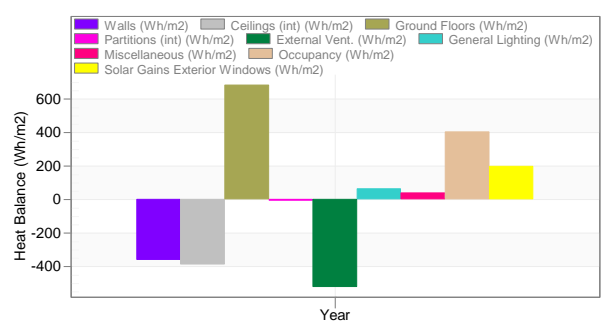
Winter Heat Balance (21 June)



Summer Day Heat Balance Summary



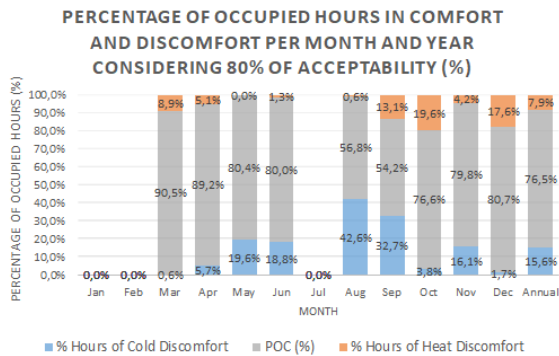
Winter Day Heat Balance Summary



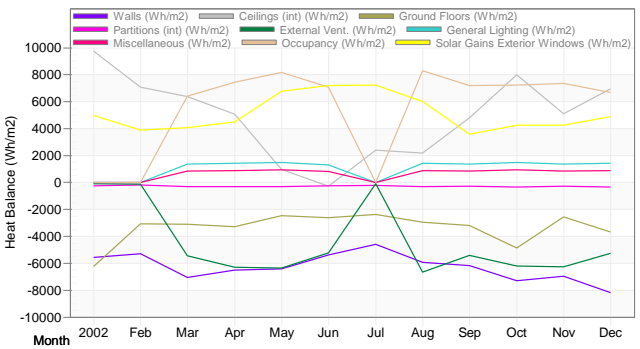
Source: Adapted from DesignBuilder (2022).

Percentage of occupied hours in comfort and discomfort and Heat balance of classroom in 1 classroom school in Nova Friburgo (RJ) – Zone 2

Comfort



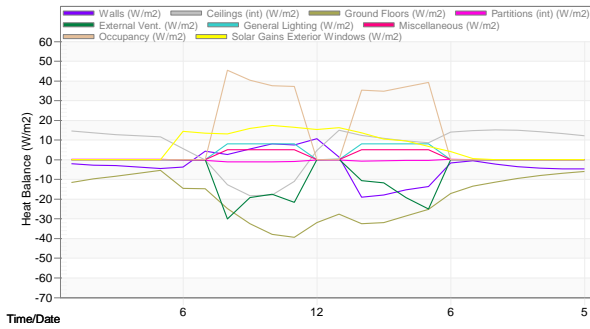
Annual Heat Balance



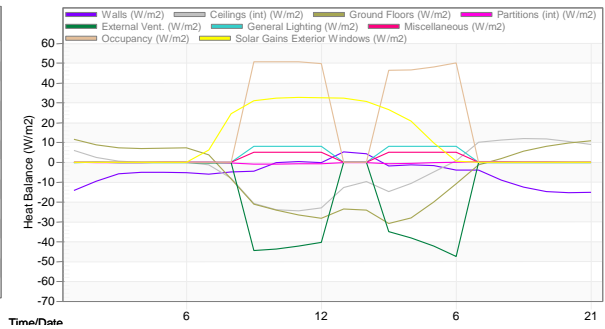
Annual Heat Balance Summary



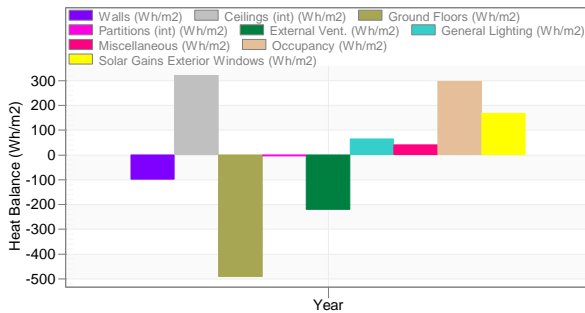
Summer Heat Balance (5 December)



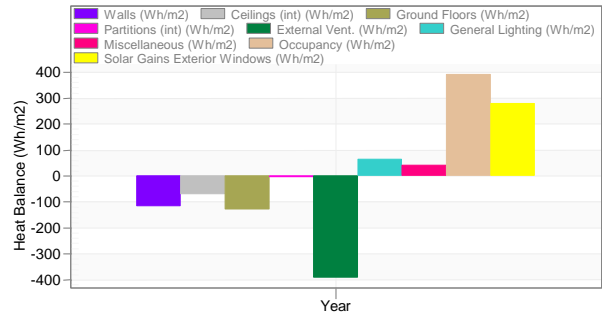
Winter Heat Balance (21 June)



Summer Day Heat Balance Summary



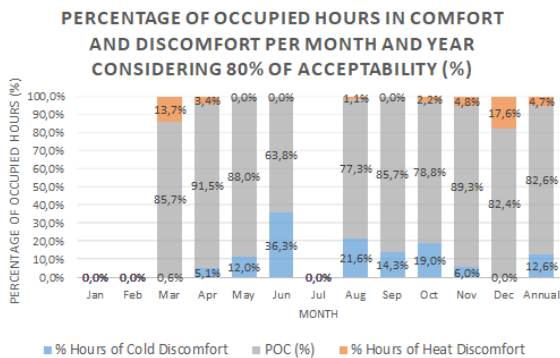
Winter Day Heat Balance Summary



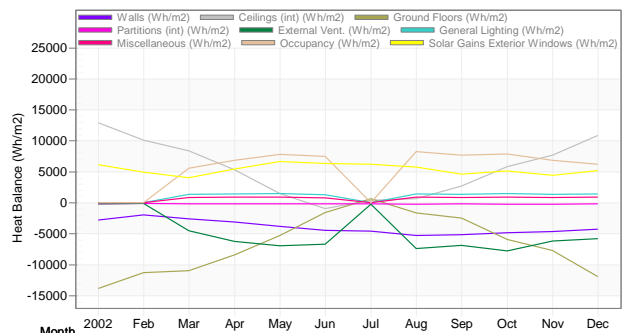
Source: Adapted from DesignBuilder (2022).

Percentage of occupied hours in comfort and discomfort and Heat balance of classroom in 1 classroom school in Florianópolis (SC) – Zone 3

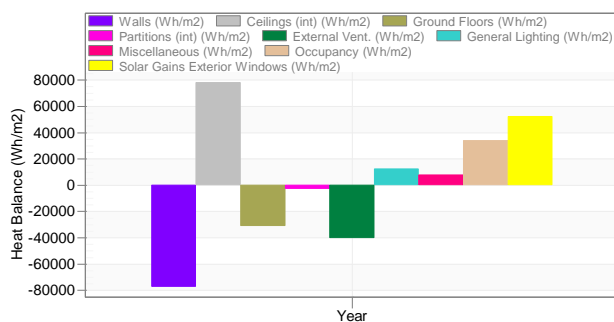
Comfort



Annual Heat Balance

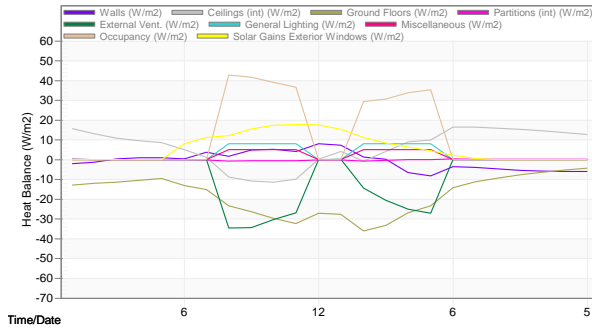


Annual Heat Balance Summary

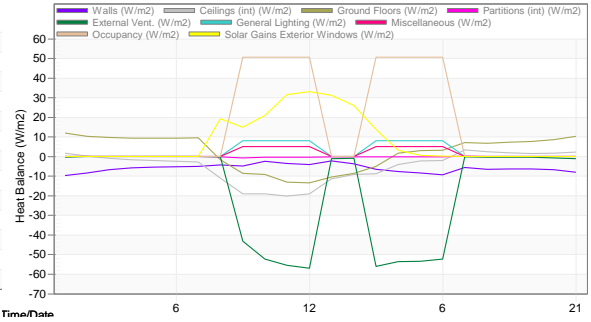




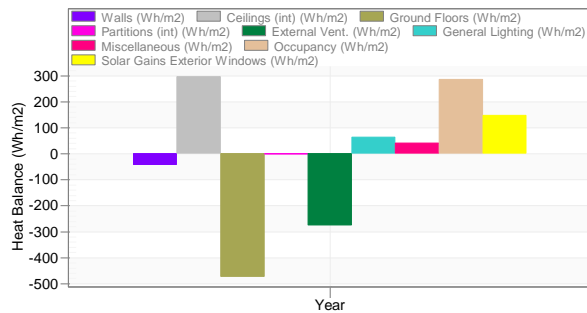
Summer Heat Balance (5 December)



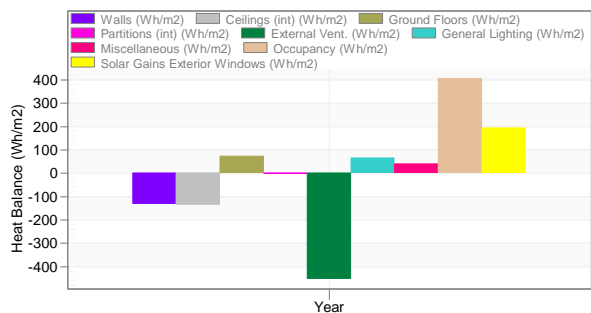
Winter Heat Balance (21 June)



Summer Day Heat Balance Summary



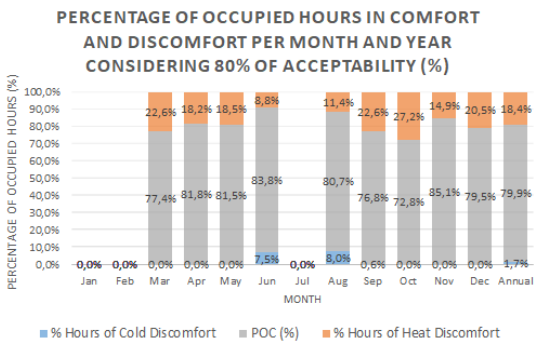
Winter Day Heat Balance Summary



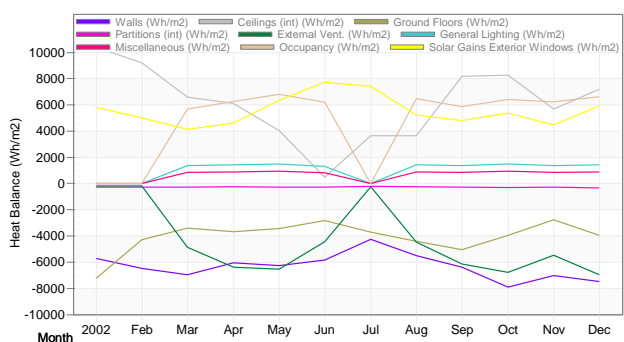
Source: Adapted from DesignBuilder (2022).

Percentage of occupied hours in comfort and discomfort and Heat balance of classroom in 1 classroom school in Brasília (DF) – Zone 4

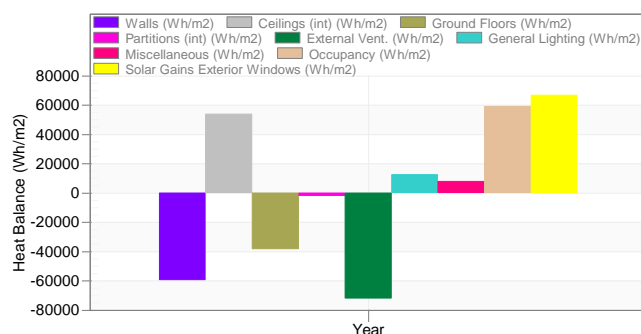
Comfort



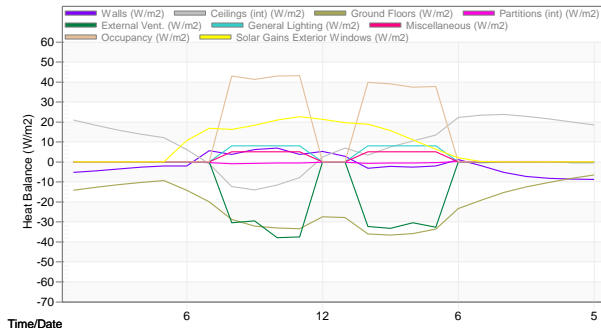
Annual Heat Balance



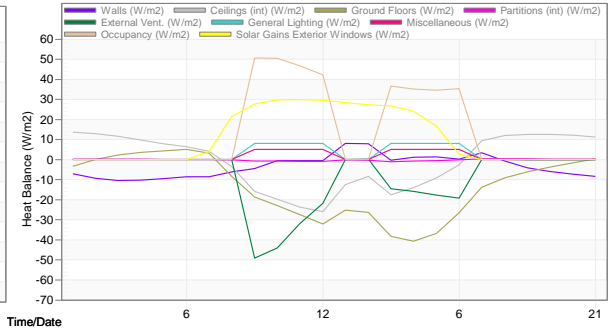
Annual Heat Balance Summary



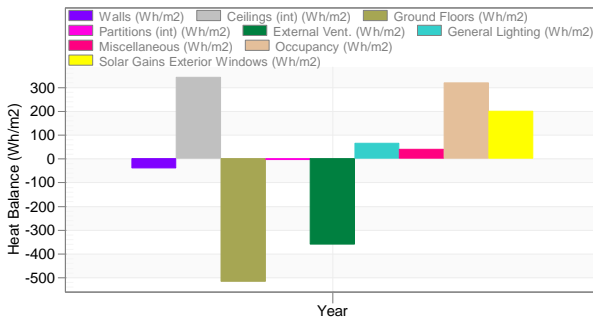
### Summer Heat Balance (5 December)



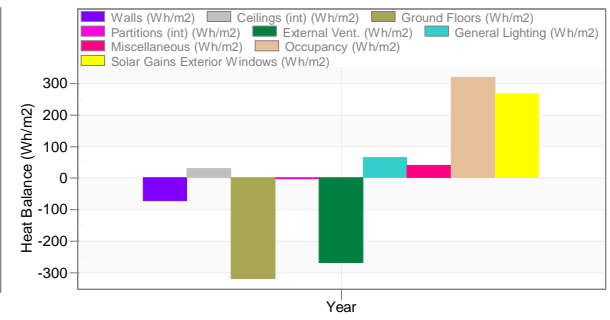
### Winter Heat Balance (21 June)



### Summer Day Heat Balance Summary



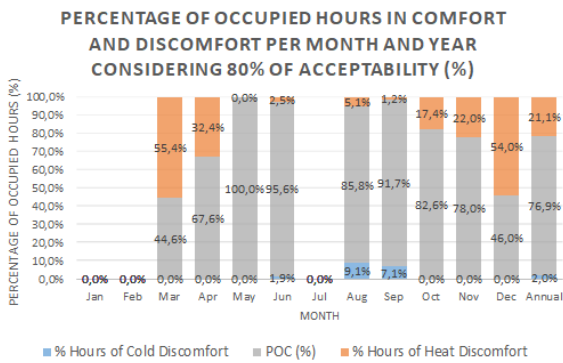
### Winter Day Heat Balance Summary



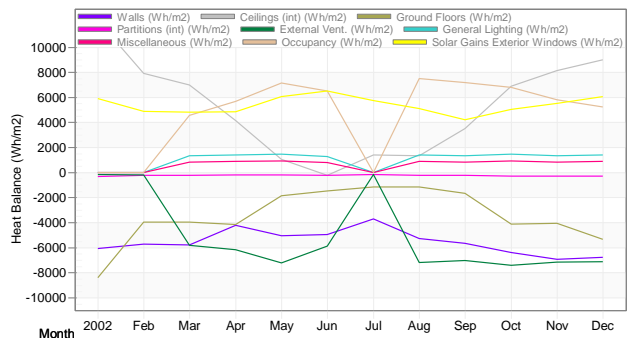
Source: Adapted from DesignBuilder (2022).

## Percentage of occupied hours in comfort and discomfort and Heat balance of classroom in 1 classroom school in Santos (SP) – Zone 5

### Comfort



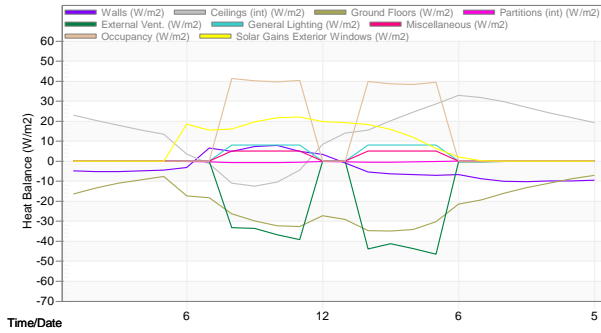
### Annual Heat Balance



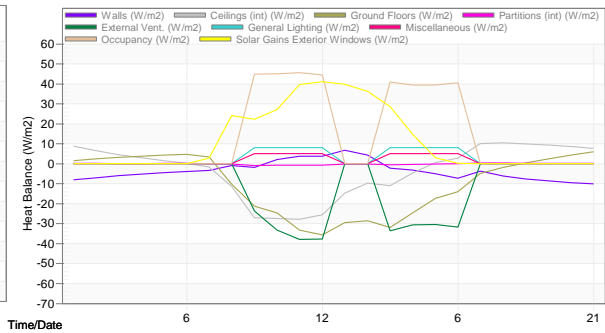
### Annual Heat Balance Summary



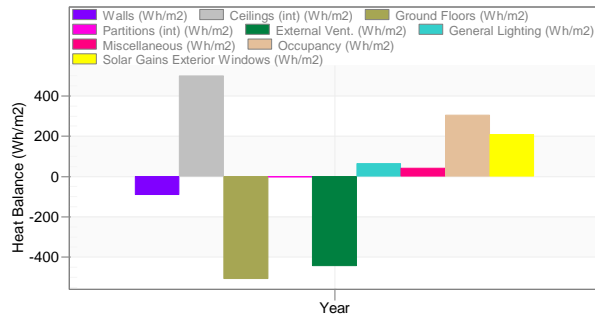
Summer Heat Balance (5 December)



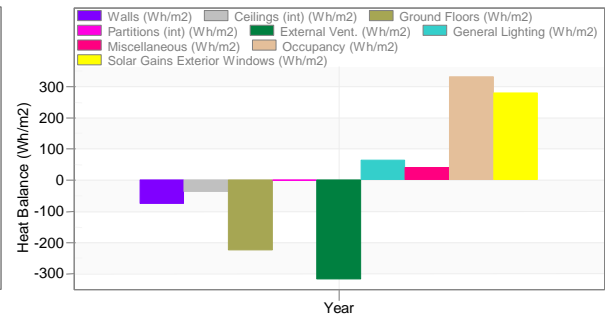
Winter Heat Balance (21 June)



Summer Day Heat Balance Summary



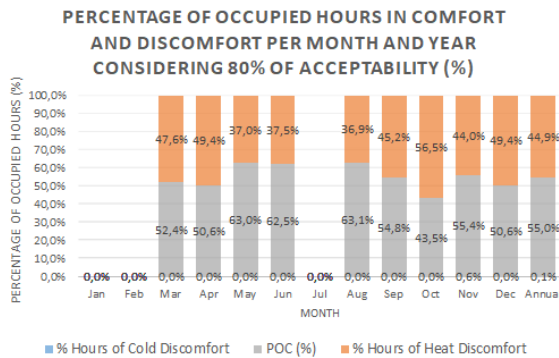
Winter Day Heat Balance Summary



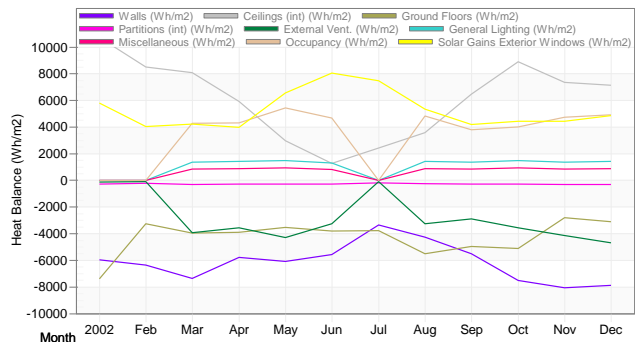
Source: Adapted from DesignBuilder (2022).

Percentage of occupied hours in comfort and discomfort and Heat balance of classroom in 1 classroom school in Goiânia (GO) – Zone 6

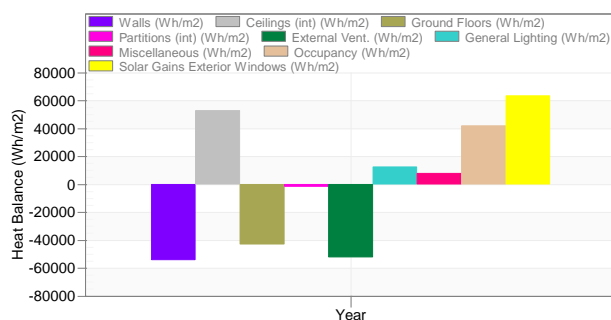
Comfort



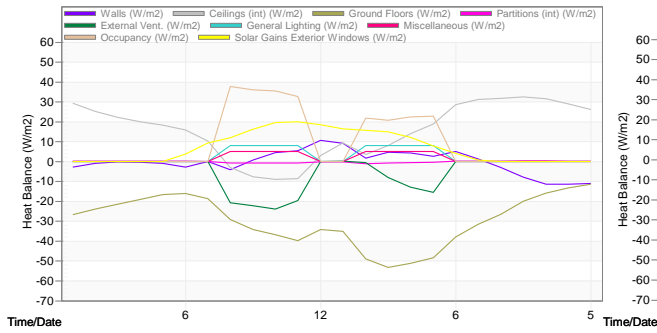
Annual Heat Balance



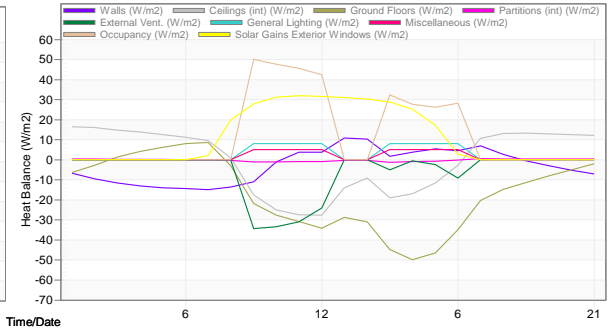
Annual Heat Balance Summary



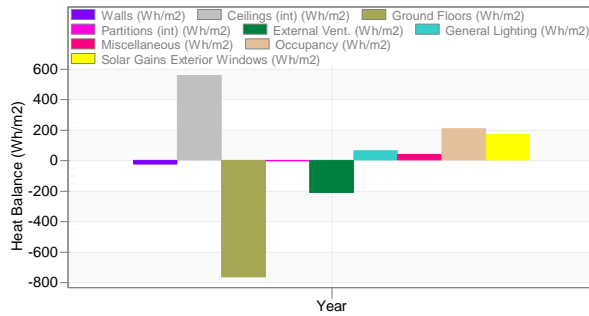
Summer Heat Balance (5 December)



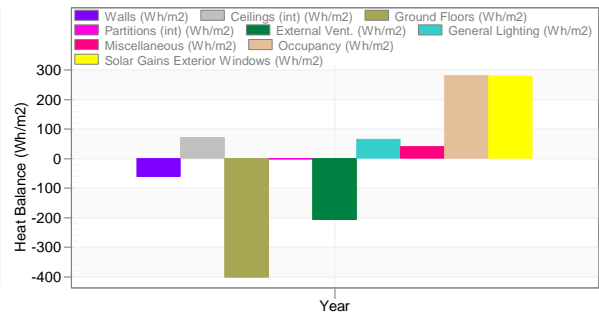
Winter Heat Balance (21 June)



Summer Day Heat Balance Summary



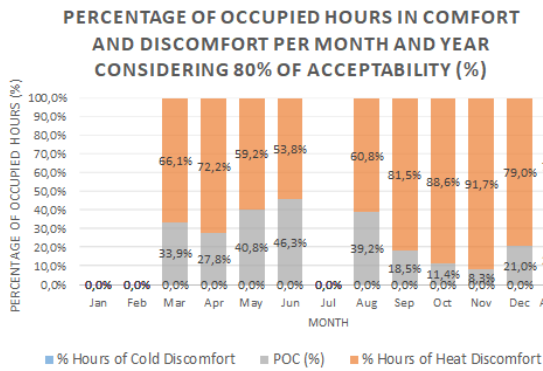
Winter Day Heat Balance Summary



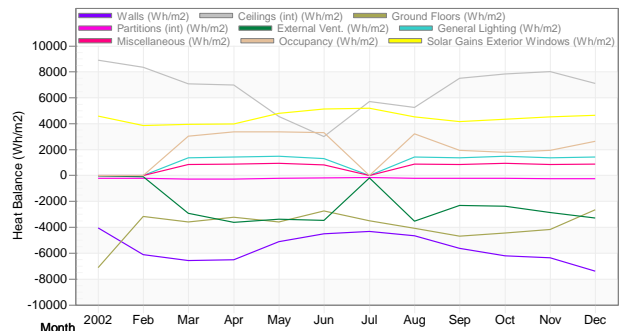
Source: Adapted from DesignBuilder (2022).

Percentage of occupied hours in comfort and discomfort of classroom in Picos (PI) – Zone 7

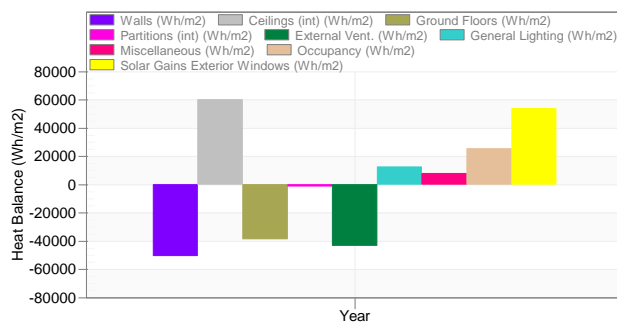
Comfort



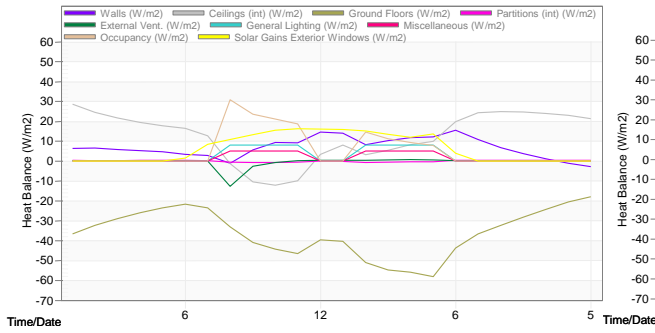
Annual Heat Balance



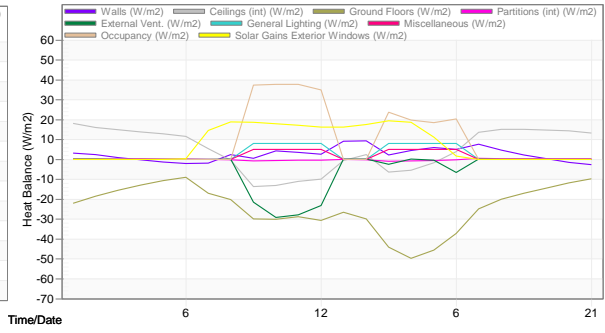
Annual Heat Balance Summary



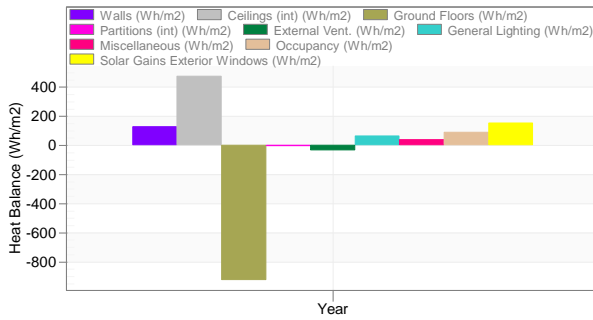
Summer Heat Balance (5 December)



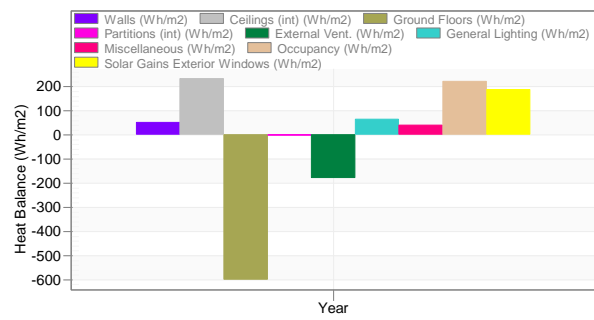
Winter Heat Balance (21 June)



Summer Day Heat Balance Summary



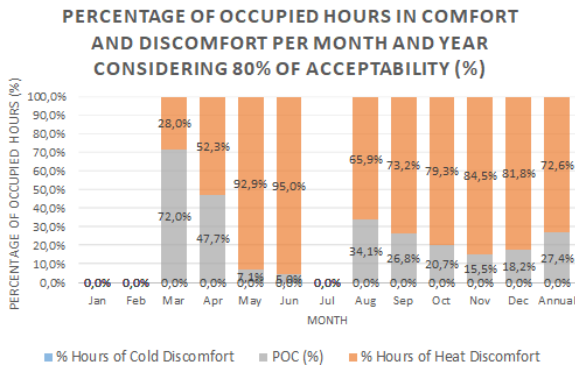
Winter Day Heat Balance Summary



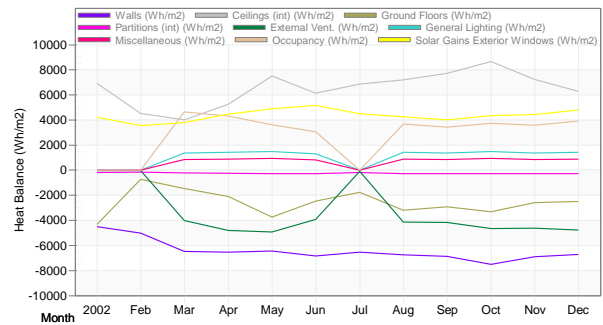
Source: Adapted from DesignBuilder (2022).

Percentage of occupied hours in comfort and discomfort and Heat balance of classroom in 1 classroom school in Belém (PA) – Zone 8

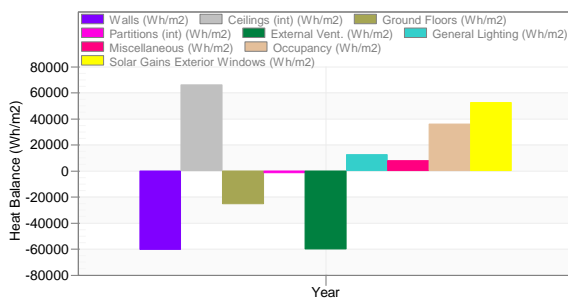
Comfort



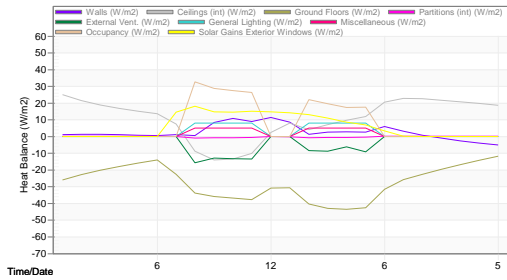
Annual Heat Balance



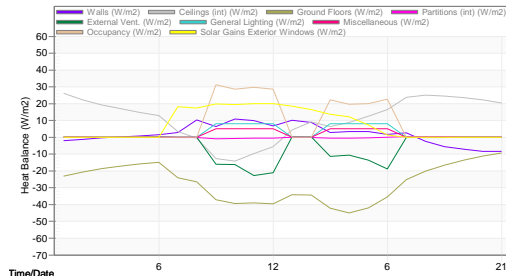
Annual Heat Balance Summary



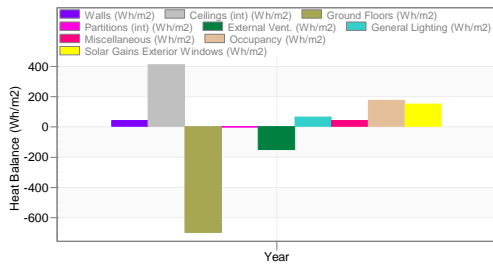
Summer Heat Balance (5 December)



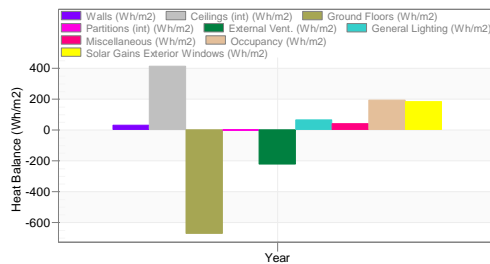
Winter Heat Balance (21 June)



Summer Day Heat Balance Summary



Winter Day Heat Balance Summary

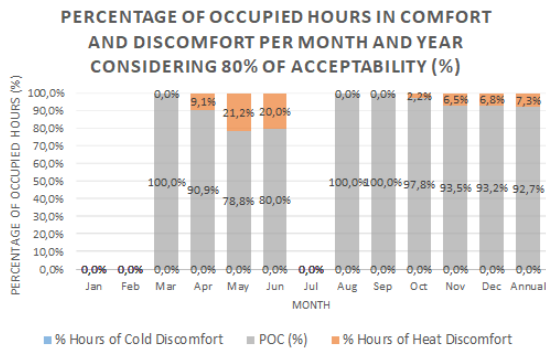


Source: Adapted from DesignBuilder (2022).

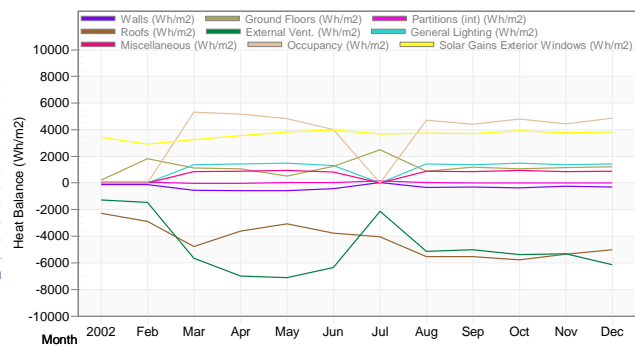
## APPENDIX E

### Percentage of occupied hours in comfort and discomfort and Annual Heat balance of classroom in 1 classroom school in Belém (PA) – Zone 8 after optimization process

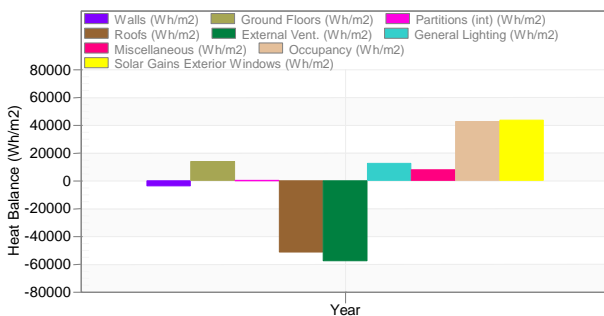
Comfort

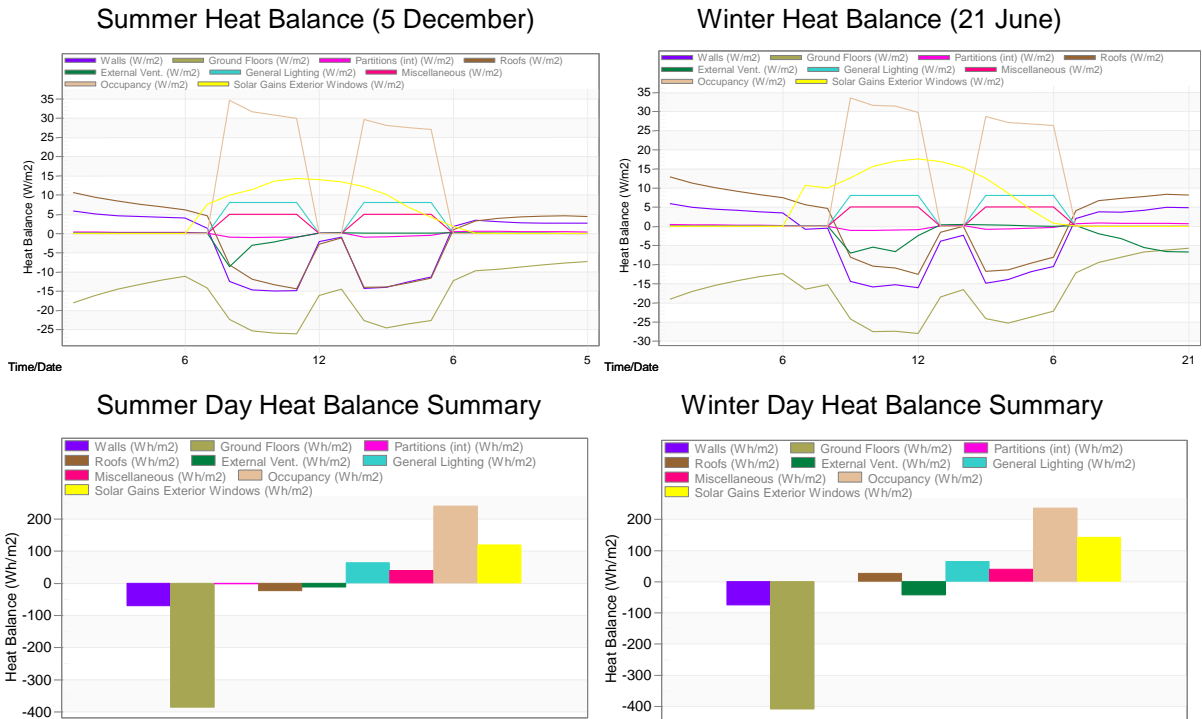


Annual Heat Balance



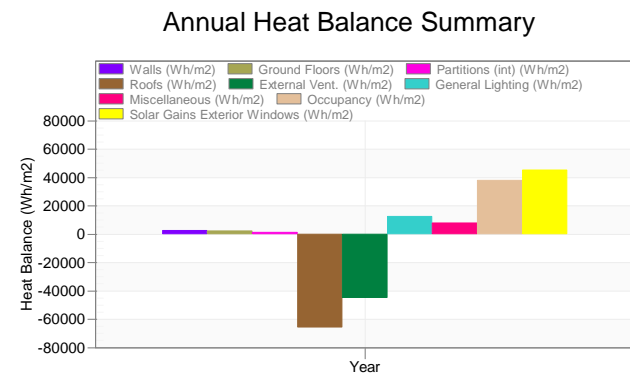
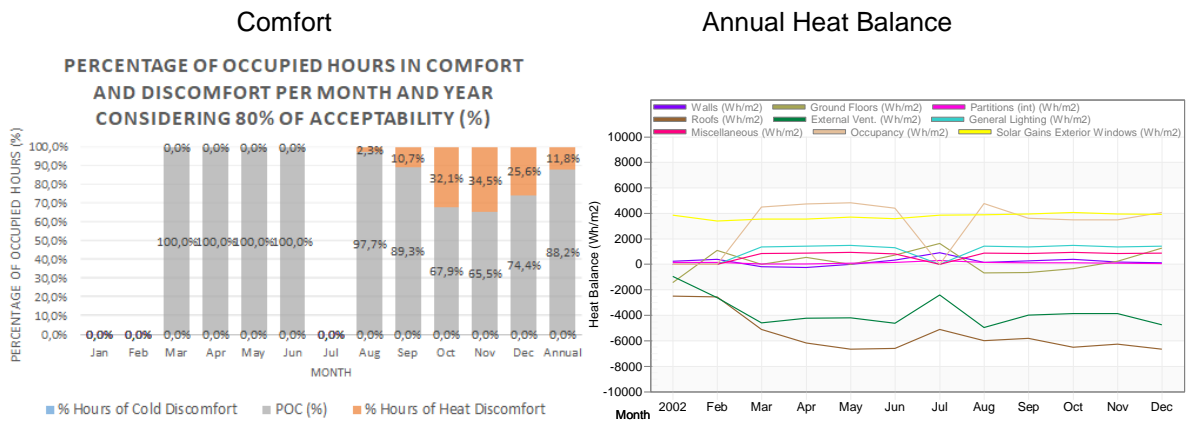
Annual Heat Balance Summary



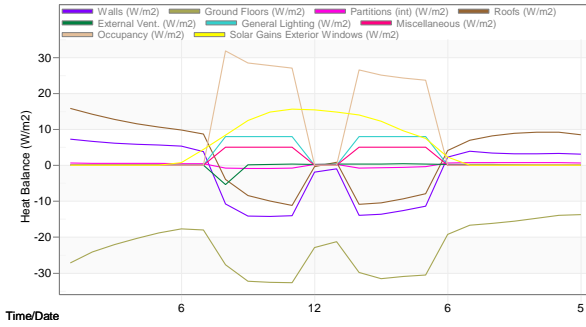


Source: Adapted from DesignBuilder (2022).

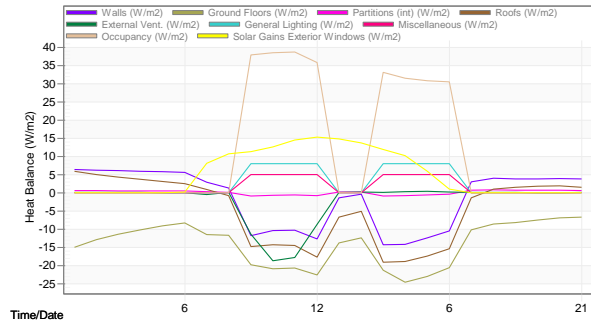
**Percentage of occupied hours in comfort and discomfort and Annual Heat balance of classroom in 1 classroom school in Picos (PI) – Zone 7 after optimization process**



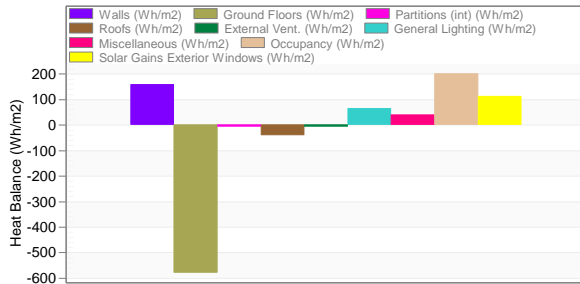
Summer Heat Balance (5 December)



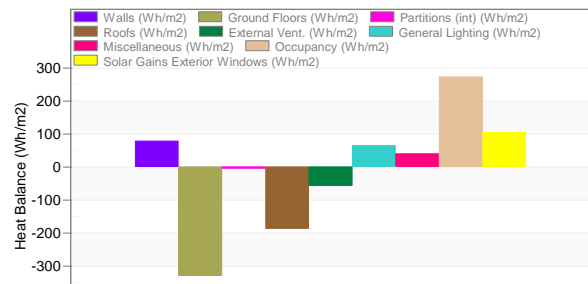
Winter Heat Balance (21 June)



Summer Day Heat Balance Summary



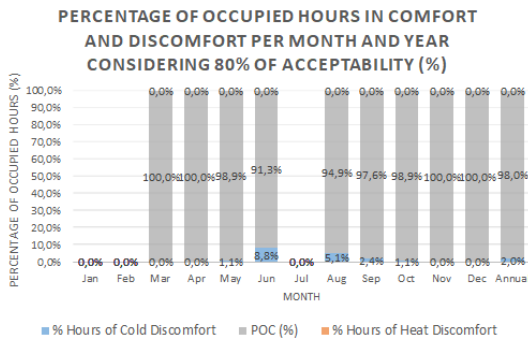
Winter Day Heat Balance Summary



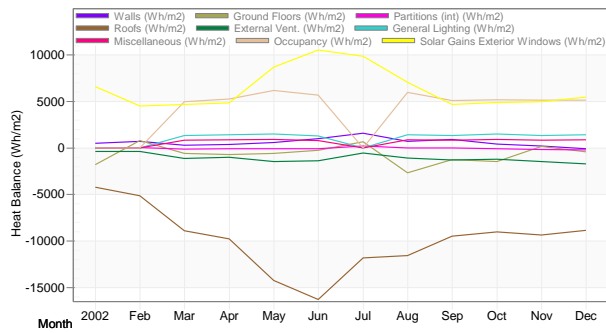
Source: Adapted from DesignBuilder (2022).

**Percentage of occupied hours in comfort and discomfort and Annual Heat balance of classroom in 1 classroom school in Goiânia (GO) – Zone 6 after optimization process**

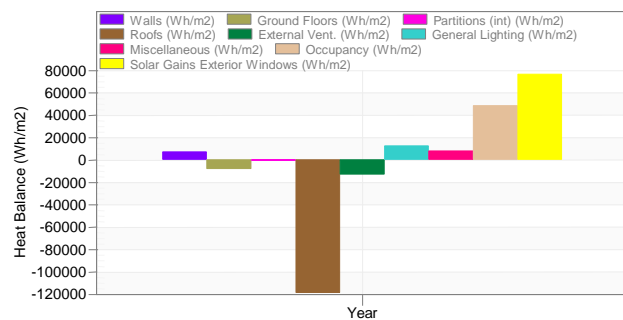
Comfort



Annual Heat Balance

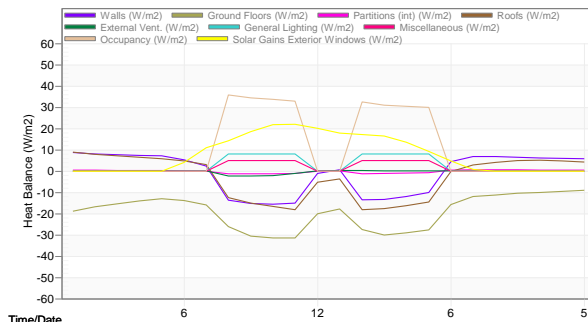


Annual Heat Balance Summary

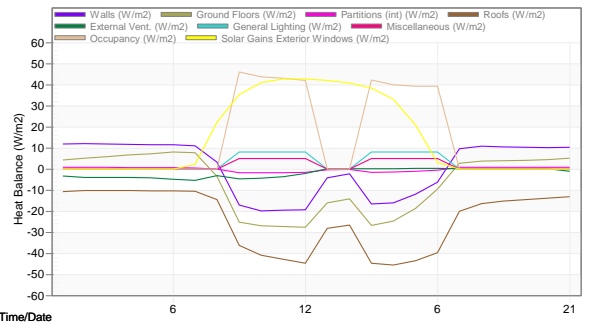




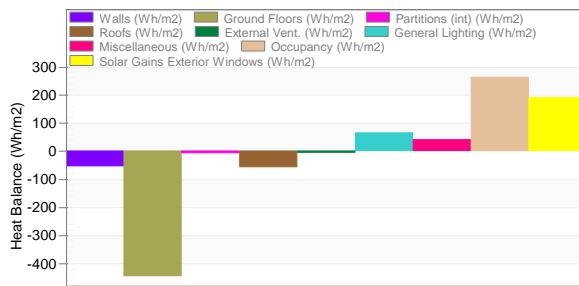
Summer Heat Balance (5 December)



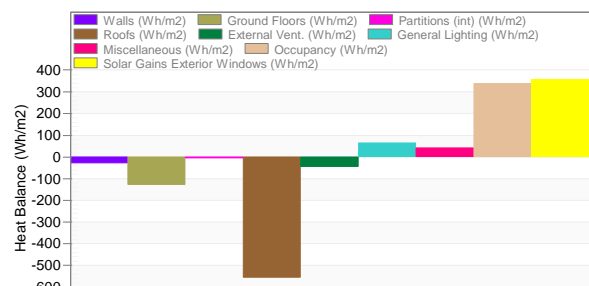
Winter Heat Balance (21 June)



Summer Day Heat Balance Summary



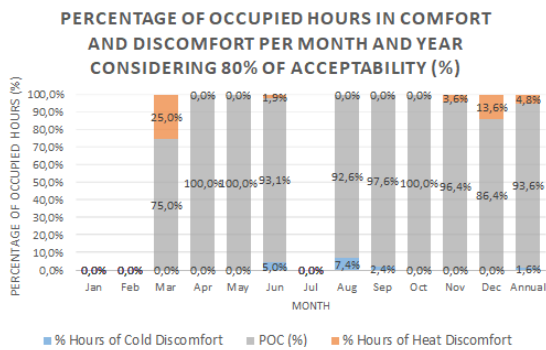
Winter Day Heat Balance Summary



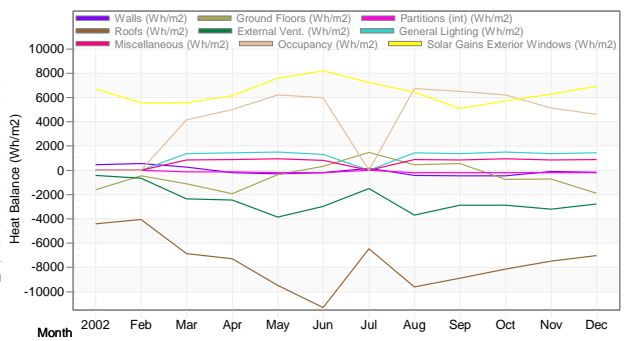
Source: Adapted from DesignBuilder (2022).

Percentage of occupied hours in comfort and discomfort and Annual Heat balance of classroom in 1 classroom school in Santos (SP) – Zone 5 after optimization process

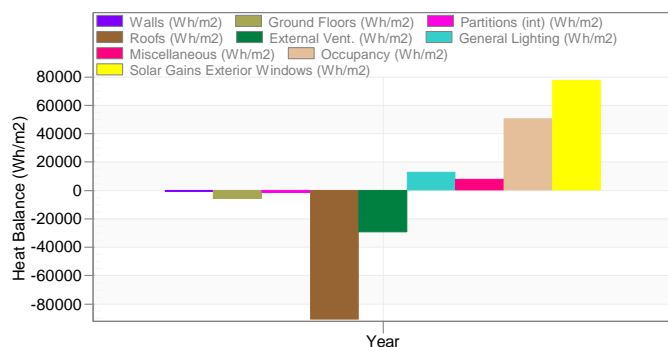
Comfort



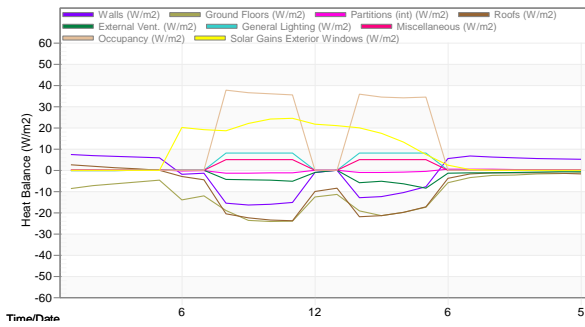
Annual Heat Balance



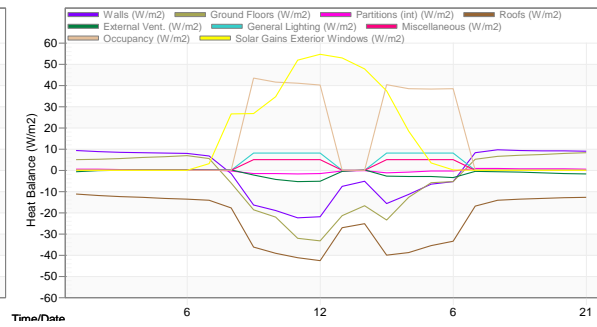
Annual Heat Balance Summary



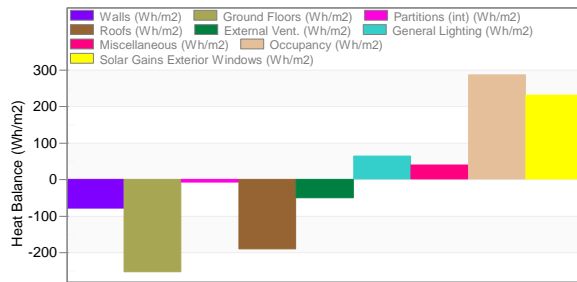
Summer Heat Balance (5 December)



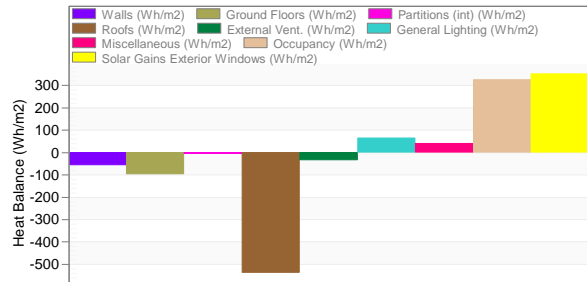
Winter Heat Balance (21 June)



Summer Day Heat Balance Summary



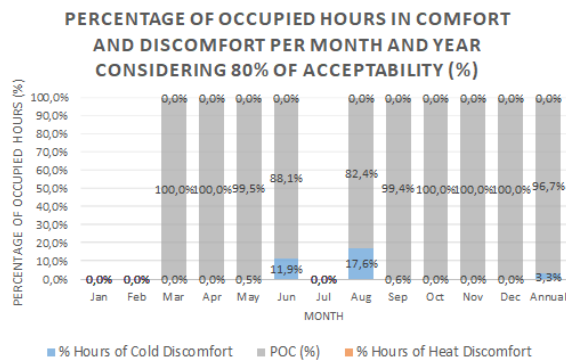
Winter Day Heat Balance Summary



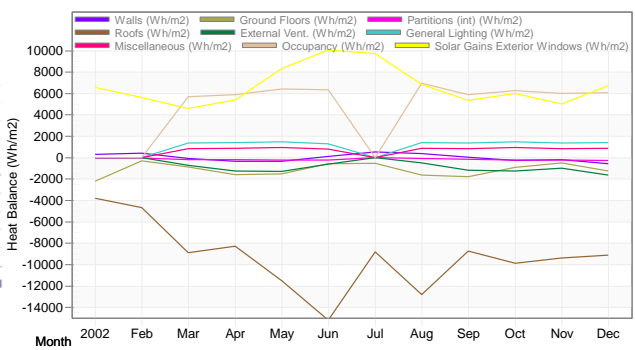
Source: Adapted from DesignBuilder (2022).

**Percentage of occupied hours in comfort and discomfort and Annual Heat balance of classroom in 1 classroom school in Brasília (DF) – Zone 4 after optimization process**

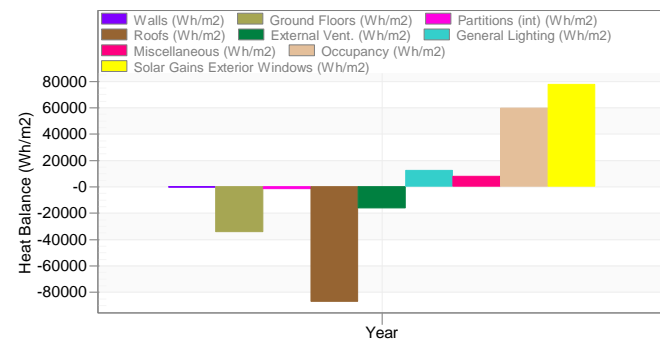
Comfort



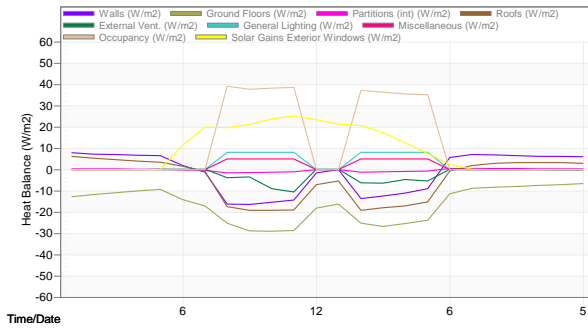
Annual Heat Balance



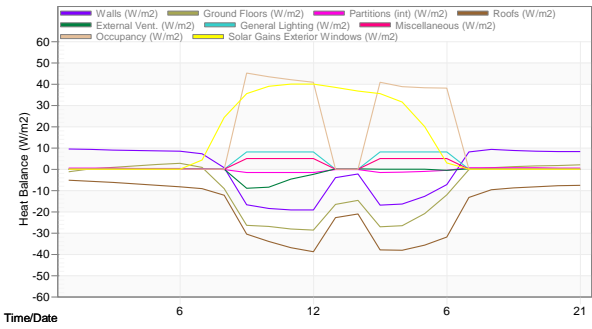
Annual Heat Balance Summary



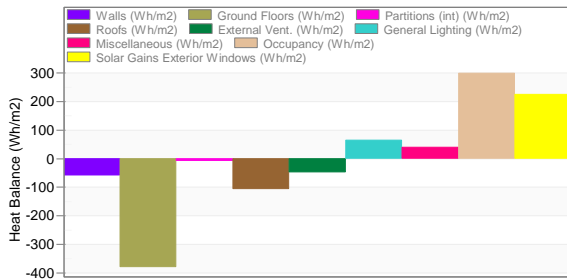
Summer Heat Balance (5 December)



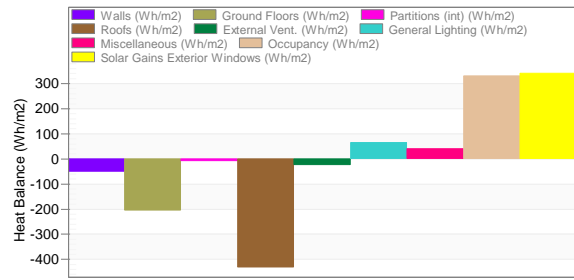
Winter Heat Balance (21 June)



Summer Day Heat Balance Summary



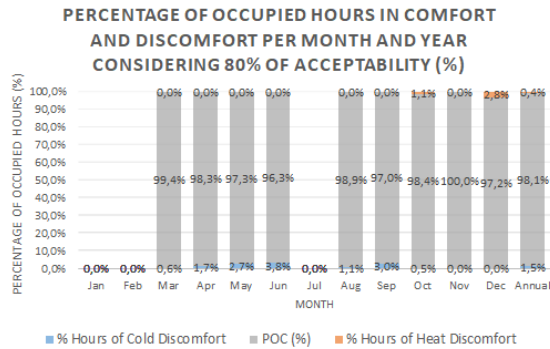
Winter Day Heat Balance Summary



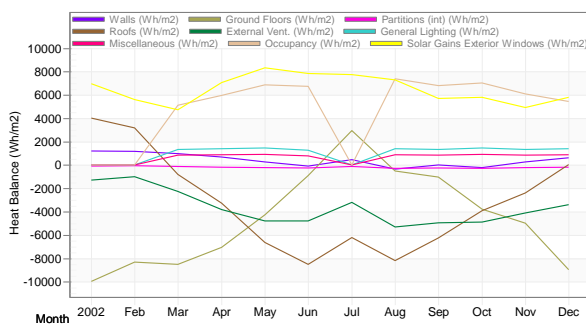
Source: Adapted from DesignBuilder (2022).

**Percentage of occupied hours in comfort and discomfort and Annual Heat balance of classroom in 1 classroom school in Florianópolis (SC) – Zone 3 after optimization process**

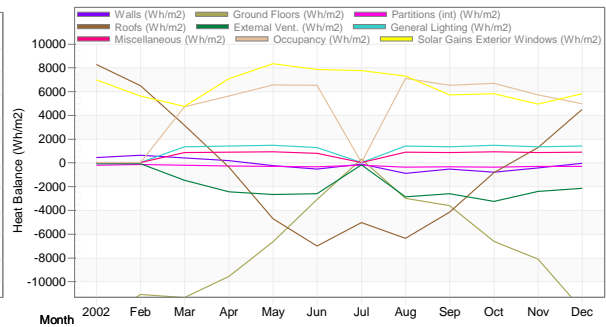
**Comfort**



Annual Heat Balance: Summer settings



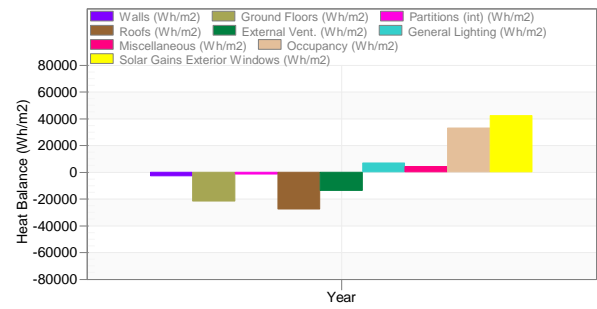
Annual Heat Balance: Winter settings



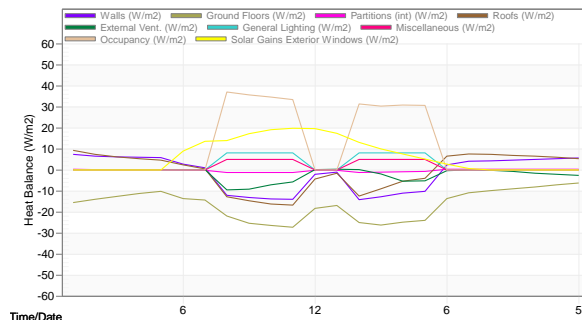
Summer Heat Balance Summary  
(Nov-Apr)



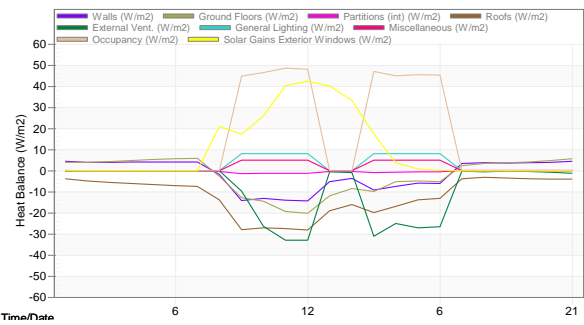
Winter Heat Balance Summary  
(May-Oct)



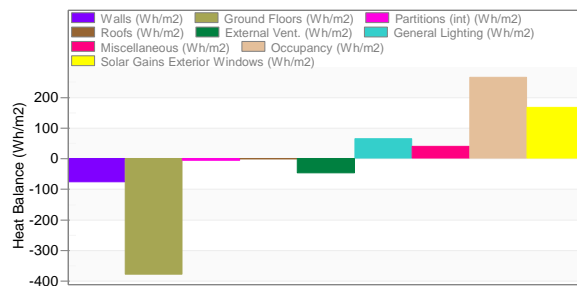
Summer Heat Balance (5 December)



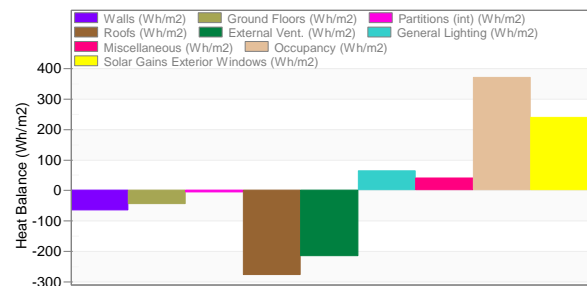
Winter Heat Balance (21 June)



Summer Day Heat Balance Summary



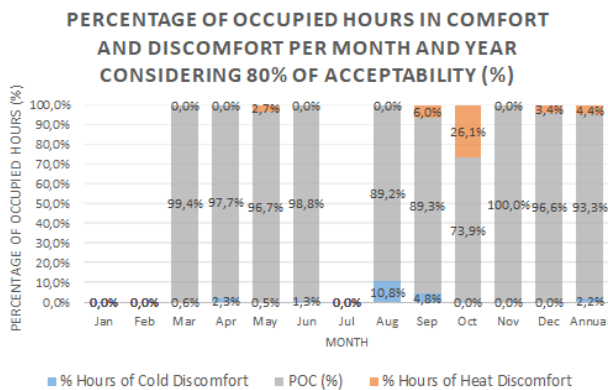
Winter Day Heat Balance Summary



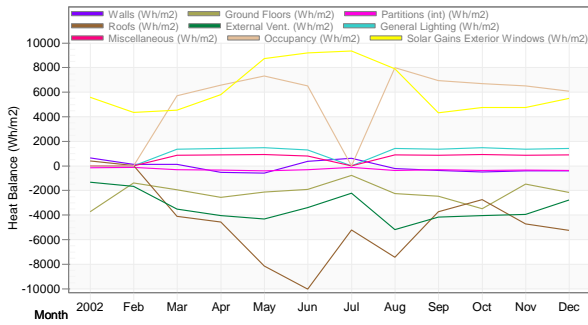
Source: Adapted from DesignBuilder (2022).

Percentage of occupied hours in comfort and discomfort and Annual Heat balance of classroom in 1 classroom school in Nova Friburgo (RJ) – Zone 2 after optimization process

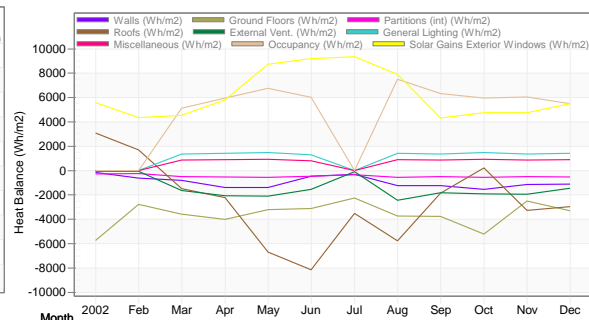
Comfort



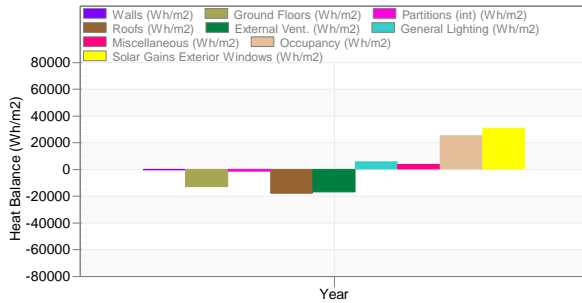
Annual Heat Balance: Summer settings



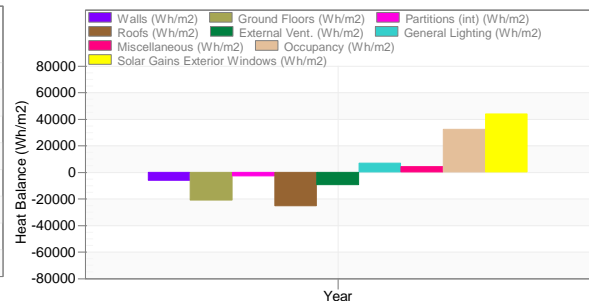
Annual Heat Balance: Winter settings



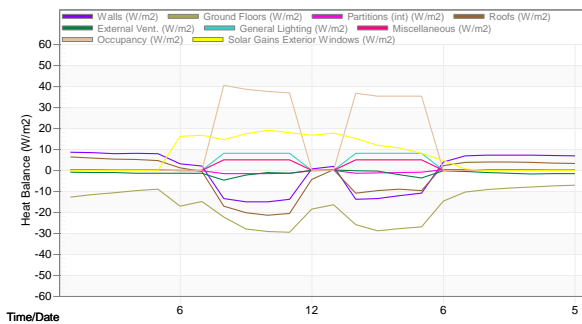
Summer Heat Balance Summary (Nov-Apr)



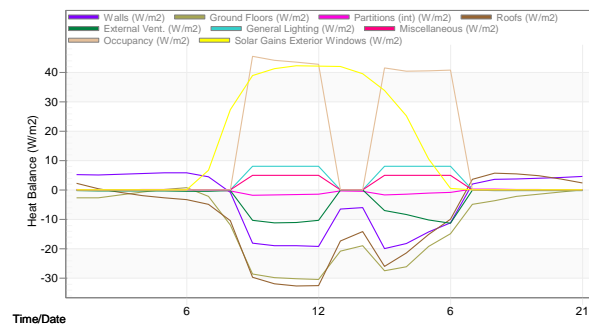
Winter Heat Balance Summary (May-Oct)



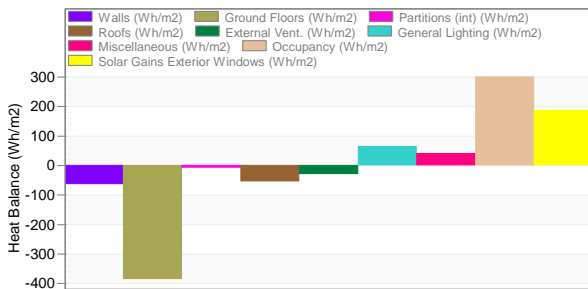
Summer Heat Balance (5 December)



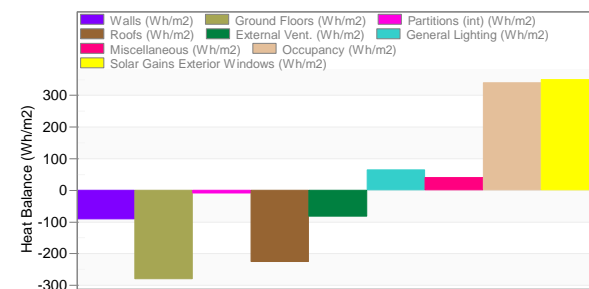
Winter Heat Balance (21 June)



Summer Day Heat Balance Summary



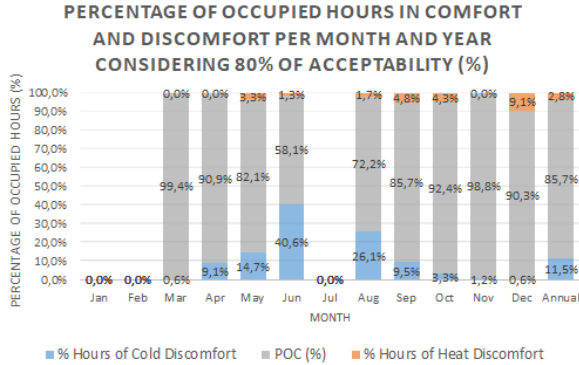
Winter Day Heat Balance Summary



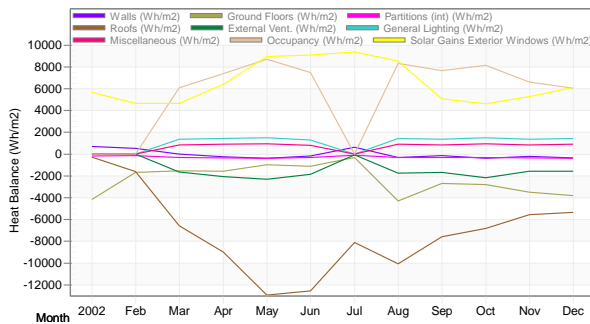
Source: Adapted from DesignBuilder (2022).

**Percentage of occupied hours in comfort and discomfort and Annual Heat balance of classroom in 1 classroom school in Caxias do Sul (RS) – Zone 1 after optimization process**

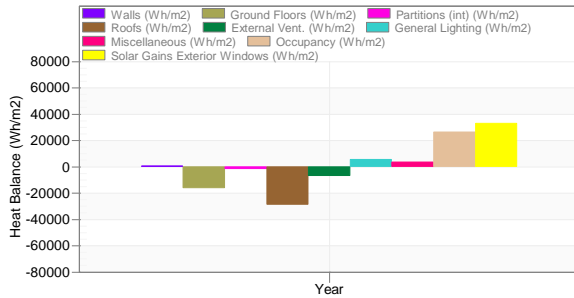
**Comfort**



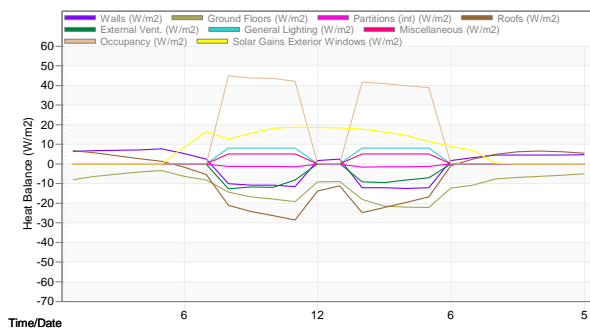
**Annual Heat Balance: Summer settings**



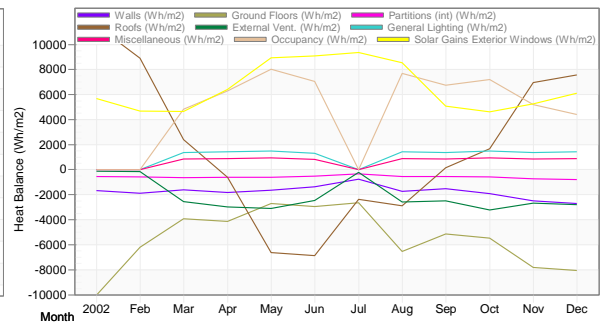
**Summer Heat Balance Summary (Nov-Apr)**



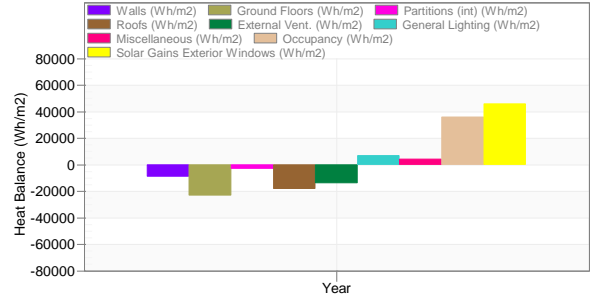
**Summer Heat Balance (5 December)**



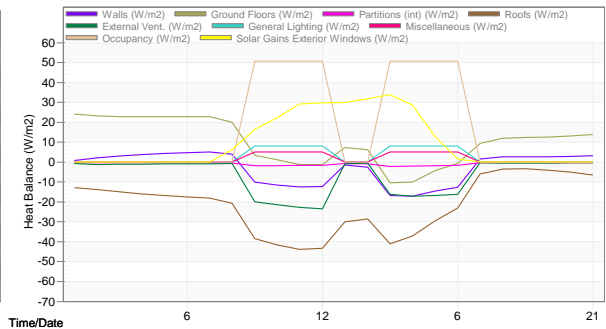
**Annual Heat Balance: Winter settings**



**Winter Heat Balance Summary (May-Oct)**



**Winter Heat Balance (21 June)**

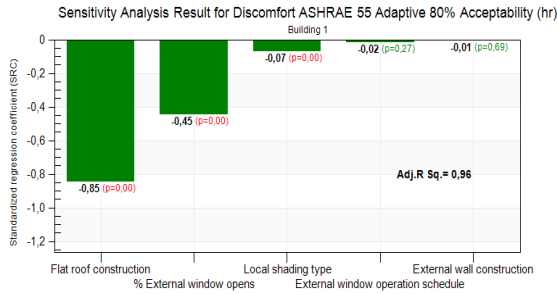


Source: Adapted from DesignBuilder (2022).

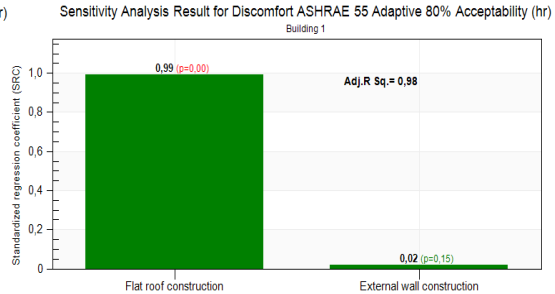
## APPENDIX F

### Sensitivity Analysis of 1 classroom school in Belém (PA) – Zone 8

#### Passive Strategies



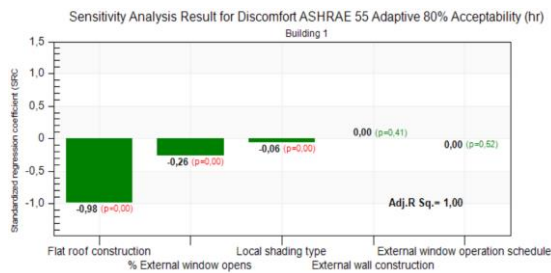
#### Reflectivity



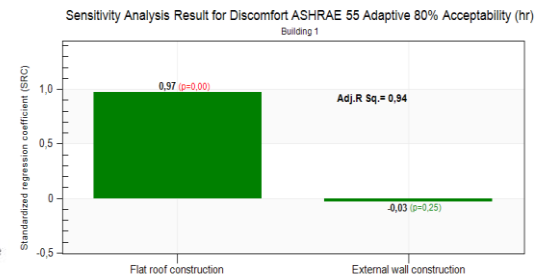
Source: Adapted from DesignBuilder (2022).

### Sensitivity Analysis of 1 classroom school in Picos (PI) – Zone 7

#### Passive Strategies



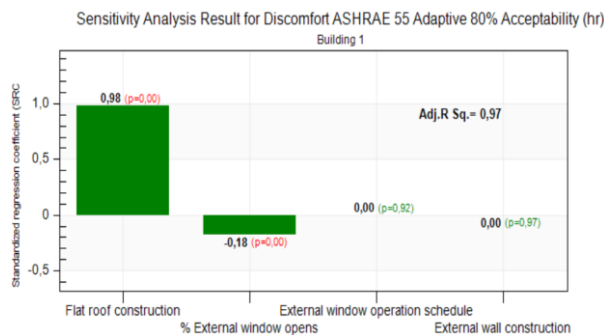
#### Reflectivity



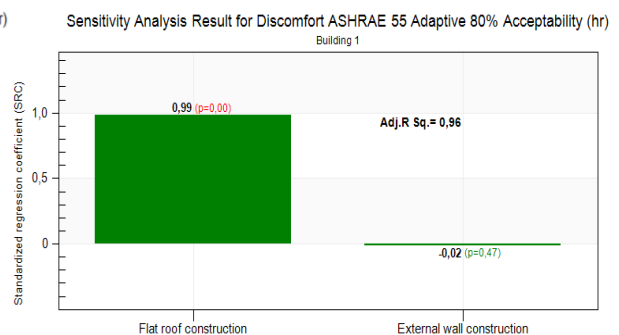
Source: Adapted from DesignBuilder (2022).

### Sensitivity Analysis of 1 classroom school in Goiânia (GO) – Zone 6

#### Passive Strategies



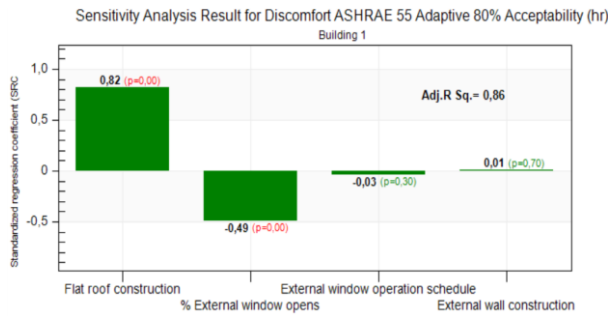
#### Reflectivity



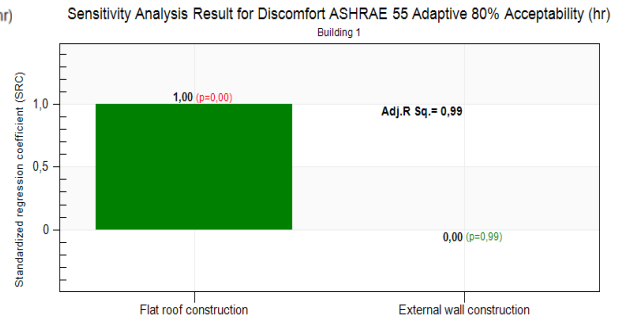
Source: Adapted from DesignBuilder (2022).

### Sensitivity Analysis of 1 classroom school in Santos (SP) – Zone 5

#### Passive Strategies



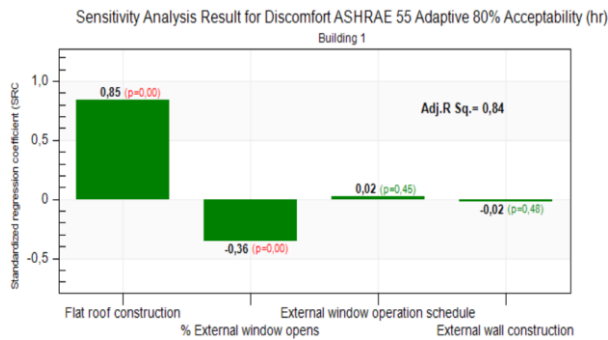
#### Reflectivity



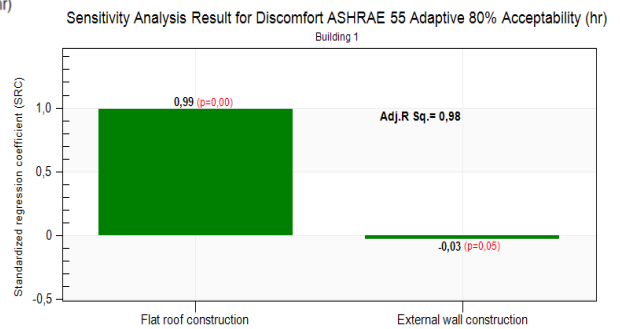
Source: Adapted from DesignBuilder (2022).

### Sensitivity Analysis of 1 classroom school in Brasília (DF) – Zone 4

#### Passive Strategies



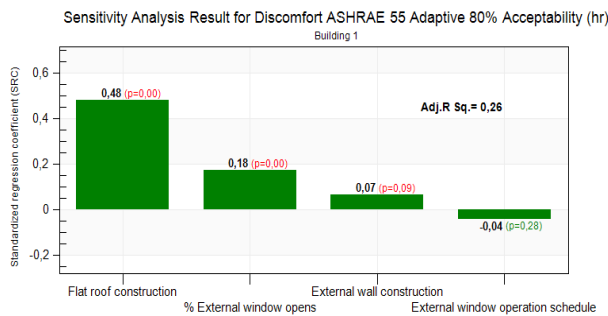
#### Reflectivity



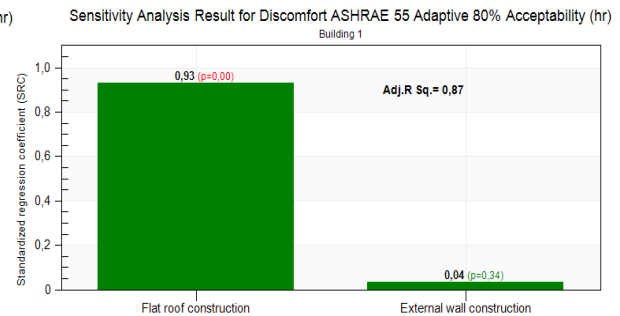
Source: Adapted from DesignBuilder (2022).

### Sensitivity Analysis of 1 classroom school in Florianópolis (SC) – Zone 3

#### Passive Strategies



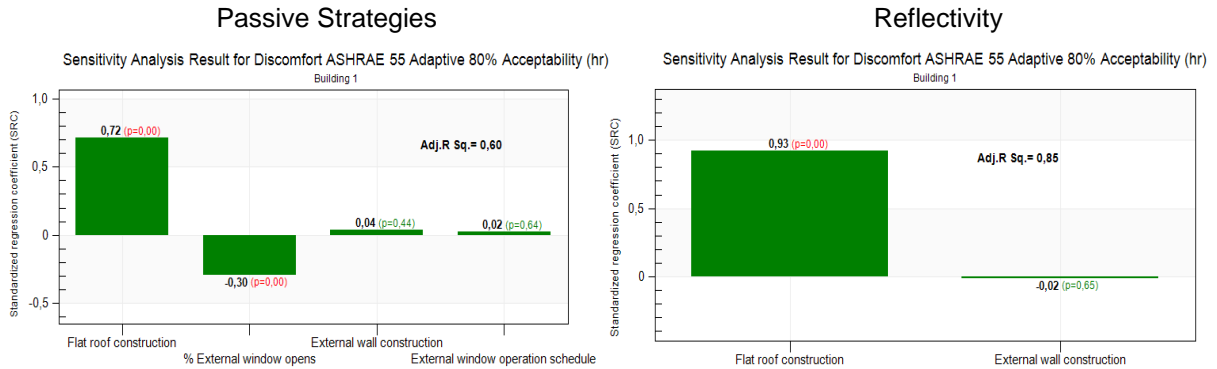
#### Reflectivity



Source: Adapted from DesignBuilder (2022).

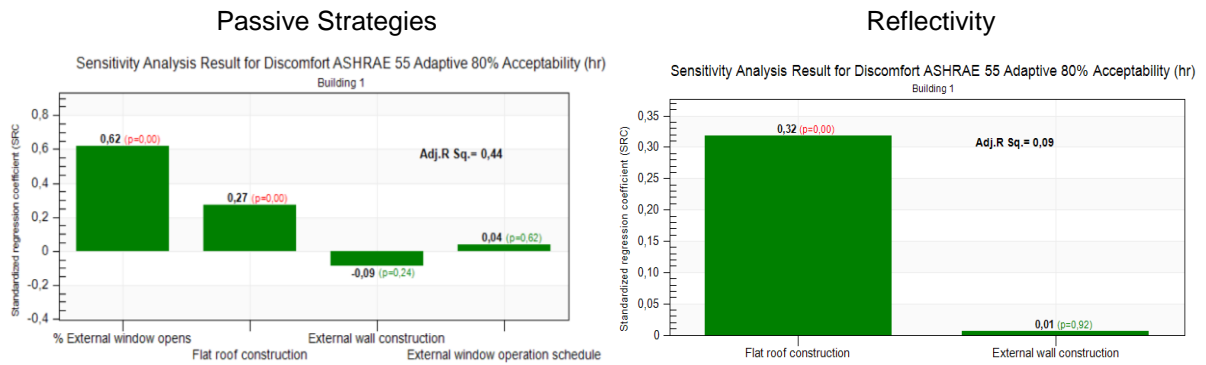


### Sensitivity Analysis of 1 classroom school in Nova Friburgo (RJ) – Zone 2



Source: Adapted from DesignBuilder (2022).

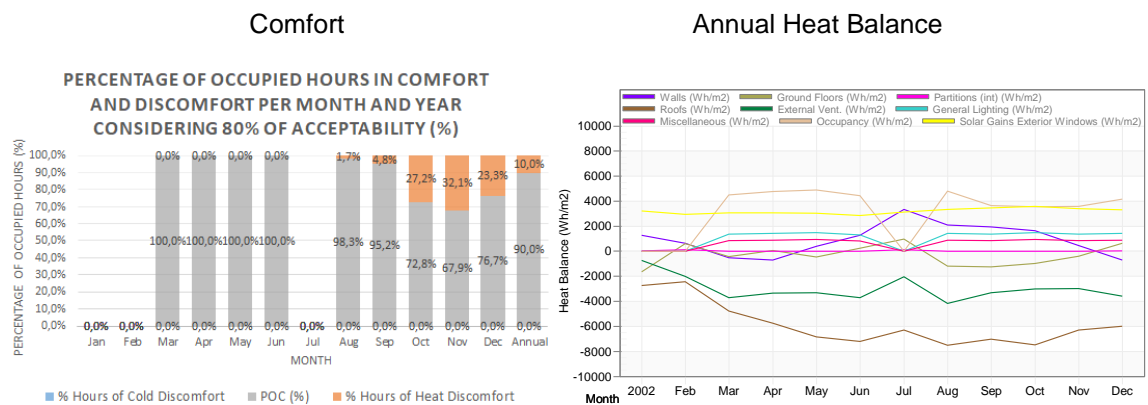
### Sensitivity Analysis of 1 classroom school in Caxias do Sul (RS) – Zone 1



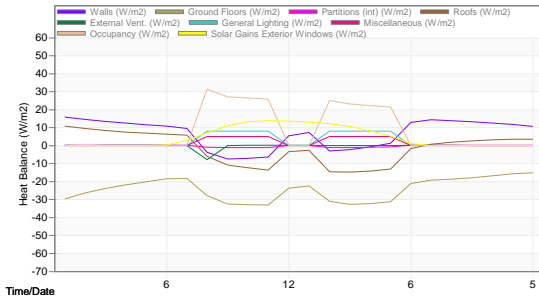
Source: Adapted from DesignBuilder (2022).

## APPENDIX G

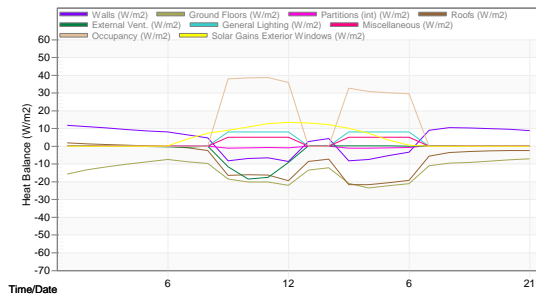
### Percentage of occupied hours in comfort and discomfort and Annual Heat balance of classroom in 1 classroom school in Picos (PI) – Zone 7 after Non Algorithm Simulations: 90% Reflectivity External Ground



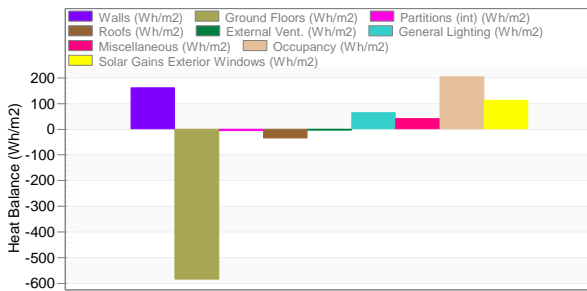
Summer Heat Balance (5 December)



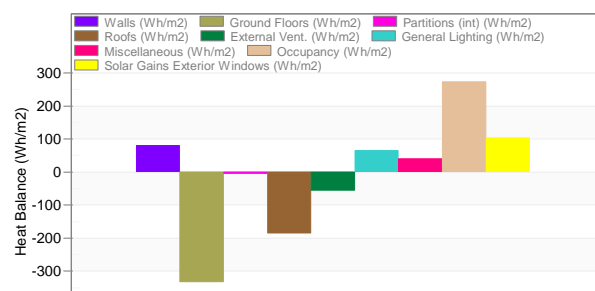
Winter Heat Balance (21 June)



Summer Day Heat Balance Summary



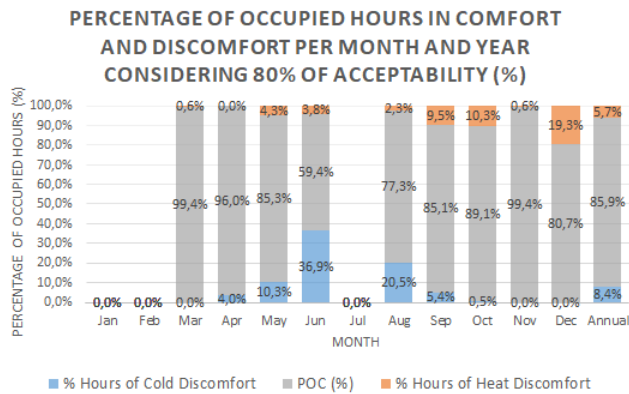
Winter Day Heat Balance Summary



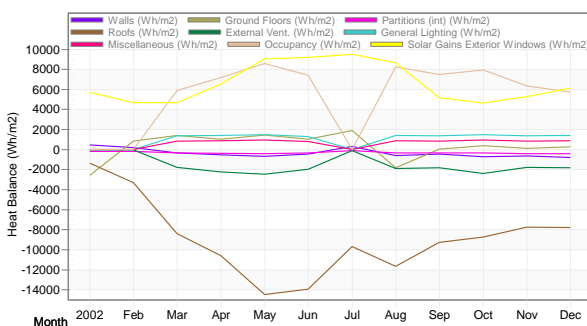
Source: Adapted from DesignBuilder (2022).

**Percentage of occupied hours in comfort and discomfort and Annual Heat balance of classroom in 1 classroom school in Caxias do Sul (RS) – Zone 1 after Non Algorithm Simulations: 30% Reflectivity External Ground**

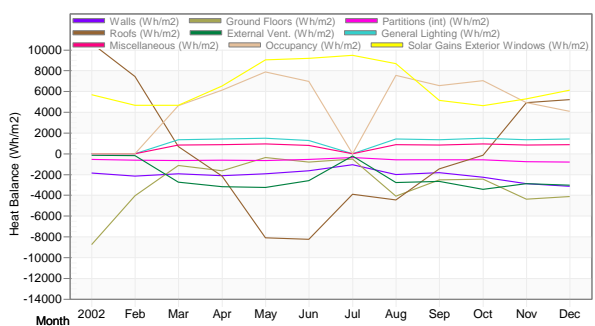
**Comfort**



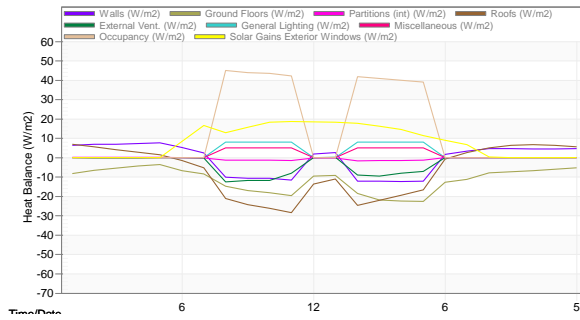
Annual Heat Balance: Summer settings



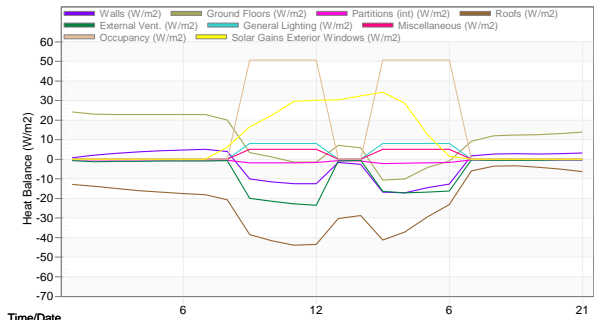
Annual Heat Balance: Winter settings



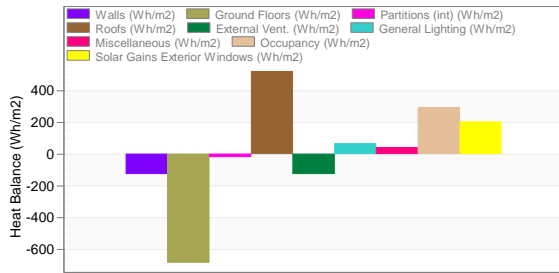
Summer Heat Balance (5 December)



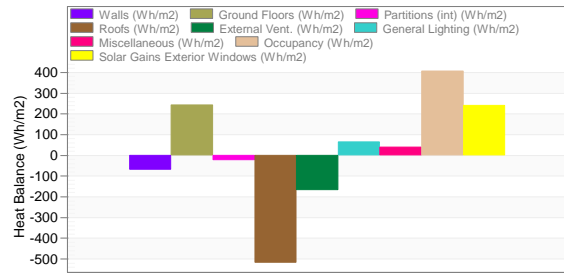
Winter Heat Balance (21 June)



Summer Day Heat Balance Summary



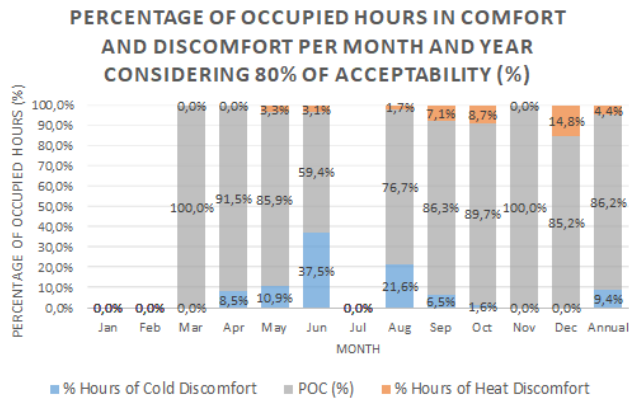
Winter Day Heat Balance Summary



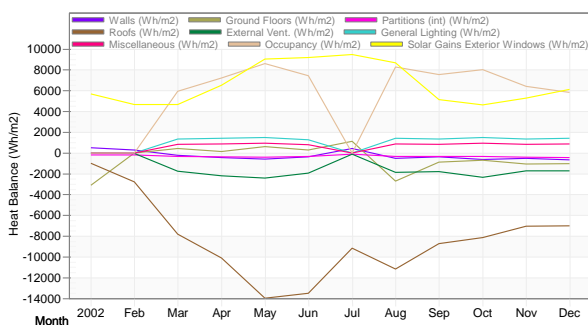
Source: Adapted from DesignBuilder (2022).

**Percentage of occupied hours in comfort and discomfort and Annual Heat balance of classroom in 1 classroom school in Caxias do Sul (RS) – Zone 1 after Non Algorithm Simulations: 50% Reflectivity External Ground**

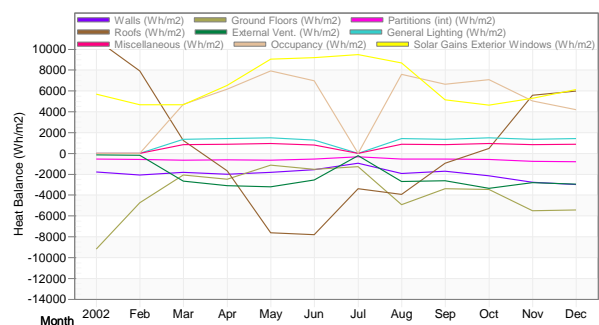
Comfort



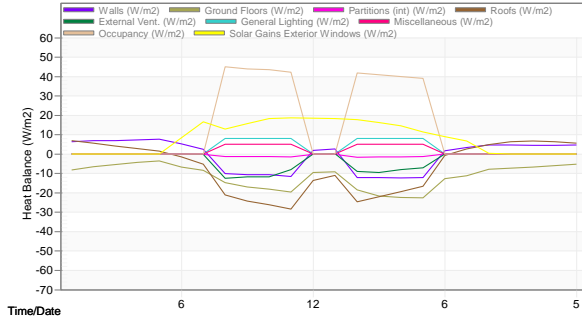
Annual Heat Balance: Summer settings



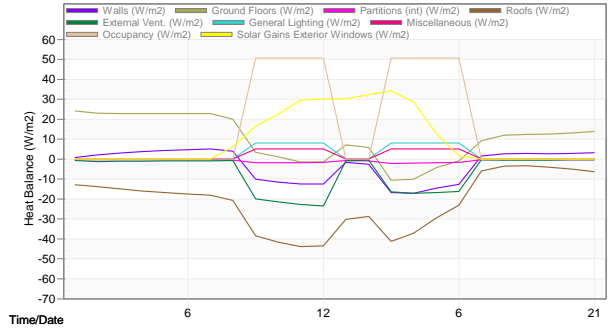
Annual Heat Balance: Winter settings



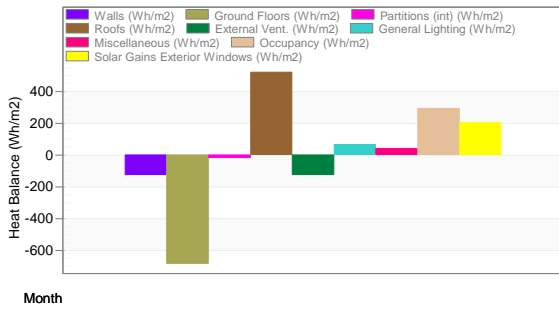
Summer Heat Balance (5 December)



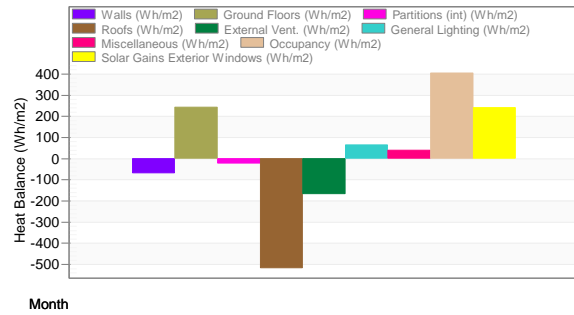
Winter Heat Balance (21 June)



Summer Day Heat Balance Summary



Winter Day Heat Balance Summary

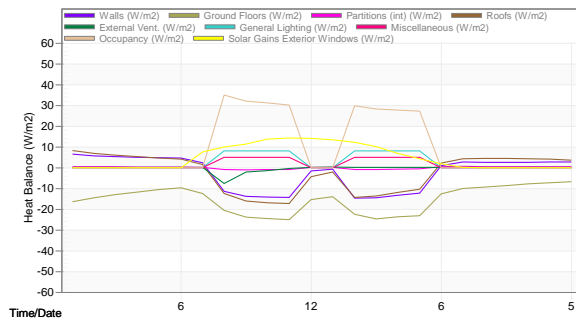


Source: Adapted from DesignBuilder (2022).

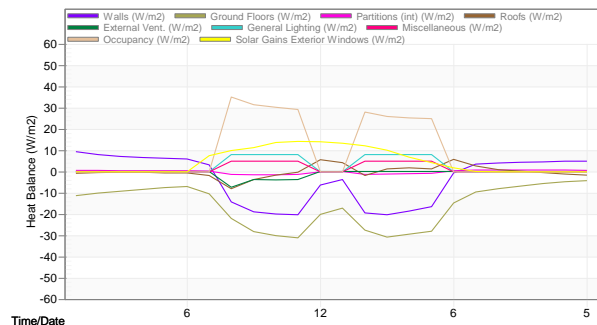
APPENDIX H

Summer Heat balances (5 December) of classroom in 1 classroom school in Belém (PA) – Zone 8 with roof type variation

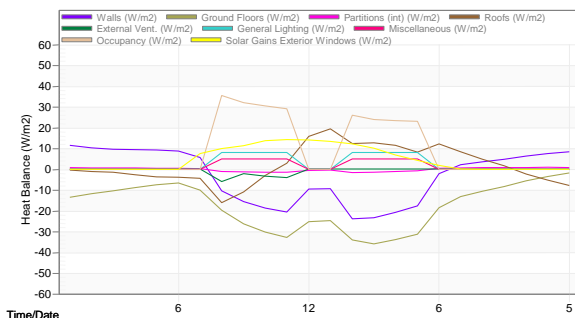
Original



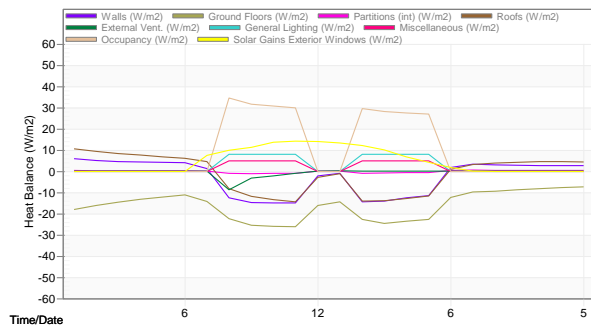
Insulated



Light

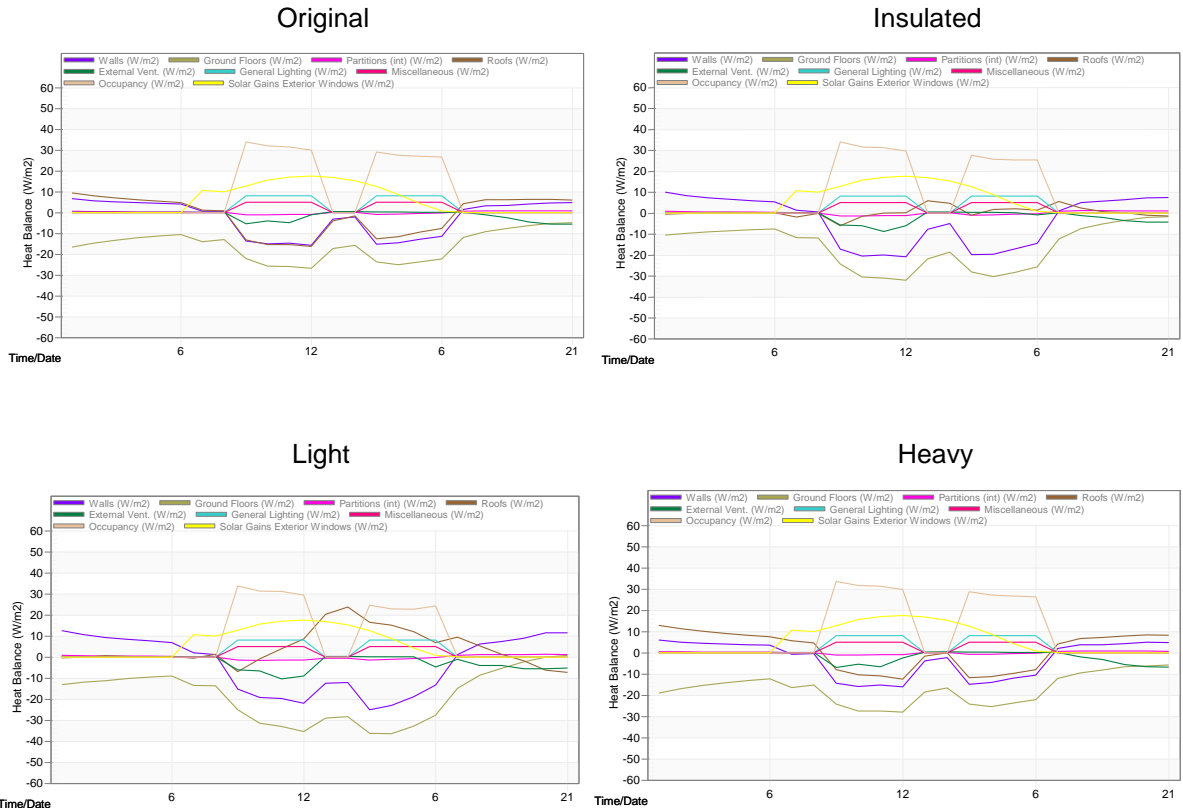


Heavy



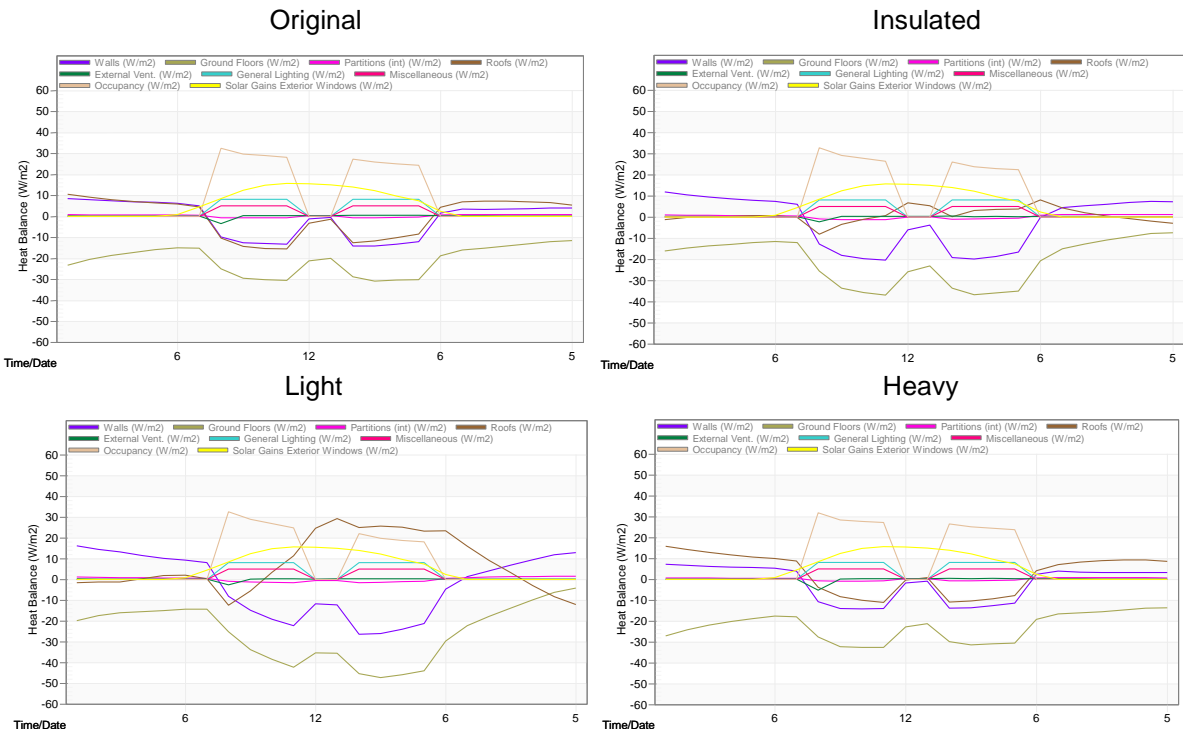
Source: Adapted from DesignBuilder (2022).

**Winter Heat balances (21 June) of classroom in 1 classroom school in Belém (PA) – Zone 8 with roof type variation**



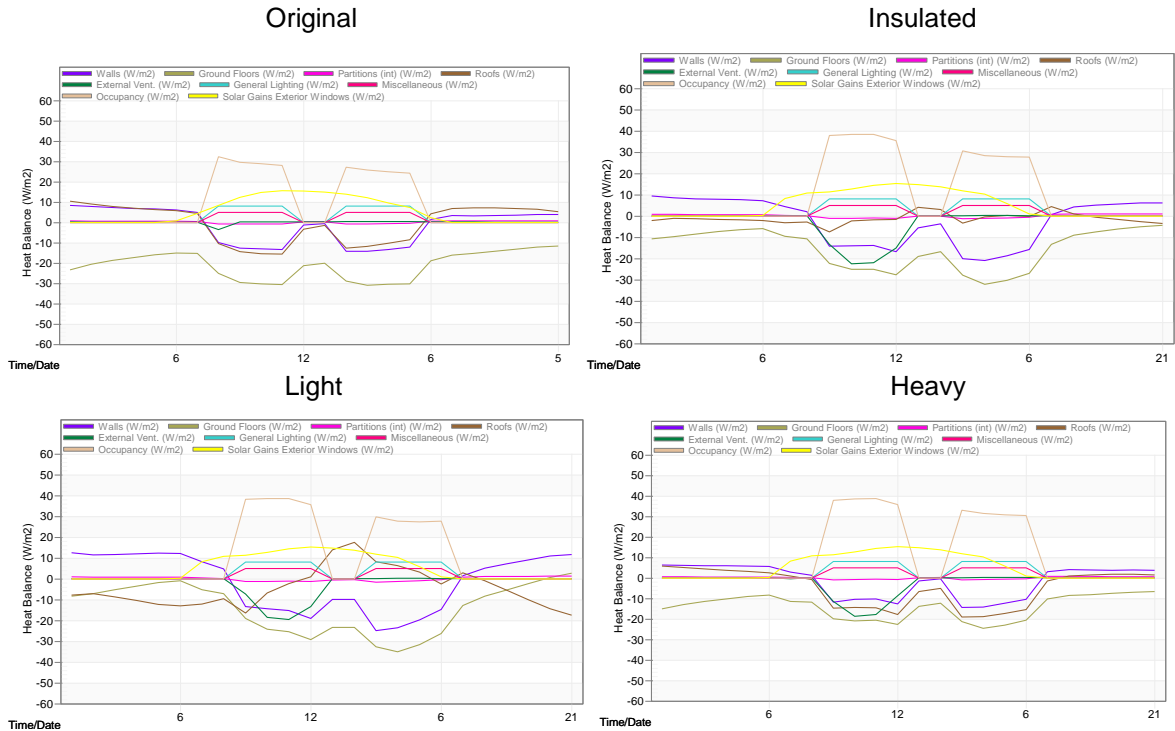
Source: Adapted from DesignBuilder (2022).

**Summer Heat balances (5 December) of classroom in 1 classroom school in Picos (PI) – Zone 7 with roof type variation**



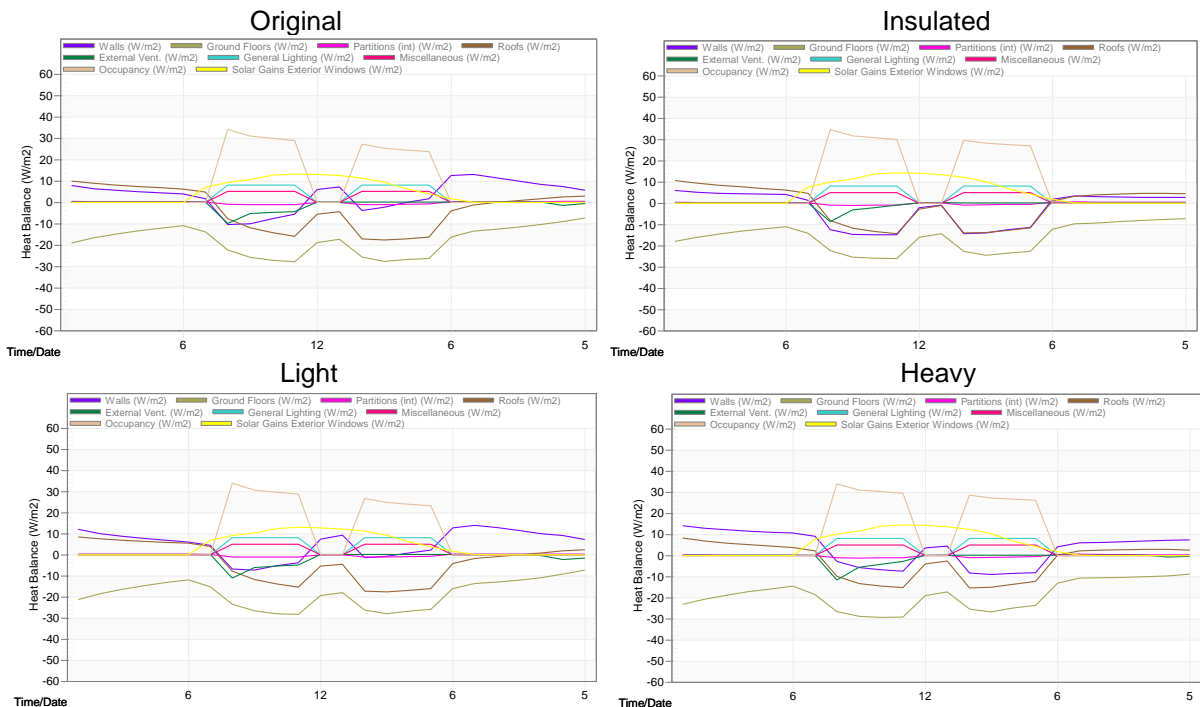
Source: Adapted from DesignBuilder (2022).

**Winter Heat balances (21 June) of classroom in 1 classroom school in Picos (PI) – Zone 7 with roof type variation**



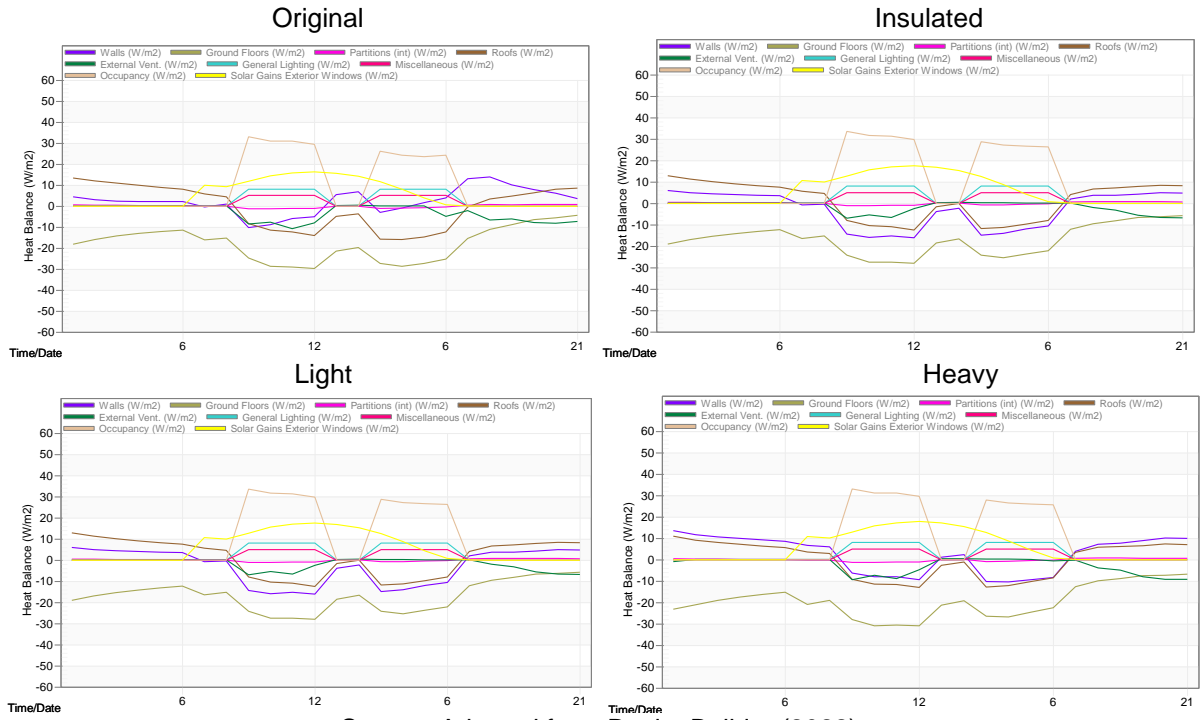
Source: Adapted from DesignBuilder (2022).

**Summer Heat balances (5 December) of classroom in 1 classroom school in Belém (PA) – Zone 8 with wall type variation**



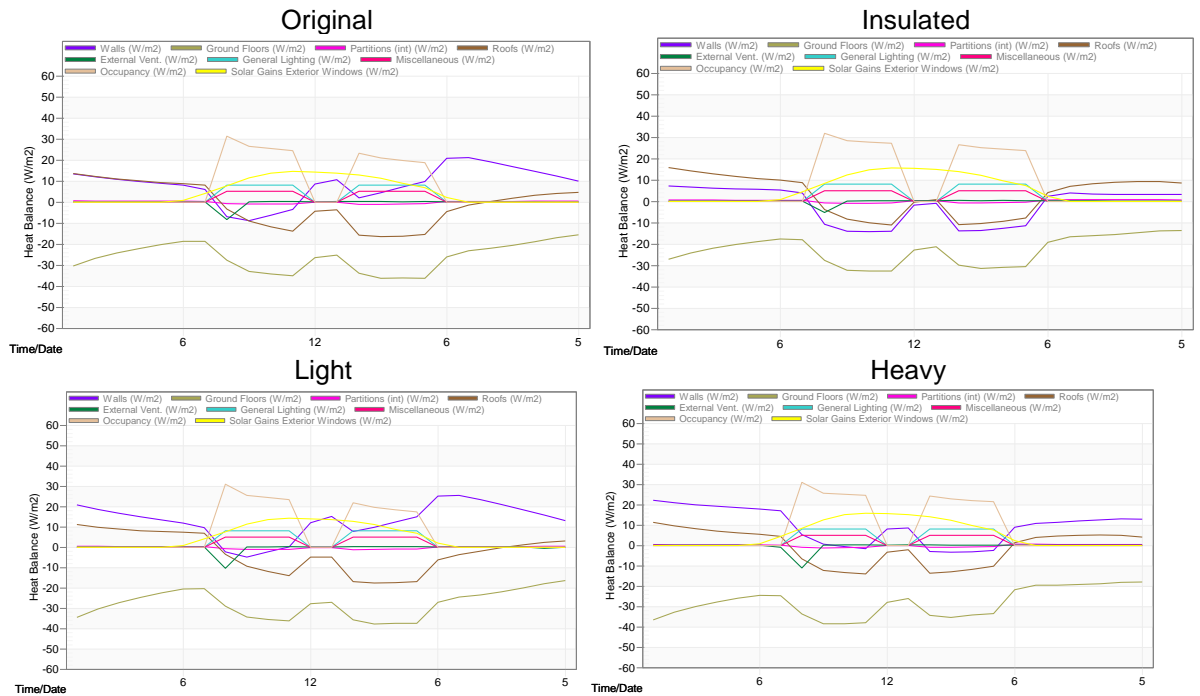
Source: Adapted from DesignBuilder (2022).

**Winter Heat balances (21 June) of classroom in 1 classroom school in Belém (PA) – Zone 8 with wall type variation**



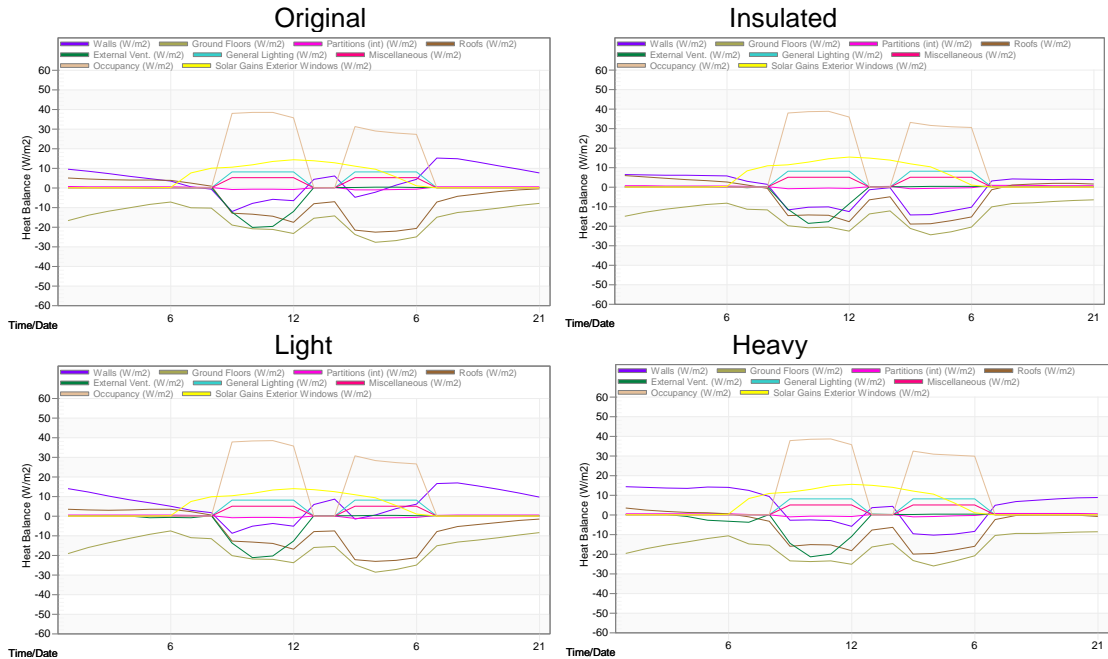
Source: Adapted from DesignBuilder (2022).

**Summer Heat balances (5 December) of classroom in 1 classroom school in Picos (PI) – Zone 7 with wall type variation**



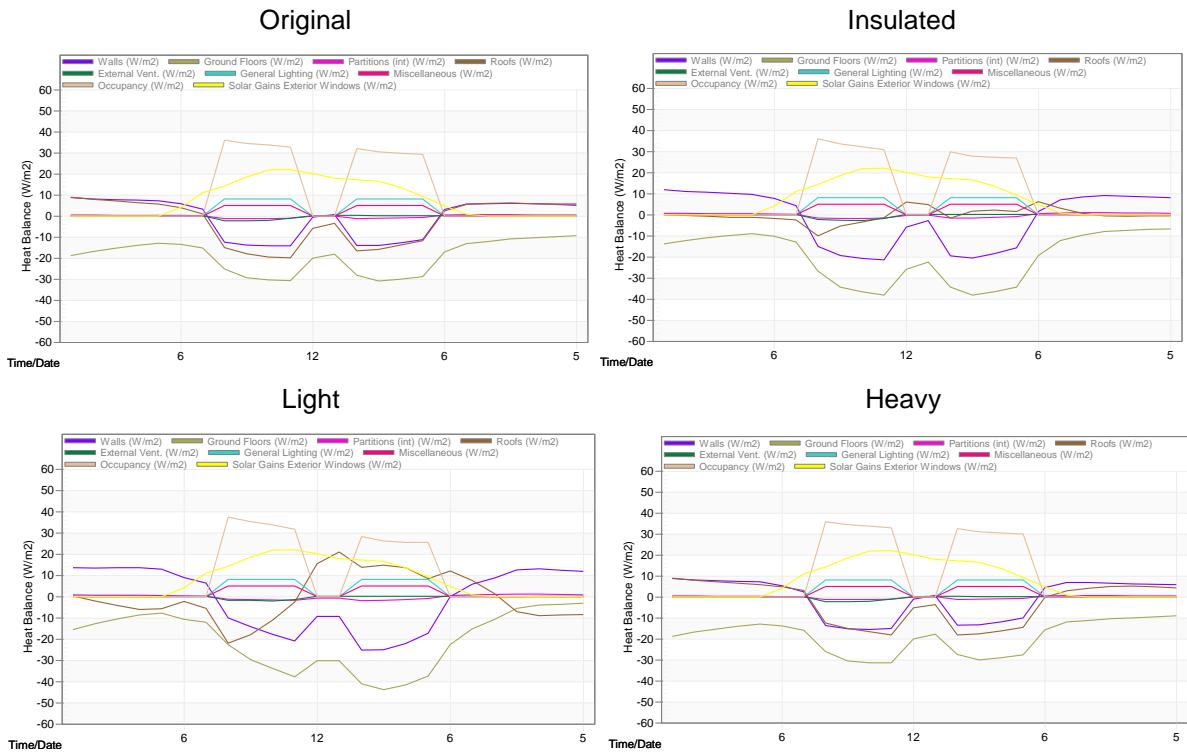
Source: Adapted from DesignBuilder (2022).

**Winter Heat balances (21 June) of classroom in 1 classroom school in Picos (PI) – Zone 7 with wall type variation**



Source: Adapted from DesignBuilder (2022).

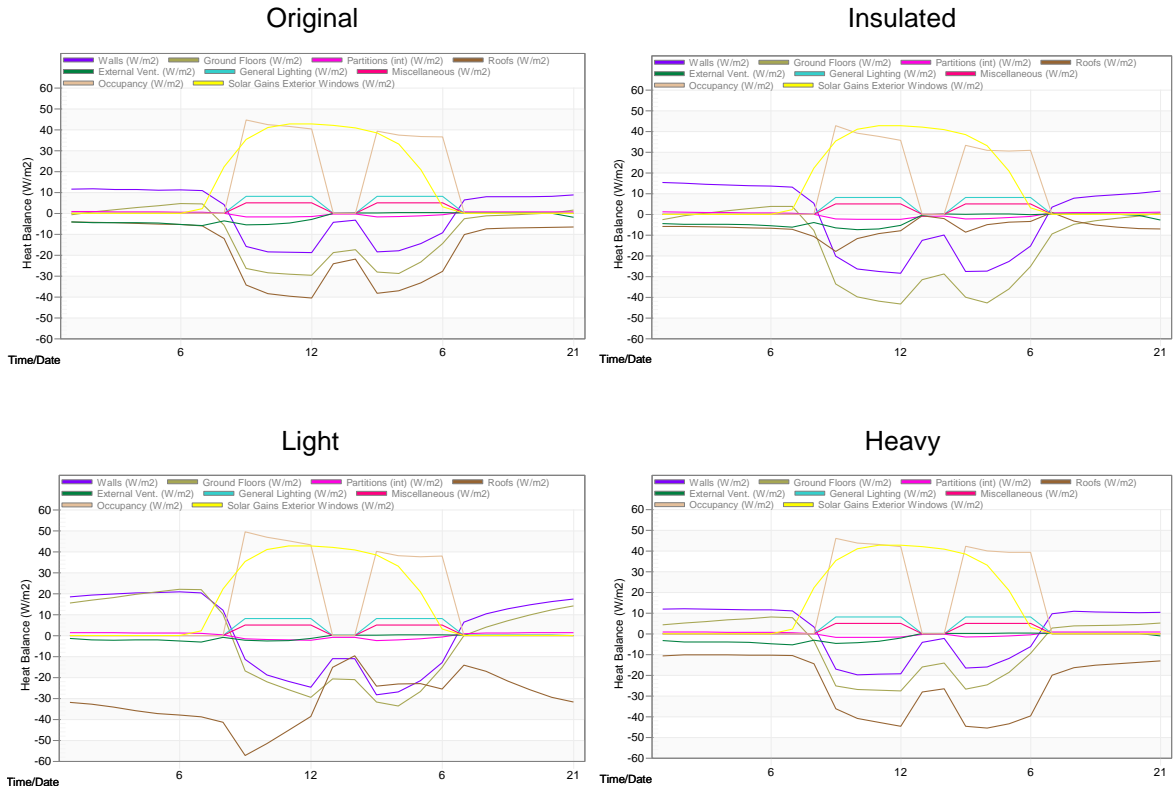
**(GO) – Zone 6 with roof type variation**



Source: Adapted from DesignBuilder (2022).

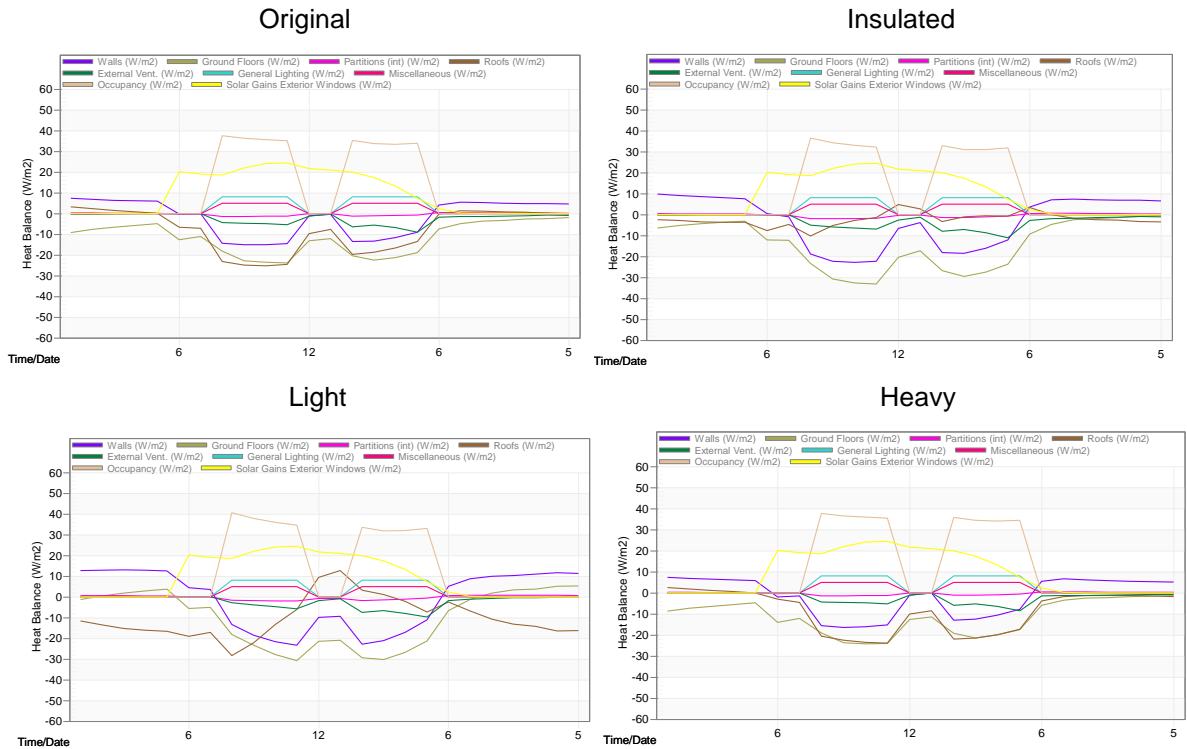


**Winter Heat balances (21 June) of classroom in 1 classroom school in Goiânia (GO) – Zone 6 with roof type variation**



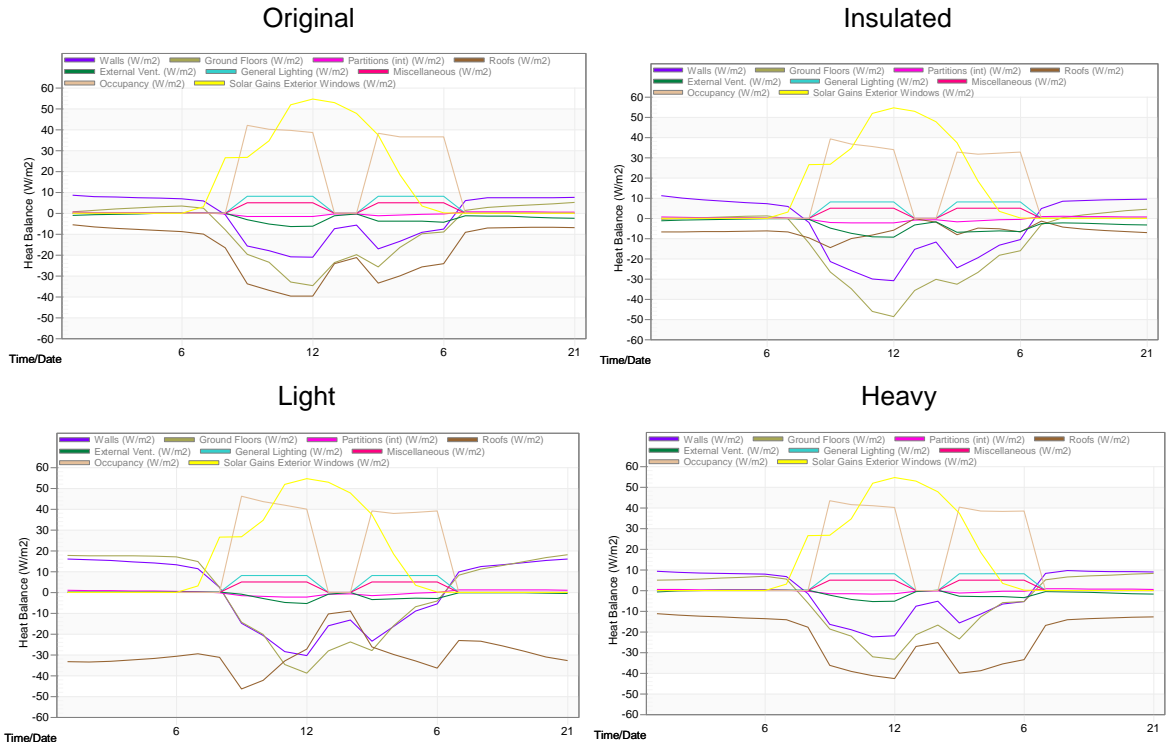
Source: Adapted from DesignBuilder (2022).

**Summer Heat balances (5 December) of classroom in 1 classroom school in Santos (SP) – Zone 5 with roof type variation**



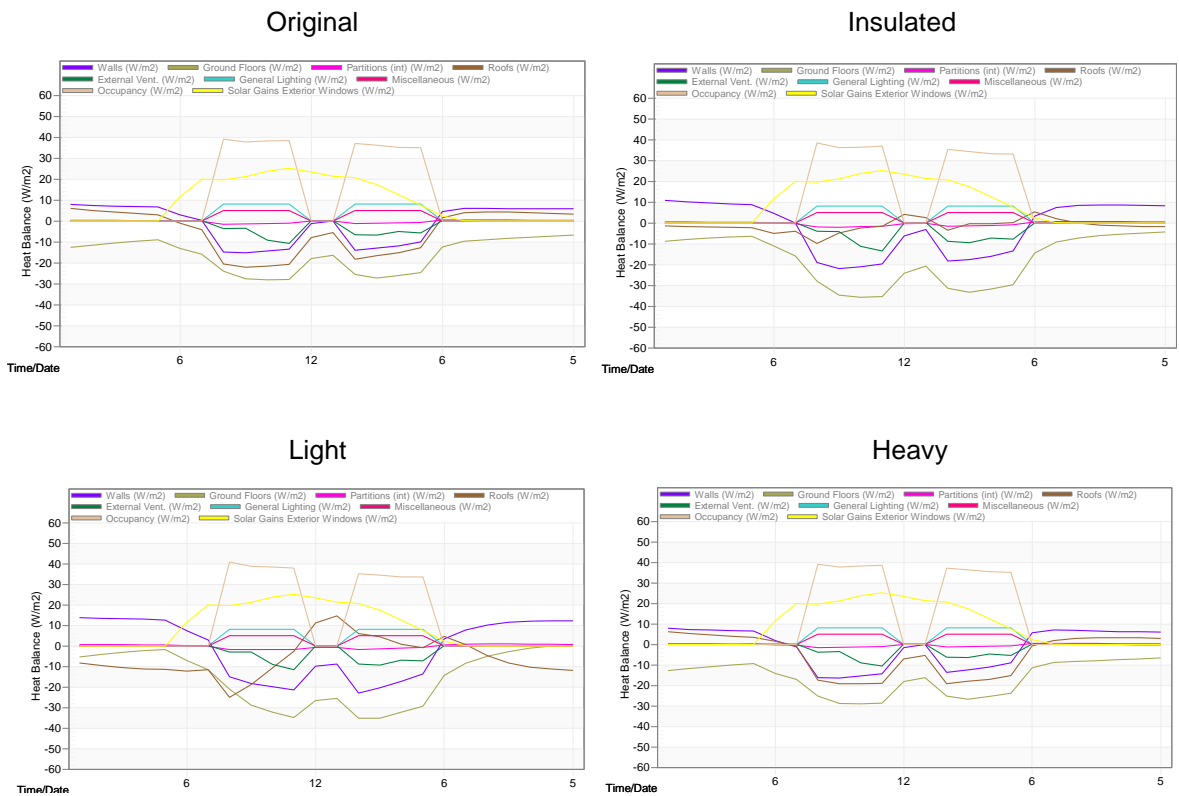
Source: Adapted from DesignBuilder (2022).

**Winter Heat balances (21 June) of classroom in 1 classroom school in Santos (SP) – Zone 5 with roof type variation**



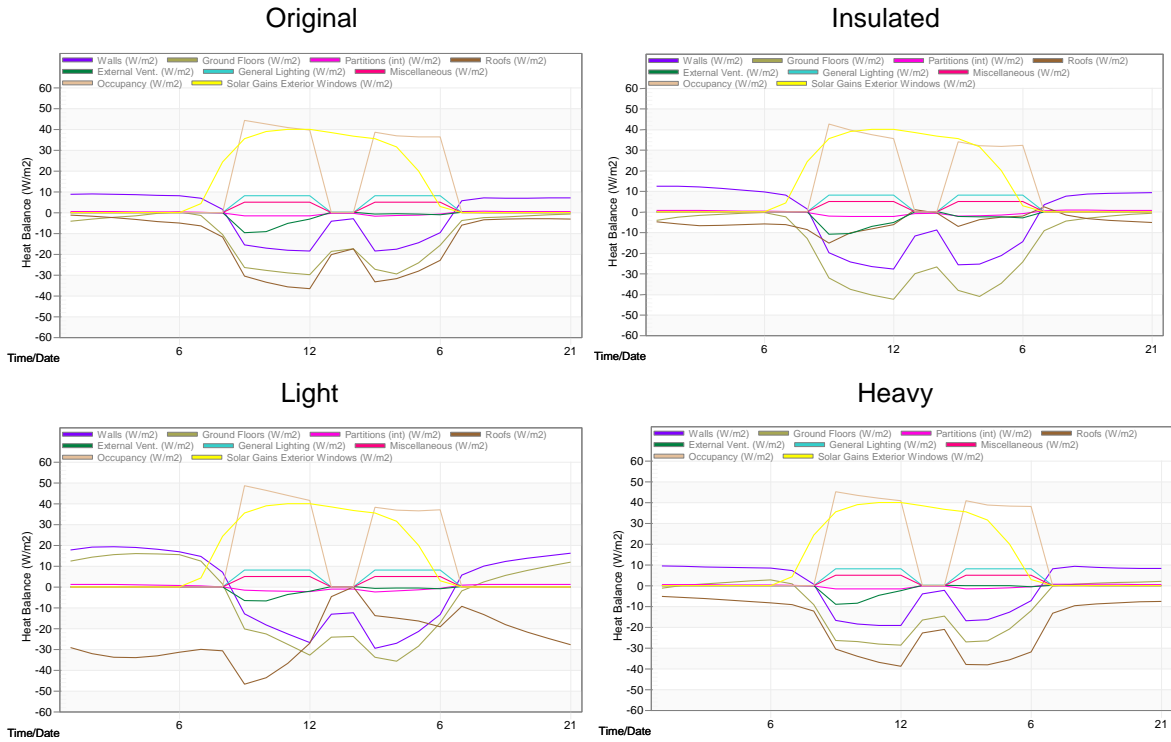
Source: Adapted from DesignBuilder (2022).

**Summer Heat balances (5 December) of classroom in 1 classroom school in Brasília (DF) – Zone 4 with roof type variation**



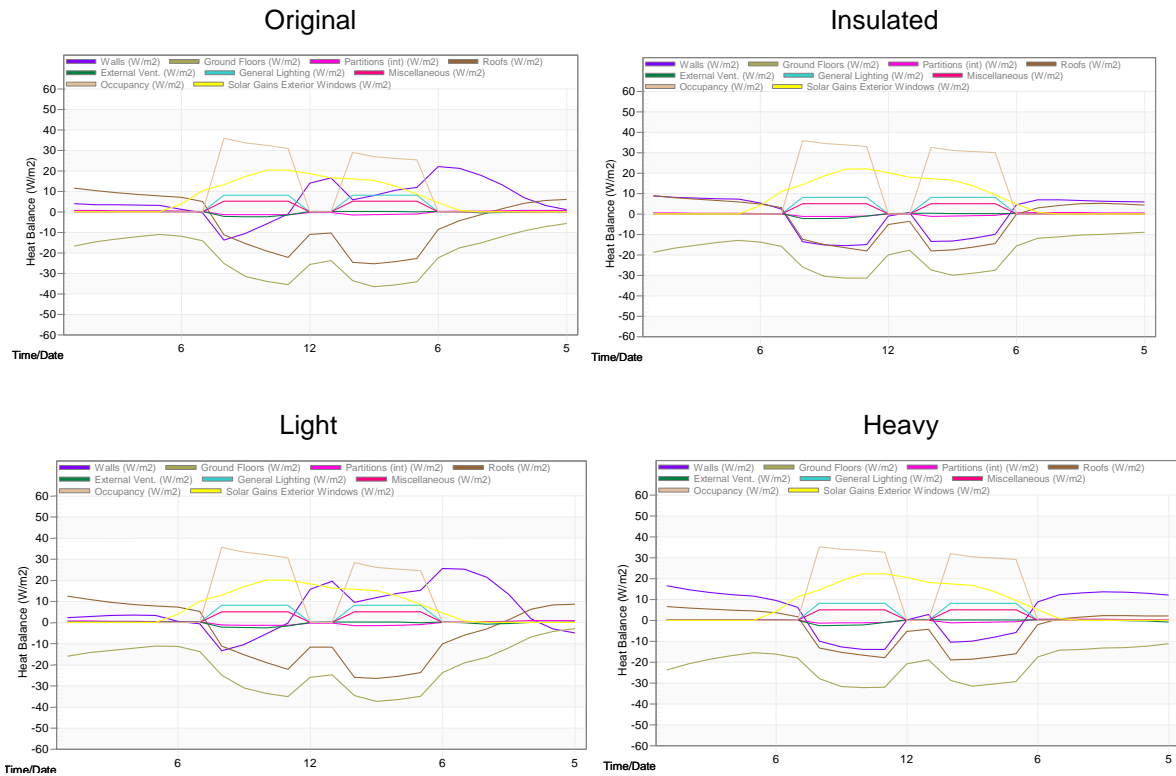
Source: Adapted from DesignBuilder (2022).

**Winter Heat balances (21 June) of classroom in 1 classroom school in Brasília (DF) – Zone 4 with roof type variation**



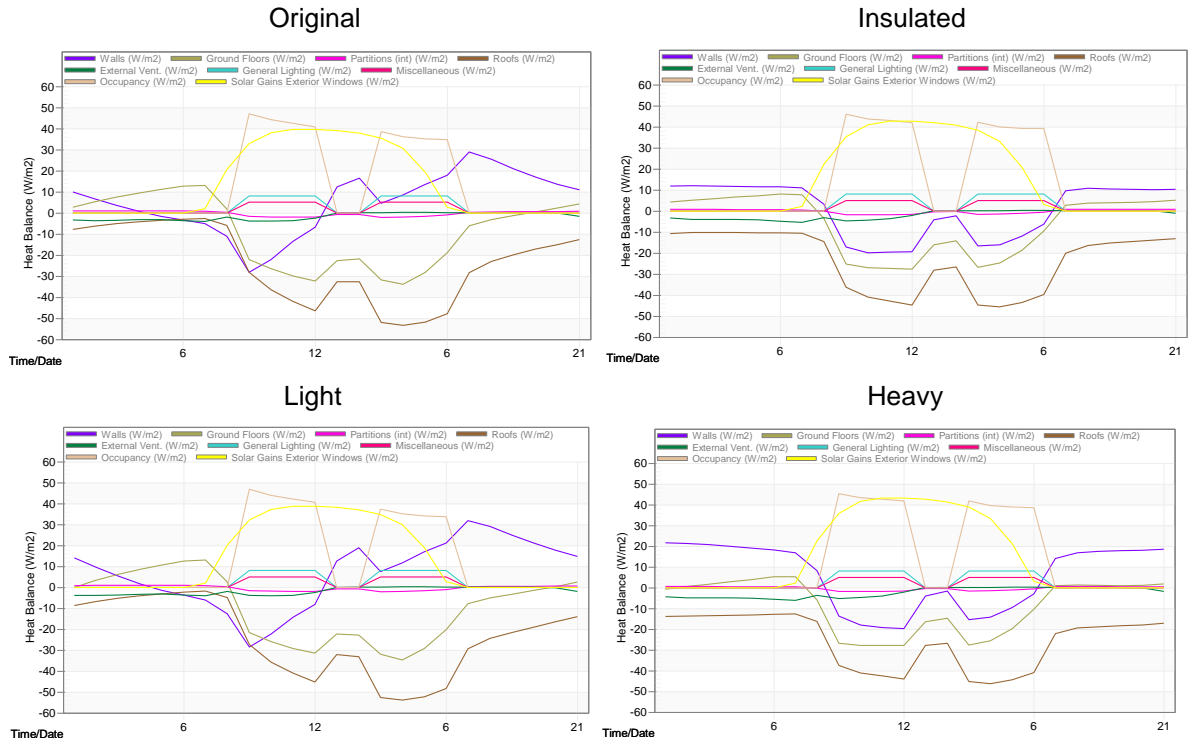
Source: Adapted from DesignBuilder (2022).

**Summer Heat balances (5 December) of classroom in 1 classroom school in Goiânia (GO) – Zone 6 with wall type variation**



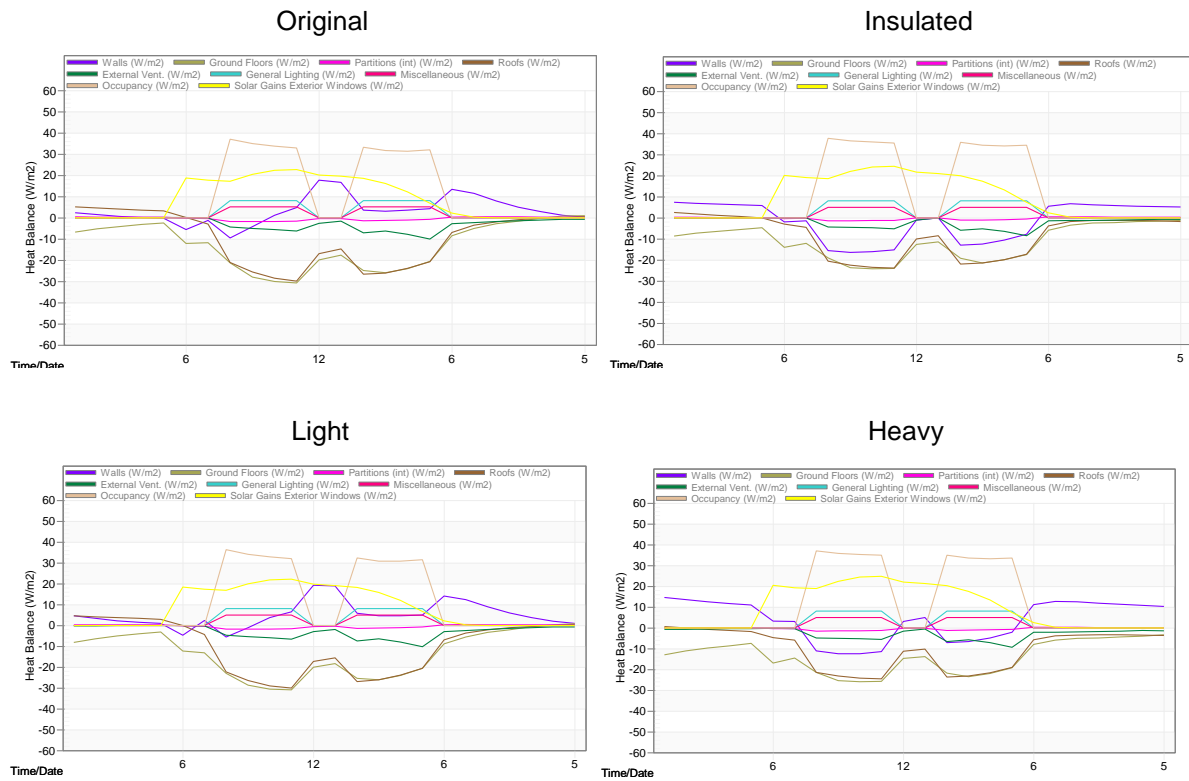
Source: Adapted from DesignBuilder (2022).

**Winter Heat balances (21 June) of classroom in 1 classroom school in Goiânia (GO) – Zone 6 with wall type variation**



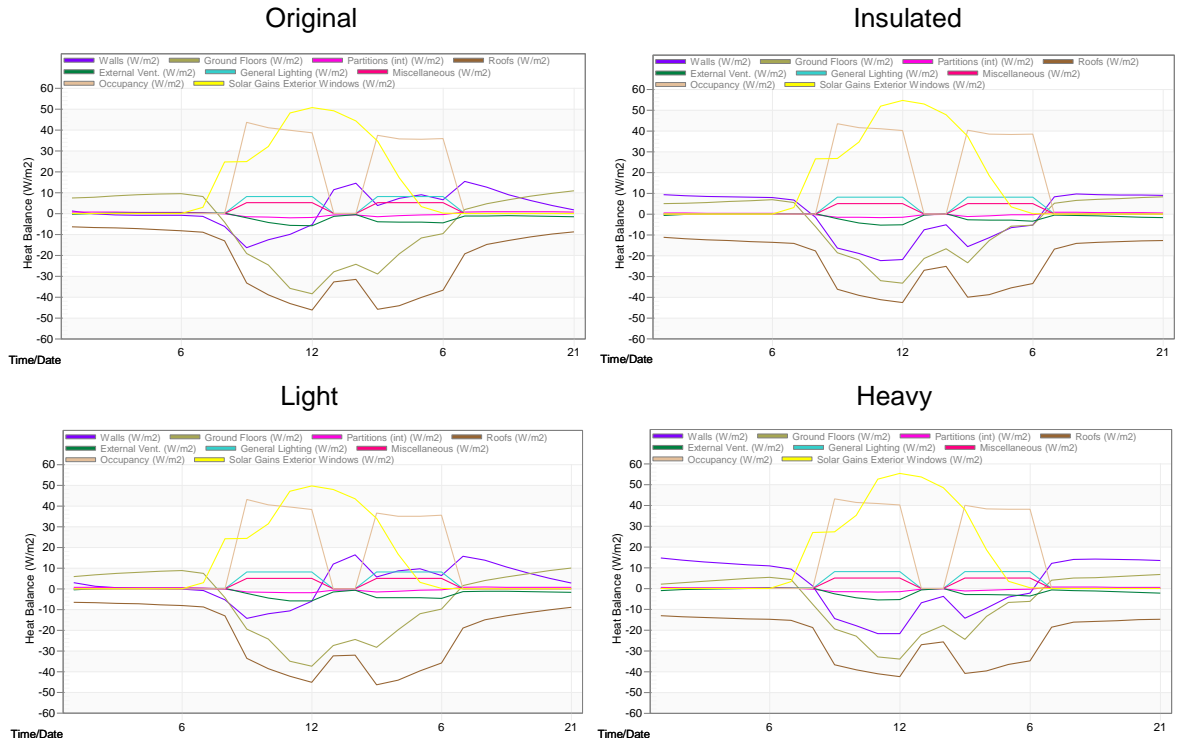
Source: Adapted from DesignBuilder (2022).

**Summer Heat balances (5 December) of classroom in 1 classroom school in Santos (SP) – Zone 5 with wall type variation**



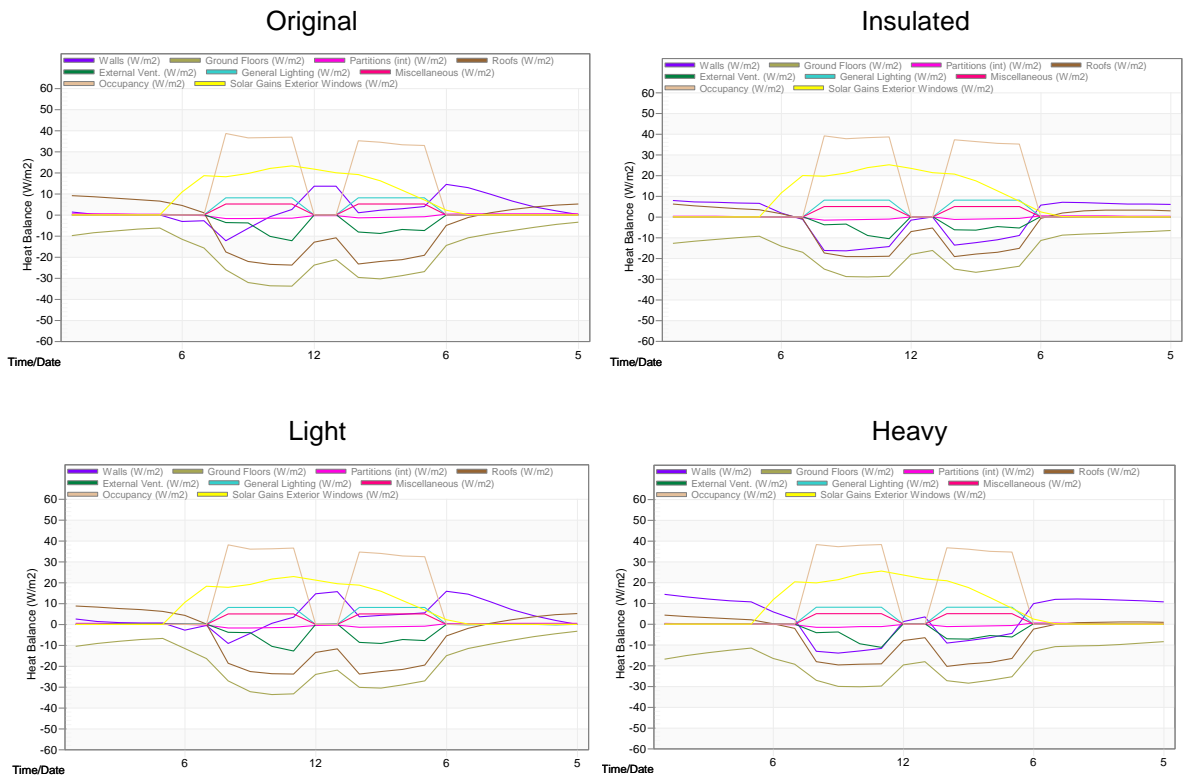
Source: Adapted from DesignBuilder (2022).

**Winter Heat balances (21 June) of classroom in 1 classroom school in Santos (SP) – Zone 5 with wall type variation**



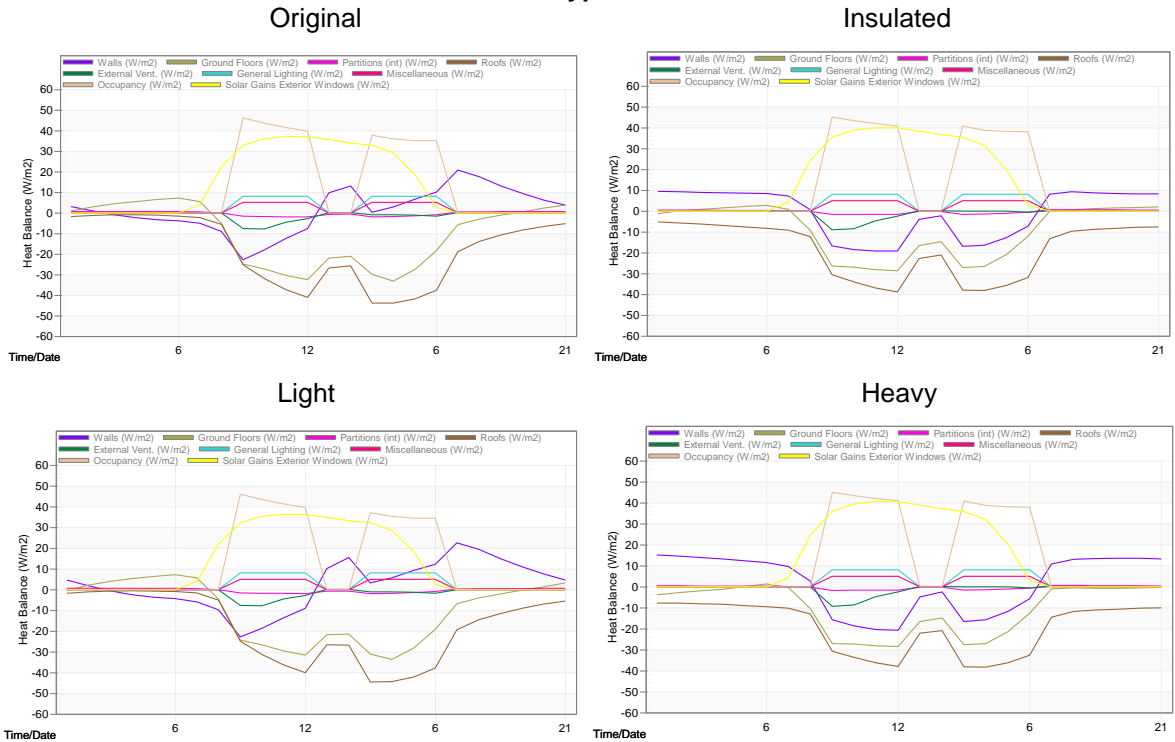
Source: Adapted from DesignBuilder (2022).

**Summer Heat balances (5 December) of classroom in 1 classroom school in Brasília (DF) – Zone 4 with wall type variation**



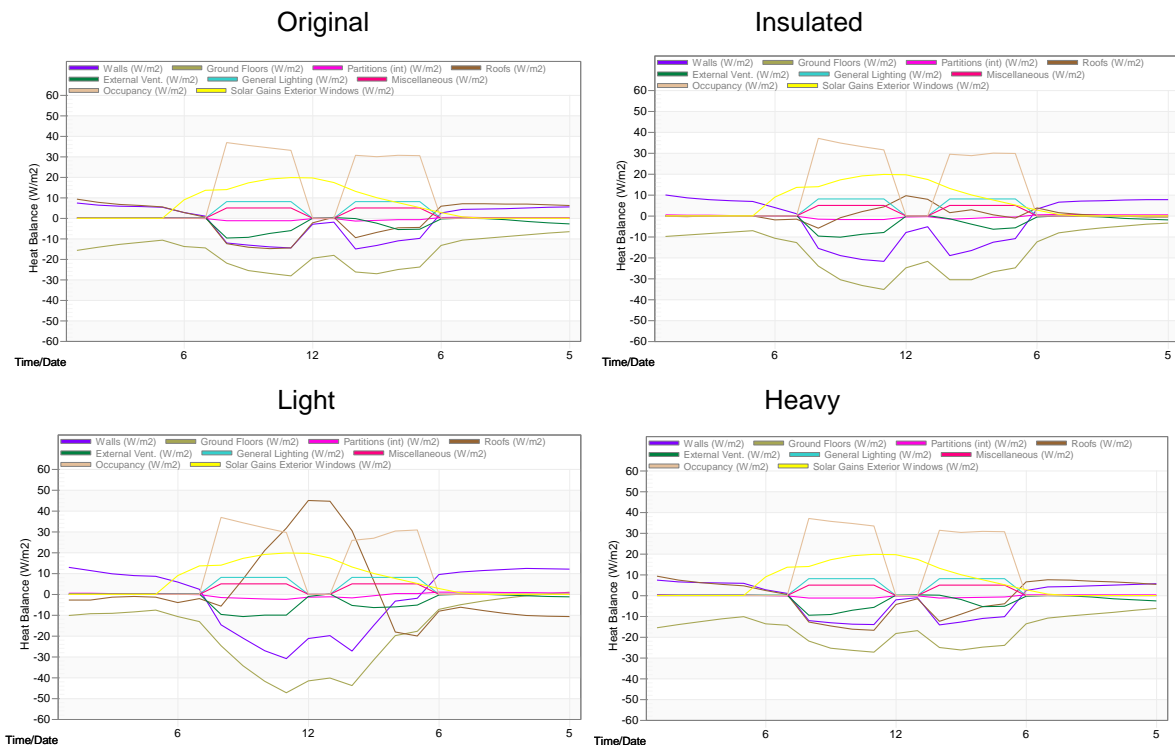
Source: Adapted from DesignBuilder (2022).

**Winter Heat balances (21 June) of classroom in 1 classroom school in Brasília (DF) – Zone 4 with wall type variation**



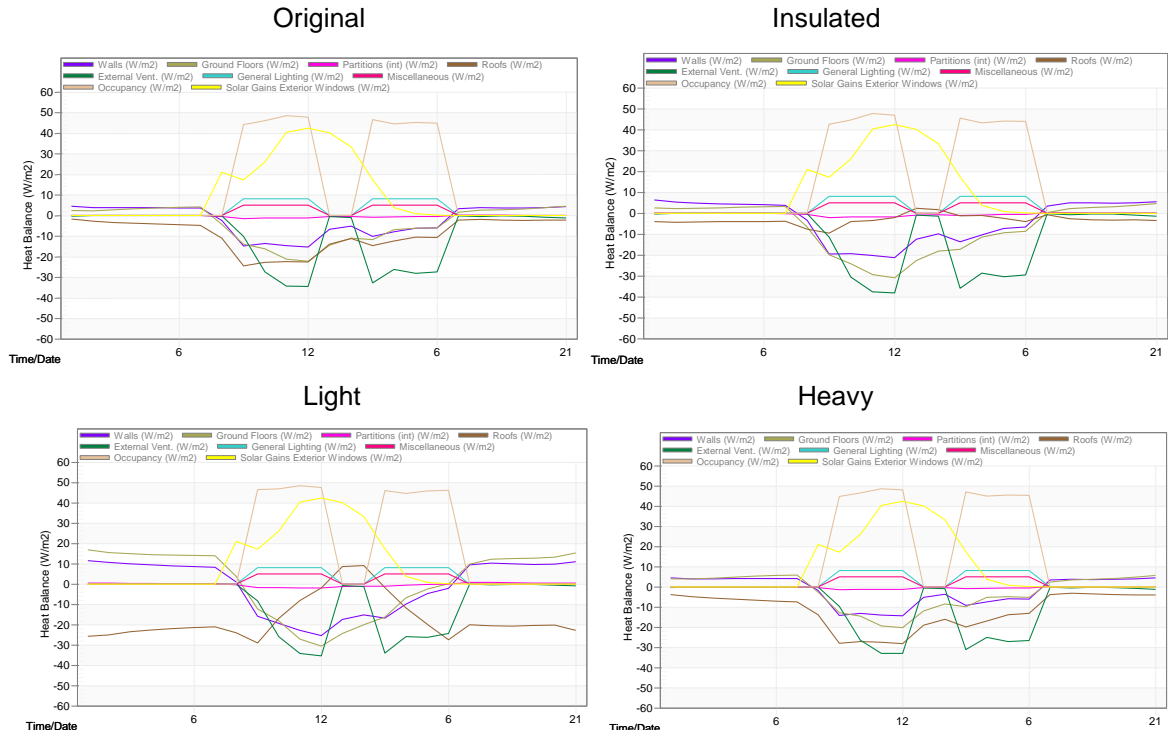
Source: Adapted from DesignBuilder (2022).

**Summer Heat balances (5 December) of classroom in 1 classroom school in Florianópolis (SC) – Zone 3 with roof type variation**



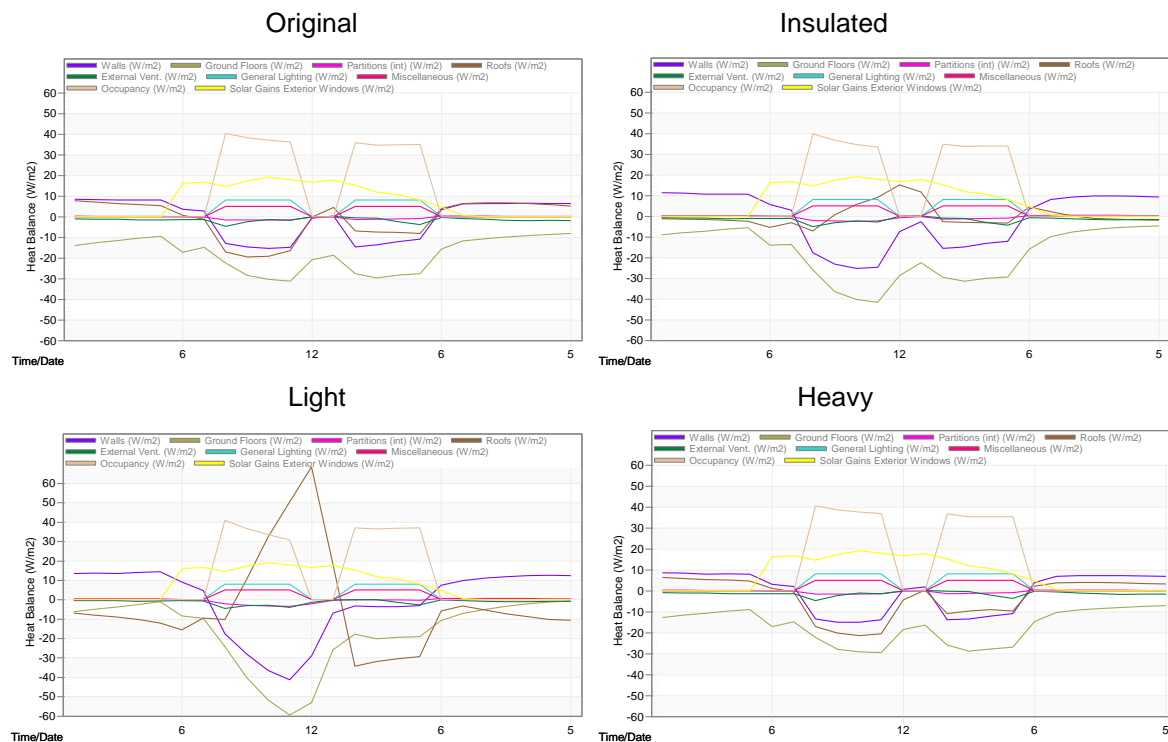
Source: Adapted from DesignBuilder (2022).

**Winter Heat balances (21 June) of classroom in 1 classroom school in Florianópolis (SC) – Zone 3 with roof type variation**



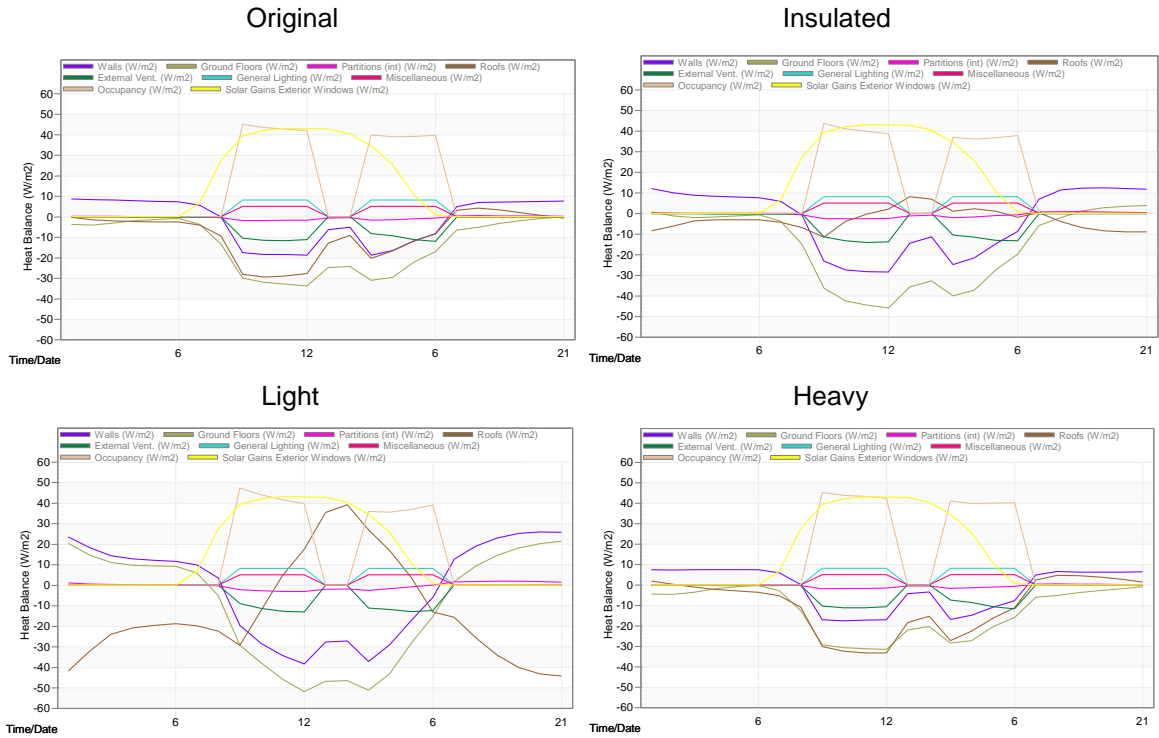
Source: Adapted from DesignBuilder (2022).

**Summer Heat balances (5 December) of classroom in 1 classroom school in Nova Friburgo (RJ) – Zone 2 with roof type variation**



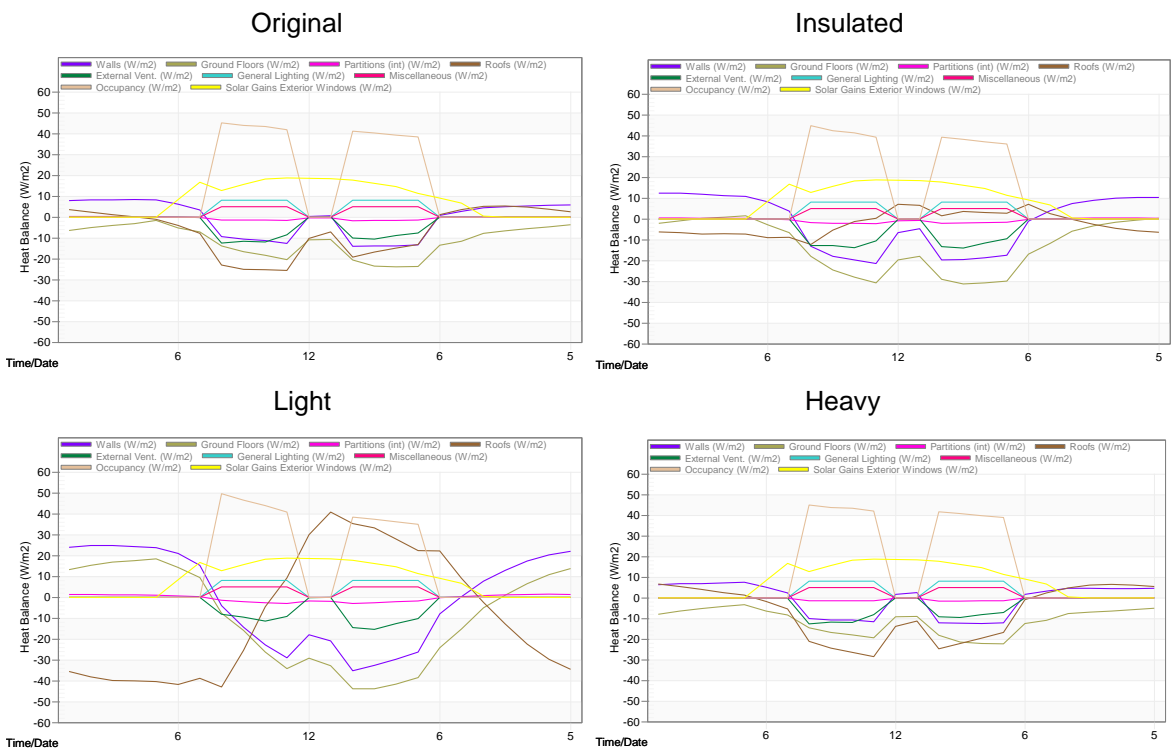
Source: Adapted from DesignBuilder (2022).

**Winter Heat balances (21 June) of classroom in 1 classroom school in Nova Friburgo (RJ) – Zone 2 with roof type variation**



Source: Adapted from DesignBuilder (2022).

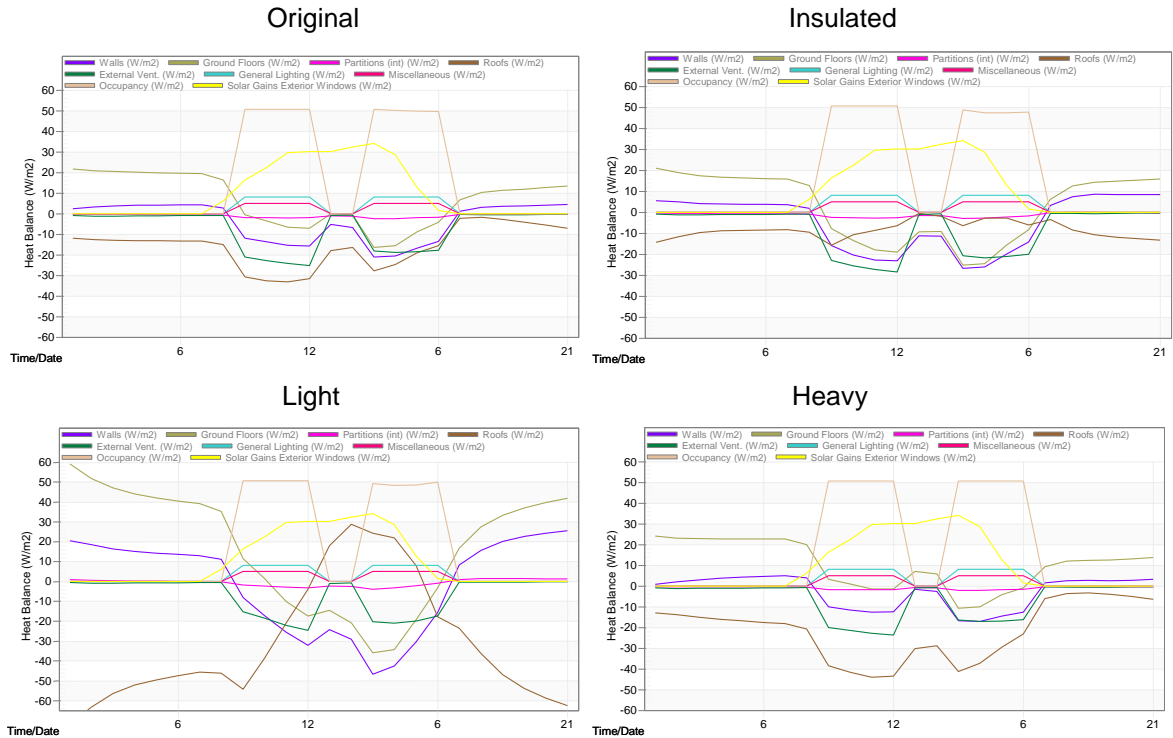
**Summer Heat balances (5 December) of classroom in 1 classroom school in Caxias do Sul (RS) – Zone 1 with roof type variation**



Source: Adapted from DesignBuilder (2022).

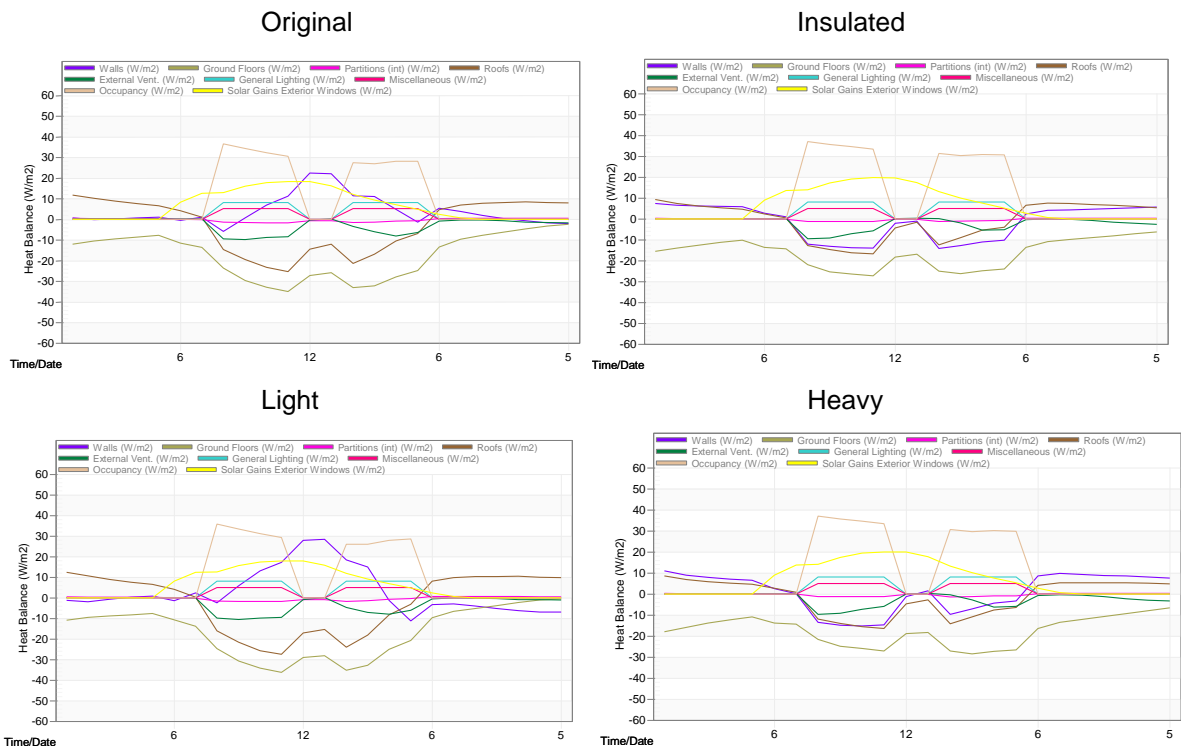


**Winter Heat balances (21 June) of classroom in 1 classroom school in Caxias do Sul (RS) – Zone 1 with roof type variation**



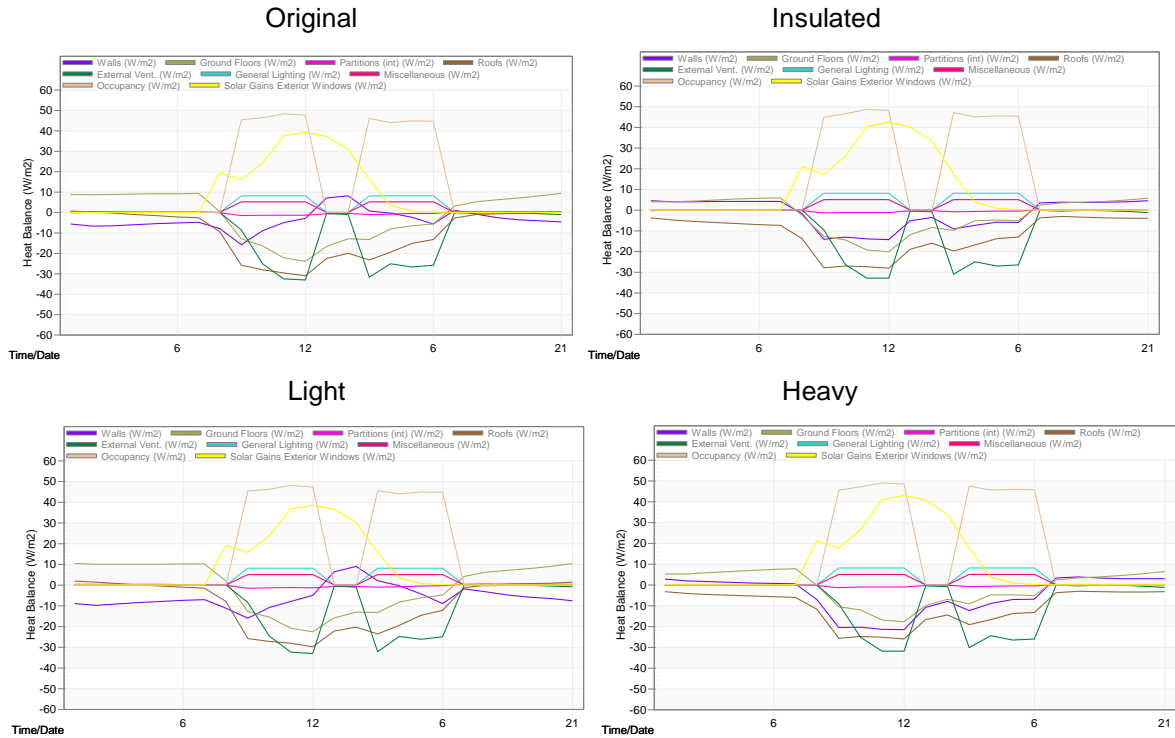
Source: Adapted from DesignBuilder (2022).

**Summer Heat balances (5 December) of classroom in 1 classroom school in Florianópolis (SC) – Zone 3 with wall type variation**



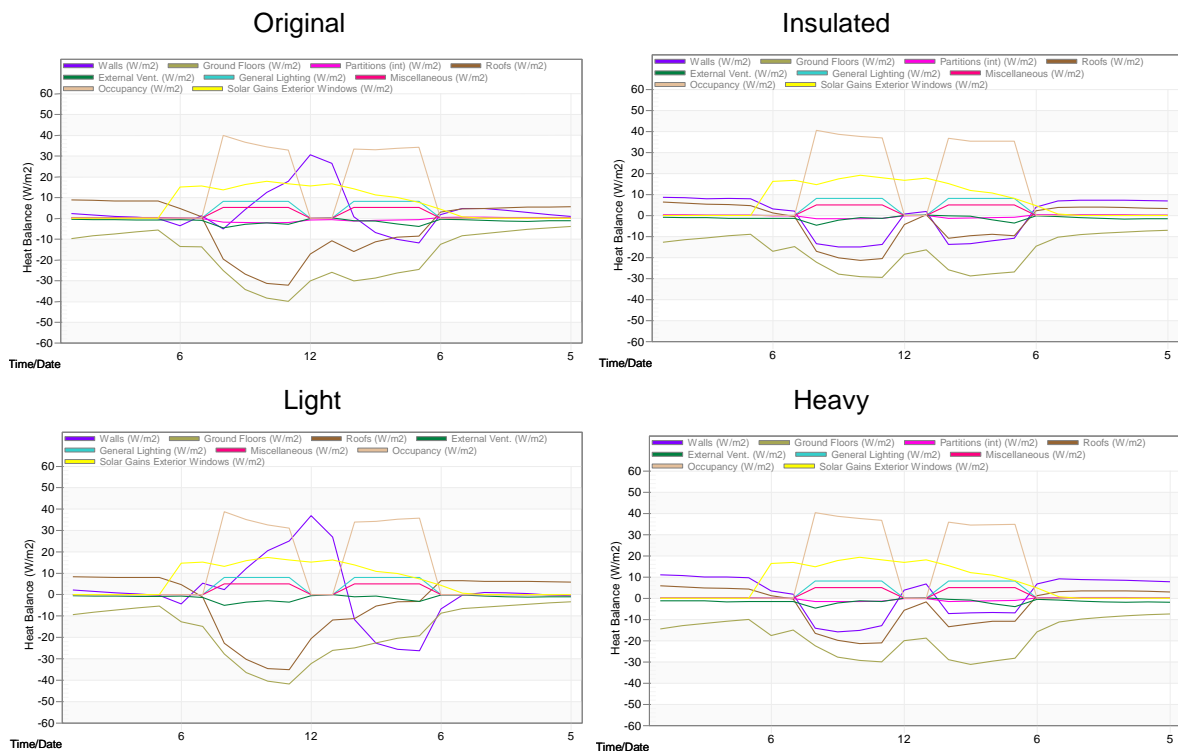
Source: Adapted from DesignBuilder (2022).

**Winter Heat balances (21 June) of classroom in 1 classroom school in Florianópolis (SC) – Zone 3 with wall type variation**



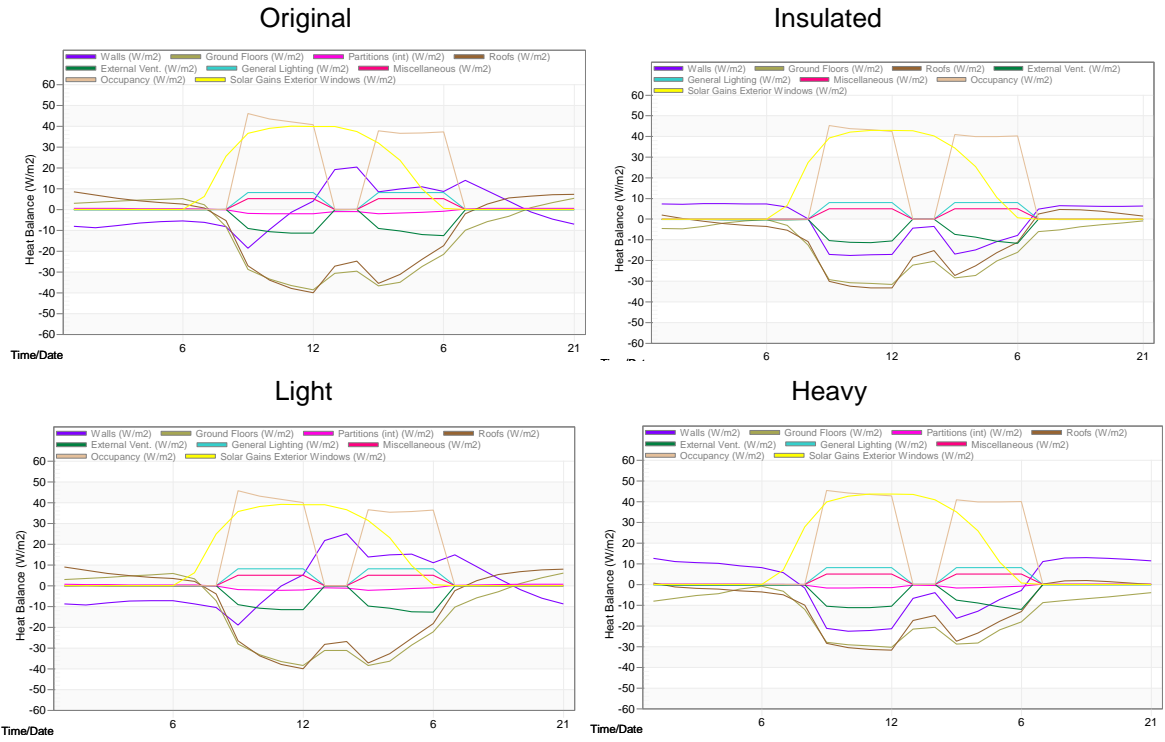
Source: Adapted from DesignBuilder (2022).

**Summer Heat balances (5 December) of classroom in 1 classroom school in Nova Friburgo (RJ) – Zone 2 with wall type variation**



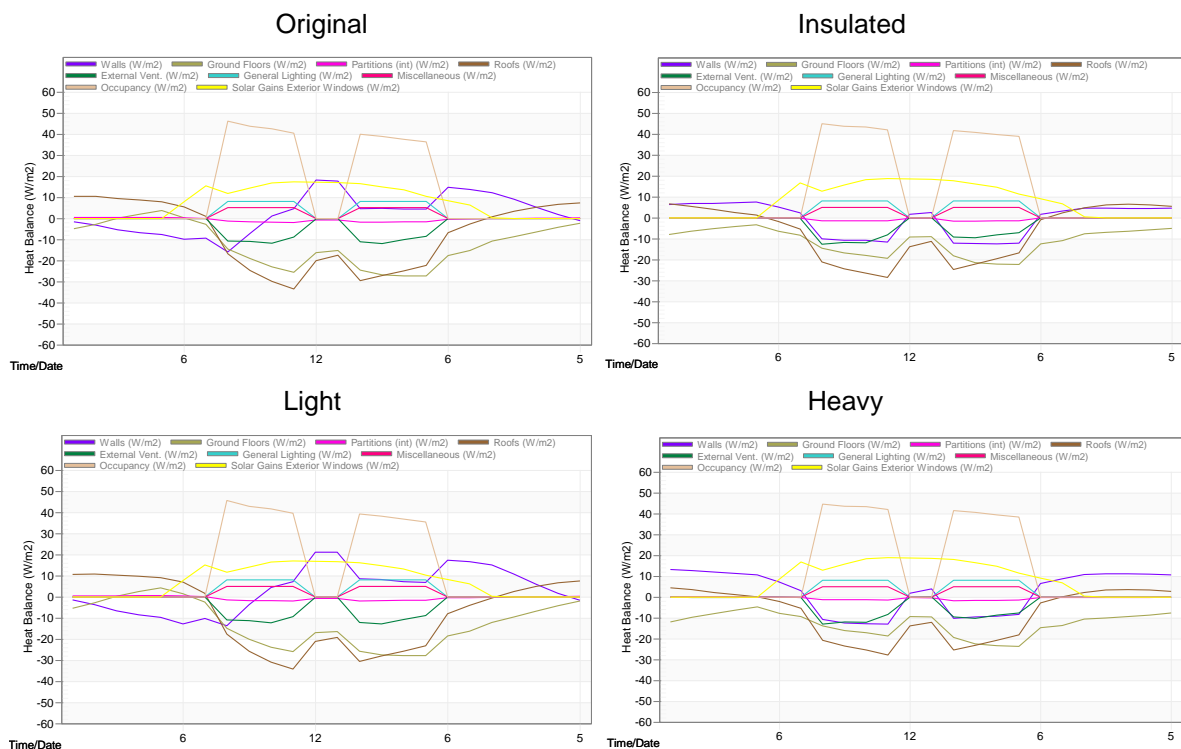
Source: Adapted from DesignBuilder (2022).

**Winter Heat balances (21 June) of classroom in 1 classroom school in Nova Friburgo (RJ) – Zone 2 with wall type variation**



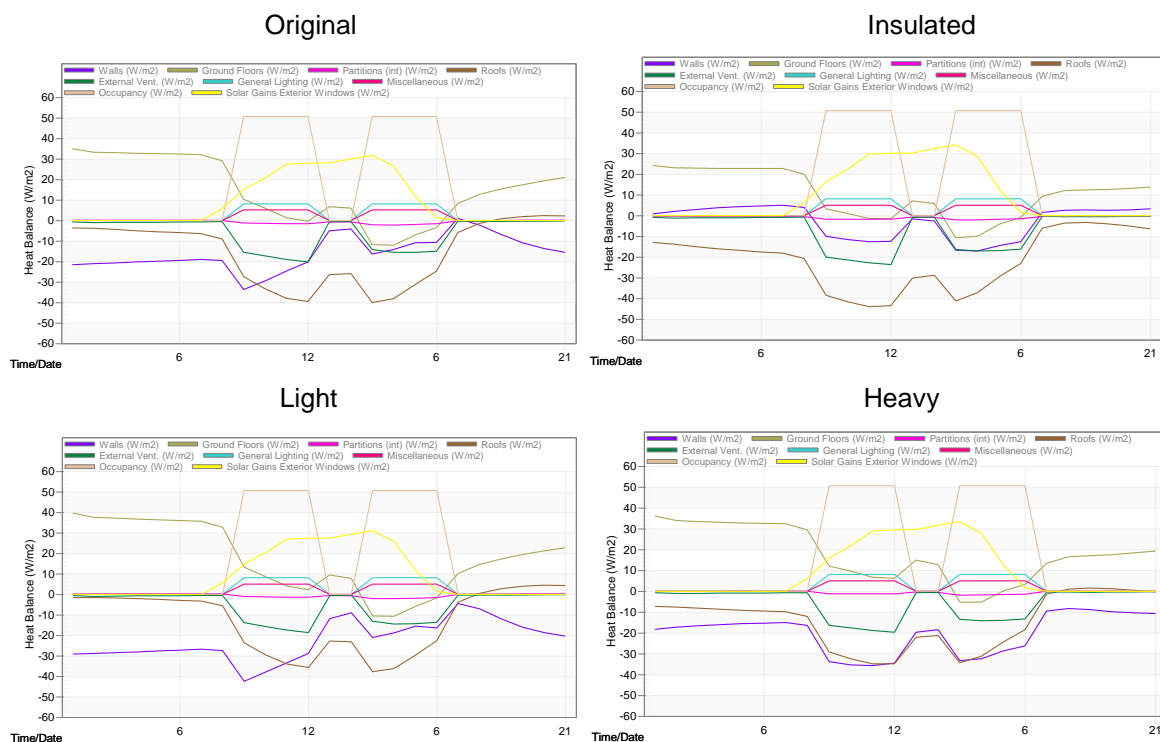
Source: Adapted from DesignBuilder (2022).

**Summer Heat balances (5 December) of classroom in 1 classroom school in Caxias do Sul (RS) – Zone 2 with wall type variation**



Source: Adapted from DesignBuilder (2022).

### Winter Heat balances (21 June) of classroom in 1 classroom school in Caxias do Sul (RS) – Zone 1 with wall type variation



Source: Adapted from DesignBuilder (2022).

## APPENDIX I

Absorbances and emissivities used in the simulations were the average values of those suggested by ABNT (2005a).

Tabela B.2 — Absortância ( $\alpha$ ) para radiação solar (ondas curtas) e emissividade ( $\epsilon$ ) para radiações a temperaturas comuns (ondas longas)

Tipo de superfície	$\alpha$	$\epsilon$
Chapa de alumínio (nova e brilhante)	0,05	0,05
Chapa de alumínio (oxidada)	0,15	0,12
Chapa de aço galvanizada (nova e brilhante)	0,25	0,25
Caixa nova	0,12 / 0,15	0,90
Concreto aparente	0,65 / 0,80	0,85 / 0,95
Telha de barro	0,75 / 0,80	0,85 / 0,95
Tijolo aparente	0,65 / 0,80	0,85 / 0,95
Reboco claro	0,30 / 0,50	0,85 / 0,95
Revestimento asfáltico	0,85 / 0,98	0,90 / 0,98
Vidro incolor	0,06 / 0,25	0,84
Vidro colorido	0,40 / 0,80	0,84
Vidro metalizado	0,35 / 0,80	0,15 / 0,84
Pintura:		
Branca	0,20	0,90
Amarela	0,30	0,90
Verde clara	0,40	0,90
"Alumínio"	0,40	0,50
Verde escura	0,70	0,90
Vermelha	0,74	0,90
Preta	0,97	0,90

## 1. Input data in both current state and optimization simulations in all climates

### 1.1 Activity

#### 1.1.1 Classroom

Occupancy was determined by the architectural layout provided by the FNDE (2023): 30 people in a 48m<sup>2</sup> room.

The writing metabolic activity was the same used by Geraldi and Ghisi (2020).

Occupancy	
<input checked="" type="checkbox"/> Occupied?	
Occupancy density (people/m <sup>2</sup> )	0,6250
Schedule	All day
Metabolic	
Activity	Writing
Factor (Men=1.00, Women=0.85, Children=0.75)	0,75
CO <sub>2</sub> generation rate (m <sup>3</sup> /s-W)	0,0000000382
Clothing	
Clothing schedule definition	1-Generic summer and winter clothing
Winter clothing (clo)	1,00
Summer clothing (clo)	0,50
Comfort Radiant Temperature Weighting	
Calculation type	1-Zone averaged
Air Velocity	
Air velocity schedule	Default Air Velocity for Comfort Calculations

DHW	
Consumption rate (l/m <sup>2</sup> -day)	2,171
Environmental Control	
Heating Setpoint Temperatures	
Heating (°C)	18,0
Heating set back (°C)	13,0
Cooling Setpoint Temperatures	
Cooling (°C)	24,0
Cooling set back (°C)	32,0
Humidity Control	
RH Humidification setpoint (%)	10,0
RH Dehumidification setpoint (%)	90,0
Ventilation Setpoint Temperatures	
Minimum Fresh Air	
Fresh air (l/s-person)	4,719
Mech vent per area (l/s-m <sup>2</sup> )	0,610
Lighting	
Target Illuminance (lux)	300
Default display lighting density (W/m <sup>2</sup> )	0

The plug power density was the same used in previous studies by Lopes (2020) on thermoenergetic simulations of FNDE schools.

Miscellaneous	
<input checked="" type="checkbox"/> On	
Power density (W/m <sup>2</sup> )	5,00
Schedule	All day
Fuel	1-Electricity from grid
Fraction lost	0,000000
Latent fraction	0,000000
Radiant fraction	0,200000

### 1.1.2 Office room

Occupancy was determined by the architectural layout provided by the FNDE (2023): 7 people in a 11,7m<sup>2</sup> room.

The typing metabolic activity was the same used by Geraldi and Ghisi (2020).

Occupancy	
<input checked="" type="checkbox"/> Occupied?	
<b>Occupancy density (people/m<sup>2</sup>)</b>	<b>0,059</b>
<b>Schedule</b>	<b>All day</b>
Metabolic	
<b>Activity</b>	Typing
Factor (Men=1.00, Women=0.85, Children=0.75)	1,00
CO2 generation rate (m <sup>3</sup> /s-W)	0,0000000382
Clothing	
Clothing schedule definition	1-Generic summer and winter clothing
Winter clothing (clo)	1,00
Summer clothing (clo)	0,50
Comfort Radiant Temperature Weighting	
Calculation type	1-Zone averaged
Air Velocity	
Air velocity schedule	Default Air Velocity for Comfort Calculations
DHW	
Consumption rate (l/m <sup>2</sup> -day)	2,171
Environmental Control	
Heating Setpoint Temperatures	
<b>Heating (°C)</b>	<b>18,0</b>
Heating set back (°C)	13,0
Cooling Setpoint Temperatures	
<b>Cooling (°C)</b>	<b>24,0</b>
Cooling set back (°C)	32,0
Humidity Control	
RH Humidification setpoint (%)	10,0
RH Dehumidification setpoint (%)	90,0
Ventilation Setpoint Temperatures	
Minimum Fresh Air	
Fresh air (l/s-person)	4,719
Mech vent per area (l/s-m <sup>2</sup> )	0,610
Lighting	
Target Illuminance (lux)	300
Default display lighting density (W/m <sup>2</sup> )	0

The plug power density was the same used by Geraldi and Ghisi (2020).

Miscellaneous	
<input checked="" type="checkbox"/> On	
<b>Power density (W/m<sup>2</sup>)</b>	<b>50,50</b>
<b>Schedule</b>	<b>All day</b>
Fuel	1-Electricity from grid
Fraction lost	0,000000
Latent fraction	0,000000
Radiant fraction	0,200000

### 1.1.3 Kitchen and Toilets

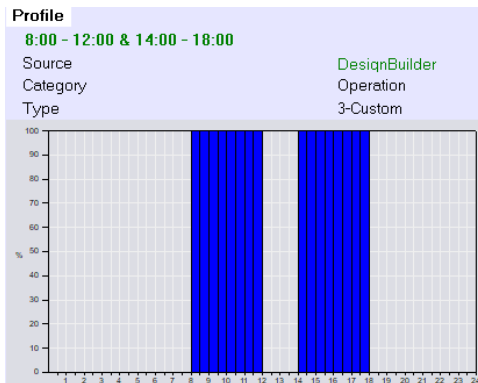
Kitchen and toilets were considered as non-occupied rooms, as suggested by INI-C/2021.

For these rooms, the plug power density was not considered, the same condition used by Geraldi and Ghisi (2020).

### 1.1.4 All school bulding

The schedule is the same considered by Geraldi and Ghisi (2021) that are in accordance with the standard schedule of school operation in Brazil, regulated by the Ministry of Education: Monday to Friday from March to June and from August to December.

General							
<b>Name</b>	<b>All day</b>						
Description	Building: OFFICE Area: OPEN PLAN OFFICE Occupancy schedule						
Source							UK NCM
Category							Offices / Workshop businesses
Region							General
Schedule type							1-7/12 Schedule
Design Days							
Design day definition method							1-End use defaults
Use end-use default							2-Occupancy
Profiles							
Month	Monday	Tuesday	Wednesday	Thursday	Friday	Saturday	Sunday
Jan	Off	Off	Off	Off	Off	Off	Off
Feb	Off	Off	Off	Off	Off	Off	Off
Mar	8:00 - 12:00 & 14:00 ...	8:00 - 12:00 & 14:00 ...	8:00 - 12:00 & 14:00 ...	8:00 - 12:00 & 14:00 ...	8:00 - 12:00 & 14:00 ...	Off	Off
Apr	8:00 - 12:00 & 14:00 ...	8:00 - 12:00 & 14:00 ...	8:00 - 12:00 & 14:00 ...	8:00 - 12:00 & 14:00 ...	8:00 - 12:00 & 14:00 ...	Off	Off
May	8:00 - 12:00 & 14:00 ...	8:00 - 12:00 & 14:00 ...	8:00 - 12:00 & 14:00 ...	8:00 - 12:00 & 14:00 ...	8:00 - 12:00 & 14:00 ...	Off	Off
Jun	8:00 - 12:00 & 14:00 ...	8:00 - 12:00 & 14:00 ...	8:00 - 12:00 & 14:00 ...	8:00 - 12:00 & 14:00 ...	8:00 - 12:00 & 14:00 ...	Off	Off
Jul	Off	Off	Off	Off	Off	Off	Off
Aug	8:00 - 12:00 & 14:00 ...	8:00 - 12:00 & 14:00 ...	8:00 - 12:00 & 14:00 ...	8:00 - 12:00 & 14:00 ...	8:00 - 12:00 & 14:00 ...	Off	Off
Sep	8:00 - 12:00 & 14:00 ...	8:00 - 12:00 & 14:00 ...	8:00 - 12:00 & 14:00 ...	8:00 - 12:00 & 14:00 ...	8:00 - 12:00 & 14:00 ...	Off	Off
Oct	8:00 - 12:00 & 14:00 ...	8:00 - 12:00 & 14:00 ...	8:00 - 12:00 & 14:00 ...	8:00 - 12:00 & 14:00 ...	8:00 - 12:00 & 14:00 ...	Off	Off
Nov	8:00 - 12:00 & 14:00 ...	8:00 - 12:00 & 14:00 ...	8:00 - 12:00 & 14:00 ...	8:00 - 12:00 & 14:00 ...	8:00 - 12:00 & 14:00 ...	Off	Off
Dec	8:00 - 12:00 & 14:00 ...	8:00 - 12:00 & 14:00 ...	8:00 - 12:00 & 14:00 ...	8:00 - 12:00 & 14:00 ...	8:00 - 12:00 & 14:00 ...	Off	Off



Items not detailed in images were not selected or had no specific setting.

## 1.2 Lighting

### 1.2.1 Classroom

Light power density was determined by the electrical project provided by the FNDE (2023): 384 watts in a 48m<sup>2</sup> room.

General Lighting	
<input checked="" type="checkbox"/> On	
<b>Power density (W/m2)</b>	<b>8,0000</b>
Schedule	All day
Luminaire type	2-Surface mount
Return air fraction	0,000
Radiant fraction	0,720
Visible fraction	0,180
Convective fraction	0,100

### 1.2.2 Office Room and Kitchen

Light power density was determined by the electrical project provided by the FNDE (2023): 64 watts in a 11.7m<sup>2</sup> room.

General Lighting	
<input checked="" type="checkbox"/> On	
<b>Power density (W/m2)</b>	<b>5,4700</b>
Schedule	All day - Building:
Luminaire type	2-Surface mount
Return air fraction	0,000
Radiant fraction	0,720
Visible fraction	0,180
Convective fraction	0,100

### 1.2.3 Toilets

Light power density was determined by the electrical project provided by the FNDE (2023): 32 watts in a 3.28m<sup>2</sup> room.

General Lighting	
<input checked="" type="checkbox"/> On	
<b>Power density (W/m2)</b>	<b>9,7500</b>
Schedule	All day
Luminaire type	2-Surface mount
Return air fraction	0,000
Radiant fraction	0,720
Visible fraction	0,180
Convective fraction	0,100

## 2 Input data in current state simulations in all climates

All information on construction, openings and HVAC were obtained from the project made available by FNDE.

### 2.1 Location: Site Details

In the simulations of the current state of the schools, the surrounding area with a grass surface of 0.2 reflectance suggested by DesignBuilder was considered.



Ground	
Surface	
<input checked="" type="checkbox"/> Texture	Grass lawn
Surface solar and visible reflectance	0,20
Snow reflected solar modifier	2,00
Snow reflected daylight modifier	2,00
Ground Modelling	
Ground modelling method	2-Kiva Basic
Kiva foundation settings	kiva settings earth common
Kiva foundation	Default kiva foundation
Monthly Temperatures	
Deep Monthly Temperatures	
Shallow Monthly Temperatures	
FCFactorMethod Monthly Temperatures	

In Kiva Foundation settings, the soil thermal properties are the default earth common of the software, the ground solar and thermal absorptivity were the ground cover values with grass and pasture described by Ferreira, Pereira and Labaki (2021) and the ground surface roughness was the value suggested by DesignBuilder Help (2022) for grass. All other values were maintained as per software default.

General	
<b>Name</b>	<b>kiva settings earth common</b>
Soil Thermal Properties	
Soil conductivity (W/m-K)	1,28
Soil density (kg/m <sup>3</sup> )	1460,00
Soil specific heat (J/kg-K)	880,00
Surface Properties	
Ground solar absorptivity	0,1800
Ground thermal absorptivity	0,9840
Ground surface roughness (m)	0,03
Extent	
Far-field width (m)	40,00
Deep-ground depth (m)	Autocalculate
Options	
Minimum cell dimension (m)	0,02
Maximum cell growth coefficient	1,50
Simulation timestep	1-Hourly
Deep-ground boundary condition	1-Autoselect

## 2.2 Construction: Ground Floor






Layers	
Number of layers	3
Outermost layer	
Material	Ceramica piso interno
Thickness (m)	0,0200
<input type="checkbox"/> Bridged?	
Layer 2	
Material	Argamassa
Thickness (m)	0,0300
<input type="checkbox"/> Bridged?	
Innermost layer	
Material	Laje de piso de concreto
Thickness (m)	0,1000
<input type="checkbox"/> Bridged?	

<b>Inner surface</b>	
Convective heat transfer coefficient (W/m <sup>2</sup> -K)	0,342
Radiative heat transfer coefficient (W/m <sup>2</sup> -K)	5,540
Surface resistance (m <sup>2</sup> -K/W)	0,170
<b>Outer surface</b>	
Convective heat transfer coefficient (W/m <sup>2</sup> -K)	19,870
Radiative heat transfer coefficient (W/m <sup>2</sup> -K)	5,130
Surface resistance (m <sup>2</sup> -K/W)	0,040
<b>No Bridging</b>	
U-Value surface to surface (W/m <sup>2</sup> -K)	9,777
R-Value (m <sup>2</sup> -K/W)	0,312
<b>U-Value (W/m<sup>2</sup>-K)</b>	<b>3,202</b>
<b>With Bridging (BS EN ISO 6946)</b>	
Thickness (m)	0,1500
Km - Internal heat capacity (KJ/m <sup>2</sup> -K)	165,0000
Upper resistance limit (m <sup>2</sup> -K/W)	0,312
Lower resistance limit (m <sup>2</sup> -K/W)	0,312
U-Value surface to surface (W/m <sup>2</sup> -K)	9,777
R-Value (m <sup>2</sup> -K/W)	0,312
<b>U-Value (W/m<sup>2</sup>-K)</b>	<b>3,202</b>

### 2.3 Construction: External and Internal Walls

The reflectivity of the external wall was calculated by a weighted average of the white surface (R=70%) and the blue surface (R=18%) according to Dornelles (2008). The final reflectivity of the wall was 60%.

<b>Surface Properties</b>	
Thermal absorptance (emissivity)	0.9000000
Solar absorptance	0.400
Visible absorptance	0.400
Roughness	3-Rough
<input type="checkbox"/> Colour	
<input checked="" type="checkbox"/> Texture	GranulatedClear02
<b>Radiance Daylighting</b>	
Material class	1-Plastic
Reflectance	0.600
Specularity	0.000
Roughness	0.000

<b>Layers</b>	
Number of layers	5
<b>Outermost layer</b>	
 Material	ORIGINAL Argamassa branco gelo
Thickness (not used in thermal calcs) (m)	0,0250
<b>Layer 2</b>	
 Material	Bloco ceramico
Thickness (m)	0,0134
<input type="checkbox"/> Bridged?	
<b>Layer 3</b>	
 Material	AR CB3E
Thickness (not used in thermal calcs) (m)	0,0632
<b>Layer 4</b>	
 Material	Bloco ceramico
Thickness (m)	0,0134
<input type="checkbox"/> Bridged?	
<b>Innermost layer</b>	
 Material	ORIGINAL Argamassa branco gelo
Thickness (not used in thermal calcs) (m)	0,0250

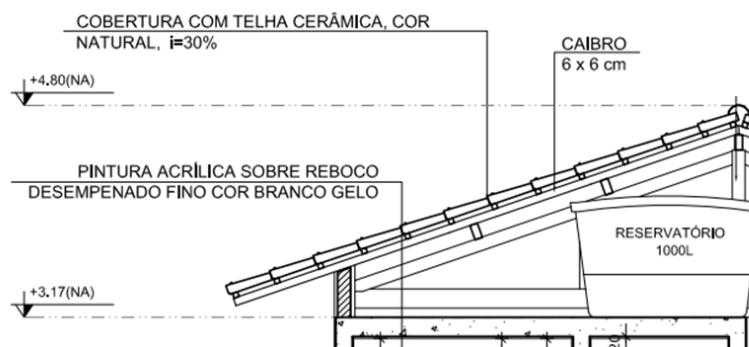
<b>Inner surface</b>	
Convective heat transfer coefficient (W/m <sup>2</sup> -K)	2,152
Radiative heat transfer coefficient (W/m <sup>2</sup> -K)	5,540
Surface resistance (m <sup>2</sup> -K/W)	0,130
<b>Outer surface</b>	
Convective heat transfer coefficient (W/m <sup>2</sup> -K)	19,870
Radiative heat transfer coefficient (W/m <sup>2</sup> -K)	5,130
Surface resistance (m <sup>2</sup> -K/W)	0,040
<b>No Bridging</b>	
U-Value surface to surface (W/m <sup>2</sup> -K)	4,028
R-Value (m <sup>2</sup> -K/W)	0,418
<b>U-Value (W/m<sup>2</sup>-K)</b>	<b>2,391</b>
<b>With Bridging (BS EN ISO 6946)</b>	
Thickness (m)	0,1400
Km - Internal heat capacity (KJ/m <sup>2</sup> -K)	69,7248
Upper resistance limit (m <sup>2</sup> -K/W)	0,418
Lower resistance limit (m <sup>2</sup> -K/W)	0,418
U-Value surface to surface (W/m <sup>2</sup> -K)	4,028
R-Value (m <sup>2</sup> -K/W)	0,418
<b>U-Value (W/m<sup>2</sup>-K)</b>	<b>2,391</b>

## 2.4 Construction: Roof

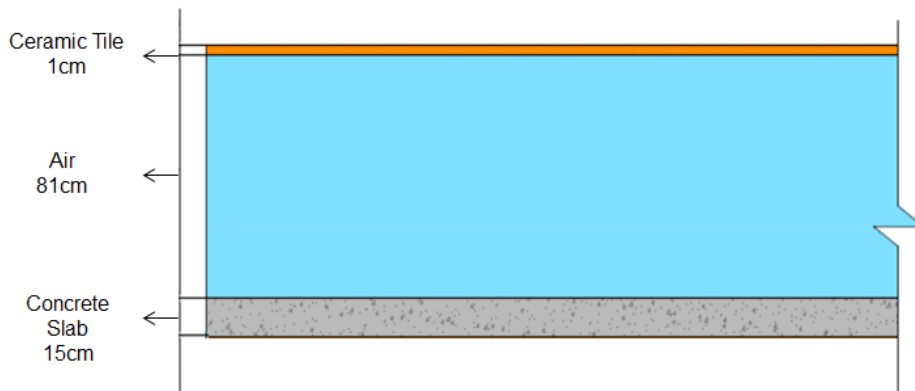
The original roof of the school was modeled with the same geometry and same composition of materials described by FNDE (2023) to obtain accurate calculations of thermal performance with DesignBuilder simulations. As the software does not provide transmittance and thermal capacity data in sloped roof models, for comparative purposes, an equivalent flat roof was modeled to obtain these data. The same equivalent model was also considered in algorithm optimization simulations.

According to Weber *et al.* (2017), a pitched roof can be represented by an equivalent horizontal model that has the air layer thickness half the maximum air layer height on the real roof. In the case of the 1-classroom school, the maximum height of the air layer is 162cm.

This is the official pitched roof design (FNDE, 2023):



Therefore, for equivalent roof design, an air layer of 81cm was used in the equivalent model as shown in figure below adapted from Weber *et al.* (2017).



According to ABNT (2005) and Weber *et al.* (2017), for roof air chambers, downward flow is considered in the summer, with resistance of 0.21 m<sup>2</sup>.°C/W.

Layers	
Number of layers	3
Outermost layer	
Material	ORIGINAL só telha ceramica
Thickness (m)	0,0100
Bridged?	
Layer 2	
Material	AR cobertura
Thickness (not used in thermal calcs) (m)	0,81
Innermost layer	
Material	Laje de piso de concreto
Thickness (m)	0,1500
Bridged?	

The reflectivity of the roof was R = 20% according to ABNT (2005a). Emissivity was the average value of ceramic tiles from ABNT (2005a).

Surface Properties	
Thermal absorptance (emissivity)	0,9000000
Solar absorptance	0,8
Visible absorptance	0,8
Roughness	3-Rough
Colour	
Texture	Red brick
Radiance Daylighting	
Material class	1-Plastic
Reflectance	0,2
Specularity	0,000
Roughness	0,002
Inner surface	
Convective heat transfer coefficient (W/m <sup>2</sup> -K)	4,460
Radiative heat transfer coefficient (W/m <sup>2</sup> -K)	5,540
Surface resistance (m <sup>2</sup> -K/W)	0,100
Outer surface	
Convective heat transfer coefficient (W/m <sup>2</sup> -K)	19,870
Radiative heat transfer coefficient (W/m <sup>2</sup> -K)	5,130
Surface resistance (m <sup>2</sup> -K/W)	0,040
No Bridging	
U-Value surface to surface (W/m <sup>2</sup> -K)	3,276
R-Value (m <sup>2</sup> -K/W)	0,445
<b>U-Value (W/m<sup>2</sup>-K)</b>	<b>2,246</b>
With Bridging (BS EN ISO 6946)	
Thickness (m)	0,9700
Km - Internal heat capacity (KJ/m <sup>2</sup> -K)	220,0000
Upper resistance limit (m <sup>2</sup> -K/W)	0,445
Lower resistance limit (m <sup>2</sup> -K/W)	0,445
U-Value surface to surface (W/m <sup>2</sup> -K)	3,276
R-Value (m <sup>2</sup> -K/W)	0,445
<b>U-Value (W/m<sup>2</sup>-K)</b>	<b>2,246</b>

## 2.5 Openings

The percentage of glazed areas in the envelope was automatically calculated by the software after the detailed design of the windows in the modeling process according to the standard architectural design of the FNDE.

The windows in the original project are tilting. Considering that this window type could be open up to 95%, an intermediate value of 45% was used in the simulations.

No local shading was considered.

Operation	
Schedule definition	1-Follow occupancy
Free Aperture	
Opening position	2-Bottom
% Glazing area opens	45,0
Discharge coefficient	0,6500

The operation of both doors and windows follows the occupancy schedule.

The type of glass was configured according to the FNDE project model and the properties described by Weber *et al.* (2017).

General	
<b>Name</b>	<b>Vidro simples 6mm</b>
Description	
Source	EnergyPlus dataset
Category	Single
Region	General
Colour	
Definition method	
Definition method	2-Simple
Simple Definition	
Total solar transmission (SHGC)	0.870
Light transmission	0.810
<b>U-Value (W/m<sup>2</sup>-K)</b>	<b>5.700</b>

## 2.6 HVAC

Non-detailed tabs have not been set or changed.

HVAC Template	
<b>Template</b>	<b>Natural ventilation - No Heating/Cooling</b>
Mechanical Ventilation	>>
Auxiliary Energy	
Pump etc energy (W/m <sup>2</sup> )	0.0000
Schedule	ASHRAE 90.1 Occupancy - School
Heating	>>
Cooling	>>
Humidity Control	>>
DHW	>>
Natural Ventilation	>

## 2.7 Model Options: Natural Ventilation

Natural Ventilation and Infiltration	
<b>Natural ventilation</b>	<b>Calculated ventilation</b> Natural ventilation and infiltration air flow rates are calculated based on opening and crack sizes, buoyancy and wind pressures.
Scheduled	Calculated
Infiltration units	1-ac/h
Airtightness method	1-Template slider

### 3. Input data only in optimization simulations:

Items not detailed in images were not selected or had no specific setting.

#### 3.1 Location: Site Details

Site Details: Picos – PI:

These are the Kiva Basic Foundation settings with cool pavement around the building. The soil thermal properties are the same used in current state simulations. The ground surface roughness was the concrete value (0,002) suggested by DesignBuilder Help (2022).

<b>Soil Thermal Properties</b>	
Soil conductivity (W/m-K)	1,28
Soil density (kg/m <sup>3</sup> )	1460,00
Soil specific heat (J/kg-K)	880,00
<b>Surface Properties</b>	
Ground solar absorptivity	0,1000
Ground thermal absorptivity	0,9000
Ground surface roughness (m)	0,002
<b>Extent</b>	
Far-field width (m)	40,00
Deep-ground depth (m)	Autocalculate
<b>Options</b>	
Minimum cell dimension (m)	0,02
Maximum cell growth coefficient	1,50
Simulation timestep	1-Hourly
Deep-ground boundary condition	1-Autoselect

Site Details: Caxias do Sul – RS:

These are the Kiva Basic Foundation settings with concrete around the building with reflectivity of 50%. The soil thermal properties are the same used in current state simulations. The ground surface roughness was the concrete value (0,002) suggested by DesignBuilder Help (2022).

Soil Thermal Properties	
Soil conductivity (W/m-K)	1,28
Soil density (kg/m <sup>3</sup> )	1460,00
Soil specific heat (J/kg-K)	880,00
Surface Properties	
Ground solar absorptivity	0,5
Ground thermal absorptivity	0,9000
Ground surface roughness (m)	0,002
Extent	
Far-field width (m)	40,00
Deep-ground depth (m)	Autocalculate
Options	
Minimum cell dimension (m)	0,02
Maximum cell growth coefficient	1,50
Simulation timestep	1-Hourly
Deep-ground boundary condition	1-Autoselect

These are the Kiva Basic Foundation settings with concrete around the building with reflectivity of 30%.

Soil Thermal Properties	
Soil conductivity (W/m-K)	1,28
Soil density (kg/m <sup>3</sup> )	1460,00
Soil specific heat (J/kg-K)	880,00
Surface Properties	
Ground solar absorptivity	0,7
Ground thermal absorptivity	0,9000
Ground surface roughness (m)	0,002
Extent	
Far-field width (m)	40,00
Deep-ground depth (m)	Autocalculate
Options	
Minimum cell dimension (m)	0,02
Maximum cell growth coefficient	1,50
Simulation timestep	1-Hourly
Deep-ground boundary condition	1-Autoselect

### 3.2 Construction

Concrete layer properties and settings used in all cases with concrete material (walls or roof in all cities):

Source	CIBSE Guide
Category	Plaster
Region	General
<b>Material Layer Thickness</b>	
Force thickness	No
<b>Thermal Properties</b>	
Detailed properties	Yes
<b>Thermal Bulk Properties</b>	
Conductivity (W/m-K)	1,7500
Specific Heat (J/kg-K)	1000,00
Density (kg/m <sup>3</sup> )	2200,00
Resistance (R-value)	No
<b>Vapour Resistance</b>	
Vapour resistance definition	1-Factor
Vapour factor	20
Vapour resistivity (MN/g.m)	10
<b>Moisture Transfer</b>	
Include moisture transfer sett...	Yes
Moisture transfer settings	Generic Conc

### 3.2.1 Insulated Walls

This type of wall is composed by 7 layers: melamine board, EPS, Mortar, concrete, air layer, concrete and mortar. This is the composition suggested by Weber *et al.* (2017) to correctly represent this type of wall commonly used in Brazil.

Layers	
Number of layers	7
Outermost layer	
Material	Placa melaminica R90
Thickness (m)	0,0060
Bridged?	
Layer 2	
Material	EPS Caxias
Thickness (m)	0,0800
Bridged?	
Layer 3	
Material	Argamassa Caxias
Thickness (m)	0,0250
Bridged?	
Layer 4	
Material	Bloco de concreto Caxias
Thickness (m)	0,0300
Bridged?	
Layer 5	
Material	Ar parede Caxias
Thickness (not used in thermal calcs) (m)	0,0800
Layer 6	
Material	Bloco de concreto Caxias
Thickness (m)	0,0300
Bridged?	
Innermost layer	
Material	Argamassa Caxias
Thickness (m)	0,0250

The thermal properties of the insulated wall is described below.

Inner surface	
Convective heat transfer coefficient (W/m <sup>2</sup> -K)	2,152
Radiative heat transfer coefficient (W/m <sup>2</sup> -K)	5,540
Surface resistance (m <sup>2</sup> -K/W)	0,130
Outer surface	
Convective heat transfer coefficient (W/m <sup>2</sup> -K)	19,870
Radiative heat transfer coefficient (W/m <sup>2</sup> -K)	5,130
Surface resistance (m <sup>2</sup> -K/W)	0,040
No Bridging	
U-Value surface to surface (W/m <sup>2</sup> -K)	0,452
R-Value (m <sup>2</sup> -K/W)	2,381
<b>U-Value (W/m<sup>2</sup>-K)</b>	<b>0,420</b>
With Bridging (BS EN ISO 6946)	
Thickness (m)	0,2760
Km - Internal heat capacity (KJ/m <sup>2</sup> -K)	122,0000
Upper resistance limit (m <sup>2</sup> -K/W)	2,381
Lower resistance limit (m <sup>2</sup> -K/W)	2,381
U-Value surface to surface (W/m <sup>2</sup> -K)	0,452
R-Value (m <sup>2</sup> -K/W)	2,381
<b>U-Value (W/m<sup>2</sup>-K)</b>	<b>0,420</b>

### 3.2.2 Light Walls

In this type of wall, only one layer of material (concrete) was configured, with a thickness of 10cm.



Inner surface	
Convective heat transfer coefficient (W/m <sup>2</sup> -K)	2,152
Radiative heat transfer coefficient (W/m <sup>2</sup> -K)	5,540
Surface resistance (m <sup>2</sup> -K/W)	0,130
Outer surface	
Convective heat transfer coefficient (W/m <sup>2</sup> -K)	19,870
Radiative heat transfer coefficient (W/m <sup>2</sup> -K)	5,130
Surface resistance (m <sup>2</sup> -K/W)	0,040
No Bridging	
U-Value surface to surface (W/m <sup>2</sup> -K)	17,500
R-Value (m <sup>2</sup> -K/W)	0,227
<b>U-Value (W/m<sup>2</sup>-K)</b>	<b>4.403</b>
With Bridging (BS EN ISO 6946)	
Thickness (m)	0,1000
Km - Internal heat capacity (KJ/m <sup>2</sup> -K)	110,0000
Upper resistance limit (m <sup>2</sup> -K/W)	0,227
Lower resistance limit (m <sup>2</sup> -K/W)	0,227
U-Value surface to surface (W/m <sup>2</sup> -K)	17,500
R-Value (m <sup>2</sup> -K/W)	0,227
<b>U-Value (W/m<sup>2</sup>-K)</b>	<b>4.403</b>

### 3.2.3 Heavy Walls

In this type of wall, only one layer of material (concrete) was configured, with a thickness of 30cm.

Inner surface	
Convective heat transfer coefficient (W/m <sup>2</sup> -K)	2,152
Radiative heat transfer coefficient (W/m <sup>2</sup> -K)	5,540
Surface resistance (m <sup>2</sup> -K/W)	0,130
Outer surface	
Convective heat transfer coefficient (W/m <sup>2</sup> -K)	19,870
Radiative heat transfer coefficient (W/m <sup>2</sup> -K)	5,130
Surface resistance (m <sup>2</sup> -K/W)	0,040
No Bridging	
U-Value surface to surface (W/m <sup>2</sup> -K)	5,833
R-Value (m <sup>2</sup> -K/W)	0,341
<b>U-Value (W/m<sup>2</sup>-K)</b>	<b>2.929</b>
With Bridging (BS EN ISO 6946)	
Thickness (m)	0,3000
Km - Internal heat capacity (KJ/m <sup>2</sup> -K)	220,0000
Upper resistance limit (m <sup>2</sup> -K/W)	0,341
Lower resistance limit (m <sup>2</sup> -K/W)	0,341
U-Value surface to surface (W/m <sup>2</sup> -K)	5,833
R-Value (m <sup>2</sup> -K/W)	0,341
<b>U-Value (W/m<sup>2</sup>-K)</b>	<b>2.929</b>

### 3.2.4 Insulated Roof

This type of wall is composed by 3 layers: steel tile filled with polyurethane, air layer and plaster board. This is the composition suggested by Weber *et al.* (2017) to correctly represent this type of roof commonly used in Brazil.

Layers	
Number of layers	3
Outermost layer	
 Material	Aco e PU
Thickness (m)	0,0420
<input type="checkbox"/> Bridged?	
Layer 2	
 Material	AR CB3E telhado caxias
Thickness (not used in thermal calcs) (m)	0,2500
Innermost layer	
 Material	Forno gesso Caxias
Thickness (m)	0,0300
<input type="checkbox"/> Bridged?	

The thermal properties of the insulated wall is described below.

<b>Inner surface</b>	
Convective heat transfer coefficient (W/m <sup>2</sup> -K)	4,460
Radiative heat transfer coefficient (W/m <sup>2</sup> -K)	5,540
Surface resistance (m <sup>2</sup> -K/W)	0,100
<b>Outer surface</b>	
Convective heat transfer coefficient (W/m <sup>2</sup> -K)	19,870
Radiative heat transfer coefficient (W/m <sup>2</sup> -K)	5,130
Surface resistance (m <sup>2</sup> -K/W)	0,040
<b>No Bridging</b>	
U-Value surface to surface (W/m <sup>2</sup> -K)	0,614
R-Value (m <sup>2</sup> -K/W)	1,769
<b>U-Value (W/m<sup>2</sup>-K)</b>	<b>0,565</b>
<b>With Bridging (BS EN ISO 6946)</b>	
Thickness (m)	0,3220
Km - Internal heat capacity (KJ/m <sup>2</sup> -K)	23,4900
Upper resistance limit (m <sup>2</sup> -K/W)	1,769
Lower resistance limit (m <sup>2</sup> -K/W)	1,769
U-Value surface to surface (W/m <sup>2</sup> -K)	0,614
R-Value (m <sup>2</sup> -K/W)	1,769
<b>U-Value (W/m<sup>2</sup>-K)</b>	<b>0,565</b>

### 3.2.5 Light Roof

In this type of roof, only one layer of material (concrete slab) was configured, with a thickness of 5cm.

<b>Inner surface</b>	
Convective heat transfer coefficient (W/m <sup>2</sup> -K)	4,460
Radiative heat transfer coefficient (W/m <sup>2</sup> -K)	5,540
Surface resistance (m <sup>2</sup> -K/W)	0,100
<b>Outer surface</b>	
Convective heat transfer coefficient (W/m <sup>2</sup> -K)	19,870
Radiative heat transfer coefficient (W/m <sup>2</sup> -K)	5,130
Surface resistance (m <sup>2</sup> -K/W)	0,040
<b>No Bridging</b>	
U-Value surface to surface (W/m <sup>2</sup> -K)	35,000
R-Value (m <sup>2</sup> -K/W)	0,169
<b>U-Value (W/m<sup>2</sup>-K)</b>	<b>5,932</b>
<b>With Bridging (BS EN ISO 6946)</b>	
Thickness (m)	0,0500
Km - Internal heat capacity (KJ/m <sup>2</sup> -K)	55,0000
Upper resistance limit (m <sup>2</sup> -K/W)	0,169
Lower resistance limit (m <sup>2</sup> -K/W)	0,169
U-Value surface to surface (W/m <sup>2</sup> -K)	35,000
R-Value (m <sup>2</sup> -K/W)	0,169
<b>U-Value (W/m<sup>2</sup>-K)</b>	<b>5,932</b>

### 3.2.6 Heavy Roof

In this type of roof, only one layer of material (concrete slab) was configured, with a thickness of 30cm.

<b>Inner surface</b>	
Convective heat transfer coefficient (W/m <sup>2</sup> -K)	4,460
Radiative heat transfer coefficient (W/m <sup>2</sup> -K)	5,540
Surface resistance (m <sup>2</sup> -K/W)	0,100
<b>Outer surface</b>	
Convective heat transfer coefficient (W/m <sup>2</sup> -K)	19,870
Radiative heat transfer coefficient (W/m <sup>2</sup> -K)	5,130
Surface resistance (m <sup>2</sup> -K/W)	0,040
<b>No Bridging</b>	
U-Value surface to surface (W/m <sup>2</sup> -K)	5,833
R-Value (m <sup>2</sup> -K/W)	0,311
<b>U-Value (W/m<sup>2</sup>-K)</b>	<b>3,211</b>
<b>With Bridging (BS EN ISO 6946)</b>	
Thickness (m)	0,3000
Km - Internal heat capacity (KJ/m <sup>2</sup> -K)	220,0000
Upper resistance limit (m <sup>2</sup> -K/W)	0,311
Lower resistance limit (m <sup>2</sup> -K/W)	0,311
U-Value surface to surface (W/m <sup>2</sup> -K)	5,833
R-Value (m <sup>2</sup> -K/W)	0,311
<b>U-Value (W/m<sup>2</sup>-K)</b>	<b>3,211</b>

### 3.2.7 Optical Properties of Walls and Roofs

These are the Optical property settings for reflectivities of 10%.

<b>Surface Properties</b>	
Thermal absorptance (emissivity)	0,9000000
Solar absorptance	0,900
Visible absorptance	0,900
Roughness	3-Rough
<input type="checkbox"/> Colour	
<input checked="" type="checkbox"/> Texture	Brushed flat concrete
<b>Radiance Daylighting</b>	
Material class	1-Plastic
Reflectance	0,100
Specularity	0,000
Roughness	0,000

These are the Optical property settings for reflectivities of 30%.

<b>Surface Properties</b>	
Thermal absorptance (emissivity)	0,9000000
Solar absorptance	0,700
Visible absorptance	0,700
Roughness	3-Rough
<input type="checkbox"/> Colour	
<input checked="" type="checkbox"/> Texture	Brushed flat concrete
<b>Radiance Daylighting</b>	
Material class	1-Plastic
Reflectance	0,300
Specularity	0,000
Roughness	0,000

These are the Optical property settings for reflectivities of 50%.

Surface Properties	
Thermal absorptance (emissivity)	0,9000000
Solar absorptance	0,500
Visible absorptance	0,500
Roughness	3-Rough
<input type="checkbox"/> Colour	
<input checked="" type="checkbox"/> Texture	Brushed flat concrete
Radiance Daylighting	
Material class	1-Plastic
Reflectance	0,500
Specularity	0,000
Roughness	0,000

These are the Optical property settings for reflectivities of 70%.

Surface Properties	
Thermal absorptance (emissivity)	0,9000000
Solar absorptance	0,300
Visible absorptance	0,300
Roughness	3-Rough
<input type="checkbox"/> Colour	
<input checked="" type="checkbox"/> Texture	Brushed flat concrete
Radiance Daylighting	
Material class	1-Plastic
Reflectance	0,700
Specularity	0,000
Roughness	0,000

These are the Optical property settings for reflectivities of 90%.

Surface Properties	
Thermal absorptance (emissivity)	0,9000000
Solar absorptance	0,100
Visible absorptance	0,100
Roughness	3-Rough
<input type="checkbox"/> Colour	
<input checked="" type="checkbox"/> Texture	White
Radiance Daylighting	
Material class	1-Plastic
Reflectance	0,900
Specularity	0,000
Roughness	0,000

### 3.3 Openings: Free Aperture for Ventilation

These are the window settings for 5% of free aperture for ventilation.

Free Aperture	
Opening position	2-Bottom
% Glazing area opens	5
Discharge coefficient	0,6500

These are the window settings for 35% of free aperture for ventilation.

Free Aperture	
Opening position	2-Bottom
% Glazing area opens	35,0
Discharge coefficient	0,6500

These are the window settings for 65% of free aperture for ventilation.

Free Aperture	
Opening position	2-Bottom
% Glazing area opens	65,0
Discharge coefficient	0,6500


These are the window settings for 95% of free aperture for ventilation.

Free Aperture	
Opening position	2-Bottom
% Glazing area opens	95.0
Discharge coefficient	0.6500

### 3.4 Electricity Generation Settings


Add Solar Collector - Hot Water

Add Solar Collector - Photovoltaic


 On Site Electricity Generation

Include electric load centres

Number of electric load centres 1

 Load centre 1 School DC with inverter


General

<b>Name</b>	<b>School DC with inverter</b>
Operation scheme	1-Base load
Electrical buss type	3-Direct Current With Inverter
 Inverter	Example Inverter - Simple


Cost

Distribution and electrical cost (GBP)	600.00
--	--------


Generator 1

DC generator type	1-Photovoltaic
 PV solar collector	Solar collector 1

Solar Collector

Solar collector type	2-Photovoltaic
Cost (GBP/m <sup>2</sup> )	600,000
Level	1-Building
 Material	Bitumen Felt
Flat surface position	1-Upper surface

Photovoltaic Options

Performance type	1-Simple
 Performance model	PV Constant Efficiency = 0.15
Heat transfer integration mode	1-Decoupled

**Data Report (Not Editable)**

**General**

**Bitumen Felt**  
 Bitumen felt or sheet  
 Source: BS EN 1252  
 Category: Asphalts an  
 Region: England an

**Material Layer Thickness**  
 Force thickness: No

**Thermal Properties**  
 Detailed properties: Yes

**Thermal Bulk Properties**  
 Conductivity (W/m-K): 0,2300  
 Specific Heat (J/kg-K): 1000,00  
 Density (kg/m3): 1100,00  
 Resistance (R-value): No

**Green Roof**  
 Green roof: No

**Embodied Carbon**  
 Embodied carbon data: Yes  
 Embodied carbon (kg...): 1,70  
 Conversion factor name: Saturated F  
 Source: ICE v1.6  
 Assumption / factor bo...: Cradle to gr  
 Equivalent carbon data...: No

**Phase Change Properties**  
 Phase change material: No

**Cost**  
 Cost type: 1-Cost per s  
 Cost per surface area (G...): 50,000  
 Cost per mass (GBP/kg): 1,000  
 Cost per volume (GBP/m...): 500,000

**Vapour Resistance**  
 Vapour resistance definit...: 1-Factor  
 Vapour factor: 50000  
 Vapour resistivity (MNs/...): 10

**Moisture Transfer**  
 Include moisture transfer ...: No

**Surface Properties**  
 Thermal absorptance (e...): 0,9000000  
 Solar absorptance: 0,870  
 Visible absorptance: 0,870  
 Roughness: 3-Rough  
 Colour:   
 Texture: Cold Spring

**Radiance Daylighting**  
 Material class: 1-Plastic  
 Absorptance: 0,870  
 Reflectance: 0,130  
 Specularity: 0,000  
 Roughness: 0,000  
 Transmissivity: 0,000  
 Fraction diffused: 0,000

**Photovoltaic Generator - Simple**

Performance Model

**General**

**Name** PV Constant Efficiency = 0.15

Fraction of surface with active solar cells	0,9
Conversion efficiency input mode	1-Fixed
Cell efficiency value	0,150
Rated electric power output (W)	48000,00
Availability schedule	On 24/7

#### 4. Input data only in passive survivability analysis:

Items not detailed in images were not selected or had no specific setting.

#### 4.1 Model Options: Simple HVAC

**HVAC**

Simple  Detailed

**Simple HVAC**  
 HVAC systems are modelled using Ideal Loads, fuel consumption is calculated from loads using seasonal efficiencies

HVAC sizing	3-Autosize
Simple HVAC autosize method	1-EnergyPlus
<input checked="" type="checkbox"/> Specify Simple/Design HVAC details	
Auxiliary energy calculations	2-Separate fans and pumps
Mechanical ventilation method	2-Ideal loads

#### 4.2 Model Options: Cooling Design Calculation Options

Calculation Options	
Simulation method	1-EnergyPlus
Temperature control	1-Air temperature
<input type="checkbox"/> Exclude all zone natural ventilation (infiltration is always included)	
<input type="checkbox"/> Exclude all zone mechanical ventilation	
<input checked="" type="checkbox"/> Exclude heat recovery	

### 4.3 Activity Tab: Environmental Control

Environmental Control	
Heating Setpoint Temperatures	
Heating (°C)	12,0
Heating set back (°C)	4,0
Cooling Setpoint Temperatures	
Cooling (°C)	26,0
Cooling set back (°C)	40,0

### 4.4 HVAC Settings

HVAC Template	
Template	Split + Separate Mechanical Ventilation
Mechanical Ventilation	
<input type="checkbox"/> On	
Auxiliary Energy	
Heating	
Cooling	
<input checked="" type="checkbox"/> Cooled	
Cooling system	Default
Fuel	1-Electricity from grid
Cooling system seasonal CoP	3,780
Supply Air Condition	
Operation	
Schedule	All day
Humidity Control	
DHW	
Natural Ventilation	
<input checked="" type="checkbox"/> On	
Mixed Mode Zone Equipment	
<input checked="" type="checkbox"/> Mixed mode on	
Wind and Rain	
Temperature Control	
Min outdoor temperature (°C)	12,0
Max outdoor temperature (°C)	26,0

## APPENDIX J

According to Sunpath studies using DesignBuilder, the 1.80m distance between module bases avoid shadings on PV system from 8:00 to 17:30 in summer and from 9:30 to 15:30 in all cities.



# Sunpath Studies to avoid Shading on PV System

Source: DesignBuilder (2023).

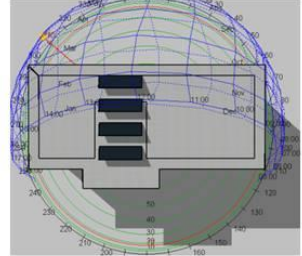
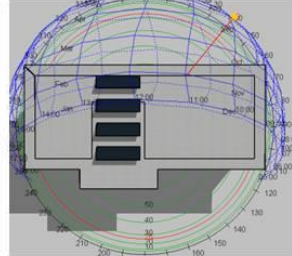
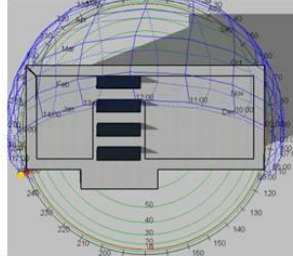
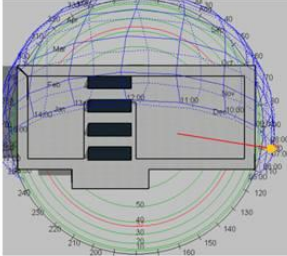
## Zone 1 – Caxias do Sul (RS)

21 December – 8:00

21 December – 18:00

21 June – 9:30

21 June – 15:30



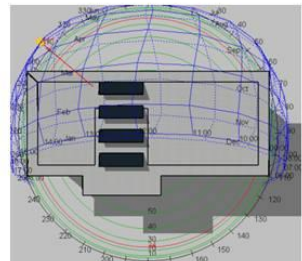
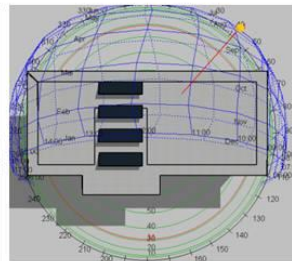
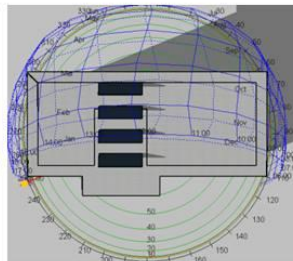
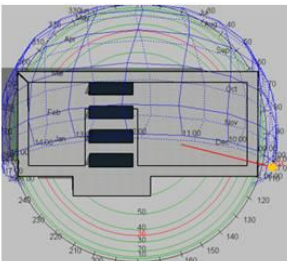
## Zone 2 – Nova Friburgo (RJ)

21 December – 8:00

21 December – 18:00

21 June – 09:30

21 June – 15:30



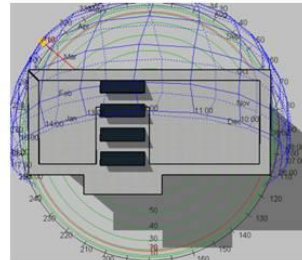
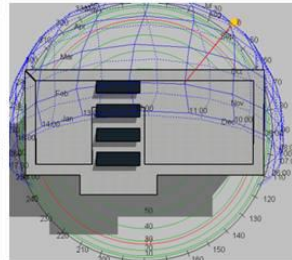
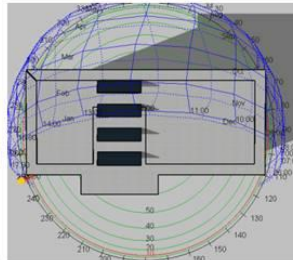
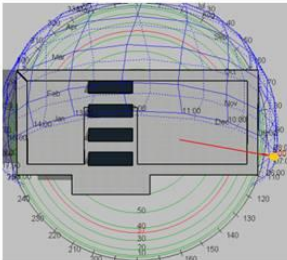
## Zone 3 – Florianópolis (SC)

21 December – 8:00

21 December – 18:00

21 June – 9:30

21 June – 15:30



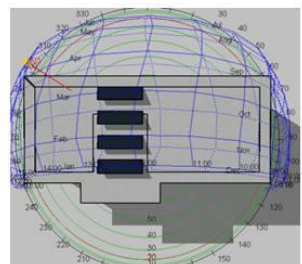
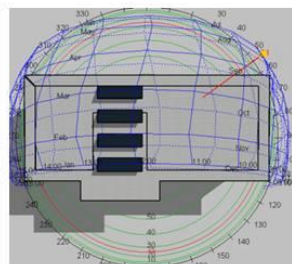
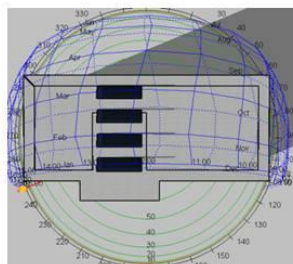
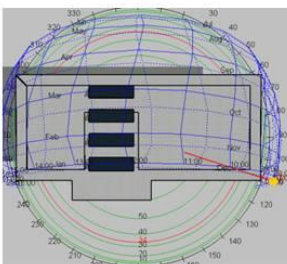
## Zone 4 – Brasília (DF)

21 December – 8:00

21 December – 18:00

21 June – 8:30

21 June – 16:00





## Sunpath Studies to avoid Shading on PV System

Source: DesignBuilder (2023).

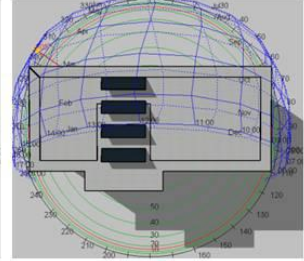
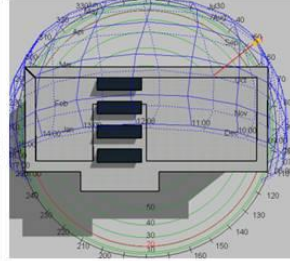
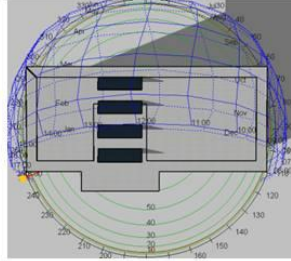
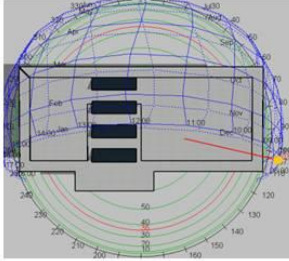
### Zone 5 – Santos (SP)

21 December – 8:00

21 December – 18:00

21 June – 8:30

21 June – 16:00



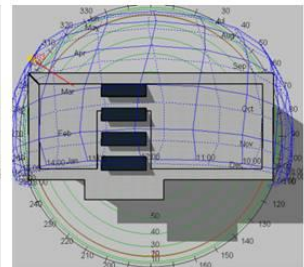
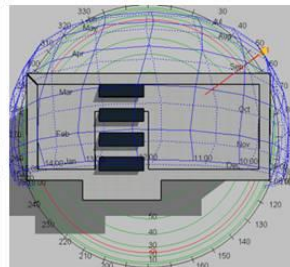
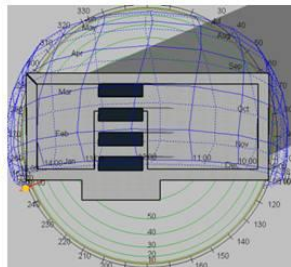
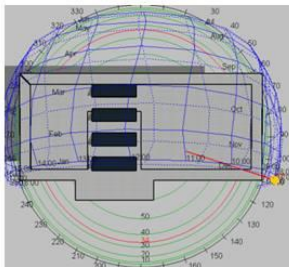
### Zone 6 – Goiânia (GO)

21 December – 8:00

21 December – 18:00

21 June – 08:30

21 June – 16:00



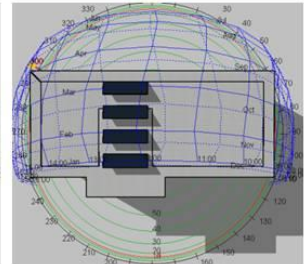
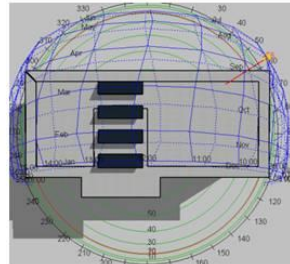
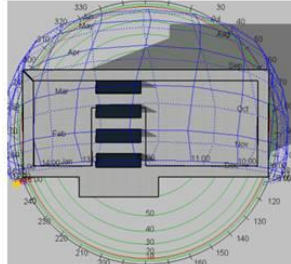
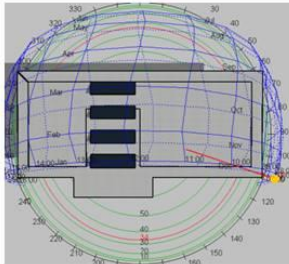
### Zone 7 – Picos (PI)

21 December – 8:00

21 December – 17:30

21 June – 8:00

21 June – 16:30



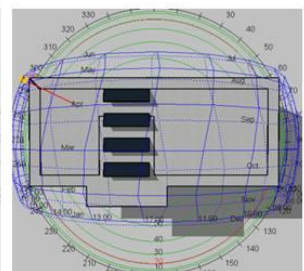
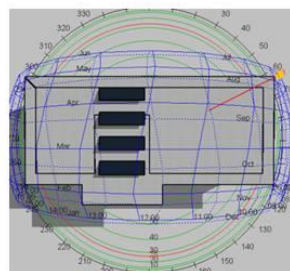
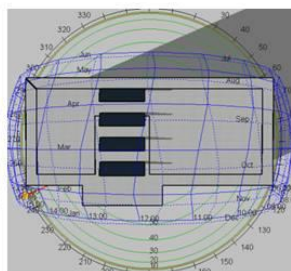
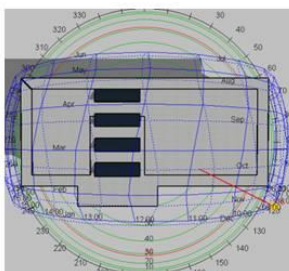
### Zone 8 – Belém (PA)

21 December – 8:00

21 December – 17:30

21 June – 8:00

21 June – 16:30

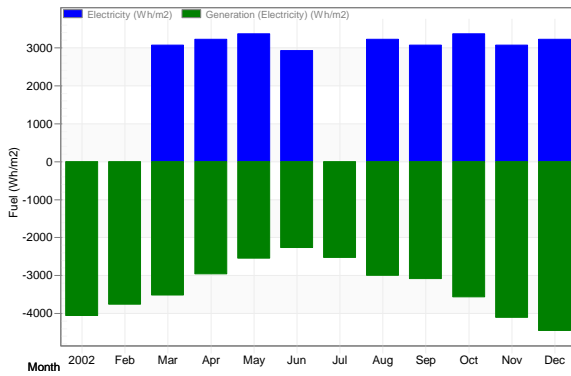


## APPENDIX K

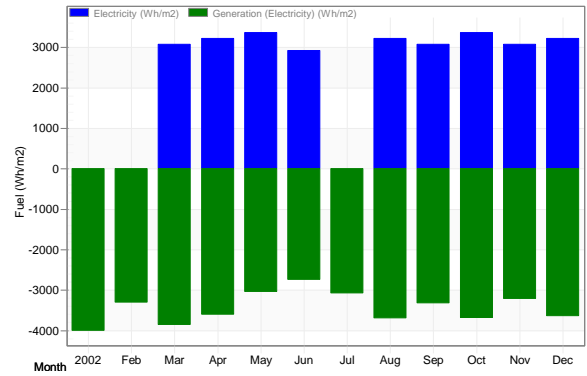
The following graphs are DesignBuilder outputs that compare loads and local energy production during the year.

### Comparison of Annual Loads and Local Energy Production

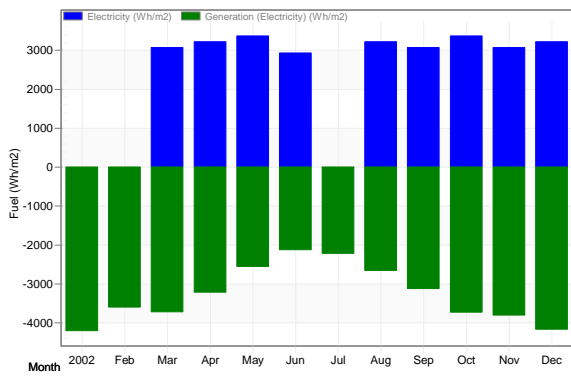
Caxias do Sul (RS) – Zone 1



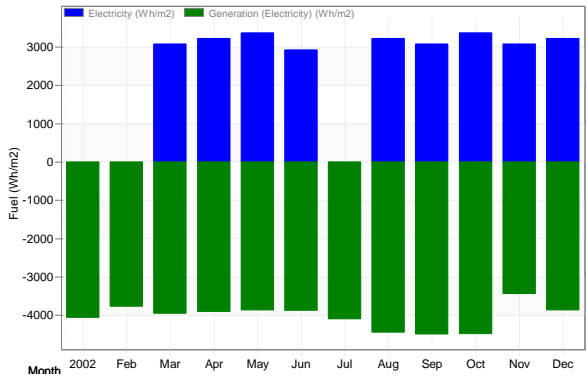
Nova Friburgo (RJ) – Zone 2



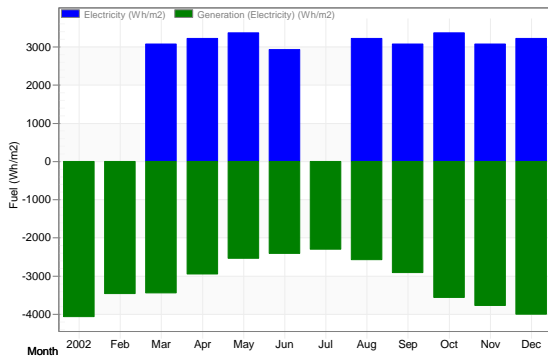
Florianópolis (SC) – Zone 3



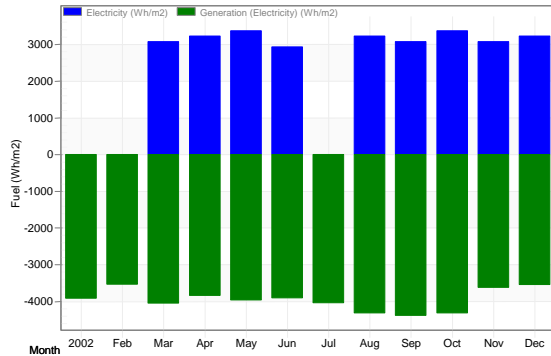
Brasília (DF) – Zone 4



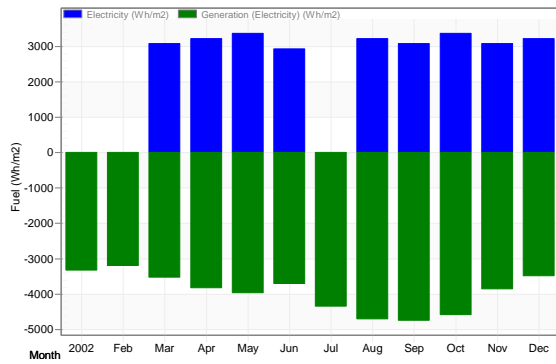
Santos (SP) – Zone 5



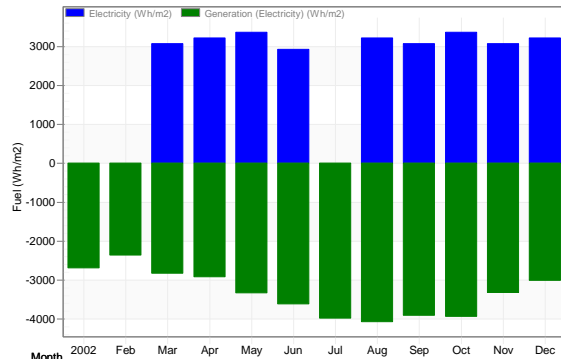
Goiânia (GO) – Zone 6



Picos (PI) – Zone 7



Belém (PA) – Zone 1

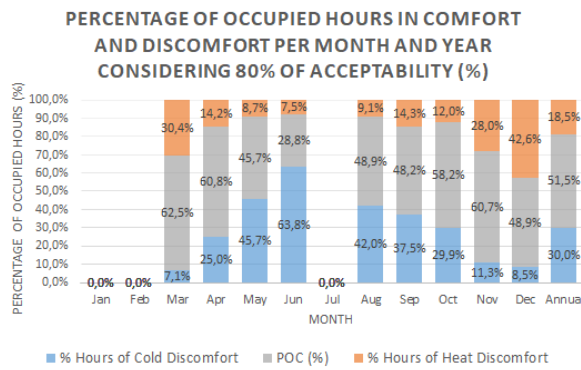


Source: DesignBuilder (2023).

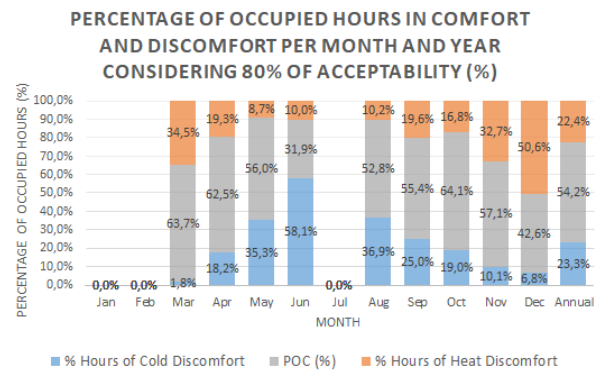
APPENDIX L

Percentage of occupied hours in comfort and discomfort in Caxias do Sul (RS) – Zone 1

2050

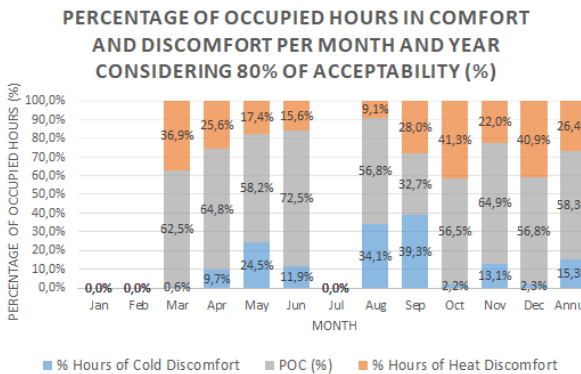


2080

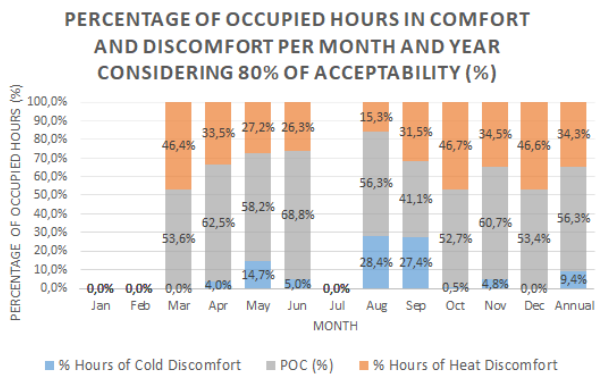


Percentage of occupied hours in comfort and discomfort in Nova Friburgo (RJ) – Zone 2

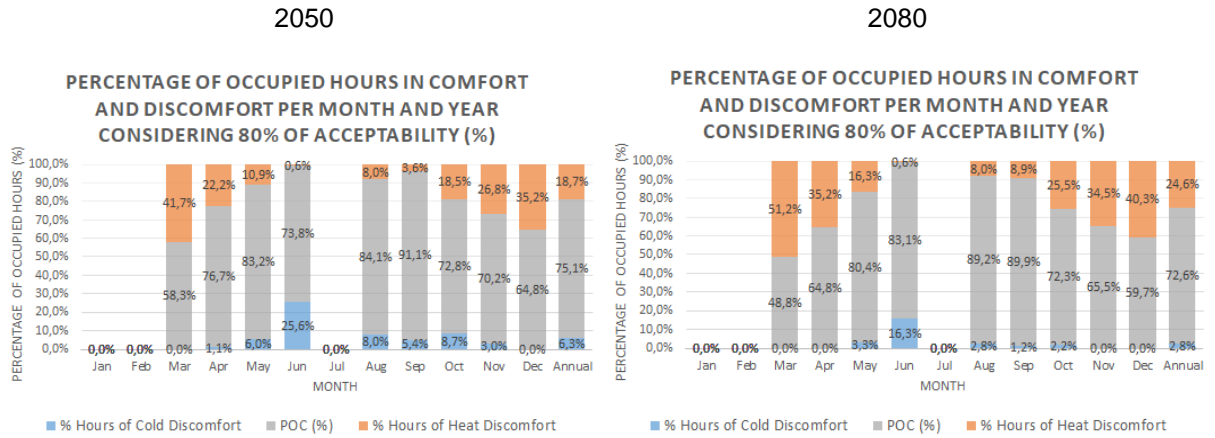
2050



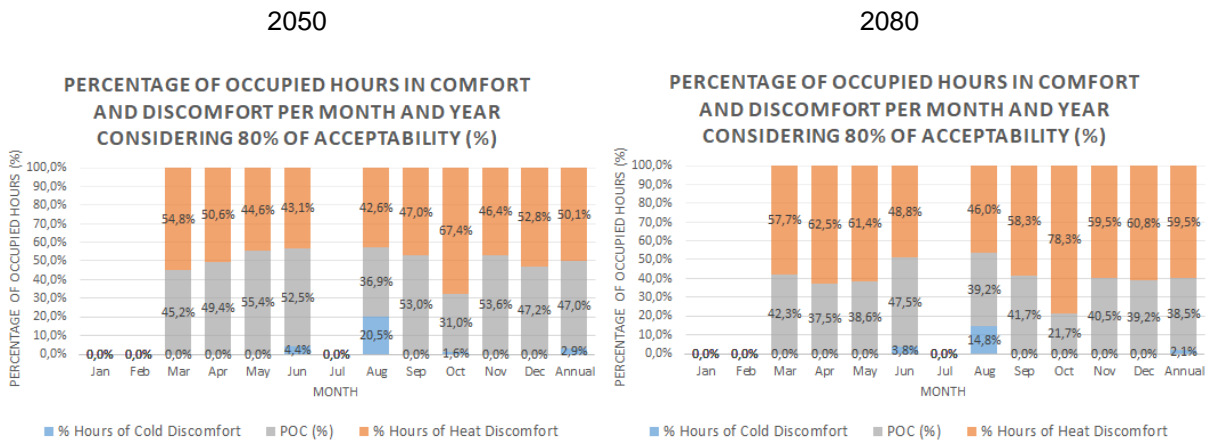
2080



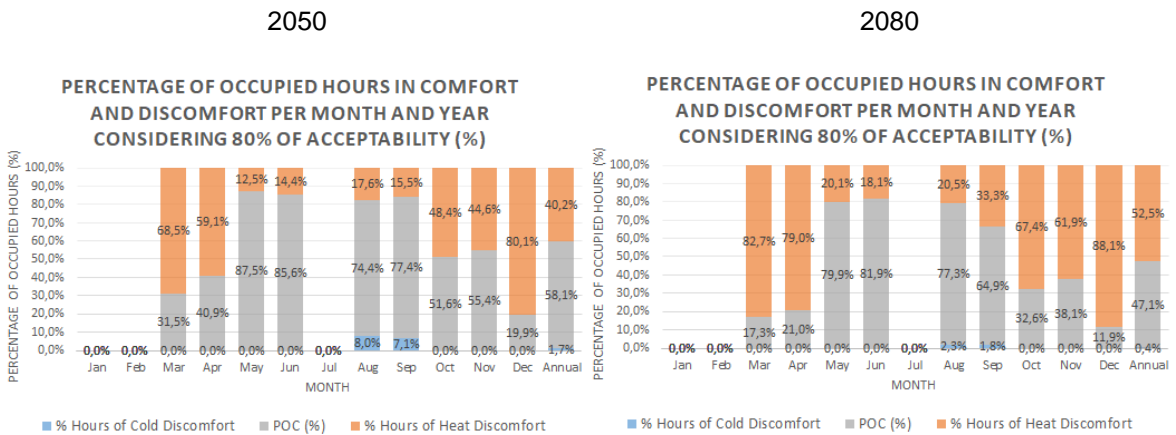
**Percentage of occupied hours in comfort and discomfort in Florianópolis (SC) – Zone 3**



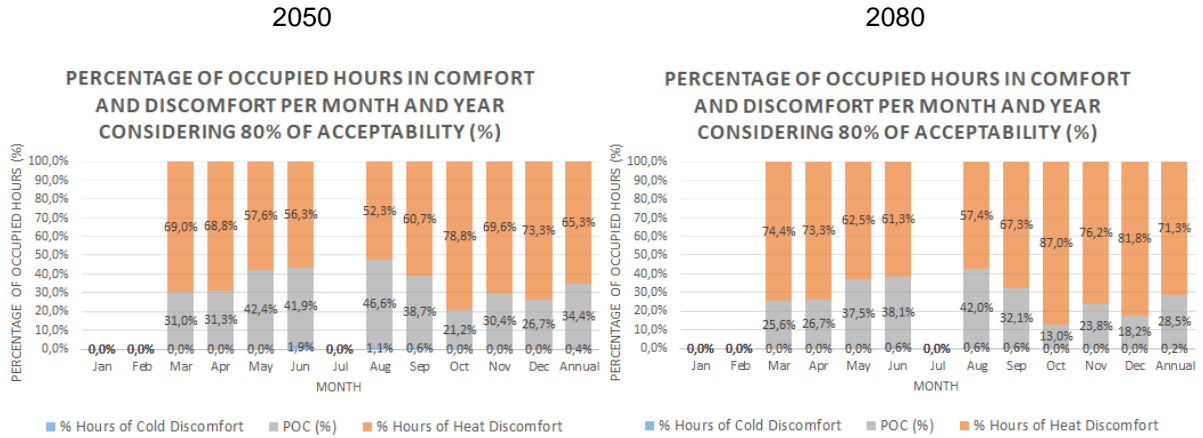
**Percentage of occupied hours in comfort and discomfort in Brasília (DF) – Zone 4**



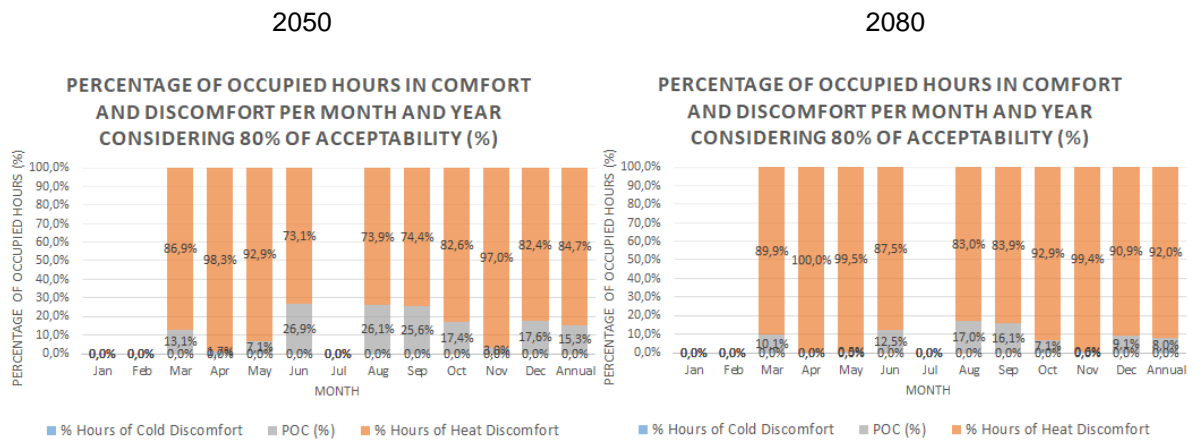
**Percentage of occupied hours in comfort and discomfort in Santos (SP) – Zone 5**



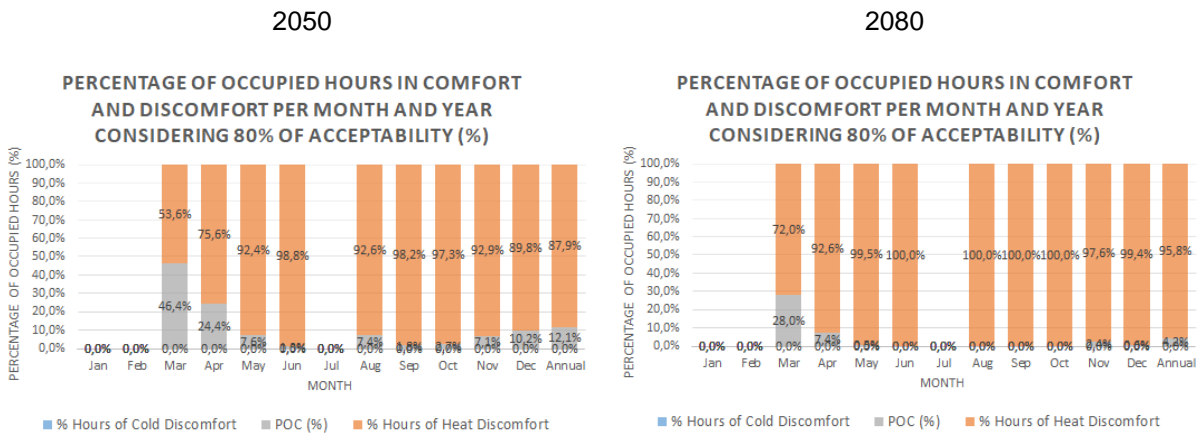
**Percentage of occupied hours in comfort and discomfort in Goiânia (GO) – Zone 6**



**Percentage of occupied hours in comfort and discomfort in Picos (PI) – Zone 7**



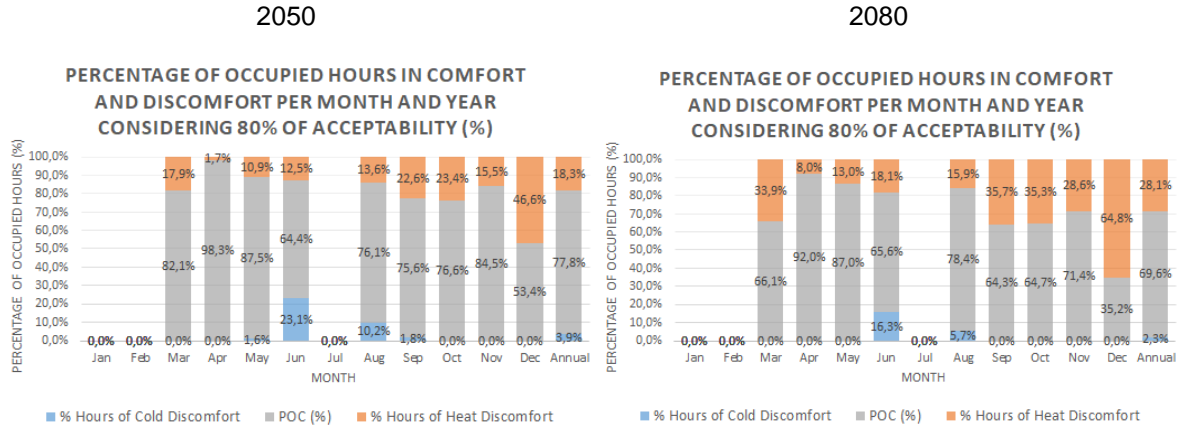
**Percentage of occupied hours in comfort and discomfort in Belém (PA) – Zone 8**



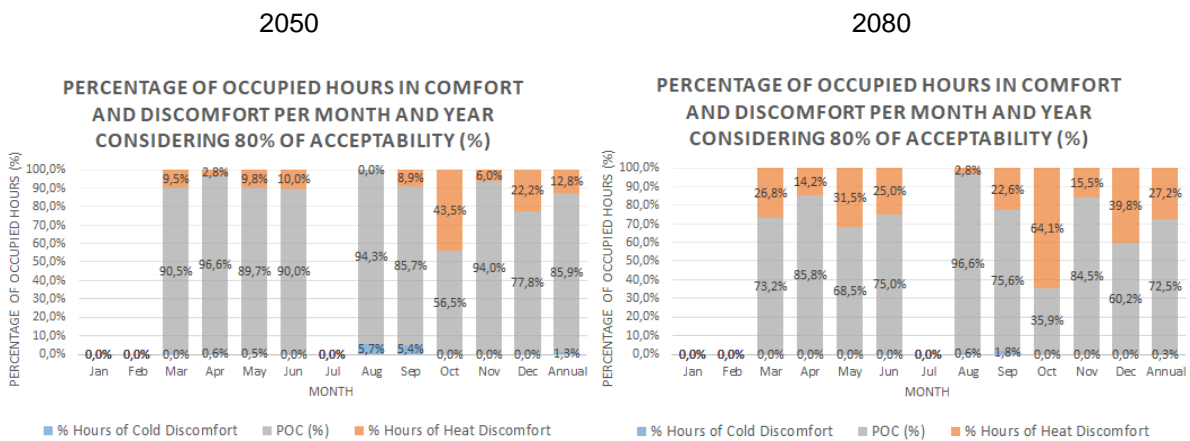


APPENDIX M

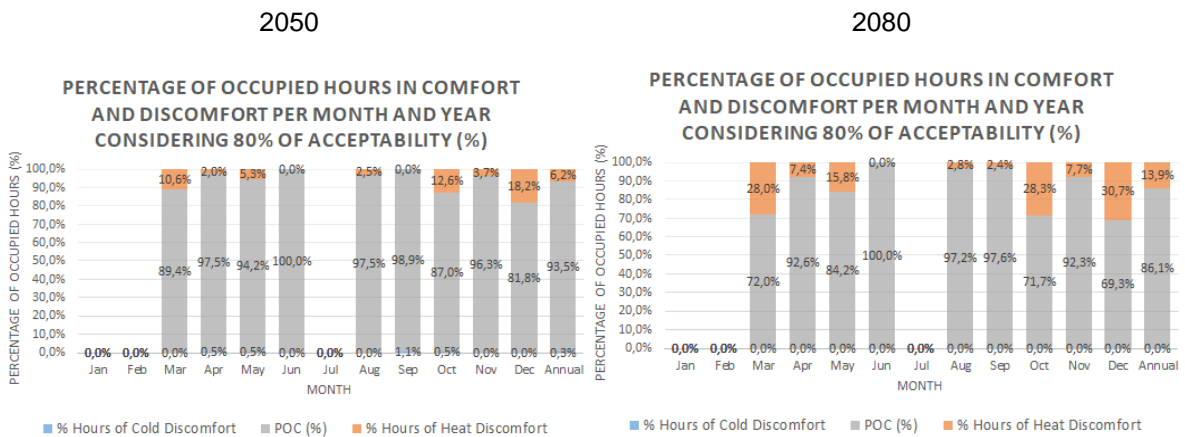
Percentage of occupied hours in comfort and discomfort in Caxias do Sul (RS) – Zone 1



Percentage of occupied hours in comfort and discomfort in Nova Friburgo (RJ) – Zone 2



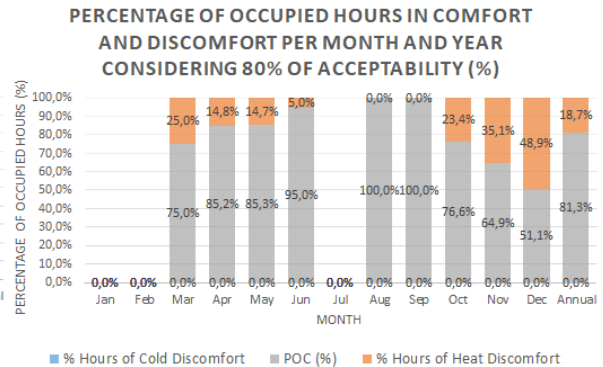
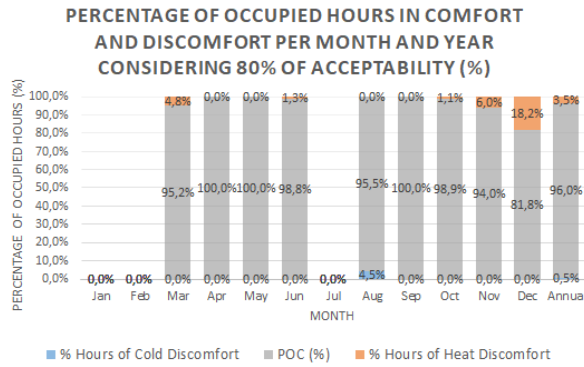
Percentage of occupied hours in comfort and discomfort in Florianópolis (SC) – Zone 3



**Percentage of occupied hours in comfort and discomfort in Brasília (DF) – Zone 4**

2050

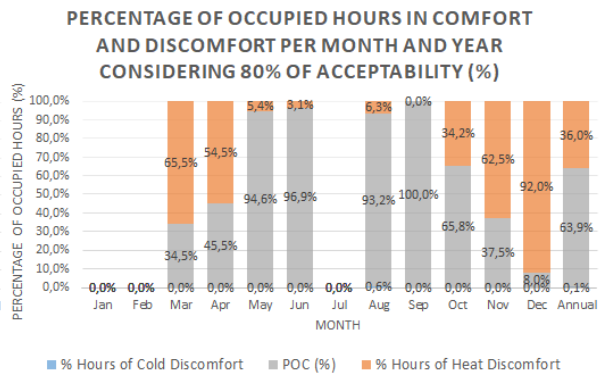
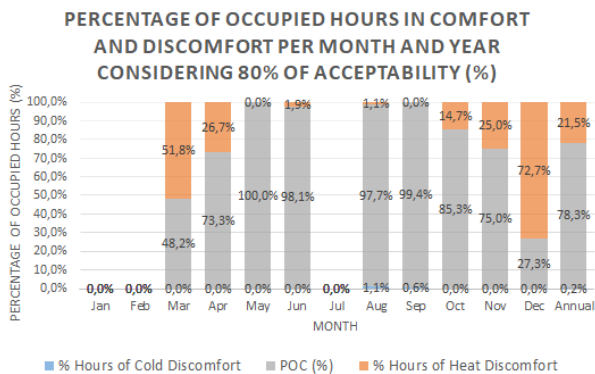
2080



**Percentage of occupied hours in comfort and discomfort in Santos (SP) – Zone 5**

2050

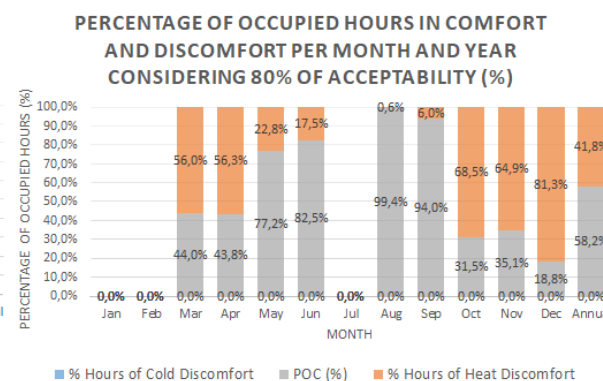
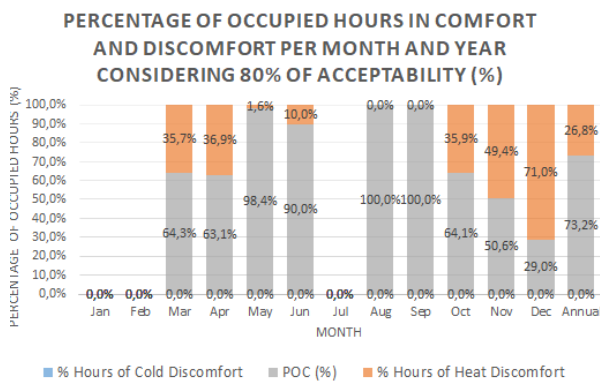
2080



**Percentage of occupied hours in comfort and discomfort in Goiânia (GO) – Zone 6**

2050

2080

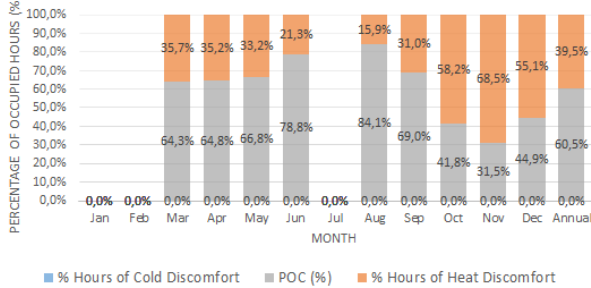


Percentage of occupied hours in comfort and discomfort in Picos (PI) – Zone 7

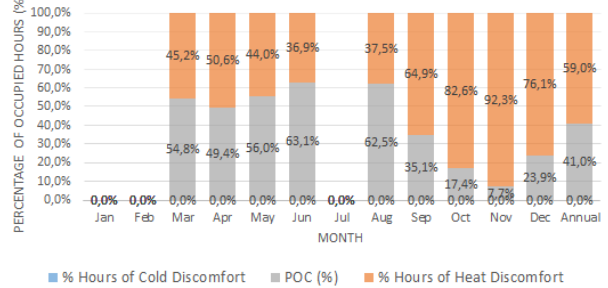
2050

2080

PERCENTAGE OF OCCUPIED HOURS IN COMFORT AND DISCOMFORT PER MONTH AND YEAR CONSIDERING 80% OF ACCEPTABILITY (%)



PERCENTAGE OF OCCUPIED HOURS IN COMFORT AND DISCOMFORT PER MONTH AND YEAR CONSIDERING 80% OF ACCEPTABILITY (%)

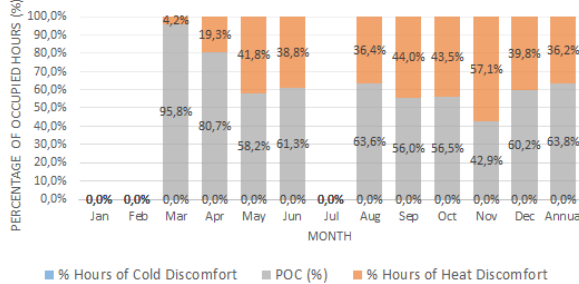


Percentage of occupied hours in comfort and discomfort in Belém (PA) – Zone 8

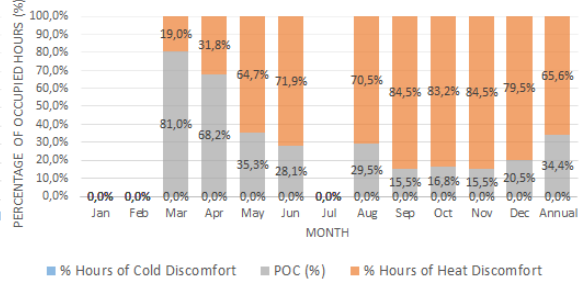
2050

2080

PERCENTAGE OF OCCUPIED HOURS IN COMFORT AND DISCOMFORT PER MONTH AND YEAR CONSIDERING 80% OF ACCEPTABILITY (%)

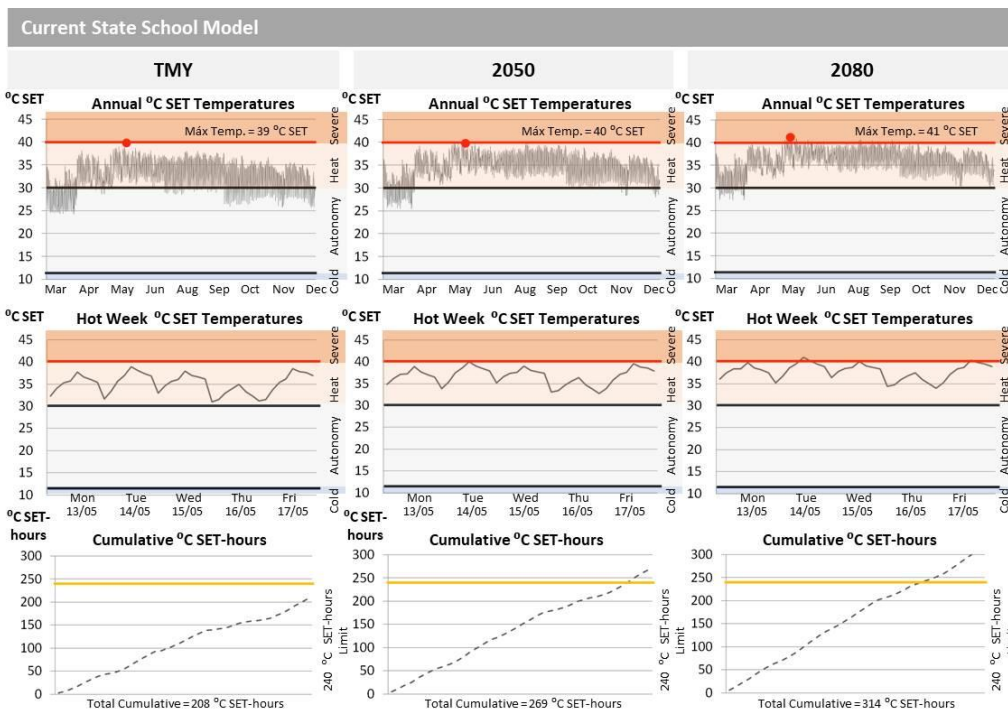


PERCENTAGE OF OCCUPIED HOURS IN COMFORT AND DISCOMFORT PER MONTH AND YEAR CONSIDERING 80% OF ACCEPTABILITY (%)

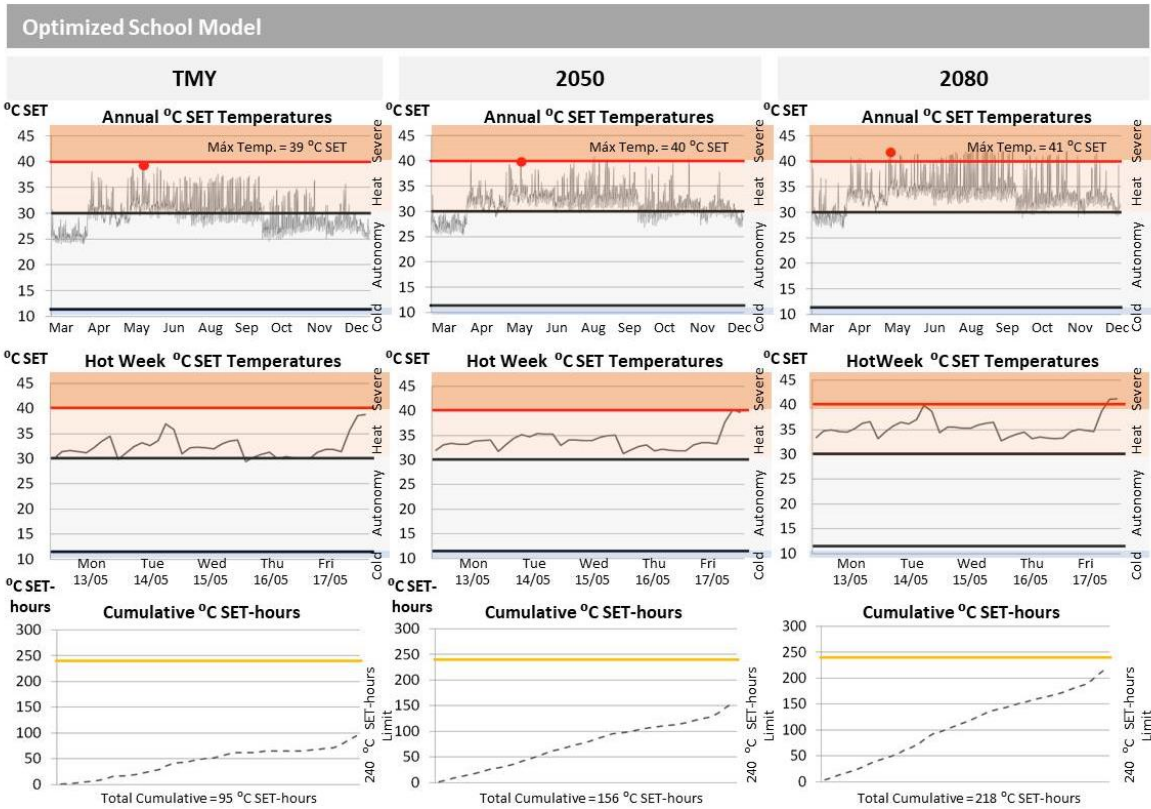


APPENDIX N

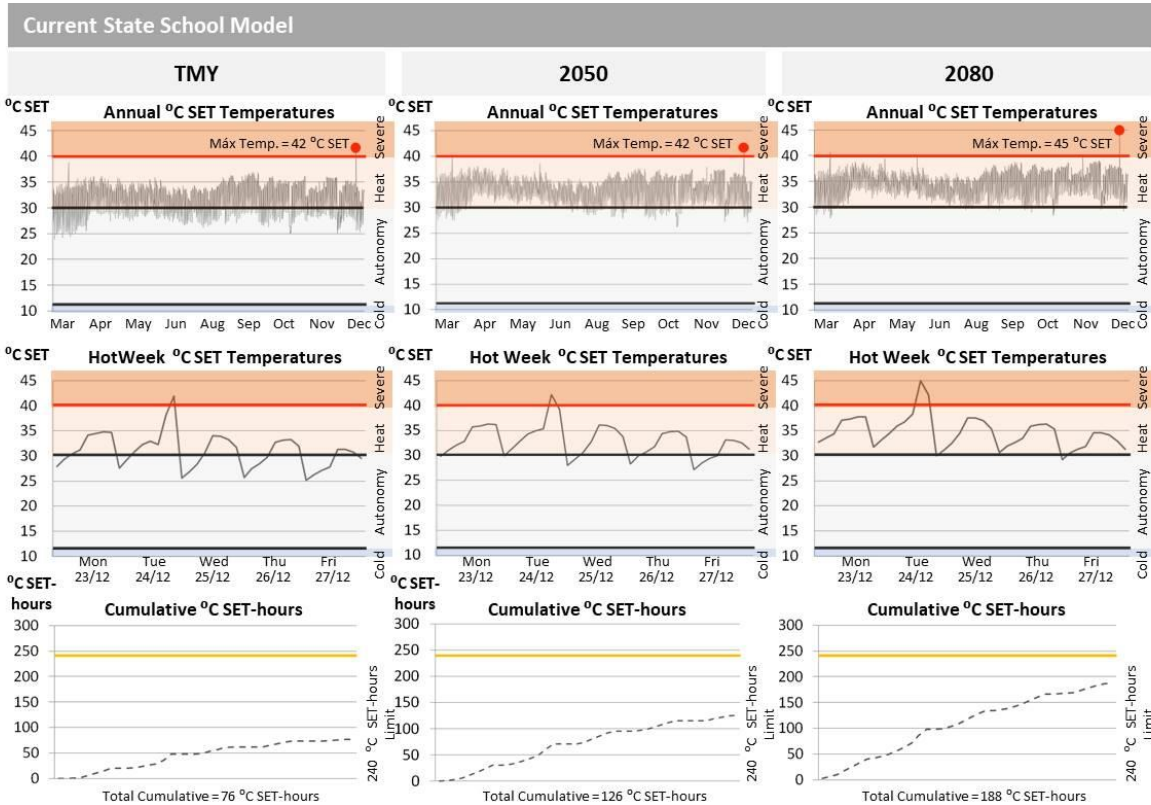
Belém (PA) – Zone 8

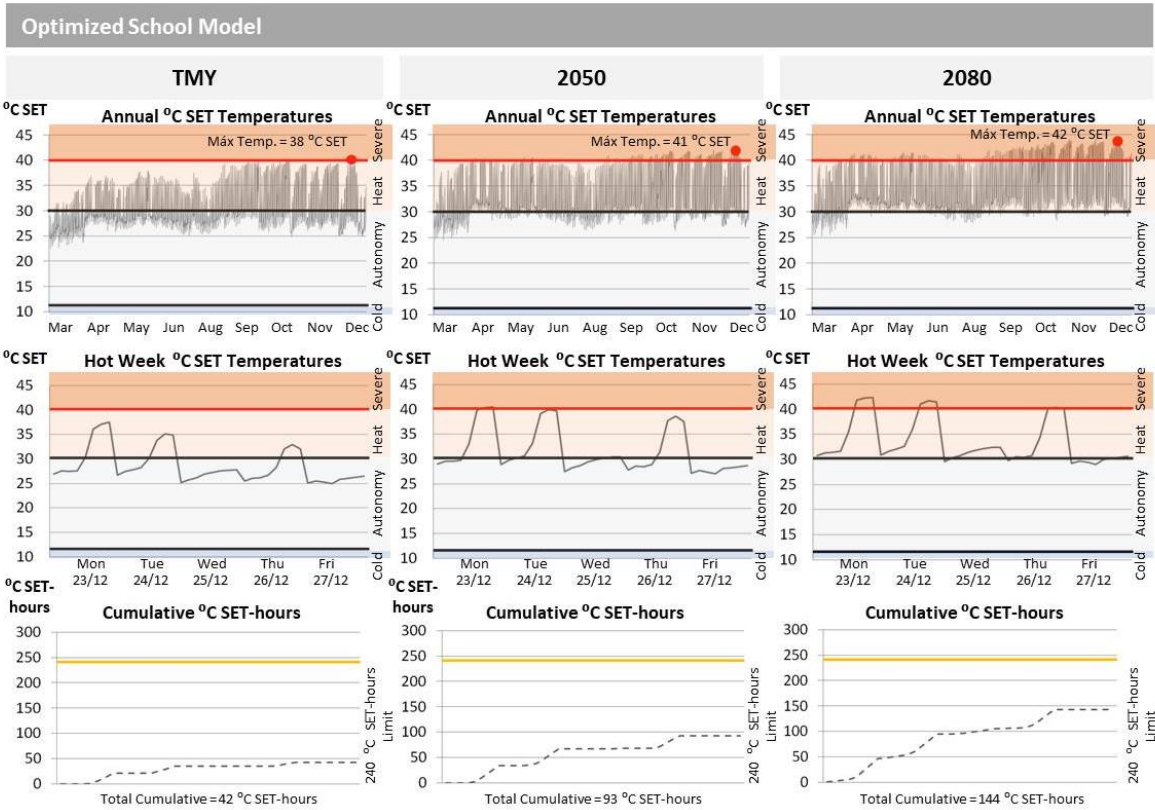




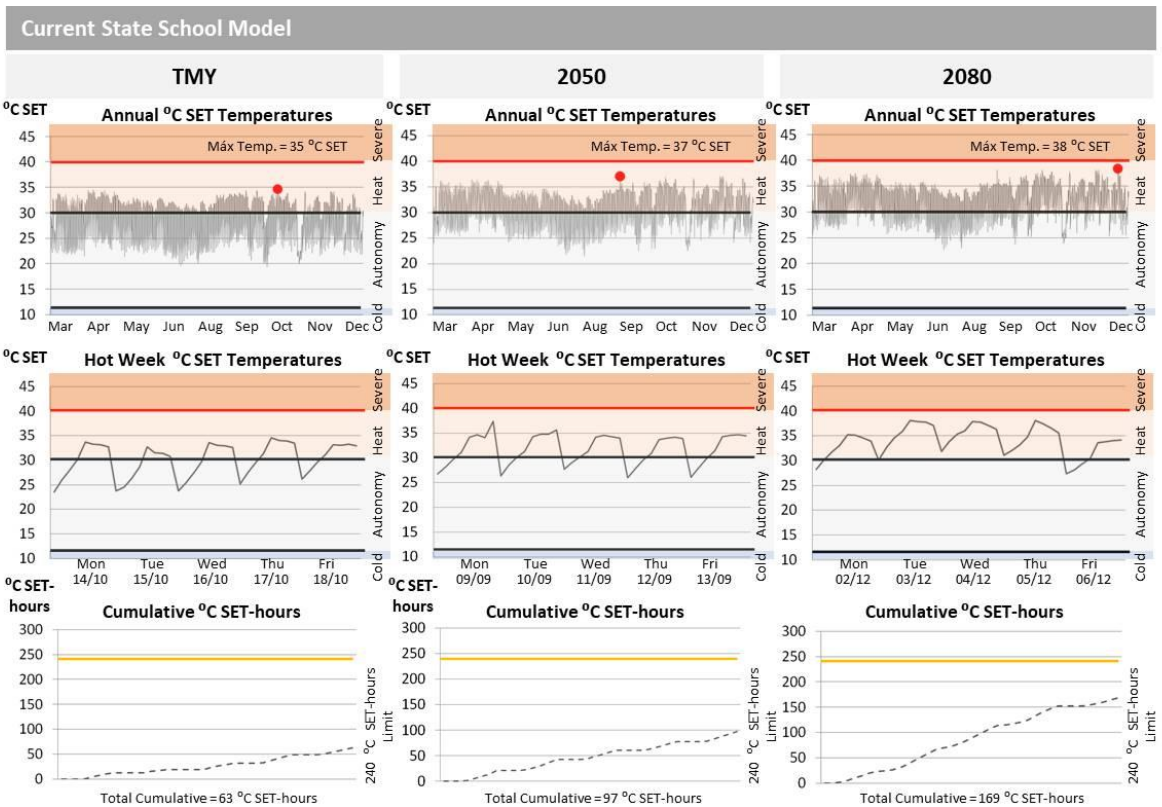


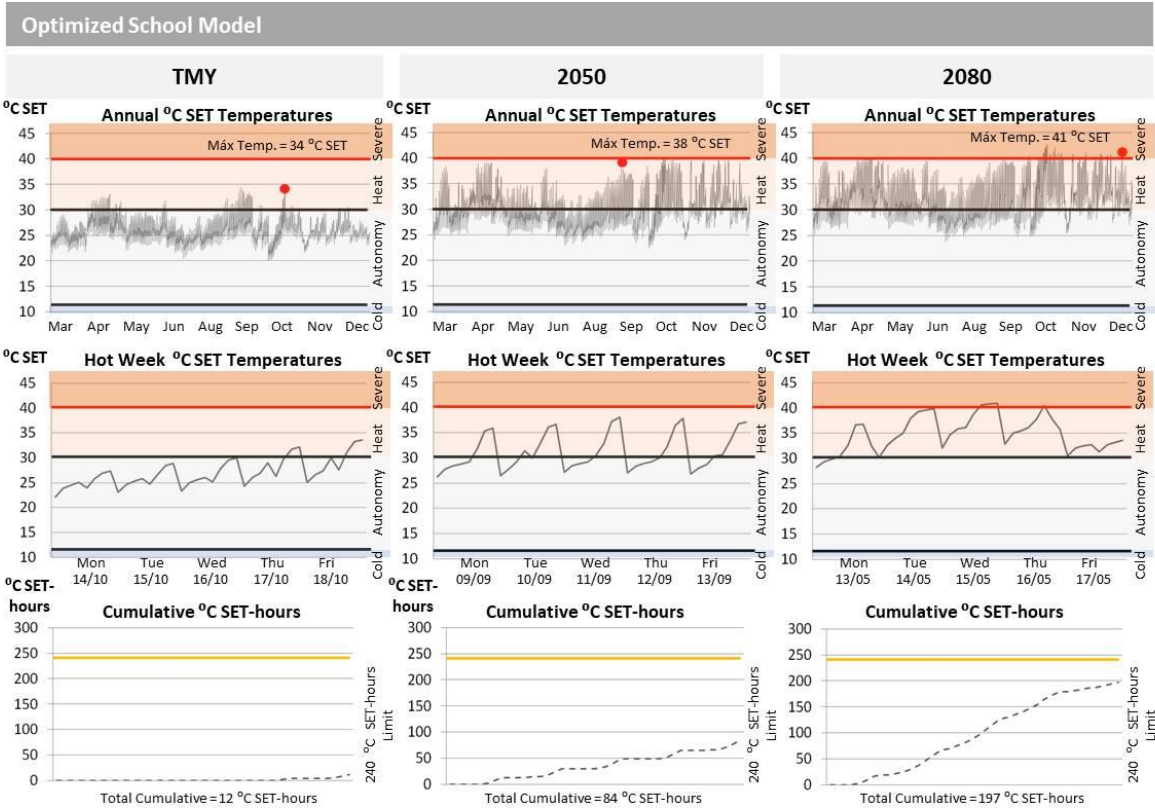
Picos (PI) – Zone 7



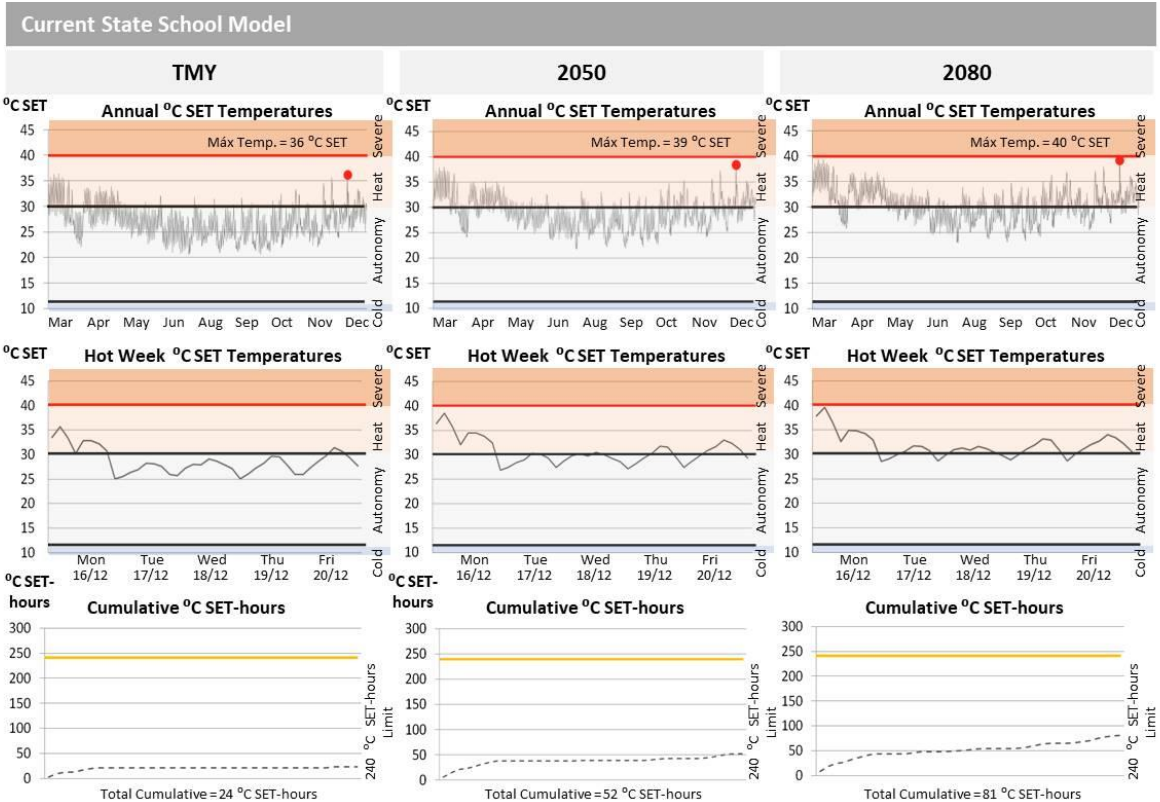


### Goiânia (GO) – Zone 6

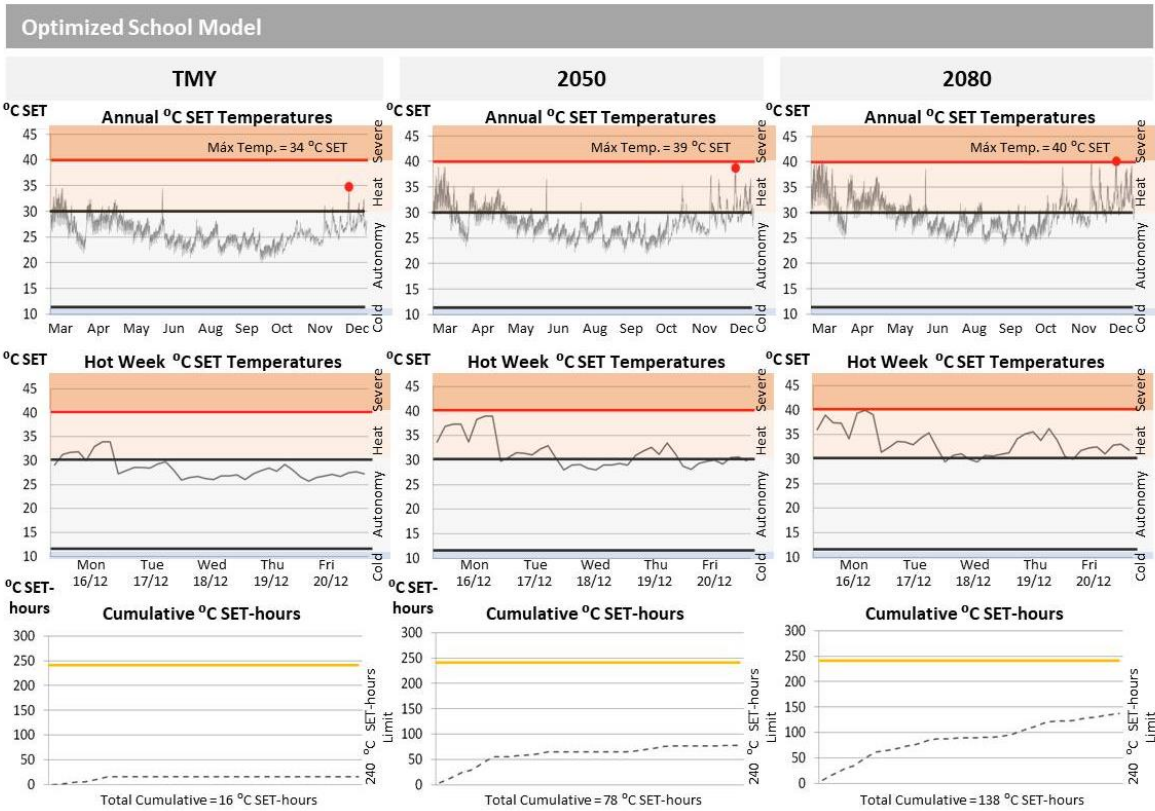




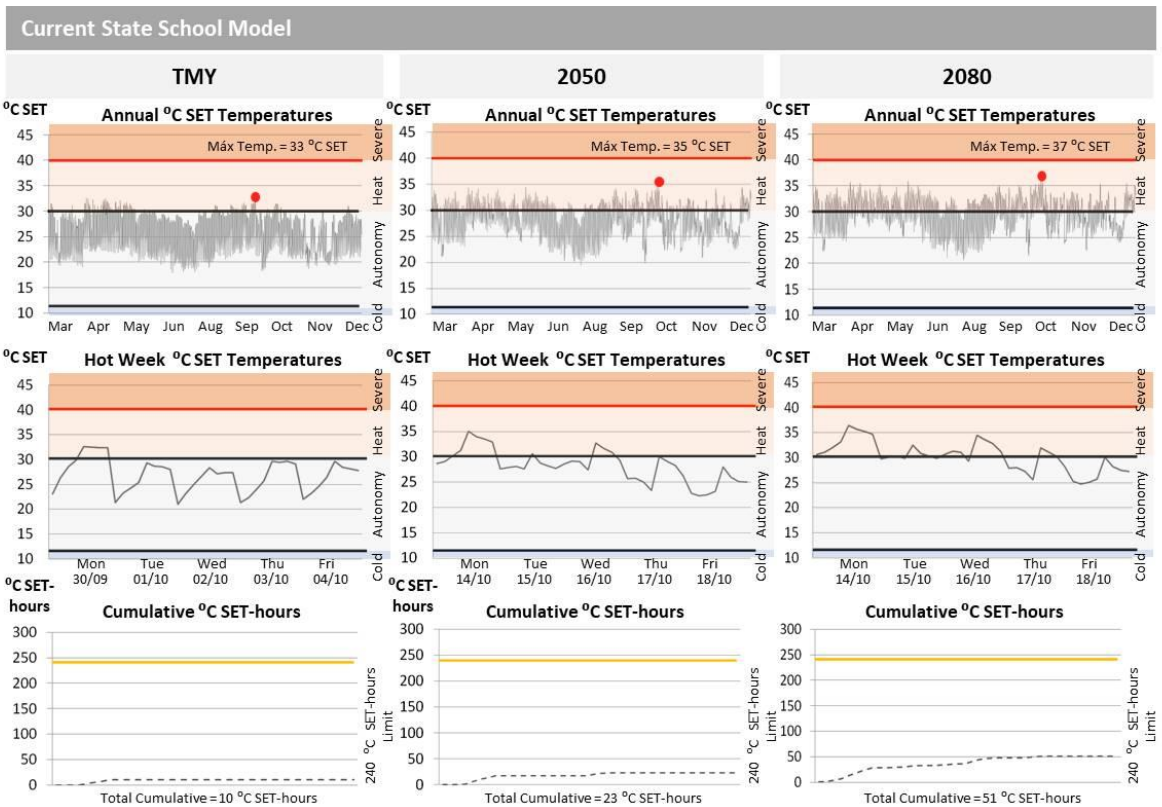
### Santos (SP) – Zone 5

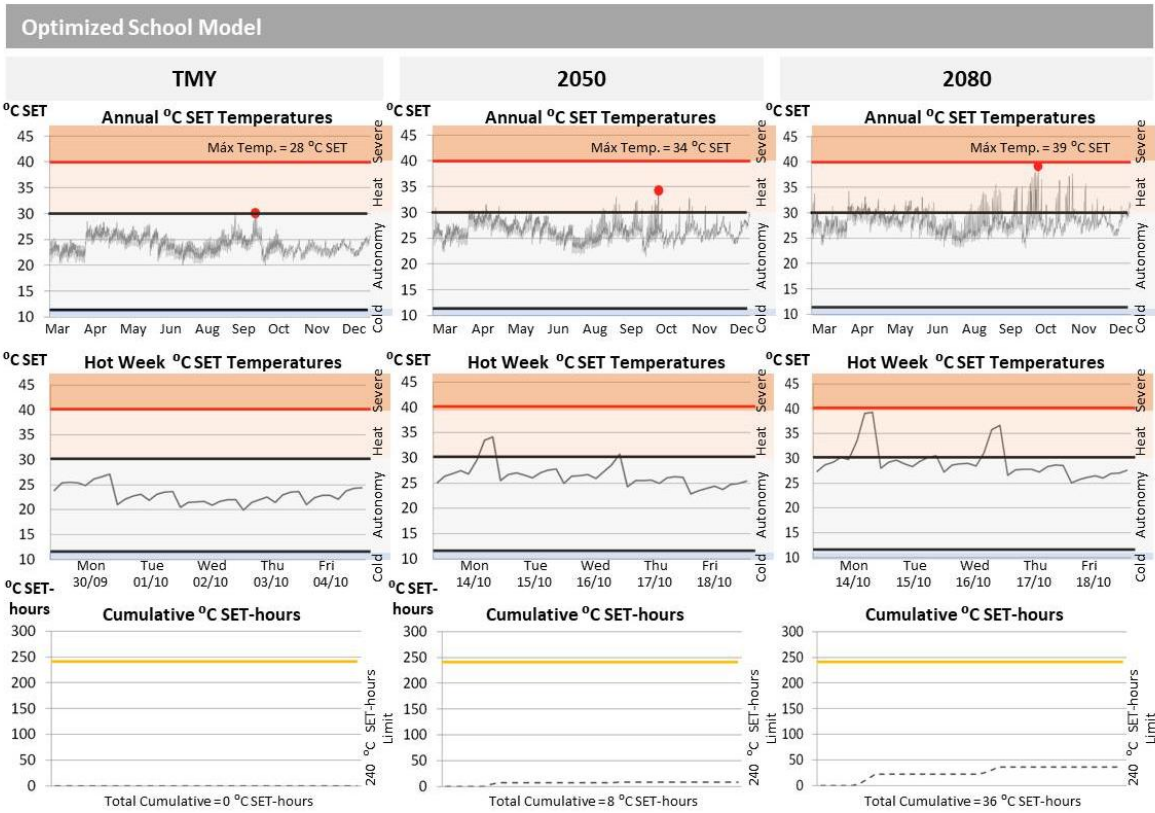




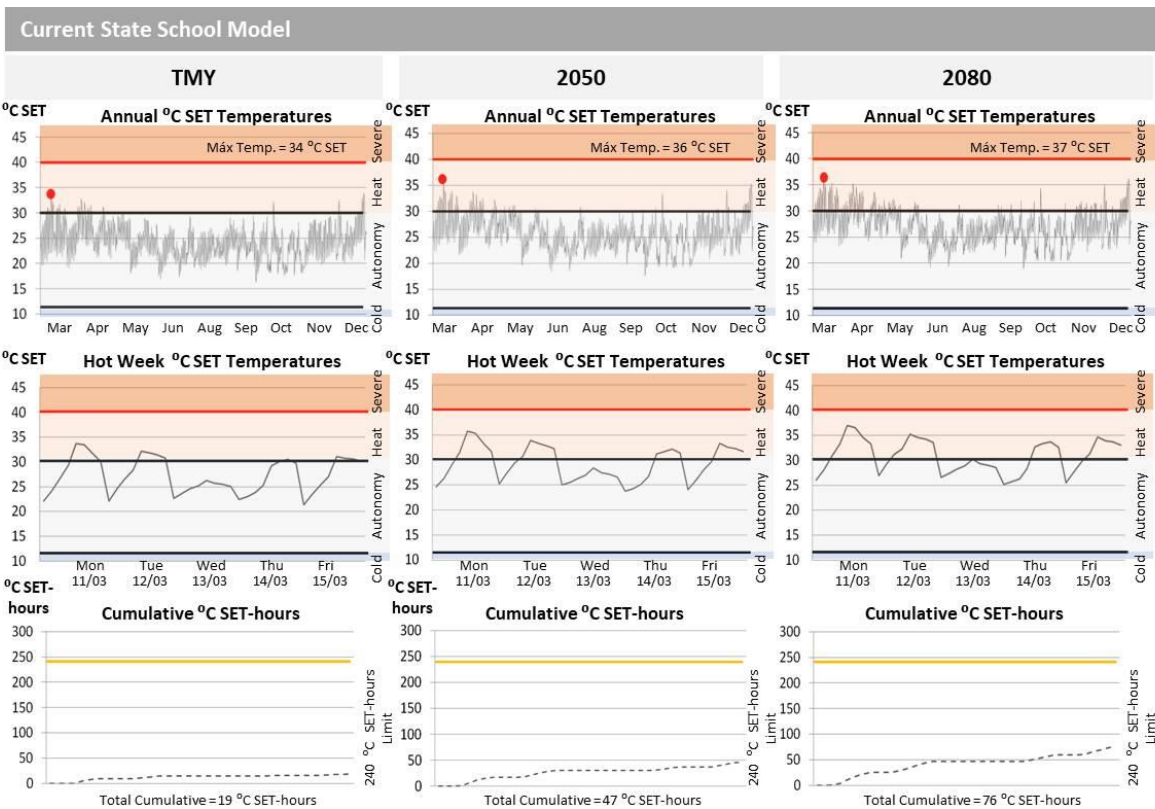


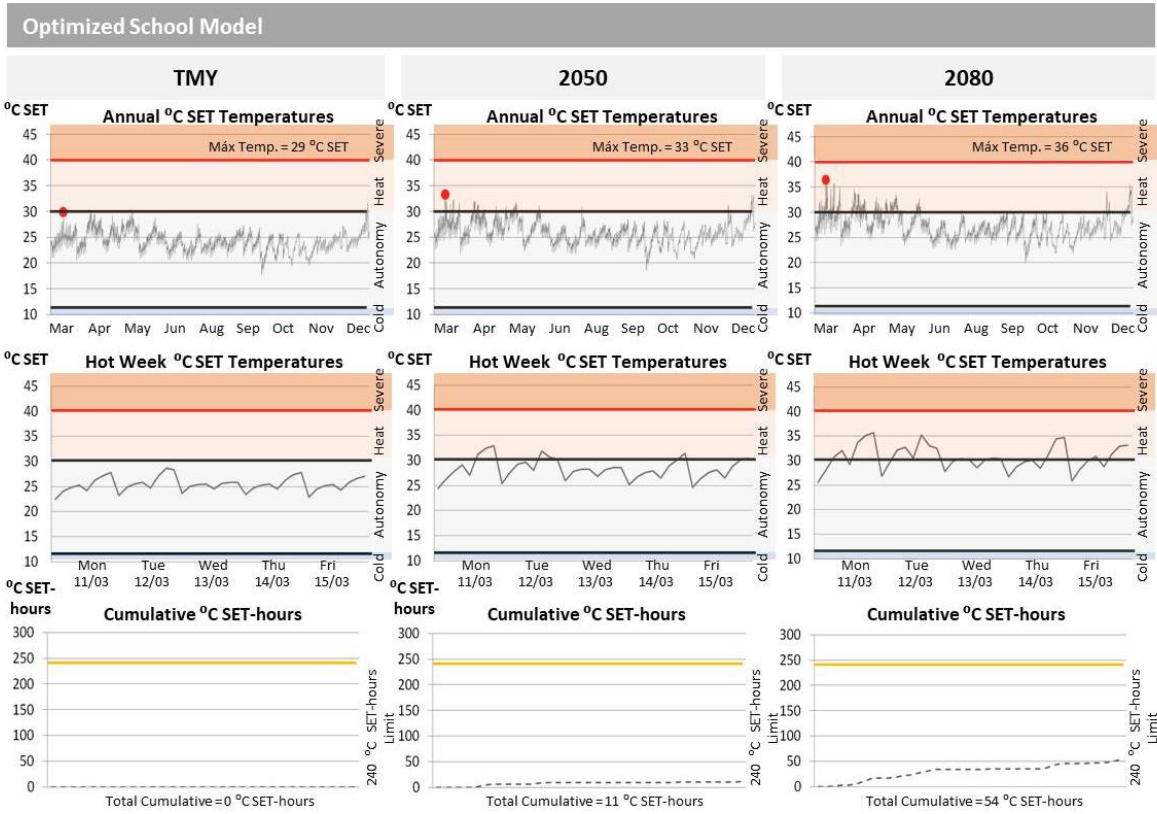
Brasilia (DF) – Zone 4



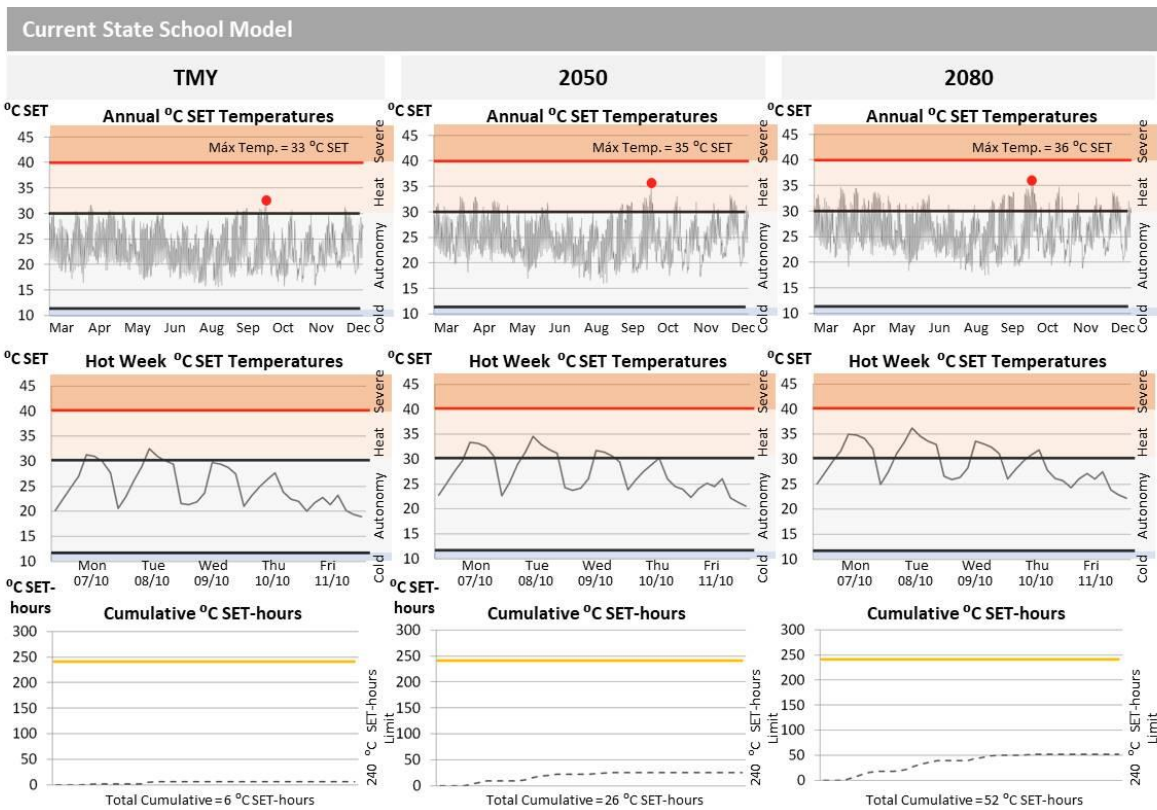


Florianópolis (SC) – Zone 3

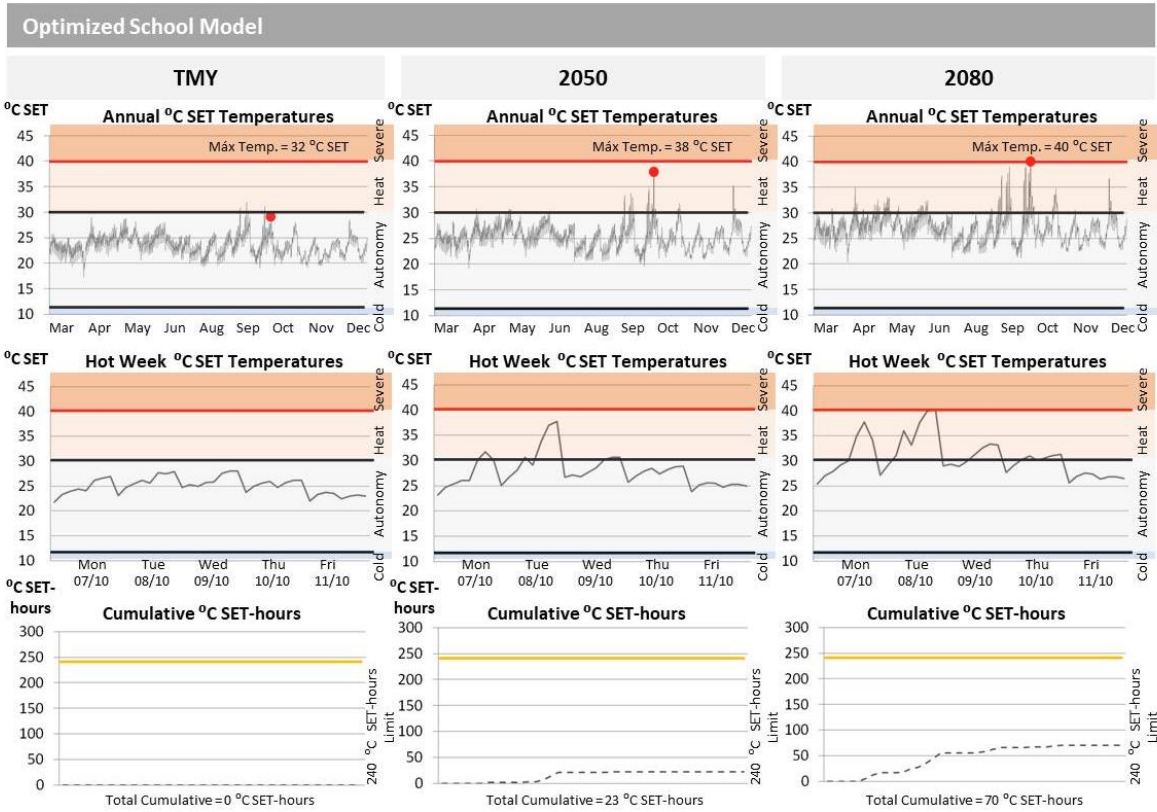




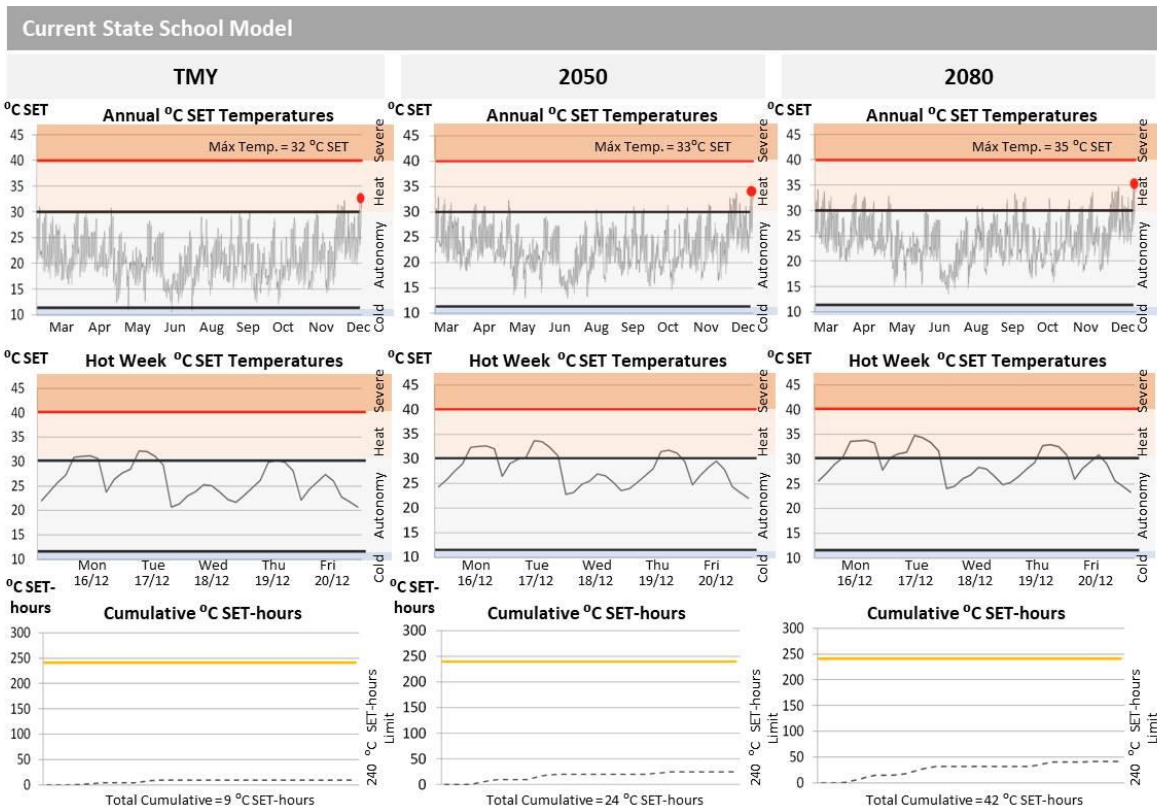
Nova Friburgo (RJ) – Zone 2

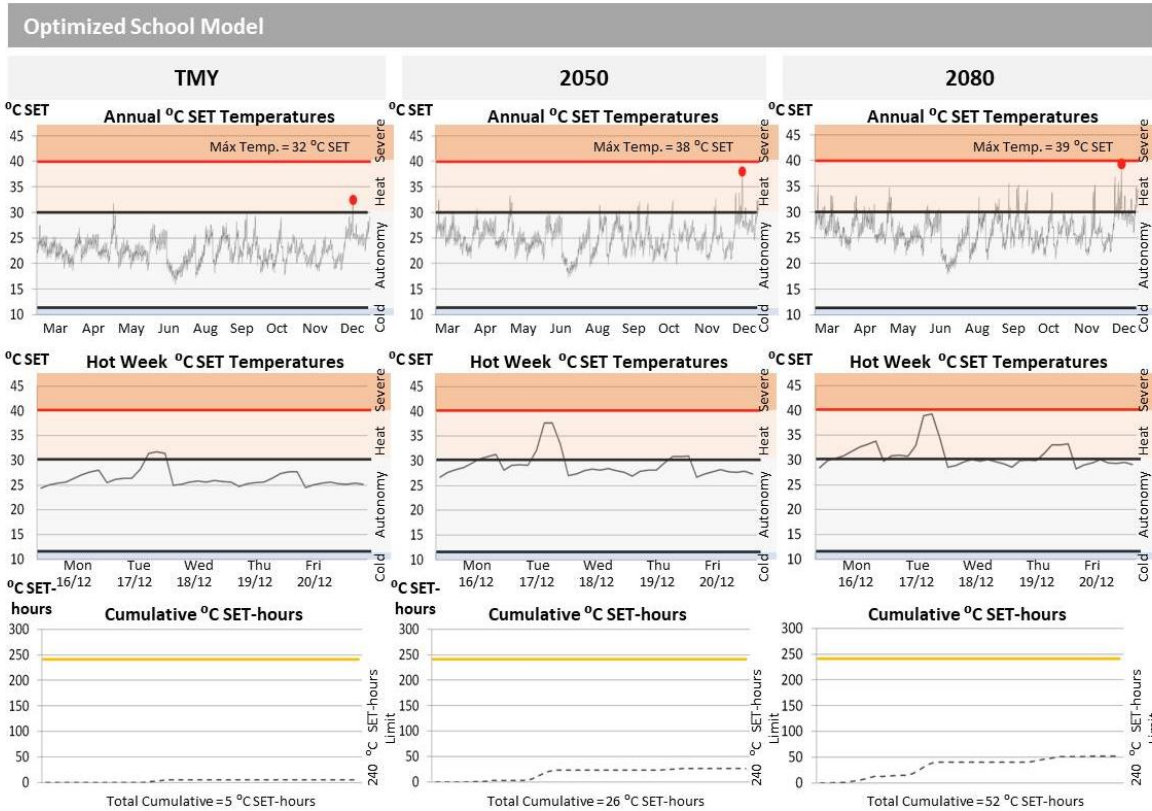






Caxias do Sul (RS) – Zone 1



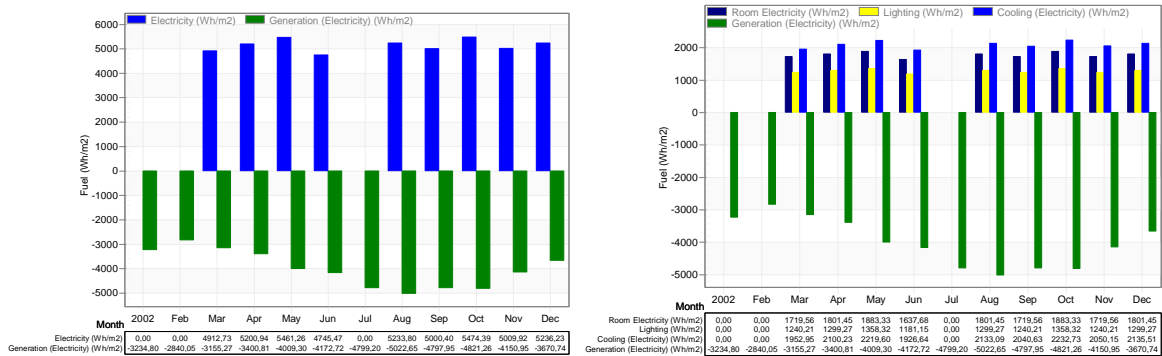


### APPENDIX O

The following graphs are DesignBuilder outputs that compare loads and local energy production, with PV System dimensioned to guarantee Passive Survivability in 2050 and 2080.

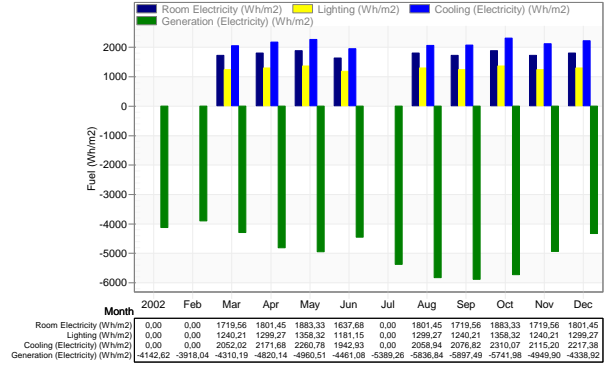
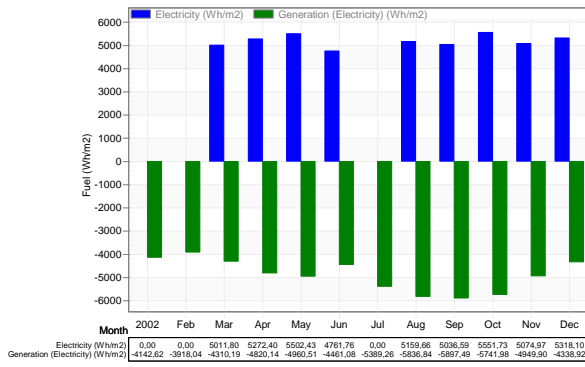
#### 2050

##### Belém (PA) – Zone 8

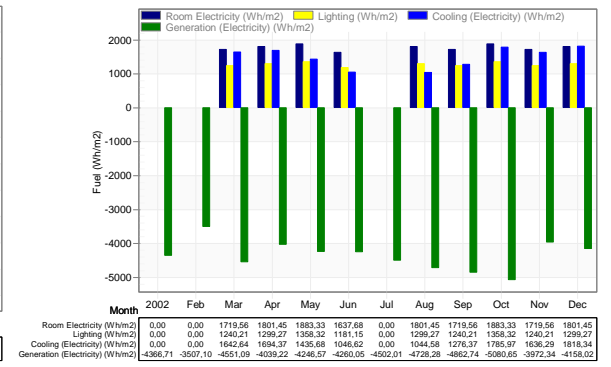
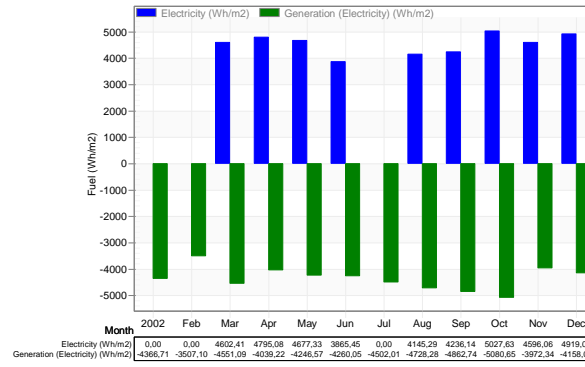


##### Picos (PI) – Zone 7

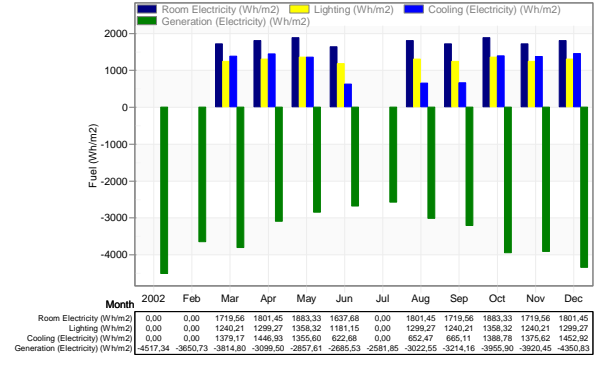
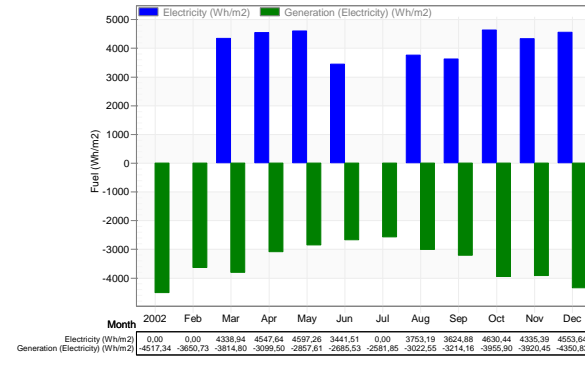




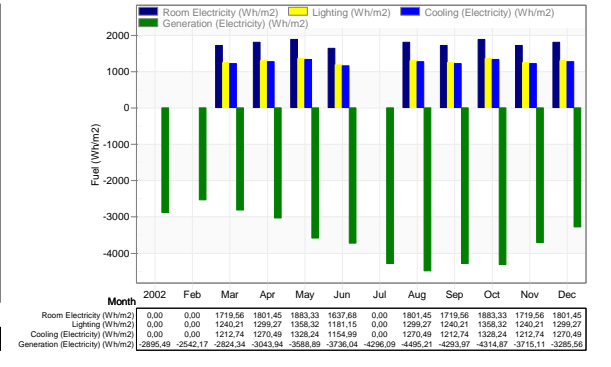
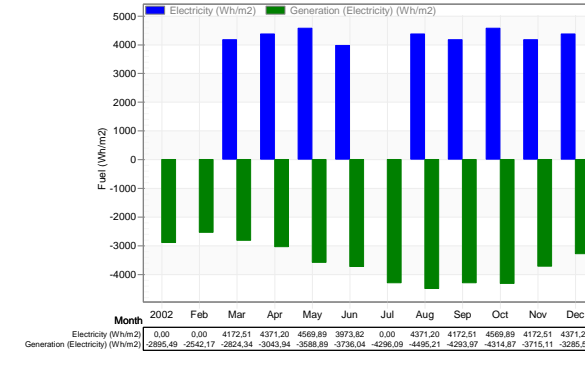
Goiania (GO) – Zone 6



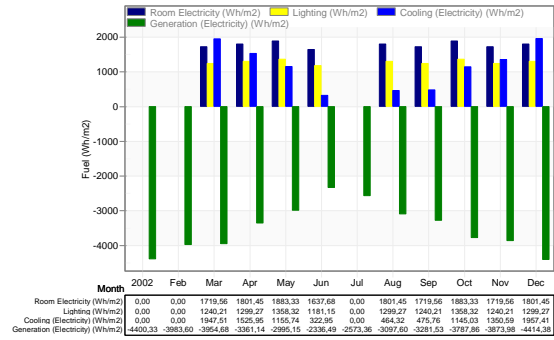
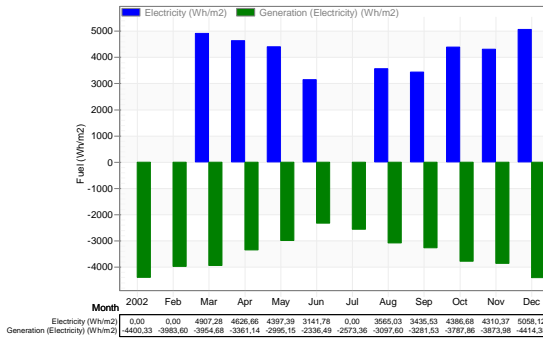
Santos (SP) – Zone 5



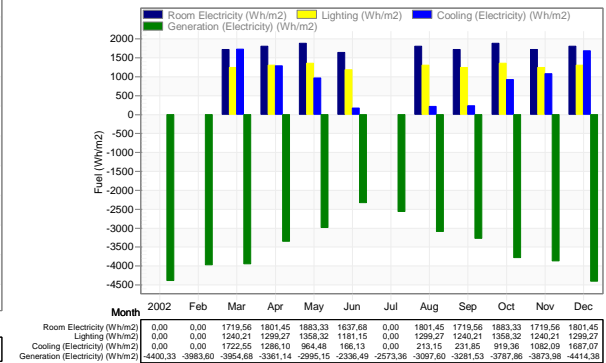
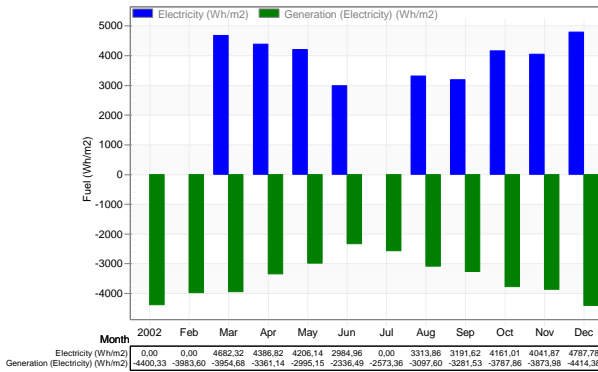
Brasilia (DF) – Zone 4



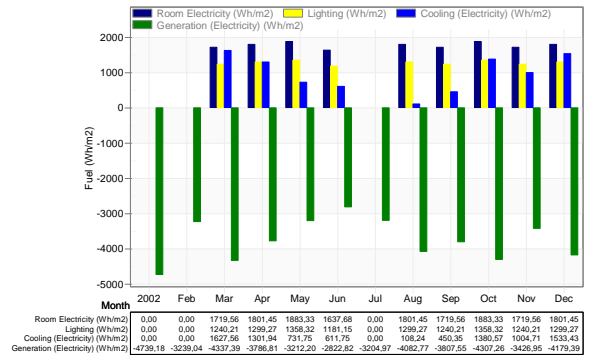
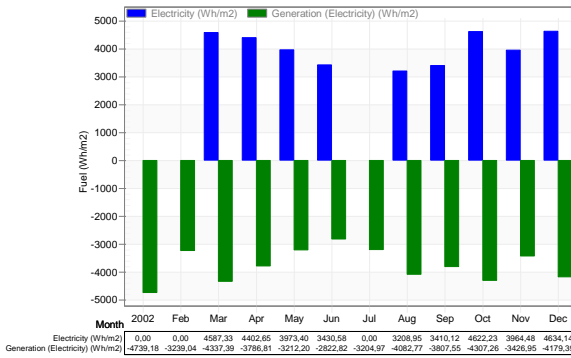
Florianópolis (SC) – Zone 3 – Winter (May to October)



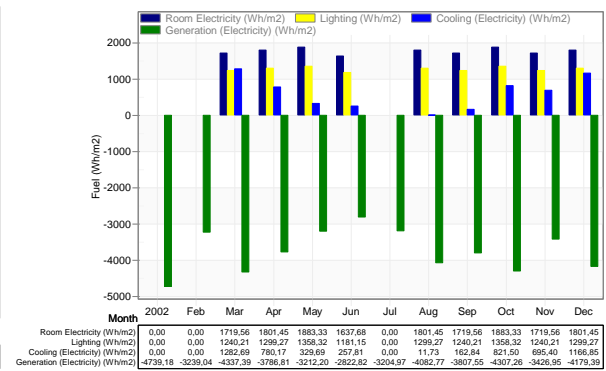
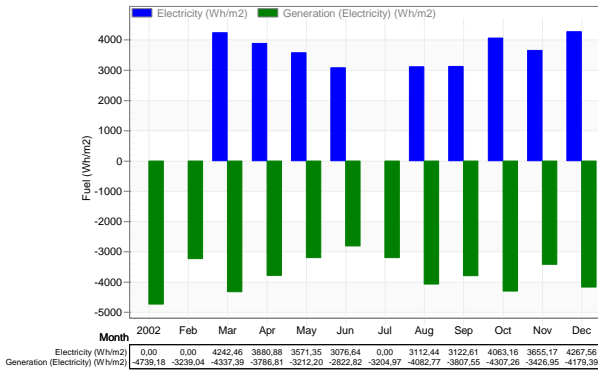
Florianópolis (SC) – Zone 3 – Summer (November to April)



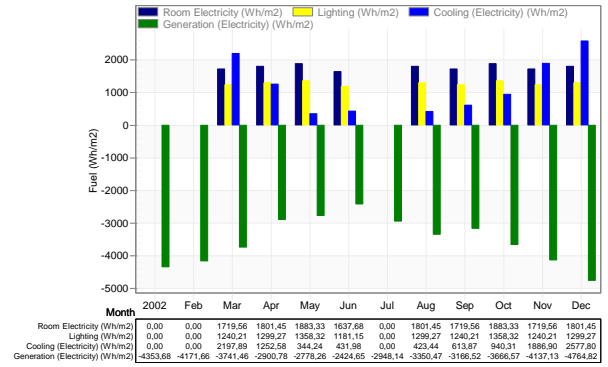
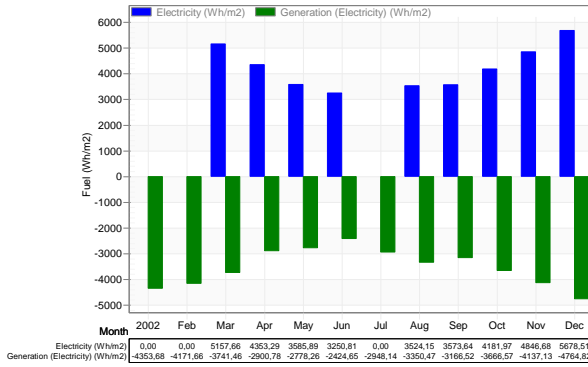
Nova Friburgo (RJ) – Zone 2 – Winter (May to October)



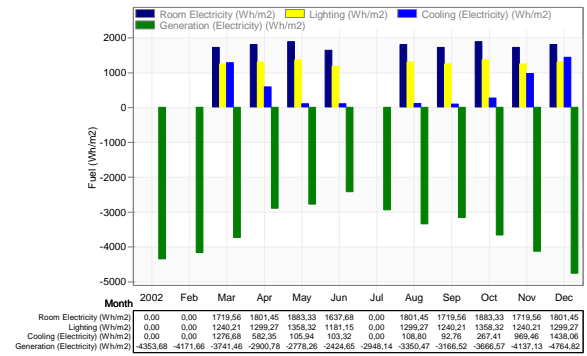
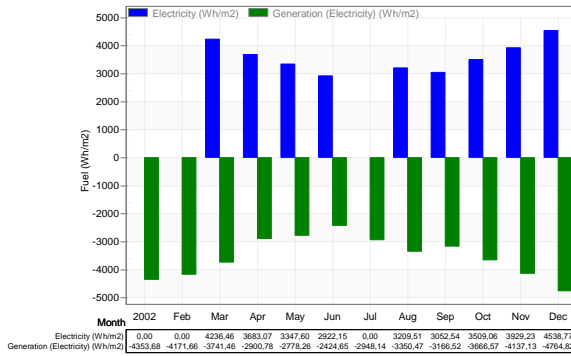
Nova Friburgo (RJ) – Zone 2 – Summer (November to April)



Caxias do Sul (RS) – Zone 1 – Winter (May to October)

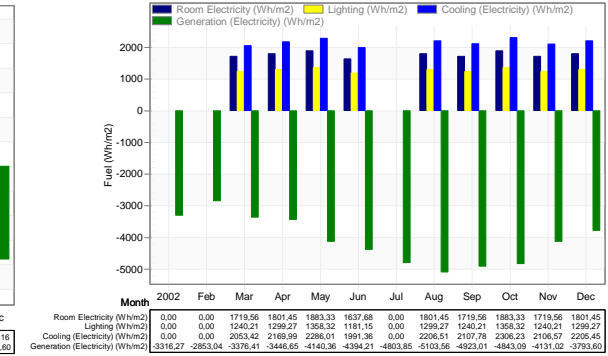
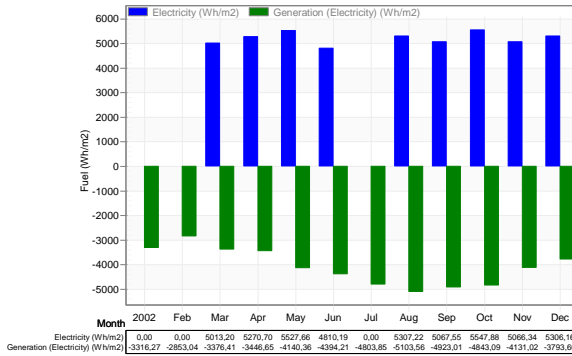


Caxias do Sul (RS) – Zone 1 – Summer (November to April)

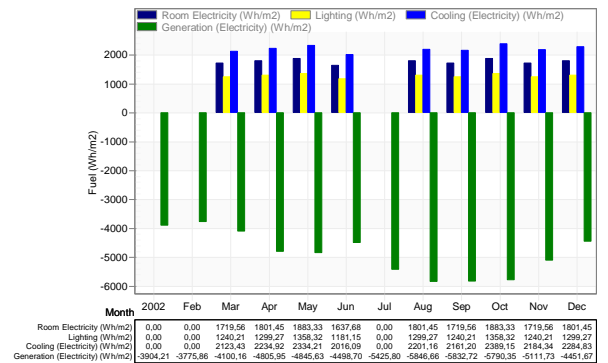
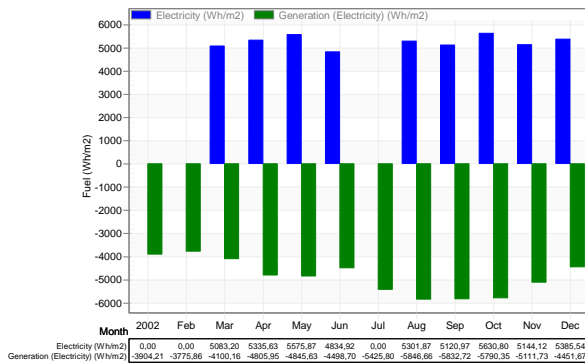


2080

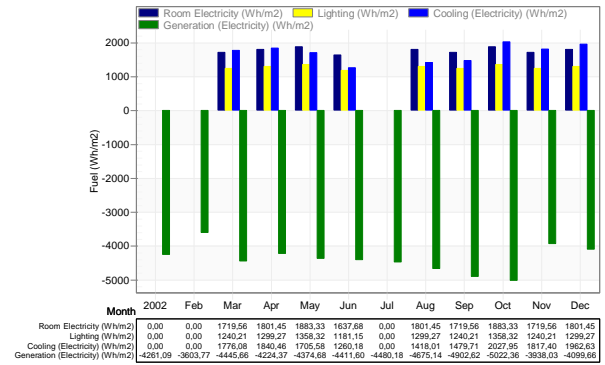
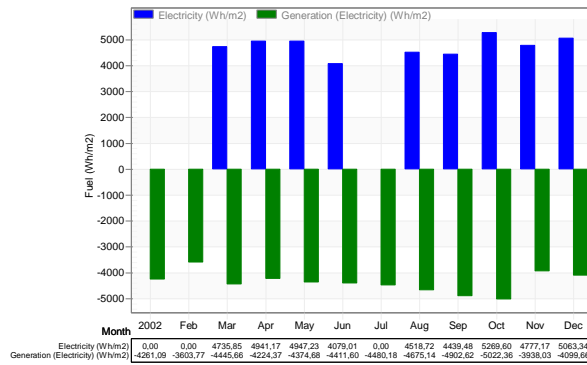
Belém (PA) – Zone 8



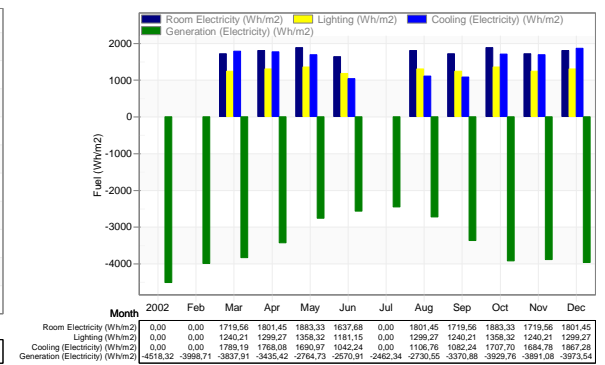
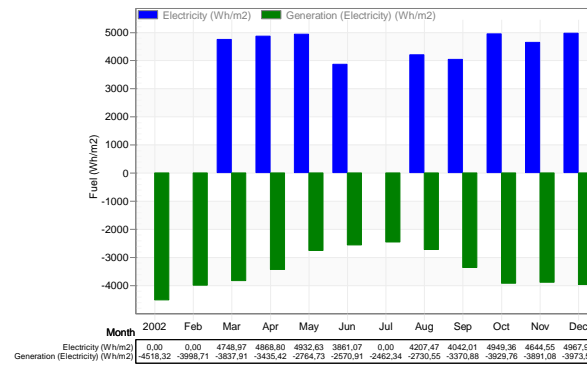
Picos (PI) – Zone 7



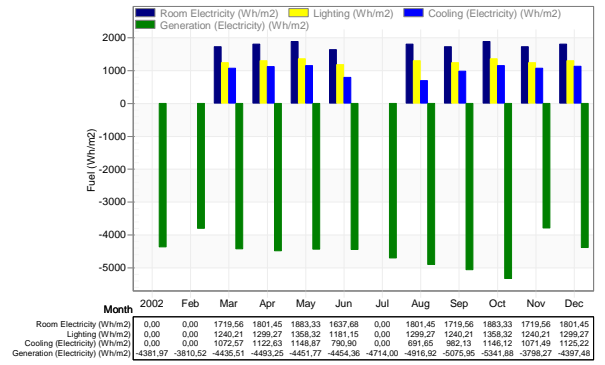
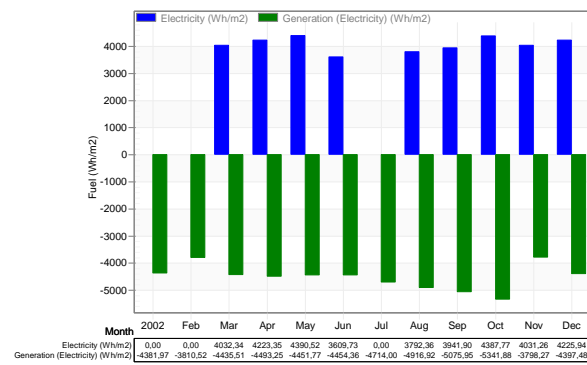
### Goiania (GO) – Zone 6



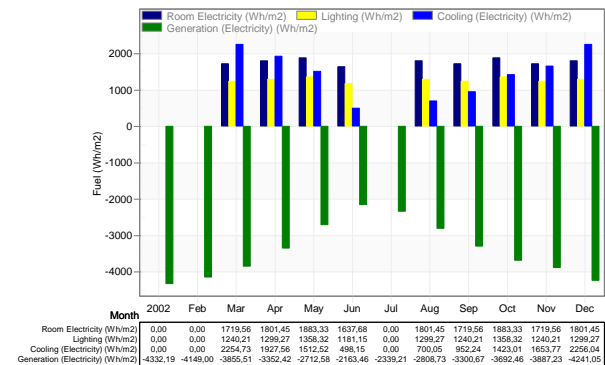
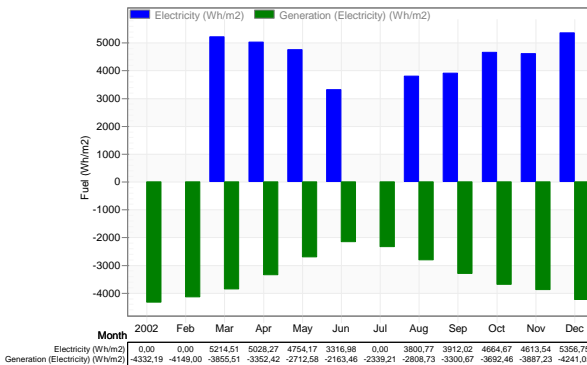
### Santos (SP) – Zone 5



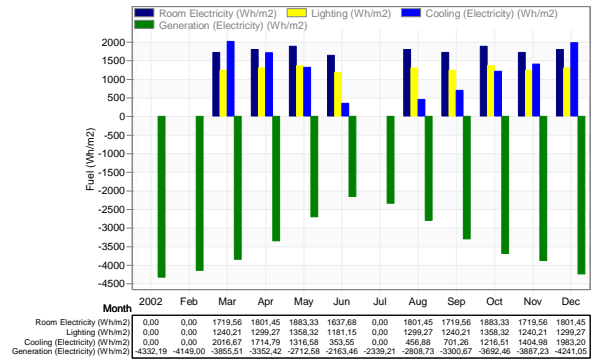
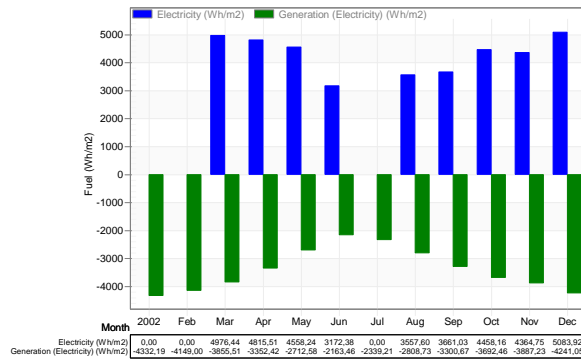
### Brasilia (DF) – Zone 4



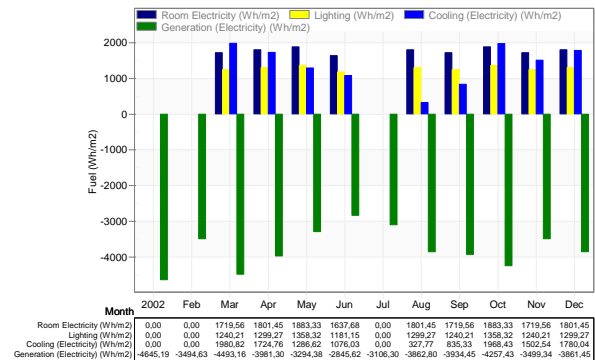
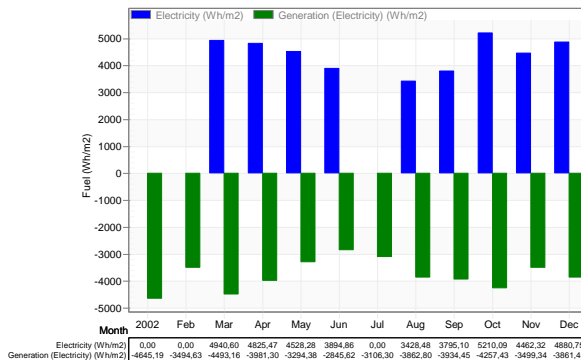
### Florianópolis (SC) – Zone 3 – Winter (May to October)



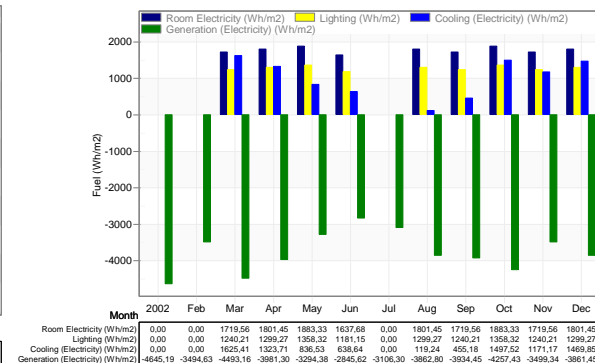
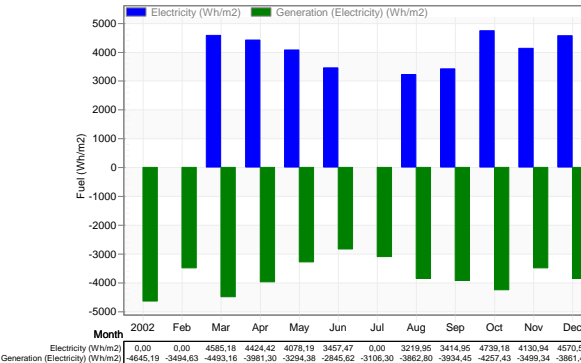
### Florianópolis (SC) – Zone 3 – Summer (November to April)



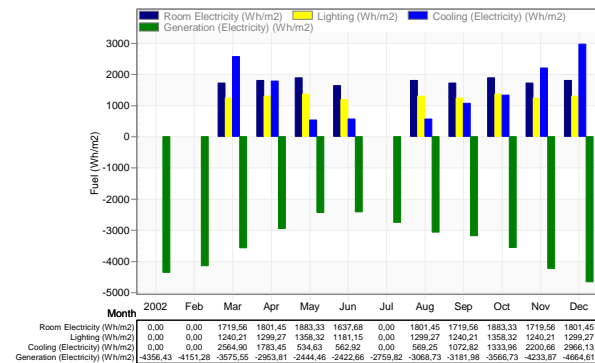
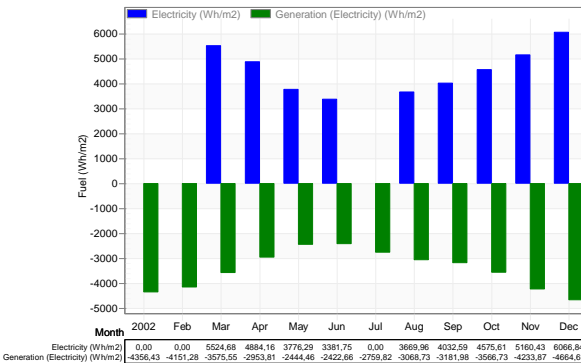
### Nova Friburgo (RJ) – Zone 2 – Winter (May to October)



### Nova Friburgo (RJ) – Zone 2 – Summer (November to April)



### Caxias do Sul (RS) – Zone 1 – Winter (May to October)



### Caxias do Sul (RS) – Zone 1 – Summer (November to April)

